

Active Suspension Development

Based on Energy Analysis

by

© Mohammad Javad Abedini Laksar

A thesis submitted to the
School of Graduate Studies
in partial fulfilment of the
requirements for the degree
of
Master of Mechanical Engineering

Faculty of Engineering and Applied Science
Memorial University of Newfoundland

May 2016

St. John's

Newfoundland

Abstract

This research focuses on developing active suspension optimal controllers for two linear and non-linear half-car models. A detailed comparison between quarter-car and half-car active suspension approaches is provided for improving two important scenarios in vehicle dynamics, i.e. ride quality and road holding. Having used a half-car vehicle model, heave and pitch motion are analyzed for those scenarios, with cargo mass as a variable. The governing equations of the system are analysed in a multi-energy domain package, i.e., 20-Sim. System equations are presented in the bond-graph language to facilitate calculation of energy usage. The results present optimum set of gains for both ride quality and road holding scenarios are the gains which has derived when maximum allowable cargo mass is considered for the vehicle. The energy implications of substituting passive suspension units with active ones are studied by considering not only the energy used by the actuator, but also the reduction in energy lost through the passive damper. Energy analysis showed less energy was dissipated in shock absorbers when either quarter-car or half-car controllers were used instead of passive suspension. It was seen that more energy could be saved by using half-car active controllers than the quarter-car ones. Results also proved that using active suspension units, whether quarter-car or half-car based, under those realistic limitations is energy-efficient and suggested.

Acknowledgement

I can clearly see myself in an art exhibition. People are praising variant paintings. And everyone claims that his favourite painting is much better than the others. Notwithstanding the arguments between the people, all these praises are just for one person and he is the artist who had painted all the paintings one after the other. I would like to show my sincere praise to God who is unique and made the variant religions.

Secondly, I would like to express my sincere gratitude to my uncle, Mr. Javad Abedini Laksar who sacrificed his life for the freedom of the country where I come from. And to my kind family for supporting me spiritually in all steps of my life, especially for living abroad.

Besides my family, I am extremely thankful and indebted to my supervisor Prof. Geoff Rideout for his continuous support of my graduate studies in completing Master of Engineering; For his patience, immense knowledge, and insightful comments and encouragement. I could not have imagined having a better supervisor for my MEng study. Without his precious support it would not be possible to conduct this research.

Contents

Abstract	ii
Acknowledgements	iii
Appendices	viii
List of Tables	ix
List of Figures	xi
Nomenclature	xxiii
1 Introduction	1
1.1 Motivation	1
1.2 Study Approach.....	2
1.3 Simulation Method.....	3
1.4 Vehicle Model.....	4
1.5 Vehicle Parameters.....	6
1.6 Active Suspension Design (LQR Approach)	9
1.7 Energy Analysis.....	11
1.8 Summary	12
2 Literature Review	14
2.1 Classical Work.....	14
2.2 Bond Graph and 20-Sim	15

2.3	Half-Car Model.....	15
2.4	Tire Damping.....	16
2.5	Actuation Limitation	17
2.6	Cargo Mass Effects.....	18
2.7	Vehicle Coupling.....	18
2.8	Vehicle Parameters.....	20
2.9	Energy Analysis.....	20
2.10	Literature Motivation	21
2.11	Summary.....	23
3	Bond Graph	24
3.1	Introduction on Bond Graph	24
3.2	Foundation of Bond Graph	25
3.3	Bond Graph Fundamental Elements.....	26
3.4	Variable of Bond Graph.....	28
3.5	Element Analysis	30
3.5.1	C-Type Elements.....	30
3.5.2	R-Type Elements	31
3.5.3	I-Type Elements.....	32
3.5.4	Sources.....	34
3.5.5	Two-Port Elements	35
3.5.6	Three-Port Elements	36
3.5.7	One-Junction.....	37
3.5.8	Zero-Junction	39

3.6	Orientation	41
3.7	Quarter-Car Active Suspension Model Analysis in Bond Graph	47
4	Development of Half-Car Model	51
4.1	Simple Linear Half-Car Model.....	51
4.2	Complex Non-Linear Half-Car Model.....	54
4.2.1	Plain Model.....	54
4.2.2	Drag Force.....	55
4.2.3	Tire Model.....	57
4.2.4	Engine Torque	57
4.2.5	Roll Friction	60
4.2.6	Slip Friction	61
4.2.7	Road Profile	63
4.2.7.1	Rough Terrain with Gaussian Noise	63
4.2.7.2	Combined Discrete Bumps	64
4.2.8	Assigned Coordinates	67
4.3	Summary	71
5	Active Suspension Gains Using Quarter-Car Approach	72
5.1	Overview.....	72
5.2	System Equations.....	74
5.3	Linear Quadratic Regulator Gains	78
5.4	Weighting Factors.....	83
5.5	Cargo Mass.....	84
5.6	Conclusion.....	87

5.6.1	Cargo Effect.....	87
5.6.1.1	Ride Quality	89
5.6.1.2	Road Holding.....	99
5.6.2	Ride Quality.....	106
5.6.3	Road Holding.....	118
5.6.3.1	Heavily Road Holding	120
5.7	Summary of Conclusions.....	123
6	Active Suspension Gains Using Half-Car Approach	124
6.1	Overview.....	124
6.2	System Equations.....	125
6.3	Linear Quadratic Regulator Gains	132
6.4	Weighting Factors.....	136
6.5	Conclusion.....	138
6.5.1	Cargo Effect.....	138
6.5.1.1	Ride Quality	138
6.5.1.2	Road Holding.....	148
6.5.2	Ride Quality.....	157
6.5.2.1	Ride Quality with Pitch Control	169
6.5.3	Road Holding.....	169
6.5.3.1	Heavily Road Holding	172
6.5.4	Comparison between Quarter-Car Controllers and Half-Car Controller.....	174
6.6	Summary of Conclusions.....	175

7	Energy	177
7.1	Introduction	177
7.2	Dissipated Energy in Shock Absorbers	179
7.3	Active Suspension Actuators.....	180
7.4	Limitation on Actuator Force.....	181
7.5	Limitation on Spring Deflection.....	186
7.6	Half-Car Model using Two Quarter-Car Active Suspension Units	189
7.7	Half-Car Model using Half-Car Active Suspension Units.....	196
8	Conclusions and Recommendations for Future Work	202
8.1	Summary of Conclusions	202
8.2	Future Work.....	206
9	Bibliography	207

Appendices

A	Cargo Mass Analysis.....	203
B	Linear Half-Car Model, Ride Quality Scenario, Quarter-Car Active Suspensions.....	206
C	Linear Half-Car Model, Ride Quality Scenario, Half-Car Active Suspensions.....	220
D	Linear Half-Car Model, Road Holding Scenario, Quarter-Car Active Suspensions....	233
E	Linear Half-Car Model, Road Holding Scenario, Half-Car Active Suspensions.....	42
F	Non-Linear Half-Car Model, Ride Quality, Quarter-Car Active Suspensions.....	271
G	Non-Linear Half-Car Model, Ride Quality, Half-Car Active Suspensions.....	279
H	Non-Linear Half-Car Model, Road Holding, Quarter-Car Active Suspensions.....	287
I	Non-Linear Half-Car Model, Road Holding, Half-Car Active Suspensions.....	297
J	Non-Linear Half-Car Model, Quarter-Car and Half-Car Approaches Comparison.....	307
K	Non-Linear Half-Car Model, Road Holding Scenario, Energy Analysis.....	315
L	Properties Matrices for Half-Car Active Suspension Approach.....	315
M	Continuous Algebraic Riccati Equation (CARE).....	340
N	Codes used in 20-Sim Model.....	342

List of Tables

1.1	Vehicle models.....	4
1.2	Vehicle parameters.....	7
3.1	Bond graph's elements, symbols, and usages.....	27
3.2	Engineering domains with corresponding effort and flow.....	28
3.3	Power, momentum, and displacement variables definition	29
3.4	Energy definition	29
3.5	C-element.....	31
3.6	R-element.....	32
3.7	I-element	33
3.8	Sources	34
3.9	Two-port elements	36
3.10	Three-port elements.....	37

3.11	Preferred position for half-arrows and strokes on bonds	44
3.12	Simplified units in bond graph.....	46
5.1	Weighting parameters for quarter-car controller	84
5.2	Studied truck dimensions.....	86
5.3	Ride quality scenario's gain matrices for different cargo masses	89
5.4	Rear energy indices for ride quality gains.....	98
5.5	Road holding scenario's gain matrices for different cargo masses.....	99
5.6	Weighting parameters for quarter-car controller	121
6.1	Weighting parameters for half-car controller.....	137
6.2	Ride quality scenario's gain matrices for different cargo masses	139
6.3	Rear energy indices for ride quality gains.....	147
6.4	Heavily road holding scenario's gain matrices for different cargo masses....	149
6.5	Ride quality indices comparison.....	175
7.1	Assigned power from engine for actuating units	182
7.2	Dissipated energy in suspension spring comparison (QCM)	194
7.3	Dissipated energy in suspension spring comparison (HCM)	199

List of Figures

1.1	Quarter-car model.....	5
1.2	Half-car model.....	7
2.1	Quarter-car vehicle model.....	16
2.2	Half-car pitch-plane bond graph.....	17
3.1	Different possibilities of having half-arrow and stroke on a bond	25
3.2	Effort and flow signal directions.....	26
3.3	C-element symbol.....	30
3.4	R-element symbol.....	31
3.5	I-element symbol.....	32
3.6	Effort and flow source symbols.....	34
3.7	Transformer and gyrator symbols	35
3.8	Modulated transformer and gyrator symbols	36
3.9	One-junction symbol.....	38

3.10	Parallel spring and damper in a simple mechanical system.....	38
3.11	Parallel spring and damper in a bond graph	39
3.12	Zero-junction symbol.....	40
3.13	Series spring and damper in a simple mechanical system	40
3.14	Series spring and damper in a bond graph.....	41
3.15	Standard half-arrow position for simple elements.....	42
3.16	Fixed causality strokes for sources	43
3.17	Constrained causality for transformers.....	43
3.18	Constrained causality for gyrators.....	43
3.19	One-junction causality constraint.....	43
3.20	Zero-element causality analysis.....	44
3.21	I-element in derivative causality	45
3.22	I-element in integral causality	46
3.23	Quarter-car active suspension model.....	47
3.24	Free body diagram for sprung mass.....	48
3.25	Free body diagram for unsprung mass	48
3.26	Bond graph for a quarter-car active suspension model.....	50

4.1	Linear half-car model	52
4.2	Half-car model bond graph	53
4.3	Plane motion bond graph	55
4.4	Aerodynamic drag force	56
4.5	Torque-speed graph for International DT 530 engine.....	58
4.6	Cruise control	59
4.7	Roll friction	61
4.8	Slip friction.....	62
4.9	Rough terrain with Gaussian noise profile	63
4.10	Single bump profile	64
4.11	Double bump profile.....	65
4.12	Triple bump profile	65
4.13	Ramp profile.....	66
4.14	Symmetric rough road profile.....	66
4.15	Custom road profile	67
4.16	Non-linear half-car model	68
4.17	Front tire coordinate system	69
4.18	Coordinate transformation.....	70

5.1	Quarter-car active suspension unit.....	74
5.2	Free body diagram for sprung mass.....	75
5.3	Free body diagram for unsprung mass.....	75
5.4	Sketch of studied truck.....	86
5.5	Pitch angle using quarter-car gains for ride quality.....	90
5.6	Front sprung mass acceleration using quarter-car gains for ride quality	91
5.7	Rear sprung mass acceleration using quarter-car gains for ride quality	91
5.8	Centre of gravity vertical acceleration using quarter-car gains ride quality.	92
5.9	Vertical acceleration using quarter-car gains for ride quality.....	93
5.10	Rear performance index using quarter-car gains for ride quality.....	94
5.11	Front performance index using quarter-car gains for ride quality.....	94
5.12	Total performance index using quarter-car gains for ride quality.....	94
5.13	Central states using quarter-car gains for ride quality.....	95
5.14	Vertical acceleration for 1 st and 5 th sets of gains for ride quality	98
5.15	Pitch angle using quarter-car gains for road holding.....	100
5.16	Performance indices using quarter-car gains for road holding.....	100
5.17	Tires' deflection using quarter-car gains for road holding.....	101

5.18	Magnified tires' deflection using quarter-car gains for road holding.....	101
5.19	Tires' velocities using quarter-car gains for road holding.....	102
5.20	Magnified tires' velocities using quarter-car gains for road holding.....	102
5.21	Central states using quarter-car gains for road holding	103
5.22	Magnified central states using quarter-car gains for road holding.....	103
5.23	Tires' velocities comparison between two sets of quarter-car gains in road holding.....	104
5.24	Tires' deflections comparison between two sets of quarter-car gains in road holding.....	105
5.25	Vehicle pitch angle over 1 st event of custom road profile in ride quality.....	106
5.26	Vehicle pitch angle over 2 nd event of custom road profile in ride quality.....	107
5.27	Vehicle pitch angle over 3 rd event of custom road profile in ride quality.....	107
5.28	Vehicle pitch angle over 4 th event of custom road profile in ride quality	108
5.29	Vehicle pitch angle over 5 th event of custom road profile in ride quality	108
5.30	Performance index using quarter-car optimum gains in ride quality.....	109
5.31	Front sprung mass acceleration over 1 st event of custom road profile.....	110
5.32	Front sprung mass acceleration over 2 nd event of custom road profile.....	110
5.33	Front sprung mass acceleration over 3 rd event of custom road profile	111
5.34	Front sprung mass acceleration over 4 th event of custom road profile	111

5.35	Front sprung mass acceleration over 5 th event of custom road profile	112
5.36	Rear sprung mass acceleration over 1 st event of custom road profile.....	112
5.37	Rear sprung mass acceleration over 2 nd event of custom road profile.....	113
5.38	Rear sprung mass acceleration over 3 rd event of custom road profile	113
5.39	Rear sprung mass acceleration over 4 th event of custom road profile	114
5.40	Rear sprung mass acceleration over 5 th event of custom road profile	114
5.41	Central states over 1 st event of custom road profile	115
5.42	Central states over 2 nd event of custom road profile	116
5.43	Central states over 3 rd event of custom road profile.....	116
5.44	Central states over 4 th event of custom road profile	117
5.45	Central states over 5 th event of custom road profile	117
5.46	Vehicle pitch angle using quarter-car gains for road holding.....	118
5.47	Vehicle performance index using quarter-car gains in road holding	119
5.48	Tires' velocities over 2 nd event of custom road profile in road holding.....	119
5.49	Tires' deflections over 2 nd event of custom road profile in road holding.....	120
5.50	Vehicle performance index using quarter-car gains in road holding	121
5.51	Tires' velocities over 3 rd event of custom road profile in road holding	122
5.52	Tires' deflections over 3 rd event of custom road profile in road holding.....	122

6.1	Half-car active suspension model	126
6.2	Free body diagram for chassis	126
6.3	Free body diagram for front unsprung mass.....	127
6.4	Free body diagram for rear unsprung mass	127
6.5	Pitch angle using half-car gains for ride quality.....	140
6.6	Front sprung mass acceleration using half-car gains for ride quality.....	141
6.7	Rear sprung mass acceleration using half-car gains for ride quality.....	141
6.8	Centre of gravity vertical acceleration using half-car gains for ride quality .	142
6.9	Vertical acceleration using half-car gains for ride quality	143
6.10	Total performance index using half-car gains for ride quality	143
6.11	Central states using half-car gains for ride quality	144
6.12	Magnified central states using half-car gains for ride quality	145
6.13	Vertical acceleration for 1 st and 5 th sets of gains for ride quality	148
6.14	Pitch angle using half-car gains for road holding.....	150
6.15	Performance indices using half-car gains for road holding	151
6.16	Tires' deflection using half-car gains for road holding	152
6.17	Magnified tires' deflection using half-car gains for road holding	152
6.18	Tires' velocities using half-car gains for road holding	153

6.19 Magnified tires' velocities using half-car gains for road holding	153
6.20 Central states using half-car gains for road holding.....	154
6.21 Magnified central states using half-car gains for road holding.....	154
6.22 Tires' velocities comparison between two sets of half-car gains in road holding.....	155
6.23 Tires' deflections comparison between two sets of half-car gains in road holding.....	156
6.24 Vehicle pitch angle over 1 st event of custom road profile in ride quality.....	157
6.25 Vehicle pitch angle over 2 nd event of custom road profile in ride quality.....	158
6.26 Vehicle pitch angle over 3 rd event of custom road profile in ride quality	158
6.27 Vehicle pitch angle over 4 th event of custom road profile in ride quality	159
6.28 Vehicle pitch angle over 5 th event of custom road profile in ride quality	159
6.29 Performance index using half-car optimum gains in ride quality	160
6.30 Front sprung mass acceleration over 1 st event of custom road profile.....	161
6.31 Front sprung mass acceleration over 2 nd event of custom road profile.....	161
6.32 Front sprung mass acceleration over 3 rd event of custom road profile	162
6.33 Front sprung mass acceleration over 4 th event of custom road profile	162
6.34 Front sprung mass acceleration over 5 th event of custom road profile	163
6.35 Rear sprung mass acceleration over 1 st event of custom road profile.....	163

6.36	Rear sprung mass acceleration over 2 nd event of custom road profile.....	164
6.37	Rear sprung mass acceleration over 3 rd event of custom road profile.....	164
6.38	Rear sprung mass acceleration over 4 th event of custom road profile	165
6.39	Rear sprung mass acceleration over 5 th event of custom road profile	165
6.40	Central states over 1 st event of custom road profile	166
6.41	Central states over 2 nd event of custom road profile	167
6.42	Central states over 3 rd event of custom road profile.....	167
6.43	Central states over 4 th event of custom road profile.....	168
6.44	Central states over 5 th event of custom road profile.....	168
6.45	Vehicle pitch angle using half-car gains for road holding	170
6.46	Vehicle performance index using half-car gains in road holding.....	170
6.47	Tires' velocities over 1 st event of custom road profile in road holding.....	171
6.48	Tires' deflections over 2 nd event of custom road profile in road holding.....	171
6.49	Vehicle performance index using half-car gains in road holding.....	172
6.50	Tires' velocities over 3 rd event of custom road profile in road holding	173
6.51	Tires' deflections over 3 rd event of custom road profile in road holding.....	173
7.1	Limitation on actuator force for 3 rd event on the road profile using quarter-car active suspension units.....	182
7.2	Limitation on actuator force for 5 th event on the road profile using quarter-	

car active suspension units.....	183
7.3 Limitation on actuator power for 3 rd event on the road profile using quarter-car active suspension units.....	183
7.4 Limitation on actuator power for 5 th event on the road profile using quarter-car active suspension units.....	184
7.5 Limitation on actuator force for 3 rd event on the road profile using half-car active suspension units.....	184
7.6 Limitation on actuator power for 3 rd event on the road profile using half-car active suspension units.....	185
7.7 Limitation on actuator force for 5 th event on the road profile using half-car active suspension units.....	185
7.8 Limitation on actuator power for 5 th event on the road profile using half-car active suspension units.....	186
7.9 Force-deflection relationship for a realistic spring.....	187
7.10 Force-deflection relationship for a realistic spring in QCM	188
7.11 Force-deflection relationship for a realistic spring in HCM	188
7.12 Performance indices using quarter-car active suspension units	189
7.13 Performance indices using half-car active suspension units.....	190
7.14 Dissipated power in suspension using quarter-car actuation units.....	191
7.15 Dissipated power in suspension using half-car actuation units	191
7.16 Dissipated power comparison in the 1 st hike (QCM)	192
7.17 Dissipated power comparison in the 2 nd hike (QCM)	192

7.18	Dissipated power comparison in the 3 rd hike (QCM)	193
7.19	Dissipated power comparison in the 4 th hike (QCM).....	193
7.20	Ride quality performance for 3 rd event of the road profile (QCM).....	195
7.21	Ride quality performance for 5 th event of the road profile (QCM).....	196
7.22	Dissipated energy comparison in the 1 st hike (HCM)	197
7.23	Dissipated power comparison in the 2 nd hike (HCM).....	197
7.24	Dissipated power comparison in the 3 rd hike (HCM)	198
7.25	Dissipated power comparison in the 4 th hike (HCM).....	198
7.26	Ride quality performance for 3 rd event of the road profile (HCM)	200
7.27	Ride quality performance for 5 th event of the road profile (HCM).....	200
8.1	Work summary	203

Nomenclature

ρ	Air Density (kg/m ³)
ρ_i	Associated Weighting Factors
ω	Centre of Gravity Angular Velocity (rad/s)
A	Cross-Sectional Area (m ²)
W_b	Dissipated Energy in Suspension Spring
a	Distance from Centre of Gravity to Front Wheels (m)
b	Distance from Centre of Gravity to Rear Wheels (m)
C_D	Drag Coefficient
DI	Dynamic Index

e	Effort
f	Flow
F_{af}	Front Actuator Force (N)
Z_f	Front Deflection (m)
El_F	Front Horsepower Index
M_{Sf}	Front Sprung Mass (kg)
b_{sf}	Front Suspension Damping Coefficient (N.s/m)
k_{sf}	Front Suspension Spring Stiffness (N/m)
b_{tf}	Front Tire Damping Coefficient (N.s/m)
k_{tf}	Front Tire Spring Stiffness (N/m)
\ddot{Z}_S	Heave Acceleration (m/s ²)
v	Longitudinal Velocity (m/s)
G	LQR Gain Matrix
N	LQR Input-State Combination Weighting Matrix

P	LQR Solution to Matrix Riccati Equation
Q	LQR State Combination Weighting Matrix
J	Performance Index or Cost Function
$\ddot{\theta}_s$	Pitch Acceleration (m/s ²)
TI	Pitch Angle Acceleration of Vehicle Centre of Gravity Index
x_{CG}	Position of Centre of Gravity with Respect of Rear Wheels (m)
k	Radius of Gyration (m)
F_{ar}	Rear Actuator Force (N)
Z_r	Rear Deflection (m)
EI_R	Rear Horsepower Index
M_{sr}	Rear Sprung Mass (kg)
b_{sr}	Rear Suspension Damping Coefficient (N.s/m)
k_{sr}	Rear Suspension Spring Stiffness (N/m)
b_{tr}	Rear Tire Damping Coefficient (N.s/m)
k_{tr}	Rear Tire Spring Stiffness (N/m)

k	Slip Ratio
x	State Variables
u	System Input
M_S	Total Sprung Mass (kg)
J_S	Vehicle Inertia (kg.m ²)
ZI	Vertical Acceleration of Vehicle Centre of Gravity Index
l	Wheelbase Distance (m)

Chapter 1

Introduction

1.1 Motivation

Ride quality, safety, and energy are three extremely important considerations for both automobile companies and customers. Cars, as one of the products most commonly used in people's lives, have changed dramatically in order to improve on these three factors. Ride quality is simply defined as a vehicle's responses to a road surface or terrain. A comfortable vehicle is one with good ride quality. This can be realized by minimizing the

effects of road improprieties on the vehicle occupants. Among these aspects, energy plays a fundamental role and can control the other two factors. Active suspension better manages the trade offs between ride comfort, handling, and road holding than does passive suspension. However, active suspensions consume energy.

The importance of vehicles in people's lives cannot be neglected. Billions of people travel every day around the world by car and the usage of automobiles is increasing dramatically. In 2009, the number of cars worldwide was estimated at about 980 million; however, this number jumped to 1.015 billion in just one year [1]. This non-stop growth shows the importance of studies in this area. Car companies, in order to be able to stay competitive, have tried to produce vehicles with better ride quality, increased safety, and improved energy efficiency. This research presents a method to optimize active suspension gains for vehicles with varying parameters such as mass, and also studies energy implications of active suspension.

1.2 Study Approach

In general, a process can be studied under two approaches, i.e., simulation and full scale testing. In the engineering domains, the simulation approach is more appropriate when the cost of the real experiment is extremely high. Simulation is an innovative method that

can forecast uncertain processes and provide answers to desired inquiries. Moreover, the results of simulation do not cause any damage to equipment, environments, or people. Even undesirable mistakes in the simulation can be a great learning experience. Simulation environments can also provide immediate feedback and different variables can be read and recorded during the process. Having considered all these benefits, this research is based on a simulation.

1.3 Simulation Method

The bond-graph approach is known as a strong method for simulating and solving governing equations for engineering systems such as mechanical, electrical, acoustical, material systems, etc. The bond graph language can make it easier to implement the classical approaches, i.e., Lagrange theorem and Newton's laws. It is a domain-independent tool and plays a great role in analyzing complicated systems that consist of various subsystems in different domains. These advantages often lead researchers to prefer this method more than others. In this research, the generated model in bond graph language is analyzed by means of a 20-Sim package [2] where governing equations can be solved in the desired state-space domain.

1.4 Vehicle Model

There are three main models: quarter-car, half-car, and full-car models. These commonly used models can be categorized as follows based on their degrees of freedom (DOF).

Table 1.1: Vehicle models

DOF	One	Two		Three	Four	Seven
Model	Quarter - Car	Quarter - Car	Half - Car	Full - Car	Half - Car	Full - Car

In this work, the half-car model is chosen. In the half-car model, the vehicle is modeled as a singular beam connected to the ground with two distinct masses in the front and rear where the suspension units are located.

In the simplest model, the 1-DOF quarter-car, the entire vehicle's mass is assumed as one point mass which can only heave. This mass is connected to the ground by an equivalent spring instead of springs for each tire. In a higher order model, the tire is modeled as an unsprung mass which is connected to a sprung mass by a parallel set of a damper and a spring. This model is presented in Figure 1.1.

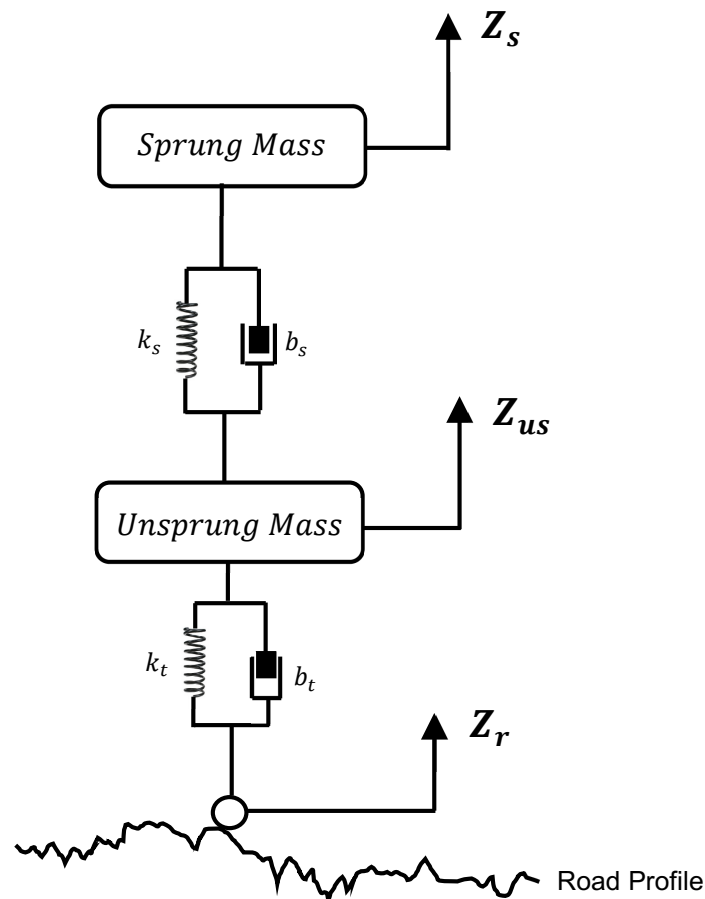


Figure 1.1: Quarter-car model

With the quarter-car model, only heave motion can be studied. In order to study both heave and pitch motion, a more complicated half-car model is needed. In this model, the front left and right suspension systems are idealized into one suspension unit, as is the rear part. Hence, a model will be generated with one equivalent suspension unit in the front and one in the rear. This model can have various degrees of freedom. Finally, in a general model, all four suspension units are modeled independently. This model can analyze heave, pitch, and roll motions.

Active suspension in a theoretical framework can be implemented in all previous discussed models by using a Linear Quadratic Regulator approach [3]. The theory is based on skyhook theory [4]. The skyhook idea mainly describes the motion of an object which is travelling suspended by an imaginary straight line, suggesting that the object can maintain a stable posture. In general, in an active suspension setup, an actuation unit is considered parallel to the suspension spring and damper, all of which is located between sprung and unsprung masses. However, in some simplified cases, unsprung mass might be negligible. In that case, the actuation unit will be in parallel with the tire stiffness and damper.

1.5 Vehicle Parameters

A half-car vehicle model is demonstrated in Figure 1.2 and the vehicle parameters are categorized in Table 1.2.

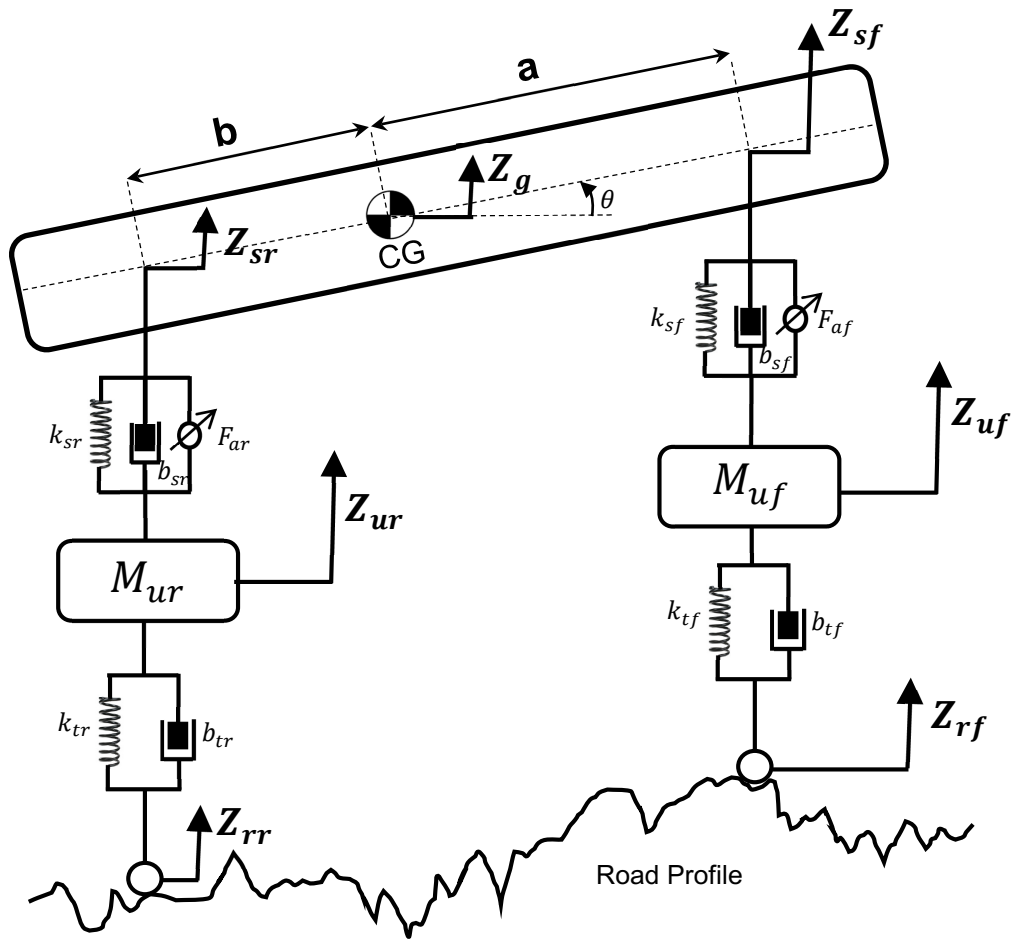


Figure 1.2: Half-car model

Table 1.2: Vehicle parameters [5]

Symbol	Magnitude	Unit	Description
M_{si}	7,257.4	kg	Sprung mass when cargo mass is zero
M_{uf}	276.29	kg	Front unsprung mass
M_{ur}	449.45	kg	Rear unsprung mass
M_C	0 - 18,000	kg	Cargo mass
J_s	20,010.63	kg . m ²	Sprung mass rotational inertia

J_{wf}	10	kg . m ²	Front wheel inertia
J_{wr}	18.76	kg . m ²	Rear wheel inertia
a_0	2.31	m	Distance between front wheel and vehicle centre of gravity when cargo mass is zero
b_0	1.42	m	Distance between rear wheel and vehicle centre of gravity when cargo mass is zero
AC	0.6	m	Height of centre of gravity above front wheel hub
BD	0.6	m	Height of centre of gravity above rear wheel hub
d	3.9	m	Truck bed length
h	2.1	m	Truck bed height
X_1	0.32	m	Distance between rear wheel and centre of gravity of cargo masses
l	3.73	m	Wheelbase distance
r_{wf}	0.413	m	Front wheel radius
r_{wr}	0.413	m	Rear wheel radius
k_{sf}	490,000	N / m	Front suspension stiffness
k_{sr}	1,580,000	N / m	Rear suspension stiffness
k_{tf}	1,680,000	N / m	Front tire stiffness
k_{tr}	3,360,000	N / m	Rear tire stiffness
b_{sf}	10,000	N . s / m	Front suspension damping
b_{sr}	21,800	N . s / m	Rear suspension damping
b_{tf}	1,500	N . s / m	Front tire damping
b_{tr}	2,000	N . s / m	Rear tire damping
A	5.20	m ²	Front area
C_d	0.8	-	Drag coefficient

μ_f	0.7	-	Front tire friction coefficient
μ_r	0.7	-	Rear tire friction coefficient
$k_{max,f}$	0.3	-	Saturation limit for front wheel slip ration
$k_{max,r}$	0.3	-	Saturation limit for rear wheel slip ration

1.6 Active Suspension Design (LQR Approach)

In dynamical systems, it is sometimes desired for a system to work at the minimum cost. This goal can be achieved through optimal control theory. These system dynamics can be described by sets of either linear or non-linear differential equations. On the other hand, cost function, which is set to be minimum, can be presented in various types of functions. The Linear Quadratic (LQ) problem is a case where system equations and cost function are linear and quadratic, respectively. The solution to such an example can be provided by a Linear-Quadratic Regulator, known as LQR. In general, a continuous linear system can be presented as follows:

$$\{\dot{x}\} = [A] \{x\} + [B] \{u\} \quad (1-1)$$

where:

x : *state variable*

u : *system input*

A, B : *system identification matrices*

For this linear system, a quadratic cost function can be defined as follows:

$$J = \int_0^{+\infty} (x^T Q x + u^T R u + 2 x^T N u) dt \quad (1-2)$$

The value of this cost function, J, can be minimized by a proportional feedback control law i.e. $u = -G \cdot x$ where G is the system gain matrix. In order to solve this LQR problem, another equation has to be solved first which is called the Continuous Algebraic Riccati Equation (CARE). CARE can be presented in either of following ways [6]:

$$A^T P + PA + Q - (PB + N)R^{-1}(B^T P + N^T) = 0 \quad (1-3)$$

$$A_{eq}^T P + PA_{eq} + Q_{eq} - PBR^{-1}B^T P = 0 \quad (1-4)$$

where:

P : *solution of CARE*

A_{eq} : $A - BR^{-1}N^T$

Q_{eq} : $Q - NR^{-1}N^T$

Having solved CARE, the gain matrix G can be presented in terms of P and system identification matrices, as follows:

$$G = R^{-1} (B^T P + N^T) \quad (1-5)$$

The first term of the equation (1-5) depends on the solution of the Riccati equation and also the weighting factors used in the cost function. The second term just cancels out the passive force in the damper and spring.

1.7 Energy Analysis

Classic passive suspension units consist of springs and dampers. Passive suspension units aim to dissipate energy via dampers (shock absorbers). Efatpenah [7] claimed that dissipated energy through shock absorbers in active suspension is less than passive; hence, a vehicle equipped with an active suspension unit will have less drop in forward velocity on a rough road in comparison with a flat road. In this research, the engine as an energy source causes longitudinal motion. In both passive and active suspension situations energy will be dissipated by dampers but in different levels. Although this amount of dissipated energy seems to be less in active suspension, some energy is needed to create the necessary force for actuators. An active suspension unit is not considered efficient if it takes a high percentage of engine power to generate adequate power for actuators. The efficiency of active suspension is analyzed in this research based on this point of view. The net energy cost of an active suspension unit can be calculated by subtracting passive damper power savings from the required actuator power.

1.8 Summary

Although much work has been done on designing and optimizing active suspension, there is an abundance of research on designing a better active actuation system which is also reasonable from an energy point of view. This research tries to present an effective force actuator control design which can improve vehicle ride quality or road holding while the required actuator force and energy remain physically reasonable.

A detailed background of previous work and the importance of the current research is explained in Chapter 2.

In Chapter 3, bond graph language and its advantages over classical methods is clarified. Fundamental elements in bond graph language are also introduced and ways to generate an appropriate bond graph for any desired system are explored in this chapter.

Two vehicle half-car models with different levels of complexity are developed in Chapter 4. Moreover, aerodynamic drag force, tire models, engine specifications, and roll and slip frictions are described in this chapter in detail. At the end of that chapter, road profiles are presented.

Active suspension gains obtained by using the quarter-car and half-car approaches are demonstrated in chapters 5 and 6, respectively. Corresponding system equations for each approach are derived using LQR method, and the proper feedback gains are obtained for both ride quality and road holding. The effects of having varying cargo masses are also studied and an optimum set of gains is introduced which can be efficient for all possible cargo masses.

In Chapter 7, all previous results are represented by comparing saved and dissipated energy for passive and active suspension setups. For this reason, some limitations are considered for required actuator force and suspension spring deflection. Energy efficiency of having active suspension units in a vehicle is quantified in this chapter.

Finally in Chapter 8, a detailed summary of the work with highlighted results are covered and potential future work is also suggested at the end of the chapter.

Chapter 2

Literature Review

2.1 Classical Work

Since the late 1980's, a great number of works have been done using bond graph approach to analyze problems in various engineering domains such as mechanical, electrical, material, and etc. In the vehicle dynamics area, one of the fundamental works back to 1983 when Hubbard and Karnopp [8] modeled a vehicle using bond graph approach. They demonstrated various types of motions, i.e., heave, pitch, and roll in their generated model. In addition, they considered a non-linear suspension with tire-force and lateral dynamics. In

1993, Hrovat [9] presented his results of studying applications of optimal control to advanced automotive suspension design and provided another good vehicle model in his paper. However, one of the most general studies on vehicles based on bond graph method was done by Margolis and Shim [10] in 2000. They developed a nonlinear full-car vehicle model and presented controlling units at each tires related to electrical brakes and steering. The model demonstrated a front steering vehicle, considering six degrees of freedom for the body. They represented a complete model for power steering system and suspension units as well, and assembled them all in one general bond graph.

2.2 Bond Graph and 20-Sim

Governing equations in Margolis' work [10] were solved by the ACSL [11]. In 2008, Barak and Gadde [12] formulated the state-space by means of bond graph approach. They used a 4 degrees of freedom model and claimed that there was no approach to study for the physical model, but the bond graph method. They discussed about the advantages of bond-graph approach in comparison with the other methods. MatLab package [13] was used to solve the governing equations.

2.3 Half-Car Model

In 2005, Kumar and Vijayarangan [14] analysed the advantages of active suspension over passive suspension using a Linear Quadratic Regulator (LQR) controller. They used a linear quarter-car model and studied on ride quality and road holding scenarios.

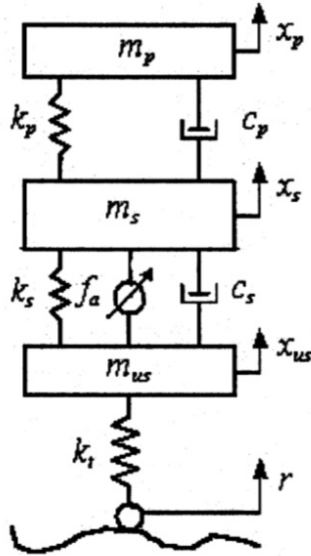


[Figure 2.1: Quarter-car vehicle model][14]

With the quarter-car model, only heave motion can be studied. In order to study both heave and pitch motion, a more complicated half-car model is needed. In this model, front left and right suspension systems are idealized into one suspension unit. So does the rear part. Hence, a model will be generated with one equivalent suspension unit in front and one in the rear. This model can have various degrees of freedom. Finally in a general model, all four suspension units are modeled independently. This model can analyze heave, pitch, and roll motions.

2.4 Tire Damping

In 2000, German Filippini *et al.* [15] considered a nonlinear full-car model. They used 20-Sim environment to implement the vehicle dynamic bond graph. However, tires damping

was neglected in their work. Based on experimental studies by Chantranuwathana *et al.* [16] tire damping coefficients and suspension dampers are on the same order of magnitude, however, tire stiffnesses are generally 10 times greater than suspension's. Having considered this point, tire damping must be included in the model. This point has missed in many other work done so far, but will be considered in this thesis.

2.5 Actuation Limitation

One of the most detailed half-car models in vehicle dynamics area was developed in 2007, when Rideout *et al.* [17] demonstrated a half-car model using the bond graph method.

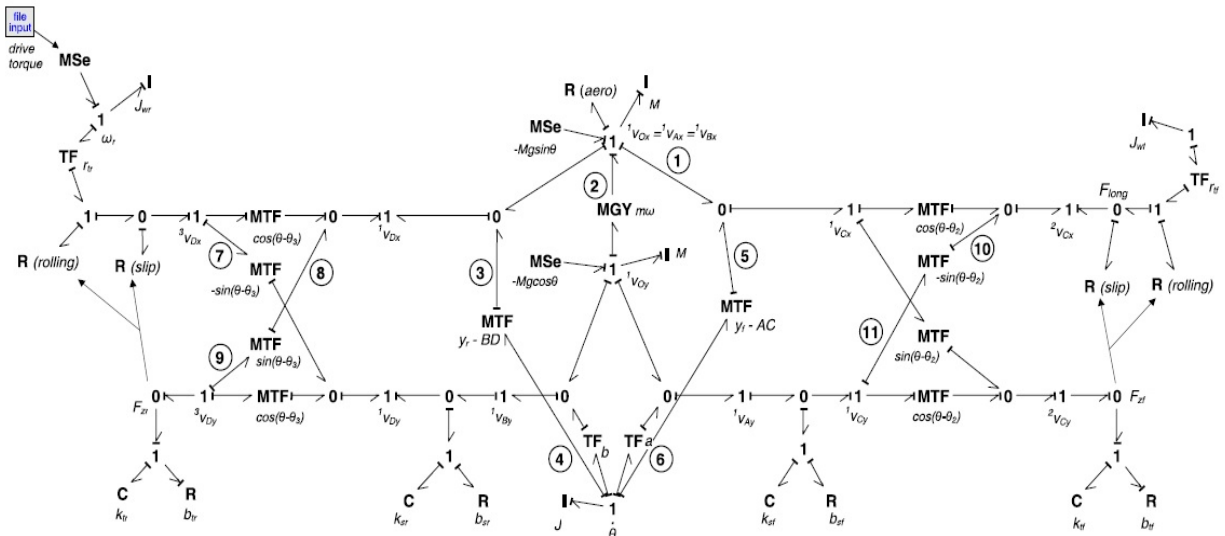


[Figure 2.2: Half-car pitch-plane bond graph][17]

In the following decade, couple of work were done by Rideout's group. In 2009, Adibi-Asl and Rideout [18] modeled and simulated a full-car model with active suspension systems. Ride improvement and handling through an active suspension system was represented in their published paper. With a 7 degrees of freedom, the benefits of using an active suspension system was studied. They did not limit the actuators' force and springs' deflection.

2.6 Cargo Mass Effects

In 2011, Wakeham and Rideout [19] studied on improving ride quality and road holding of a vehicle by means of Linear Quadratic Regulator controller. Vertical and pitch acceleration, and road holding of a pitch plane were analyzed based on a half-car model. There is an abundance in the research on limiting the actuator force and suspension deflection. The LQR gains were also derived for a vehicle with no cargo mass.

2.7 Vehicle Coupling

Krtolica and Hrovat [20] claimed there is a coupling relationship between front and rear part of vehicle and it is related to mass inertia, sprung mass, and location of centre of gravity. For a coupled vehicle, deflections of front and rear parts of the vehicle are related to each other.

Based on their work front and rear part of a vehicle is sufficiently decoupled when equation 2.1 is satisfied within 20%. In other words, the vehicle's front and rear parts can be assumed decoupled when its pitch inertia is between 0.8 and 1.2 times the product of the sprung mass and the distances from wheels to center of gravity.

$$(0.8) M_s \cdot a \cdot b < J_s < (1.2) M_s \cdot a \cdot b \quad (2-1)$$

Where:

M_s : *sprung mass*

J_s : *vehicle inertia*

a : *distance from centre of gravity to front wheels*

b : *distance from centre of gravity to rear wheels*

This criteria is also discussed in Gillespie's book [21]. He suggested an indicator called Dynamic Index (DI) which can distinguish coupling from decoupling situations. Front and rear parts of a vehicle are considered decoupled when DI=1. Otherwise, a coupling exists in the system.

$$DI = \frac{k^2}{x_{CG} \cdot (l - x_{CG})} = \frac{J_s / M_s}{x_{CG} \cdot (l - x_{CG})} \quad (2-2)$$

where:

k : *radius of gyration*

J_s : *sprung mass rotational inertia*

M_s : *sprung mass*

x_{CG} : *distance between rear wheel and centre of gravity*

l : *wheelbase distance*

2.8 Vehicle Parameters

Vehicle parameters for this research has been mainly taken from two sources: A fact book about heavy trucks' specifications published by Fancher *et al.* [22] and a paper published by Rideout *et al.* [17]. These parameters were listed in chapter 1 in detail.

2.9 Energy Analysis

In 2010, Efatpenah *et al.* [7] studied energy requirements for passive and active suspension units. A quarter-car model was implemented in bond graph language and it was developed to study the energy flow through the vehicle. They claimed vehicle's longitudinal velocity drops less when passive suspension unit is replaced by active suspension. Aerodynamic drag force was considered as the only source of non-conservative energy loss which dictates the maximum longitudinal speed. Achieved results from the simulation presented the total energy loss, considering all energy losses in all parts of the model, in the

vehicle with passive suspension units is greater than when active suspension is used. This gap was mainly because of the great difference in the amount of dissipated energy in shock absorbers for passive and active suspension situations.

2.10 Literature Motivation

In this work, heave motion is mainly studied. Using a full-car model would add unnecessary complexity to the simulations and calculations. Hence the model used by Margolis and Shim [10] is not the best model for this research. The governing equations are presented in bond graph language and 20-Sim package is used for the simulating a half-car vehicle model. Some non-linear terms such as aerodynamic drags and tire models are included in the model while these points are neglected in Kumar's [14] work. In a half-car model the vehicle is assumed like a singular beam connected to ground by means of two distinct masses in front and rear which is known as unsprung mass. Since analysing the active suspension performance does not do anything with the roll motion, the full-car model is not used in this work. In order to have more realistic model, appropriate damper units are added in parallel with the tire stiffness units in the front and rear part of the vehicle.

This research tries to present a realistic force actuator system which can improve vehicle ride quality and road holding while the required actuator force and suspension deflection is controlled. The effects of having various cargo masses on ride quality and road holding scenarios are studied and optimum set of gain is presented.

The studied vehicle in this research is in decoupled region while there is no cargo mass. By increasing cargo mass it first goes to coupled region and then back to decoupled region again. Appendix J presents this behavior in detail. Having considered this point, appropriate set of gains is suggested for suspension units. When the vehicle is laden with no cargo mass, dynamic index (DI) is less than 1. Hence, front and rear parts of the vehicle seem to be coupled. By increasing cargo mass, DI is merging until it reaches 1 at cargo mass around 7000kg. At this point, front and rear part of vehicle is decoupled. For a coupled vehicle, front and rear states are related to each other. Therefore, the designed quarter-car controller for each part of the vehicle can affect the other part. Hence, a better performance could be expected when the vehicle is decoupled as the quarter-car controllers are designed independently. However, by escalating more cargo mass, DI is increasing and it goes to the coupled region again. Designing a controller which can be dependable for all possible cargo masses is also studied in this research.

Finally, the dissipated energy in shock absorbers for passive and active suspensions is compared for a more realistic model, i.e., half-car model. Moreover, slip and roll frictions are also considered in the generated model besides the aerodynamic drag force.

2.11 Summary

This research focuses on renewed exploration into active suspension. Having used a half-car model, heave and pitch motions are analyzed for ride quality and road holding purposes, while cargo mass could vary. Furthermore, in active suspension situation, front vehicle's states and rear's can be distinctly modeled as either two independent quarter-car models, or one half-car one. A detailed comparison in this research clarifies advantages and disadvantages of each approach. Eventually, net energy cost of active suspension is evaluated and efficiency of substituting a passive suspension unit with an active one is discussed.

Chapter 3

Bond Graph Method

3.1 Introduction on Bond Graph

Physical systems can be described in different ways. One of the graphical methods to describe dynamical systems is bond graphs. This tool is based on energy structure of the studied system and its subsystems. This fact helps it be able to describe complicated multi-domain systems using a single set of generated elements. On another word, an engineering system consists of one or more subsystems can be described efficiently using the analogy

between equations and physical concepts. These subsystems could be any engineering system such as mechanical, electrical, hydraulic, thermal, acoustical, etc.

The bond graphs language was used by Paynter [23] for the first time (1961). A few years after, it was developed and was re-presented by Karnopp, Margolis, and Rosenberg [24]. Finally Breedveld [25,26] did some formulation on the framework and opened a new window in system theory studies by evolving bond graphs (1984-1985).

3.2 Foundation of Bond Graph

Bond graph method, as a graphical domain-independent tool, consists of elements and bonds. Each bond connects two elements together and represents relationship between flow and effort of those attached elements. They are also known as energy interactions between physical structures of a system. Each bond has one half-arrow and one stroke at ends. These two symbols could come both at one end of a bond, or one per end.



Figure 3.1: Different possibilities of having half-arrow and stroke on a bond

This stroke at one end of a port shows direction of effort and flow signals between the elements. Causality of a bond which shows the direction of the effort between two elements is defined by position of the stroke. Figure 3.2 represents the signal direction of the effort and flow based on the position of stroke on the bond.

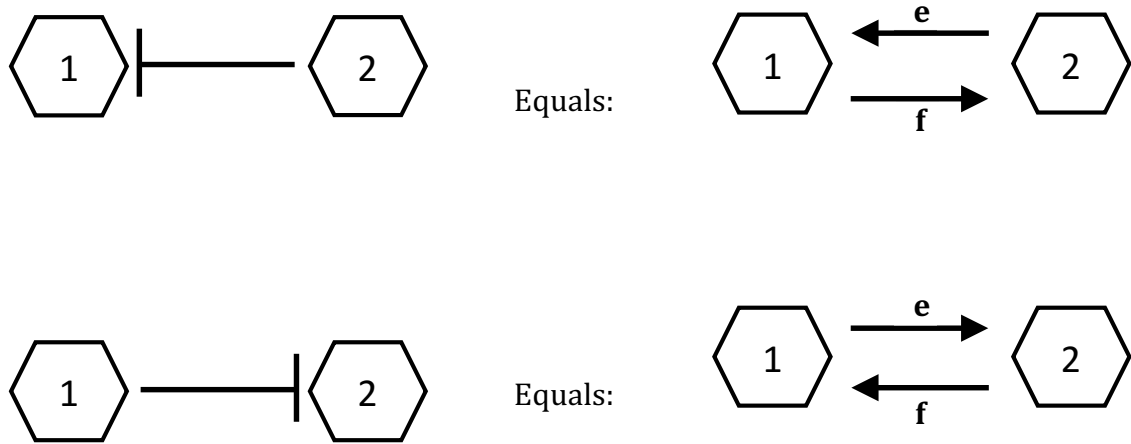


Figure 3.2: Effort and flow signal directions

3.3 Bond Graph Fundamental Elements

In bond graph language, elements can be categorized based on the number of their allowable ports. Some elements cannot connect to more than one element and they are called 1-port elements. Some can connect to two or more elements at the same time. Table 3.1 shows the most common elements based on their allowable ports.

Table 3.1: Bond graph's elements, symbols, and usages

Number of Ports	Name of Elements	Symbol	Usage
1	Resistor	R	Energy dissipater
	Capacitor	C	Storage element for q-type variables
	Inertia	I	Storage element for p-type variables
	Effort Source	Se	Sources
	Flow Source	Sf	
2	Transformer	TF	Representing the passive or active mathematical relationship between flows and efforts of two separated elements.
	Gyrator	GY	
3	Modulated Transformer	MTF	
	Modulated Gyrator	MGY	
3 or more	One-junction	0	
	Zero-junction	1	

3.4 Variables of Bond Graph

Power factors i.e., effort and flow are listed in Table 3.2 for some different physical domains. There are also some other important variables in bond graph language rather than effort and flow. Momentum (p) and displacement (q) are two basic variables which can be derived by time integration over effort and flow, respectively. Power (P) variable also can be defined by multiplication of effort and power.

Table 3.2: Engineering domains with corresponding effort and flow.

Physical Domain		Effort (e)	Flow (f)
Mechanical	Translation	Force (F)	Velocity (V)
	Rotation	Torque (τ)	Angular Velocity (ω)
Electrical		Voltage (V)	Current (i)
Thermal		Temperature (T)	Entropy Change Rate (\dot{S})
		Pressure (P)	Volume Change Rate (\dot{V})
Hydraulic		Pressure (P)	Volume Flow Rate (\dot{Q})
Chemical		Chemical Potential (μ)	Mole Flow Rate (\dot{N})
		Enthalpy (h)	Mass Flow Rate (\dot{m})
Magnetic		Magneto-Motive Force (e_m)	Magnetic Flux (φ)

Table 3.3: Power, momentum, and displacement variables definition

Variable		Definition
Power	$P(t)$	$P(t) = e(t) \cdot f(t)$
Momentum	$p(t)$	$p(t) = \int^t e(t).dt$
Displacement	$q(t)$	$q(t) = \int^t f(t).dt$

Energy in general is defined based on time integration of power. This variable can be represented in two different equations in terms of either effort or flow.

Table 3.4: Energy definition

Variable	Definition	Alternative Definition
Energy	$E(t) = \int^t P(t).dt$	$E(t) = \int^t e(t).dq(t)$
		$E(t) = \int^t f(t).dp(t)$

3.5 Element Analysis

3.5.1 C-type Elements

One-port C-element shows a constitutive relation through a state variable q called displacement.

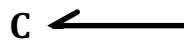


Figure 3.3: C-element symbol

Mathematical relationship between effort and displacement variables represented by a C-element can be shown as follows:

$$e = \phi_C^{-1}(q) \quad (3-1)$$

This element can store or give up potential energy. Physical device for this type of element can be translational springs, rotational springs, torsion bars, electrical capacitors, accumulators, gravity tanks, and etc.

Table 3.5: C-element

Physical Domain	Device	Symbol	Relationship	Schematic
Mechanical	Spring	K^{-1}	$F = K \int V . dt$	
Electrical	Capacitor	C	$E = \frac{1}{C} \int i . dt$	
Hydraulic	Gravity Tank	C_T	$F = \frac{1}{C_T} \int Q . dt$	

3.5.2 R-type Elements

One-port R-element quantity shows a constitutive relationship between effort and flow variables.



Figure 3.4: R-element symbol

Mathematical relationship between effort and flow variables represented by an R-element can be shown as follows:

$$e = \phi_R^{-1}(f) \quad (3-2)$$

This element can dissipate energy. Physical device for this type of element can be mechanical dampers, electrical resistors, porous plugs in pipes, and etc.

Table 3.6: R-element

Physical Domain	Device	Symbol	Relationship	Schematic
Mechanical	Damper	b	$F = b \cdot V$	
Electrical	Resistor	R	$E = R \cdot i$	
Hydraulic	Porous Plugs	R	$P = R \cdot Q$	

3.5.3 I-type Elements

One-port I-element as a conserved quantity shows a constitutive relation through a state variable p called momentum.



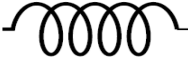
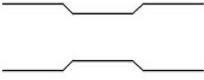
Figure 3.5: I-element symbol

Mathematical relationship between flow and momentum variables represented by an I-element can be shown as follows:

$$f = \phi_I^{-1}(p) \quad (3-3)$$

This element also stores kinetic energy. Physical device for this type of element can be masses, inertances, inductors, and etc.

Table 3.7: I-element

Physical Domain	Device	Symbol	Relationship	Symbol
Mechanical	Mass	m	$\dot{F} = m \cdot V$	
Electrical	Inductor	L	$\dot{E} = L \cdot i$	
Hydraulic	Constricted pipe	Q	$\dot{P} = I_f \cdot Q$	

3.5.4 Sources

Sources as active ports represent the interaction of a system with its environment.



Figure 3.6: Effort and flow source symbols

These elements represent boundary conditions where energy is exchanged between the system and its environment. Physical device for this type of element can be velocity sources, external forces, current sources, voltage sources, and etc.

Table 3.8: Sources

Source Type	Symbol	Relationship	Given Variable	Arbitrary Variable
Effort	Se	$e = E(t)$	$e(t)$	$f(t)$
Flow	Sf	$f = F(t)$	$f(t)$	$e(t)$

3.5.5 Two-Ports Elements

Transformers and gyrators as power continuous elements are two common examples in this category. In transformers either efforts or flows between two elements are transduced by a modulus m . While in a gyrator, effort of one element is related to flow of another element by a modulus r .

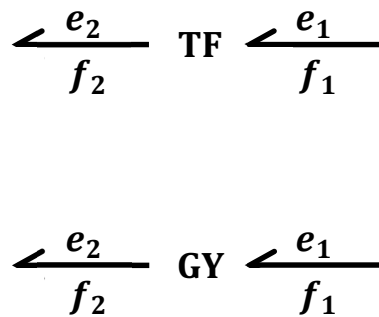


Figure 3.7: Transformer and gyrator symbols

The power-conserving nature of these elements can be shown as follows:

$$e_1 \cdot f_1 = e_2 \cdot f_2 \quad (3-4)$$

Physical devices for this type of element can be mechanical gears, cantilevers, electrical transformers, motors, pumps, generators, turbines, and etc.

Table 3.9: Two-port elements

Element	Symbol	Constant Modulus	Relationship
Transformer	TF	m	$e_1 = m \cdot e_2$ $f_2 = m \cdot f_1$
Gyrator	GY	r	$e_1 = r \cdot f_2$ $e_2 = r \cdot f_1$

3.5.6 Three-Port Elements

Modulated transformers and gyrators as three-port elements do the same roles as transformers and gyrators in bond graph theory in terms of representing a relationship between efforts and flows of two elements. The only difference is modulus in these types of elements are not constant and can be varied while the system is running. In other words, the moduli in these elements are functions of time and can be imported to the element by a signal coming from another element.

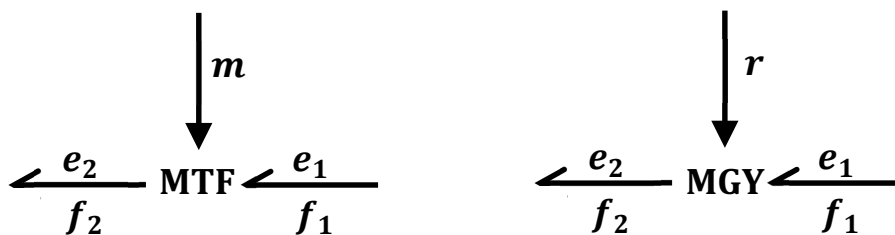


Figure 3.8: Modulated transformer and gyrator symbols

As with constant modulus TF and GY elements, power is conserved:

$$e_1 \cdot f_1 = e_2 \cdot f_2 \quad (3-5)$$

Physical devices for this type of element can be mechanical gears, cantilevers, electrical transformers, motors, pumps, generators, turbines, and etc.

Table 3.10: Three-port elements

Element	Symbol	Signal Modulus	Relationship
Transformer	<i>MTF</i>	<i>m</i>	$e_1 = m \cdot e_2$ $f_2 = m \cdot f_1$
Gyrator	<i>MGY</i>	<i>r</i>	$e_1 = r \cdot f_2$ $e_2 = r \cdot f_1$

3.5.7 One-Junction

This type of junction neither stores nor dissipates energy, but connects two or more elements in a power continuous way. Elements connected to a one-junction have same flow,

and efforts sum to zero them based on positions of half-arrows on the bonds. This junction is also known as a common flow junction. In mechanical systems, it represents Newton's third law and balance forces between elements.

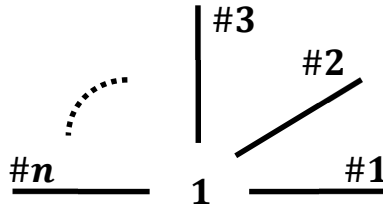


Figure 3.9: One-junction symbol

Mathematical relationship between power variables i.e., efforts and flows of bonds connected to any one-junction can be shown as follows:

$$f_1(t) = f_2(t) = f_3(t) = \dots = f_n(t) \quad (3-6)$$

$$\sum_{i=1}^n e_i(t) = 0 \quad (3-7)$$

An example in the mechanical domain is springs and dampers in a parallel situation. They will have the same velocity while forces can be different in each element.

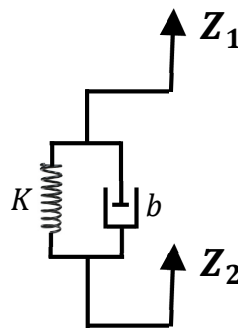


Figure 3.10: Parallel spring and damper in a simple mechanical system

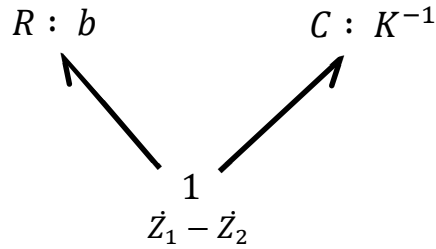


Figure 3.11: Parallel spring and damper in a bond graph

In mechanical systems, effort and flow variables can be substituted by force and velocity separately. Mathematical relationship between power variables for this simple system can be described as follows:

$$V_{spring} = V_{damper} = \dot{Z}_1 - \dot{Z}_2 \quad (3-8)$$

$$F_{spring} = K \cdot (Z_1 - Z_2) \quad (3-9)$$

$$F_{damper} = b \cdot (\dot{Z}_1 - \dot{Z}_2) \quad (3-10)$$

3.5.8 Zero-Junction

This type of junction either neither store nor dissipate energy, but connects two or more elements in a power continuous way. Elements connected to a zero-junction have same effort, and flow is shared between them based on positions of half-arrows on the bonds. This junction is also known as common effort junction.

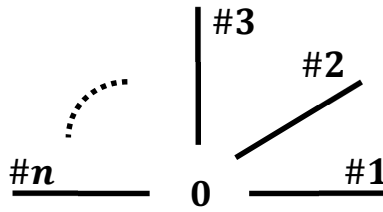


Figure 3.12: Zero-junction symbol

Mathematical relationship between power variables i.e., efforts and flows of bonds connected to any zero-junction can be shown as follows:

$$e_1(t) = e_2(t) = e_3(t) = \dots = e_n(t) \quad (3-11)$$

$$\sum_{i=1}^n f_i(t) = 0 \quad (3-12)$$

An example in mechanical domain is springs and dampers in series. The same force is present in each and all of them, while they could have different velocities.

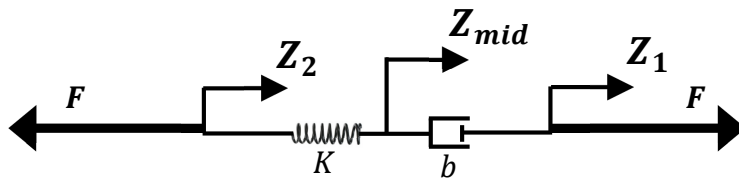


Figure 3.13: Series spring and damper in a simple mechanical system

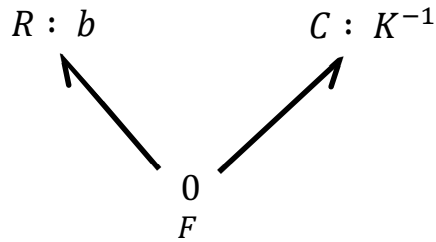


Figure 3.14: Series spring and damper in a bond graph

In mechanical systems, effort and flow variables can be substituted by force and velocity separately. Mathematical relationship between power variables for this simple system can be described as follows:

$$F_{spring} = F_{damper} \quad (3-13)$$

$$F_{spring} = K \cdot (Z_{mid} - Z_2) \quad (3-14)$$

$$F_{damper} = b \cdot (\dot{Z}_1 - \dot{Z}_{mid}) \quad (3-15)$$

3.6 Orientation

Elements in bond graph language can have one or more ports in order to connect with each other. These connections are shown by bonds. Each bond has two symbols, i.e., half-arrow and casual stroke. Direction of half-arrow shows the direction of positive power flow. With this definition, incoming bonds to one element make it consume power if this power is

positive. On the other hand, if effort and flow don't have the same signs, the power won't be positive. Hence, power flows in opposite direction of half-arrow.

Figure 3.15 shows standard mostly-common-used half-arrow position for previously-discussed elements. In springs, typically both force and velocity would be defined as positive in the same direction, eg. tensile. If a positive (eg. tensile) force is extending the spring, then both force and velocity are positive, and power flows into the spring, increasing its stored potential energy. Hence, the positive power flow direction is as shown in Figure 3.15.



Figure 3.15: Standard half-arrow position for simple elements

Source element half-arrows can be in either direction. However, the position of causal strokes on their bonds is fixed based on if they deliver either effort or flow to system.



Figure 3.16: Fixed causality strokes for sources



Figure 3.17: Constrained causality for transformers



Figure 3.18: Constrained causality for gyrators

One-junctions, as common flow elements, can have just one flow as their inputs. As it was discussed earlier in section 3.2, stroke on a bond represents the direction of effort and flow for that bond. Figure 3.19 demonstrates the most common notation for strokes on a one-junction bonds. The elements connected there will use the one-junction flow as an input to their consecutive laws. The only different bond in the Figure is the lowest one which will define the flow.

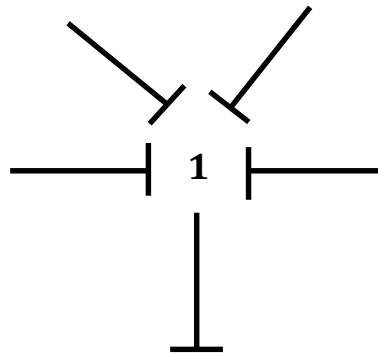


Figure 3.19: One-junction causality constraint

On the other hand, common effort elements which are known as zero-junctions, can just have one effort as input. This is schematically shown in Figure 3.20.

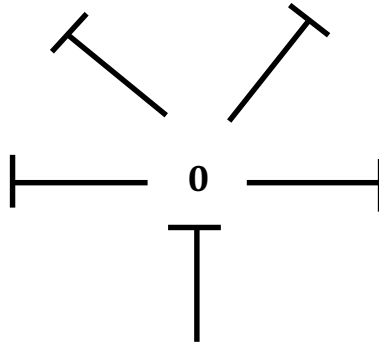


Figure 3.20: Zero-element causality analysis

Table 3.11 briefly shows preferred position of half-arrows and strokes on elements' ports. Although some causalities are fixed, energy-storing elements, C-, and I-elements, can take strokes on either end of their bonds. Based on the position of their casual stroke they can be categorized in either integral or derivative causality group. Integral causality is preferable for these elements. In integral causality, C-elements take the flow and return the effort, and in I-elements flow is returned and effort to the input.

Table 3.11 Preferred position for half-arrows and strokes on bonds

Element	Example	Description
Sources	Sf ——	Fixed causality
	Se ——	Fixed causality
R-element	R ←——	If power is positive
C-element	C ←——	If power is positive
	C ——	Integral causality

I-element	I ←	If power is positive
	I	Integral causality

Figure 3.21 shows derivative causality for an I-element. Based on the following bond, output and input for this element are force and velocity, respectively. Effort as an output of this I-element is related to differentiation of flow i.e., velocity. Hence, it is called derivative causality.

$$e = m \cdot \frac{df}{dt} \quad (3-16)$$



Figure 3.21: I-element in derivative causality

Figure 3.22 shows integral causality for an I-element. Based on the following bond, output and input for this element are velocity and force, respectively. Flow as an output of this I-element is related to differentiation of effort i.e., force. Hence, it is called integral causality.

$$f = \frac{1}{m} \int e \cdot dt$$

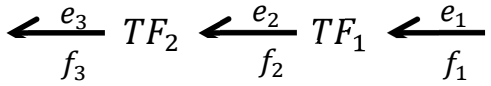
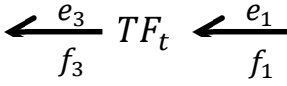
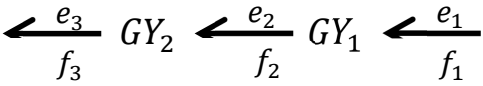
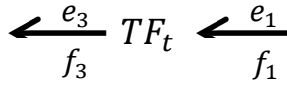
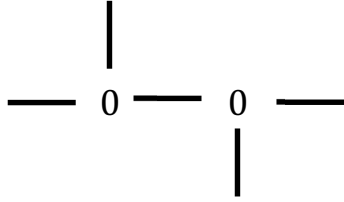
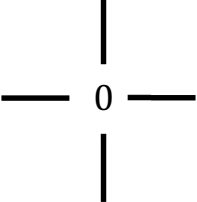
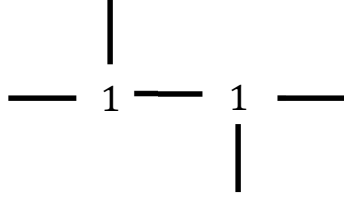
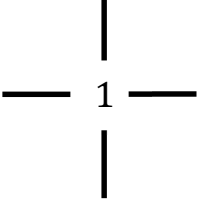
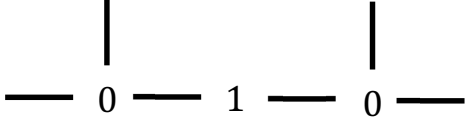
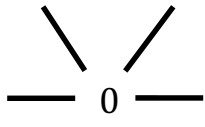


(3-17)

Figure 3.22: I-element in integral causality

Sometimes it is possible to simplify a generated bond graph. Table 3.12 represents some techniques on how to combine two or more possible elements into one.

Table 3.12: Simplified units in bond graph

Initial unit	Simplified unit
	
	
	
	
	

3.7 Quarter-Car Active Suspension Model Analysis in Bond Graph

A quarter-car active suspension model is shown in Figure 3.23. In this model, M_s represents sprung mass of vehicle which in this case will be approximately a quarter of total body mass, frame and engine. M_{us} represents unsprung mass and refers mostly to suspension components and tire mass and brake assemblies. In the following model, sprung mass and unsprung mass are connected to each other with a parallel set of suspension stiffness k_s , and suspension damper b_s . There is an active suspension force F_a which is applied on the suspension section as well. Furthermore, tire stiffness k_t , and tire damper b_t are also made another parallel set between the tire and road. Road profile here is assumed as input of the system.

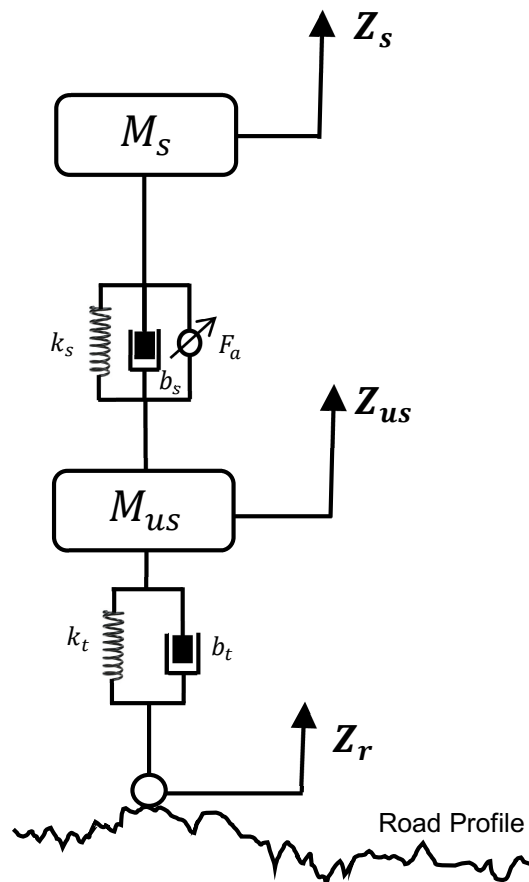


Figure 3.23: Quarter-car active suspension model

Free body diagrams for this system can be drawn as follows:

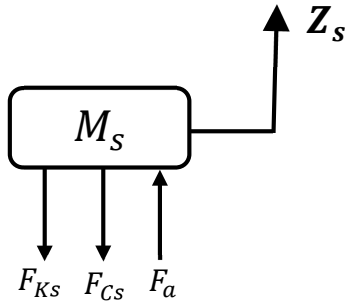


Figure 3.24: Free body diagram for sprung mass

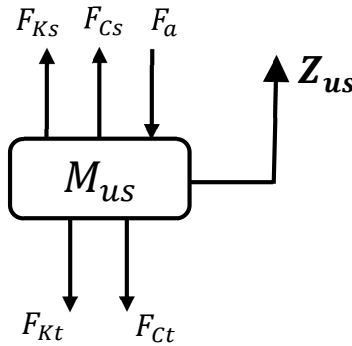


Figure 3.25: Free body diagram for unsprung mass

Based on these free body diagrams in Figures 3.24 and 3.25, governing equation for the system can be derived by satisfying Newtonian's law in vertical direction.

For sprung mass:

$$\sum F_y = M_s \ddot{Z}_s \quad \rightarrow \quad F_a - F_{Ks} - F_{Cs} = M_s \ddot{Z}_s \quad (3-18)$$

where:

$$F_{Ks} = K (Z_s - Z_{us}) \quad (3-19)$$

$$F_{Cs} = b (\dot{Z}_s - \dot{Z}_{us}) \quad (3-20)$$

For unsprung mass:

$$\sum F_y = M_{us} \ddot{Z}_{us} \quad \rightarrow \quad F_{Ks} + F_{Cs} - F_a - F_{Kt} - F_{Ct} = M_{us} \ddot{Z}_{us} \quad (3-21)$$

where:

$$F_{Kt} = K (Z_{us} - Z_r) \quad (3-22)$$

$$F_{Ct} = b (\dot{Z}_{us} - \dot{Z}_r) \quad (3-23)$$

In order to analyze any engineering system (mechanical, electrical, hydraulic, acoustical, material and etc) with bond graph, it first needs to be converted in bond graph language i.e., elements and bonds. Following steps are recommendations to bring a mechanical system into bond graph domain.

- Indicating positive direction of distinct absolute velocity components on free body diagrams.
- Using one-junction for distinct velocities and references.
- Attaching elements with same velocity to their proper one-junction.
- Establishing relative velocities using zero-junctions if it's needed.
- Simplifying the model.
- Assigning proper half-arrows on bonds.
- Assigning proper causality strokes on bonds based on following priorities:
 - ❖ Fixed causality. (sources)

Chapter 4

Development of Half-Car Model

4.1 Simple Linear Half-Car Model

In this model, vehicle is assumed like a singular beam connected to ground by means of two distinct masses in front and rear parts, known as unsprung masses. Front left and right suspension systems are idealized into one suspension unit. So does the rear part. The generated model based on these assumptions has two distinct suspension units in the front and rear, and can present both heave and pitch motions.

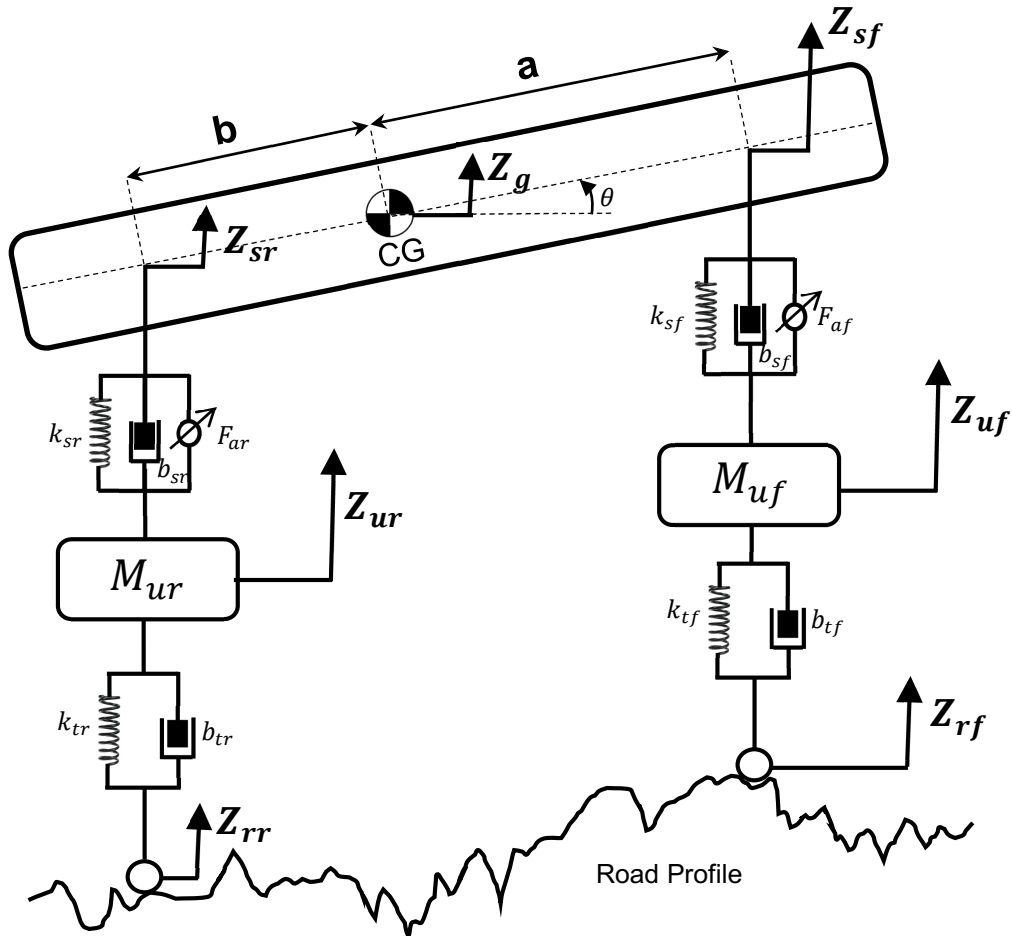


Figure 4.1: Linear half-car model

This model can be basically separated into three main parts: front suspension unit, rear suspension unit, and main vehicle body. The suspension units have been covered in detail in chapter 3. For the main vehicle body, the governing equations can be presented as follows:

$$V_{sf} = V_g + a \cdot \omega \quad (4-1)$$

$$V_{sr} = V_g - b \cdot \omega \quad (4-2)$$

where:

V_{sf} : front sprung mass velocity

V_{sr} : rear sprung mass velocity

V_g : centre of gravity velocity

a : distance between centre of gravity and front wheels

b : distance between centre of gravity and rear wheels

ω : centre of gravity angular velocity

The Bond graph for this model is combination of bond graphs for the suspension units and the main body, presented in Figure 4.2.

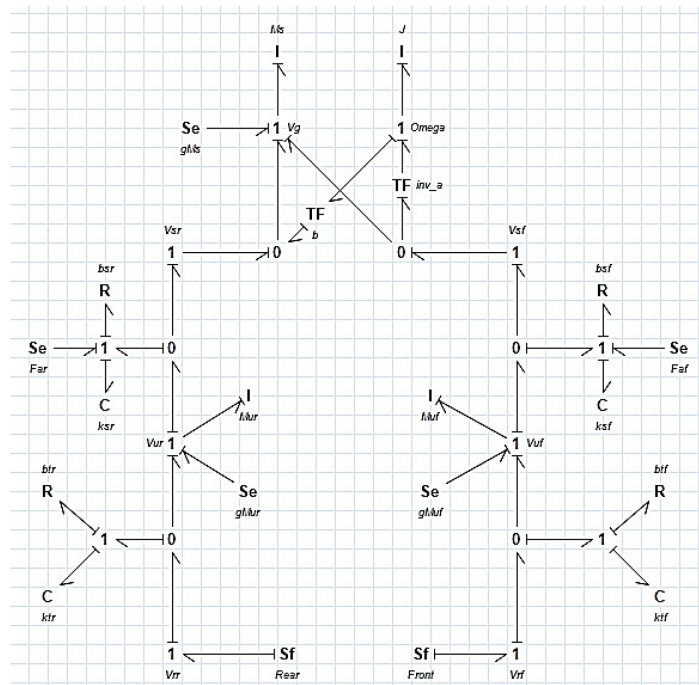


Figure 4.2: Half-car model bond graph

Gravity forces for unsprung masses have been added to the suspension bond graphs. In passive suspension, no external force exerts on sprung masses while in active, actuators apply some amount of force on sprung masses. Moreover, pitch angle in this model is assumed very small. This assumption leads us to consider just vertical motions for front and rear wheels. Hence, the model will be sufficiently linear.

4.2 Complex Non-Linear Half-Car Model

In order to have more realistic study on a half-car model, some features have to be considered and added to the previously mentioned bond graph (Figure 4.2). These considerations increase order of system and make it non-linear. In the following section, some of these considerations are discussed.

4.2.1 Plane Motion

Plane motion dynamics involves a rigid body that can rotate and move translationally. In vehicle dynamics, engine makes automobile move forward while road roughness makes it heave or pitch. When the inertial vehicle body is constrained to translate in two dimensions i.e. x and y , and to rotate about z -axis, plane motion is resulted. Governing equation for plane motion can be written as follows:

$$\sum F_x + (M \cdot \omega) V_y = M \dot{V}_x \quad (4-3)$$

$$\sum F_y - (M \cdot \omega) V_x = M \dot{V}_y \quad (4-4)$$

This set of equations relate horizontal and vertical motions of a rigid body to each other. Graphical presentation for these governing equations in bond graph language is demonstrated in Figure 4.3 where effort sources for horizontal, vertical, and pitch motions are $\sum F_x$, $\sum F_y$, and $\sum \tau$, respectively.

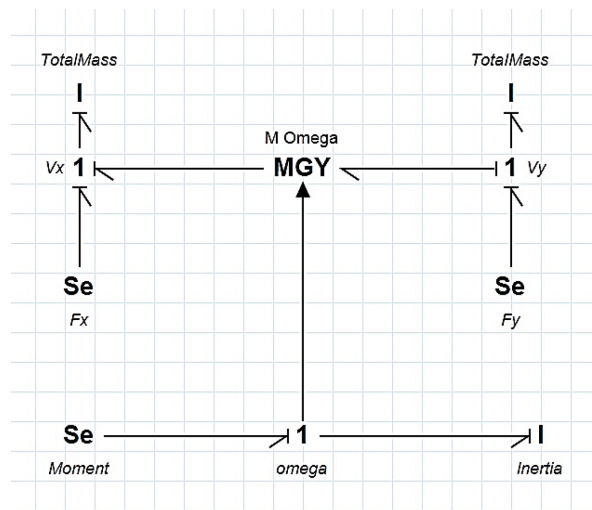


Figure 4.3: Plane motion bond graph

4.2.2 Drag Force

Drag force refers to an aerodynamic force opposes a vehicle's motion through the air.

This force can be expressed as follows:

$$F_D = \frac{1}{2} C_D A \rho v^2 \quad (4-5)$$

where:

C_D : drag coefficient

A : cross sectional area

ρ : air density

v : longitudinal velocity

The aerodynamic drag force exerts on horizontal component of body-fixed coordinate. Figure 4.4 indicates an appropriate location for drag force in bond graph language approach.

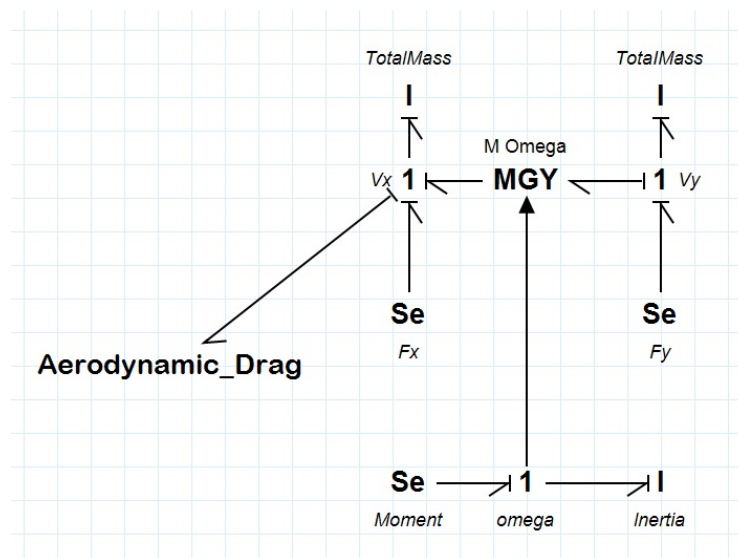


Figure 4.4: Aerodynamic drag force

4.2.3 Tire Model

A linear tire does the same behaviour in both compression and tension and generate the same amount of force in both situations. This force is proportional to deflection. A non-linear tire can be modeled in particular ways. One specific way is when the tire is set to generate force in just tension. For this tire, when spring deflection is negative, it does not produce any restoring force. This non-linearity can be added to model by manipulating tire code in 20sim model as shown:

- parameters
- real c = 0.0001; // c = 1/k, where k is tire stiffness

- equations
- state = int(p.f); // pf = flow, where flow is tire deflection velocity for this element
- if state <=0 then
- p.e = 0; // no restoring force in compression
- else
- p.e = state / c; // p.e = effort, where effort is force in mechanical domains
- end;

4.2.4 Engine Torque

Engine, as power source of a vehicle, produces power to a rotating shaft which can exert a given amount of torque at a given speed (RPM). Figure 4.5 indicates torque-speed of an International DT 530 engine. As it is seen, the peak torque and horsepower for this type of engine is 950 lb-ft (1288 N-m) and 310 hp, respectively.

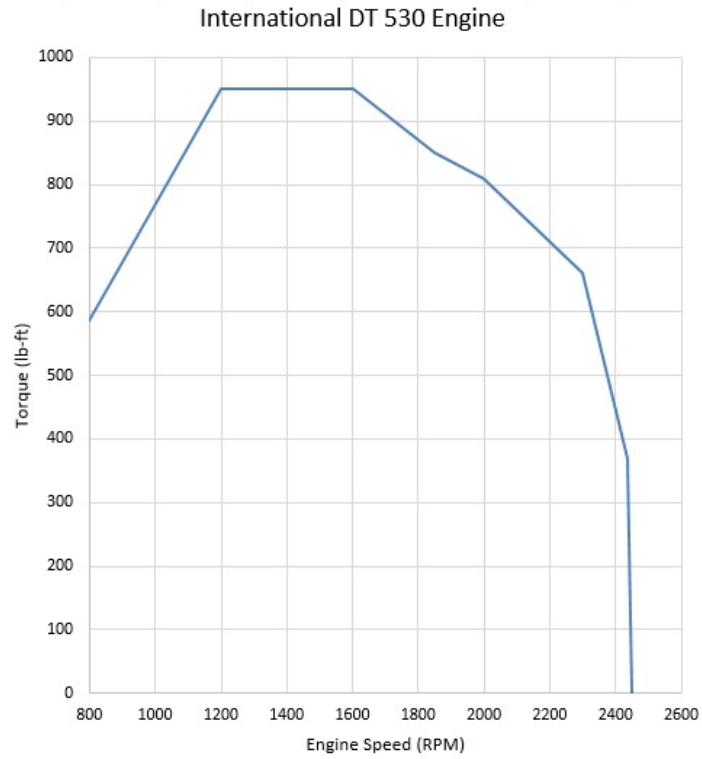


Figure 4.5: Torque-speed graph for International DT 530 engine

Applied torque on vehicle wheels is a function of the produced engine torque. This mathematical relationship can be expressed as follows:

$$T_w = r_G \cdot r_{FD} \cdot T_e \quad (4-6)$$

where:

T_w : wheel torque

r_G : gear ratio

r_{FD} : final drive ratio

T_e : engine torque

Figure 4.6 demonstrates cruise control simulation. Error signal ($V_{desired} - V_{vehicle}$) is controlled by a PD controller. The output of PD controller has to be between zero and maximum torque that the engine can produce. This signal, at that instant, needs to be multiplied by gear and final drive ratio consecutively. The final signal represents applied torque on centre of a wheel. Then the forward velocity of the wheel can be easily evaluated by multiplying the tire radius by its angular velocity.

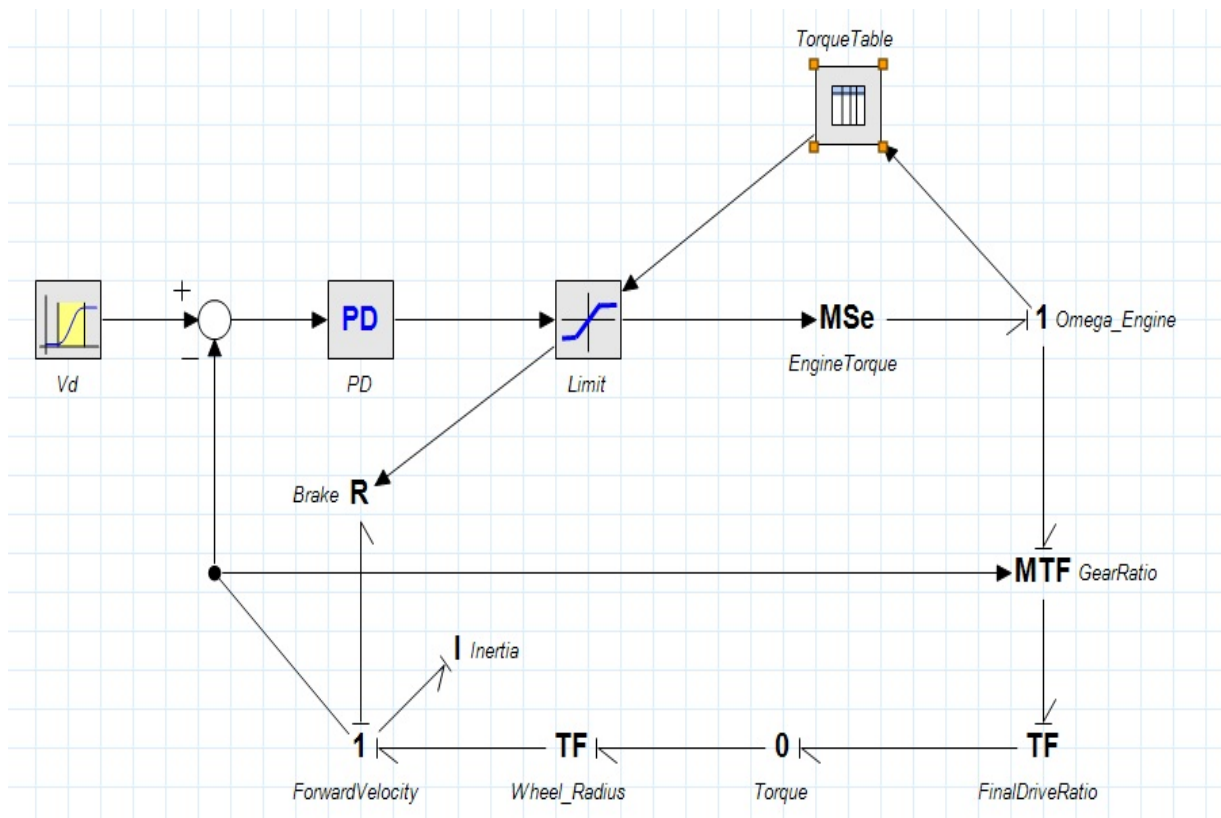


Figure 4.6: Cruise control

4.2.5 Roll Friction

In vehicle dynamics, due to constant deformation of a wheel, some amount of energy is lost when it is rolling on the road. This resisting force is known as roll friction or roll resistance. The amount of this force is a function of normal tire load, longitudinal velocity and tire pressure. This relationship can be represented as follows:

$$F_{roll} = \text{sign}(v) \cdot [C_1 + C_2 \cdot F_z + C_3 \cdot \frac{F_z}{P} + C_4 \cdot \frac{F_z^2}{P}] \quad (4-7)$$

where:

F_z : *tire force normal to the road*

v : *longitudinal velocity*

P : *tire pressure*

C_i : *rolling friction constants*

Graphical demonstration for roll friction of rear part of a vehicle in bond graph language is demonstrated in Figure 4.7.

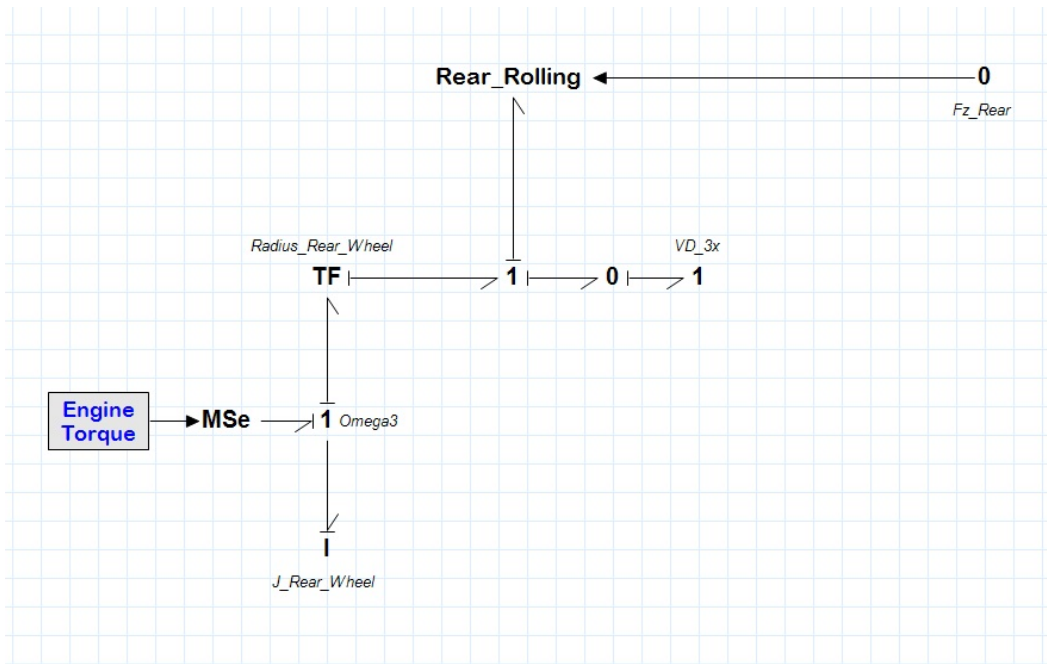


Figure 4.7: Roll friction

4.2.6 Slip Friction

The velocity of tire, if it is rigid can be evaluated by multiplying tire radius by its angular velocity i.e. $r\omega$. However, true forward velocity v is different from $r\omega$ since tire is not completely rigid in reality. This difference can be described as slip ratio. The slip ratio demonstrates portion of the difference in real longitudinal velocity from its theoretical expected value. Having defined slip ratio k , slip resistance can be expressed as follows:

$$k = \frac{r\omega - v}{v} \quad (4-8)$$

$$F_{slip} = \frac{\text{sign}(k) \mu |F_z| |k|}{k_{max}} \quad (4-9)$$

4.2.7 Road Profile

A road profile basically consists of road slopes connected by vertical curves which provide a gradual change from one road slope to another. This leads a vehicle faces continuous geometrical road where it can smoothly navigate grade changes as it travels. Two scenarios to be studied, a rough terrain, which is a standard Gaussian noise as the road profile, and a custom combination of discrete bumps cases. These two cases are clarified in details in the following.

4.2.7.1 Rough Terrain with Gaussian Noise

This scenario is modeled with a continuous motion profile shown in Figure 4.9. This input is generated based on a random Gaussian noise and has used as a rough terrain input in order to study the effect of cargo mass on actuator forces for different associated gains.

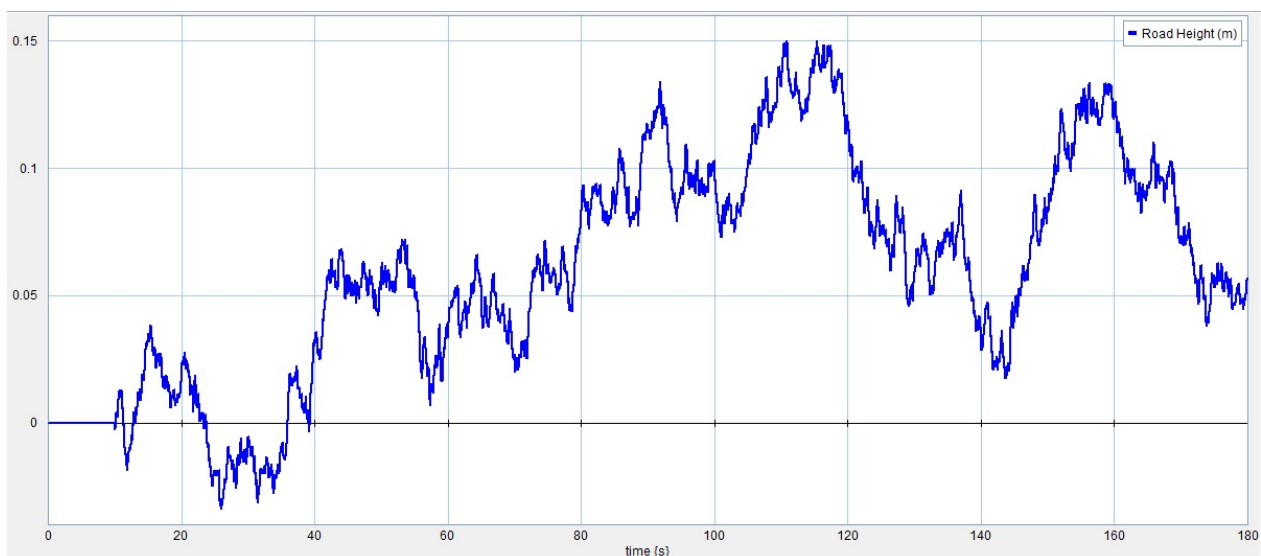


Figure 4.9: Rough terrain with Gaussian noise profile

The same profile has been sent to the front and rear wheels, considering a delay for rear wheels due to studied constant forward velocity of 20 m/s (72 km/h). The amount of this delay can be evaluated by dividing wheelbase distance by assumed forward velocity.

$$t_{delay} = \frac{\text{wheelbase distance}}{\text{forward velocity}} = \frac{3.73 \text{ (m)}}{20 \text{ (m/s)}} = 0.1865 \text{ (s)} \quad (4-10)$$

4.2.7.2 Combined Discrete Bumps

Many possible events can be considered inside a road profile depending on the purpose of study. For instance, in order to examine generated engine power of a vehicle, a road profile consisting of a ramp can be beneficial. Or a road profile containing of bumps can be operated in order to study on vehicle suspension performance. A good general road profile consists of all possible curves, including bumps, ramps, and noise all together. Having considered this point, a custom road profile was generated including the most common road curves in reality. Figures 4.10 to 4.14 presents this profile. The first part of the profile consists of a significant single bump shown in Figure 4.10.

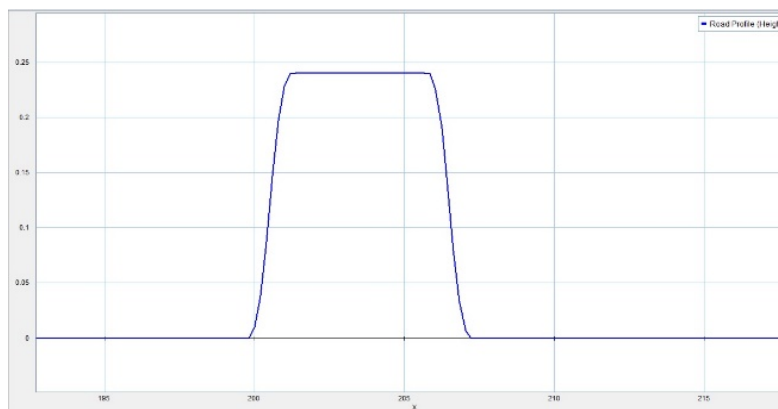


Figure 4.10: Single bump profile

A same bump profile copied and added to the first bump and make a double bump shown in Figure 4.11. Likewise, a profile with three bumps was developed and added to the path consequently.

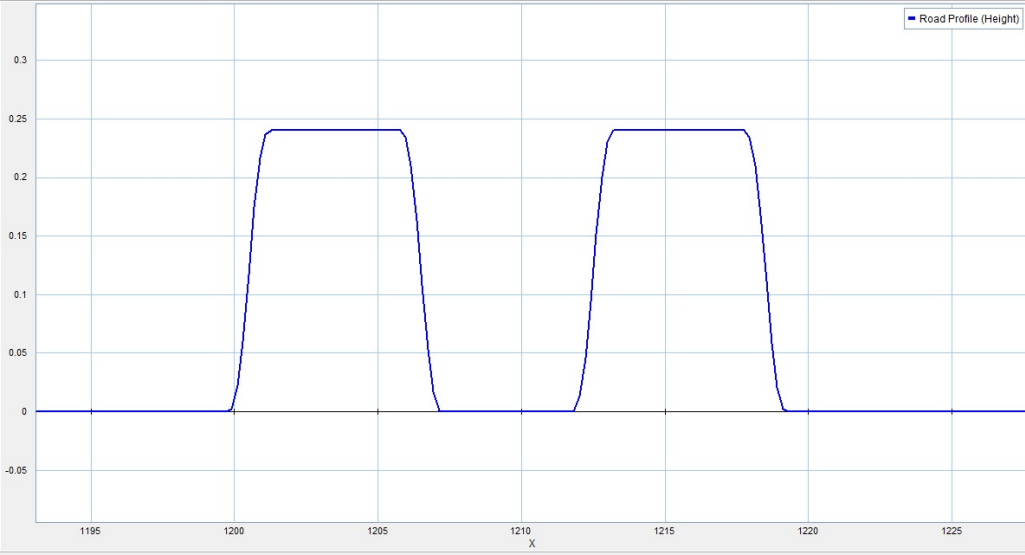


Figure 4.11: Double bump profile

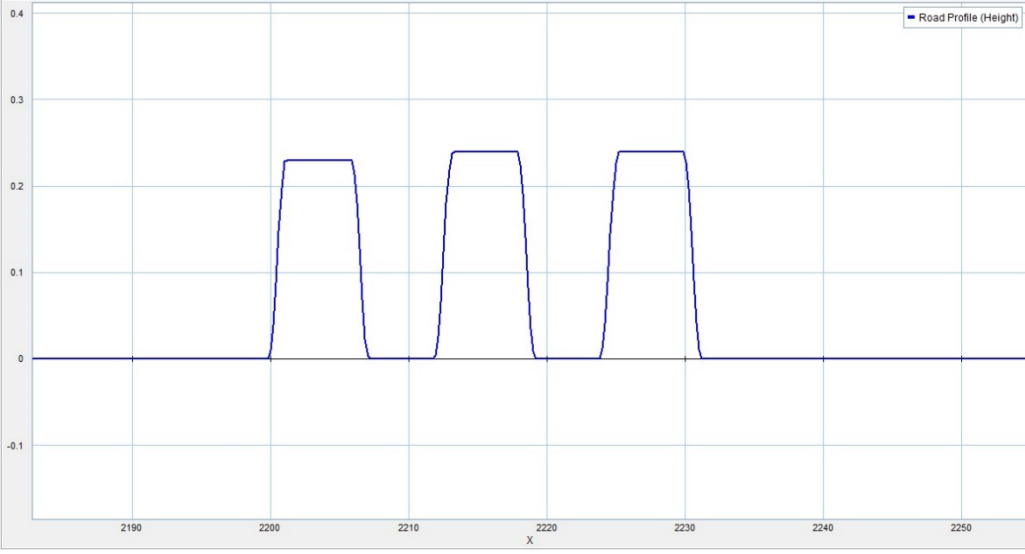


Figure 4.12: Triple bump profile

The custom road profile continued considering a ramp with constant slope of 7% over 500 meters. And finally a symmetric noise with an amplitude of the same order as the Gaussian noise in previous section was developed and added to the profile.

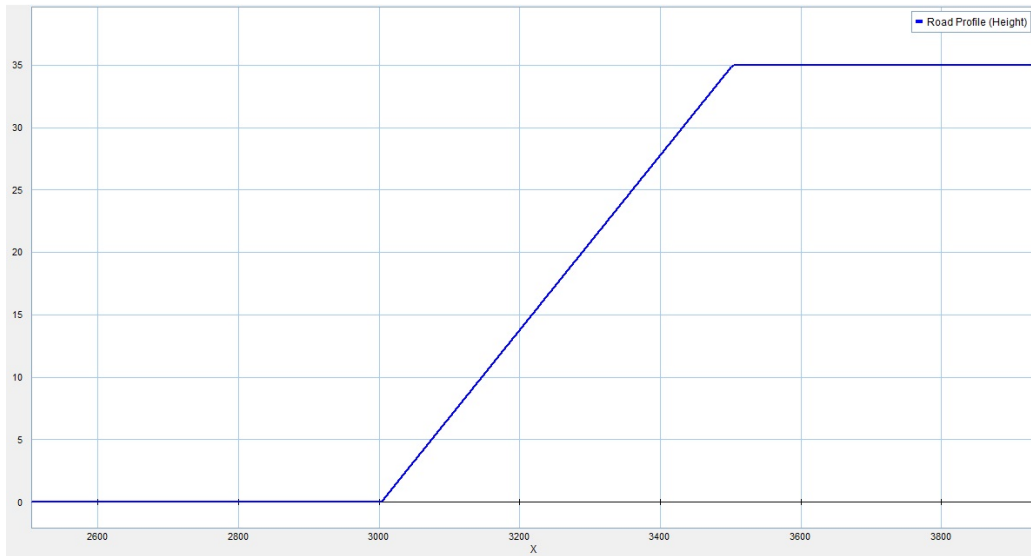


Figure 4.13: Ramp profile

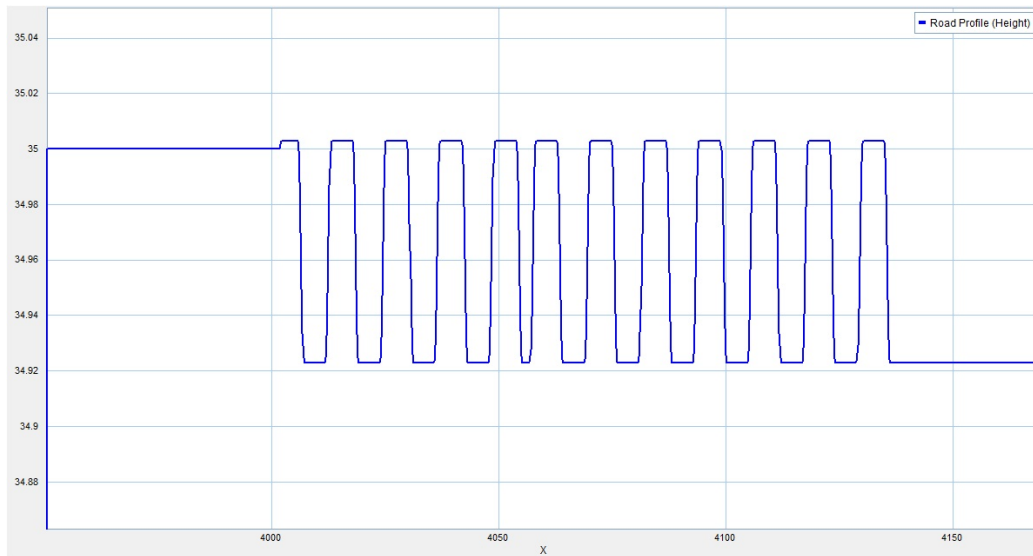


Figure 4.14: Symmetric rough road profile

Combining all those previously mentioned profiles together makes a general road profile which can be studied for various purposes. Figure 4.15 schematically represents the custom generated road profile but not in appropriate scale.

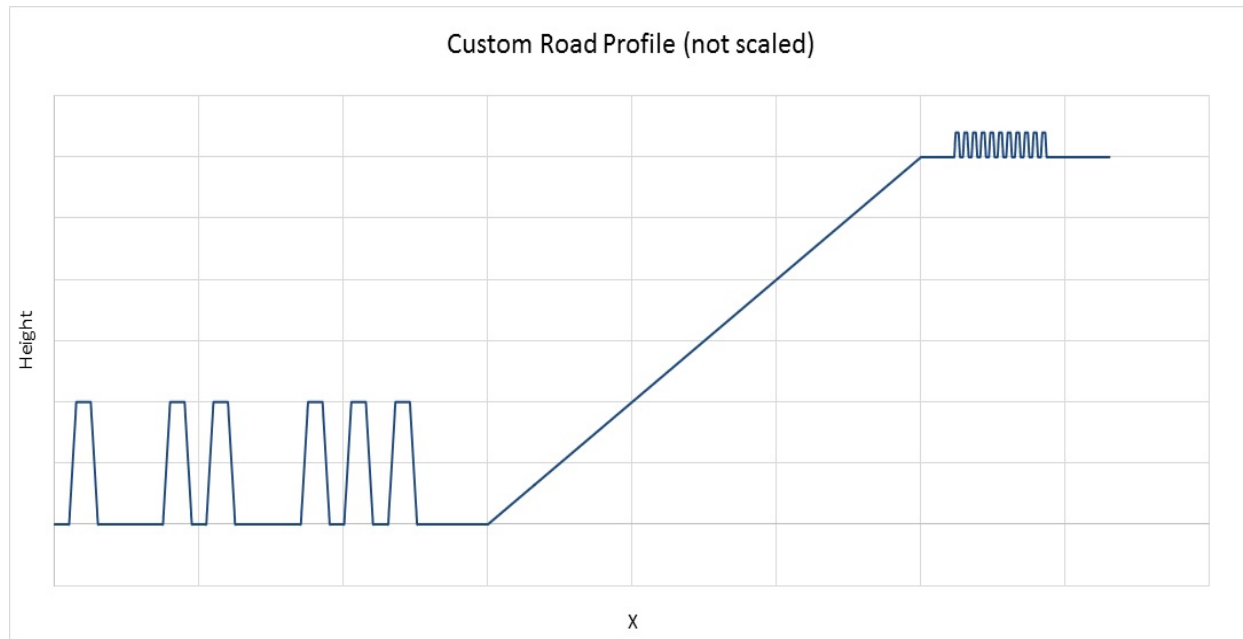


Figure 4.15: Custom road profile

4.2.8 Assigned Coordinates

Figure 4.16 demonstrates a complex non-linear half-car model. In order to describe this system in mechanical domain three local coordinates are required rather than a general one. The first local coordinate needs to be placed at the vehicle's centre of gravity. The horizontal axis of this coordinate is along the vehicle body and the vertical axis is considered perpendicular to the horizontal axis so that the pitch angle obtained from right-hand rule

will be positive in counter clockwise direction. Once this coordinate defined, the other two local coordinates can be placed in front and rear tires' centres, respectively. For these coordinates, the vertical axes are perpendicular to road profile and the right-hand rule point-out the same direction as the first local coordinate, hence the positive direction for horizontal axes can be properly assigned and considered.

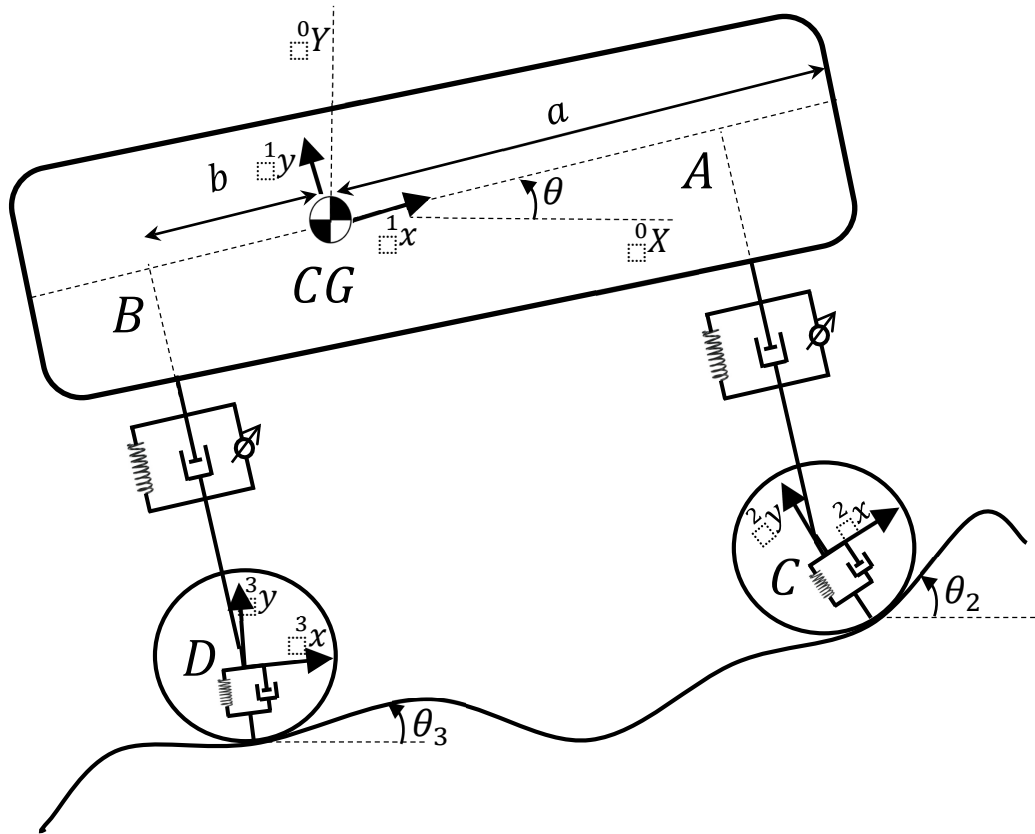


Figure 4.16: Non-linear half-car model

Figure 4.17 highlights the front part of the vehicle and the two local coordinates can be clearly distinguished. First local coordinate, placed at CG, makes an angle between its

horizontal axis and the horizontal axis of general coordinate. The angle which is labeled θ here is known as vehicle pitch angle. Suspension systems are along with the vertical axis of this coordinate, hence it will be more convenient if they are studied in this coordinate. The second local coordinate, placed in front tire origin, will be useful when the vehicle faces bumps on its way or when it travels off road on a rough terrain. In this situation, this coordinate makes an angle with the first local coordinate. Tire states i.e. deflection and velocity can be presented in its own local coordinates since they are along with the vertical axes. Figure 4.18 indicates these two local coordinates at the same time and place. Having focused on this Figure, appropriate relationship between the local coordinate systems can be expressed. So the whole system can be described in just one local coordinate system.

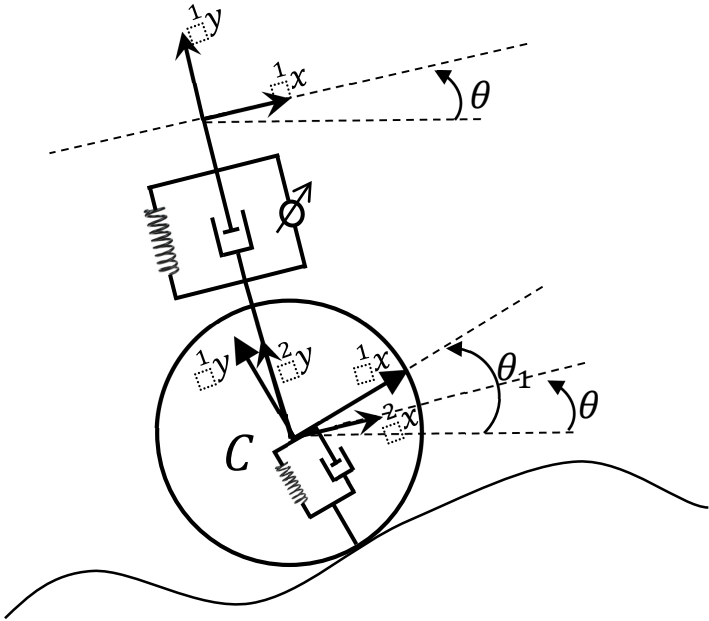


Figure 4.17: Front tire coordinate system

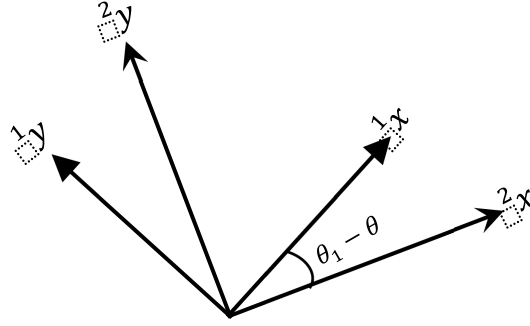


Figure 4.18: Coordinate transformation

An appropriate matrix transformation is required to be applied on the second and third coordinate systems in order to describe tire forces in the first local coordinate. This transformation matrix can be presented as follows:

$$[R_f] = \begin{bmatrix} \cos(\theta - \theta_2) & -\sin(\theta - \theta_2) \\ \sin(\theta - \theta_2) & \cos(\theta - \theta_2) \end{bmatrix}$$

$$[R_f]^{-1} = \begin{bmatrix} \cos(\theta - \theta_2) & \sin(\theta - \theta_2) \\ -\sin(\theta - \theta_2) & \cos(\theta - \theta_2) \end{bmatrix}$$

$$[R_r] = \begin{bmatrix} \cos(\theta - \theta_3) & -\sin(\theta - \theta_3) \\ \sin(\theta - \theta_3) & \cos(\theta - \theta_3) \end{bmatrix}$$

$$[R_r]^{-1} = \begin{bmatrix} \cos(\theta - \theta_3) & \sin(\theta - \theta_3) \\ -\sin(\theta - \theta_3) & \cos(\theta - \theta_3) \end{bmatrix}$$

For instant velocity vector of point C can be transformed from one coordinate to another by using the appropriate corresponding transformation matrix, as follows:

$${}^2[V_C] = [R_f] {}^1[V_C] \qquad \begin{bmatrix} V_{Cx} \\ V_{Cy} \end{bmatrix} = \begin{bmatrix} \cos(\theta - \theta_2) & -\sin(\theta - \theta_2) \\ \sin(\theta - \theta_2) & \cos(\theta - \theta_2) \end{bmatrix} \begin{bmatrix} V_{Cx} \\ V_{Cy} \end{bmatrix}$$

$${}^1[V_C] = [R_f]^{-1} {}^2[V_C] \qquad \begin{bmatrix} V_{Cx} \\ V_{Cy} \end{bmatrix} = \begin{bmatrix} \cos(\theta - \theta_2) & \sin(\theta - \theta_2) \\ -\sin(\theta - \theta_2) & \cos(\theta - \theta_2) \end{bmatrix} \begin{bmatrix} V_{Cx} \\ V_{Cy} \end{bmatrix}$$

4.3 Summary

As it was discussed in Chapter 2, the best vehicle model for studying pitch and heave motions is a half-car model. In this chapter, two half-car vehicle models were presented, as follows:

- Simple linear half-car model.
- Complex non-linear half-car model.

The main purpose of presenting a linear half-car model is to study on effects of having various cargo masses for the studied vehicle. This research is mainly based on the complex half-car vehicle model where the different nonlinearity terms are considered. These non-linear terms were studied in this chapter in detail.

In addition to appropriate vehicle models, feasible road profiles are also needed for the simulation. Hence, two sample road profiles were expressed in this chapter, as follows:

- Regular rough terrain with Gaussian noise.
- Combined discrete bumpy road profile.

The first road profile is a realistic off-road terrain. However, the second road profile contains different severe events that a vehicle may face on its way. The previously mentioned vehicle models will be run over these two road profiles in the following chapters.

Chapter 5

Active Suspension Gains

Using Quarter-Car Approach

5.1 Overview

The idea behind using a controller for a system is to force the system to operate in ideal states. This can occur by using different types of controllers and methods. The system will be at its optimum efficiency when it is performing at those desired ideal states. In vehicle dynamics, an actuator is needed in order to control the suspension of a vehicle. The best

place to put this actuator unit is between the vehicle's sprung and unsprung masses, because tires cannot be adjusted quickly and the vehicle body, in reality, cannot be actuated in the stationary world. Based on the desired goal of having an actuating unit, various types of controllers can be used. A simple PID (Proportional, Integral, Derivative) controller can easily adjust displacement or velocity. If a vehicle is travelling off road or hitting bumps at a high speed, it is important to improve the handling. This can be done by minimizing the variations in tire spring deflection. Two important scenarios are studied in this chapter: ride quality and road holding. In ride quality, the goal of active suspension is to minimize sprung mass acceleration, while in road holding, minimizing the variations in tire spring deflection is the concerns. There are many approaches to satisfying these goals; however, Butsuen [27] claimed that Optimal Linear Quadratic Regulators suit these goals very well. This method is used in this research for a half-car vehicle model.

In this chapter, system equations will be derived and presented in a matrix form for the desired state variables of a quarter-car. Then, the performance index with appropriate weighting factors corresponding to the studied scenario will be defined. With help of the LQR approach, the controller gain vector will be evaluated for a quarter-car model. This procedure will be applied for both the front and rear parts of a vehicle and two quarter-car-based actuators will be presented. Finally, ride quality and road holding scenarios will be studied on a half-car model using two quarter-car actuators in the front and rear. Furthermore, the effects of various cargo masses on active suspension performance will be studied.

5.2 System Equations

A quarter-car active suspension model is shown in Figure 5.1. M_s and M_{us} represent the vehicle sprung mass, i.e., half of the total body mass, frame and engine, and the unsprung mass, i.e., suspension components, tire mass and brake assemblies, respectively. In the following model, sprung and unsprung masses are connected to each other with a parallel set of suspension stiffness k_s , suspension damper b_s , and an active suspension force F_a . Furthermore, tire stiffness k_t , and tire damper b_t are also made another parallel set between the tire and road. The road profile here is assumed as the input of the system.

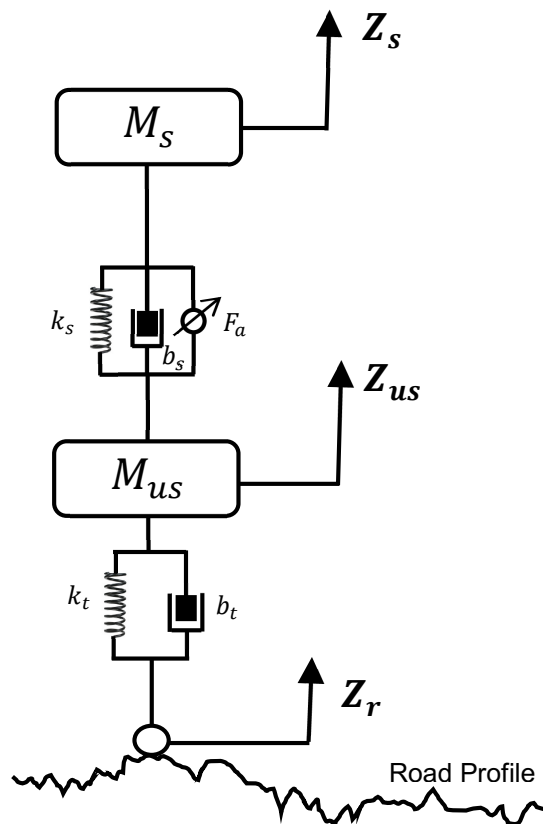


Figure 5.1: Quarter-car active suspension model

Free body diagrams for this system can be drawn as follows:

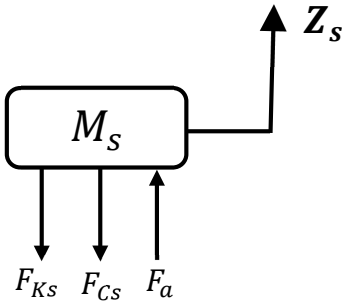


Figure 5.2: Free body diagram for sprung mass

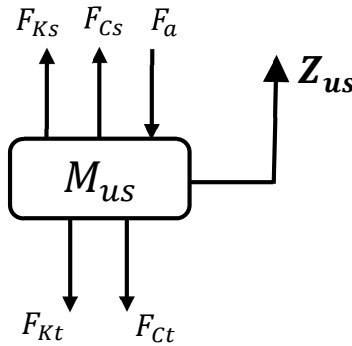


Figure 5.3: Free body diagram for unsprung mass

Based on the free body diagrams shown in Figures 5.2 and 5.3, the governing equations for the system can be derived by satisfying Newton's second law in the vertical direction.

For sprung mass:

$$\sum F_y = M_s \ddot{Z}_s \quad \rightarrow \quad F_a - F_{Ks} - F_{Cs} = M_s \ddot{Z}_s \quad (5-1)$$

where:

$$F_{Ks} = k_s (Z_s - Z_{us}) \quad (5-2)$$

$$F_{Cs} = b_s (\dot{Z}_s - \dot{Z}_{us}) \quad (5-3)$$

For unsprung mass:

$$\sum F_y = M_{us} \ddot{Z}_{us} \quad \rightarrow \quad F_{Ks} + F_{Cs} - F_a - F_{Kt} - F_{Ct} = M_{us} \ddot{Z}_{us} \quad (5-4)$$

Where:

$$F_{Kt} = k_t (Z_{us} - Z_r) \quad (5-5)$$

$$F_{Ct} = b_t (\dot{Z}_{us} - \dot{Z}_r) \quad (5-6)$$

After substituting forces into governing equations, the motion equations of the system can be obtained as follows:

$$F_a - k_s (Z_s - Z_{us}) - b_s (\dot{Z}_s - \dot{Z}_{us}) = M_s \ddot{Z}_s \quad (5-7)$$

$$k_s (Z_s - Z_{us}) + b_s (\dot{Z}_s - \dot{Z}_{us}) - F_a - k_t (Z_{us} - Z_r) - b_t (\dot{Z}_{us} - \dot{Z}_r) = M_{us} \ddot{Z}_{us} \quad (5-8)$$

This set of equations can be represented as a classical control equation when appropriate state variables are defined. Vehicle states considered for this quarter-car model consist of suspension deflection, sprung mass velocity, tire deflection, and unsprung mass velocity. Vector x contains state variables.

$$[x] = \begin{bmatrix} Z_s - Z_{us} \\ \dot{Z}_s \\ Z_{us} - Z_r \\ \dot{Z}_{us} \end{bmatrix} \quad (5-9)$$

where:

$Z_s - Z_{us}$: suspension deflection

\dot{Z}_s : sprung mass velocity

$Z_{us} - Z_r$: tire deflection

\dot{Z}_{us} : unsprung mass velocity

For this linear system, a first-order control differential equation can be considered such as $\{\dot{x}\} = [A]\{x\} + [B]\{F_a\} + [L]\{\dot{Z}_r\}$ where A, B, and L matrices are obtained by system equations. By solving this equation a general solution in terms of the state variables will be derived demonstrating a direct relationship between system inputs and outputs. System equations can be redefined in matrix form as follows:

$$\begin{Bmatrix} \dot{Z}_s - \dot{Z}_{us} \\ \ddot{Z}_s \\ \dot{Z}_{us} - \dot{Z}_r \\ \ddot{Z}_{us} \end{Bmatrix} = [A] \begin{Bmatrix} Z_s - Z_{us} \\ \dot{Z}_s \\ Z_{us} - Z_r \\ \dot{Z}_{us} \end{Bmatrix} + [B] \{F_a\} + [L] \{\dot{Z}_r\} \quad (5-10)$$

where:

$$[A] = \begin{bmatrix} 0 & 1 & 0 & 0 \\ -\frac{k_s}{M_s} & -\frac{b_s}{M_s} & 0 & \frac{b_s}{M_s} \\ 0 & 0 & 0 & 0 \\ \frac{k_s}{M_{us}} & \frac{b_s}{M_{us}} & -\frac{k_t}{M_{us}} & -\frac{b_s - b_t}{M_{us}} \end{bmatrix} \quad (5-11)$$

$$[B] = \begin{bmatrix} 0 \\ 1/M_s \\ 0 \\ -1/M_{us} \end{bmatrix} \quad (5-12)$$

$$[L] = \begin{bmatrix} 0 \\ 0 \\ -1 \\ b_t/M_{us} \end{bmatrix} \quad (5-13)$$

5.3 Linear Quadratic Regulator Gains

The Linear Quadratic (LQ) problem is a case where system equations and cost functions are linear and quadratic, respectively. The solution for such an example can be provided by a Linear-Quadratic Regulator, known as LQR. In order to use this method, an appropriate performance index needs to be defined. This index can be defined by integrating

some factors over time which are intended to be minimized. It can also be presented in terms of state variables and input matrices.

$$J = \int_0^{+\infty} \left\{ \ddot{Z}_s^2 + \rho_1 \cdot (Z_s - Z_{us})^2 + \rho_2 \cdot \dot{Z}_s^2 + \rho_3 \cdot (Z_{us} - Z_r)^2 + \rho_4 \cdot \dot{Z}_{us}^2 \right\} \cdot dt \quad (5-14)$$

$$J = \int_0^{+\infty} (x^T \cdot Q \cdot x + 2x^T \cdot N \cdot u + u^T \cdot R \cdot u) \cdot dt \quad (5-15)$$

By using equation (5-7), \ddot{Z}_s can be derived and then substituted in the performance index. After some simplification, the performance index can be presented based on state variables as follows:

$$\ddot{Z}_s = \frac{1}{M_s} \left\{ F_a - k_s (Z_s - Z_{us}) - b_s (\dot{Z}_s - \dot{Z}_{us}) \right\} \quad (5-16)$$

$$J = \int_0^{+\infty} \left\{ \frac{1}{M_s^2} \left\{ F_a - k_s (Z_s - Z_{us}) - b_s (\dot{Z}_s - \dot{Z}_{us}) \right\}^2 + \rho_1 \cdot (Z_s - Z_{us})^2 + \rho_2 \cdot \dot{Z}_s^2 + \rho_3 \cdot (Z_{us} - Z_r)^2 + \rho_4 \cdot \dot{Z}_{us}^2 \right\} \cdot dt \quad (5-17)$$

After substituting equation (5-16) into equation (5-17), the performance index can be expressed as follows:

$$J = \int_0^{+\infty} \left\{ \frac{1}{M_s^2} \left\{ F_a^2 + k_s^2 (Z_s - Z_{us})^2 + b_s^2 (\dot{Z}_s - \dot{Z}_{us})^2 - 2 F_a k_s (Z_s - Z_{us}) + 2 k_s b_s (Z_s - Z_{us}) (\dot{Z}_s - \dot{Z}_{us}) - 2 F_a b_s (\dot{Z}_s - \dot{Z}_{us}) \right\} + \rho_1 \cdot (Z_s - Z_{us})^2 + \rho_2 \cdot \dot{Z}_s^2 + \rho_3 \cdot (Z_{us} - Z_r)^2 + \rho_4 \cdot \dot{Z}_{us}^2 \right\} \cdot dt \quad (5-18)$$

Once the performance index is defined, an optimal gain G can be evaluated. For this reason, the coefficient of modified performance index (5-15) has to be matched with corresponding coefficients of the expanded performance index (5-18).

$$\int_0^{+\infty} (x^T Q x + 2x^T N u + u^T R u) dt = \int_0^{+\infty} \left\{ \frac{1}{M_s^2} \{ F_a^2 + k_s^2 (Z_s - Z_{us})^2 + b_s^2 (\dot{Z}_s - \dot{Z}_{us})^2 - 2F_a k_s (Z_s - Z_{us}) + 2k_s b_s (Z_s - Z_{us})(\dot{Z}_s - \dot{Z}_{us}) - 2F_a b_s (\dot{Z}_s - \dot{Z}_{us}) \} + \rho_1 (Z_s - Z_{us})^2 + \rho_2 \dot{Z}_s^2 + \rho_3 (Z_{us} - Z_r)^2 + \rho_4 \dot{Z}_{us}^2 \right\} dt \quad (5-19)$$

In order to avoid the complexity involved in matching coefficients, partial derivatives can be used and Q, N, and R matrices can be indicated as follows:

$$q_{ij} = \frac{1}{2} \frac{\partial w^2}{\partial x_i \partial x_j} \quad (5-20)$$

$$n_{i1} = \frac{1}{2} \frac{\partial w^2}{\partial x_i \partial F_a} \quad (5-21)$$

$$r = \frac{1}{2} \frac{\partial w^2}{\partial F_a^2} \quad (5-22)$$

where:

$$w = \frac{1}{M_s^2} \{ F_a^2 + k_s^2 (Z_s - Z_{us})^2 + b_s^2 (\dot{Z}_s - \dot{Z}_{us})^2 - 2F_a k_s (Z_s - Z_{us}) + 2k_s b_s (Z_s - Z_{us})(\dot{Z}_s - \dot{Z}_{us}) - 2F_a b_s (\dot{Z}_s - \dot{Z}_{us}) \} + \rho_1 (Z_s - Z_{us})^2 + \rho_2 \dot{Z}_s^2 + \rho_3 (Z_{us} - Z_r)^2 + \rho_4 \dot{Z}_{us}^2 \quad (5-23)$$

$$[Q] = [q_{ij}]$$

$$[N] = [n_{1j}]$$

$$[R] = [r \quad]$$

For instance, q_{12} can be evaluated as follows:

$$q_{12} = \frac{1}{2} \frac{\partial w^2}{\partial x_1 \partial x_2} = \frac{1}{2} \frac{\partial w^2}{\partial (Z_s - Z_{us}) \partial \dot{Z}_s} = \frac{1}{2} \frac{\partial}{\partial (Z_s - Z_{us})} \left(\frac{\partial w}{\partial \dot{Z}_s} \right) \quad (5-24)$$

$$\frac{\partial w}{\partial \dot{Z}_s} = \frac{1}{M_s^2} \{ 2 b_s^2 (\dot{Z}_s - \dot{Z}_{us}) + 2 k_s b_s (Z_s - Z_{us}) \} + 2 \rho_2 \dot{Z}_s \quad (5-25)$$

$$\frac{\partial}{\partial (Z_s - Z_{us})} \left(\frac{\partial w}{\partial \dot{Z}_s} \right) = \frac{1}{M_s^2} \{ 2 k_s b_s \} \quad (5-26)$$

$$\frac{1}{2} \frac{\partial}{\partial (Z_s - Z_{us})} \left(\frac{\partial w}{\partial \dot{Z}_s} \right) = \frac{k_s b_s}{M_s^2} \quad (5-27)$$

Hence:

$$q_{12} = \frac{k_s b_s}{M_s^2} \quad (5-28)$$

Similarly, matrices Q, N, and R are evaluated by using a Maple package [28] and can be expressed as follows:

$$[Q] = \begin{bmatrix} \rho_1 + \frac{k_s^2}{M_s^2} & \frac{b_s k_s}{M_s^2} & 0 & \frac{-b_s k_s}{M_s^2} \\ \frac{b_s k_s}{M_s^2} & \rho_2 + \frac{b_s^2}{M_s^2} & 0 & \frac{-b_s^2}{M_s^2} \\ 0 & 0 & \rho_3 & 0 \\ \frac{-b_s k_s}{M_s^2} & \frac{-b_s^2}{M_s^2} & 0 & \rho_4 + \frac{b_s^2}{M_s^2} \end{bmatrix} \quad (5-29)$$

$$[N] = \begin{bmatrix} -k_s/M_s^2 \\ -b_s/M_s^2 \\ 0 \\ b_s/M_s^2 \end{bmatrix} \quad (5-30)$$

$$[R] = [1/M_s^2] \quad (5-31)$$

Once these matrices have been evaluated, a proportional feedback controller such as $u = -G \cdot x$ can be presented in order to minimize the cost function. Matrix G is known as the system's gain matrix and can be indicated as follows:

$$G = R^{-1} (B^T P + N^T) \quad (5-32)$$

where P is the solution of the Continuous Algebraic Riccati Equation (CARE). CARE for this system can be demonstrated as follows:

$$(A - BR^{-1}N)^T P + P(A - BR^{-1}N) + Q - N^T R^{-1} N - PBR^{-1}B^T P = 0 \quad (5-33)$$

In order to find a valid solution for CARE, the (A,B) pair must be stabilizable and the (Q,A) pair must have no observable modes on the imaginary axis in the continuous-time domain, which are both satisfied for this system. The Maple package could not solve the Riccati equation for this system as there was an error in the command “CARE” approved by the company. Hence, another multi-paradigm numerical computing environment was required in order to solve the CARE. A MatLab package, developed by MathWorks, was the software used to solve the Riccati equation. A CARE command in MatLab can evaluate the solution of the Riccati equation and gain matrix simultaneously. The obtained gain matrix from the CARE command validates the results achieved from equation 5-32.

This procedure was accomplished separately for the front and rear part of the vehicle and two sets of gains were obtained in order to use in two various optimal quarter-car controllers in the front and rear.

5.4 Weighting Factors

Ride quality and road holding scenarios are the two scenarios studied in this research. Various scenarios can be applied on LQR by manipulating the weighting parameters of the performance index. In ride quality, the coefficient for vertical acceleration is the considered unit. Since the intention is to control and minimize vertical acceleration, the coefficients for

suspension and tire velocities are considered less than the suspension and tire deflection's. When two optimal quarter-car controllers are operated instead of optimal half-car controllers, pitch acceleration cannot be controlled directly. In the road holding scenario, the vertical suspension acceleration coefficient is the considered unit while other relative parameters are much greater. These weighting factors are classified in Table 5.1.

Table 5.1: Weighting parameters for quarter-car controller

Performance Index		Scenario 1	Scenario 2
Weighting Parameters		Ride Quality	Road Holding
Suspension Deflection	ρ_1	0.4	1.6
Sprung Mass Velocity	ρ_2	0.16	1
Tire Deflection	ρ_3	0.4	1.8
Unsprung Mass Velocity	ρ_4	0.16	1.2

5.5 Cargo Mass

Gains obtained by the LQR approach consist of two terms: $R^{-1}B^T P$ and $R^{-1}N^T$. The first term varies as the weighting parameters change in different scenarios; however, the second term cancels out passive forces in the spring and damper. By gaining cargo mass, the vehicle's centre of gravity moves to the rear part of the vehicle. On the other hand, the total

vehicle mass and inertia will increase. Hence, the sprung masses for the front and rear parts will be affected by these two changes simultaneously. For instance, the sprung mass for the rear part is related to the total vehicle body mass with relationship of a/l , where a and l are the distance from CG to the front wheels, and wheelbase distance, respectively. Increasing the cargo mass results in having higher " a ". Hence, the sprung mass in the rear part will be increased more than the front sprung mass.

$$M_{sr} = \frac{a}{l} M_s \quad (5-34)$$

$$M_{sf} = \frac{b}{l} M_s \quad (5-35)$$

where:

M_s : total sprung mass

M_{sf} : front sprung mass

M_{sr} : rear sprung mass

a : distance from CG to front wheels

b : distance from CG to rear wheels

l : wheelbase distance from rear wheels to front wheels

A graphical schematic of a Class VI delivery truck based on an International 4700-series vehicle is presented in Figure 5.14. Table 5.2 categorizes dimensions of this studied truck while other properties of the vehicle have already been outlined in Chapter 2.

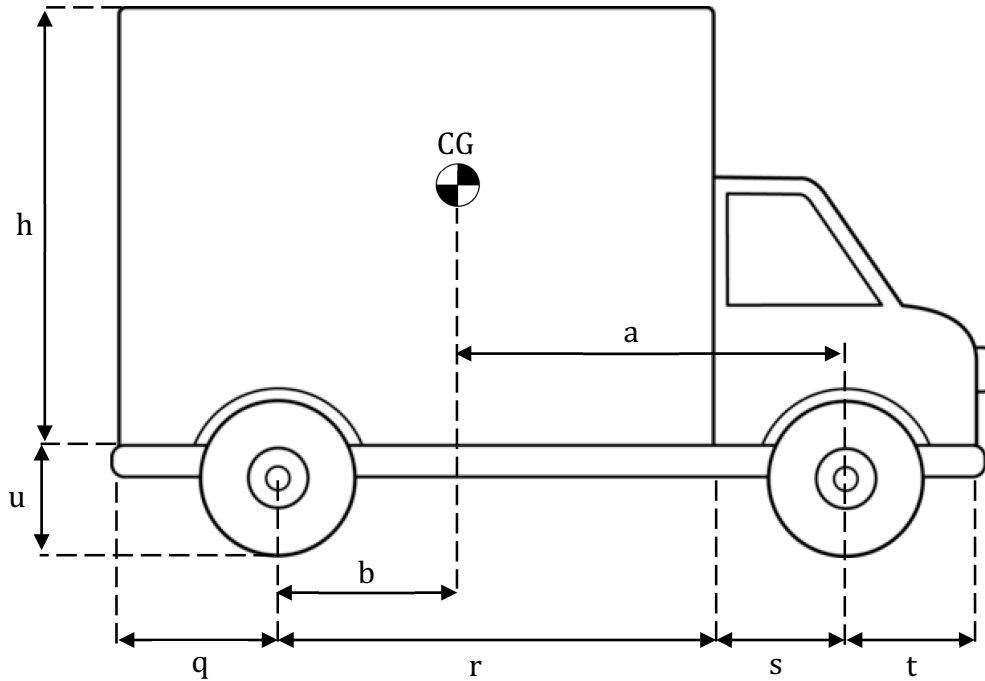


Figure 5.4: Sketch of studied truck

Table 5.2: Studied truck dimensions [29]

Parameter	Symbol	Value (mm)
Wheelbase Distance	$a + b$	3730
Maximum Length	$q + r + s + t$	6515
Front Overhang	t	998
Rear Overhang	q	1665

Front Axle to Front Body	s	1410
Overall Height (Unladen)	$h + u$	2335
Truck Width	---	3450
Maximum Chassis Cab Width	---	2060
Truck Bed Height	h	2100
Truck Bed Length	$q + r$	3985

5.6 Conclusion

5.6.1 Cargo Effect

The gain matrix is evaluated based on the system parameters. However, once the gain matrix is evaluated it cannot be changed if the system parameters change during the simulation. One of the important system parameters is cargo mass as it can vary within a huge range. The question that comes to mind is for which system parameter does the LQR approach need to be applied and gains have to be derived. For clarification, two systems are considered that have two independent quarter-car actuators in the front and rear part of each model. The gain matrix for the first system was obtained when no cargo mass was considered, while for the second system, it was found when the maximum possible cargo

mass was used. The concern is which system performs better for all possible cargo masses. In order to present an appropriate answer to this question, five scenarios were studied, as follows:

- I. Cargo mass : 0
- II. Cargo mass: 4500 kg
- III. Cargo mass: 9000 kg
- IV. Cargo mass: 13500 kg
- V. Cargo mass: 18000 kg

For each scenario, a new centre of gravity and effective sprung masses for the front and rear parts of the vehicle were obtained, and gain matrices were found afterwards. These data can be found in Appendix A. Then, each system runs under the same conditions for all five sets of gains and desired data were observed and recorded. For instance, for the first scenario, when there was no cargo mass, a half-car model with two optimal quarter-car active controllers for the front and rear part was designed. In the next step, the first set of gains, which corresponds to the first scenario with no cargo mass, was considered for the model. Then, the model was run and the desired output was captured. Once the desired data were recorded, the system was run again under the same conditions with a new set of gains corresponding to the second scenario, when the cargo mass is 9000 kg, and the desired output was recorded again. Similarly, this simulation was done for the three remaining scenarios, and for each run, the same output was captured. This procedure was exactly followed for other cases after generating an appropriate model for each scenario. By

comparing these 25 captured results, the best set of gains was introduced in order to be used for the following models.

5.6.1.1 Ride Quality

In ride quality, the main purpose is to minimize sprung mass acceleration. In this section, a linear half-car model with two quarter-car active suspension units was considered. The desired outputs for the system were defined as sprung mass accelerations in the front and rear, total performance index, and required actuator forces in the front and rear. Models were run under the same initial conditions over the rough terrain profile outlined in Chapter 4. Table 5.3 shows the obtained gains for each studied scenario.

Table 5.3: Ride quality scenario's gain matrices for different cargo masses

Gain Matrix		Cargo = 0	Cargo = 4500 kg	Cargo = 9000 kg	Cargo = 13500 kg	Cargo = 18000 kg
Front	G_1	-488,253	-488,008	-487,764	-487,519	-487,276
	G_2	-6,703	-6,242	-5,782	-5,319	-4,862
	G_3	1,312	1,442	1,563	1,677	1,784
	G_4	9,637	9,541	9,438	9,329	9,215
Rear	G_1	-1,577,157	-1574,555	-1571,953	-1569,353	-1566,749

	G_2	-16,436	-11,528	-6,620	-1,717	3,191
	G_3	2,018	3,072	3,893	4,625	5,317
	G_4	21,110	19,817	18,330	16,774	15,182

In the first case scenario, the linear model is studied while no cargo was considered. Two quarter-car active suspension units are used independently for the vehicle's front and rear parts. Parameters were set for the ride quality and the model ran for 180 seconds on the first road profile outlined in Chapter 4 [4.2.7.1]. Figure 5.5 represents the vehicle's pitch angle and could also verify that the vehicle follows the road perfectly. Dark blue and light pink lines demonstrate the active and passive suspension responses, respectively. As is seen, ride quality gains can minimize pitch angle as well.

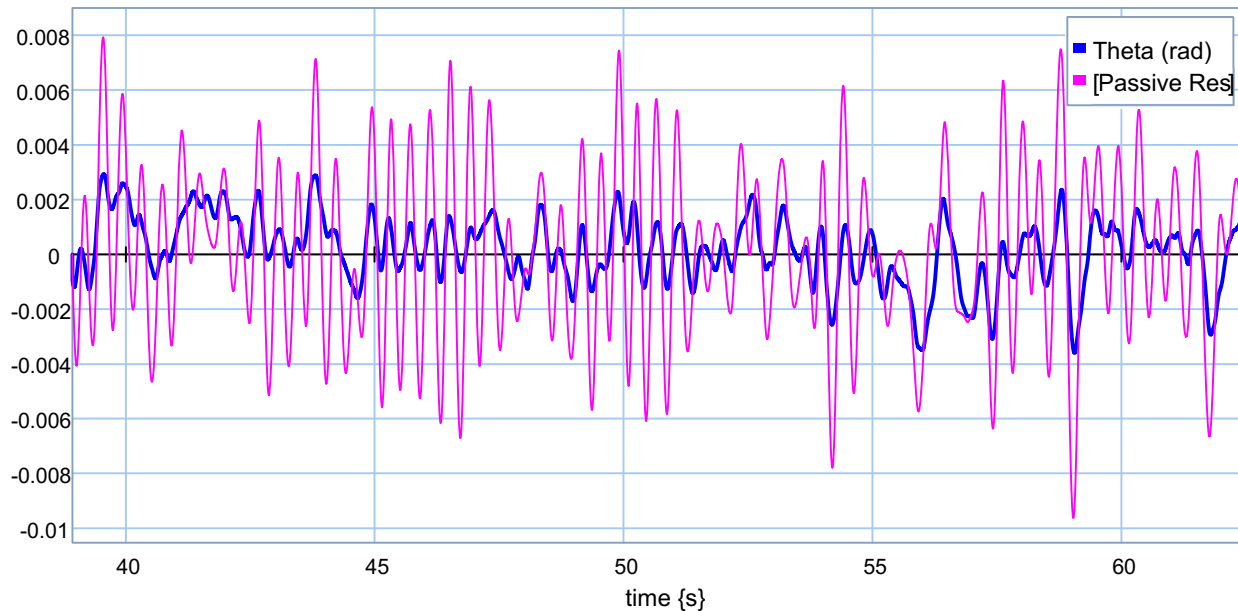


Figure 5.5: Pitch angle using quarter-car gains for ride quality

Figures 5.6 and 5.7 compare the front and rear sprung mass accelerations. As is seen, ride quality gains can control sprung masses' accelerations very well. They can also minimize the vertical acceleration of the vehicle's centre of gravity. This trend is presented in Figure 5.8.

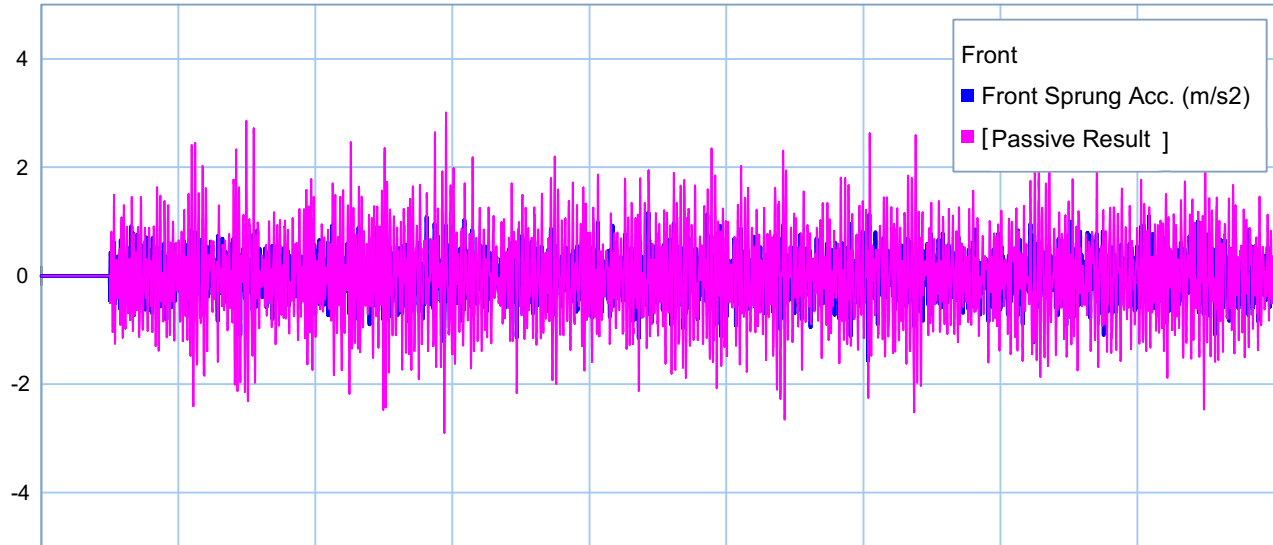


Figure 5.6: Front sprung mass acceleration using quarter-car gains for ride quality

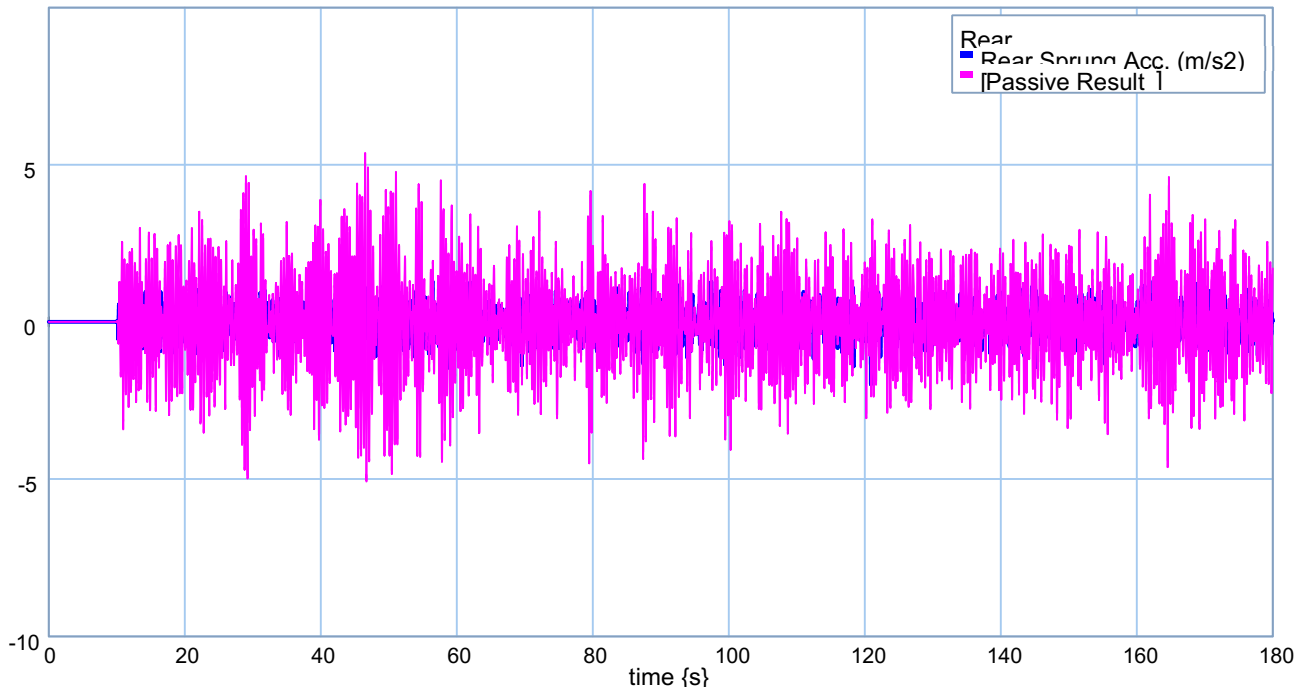


Figure 5.7: Rear sprung mass acceleration using quarter-car gains for ride quality

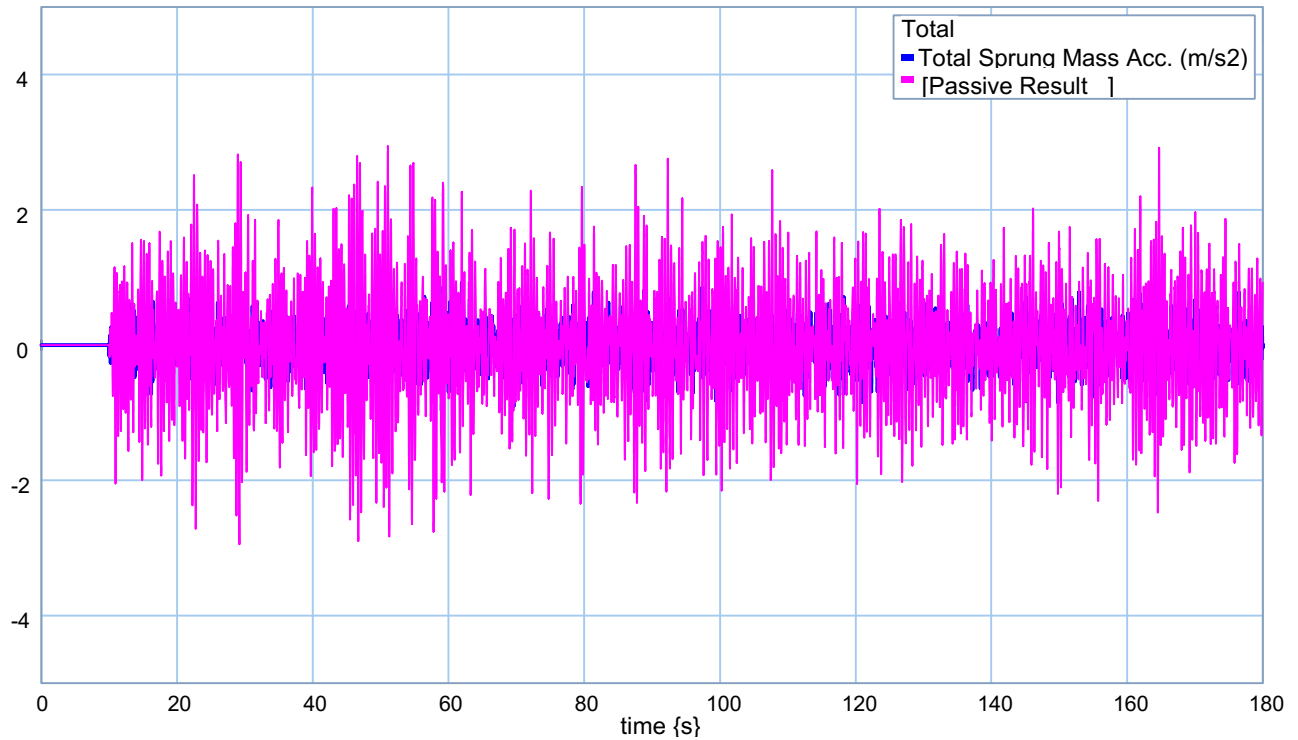


Figure 5.8: centre of gravity vertical acceleration using quarter-car gains for ride quality

In order to have a better visual comparison, Figure 5.9 displays the vertical acceleration of the vehicle front, rear and centre parts. This improvement can also be proved by comparing the performance indices for passive and active suspension. Figures 5.10 to 5.12 present this index for the front, rear and centre parts. As is seen, active suspension can minimize the performance indices.

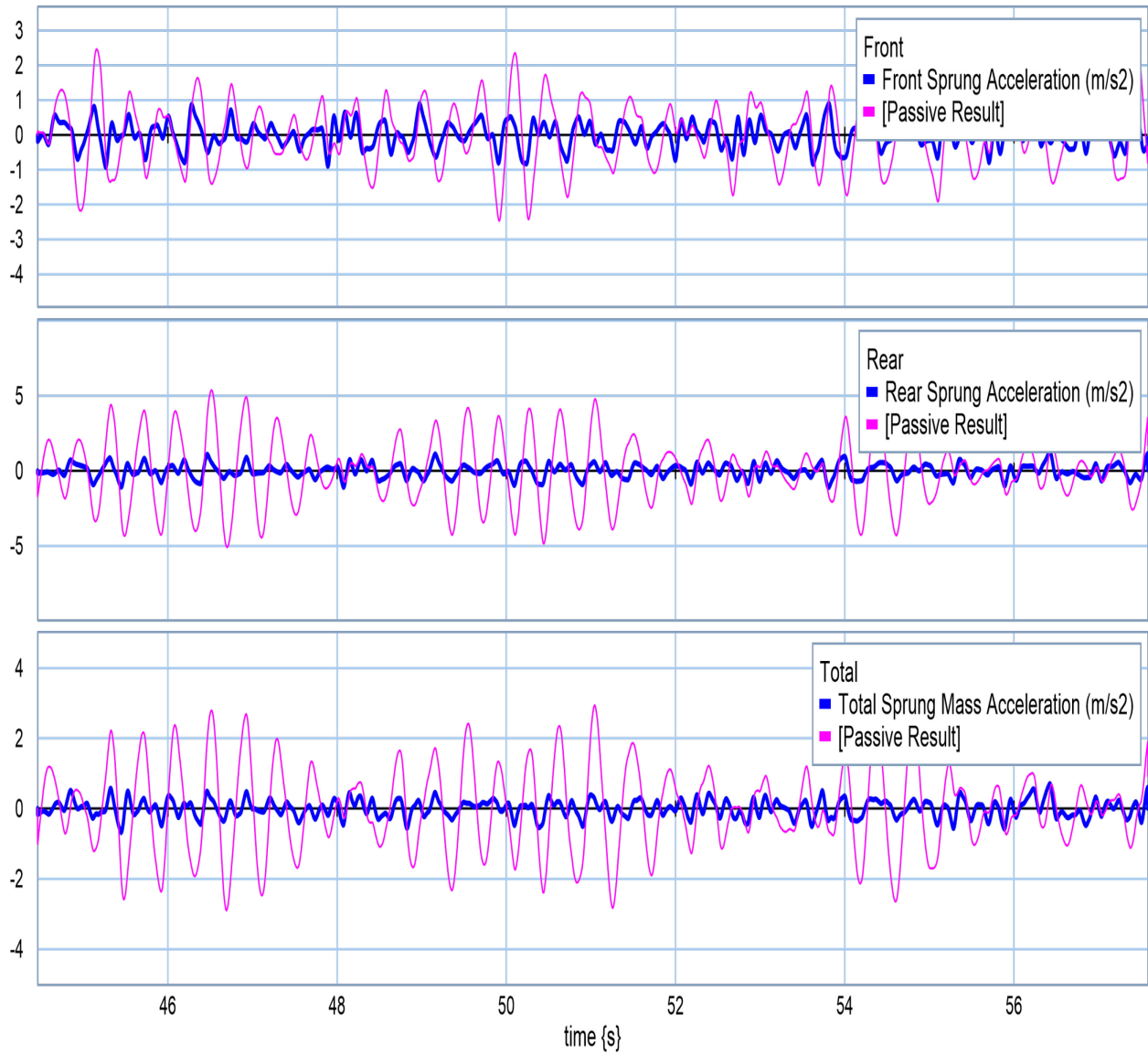


Figure 5.9: Vertical acceleration using quarter car gains for ride quality

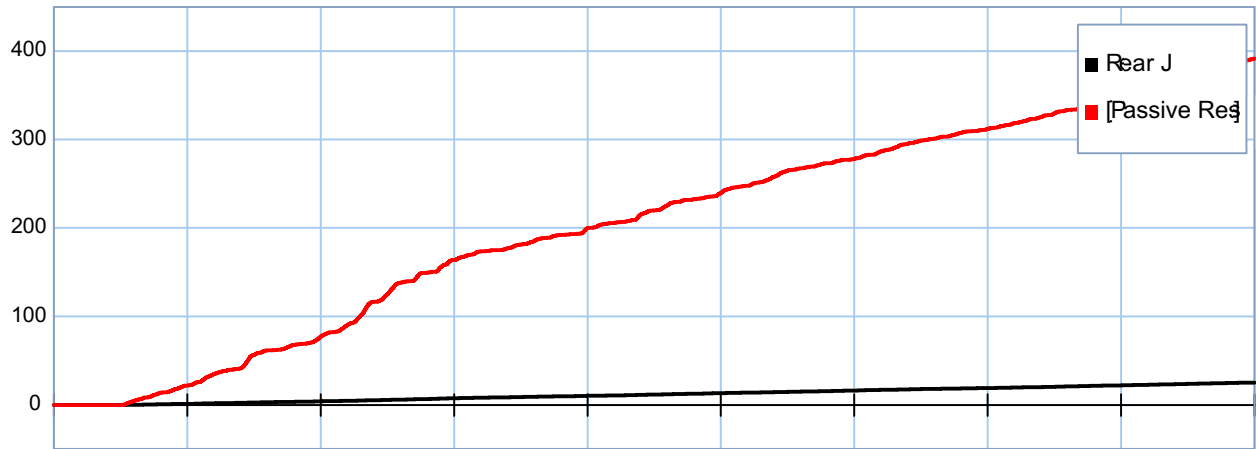


Figure 5.10: Rear performance index using quarter-car gains for ride quality

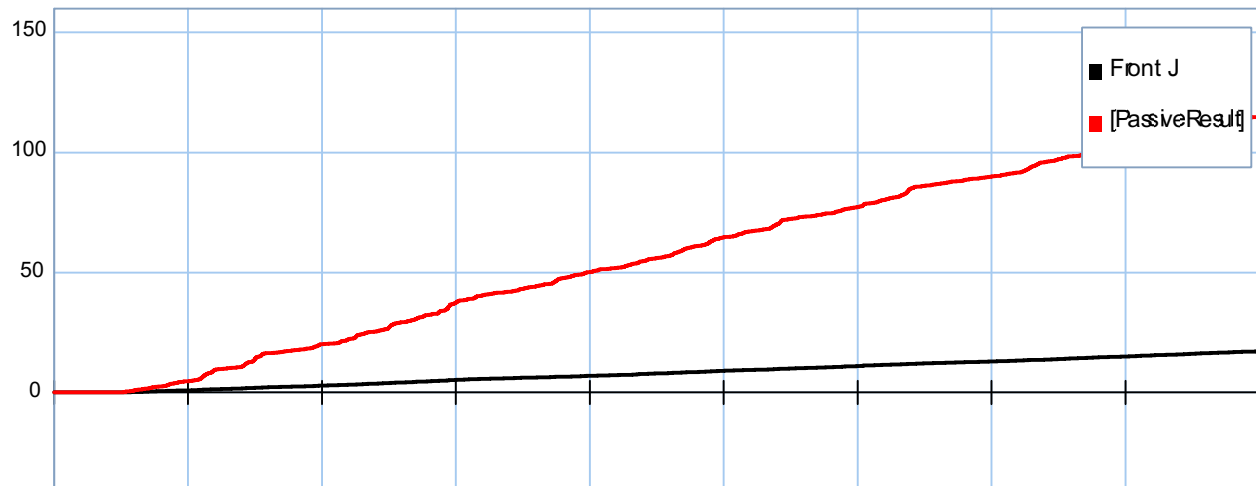


Figure 5.11: Front performance index using quarter-car gains for ride quality

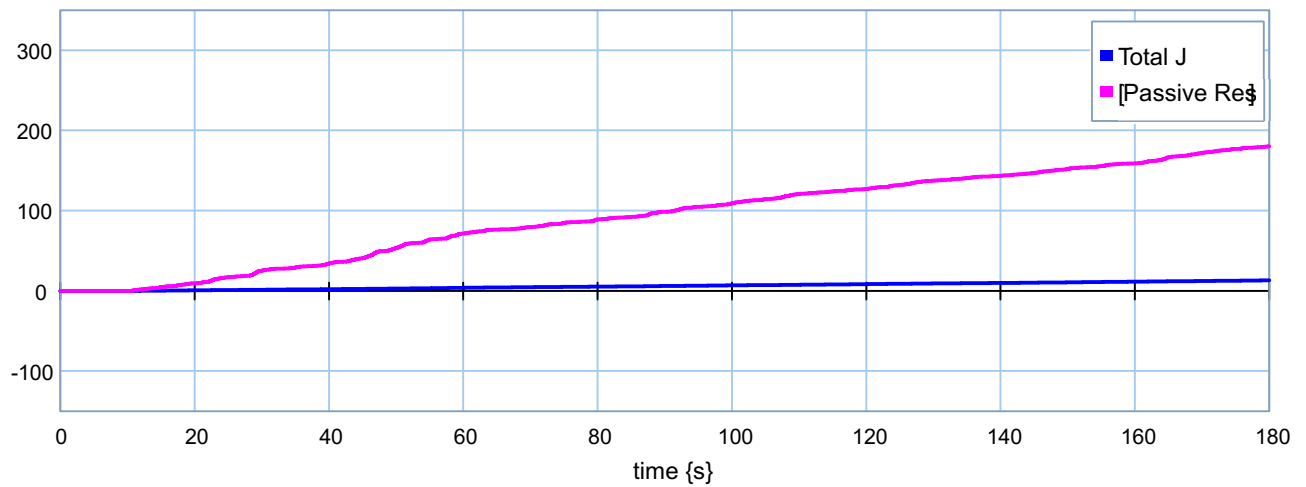


Figure 5.12: Total performance index using quarter-car gains for ride quality

Two independent actuators are used for the vehicle's front and rear parts in order to improve the ride quality by minimizing the front and rear sprung masses' accelerations. However, central states such as vertical and pitch accelerations are also improved indirectly. Figure 5.13 compares these states for passive and active suspension studies.

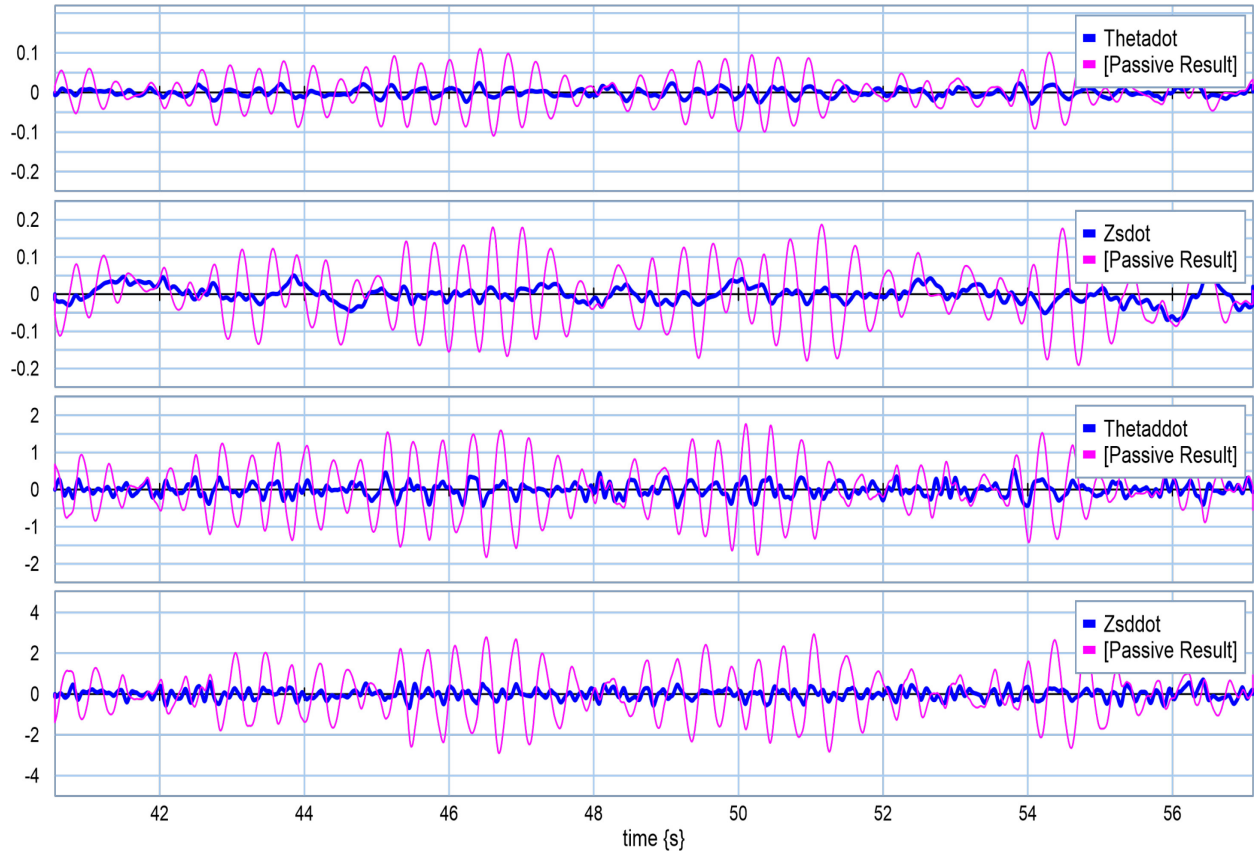


Figure 5.13: Central states using quarter-car gains for ride quality

Similarly, for the second scenario with the 4500 kilogram cargo mass, an appropriate set of gains for ride quality was applied and a very large improvement was observed. In Appendix B, all the graphs based on varying cargo masses i.e. 4500 kg., 9000 kg., 13500 kg., and 18000 kg. are covered. As was expected based on theory, actuator units with parameters set for ride quality could help the vehicle provide more comfort for passengers.

Each set of gains used in actuation units were designed based on primitive assumptions about the amount of cargo mass. When one set of gains is obtained, it cannot be changed during the simulation. An important question in this part which has to be answered is related to the efficiency of the set of gains used when the cargo mass is not the same as was assumed. Presenting an optimum set of gains which can be used for all possible cargo masses is a critical point here. In order to address this concern, first, the behaviour of each model was studied while the cargo mass was varying from 0 to 18000 kg.

For this reason, all five models ran five times for 180 seconds over the first road profile [4.2.7.1] with five different sets of gains. The final value of the performance index for all of the five cases for each model was recorded and compared to each other. For each model, the recorded values of the performance indices in the corresponding five various scenarios were too close to each other. Hence, another index needed to be defined in order to present the optimum gains. In order to define this index, the required forces for the front and rear actuators were recorded during the simulation. Then the required horsepower was

calculated by multiplying this actuator force by its vertical velocity. The new index can be called the energy index and can be represented as follows:

$$EI_F = \int FrontHorsePower^2 . dt \quad (5-36)$$

$$EI_R = \int RearHorsePower^2 . dt \quad (5-37)$$

This index could be also presented based on actuator forces. The advantage of exploring this index based on energy is the less running time required for each simulation. This happens because of the significant difference between the amount of the required forces and energies.

For instance, Table 5.4 classifies the rear energy indices for each simulation. As can be seen, for all the studied models, the minimum energy indices were recorded when the highest set of gains was used. In other words, using the fifth set of gains is more energy-efficient for all models. For the first model, the significant difference between the first and last energy indices is huge enough to design an active suspension based on the fifth set of gains.

Figure 5.14 magnifies the vertical acceleration of the centre of gravity of the truck over two seconds when the road was more severe. However, as is seen, there is not much difference between the behaviour of the system while the first and fifth sets of gains were

used. This behaviour was seen in other models as well. More graphs and tables can be found in Appendix B.

Table 5.4: Rear energy indices for ride quality gains

EI for models		G_1	G_2	G_3	G_4	G_5
EI_R	#1	172.7588	103.0163	63.8079	37.9467	19.3130
	#2	183.7089	120.6653	81.4992	53.2877	31.5688
	#3	202.3722	137.6571	96.6151	66.3597	42.6151
	#4	222.8639	154.0624	115.2604	82.1805	53.1029
	#5	243.5568	171.1507	135.0158	98.2340	63.1898

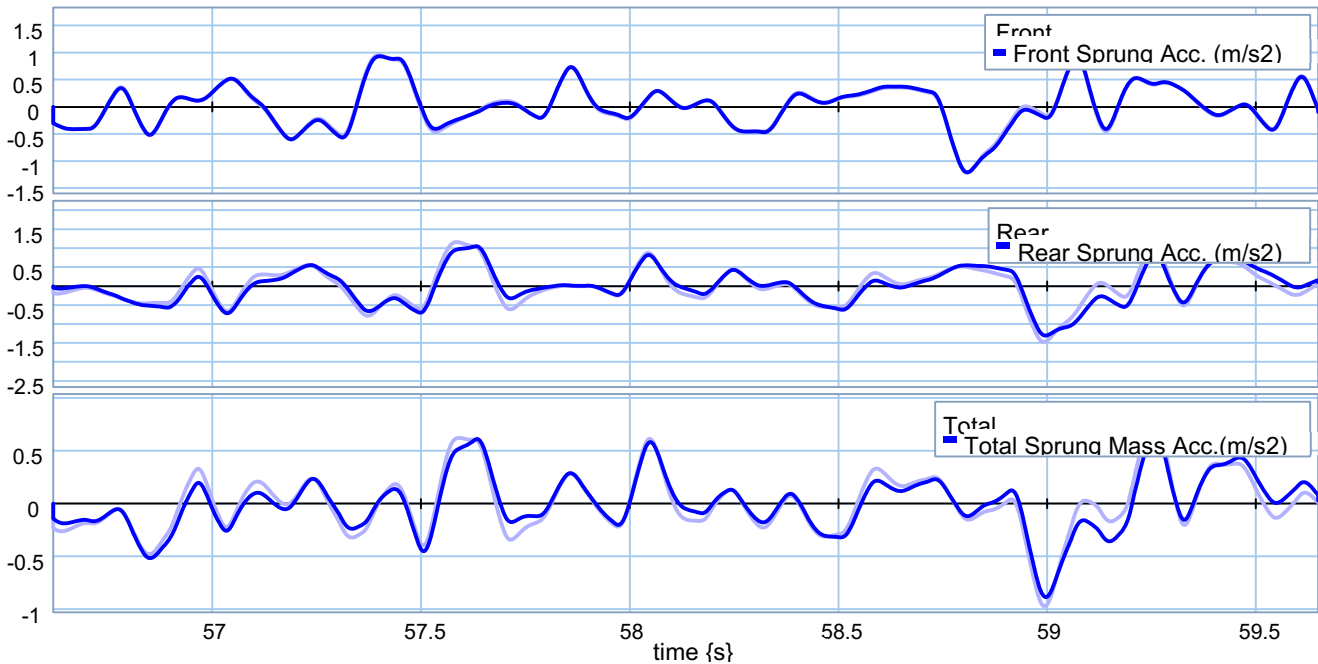


Figure 5.14: Vertical acceleration for first and fifth sets of gains for ride quality

5.6.1.2 Road Holding

The same procedure explained in the previous section was performed while the weighting parameters in the cost function were changed for the road holding scenario. In the road holding scenario, the main purpose could be defined as minimizing the tire deflection and velocity. The five generated models ran for 180 seconds under the same initial conditions over the rough terrain profile outlined in Chapter 4 [4.2.7.1]. Table 5.5 classified evaluated gains for each studied case.

Table 5.5: Road holding scenario's gain matrices for different cargo masses

Gain Matrix		Cargo = 0	Cargo = 4500 kg	Cargo = 9000 kg	Cargo = 13500 kg	Cargo = 18000 kg
Front	G_1	-486,505	-486,017	-485,529	-485,037	-484,552
	G_2	-4,809	-4,083	-3,358	-2,628	-1,907
	G_3	-34	-266	-513	-772	-1,036
	G_4	8,122	7,738	7,347	6,948	6,550
Rear	G_1	-1574,315	-1569,111	-1563,907	-1558,706	-1553,499
	G_2	-13,355	-5,621	2,120	9,860	17,617
	G_3	-542	-3,467	-6,607	-9,808	-13,040
	G_4	18,486	14,160	9,721	5,252	763

Important graphs for each run were generated and can be found in Appendix D. For instance, the first model with the first set of gains for both the front and rear quarter-car active suspension units is studied in this section. Figure 5.15 demonstrates a great deduction in pitch angle while active suspension units were used. Moreover, Figure 5.16 shows a significant drop in the performance index.

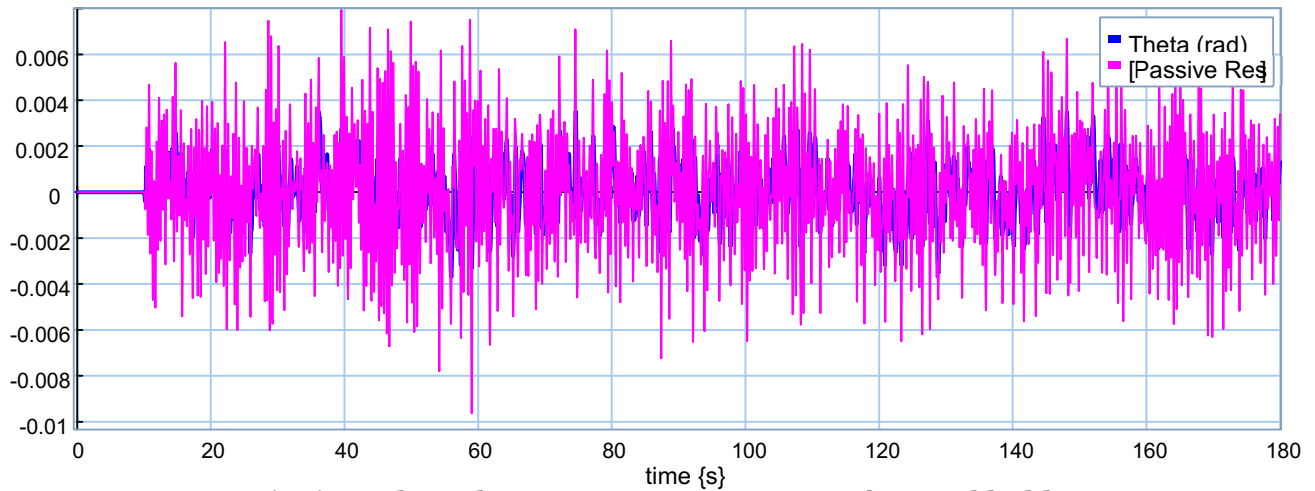


Figure 5.15: Pitch angle using quarter-car gains for road holding

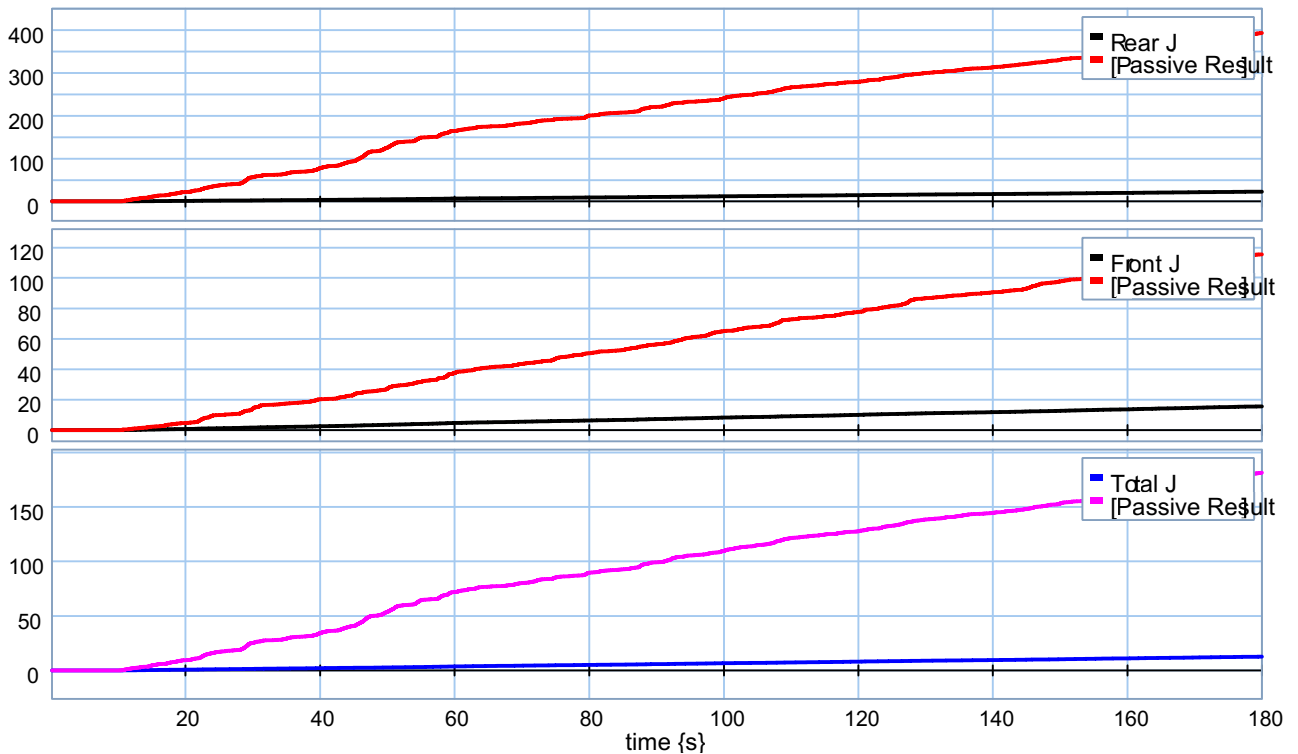


Figure 5.16: Performance indices using quarter-car gains for road holding

As was outlined, the purpose of the road holding scenario can be satisfied by the tires' declining vertical velocity and deflection. Figures 5.17 to 5.20 demonstrate the efficiency of using active suspension over the passive suspension mode.

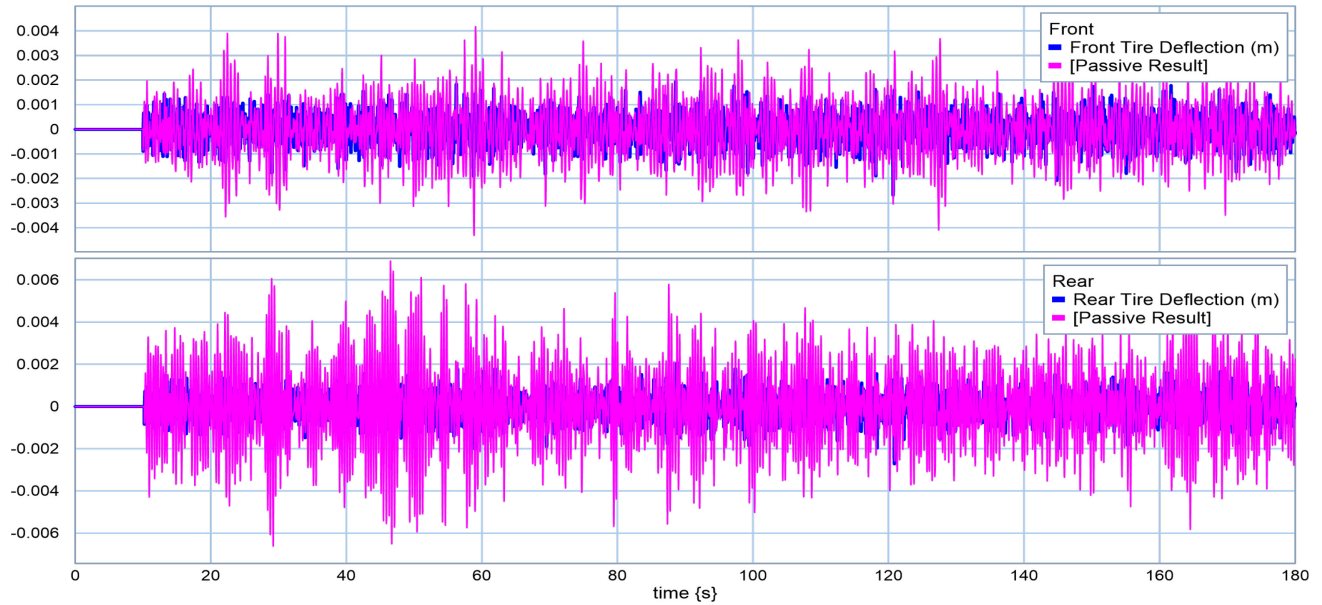


Figure 5.17: Tires' deflections using quarter-car gains for road holding

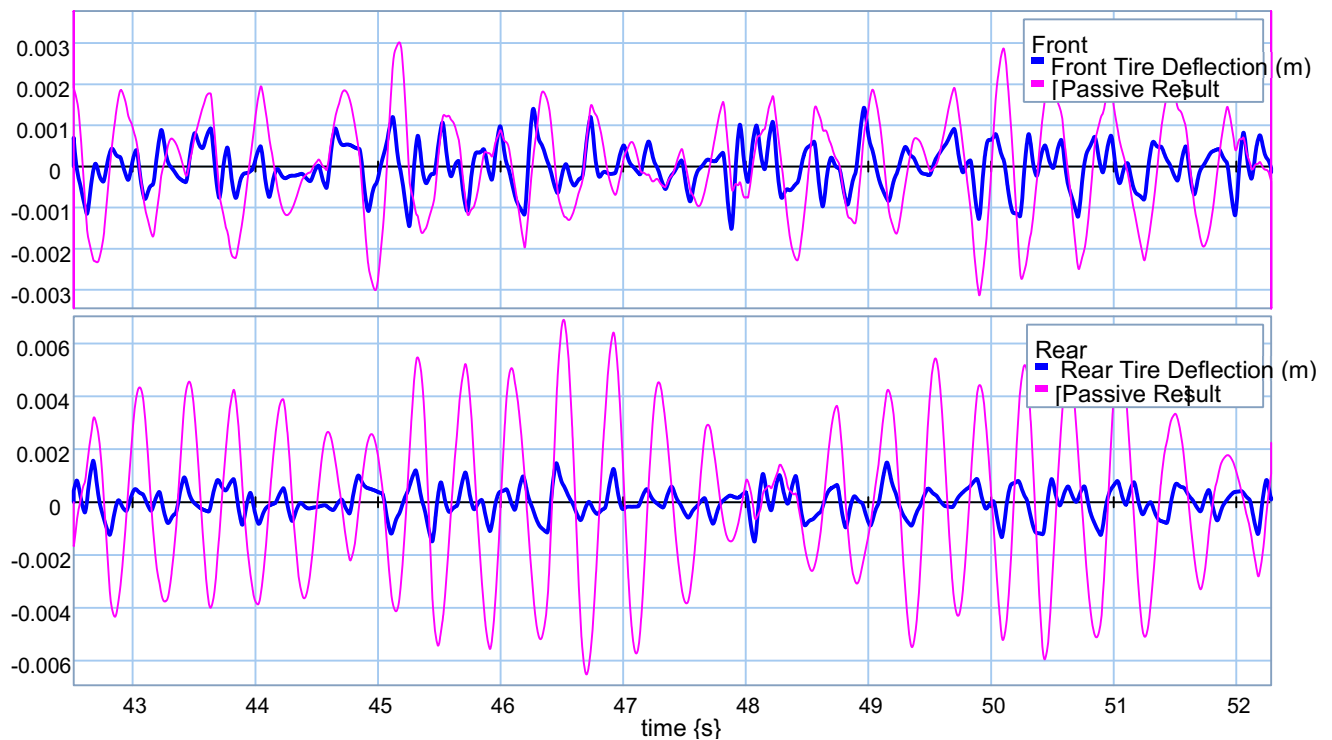


Figure 5.18: Magnified tires' deflections using quarter-car gains for road holding

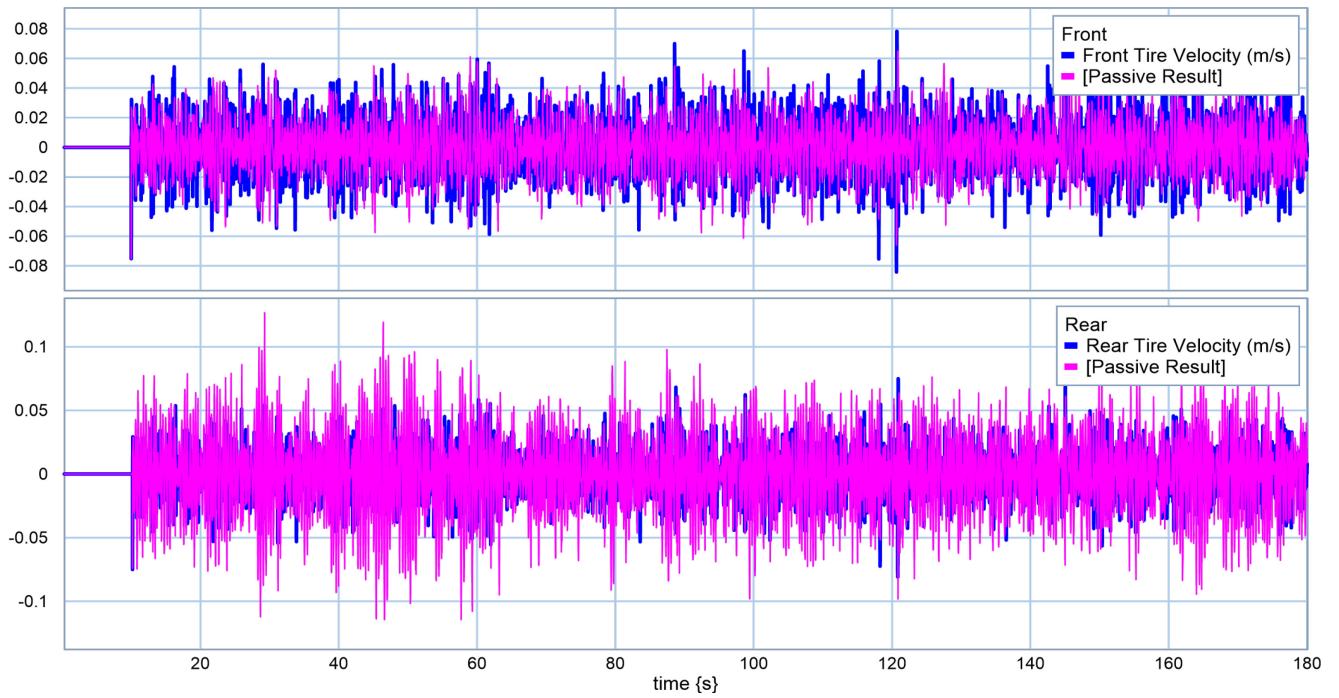


Figure 5.19: Tires' velocities using quarter-car gains for road holding

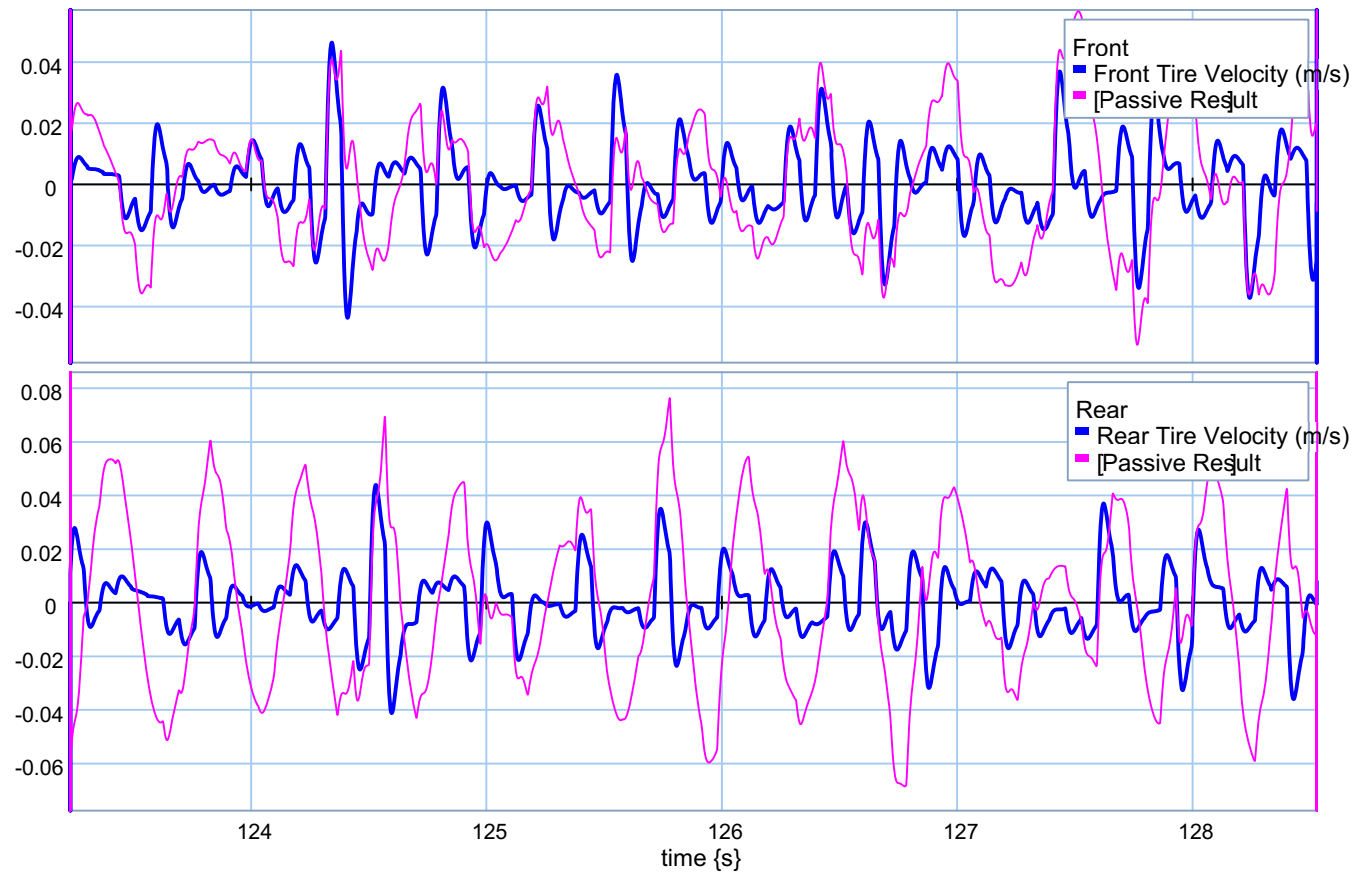


Figure 5.20: Magnified tires' velocities using quarter-car gains for road holding

Although in road holding, minimizing the vertical and pitch acceleration are not looked for, Figures 5.21 and 5.22 show a great reduction in these states, which could improve the ride quality of the vehicle.

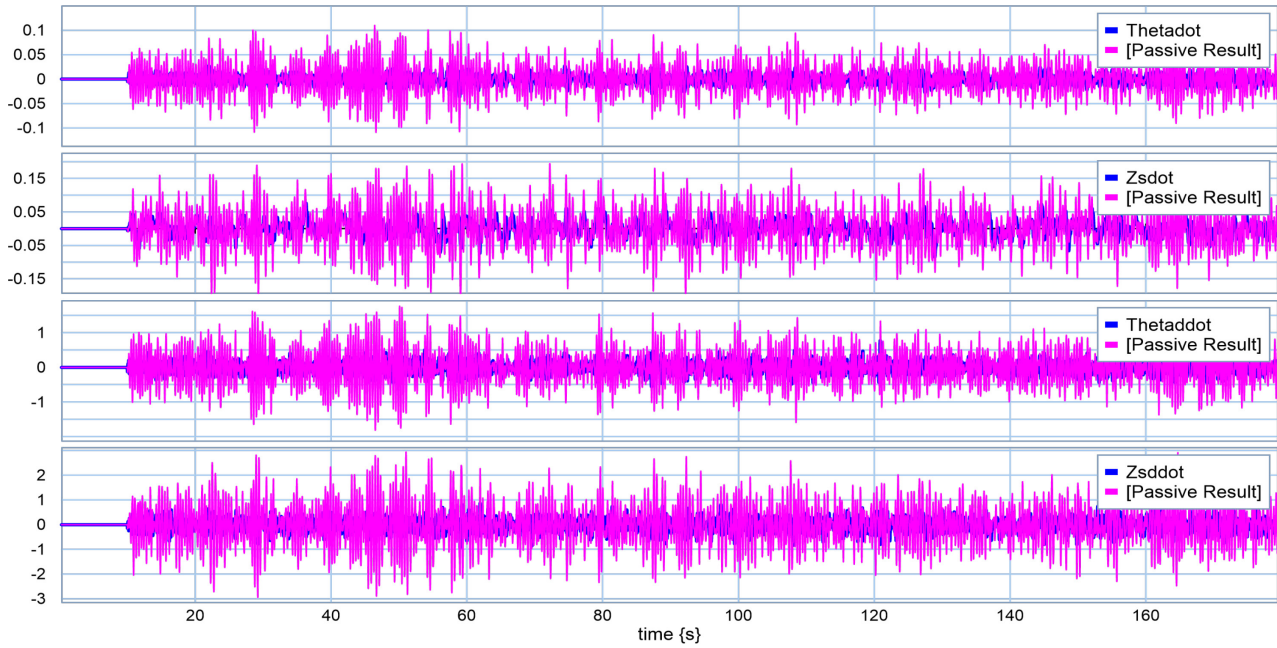


Figure 5.21: Central states using quarter-car gains for road holding

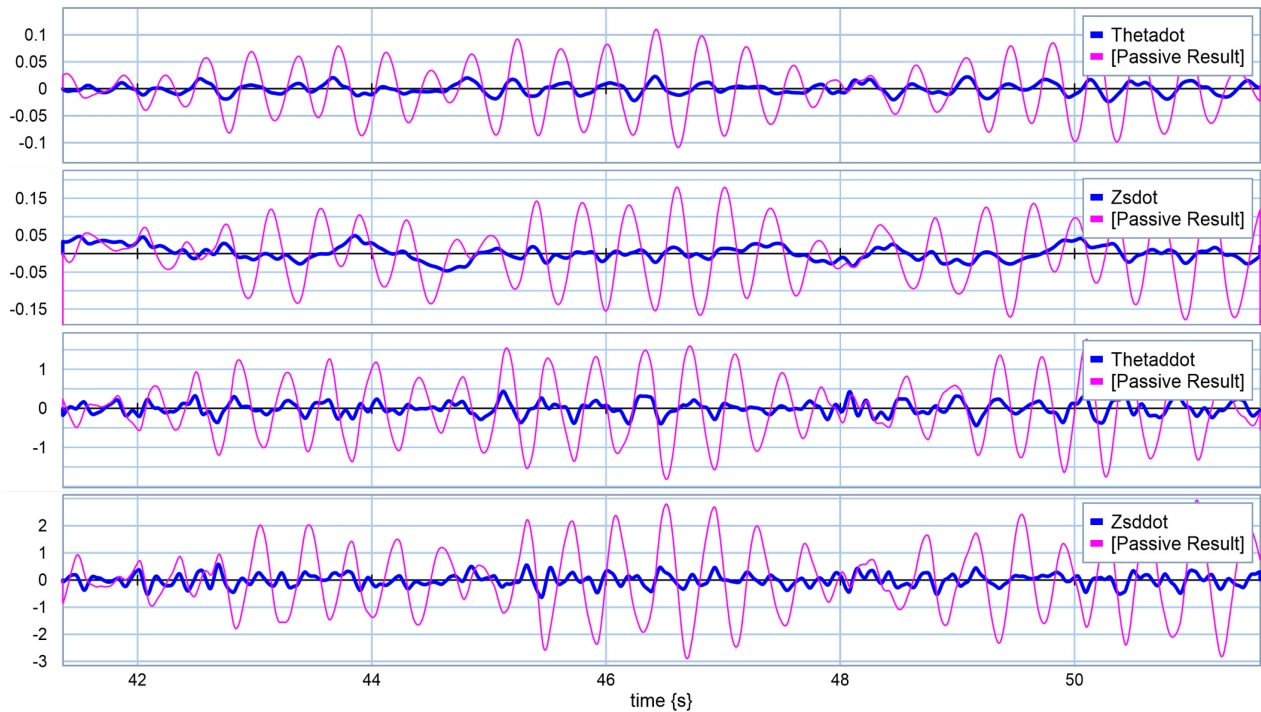


Figure 5.22: Magnified central states using quarter-car gains for road holding

Similar to what was outlined in the previous section for ride quality, an optimum set of gains needs to be presented which can be used for all possible cargo masses. For this reason, each model ran five times under the same initial conditions but with different sets of gains. The improvement in road holding was compared for each model by recording and correlating performance indices. Since the performance indices for all studied sets of gains were close to each other in each model, another index had to be used in order to present the optimum gain, i.e., energy index. Hence, the energy indices outlined in equations (5-36,37) were recorded for all runs and the results showed that for all five models the lower energy index was recorded while the fifth set of gains was used. Figures 5.23 and 5.24 compare tire velocity and deflection for the first model when the first and fifth sets of gains were used. As is seen, there is not much difference in improvement when the first set of gains was used instead of the fifth. Hence, by using the fifth set of gains, the road holding scenario would be satisfied with consuming less energy.

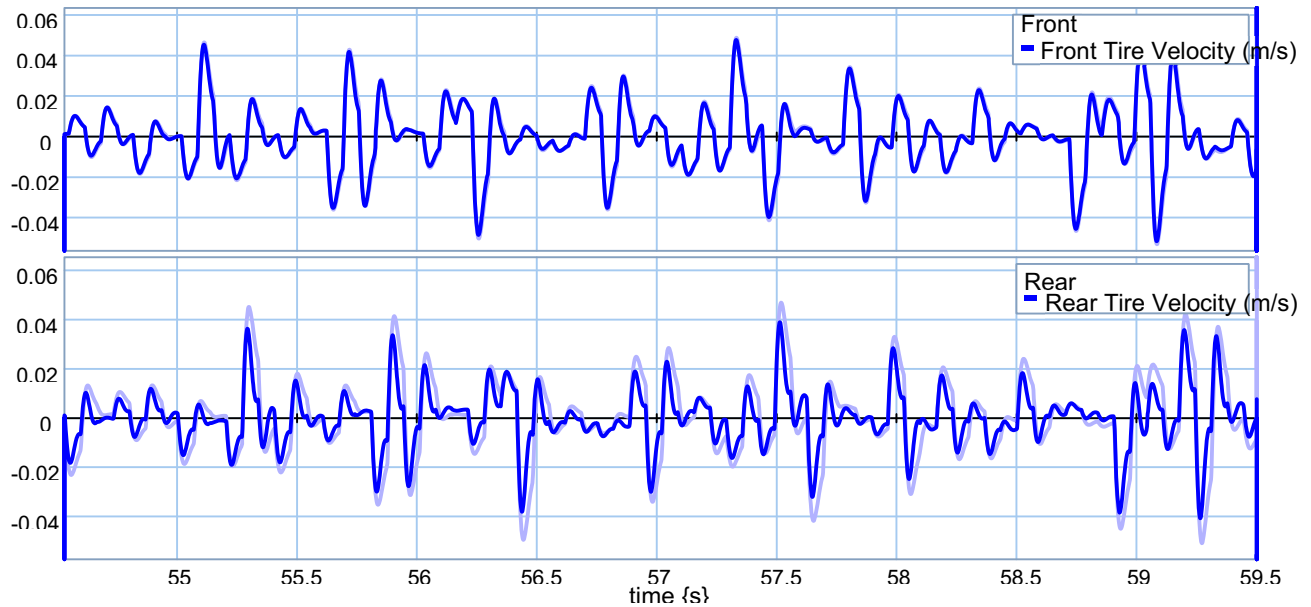


Figure 5.23: Tires' velocities comparison between two sets of quarter-car gains

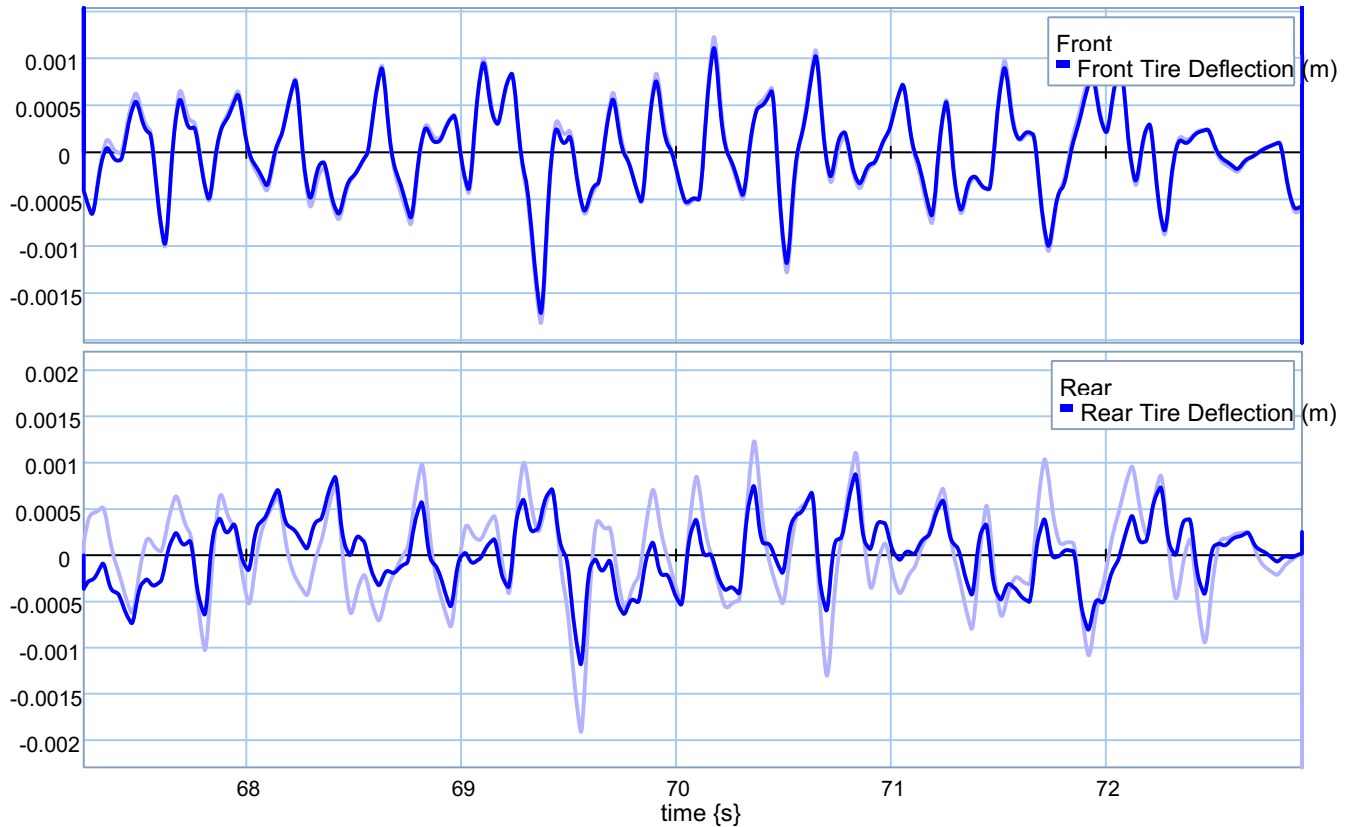


Figure 5.24: Tires' velocities comparison between two sets of quarter-car gains in road holding

Based on these two sections, for both the ride quality and road holding scenarios, the fifth set of gains is presented as the optimum gains for the quarter-car active suspension situation. These optimum gains are used in the next section for a non-linear half-car model.

5.6.2 Ride Quality

Once the best set of gains was developed, and non-linear half-car models were generated for five various cargo masses. The chosen gain matrix i.e. the fifth set of gains, was used in all five models and the results were compared with passive suspension. The road profile for this simulation was the custom road profile outlined in Chapter 4 [4.2.7.2] that consists of five fundamental events. Figures 5-25 to 5-29 compare the vehicle pitch angle for passive and active suspension situations.

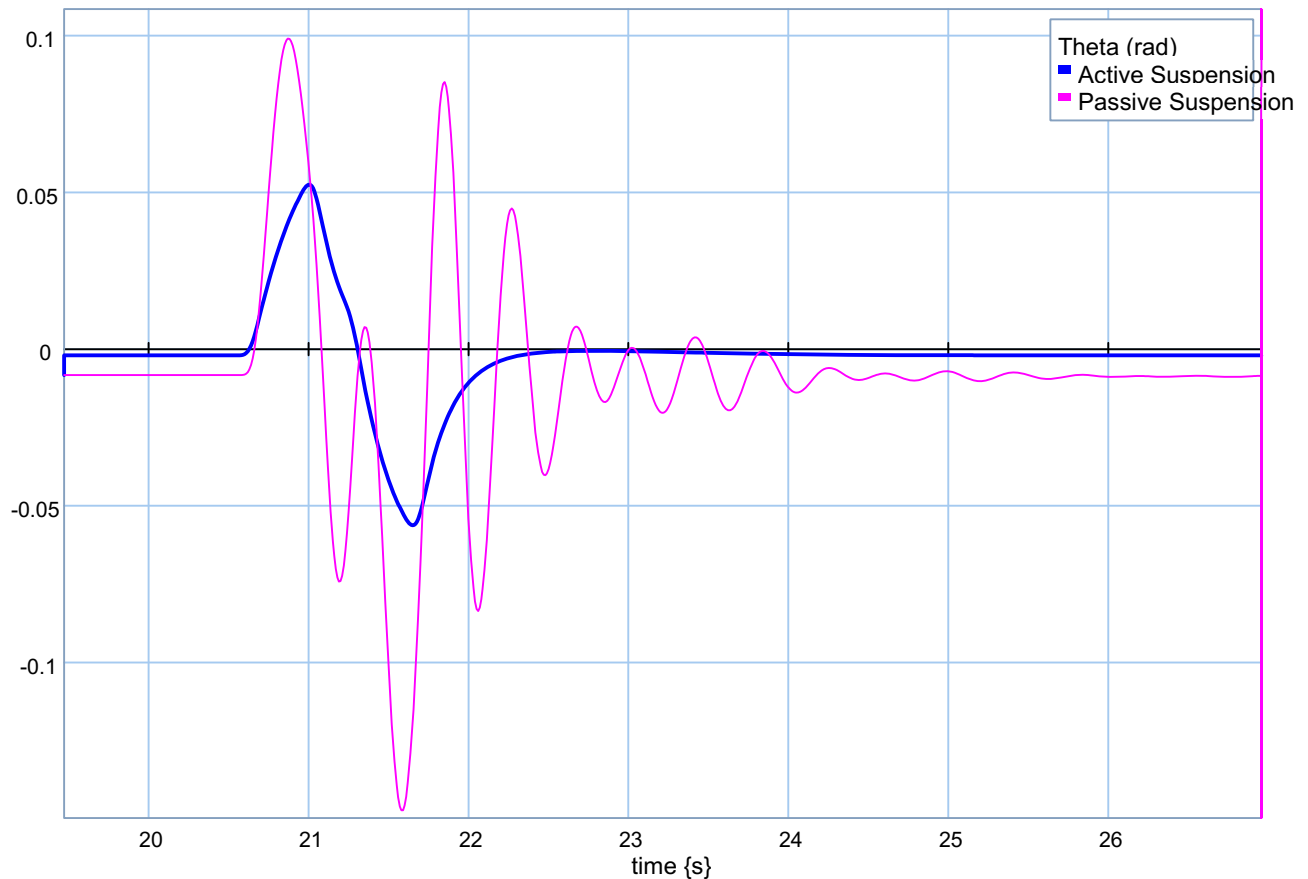


Figure 5.25: Vehicle pitch angle over 1st event of custom road profile in ride quality

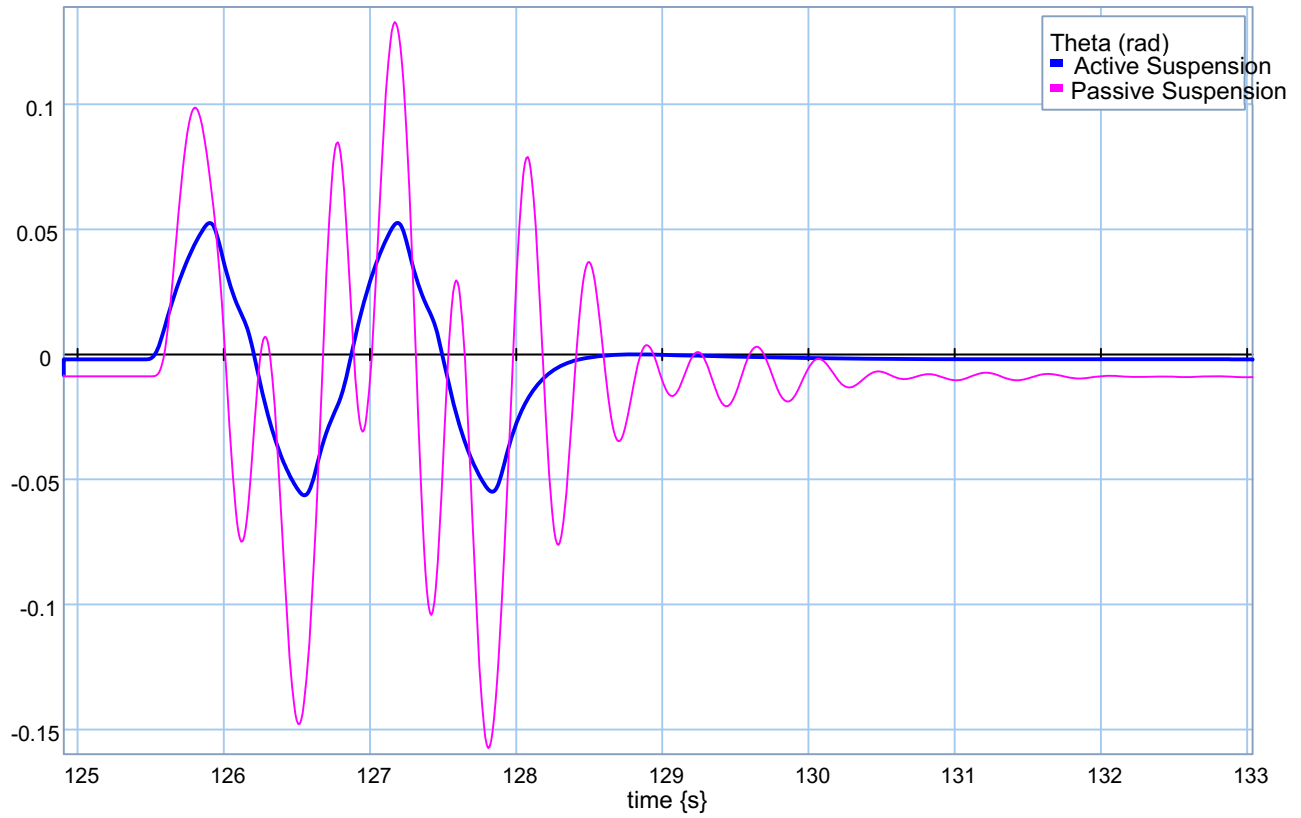


Figure 5.26: Vehicle pitch angle over 2nd event of custom road profile in ride quality

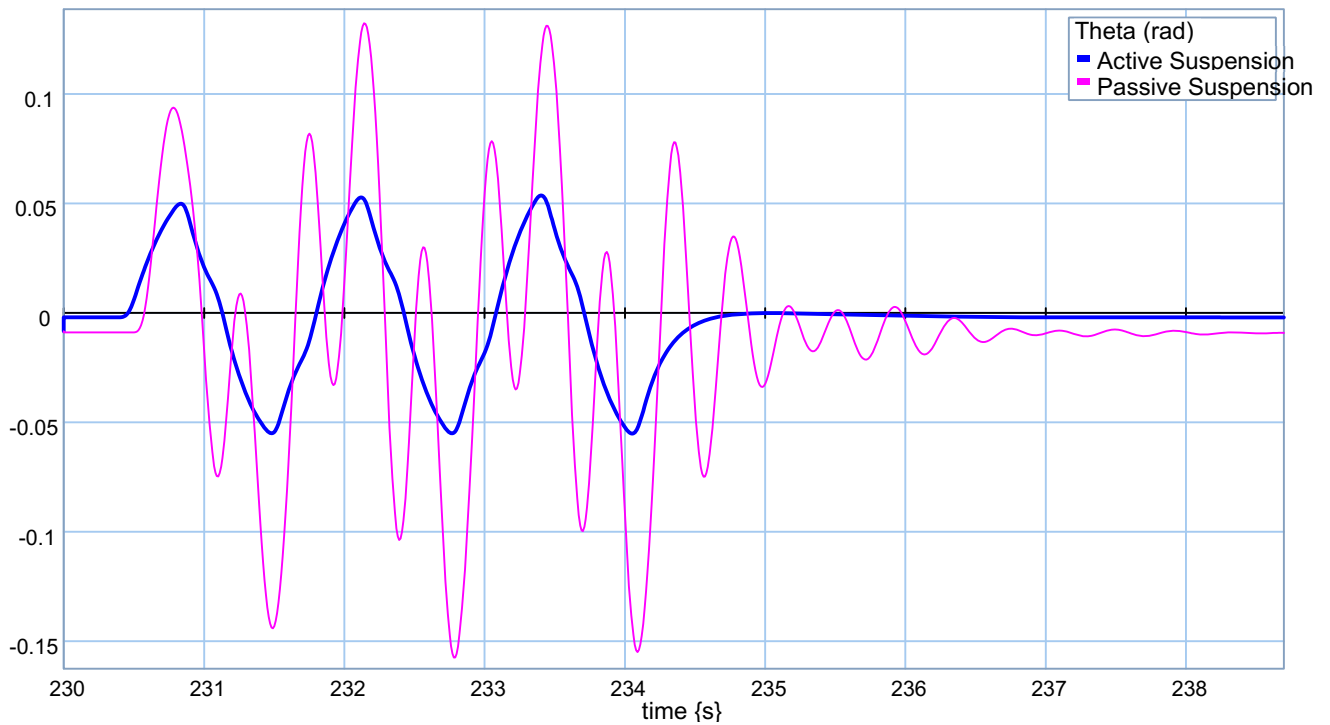


Figure 5.27: Vehicle pitch angle over 3rd event of custom road profile in ride quality

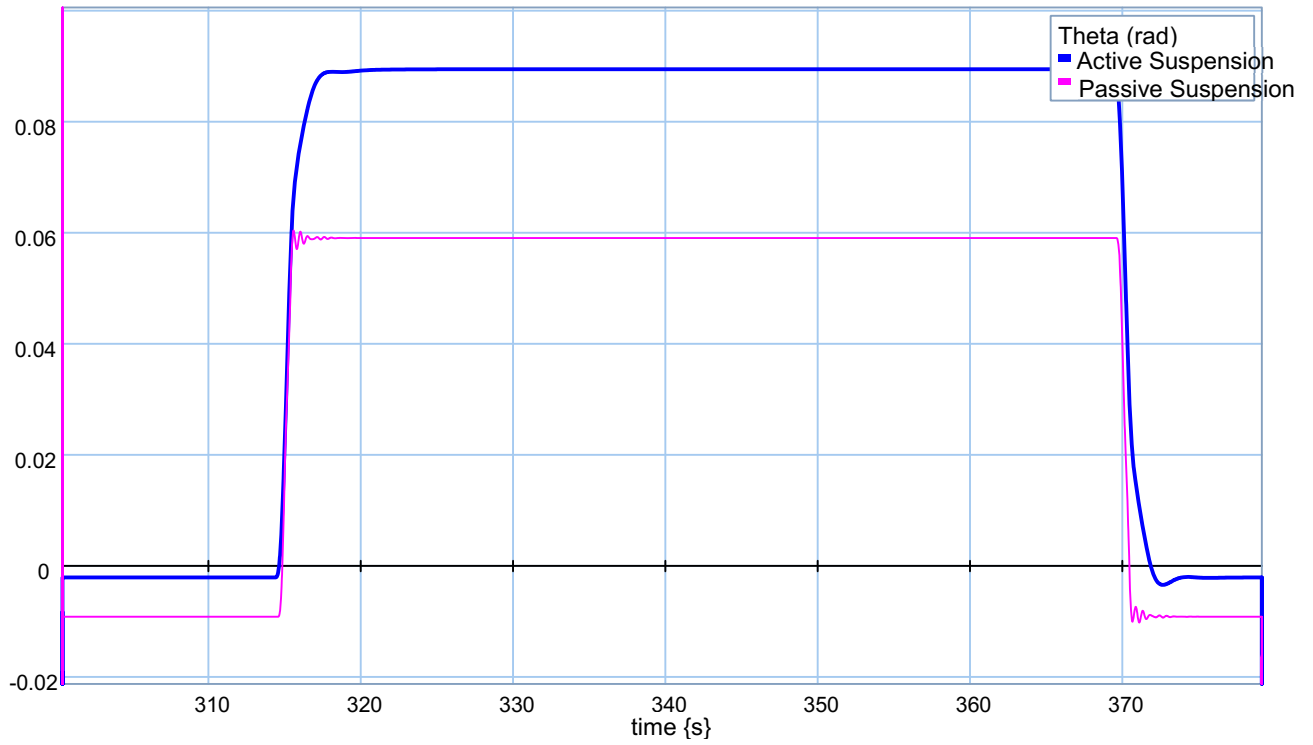


Figure 5.28: Vehicle pitch angle over 4th event of custom road profile in ride quality

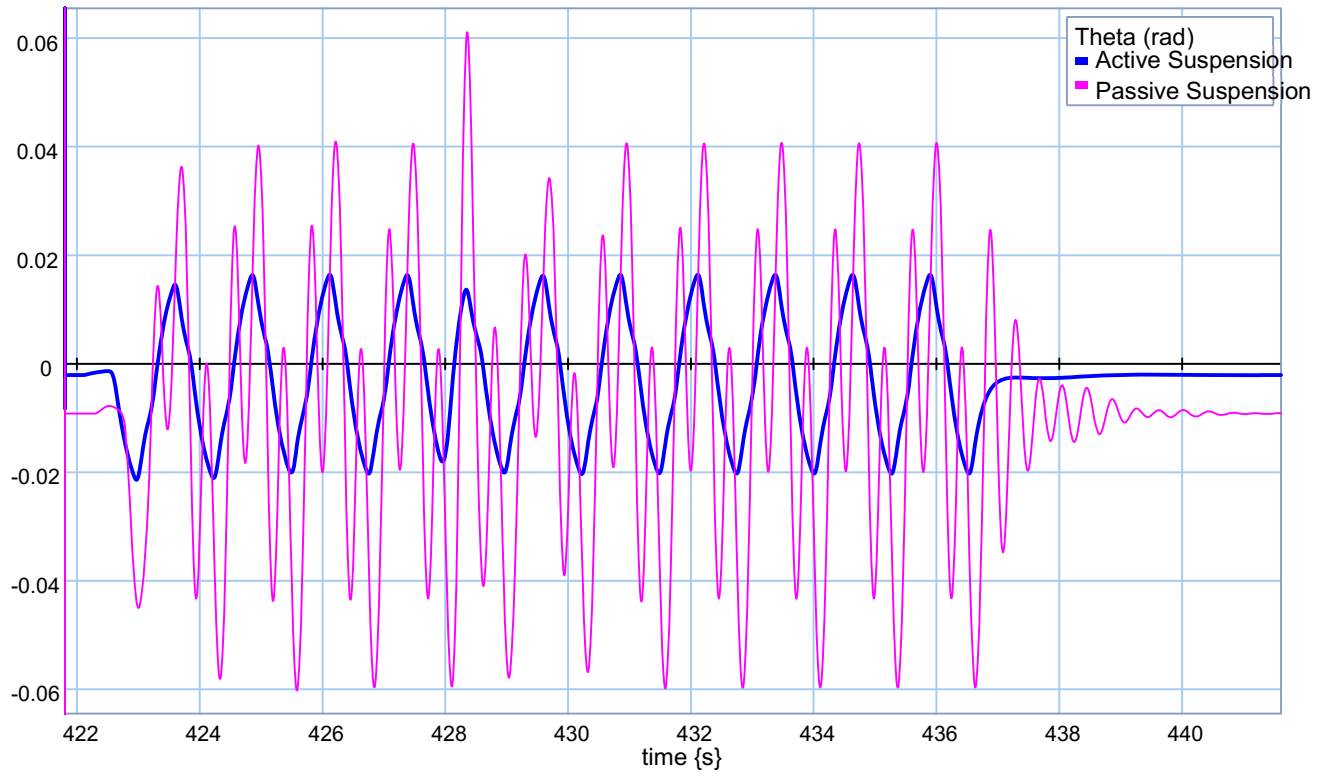


Figure 5.29: Vehicle pitch angle over 5th event of custom road profile in ride quality

In order to improve the ride quality, the vehicle's vertical acceleration needs to be controlled. In order to do so, the performance index (cost function) was defined. The lower the performance index, the better ride quality the vehicle has. Figure 5.30 compared this index for the front, rear and centre parts of the vehicle in passive and active suspension situations.

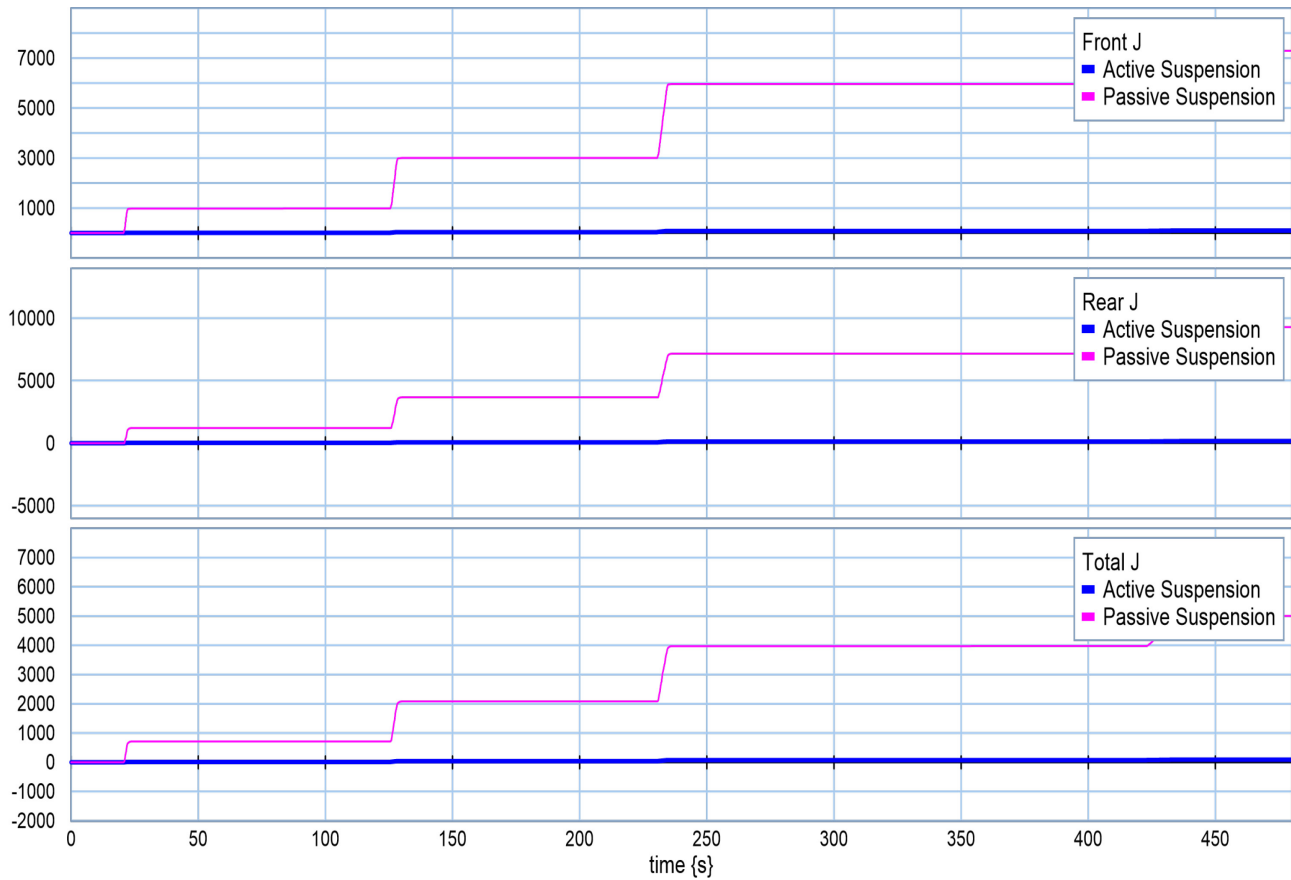


Figure 5.30: Performance index using quarter-car optimum gains in ride quality

Figures 5.31 to 5.40 present how these two quarter-car actuators improved the vehicle's ride quality by minimizing the vertical accelerations.

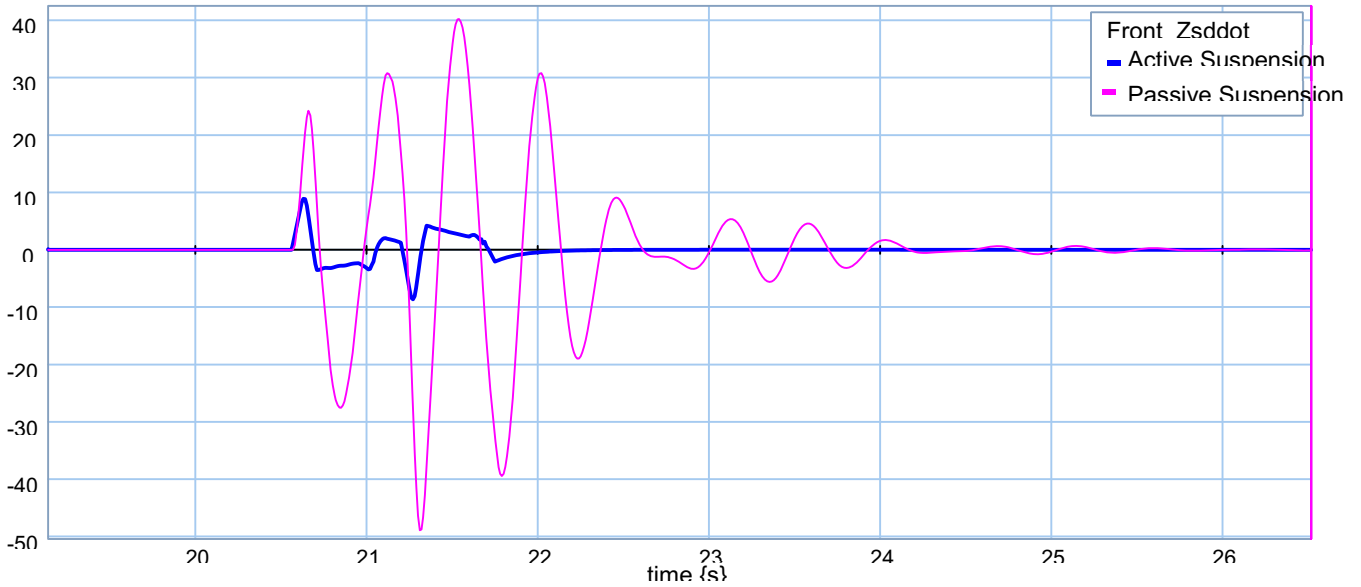


Figure 5.31: Front sprung mass acceleration over 1st event of custom road profile

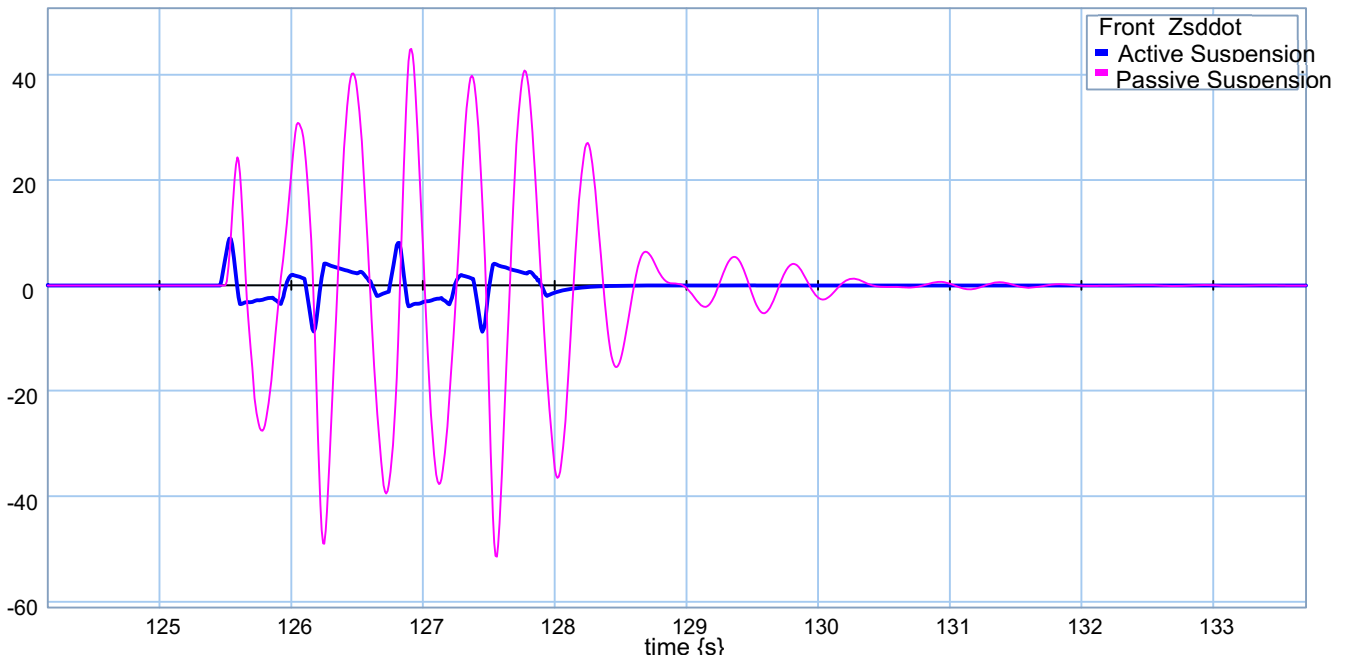


Figure 5.32: Front sprung mass acceleration over 2nd event of custom road profile

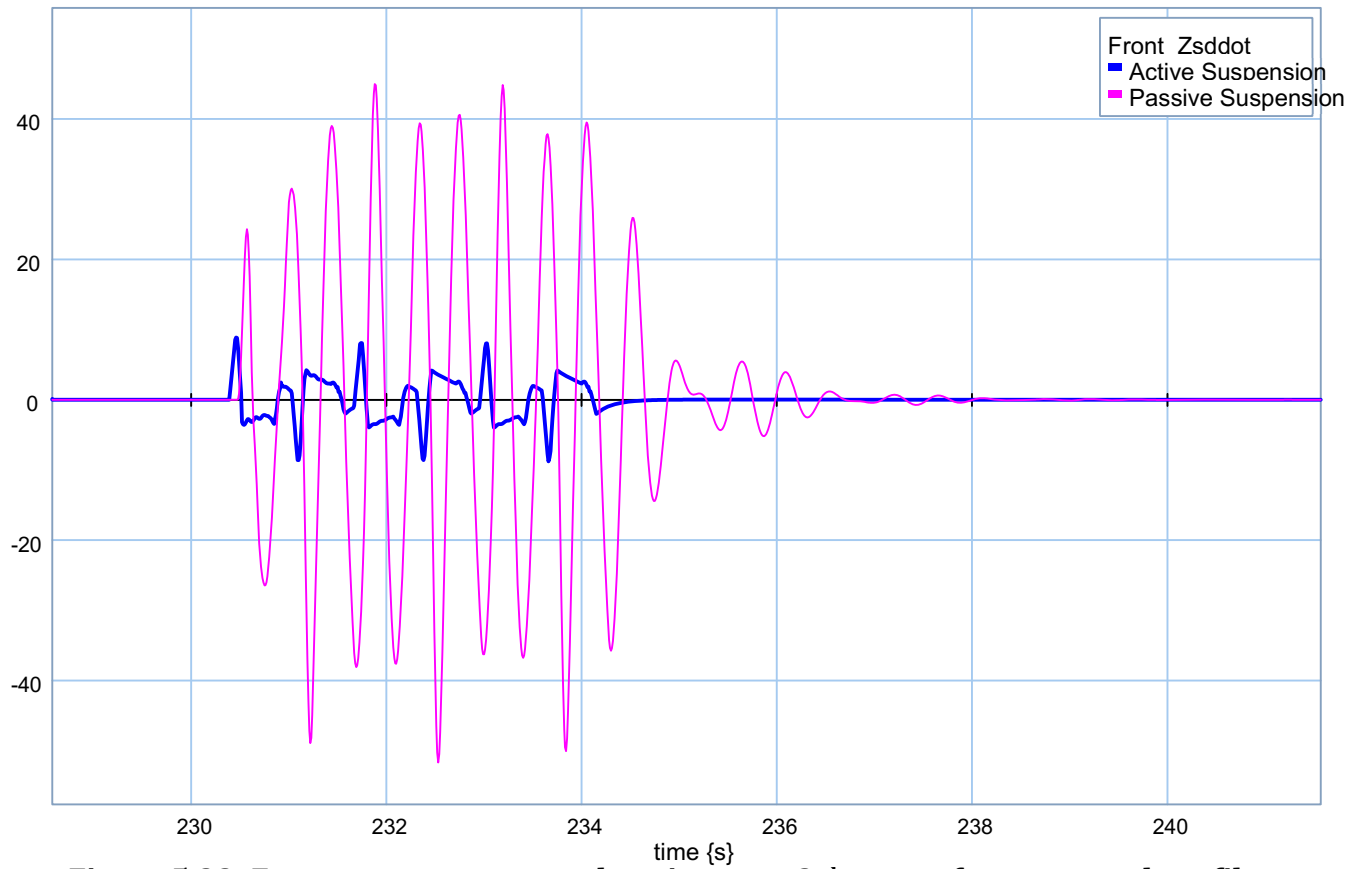


Figure 5.33: Front sprung mass acceleration over 3rd event of custom road profile

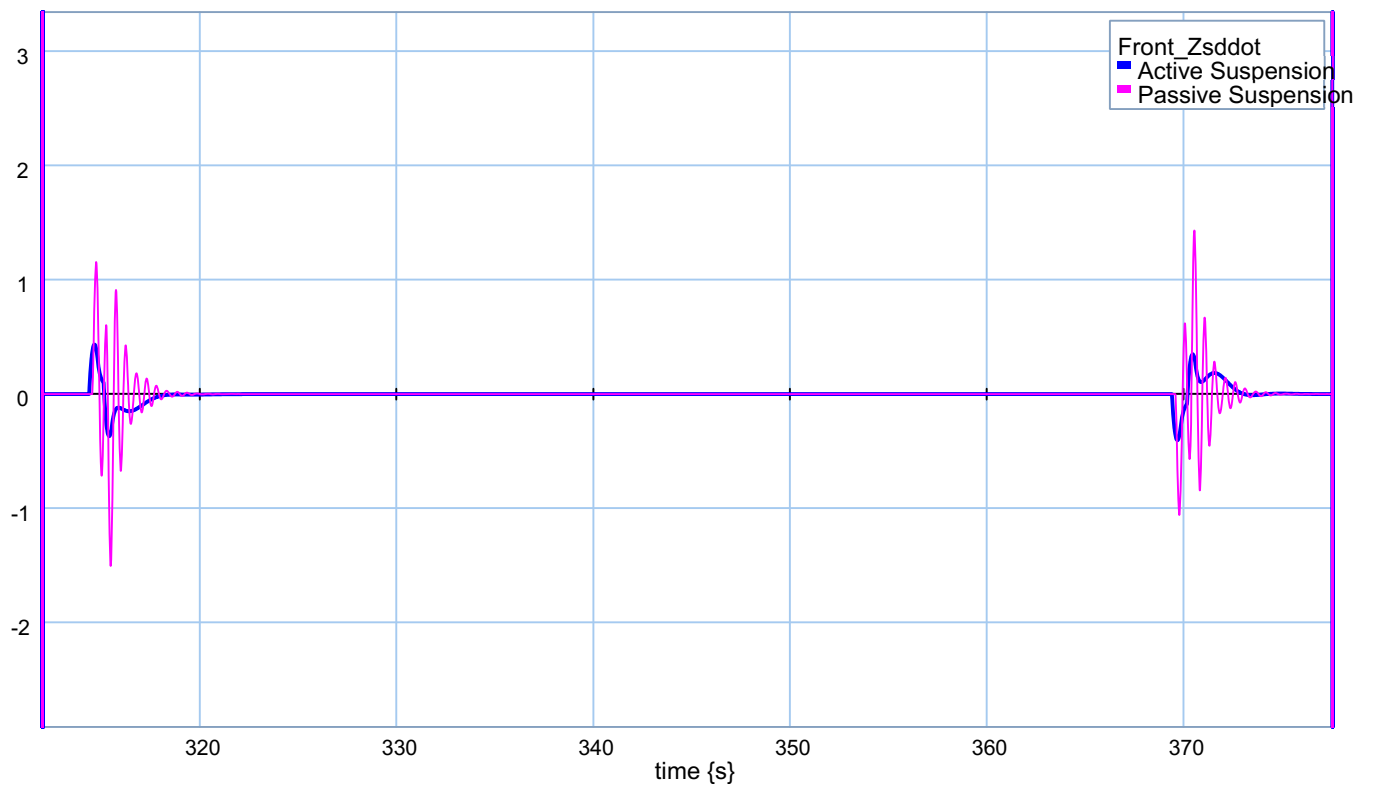


Figure 5.34: Front sprung mass acceleration over 4th event of custom road profile

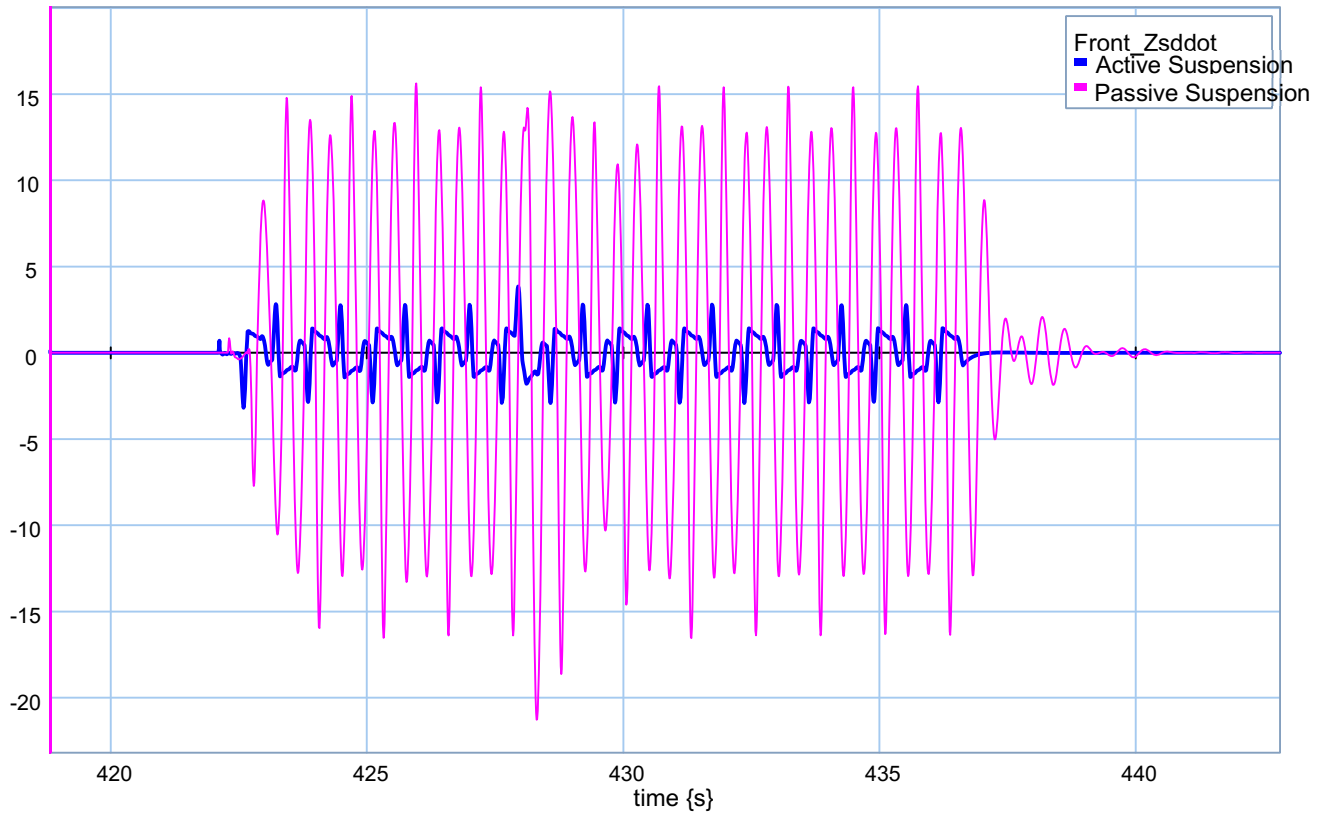


Figure 5.35: Front sprung mass acceleration over 5th event of custom road profile

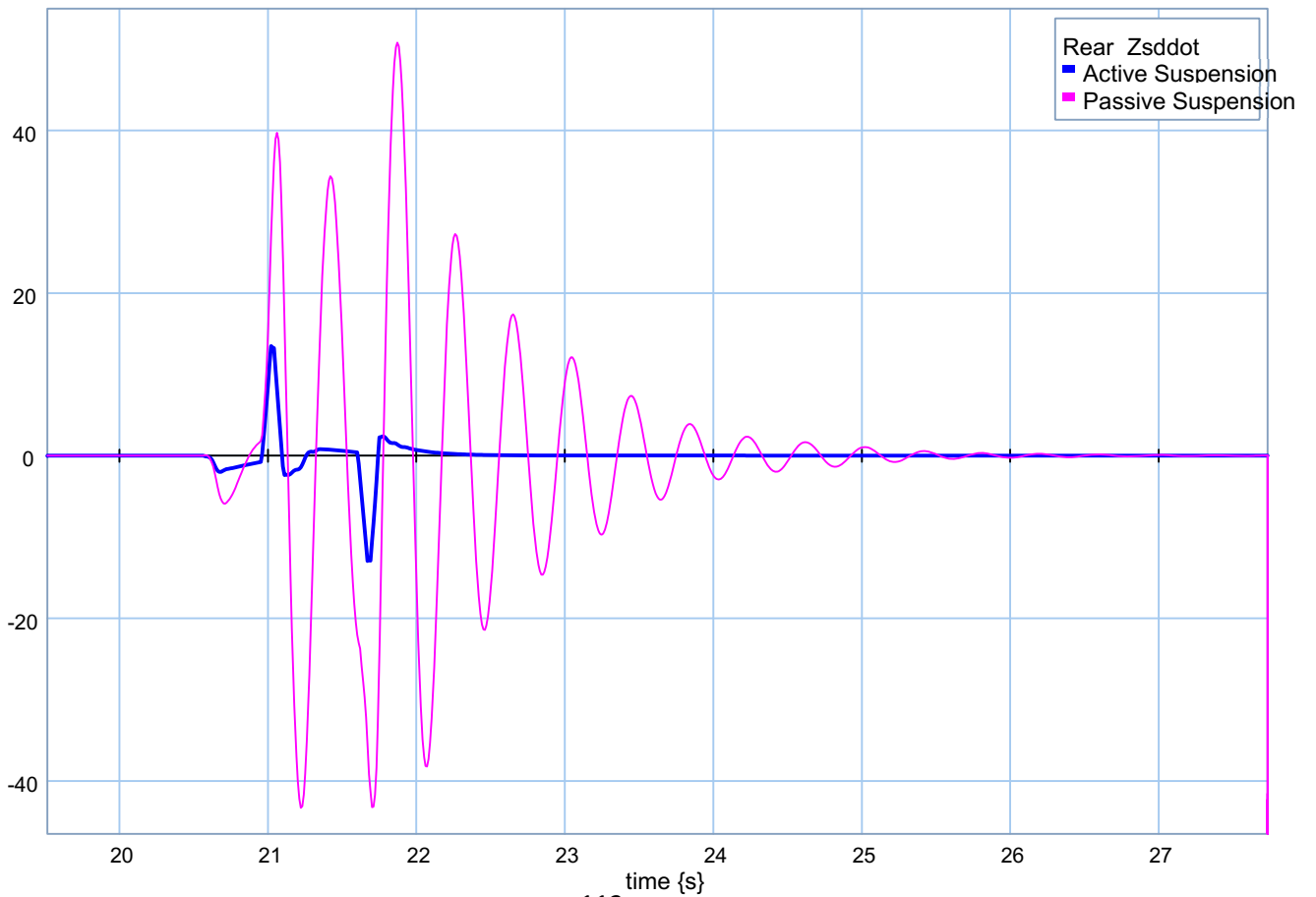


Figure 5.36: Rear sprung mass acceleration over 1st event of custom road profile

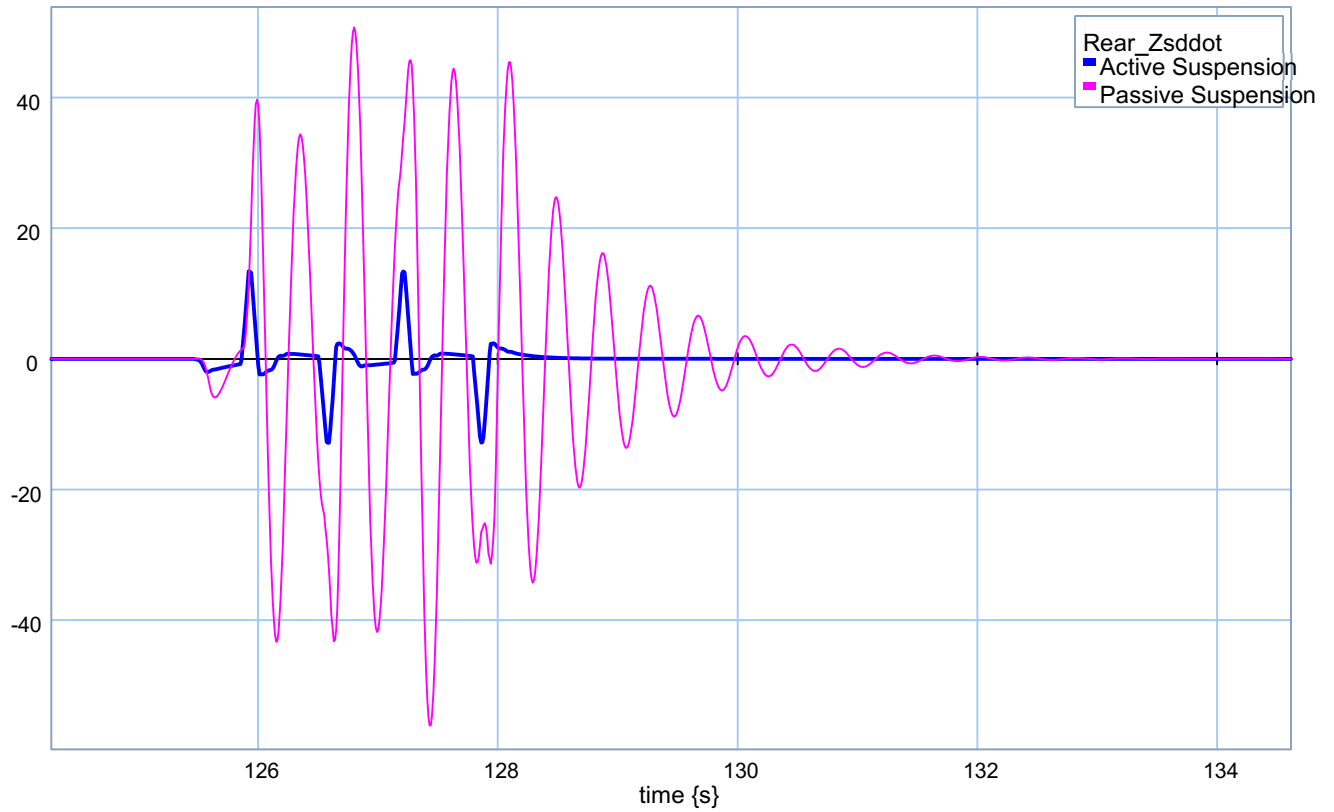


Figure 5.37: Rear sprung mass acceleration over 2nd event of custom road profile

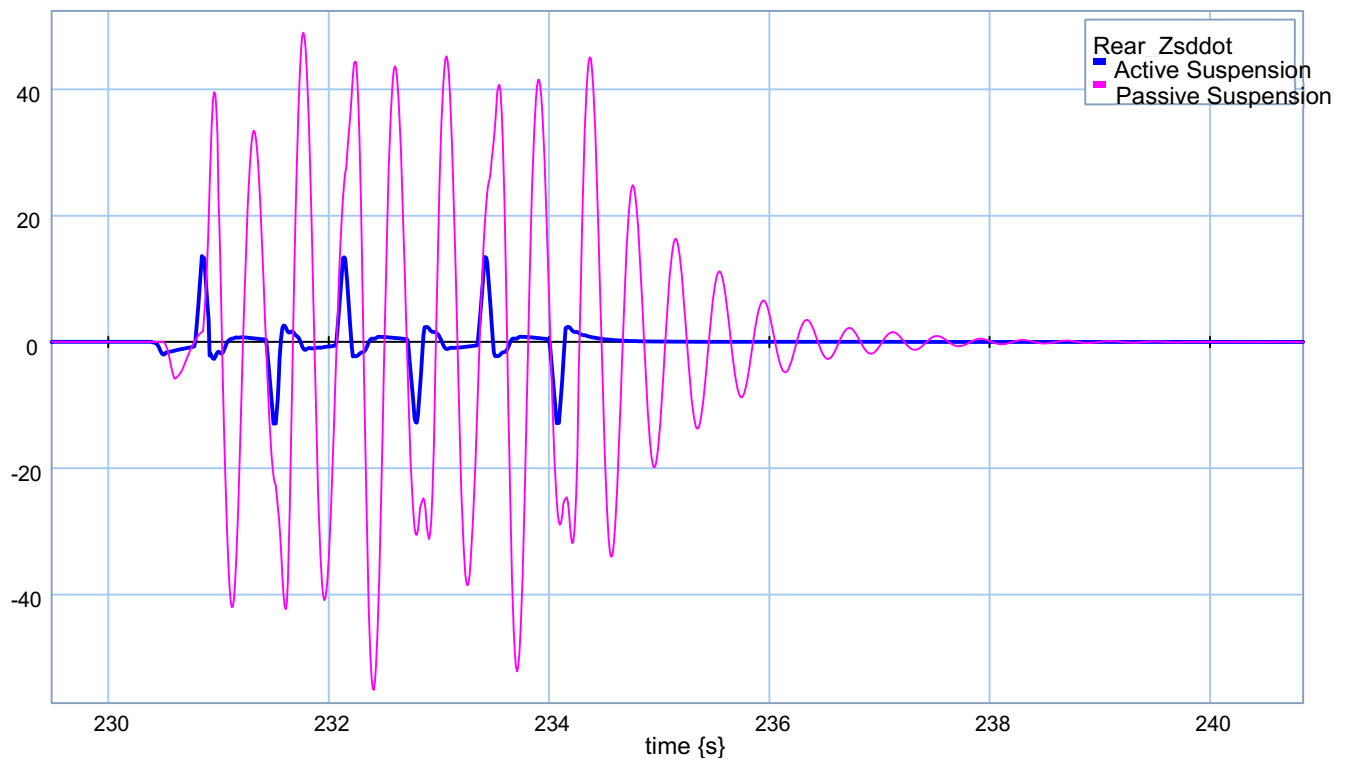


Figure 5.38: Rear sprung mass acceleration over 3rd event of custom road profile

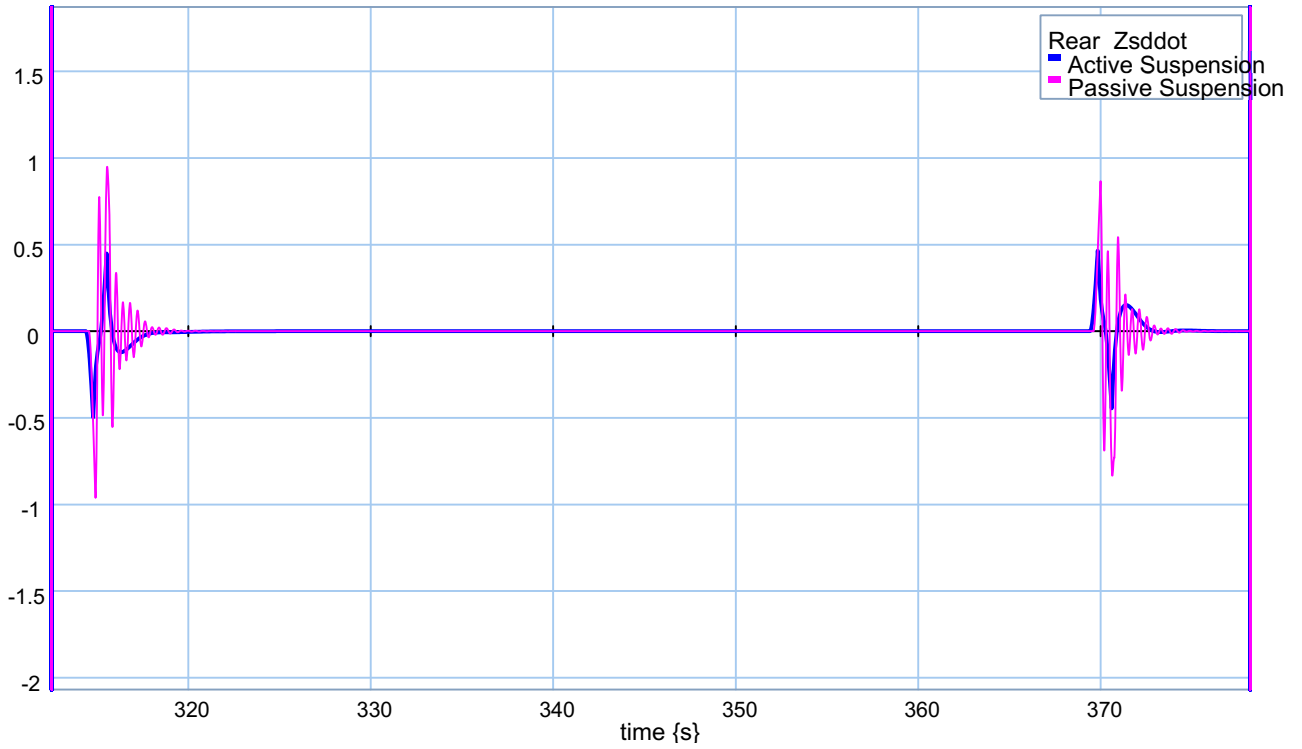


Figure 5.39: Rear sprung mass acceleration over 4th event of custom road profile

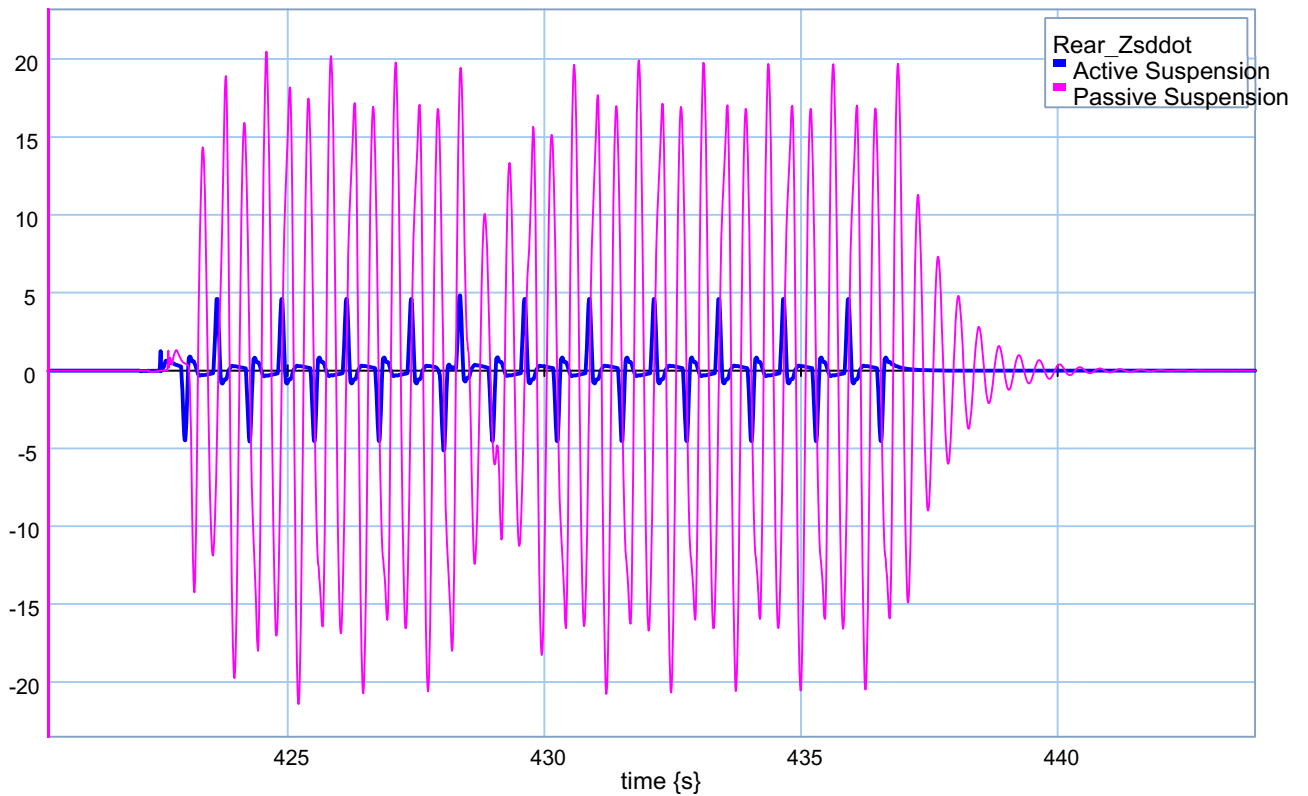


Figure 5.40: Rear sprung mass acceleration over 5th event of custom road profile

In this model, two independent quarter-car actuators were used for the front and rear parts of the vehicle. By setting the optimum gains, these actuators could control the front and rear vertical acceleration. Moreover, the vertical and pitch acceleration of the vehicle's centre of gravity was also controlled indirectly. Figure 5.41 to 5.45 demonstrate vertical and pitch acceleration for the vehicle's centre of gravity in passive and active suspension modes.

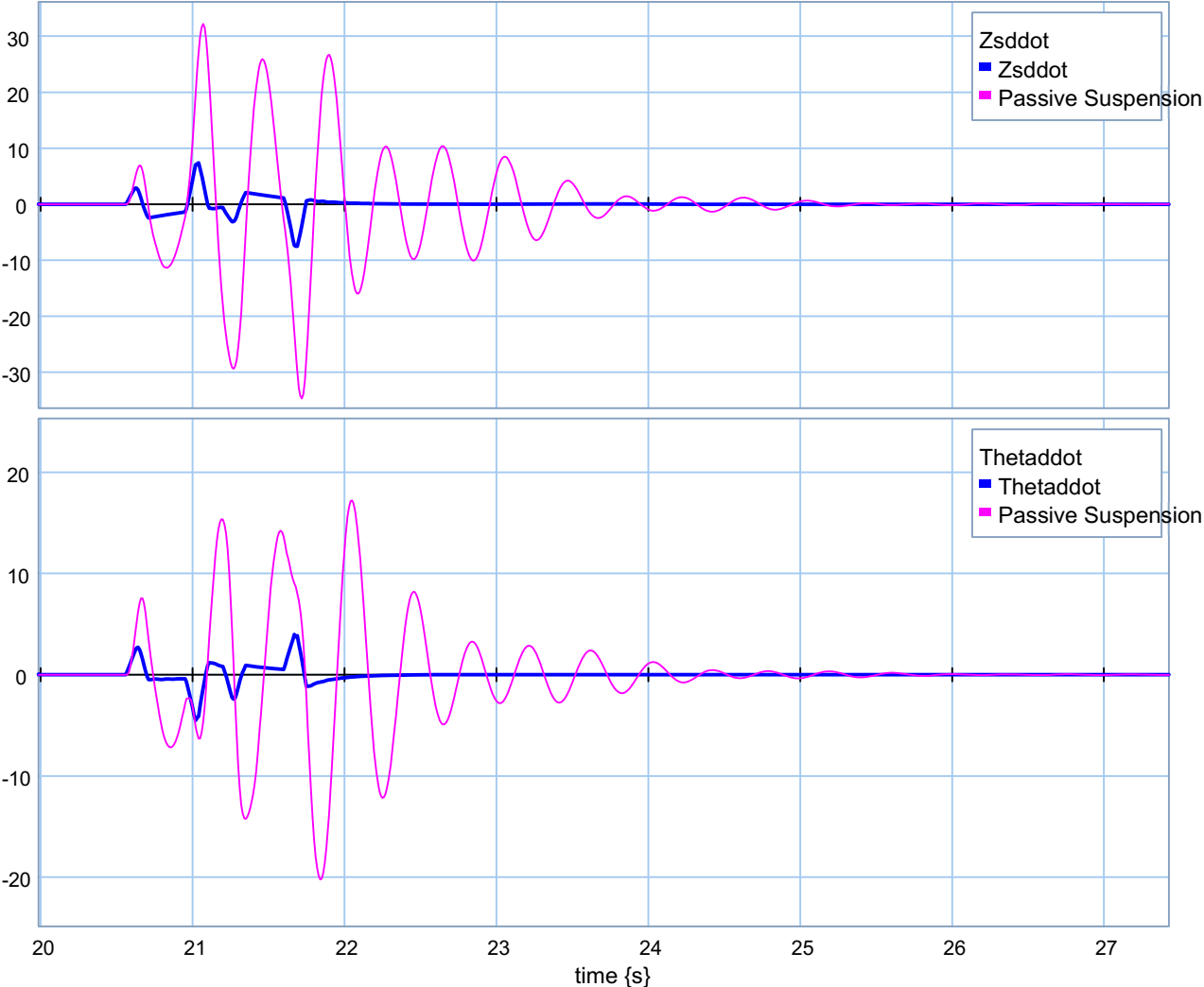


Figure 5.41: Central states over 1st event of custom road profile

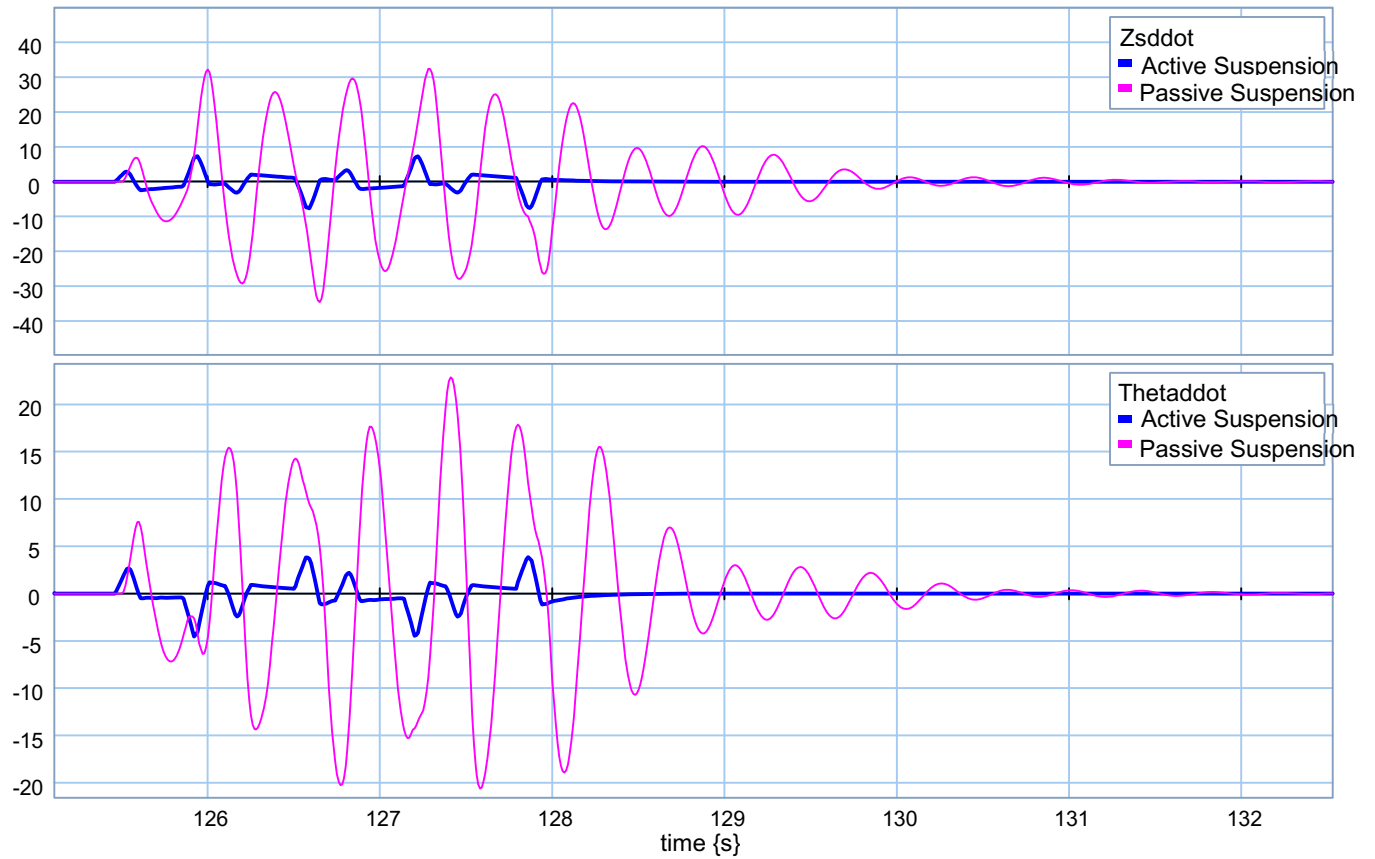


Figure 5.42: Central states over 2nd event of custom road profile

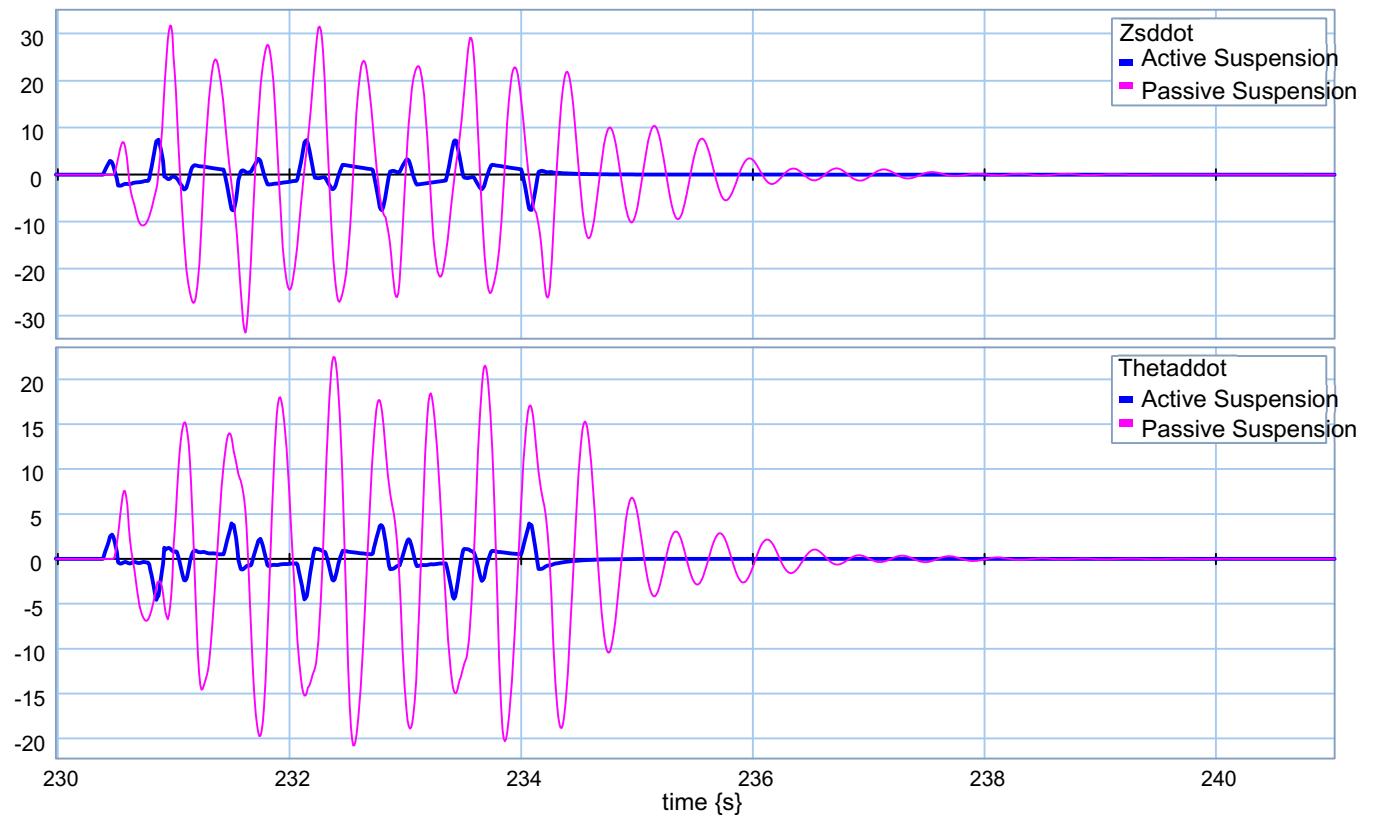


Figure 5.43: Central states over 3rd event of custom road profile

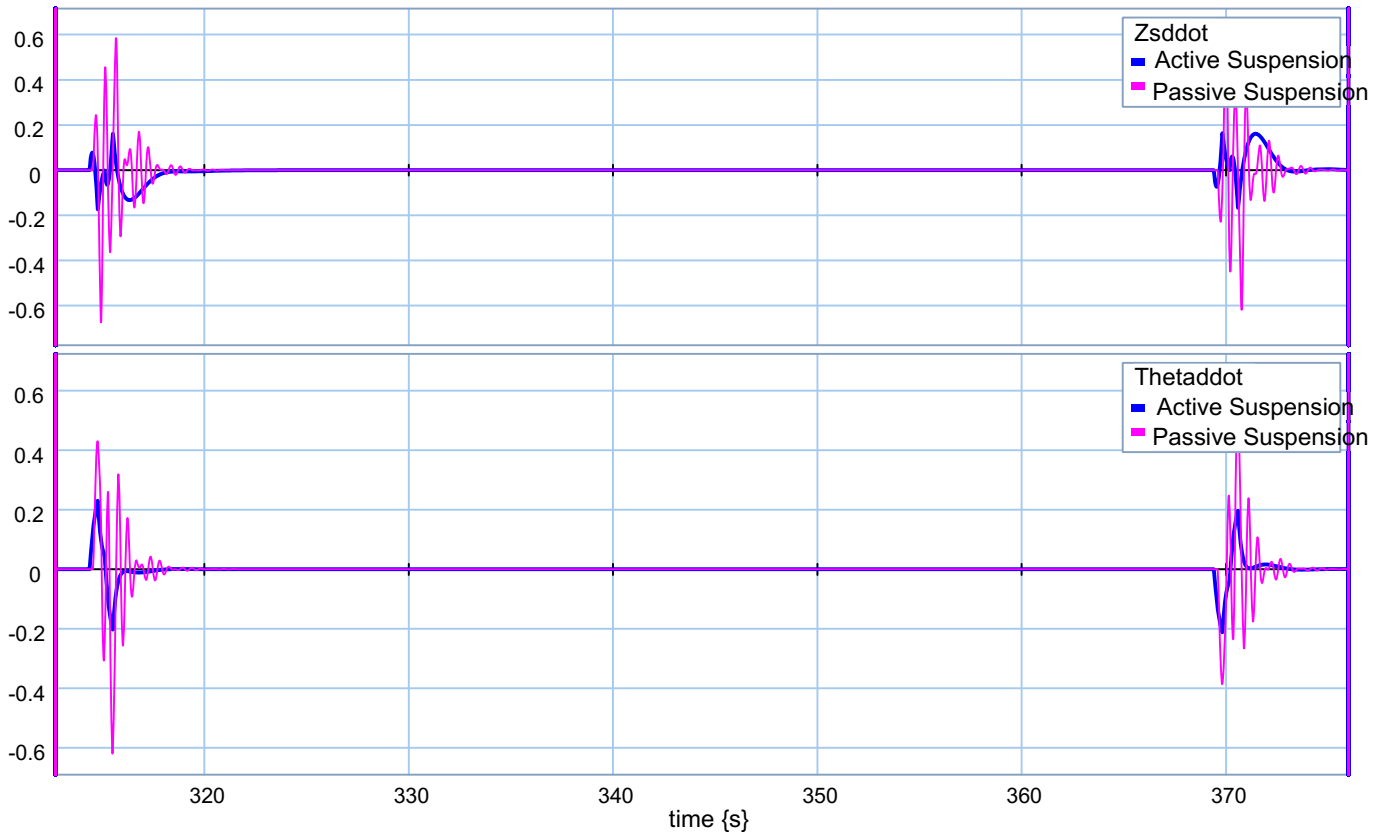


Figure 5.44: Central states over 4th event of custom road profile

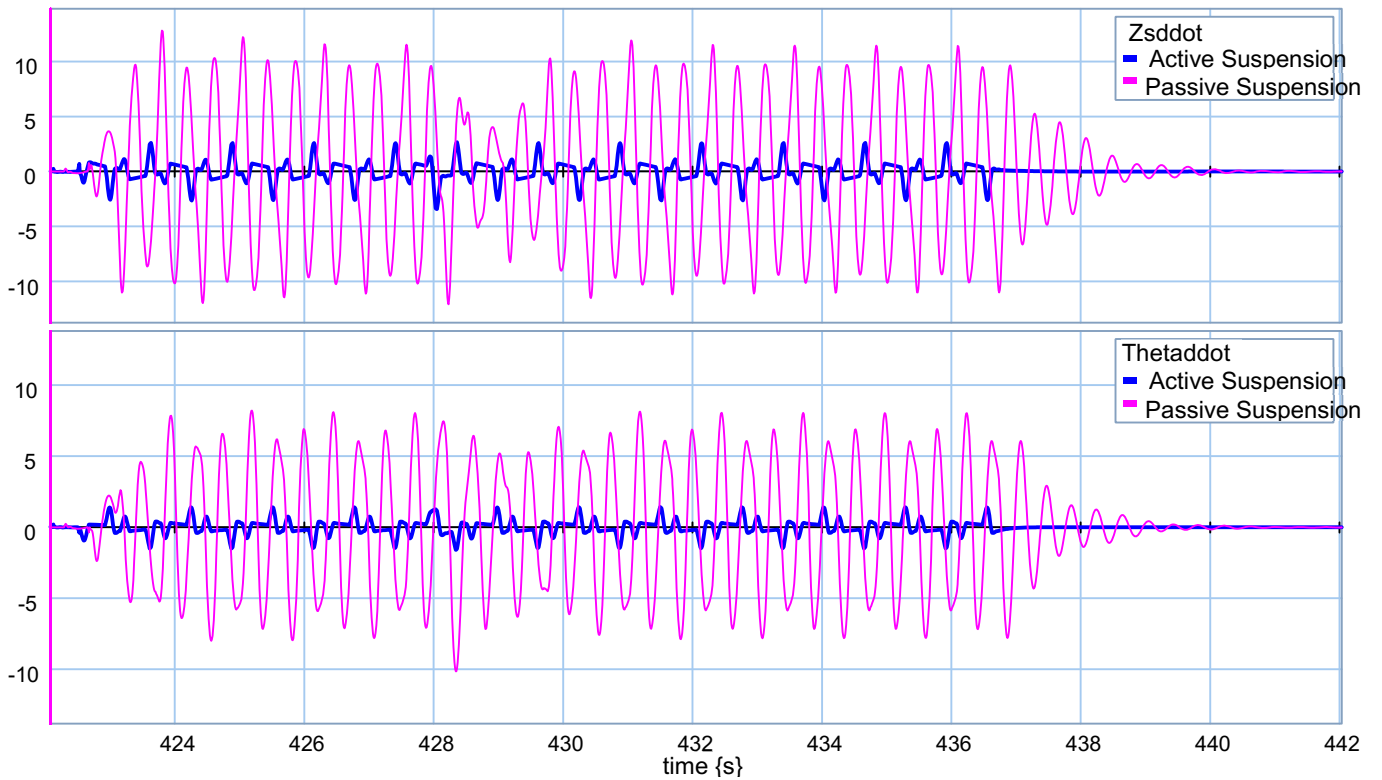


Figure 5.44: Central states over 5th event of custom road profile

5.6.3 Road Holding

Similar to what was shown in the previous section, five non-linear half-car models were generated corresponding to the five sample cargo masses. The two quarter-car actuators with suggested optimum gains outlined in section 5.6.1.2 were used in the front and rear parts of the vehicle and models were run under the same conditions over the custom road profile. The desired results corresponding to the road holding scenario were captured and compared with the situation when there were no actuators used in the vehicle (passive suspension). For instance, the results of first model are given in this section. Appendix H covers all the graphs for this scenario.

Figures 5.46 and 5.47 demonstrate that the vehicle followed the road profile very well and active suspension could decrease the front and rear performance indices.

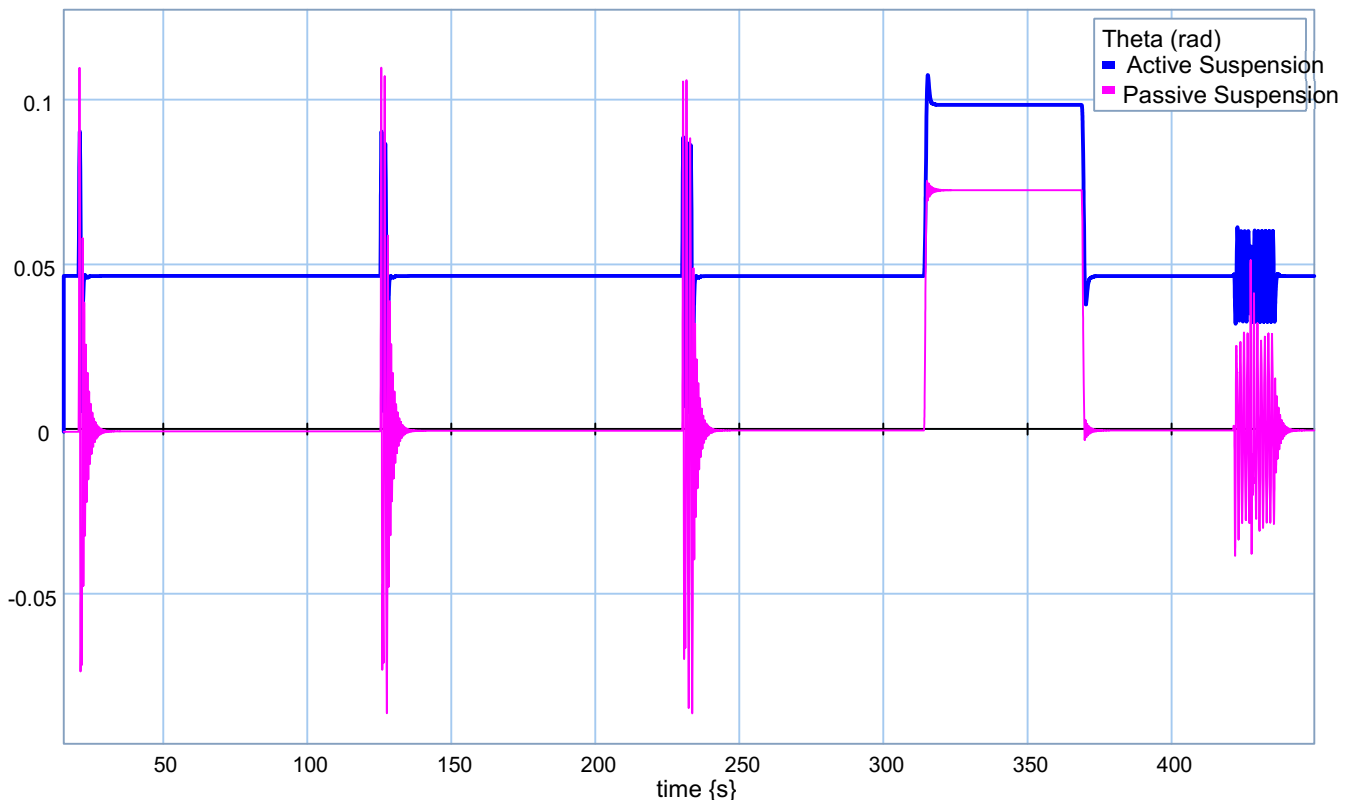


Figure 5.46: Vehicle pitch angle using quarter-car gains in road holding

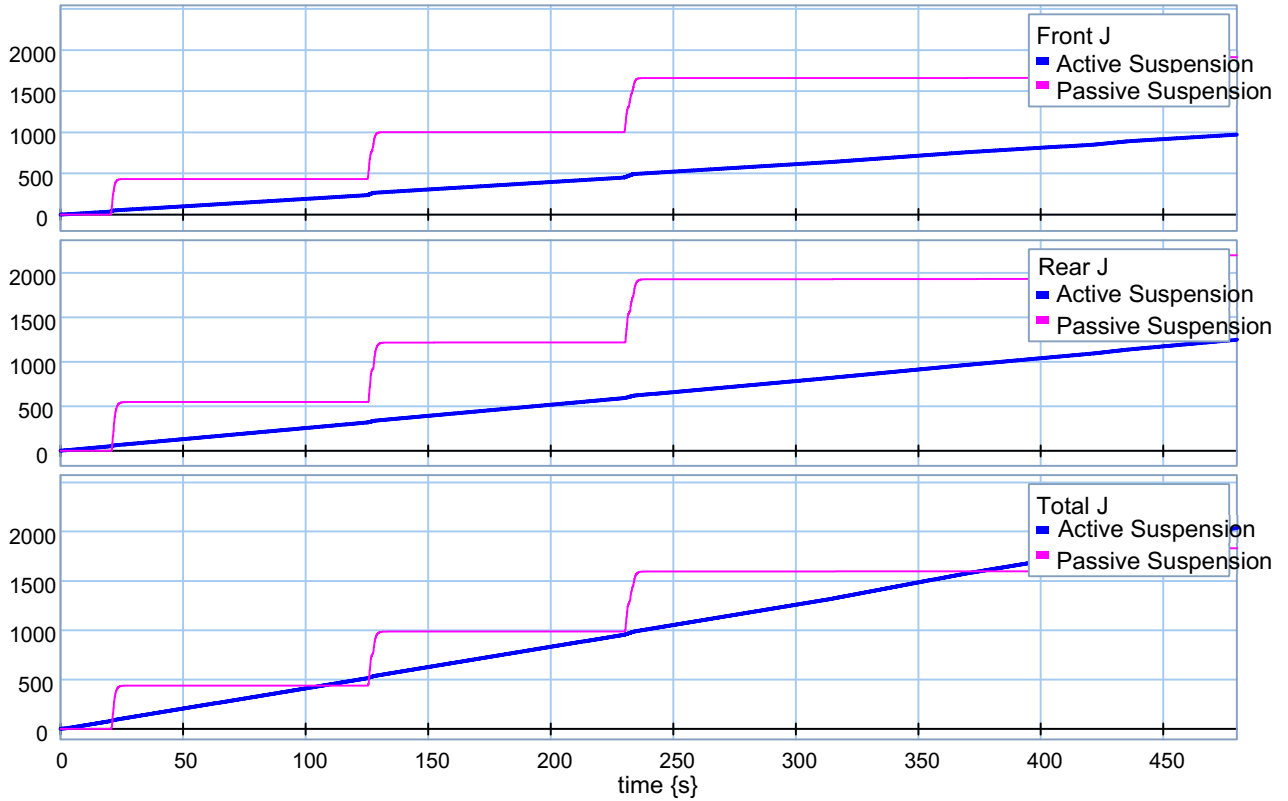


Figure 5.47: Vehicle performance index using quarter-car gains in road holding

Figures 5.48 and 5.49 represent the effect of having active suspension on the tires' vertical velocity and deflection.

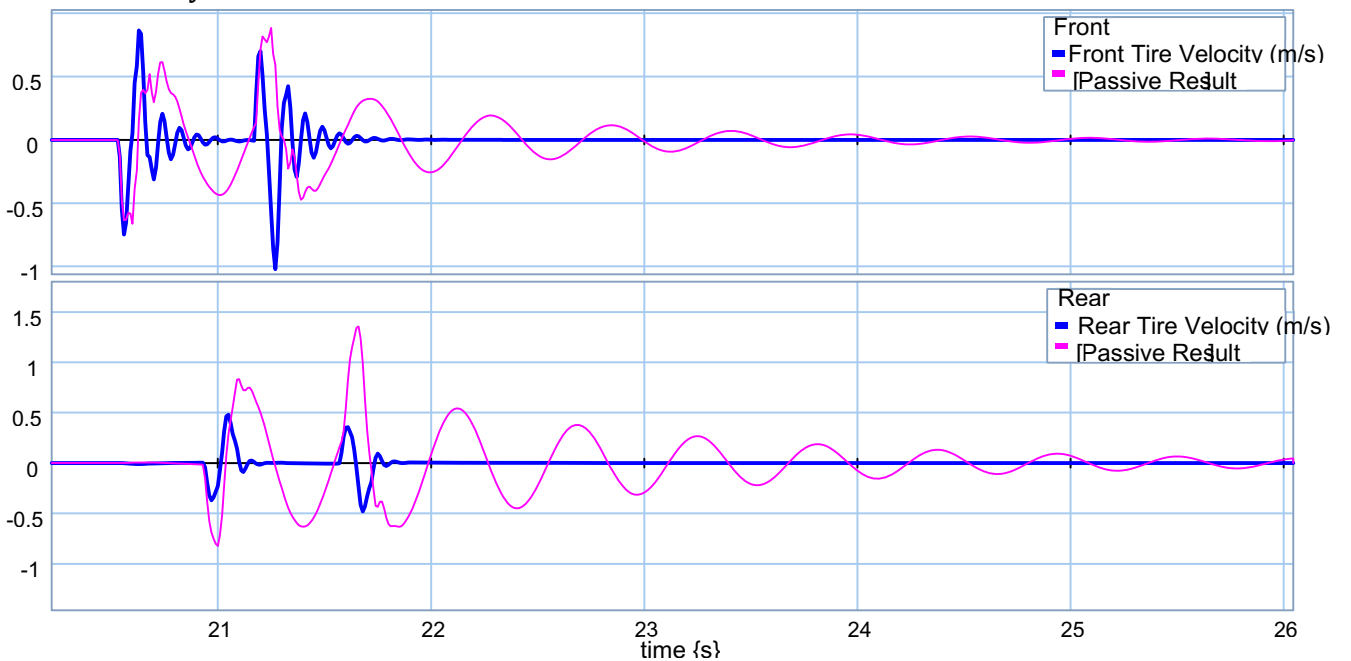


Figure 5.48: Tires' velocities over 2nd event of custom road profile in road holding

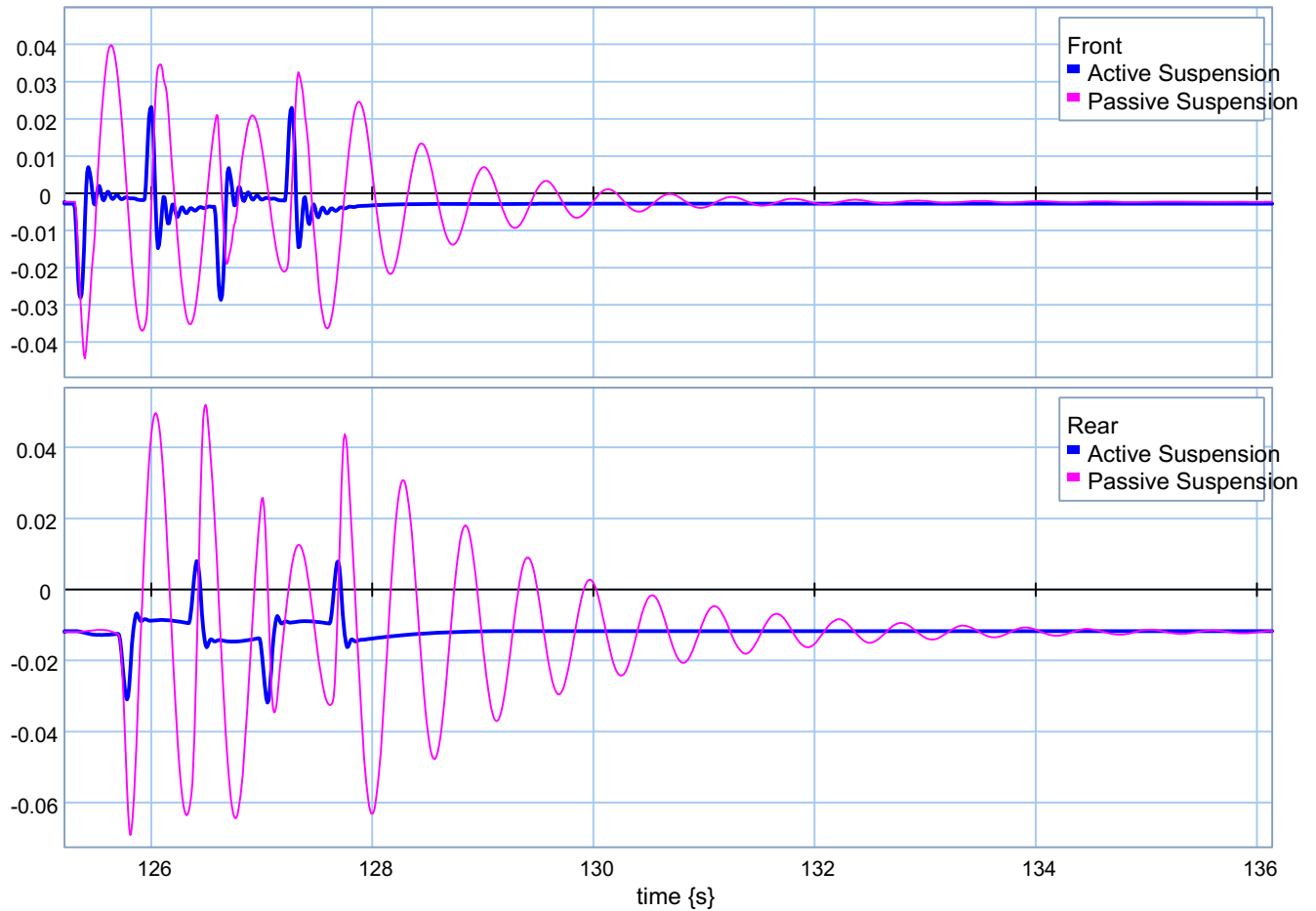


Figure 5.49: Tires' deflections over 2nd event of custom road profile in road holding

5.6.3.1 Heavily Road Holding

In this section, the effects of weighting parameters on road holding performance are studied. In order to control tires' vertical velocities and deflections, the first and third coefficients have to be greater than the other ones. As was presented earlier in this chapter [eq. 5-14], these two coefficients control the suspension and tire deflection, respectively. In the heavily road holding scenario, these coefficients are multiplied by one hundred. The new weighting factors are presented in Table 5.6.

Table 5.6: Weighting parameters for quarter-car controller

Performance Index Weighting Parameters		Scenario 2	
		Road Holding	Heavily Road Holding
Suspension Deflection	ρ_1	1.6	160
Sprung Mass Velocity	ρ_2	1	1
Tire Deflection	ρ_3	1.8	180
Unsprung Mass Velocity	ρ_4	1.2	120

This modification helps the vehicle improve its road holding ability. Figure 5.50 compares the new performance index with the passive and previously studied road holding scenario. As is seen, in the heavily road holding scenario, the performance index dropped dramatically, which would result in better performance.

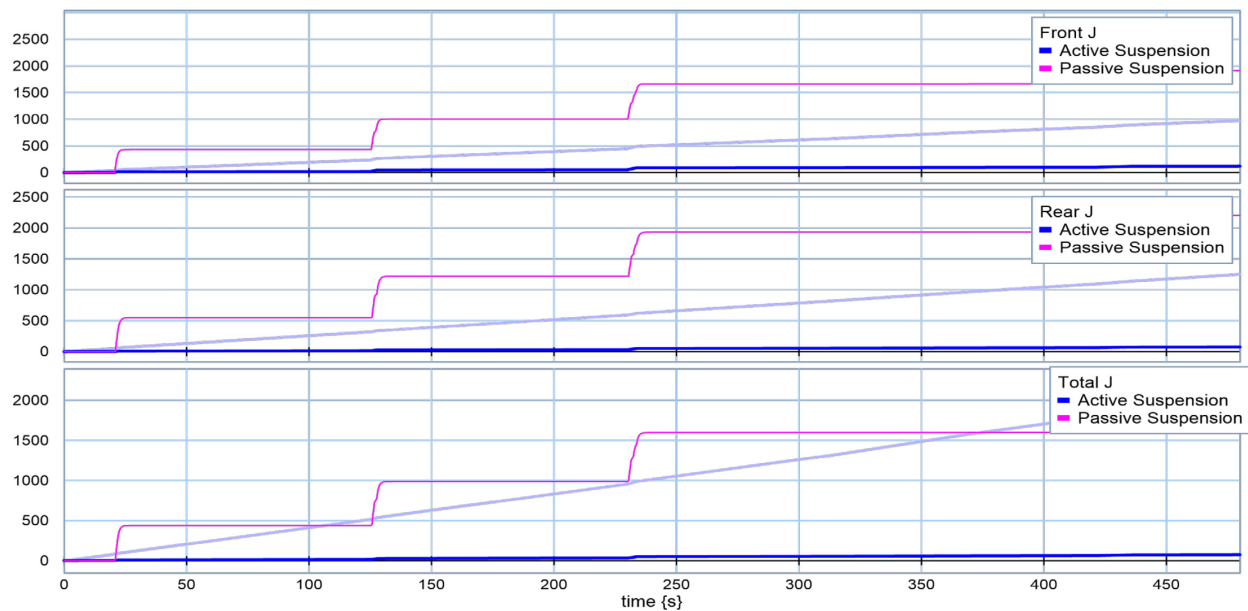


Figure 5.50: Vehicle performance index using quarter-car gains in road holding

Figures 5.51 and 5.52 demonstrate the advantages of using heavily road holding gains for minimizing tires' vertical velocities and deflections.

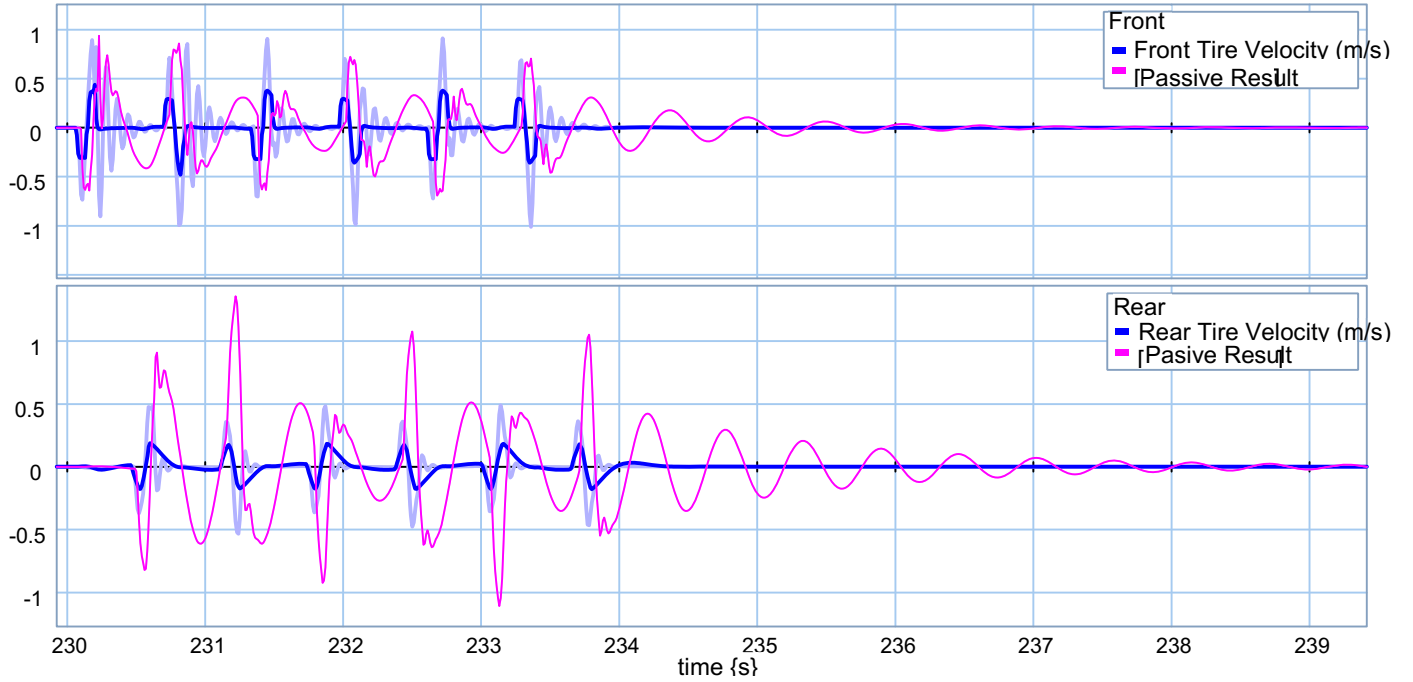


Figure 5.51: Tires' velocities over 3rd event of custom road profile in road holding

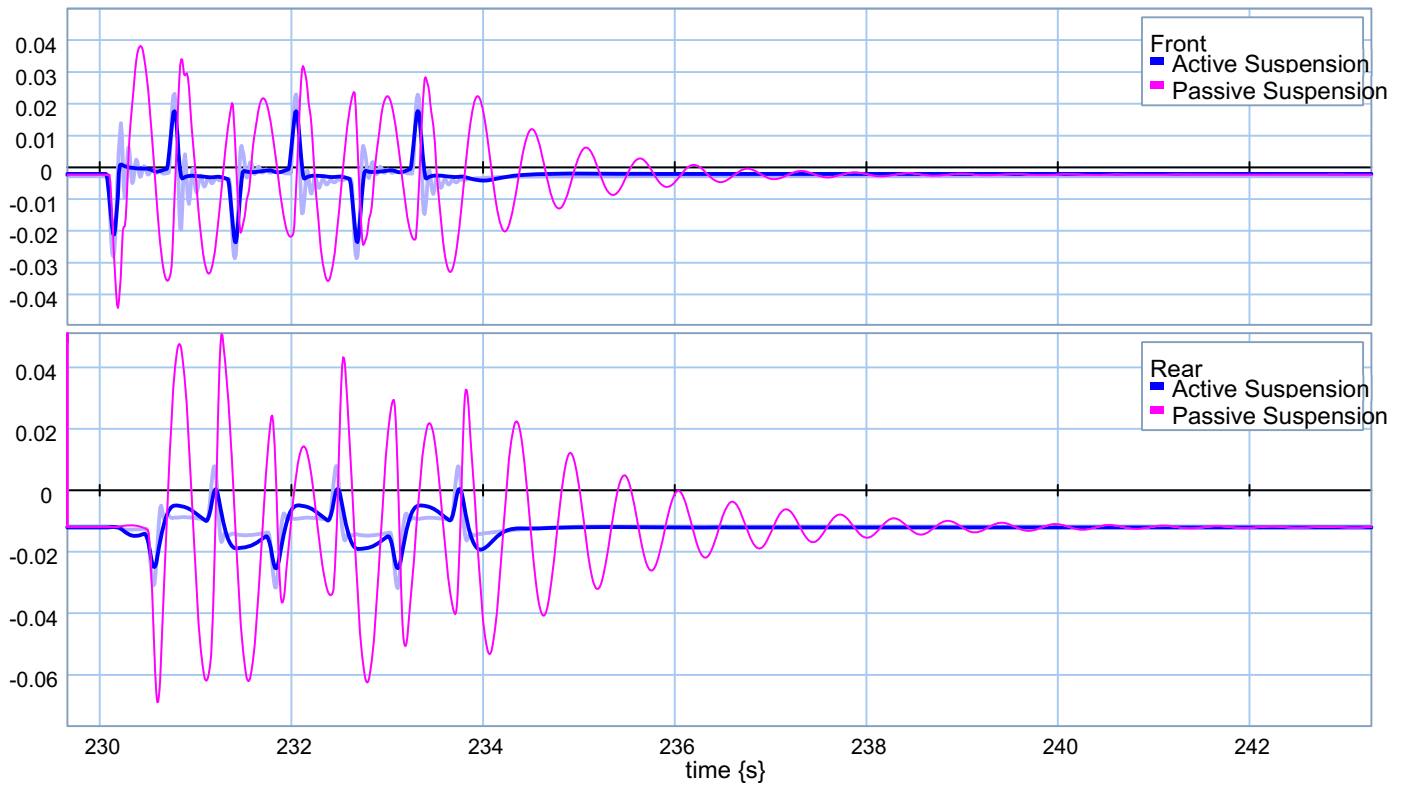


Figure 5.52: Tires' deflections over 3rd event of custom road profile in road holding

5.7 Summary of Conclusions

In the first part, the linear half-car model ran several times over the rough terrain outlined in Chapter 4 while different cargo masses and gain matrices were considered. Having defined the energy indices, an optimum set of gains were presented. These steps were done for both scenarios, i.e., ride quality, and road holding.

$$Energy\ Index = \int Actuator\ HorsePower^2 . dt \quad (5-38)$$

Once the optimum set of gains was presented, the complex non-linear half-car model ran over the severe bumpy road profile outlined in Chapter 4. For every single road events, the results were presented in detail. This procedure was done for each scenarios and the effects of having two separated quarter-car controllers in the front and rear suspension units were studied. Results proved that for both scenarios, using active suspension units are superior to the passive ones.

In the last part, the effects of changing weighting factors were analysed and a new sub-scenario was presented, i.e., heavily road holding scenario. This scenario could present a better performance than the regular road holding scenario.

Chapter 6

Active Suspension Gains Using Half-Car Approach

6.1 Overview

As it was discussed in the previous chapter, with using some sort of controllers and actuation method, a system can be forced to perform in desired states. This could result in having optimum efficiency in the system. Ride quality and road holding scenarios will be studied in this chapter based on the achieved gains for a half-car controller. System

equations will also be derived and presented in matrix form for desired state variables of a half-car. Then, performance index with appropriate weighting factors, corresponding to the studied scenario, will be defined. And with help of LQR approach, controller gain vector will be evaluated for a half-car model. At the end of the chapter, results achieved from this approach will be compared with ones from quarter-car approach, and the best approach will be introduced after.

6.2 System Equations

A half-car active suspension model is shown in Figure 6.1. M_{uf} and M_{ur} represent vehicle unsprung masses in the front and rear, respectively. Unsprung mass basically consists of suspension components, tire mass and brake assemblies. Vehicle sprung mass M_s , is located in the centre of gravity of the vehicle. It mainly represents the total body mass, frame and engine. Road profile is also assumed as the input of the system.

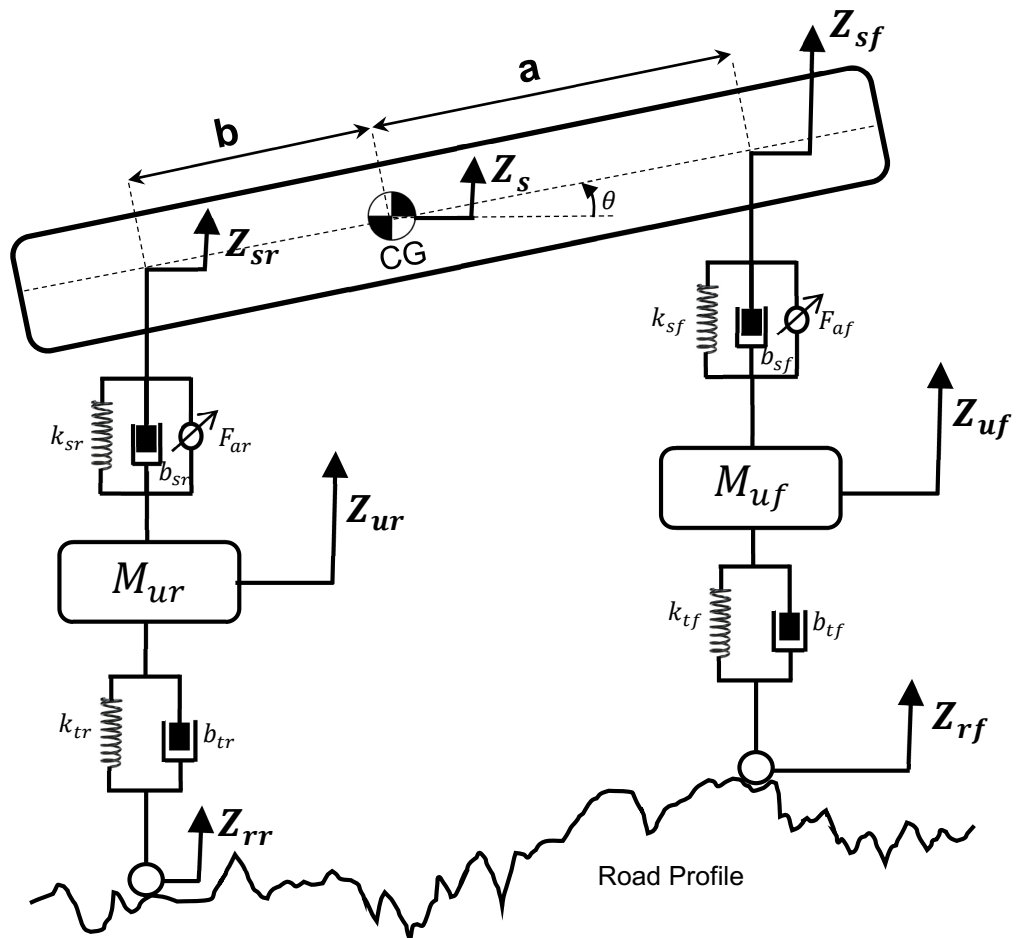


Figure 6.1: Half-car active suspension model

Free body diagrams for this system can be drawn as below in Figures 6.2 – 6.4:

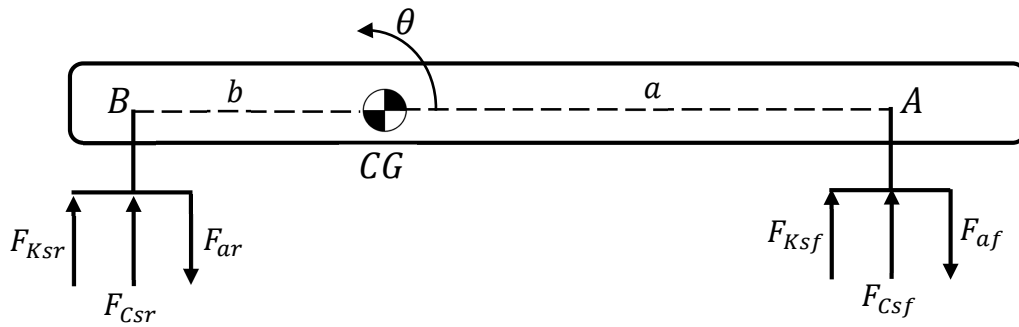


Figure 6.2: Free body diagram for chassis

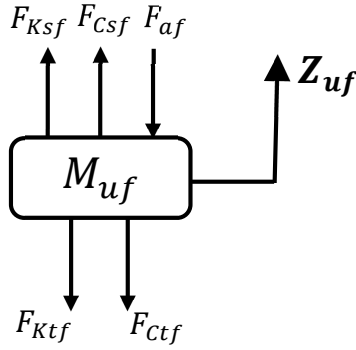


Figure 6.3: Free body diagram for front unsprung mass

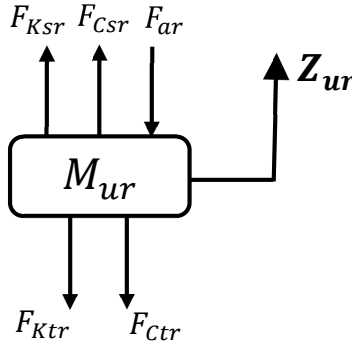


Figure 6.4: Free body diagram for rear unsprung mass

Based on these free body diagrams, governing equations for the system can be derived by satisfying Newton's second law in vertical direction and rotation.

$$\sum F_y = M_s \ddot{Z}_{CG} \quad \rightarrow \quad F_{af} + F_{ar} - F_{Ksf} - F_{Csf} - F_{Ksr} - F_{Csr} = M_s \ddot{Z}_{CG} \quad (6-1)$$

$$F_{af} + F_{ar} - k_{sf}(Z_A - Z_{uf}) - b_{sf}(\dot{Z}_A - \dot{Z}_{uf}) - k_{sr}(Z_B - Z_{ur}) - b_{sr}(\dot{Z}_B - \dot{Z}_{ur}) = M_s \ddot{Z}_{CG} \quad (6-2)$$

$$\sum M_{CG} = I_{CG} \ddot{\theta}_{CG} \quad \rightarrow \quad a. (F_{af} - F_{Ksf} - F_{Csf}) - b. (F_{ar} - F_{Ksr} - F_{Csr}) = J_S \ddot{\theta} \quad (6-3)$$

$$a. \{F_{af} - k_{sf}(Z_A - Z_{uf}) - b_{sf}(\dot{Z}_A - \dot{Z}_{uf})\} - b. \{F_{ar} - k_{sr}(Z_B - Z_{ur}) - b_{sr}(\dot{Z}_B - \dot{Z}_{ur})\} = J_S \ddot{\theta} \quad (6-4)$$

$$\left. \begin{array}{l} Z_A = Z_{CG} + a. \theta \\ Z_B = Z_{CG} - b. \theta \end{array} \right\} Z_{CG} = Z_A - a. \theta = Z_B + b. \theta \quad (6-5)$$

$$\rightarrow \theta = \frac{Z_A - Z_B}{a + b} \quad (6-6)$$

$$\ddot{\theta} = \frac{\ddot{Z}_A - \ddot{Z}_B}{a + b} \quad (6-7)$$

$$\ddot{Z}_A = \ddot{Z}_{CG} + a. \ddot{\theta} = \ddot{Z}_{CG} + a. \frac{\ddot{Z}_A - \ddot{Z}_B}{a + b} \quad (6-8)$$

$$\sum F_y = M_{ur} \ddot{Z}_{ur} \quad \rightarrow \quad F_{Ksr} + F_{Csr} - F_{ar} - F_{Ktr} - F_{Ctr} = M_{us} \ddot{Z}_{us} \quad (6-9)$$

$$k_{sr}(Z_B - Z_{ur}) + b_{sr}(\dot{Z}_B - \dot{Z}_{ur}) - F_{ar} - k_{tr}(Z_{ur} - Z_{rr}) - b_{tr}(\dot{Z}_{ur} - \dot{Z}_{rr}) = M_{ur} \ddot{Z}_{ur} \quad (6-10)$$

$$\sum F_y = M_{uf} \ddot{Z}_{uf} \quad \rightarrow \quad F_{Ksf} + F_{Csf} - F_{af} - F_{Ktf} - F_{Ctf} = M_{uf} \ddot{Z}_{uf} \quad (6-11)$$

$$k_{sf}(Z_A - Z_{uf}) + b_{sf}(\dot{Z}_A - \dot{Z}_{uf}) - F_{af} - k_{tf}(Z_{uf} - Z_{rf}) - b_{tf}(\dot{Z}_{uf} - \dot{Z}_{rf}) = M_{uf} \ddot{Z}_{uf} \quad (6-12)$$

$$F_{Ks} = k_s (Z_s - Z_{us}) \quad (6-13)$$

$$F_{Cs} = b_s (\dot{Z}_s - \dot{Z}_{us}) \quad (6-14)$$

where:

$$F_{Kt} = k_t (Z_{us} - Z_r) \quad (6-15)$$

$$F_{Ct} = b_t (\dot{Z}_{us} - \dot{Z}_r) \quad (6-16)$$

After substituting forces into the governing equation, motion equations of the system can be obtained as follows:

$$\dot{Z}_{sf} = \dot{Z}_{CG} + a. \dot{\theta} \quad (6-17)$$

$$\dot{Z}_{sr} = \dot{Z}_{CG} - b. \dot{\theta} \quad (6-18)$$

$$\ddot{Z}_{uf} = \frac{1}{M_{uf}} \{k_{sf}(Z_A - Z_{uf}) + b_{sf}(\dot{Z}_A - \dot{Z}_{uf}) - F_{af} - k_{tf}(Z_{uf} - Z_{rf}) - b_{tf}(\dot{Z}_{uf} - \dot{Z}_{rf})\} \quad (6-19)$$

$$\ddot{Z}_{ur} = \frac{1}{M_{ur}} \{k_{sr}(Z_B - Z_{ur}) + b_{sr}(\dot{Z}_B - \dot{Z}_{ur}) - F_{ar} - k_{tr}(Z_{ur} - Z_{rr}) - b_{tr}(\dot{Z}_{ur} - \dot{Z}_{rr})\} \quad (6-20)$$

$$\ddot{Z}_{CG} = \frac{1}{M_S} \{F_{af} + F_{ar} - k_{sf}(Z_A - Z_{uf}) - b_{sf}(\dot{Z}_A - \dot{Z}_{uf}) - k_{sr}(Z_B - Z_{ur}) - b_{sr}(\dot{Z}_B - \dot{Z}_{ur})\} \quad (6-21)$$

$$\ddot{\theta} = \frac{1}{J_S} \{a\{F_{af} - k_{sf}(Z_A - Z_{uf}) - b_{sf}(\dot{Z}_A - \dot{Z}_{uf})\} - b\{F_{ar} - k_{sr}(Z_B - Z_{ur}) - b_{sr}(\dot{Z}_B - \dot{Z}_{ur})\}\} \quad (6-22)$$

These sets of equations can be represented as classical control equation when appropriate state variables are defined. Vehicle states considered for this half-car model can be presented in the form of a vector, as follows:

$$\{x\} = \begin{pmatrix} Z_{sf} - Z_{uf} \\ \dot{\theta} \\ Z_{uf} - Z_{rf} \\ \dot{Z}_{uf} \\ Z_{sr} - Z_{ur} \\ \dot{Z}_{CG} \\ Z_{ur} - Z_{rr} \\ \dot{Z}_{ur} \end{pmatrix} \quad (6-23)$$

where:

$Z_{sf} - Z_{uf}$: front suspension deflection

\dot{Z}_{sf} : front sprung mass velocity

$Z_{uf} - Z_{rf}$: front tire deflection

\dot{Z}_{uf} : front unsprung mass velocity

$Z_{sr} - Z_{ur}$: rear suspension deflection

\dot{Z}_{sr} : rear sprung mass velocity

$Z_{ur} - Z_{rr}$: rear tire deflection

\dot{Z}_{ur} : rear unsprung mass velocity

For this linear system, the first-order control differential equation can be considered such as $\{\dot{x}\} = [A]\{x\} + [B]\{F_a\} + [L]\{\dot{Z}_r\}$ where A, B, and L matrices are obtained from system equations. By solving this equation a general solution in terms of the state variables can be presented demonstrating direct relationship between system inputs and outputs. System equations can also be redefined in matrix form as follows:

$$\begin{pmatrix} \dot{Z}_{sf} - \dot{Z}_{uf} \\ \ddot{\theta} \\ \dot{Z}_{uf} - \dot{Z}_{rf} \\ \ddot{Z}_{uf} \\ \dot{Z}_{sr} - \dot{Z}_{ur} \\ \ddot{Z}_{CG} \\ \dot{Z}_{ur} - \dot{Z}_{rr} \\ \ddot{Z}_{ur} \end{pmatrix} = [A] \begin{pmatrix} Z_{sf} - Z_{uf} \\ \dot{\theta} \\ Z_{uf} - Z_{rf} \\ \dot{Z}_{uf} \\ Z_{sr} - Z_{ur} \\ \dot{Z}_{CG} \\ Z_{ur} - Z_{rr} \\ \dot{Z}_{ur} \end{pmatrix} + [B] \begin{Bmatrix} F_{af} \\ F_{ar} \end{Bmatrix} + [L] \begin{Bmatrix} \dot{Z}_{rf} \\ \dot{Z}_{rr} \end{Bmatrix} \quad (6-24)$$

where:

$$[A] = \begin{bmatrix} 0 & a & 0 & -1 & 0 & 1 & 0 & 0 \\ -a.k_{sf}/J_S & (-a^2.b_{sf} - b^2.b_{sr})/J_S & 0 & a.b_{sf}/J_S & a.k_{sr}/J_S & (-a.b_{sf} + b.b_{sr})/J_S & 0 & -b.b_{sr}/J_S \\ 0 & 0 & 0 & 1 & 0 & 0 & 0 & 0 \\ k_{sf}/M_{uf} & a.b_{sf}/M_{uf} & -k_{sf}/M_{uf} & (-b_{sf} - b_{sr})/M_{uf} & 0 & a.b_{sf}/M_{uf} & 0 & 0 \\ 0 & -b & 0 & 0 & 0 & 1 & 0 & -1 \\ -k_{sf}/M_S & (-a.b_{sf} + b.b_{sr})/M_S & 0 & b_{sf}/M_S & -k_{sr}/M_S & (-b_{sf} - b_{sr})/M_S & 0 & b_{sr}/M_S \\ 0 & 0 & 0 & 0 & 0 & 0 & 0 & 1 \\ 0 & -b.b_{sr}/M_{ur} & 0 & 0 & k_{sr}/M_{ur} & b_{sr}/M_{ur} & -k_{tr}/M_{ur} & (-b_{tr} - b_{sr})/M_{ur} \end{bmatrix} \quad (6-25)$$

$$[B] = \begin{bmatrix} 0 & 0 \\ a/J_s & -b/J_s \\ 0 & 0 \\ -1/M_{uf} & 0 \\ 0 & 0 \\ 1/M_s & 1/M_s \\ 0 & 0 \\ 0 & -1/M_{ur} \end{bmatrix} \quad (6-26)$$

$$[L] = \begin{bmatrix} 0 & 0 \\ 0 & 0 \\ -1 & 0 \\ -b_{uf}/M_{uf} & 0 \\ 0 & 0 \\ 0 & 0 \\ 0 & -1 \\ 0 & b_{ur}/M_{ur} \end{bmatrix} \quad (6-27)$$

6.3 Linear Quadratic Regulator Gains

Similar to chapter 5, in order to use LQR method, first an appropriate performance index “J” needs to be defined. This index can be defined by integrating some factors over time which are intended to be minimized. It can also be presented in terms of state variables and input matrices.

$$J = \int_0^{+\infty} \left\{ \ddot{Z}_{CG}^2 + \rho_1 \ddot{\theta}^2 + \rho_2 X_1^2 + \rho_3 X_2^2 + \rho_4 X_3^2 + \rho_5 X_4^2 + \rho_6 X_5^2 + \rho_7 X_6^2 + \rho_8 X_7^2 + \rho_9 X_8^2 \right\} . dt \quad (6-28)$$

$$J = \int_0^{+\infty} (x^T . Q . x + 2 x^T . N . u + u^T . R . u) . dt \quad (6-29)$$

where:

$$X_1 = Z_{sf} - Z_{uf} \quad : \quad \text{front suspension deflection}$$

$$X_2 = \dot{\theta} \quad : \quad \text{pitch angular velocity}$$

$$X_3 = Z_{uf} - Z_{rf} \quad : \quad \text{front tire deflection}$$

$$X_4 = \dot{Z}_{uf} \quad : \quad \text{front unsprung vertical velocity}$$

$$X_5 = Z_{sr} - Z_{ur} \quad : \quad \text{rear suspension deflection}$$

$$X_6 = \dot{Z}_{CG} \quad : \quad \text{centre of gravity vertical velocity}$$

$$X_7 = Z_{ur} - Z_{rr} \quad : \quad \text{rear tire deflection}$$

$$X_8 = \dot{Z}_{ur} \quad : \quad \text{rear unsprung vertical velocity}$$

By using equations (6-21, 22), \ddot{Z}_{CG} and $\ddot{\theta}$ can be derived and then substituted in the performance index. After some simplification, performance index can be presented based on state variables as follows:

$$\ddot{Z}_{CG} = \frac{1}{M_S} \left\{ F_{af} + F_{ar} - k_{sf} X_1 - (a . b_{sf} - b . b_{sr}) X_2 + b_{sf} X_4 - k_{sr} X_5 - (b_{sf} + b_{sr}) X_6 + b_{sr} X_8 \right\} \quad (6-30)$$

$$\ddot{\theta} = \frac{1}{J_S} \left\{ a.F_{af} - b.F_{ar} - a.k_{sf}.X_1 - (a^2.b_{sf} + b^2.b_{sr}).X_2 + a.b_{sf}.X_4 + b.k_{sr}.X_5 \right. \\ \left. - (a.b_{sf} - b.b_{sr}).X_6 - b.b_{sr}.X_8 \right\} \quad (6-31)$$

After substituting equations (6-30, 31) into equation (6-28), the performance index can be presented. Once the performance index is defined, an optimal gain G can be evaluated. For this reason, the coefficient of modified performance index (6-29) has to be matched with corresponding coefficients of the expanded performance index (6-28). In order to avoid complexity involved in matching coefficients, partial derivatives can be used and Q, N, and R matrices can be indicated as follows [26]:

$$q_{ij} = \frac{1}{2} \frac{\partial w^2}{\partial x_i \partial x_j} \quad (6-32)$$

$$n_{ij} = \frac{1}{2} \frac{\partial w^2}{\partial x_i \partial F_{a_j}} \quad (6-33)$$

$$r_{ij} = \frac{1}{2} \frac{\partial w^2}{\partial F_{a_i} \partial F_{a_j}} \quad (6-34)$$

where:

$$w = \frac{1}{M_S^2} \left\{ F_{af} + F_{ar} - k_{sf}X_1 - (a.b_{sf} - b.b_{sr}).X_2 + b_{sf}X_4 - k_{sr}X_5 - (b_{sf} + b_{sr})X_6 + \right. \\ \left. b_{sr}.X_8 \right\}^2 + \rho_1 \left(\frac{1}{J_S^2} \right) \left\{ a.F_{af} - b.F_{ar} - a.k_{sf}.X_1 - (a^2.b_{sf} + b^2.b_{sr}).X_2 + a.b_{sf}.X_4 + \right. \\ \left. b.k_{sr}.X_5 - (a.b_{sf} - b.b_{sr}).X_6 - b.b_{sr}.X_8 \right\}^2 + \rho_2.X_1^2 + \rho_3.X_2^2 + \rho_4.X_3^2 + \rho_5.X_4^2 + \\ \rho_6.X_5^2 + \rho_7.X_6^2 + \rho_8.X_7^2 + \rho_9.X_8^2 \quad (6-35)$$

$$[Q] = [q_{ij}] \quad (6-36)$$

$$[N] = [n_{ij}] \quad (6-37)$$

$$[R] = [r_{ij}] \quad (6-38)$$

For instance, q_{18} can be evaluated as follows:

$$q_{18} = \frac{1}{2} \frac{\partial w^2}{\partial x_1 \partial x_8} = \frac{1}{2} \frac{\partial w^2}{\partial (Z_{sf} - Z_{uf}) \partial Z_{ur}} = \frac{1}{2} \frac{\partial}{\partial (Z_{sf} - Z_{uf})} \left(\frac{\partial w}{\partial Z_{ur}} \right) \quad (6-39)$$

$$\begin{aligned} \frac{dw}{dz_{ur}} = & -2 \left(\rho I \cdot \left(\frac{1}{J} \left(\left(- \left(\frac{a \cdot k_{sf}}{J} \right) \cdot N1 - \left(\frac{(a^2) \cdot b_{sf} + (b^2) \cdot b_{sr}}{J} \right) \cdot N2 + \left(\frac{a \cdot b_{sf}}{J} \right) \right. \right. \right. \right. \\ & \cdot N4 + \left(\frac{b \cdot k_{sr}}{J} \right) \cdot N5 + \left(\frac{-a \cdot b_{sf} + b \cdot b_{sr}}{J} \right) \cdot N6 - \left(\frac{b \cdot b_{sr}}{J} \right) \cdot N8 + \left(\frac{a}{J} \right) \cdot Faf \\ & \left. \left. \left. \left. - \left(\frac{b}{J} \right) \cdot Far \right) (b \cdot b_{sr}) \right) \right) \right) + 2 \left(\rho^9 \cdot N8 - \frac{2 \left(\left(\frac{k_{sf}}{Ms} \right) \cdot N1 \right) b_{sr}}{Ms} \right. \\ & \left. - \frac{2 \left(\left(\frac{a \cdot b_{sf} + b \cdot b_{sr}}{Ms} \right) \cdot N2 \right) b_{sr}}{Ms} + \frac{2 \left(\left(\frac{b_{sf}}{Ms} \right) \cdot N4 \right) b_{sr}}{Ms} \right. \\ & \left. - \frac{2 \left(\left(\frac{k_{sr}}{Ms} \right) \cdot N5 \right) b_{sr}}{Ms} - \frac{2 \left(\left(\frac{b_{sf} + b_{sr}}{Ms} \right) \cdot N6 \right) b_{sr}}{Ms} + \frac{2 \left(\left(\frac{b_{sr}}{Ms} \right) \cdot N8 \right) b_{sr}}{Ms} \right. \\ & \left. + \frac{2 b_{sr} Faf}{Ms^2} + \frac{2 b_{sr} Far}{Ms^2} \right) \quad (6-40) \end{aligned}$$

$$\frac{1}{2} \frac{\partial}{\partial (Z_s - Z_{us})} \left(\frac{\partial w}{\partial Z_s} \right) = \rho_1 \left(\frac{(b \cdot b_{sr}) \cdot (a \cdot k_{sf})}{J_s^2} \right) - \left(\frac{b_{sr} \cdot k_{sf}}{M_s^2} \right) \quad (6-41)$$

Hence:

$$q_{18} = \rho_1 \left(\frac{(b \cdot b_{sr}) \cdot (a \cdot k_{sf})}{J_s^2} \right) - \left(\frac{b_{sr} \cdot k_{sf}}{M_s^2} \right) \quad (6-42)$$

Similarly, matrices Q, N, and R have been evaluated by using Maple package and are outlined in Appendix L at the end of this work. Once these matrices have been evaluated, a proportional feedback controller, i.e., $u = -G.x$ can be presented in order to minimize the cost function. Matrix G is known as system's gain matrix and can be indicated as follows:

$$G = R^{-1} (B^T P + N^T) \quad (6-43)$$

Where P is the solution of Continuous Algebraic Riccati Equation (CARE). CARE for this system can be demonstrated as follows:

$$(A - BR^{-1}N)^T P + P(A - BR^{-1}N) + Q - N^T R^{-1} N - PBR^{-1}B^T P = 0 \quad (6-44)$$

The evaluated gain matrix, has two rows and eight columns. The elements in the first and second rows are optimal gains for the front and rear parts of the vehicle, respectively.

6.4 Weighting Factors

When an optimal half-car controller is operated instead of two optimal quarter-car controllers, pitch acceleration can be controlled directly. In order to have a better control on pitch angle acceleration, the corresponding weighting factor ρ_1 must be chosen greater. In this research, it is assumed that this coefficient is "20" times greater than what Wakeham *et al*, suggested in 2011[17]. In road holding scenario, the coefficient for vertical suspension

acceleration is considered unit while other relative parameters are much greater. These weighting factors are classified in Table 6.1.

Table 6.1: Weighting parameters for half-car controller

Performance Index Weighting Parameters		Scenario 1		Scenario 2	
		Ride Quality	Modified Ride Quality, Pitch Weighted	Road Holding	Heavily Road Holding
Pitch Angle Acceleration	ρ_1	1	20	1	1
Front Suspension Deflection	ρ_2	0.4	0.4	1.6	160
Pitch Angle Angular Velocity	ρ_3	0.16	0.16	1	1
Front Tire Deflection	ρ_4	0.4	0.4	1.8	180
Front Unsprung Mass Velocity	ρ_5	0.16	0.16	1.2	120
Rear Suspension Deflection	ρ_6	0.4	0.4	1.6	160
Vertical Velocity of CG	ρ_7	0.16	0.16	1	1
Rear Tire Deflection	ρ_8	0.4	0.4	1.8	180
Rear Unsprung Mass Velocity	ρ_9	0.16	0.16	1.2	120

6.5 Conclusion

6.5.1 Cargo Effect

Once gain matrix is evaluated, it cannot be changed if the system parameters change during the simulation. One of the important system parameter is cargo mass as it can vary within a huge range. The question that comes to mind is for which system parameter, does the LQR approach need to be applied and gains have to be derived. In order to present an appropriate answer for this concern, five scenarios with five various cargo masses are studied. Like what was done for two quarter-car controllers, in this section, for a half-car based controller, each model ran 5 times with 5 considered sets of gains and desired results have recorded for all 25 runs. By comparing these 25 captured results, the best set of gain was introduced in order to use for the following models.

6.5.1.1 Ride Quality

In this section, a linear half-car model with half-car active suspension controller is considered. The desired outputs for the system were defined as sprung mass acceleration, pitch angle acceleration, total performance index, and required actuator forces in the front and rear. Models were run under the same initial conditions over the rough terrain profile outlined in chapter 4. Table 6.2 represents obtained gains for each studied scenarios.

Table 6.2: Ride quality scenario's gain matrices for different cargo masses

Gain Matrix		Cargo = 0	Cargo = 4500 kg	Cargo = 9000 kg	Cargo = 13500 kg	Cargo = 18000 kg
Front	G_1	-487,370	-485,121	-483,304	-481,725	-480,275
	G_2	-22,800	-12,356	-7,823	-3,913	15
	G_3	1,948	2,026	2,504	2,651	2,544
	G_4	8,668	7,700	6,833	6,001	5,184
	G_5	2,765	2,703	2,284	1,833	1,431
	G_6	-4,193	-1,231	316	1,314	2,147
	G_7	15,814	21,386	23,172	23,669	23,693
	G_8	390	682	858	997	1,123
Rear	G_1	-4,139	-5,923	-6,770	-7,237	-7,580
	G_2	-25,089	-27,503	-28,087	-29,596	-31,719
	G_3	-10,366	-19,057	-26,440	-31,844	-35,840
	G_4	540	983	1,278	1,516	1,731
	G_5	-1578,430	-1575,341	-1572,002	-1568,746	-1565,602

	G_6	-23,930	-20,884	-15,619	-9,904	-4,250
	G_7	-9,081	-10,329	-9,961	-9,301	-8,585
	G_8	23,390	18,696	16,965	15,208	13,433

In the first case scenario, the linear model is studied while no cargo was considered. The half-car controller is used for the vehicle's front and rear parts. Parameters were set for the ride quality and the model ran for 180 seconds on the first road profile outlined in chapter 4 [4.2.7.1]. Figure 6.5 represents the vehicle's pitch angle and could also verify that vehicle follows the road perfectly. As it is seen, half-car gains in this scenario cannot minimize pitch angle like how quarter-car gains did in the previous chapter.

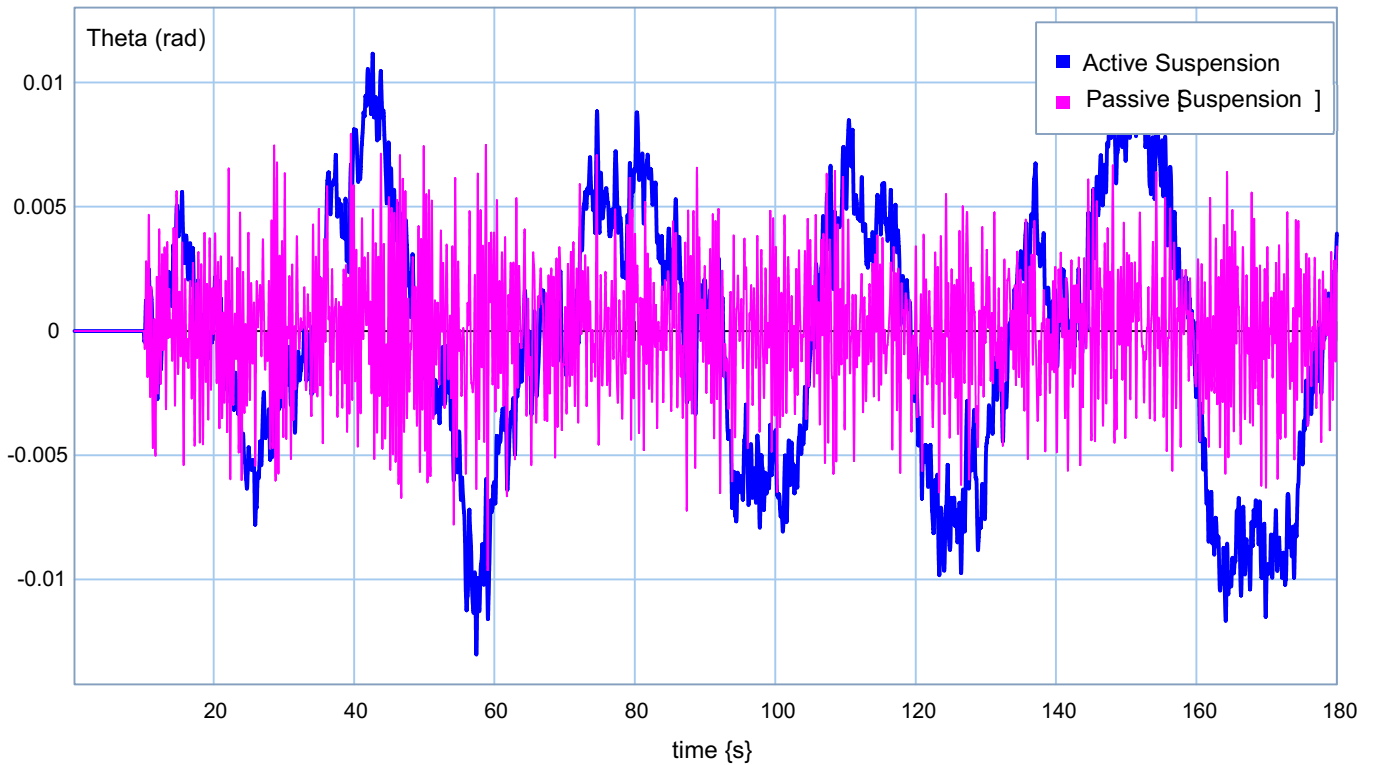


Figure 6.5: Pitch angle using half-car gains for ride quality

Figures 6.6 and 6.7 compare the front and rear sprung mass accelerations. As it is seen, ride quality gains can control sprung masses' accelerations very well. Figure 6.8 demonstrates how it can minimize the vertical acceleration of the vehicle's centre of gravity.

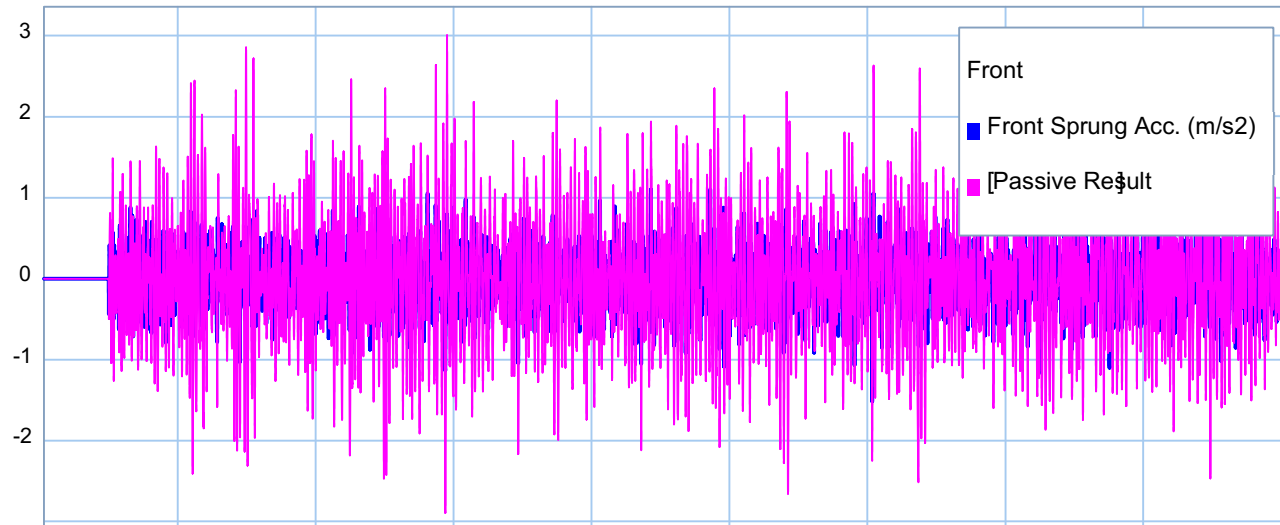


Figure 6.6: Front sprung mass acceleration using half-car gains for ride quality

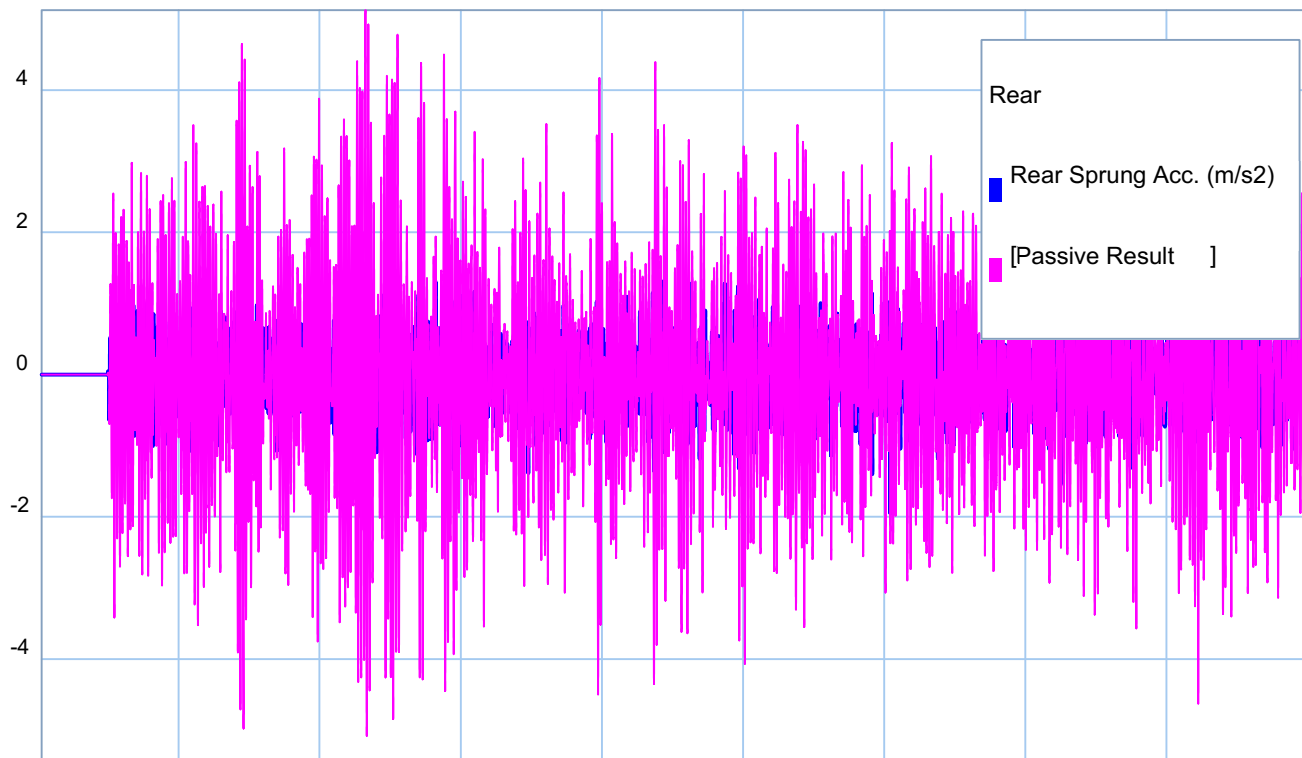


Figure 6.7: Rear sprung mass acceleration using half-car gains for ride quality

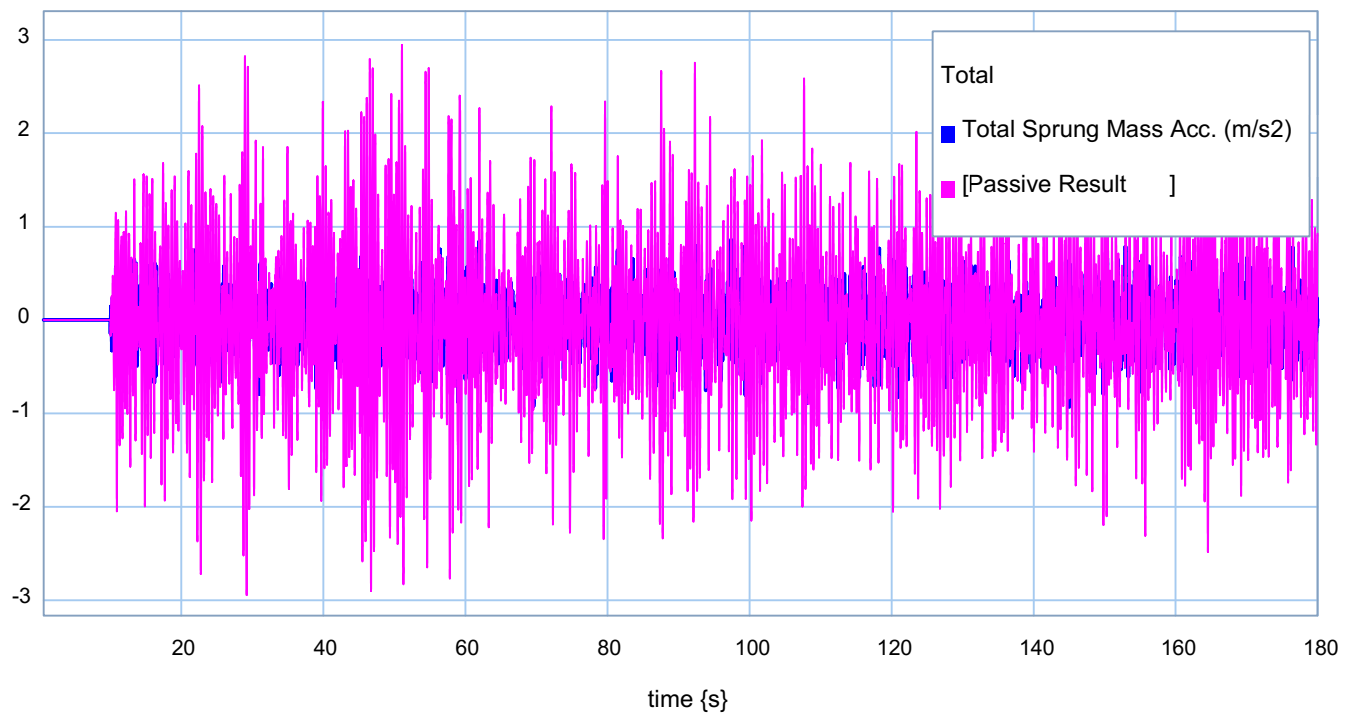


Figure 6.8: centre of gravity vertical acceleration using half-car gains for ride quality

In order to have a better visual comparison, Figure 6.9 displays the vertical acceleration of the vehicle's front, rear and centre parts. This improvement can also be proved by comparing performance indices for passive and active suspension.

Figure 6.10 present the performance index for the front, rear and centre parts. As it is seen, active suspension can reduce the performance indices.

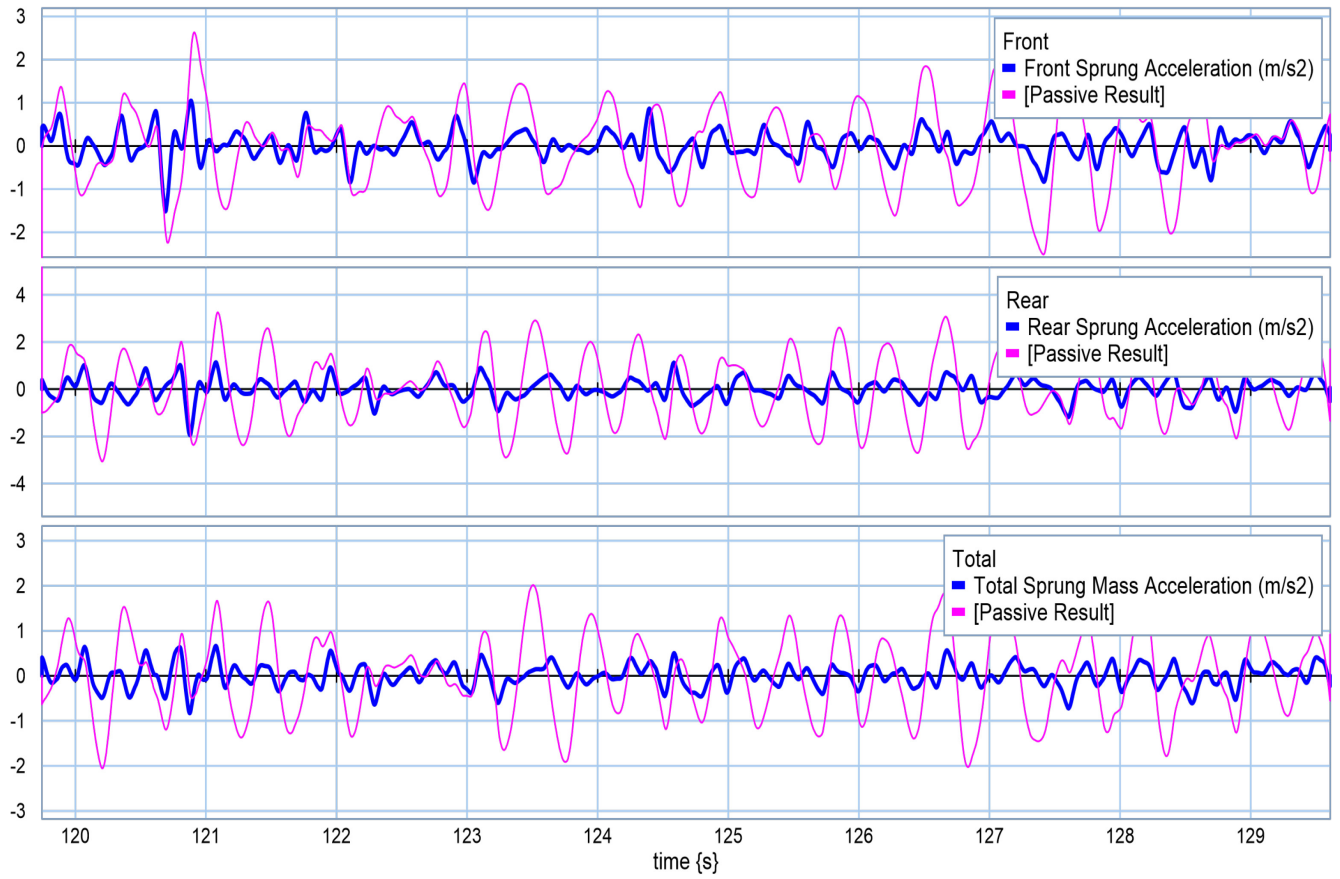


Figure 6.9: Vertical acceleration using half-car gains for ride quality

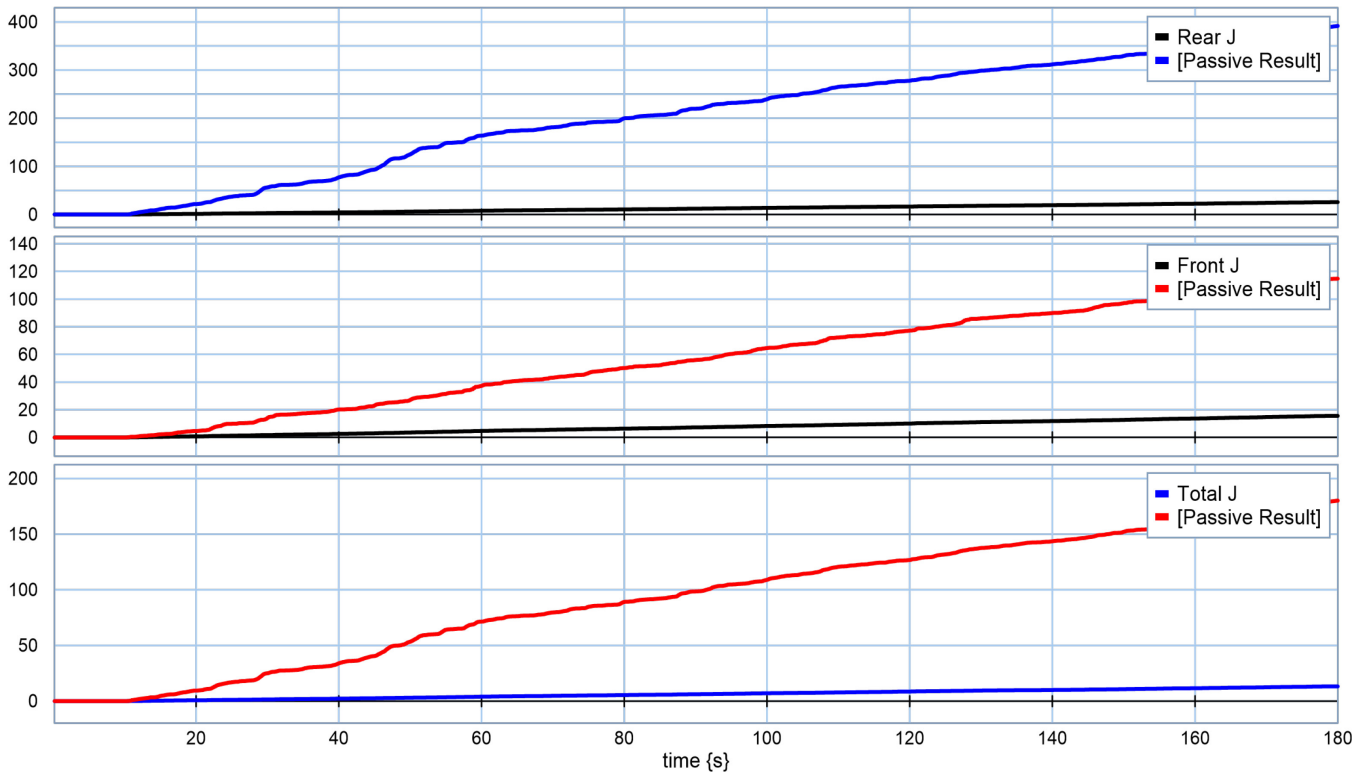


Figure 6.10: Total performance index using half-car gains for ride quality

In quarter-car approach, two independent actuators are used for the vehicle's front and rear parts in order to improve the ride quality by minimizing the front and rear sprung masses' accelerations, and central states such as vertical and pitch accelerations are improved indirectly. In half-car approach, the same improvement was seen, but in this case central states were controlled directly through the cost function. Figures 6.11 and 6.12 compare these states for passive and active suspension studies.

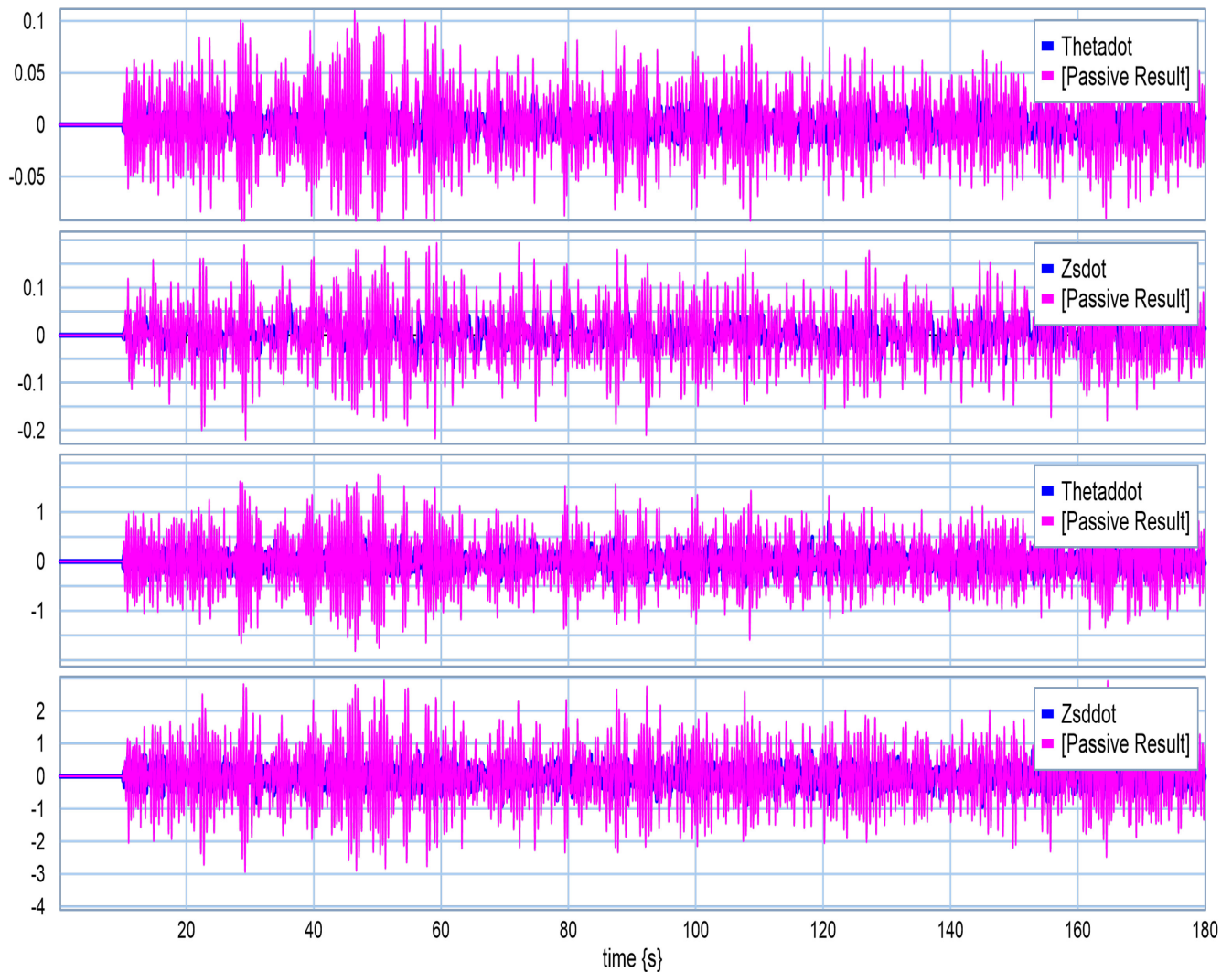


Figure 6.11: Central states using half-car gains for ride quality

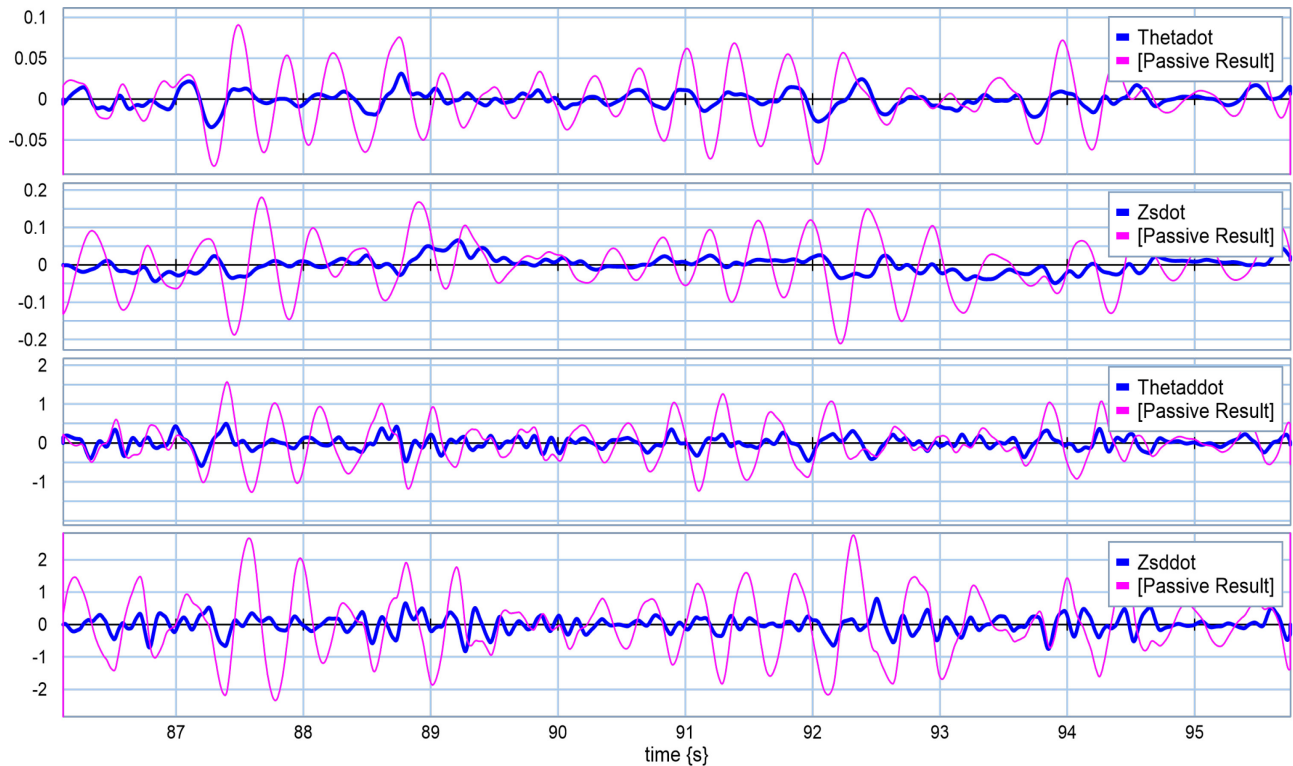


Figure 6.12: Central states using half-car gains for ride quality

Similarly, for the second scenario with the 4500 kilogram cargo mass, an appropriate set of gains for ride quality was applied and a great improvement was observed. In Appendix C, all the graphs based on varying cargo masses i.e. 4500 kg, 9000 kg, 13500 kg., and 18000 kg. are covered. As was expected based on theory, actuator units with parameters set for ride quality could help the vehicle provide more comfort for passengers.

The question has to be answered here is related to the efficiency of the set of gains used when the cargo mass is not the same as was assumed. Presenting an optimum set of gains which can be used for all possible cargo masses is a critical point here. In order to address this concern, first, the behaviour of each model was studied while the cargo mass was varying from 0 to 18000 kg.

For this reason, all five models ran five times for 180 seconds over the first road profile [4.2.7.1] with five different sets of gains. The final value of the performance index for all of the five cases for each model was recorded and compared to each other. For each model, the recorded values of the performance indices in the corresponding five various scenarios were too close to each other. Hence, another index needed to be defined in order to present the optimum gains. The new index can be called the energy index and similar to the previous chapter, it can be represented as follows:

$$EI_F = \int FrontHorsePower^2 . dt \quad (6-45)$$

$$EI_R = \int RearHorsePower^2 . dt \quad (6-46)$$

Table 6.3 classifies the rear energy indices for each simulation. As can be seen, for all the studied models, the minimum energy indices were recorded when the highest set of gains was used. In other words, using the fifth set of gains is more energy-efficient for all models. For the first model, the significant difference between the first and last energy indices is huge enough to design an active suspension based on the fifth set of gains.

Figure 6.13 magnifies the vertical acceleration of the centre of gravity of the truck over two seconds when the road was more severe. However, as is seen, there is not much difference between the behaviour of the system while the first and fifth sets of gains were

used. This behaviour was seen in other models as well. More graphs and tables can be found in Appendix C.

Table 6.3: Rear energy indices for ride quality gains

EI for models		G_1	G_2	G_3	G_4	G_5
EI_R	#1	132.5266	97.8432	83.5307	62.3209	40.5487
	#2	179.1505	135.5154	115.2154	89.2644	61.0051
	#3	226.1540	168.9507	142.2645	116.2662	81.5970
	#4	275.0482	208.2644	173.0115	142.0481	105.5562
	#5	316.6096	242.2605	203.5465	175.2405	124.0254

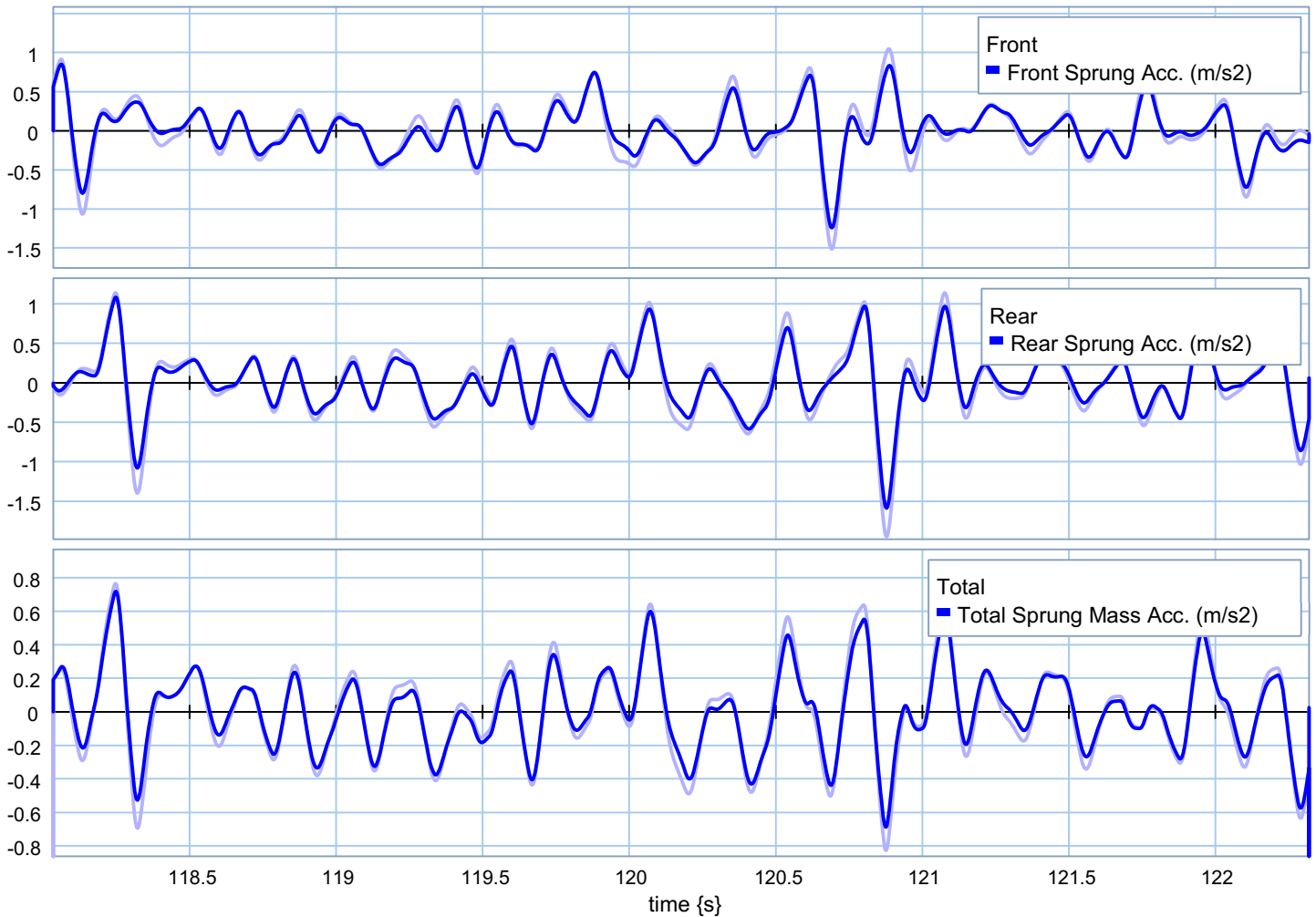


Figure 6.13: Vertical acceleration for first and fifth sets of gains for ride quality

6.5.1.2 Road Holding

The same procedure explained in the previous section was exactly performed while the weighting parameters in the cost function were changed for the road holding scenario. The five generated models ran for 180 seconds under the same initial conditions over the rough terrain profile outlined in Chapter 4 [4.2.7.1]. Table 6.4 classified evaluated gains for each studied case.

Table 6.4: Heavily road holding scenario's gain matrices for different cargo masses

Gain Matrix		Cargo = 0	Cargo = 4500 kg	Cargo = 9000 kg	Cargo = 13500 kg	Cargo = 18000 kg
Front	G_1	-415,002	-378,497	-349,210	-321,907	-295,477
	G_2	27,367	61,743	92,156	122,287	152,831
	G_3	-511,009	-766,806	-963,725	-1140,761	-1306,672
	G_4	-53,280	-82,874	-108,267	-132,102	-155,167
	G_5	14,201	-3,591	-14,123	-21,845	-28,388
	G_6	21,879	29,769	37,014	44,655	52,556
	G_7	183,734	138,528	116,687	105,704	99,835
	G_8	10,522	17,203	21,631	25,392	28,914
Rear	G_1	-48,885	-53,960	-56,660	-59,508	-62,589
	G_2	-52,268	-72,740	-90,291	-107,150	-123,887
	G_3	93,535	131,121	155,708	177,626	198,502
	G_4	17,515	27,999	35,066	41,114	46,797
	G_5	-1506,194	-1439,272	-1378,232	-1319,097	-1260,642

	G_6	-10,417	16,923	43,839	70,750	98,142
	G_7	-512,201	-661,663	-836,286	-1014,479	-1192,412
	G_8	-50,454	-103,315	-153,858	-203,802	-253,588

Important graphs for each run were generated and can be found in Appendix E. For instance, the first model with the first set of gains for the half-car based controller is studied in this section. Figure 6.14 demonstrates a great deduction in pitch angle while active suspension units were used. Moreover, Figure 6.15 shows a significant drop in the performance index.

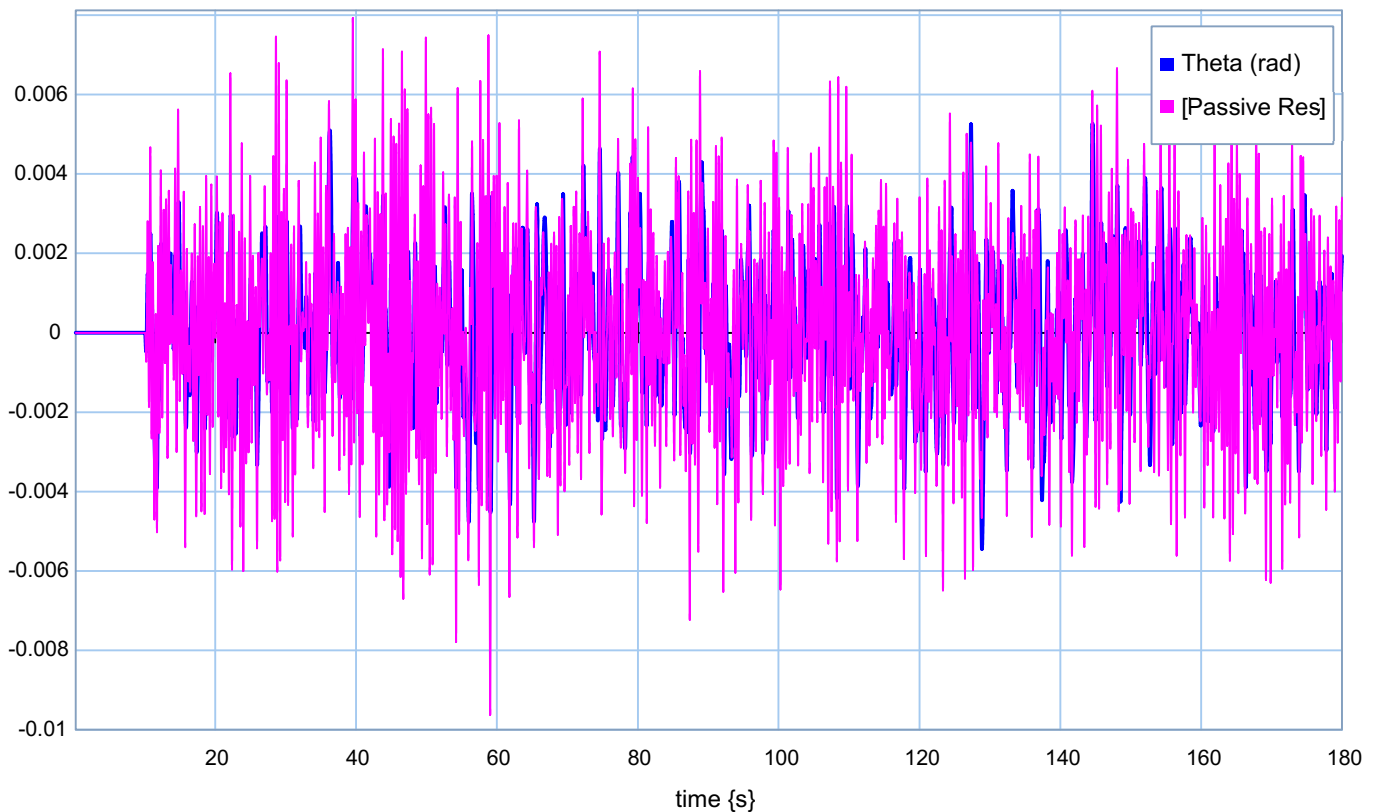


Figure 6.14: Pitch angle using half-car gains for road holding

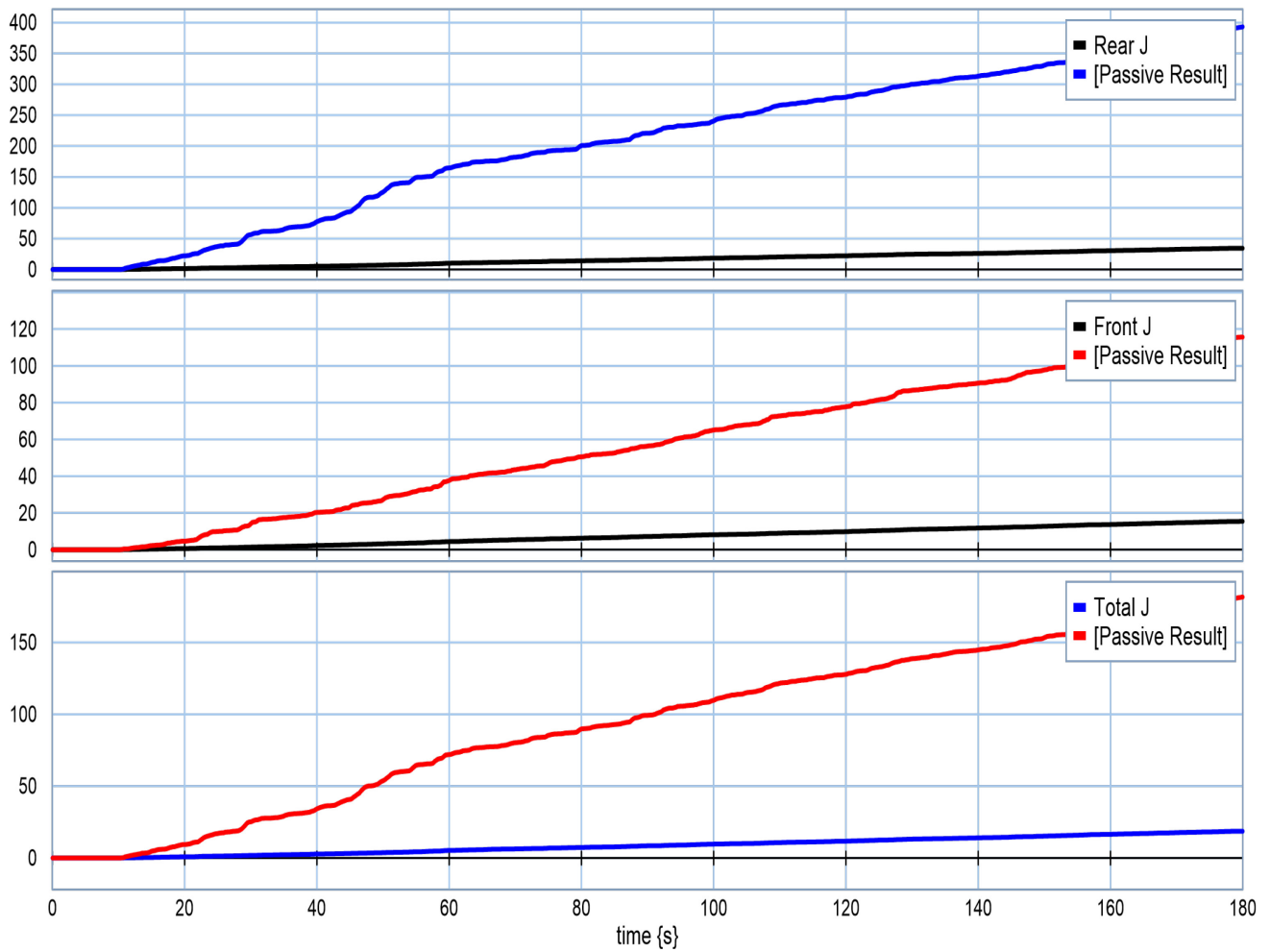


Figure 6.15: Performance indices using half-car gains for road holding

Figures 6.16 to 6.19 demonstrate the efficiency of using active suspension over the passive situation by declining the tires' vertical velocity and deflection.

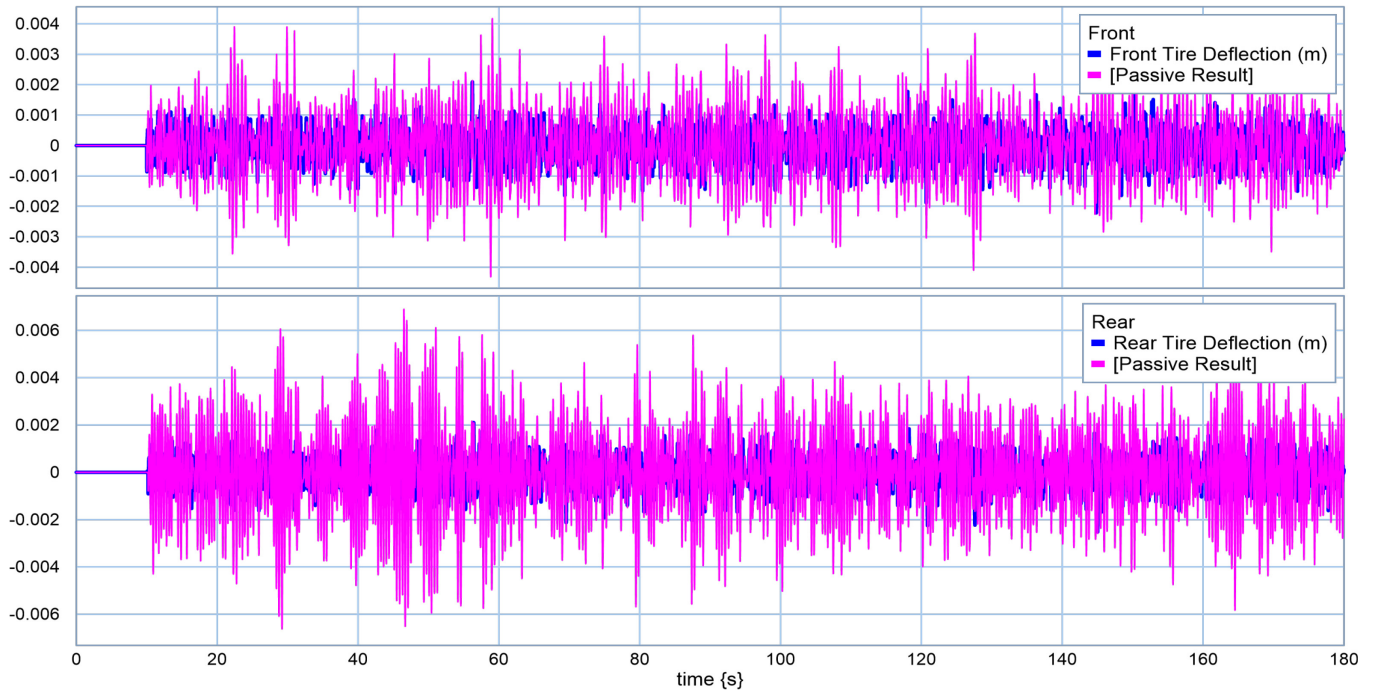


Figure 6.16: Tires' deflections using half-car gains for road holding

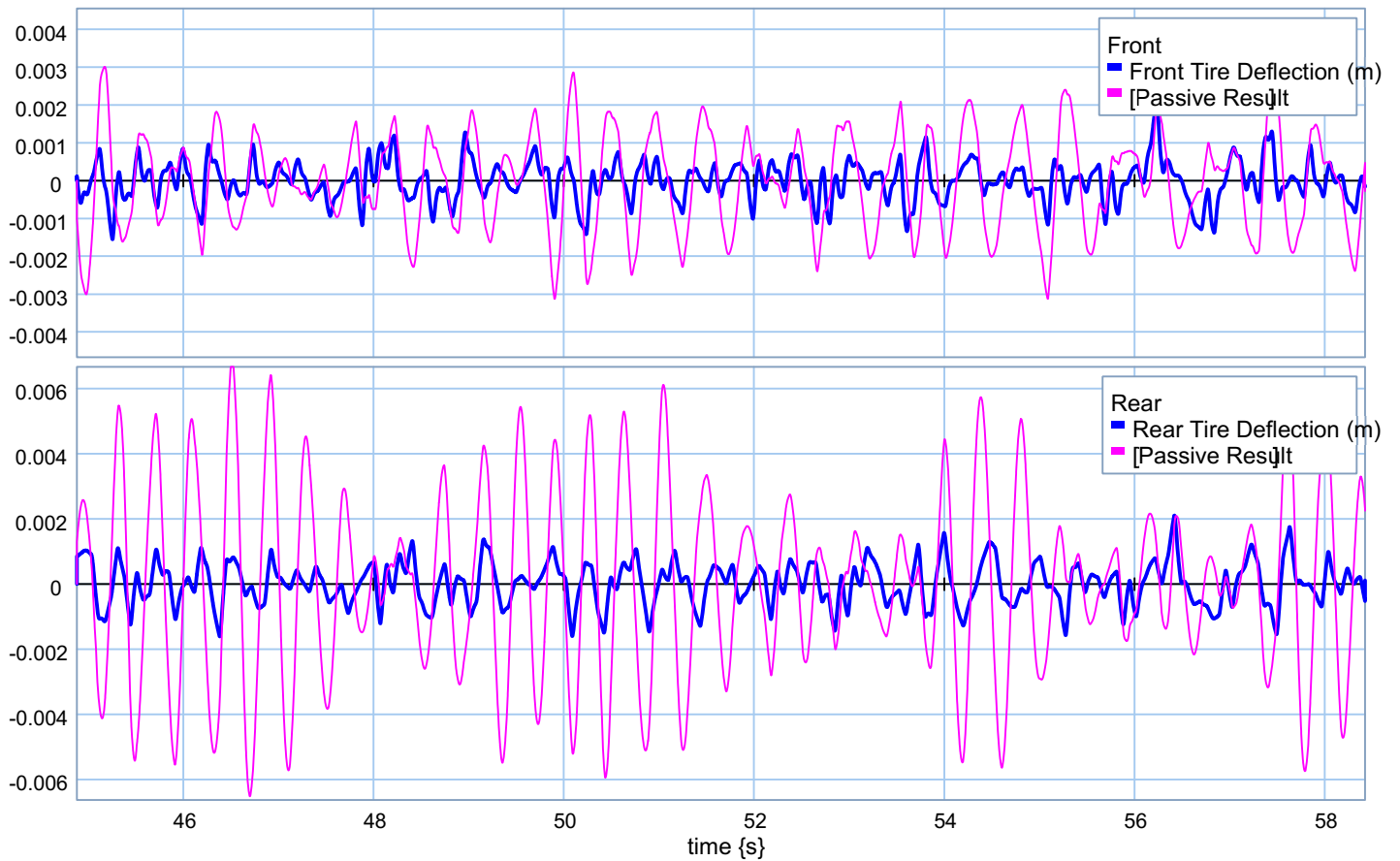


Figure 6.17: Magnified tires' deflections using half-car gains for road holding

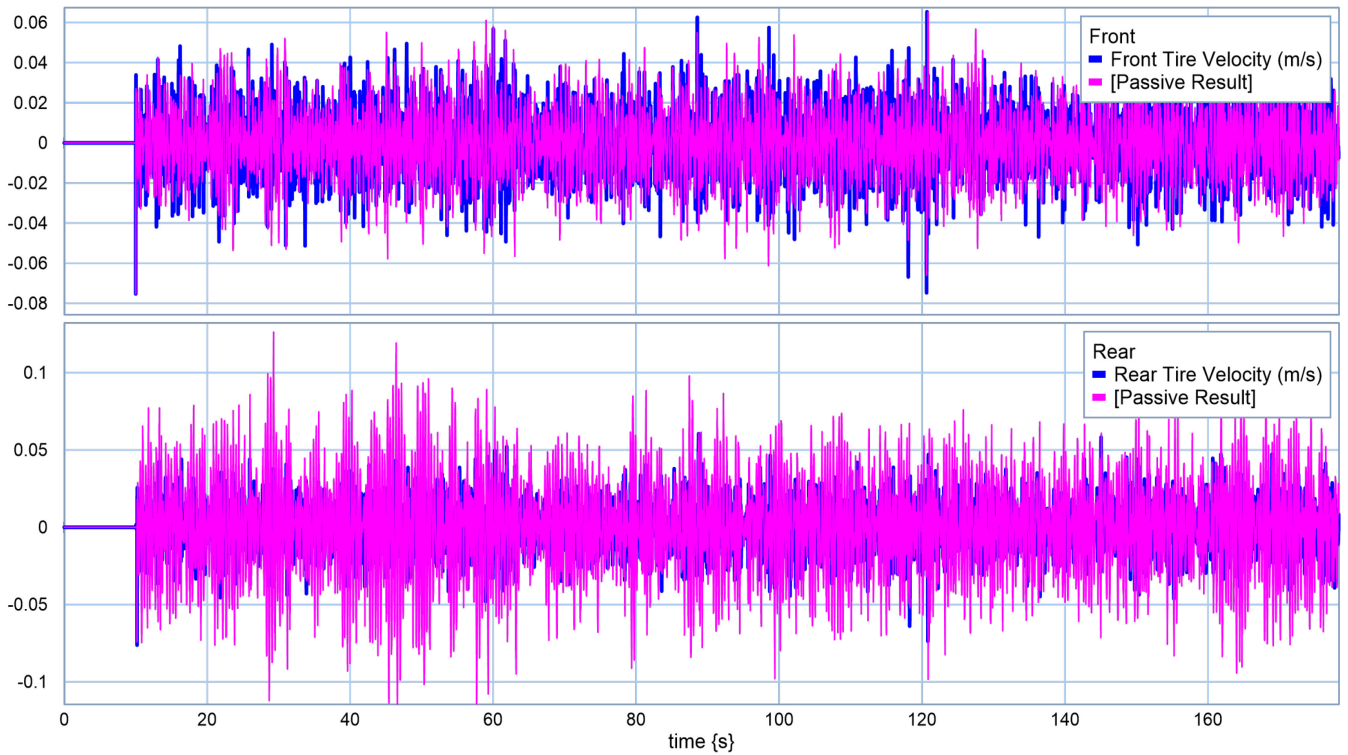


Figure 6.18: Tires' velocities using half-car gains for road holding

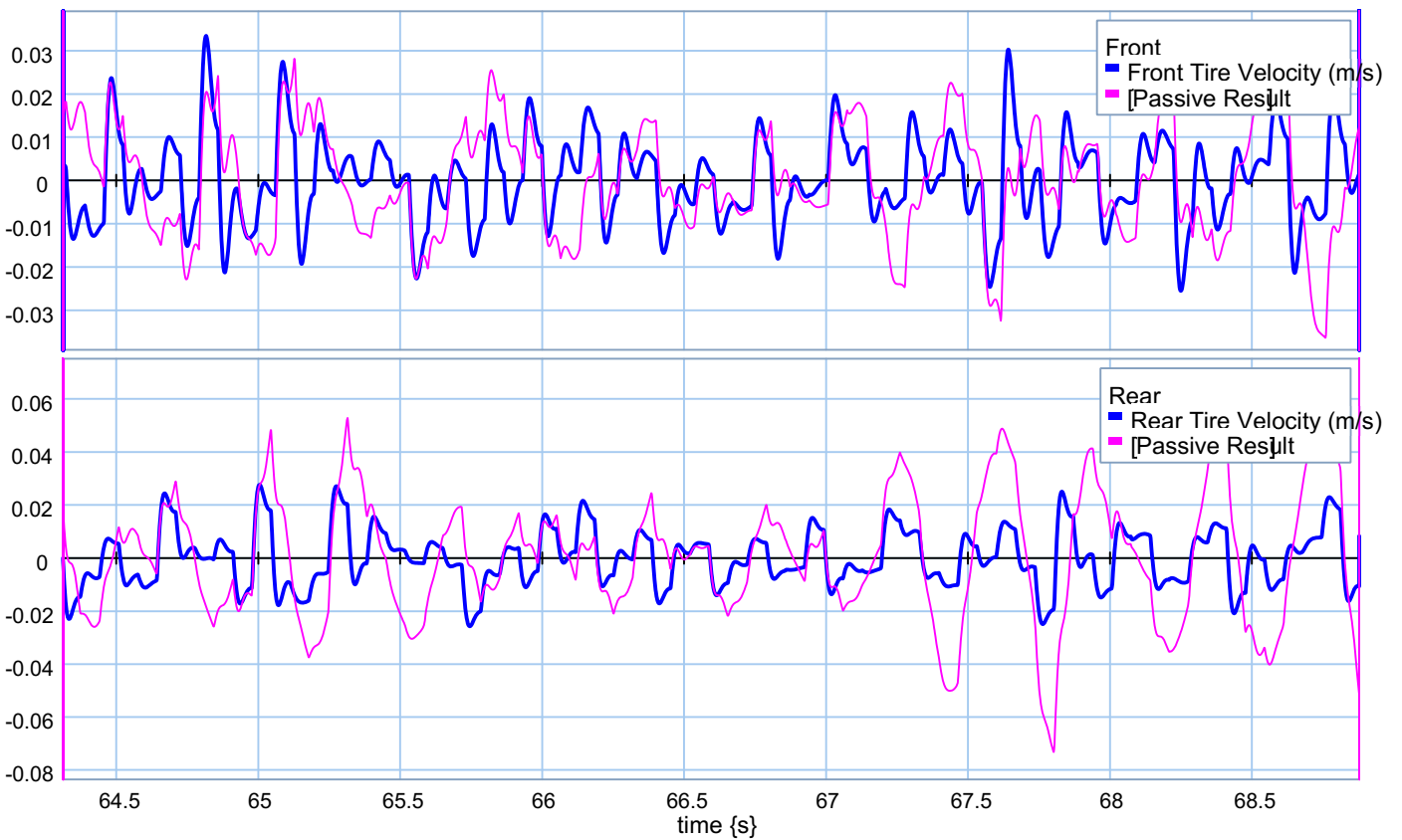


Figure 6.19: Magnified tires' velocities using half-car gains for road holding

Although in road holding, minimizing the vertical and pitch acceleration are not looked for, Figures 6.20 and 6.21 present a great reduction in these states which could improve the ride quality of the vehicle.

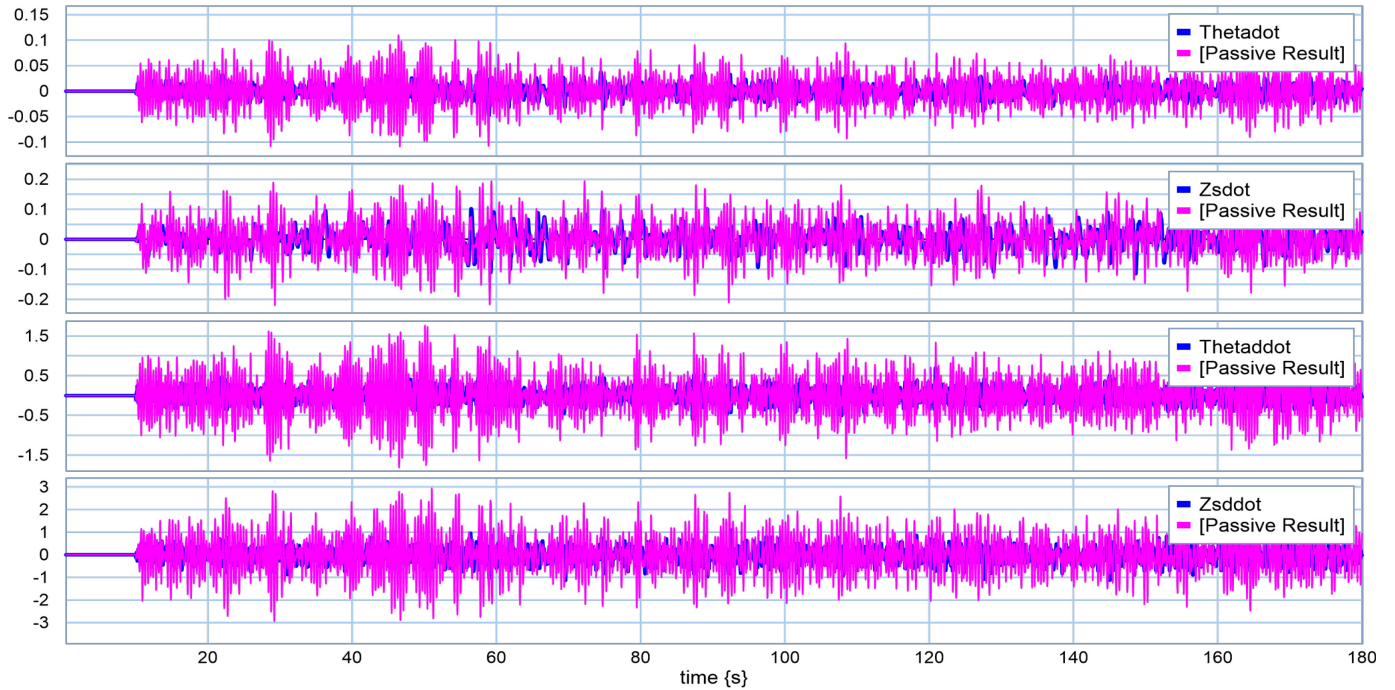


Figure 6.20: Central states using half-car gains for road holding

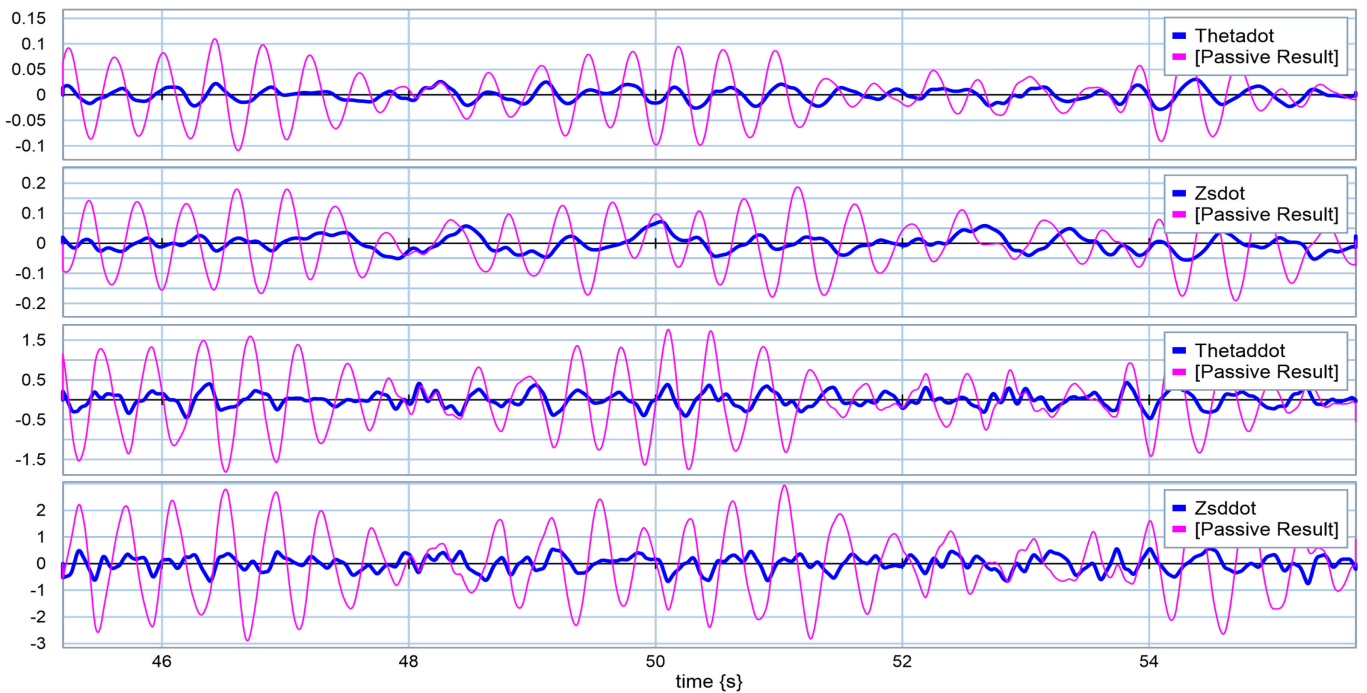


Figure 6.21: Magnified central states using half-car gains for road holding

Similar to what was outlined in previous section for ride quality, an optimum set of gains needs to be presented which can be used for all possible cargo masses. Since the performance indices for all studied sets of gains were close to each other in each model, another index had to be used in order to present the optimum gain, i.e., energy index. Hence, the energy indices outlined in equations 6.46 and 6.47 were recorded for all runs and the results presented that for all five models the lower energy index was recorded while the fifth set of gains was used. Figures 6.22 and 6.23 compare tire velocity and deflection for the first model when the first and fifth sets of gains were used. As is seen, there is not much difference in improvement when the first set of gains was used instead of the fifth. Hence, by using the fifth set of gains, the road holding scenario would be satisfied with consuming less energy.

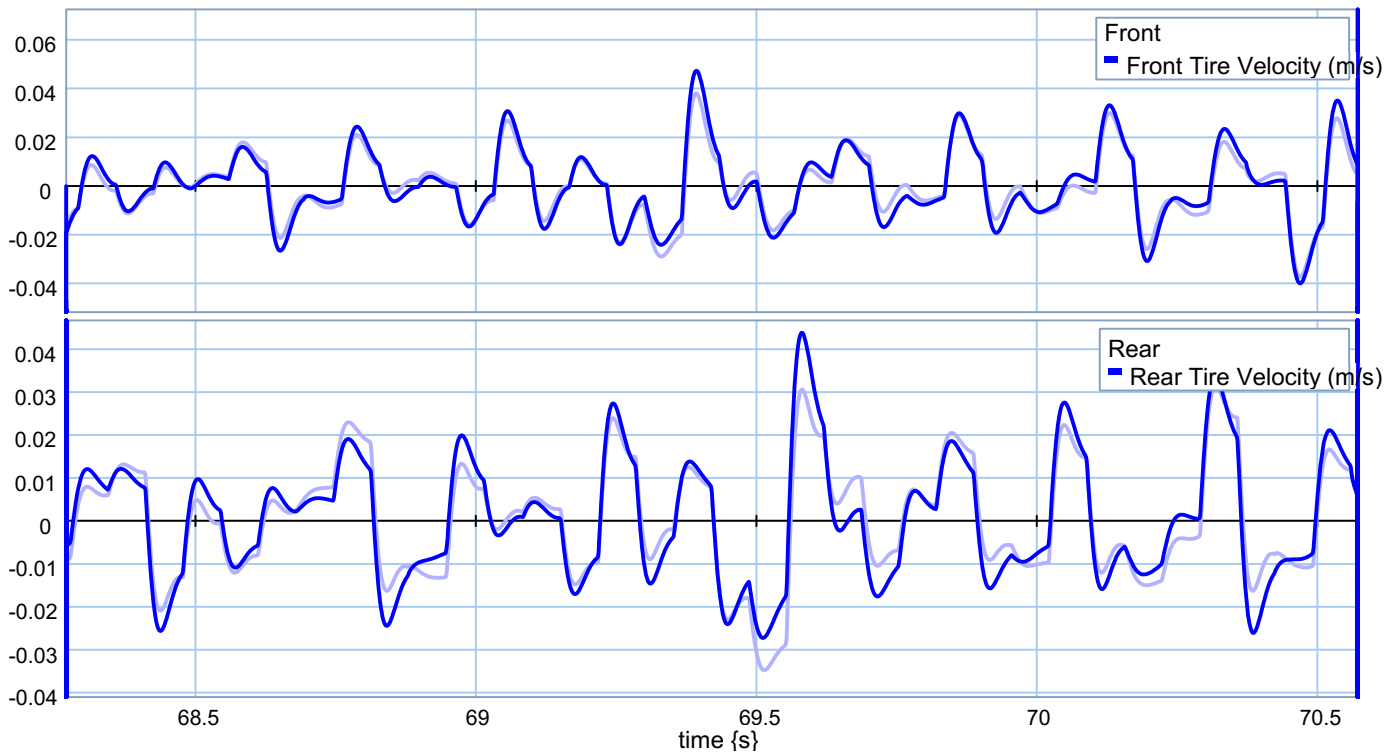


Figure 6.22: Tires' velocities comparison between two sets of half-car gains

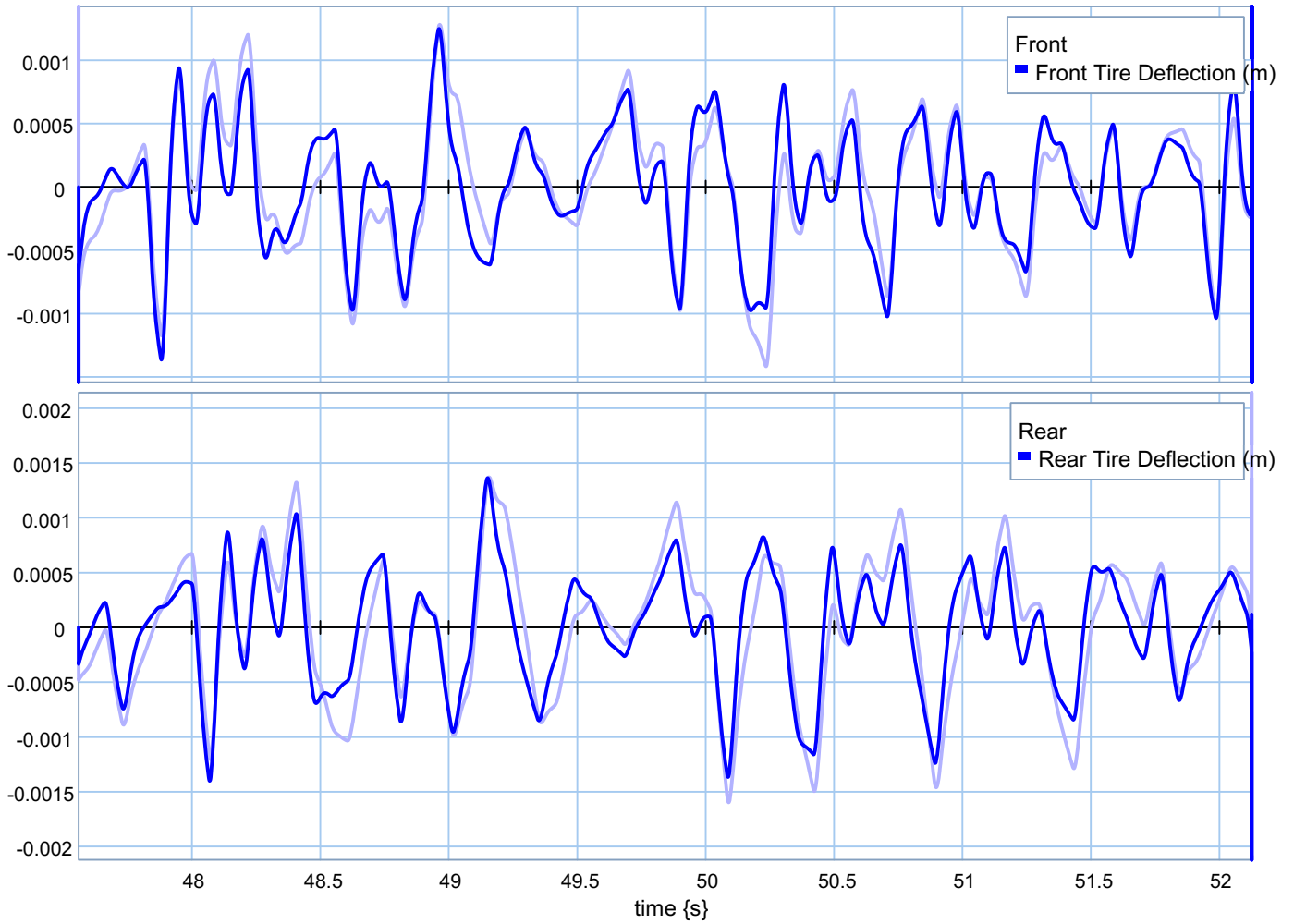


Figure 6.23: Tires' deflections comparison between two sets of half-car gains in road holding

Based on these two sections, for both the ride quality and road holding scenarios, the fifth set of gains is presented as the optimum gains for the half-car based active suspension. These optimum gains are used in the next section for a non-linear half-car model.

6.5.2 Ride Quality

Once the best set of gains was developed, and non-linear half-car models were generated for five various cargo masses. The chosen gain matrix, i.e., the fifth set of gains, was used in all five models and the results were compared with passive suspension. The road profile for this simulation was the custom road profile outlined in Chapter 4 [4.2.7.2] that consists of five fundamental events. Figures 6-24 to 6-28 compare the vehicle pitch angle for passive and active suspension situations.

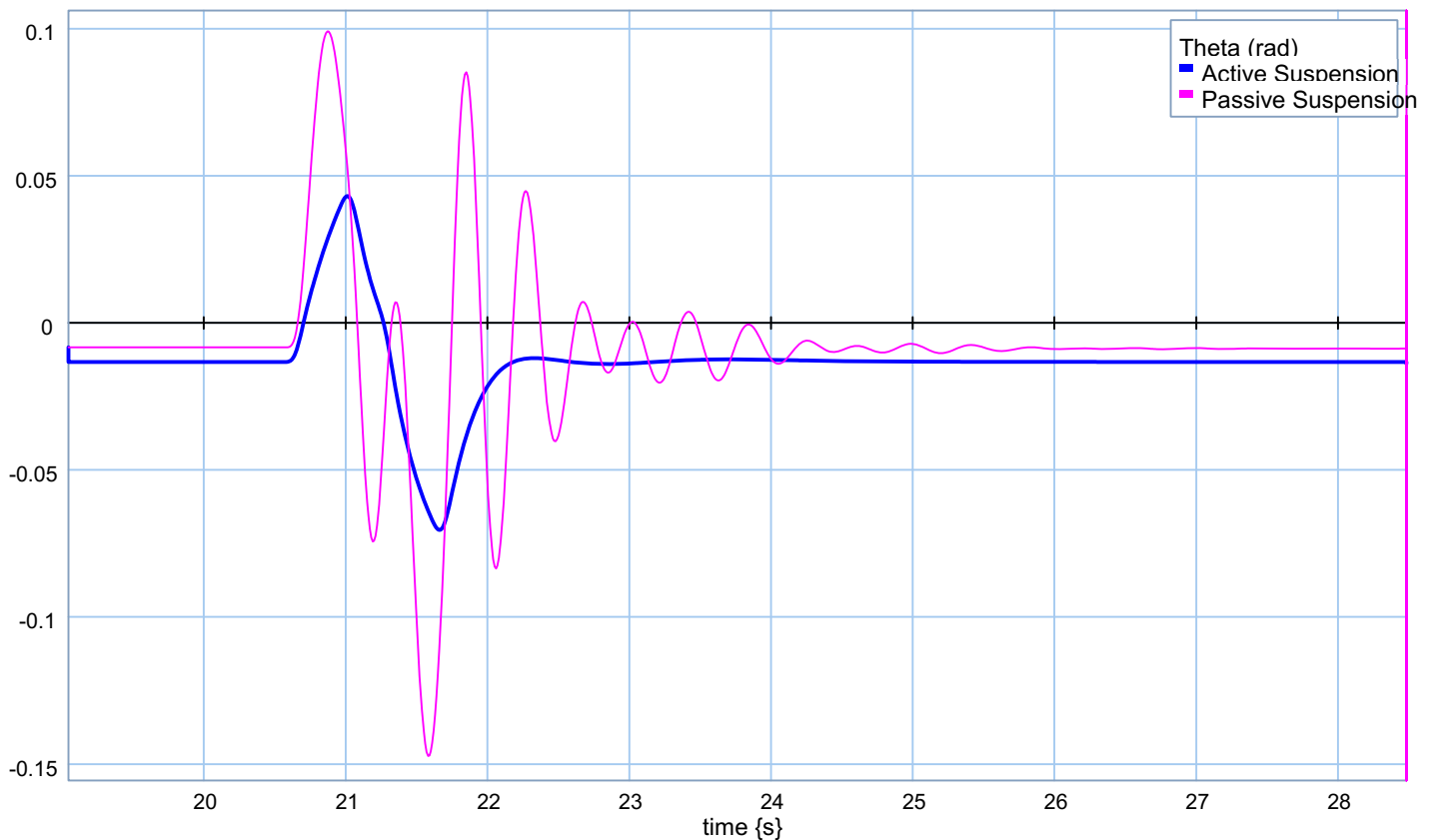


Figure 6.24: Vehicle pitch angle over 1st event of custom road profile in ride quality

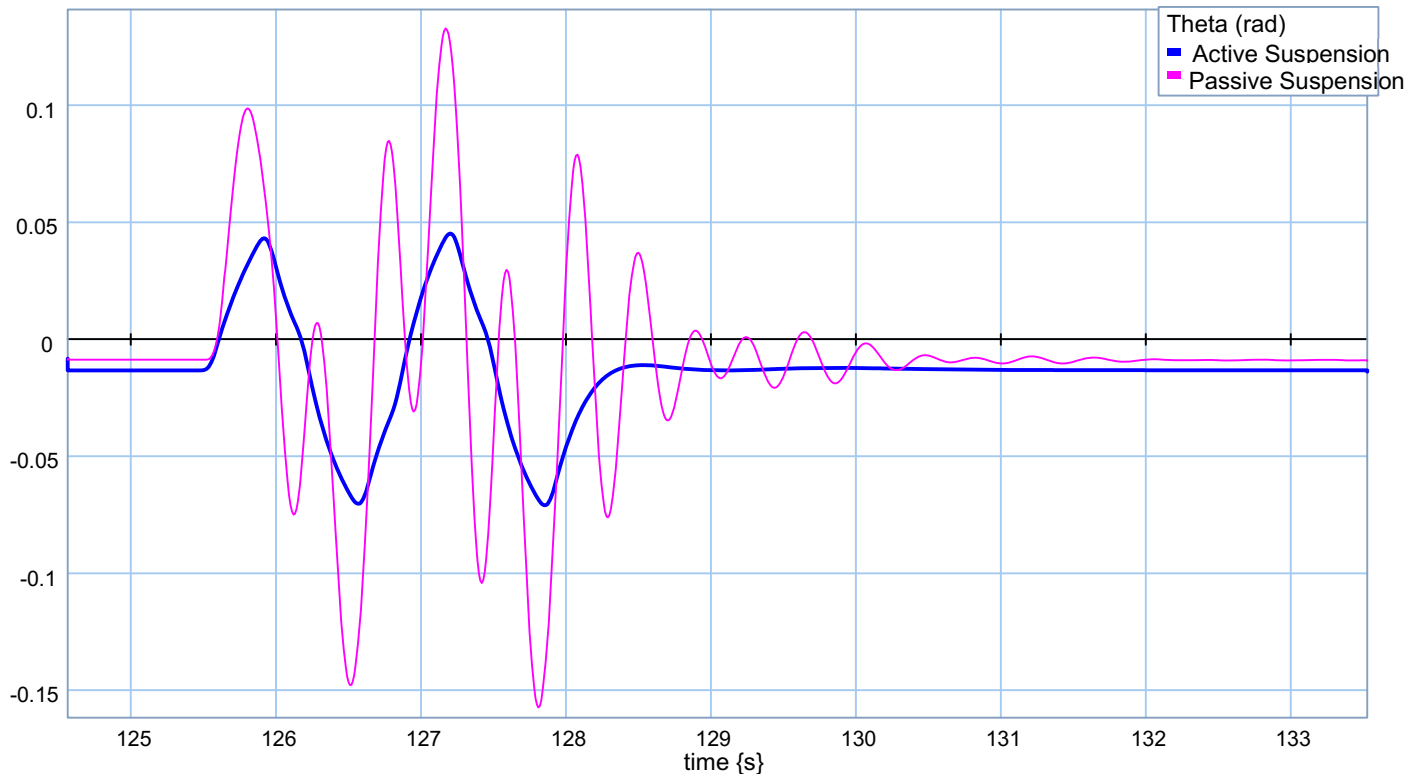


Figure 6.25: Vehicle pitch angle over 2nd event of custom road profile in ride quality

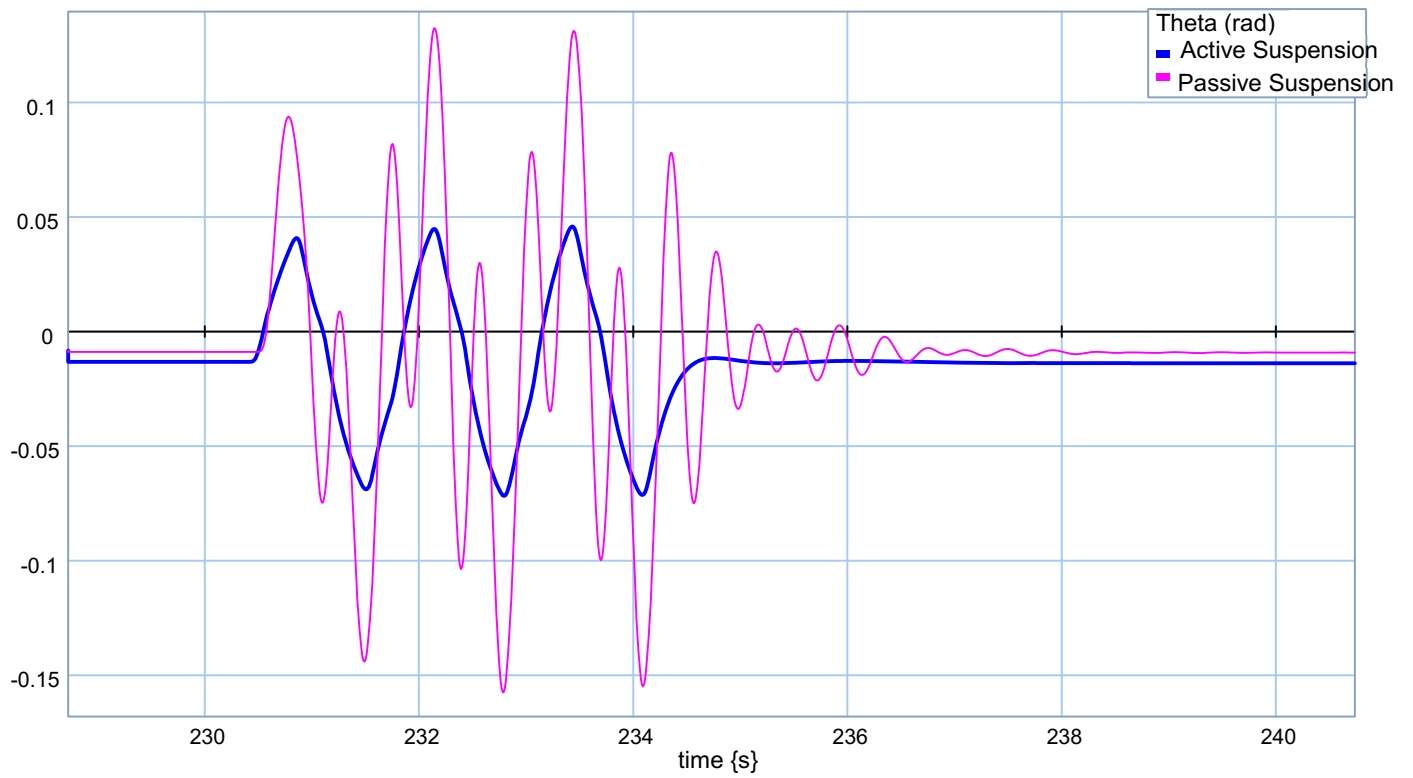


Figure 6.26: Vehicle pitch angle over 3rd event of custom road profile in ride quality

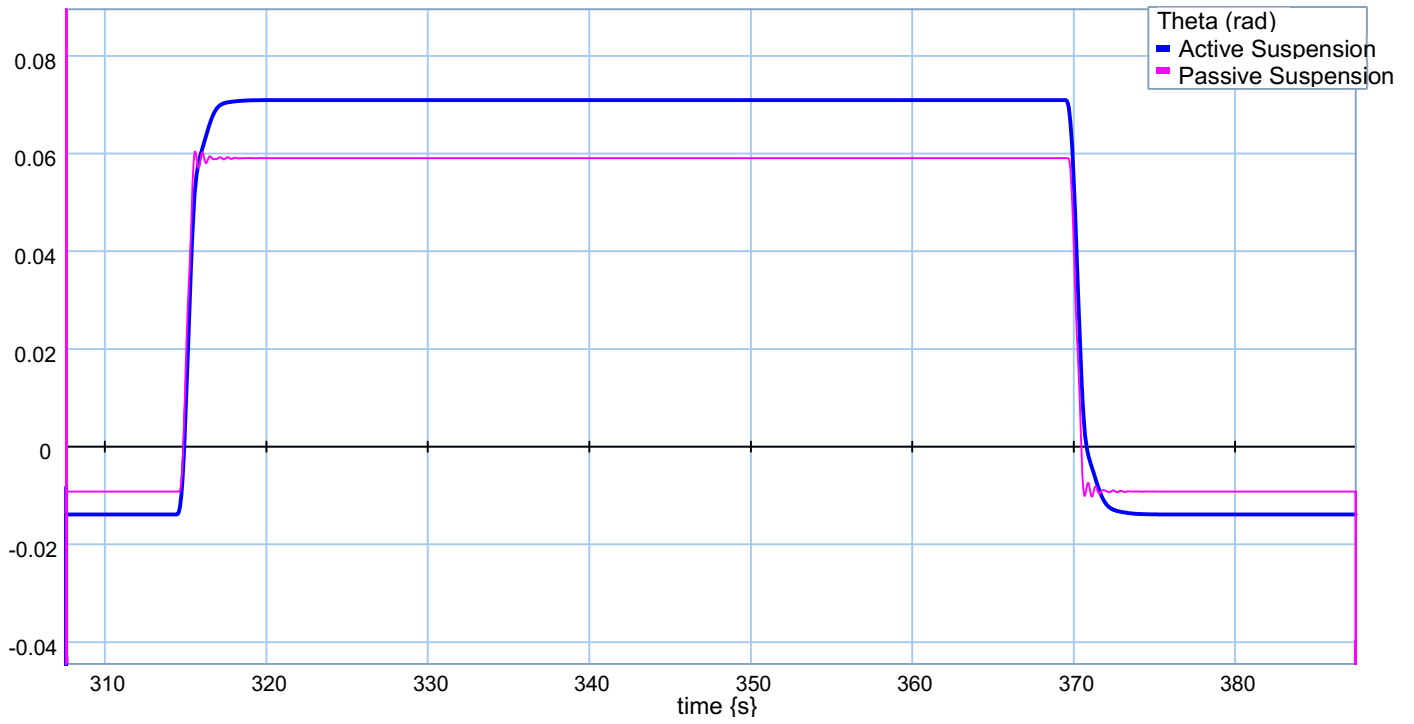


Figure 6.27: Vehicle pitch angle over 4th event of custom road profile in ride quality

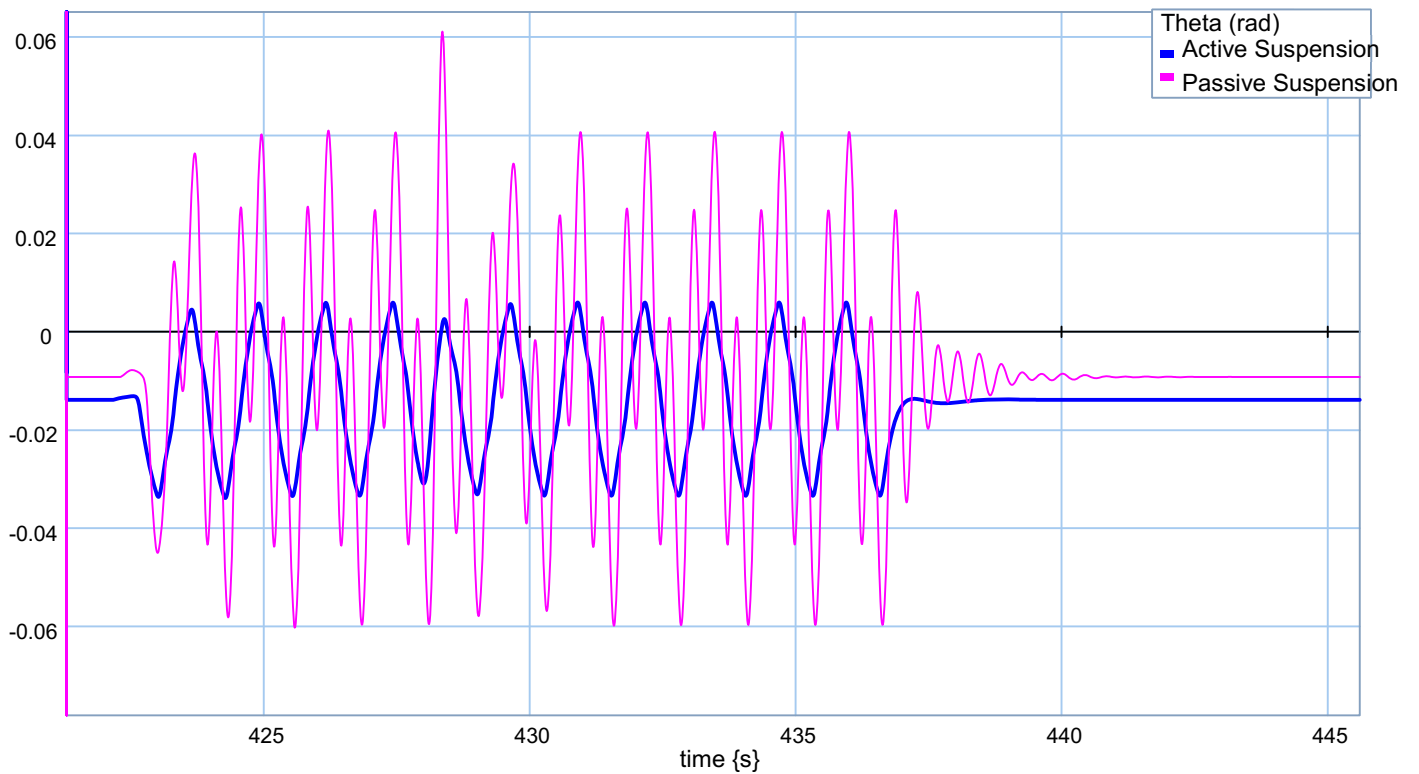


Figure 6.28: Vehicle pitch angle over 5th event of custom road profile in ride quality

The lower the performance index, the better ride quality the vehicle has. Figure 6.29 compared this index for the front, rear and centre parts of the vehicle in passive and active suspension situations.

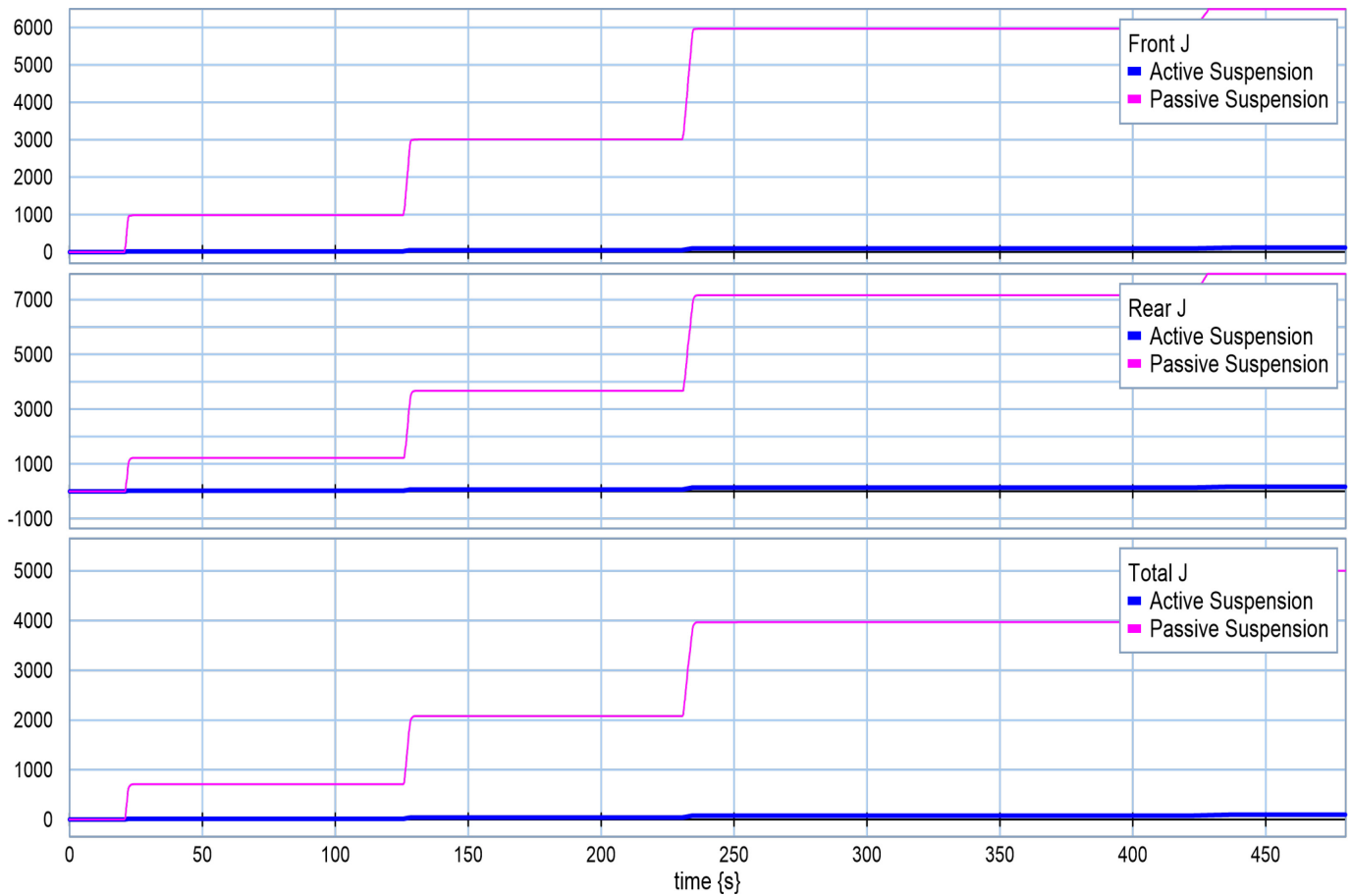


Figure 6.29: Performance index using half-car optimum gains in ride quality

Figures 6.30 to 6.39 present how perfectly the half-car controller improved vehicle ride quality by minimizing the vertical accelerations.

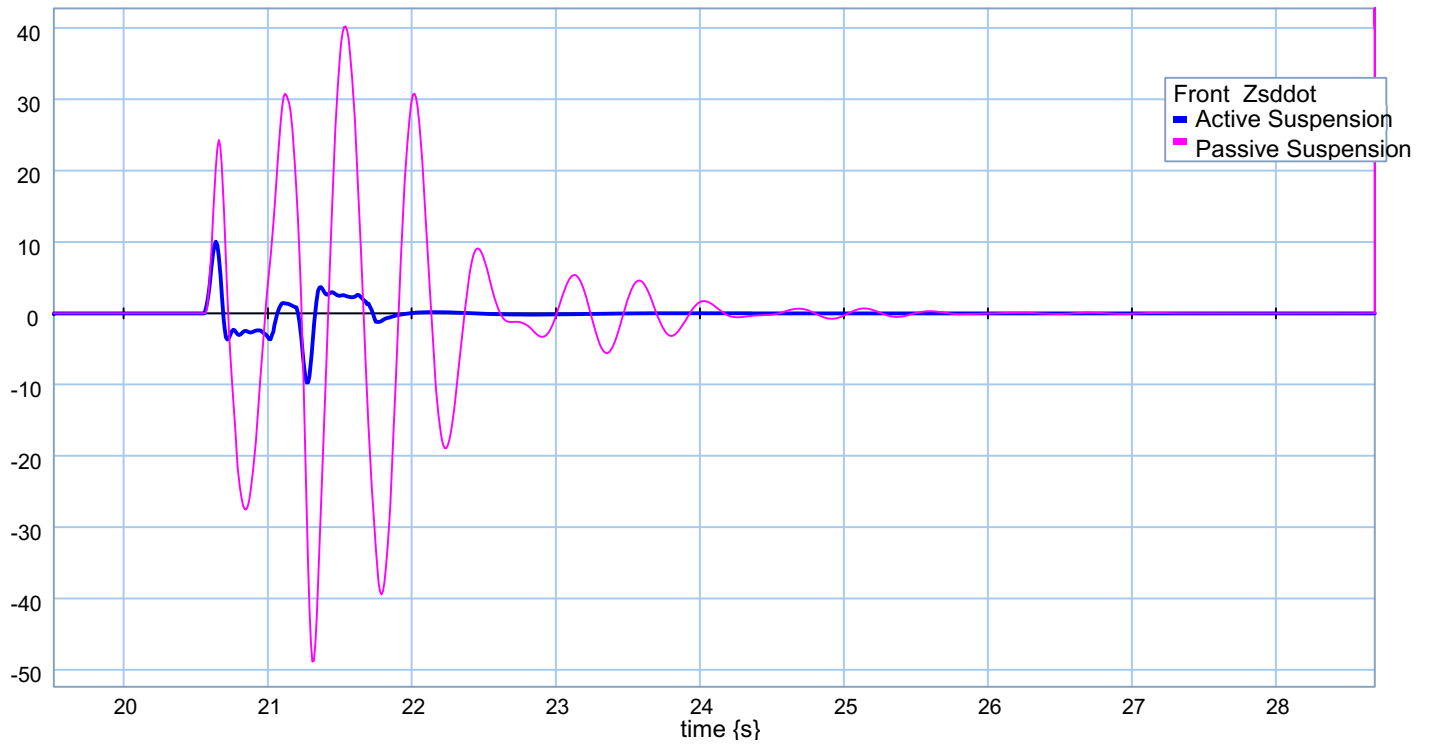


Figure 6.30: Front sprung mass acceleration over 1st event of custom road profile

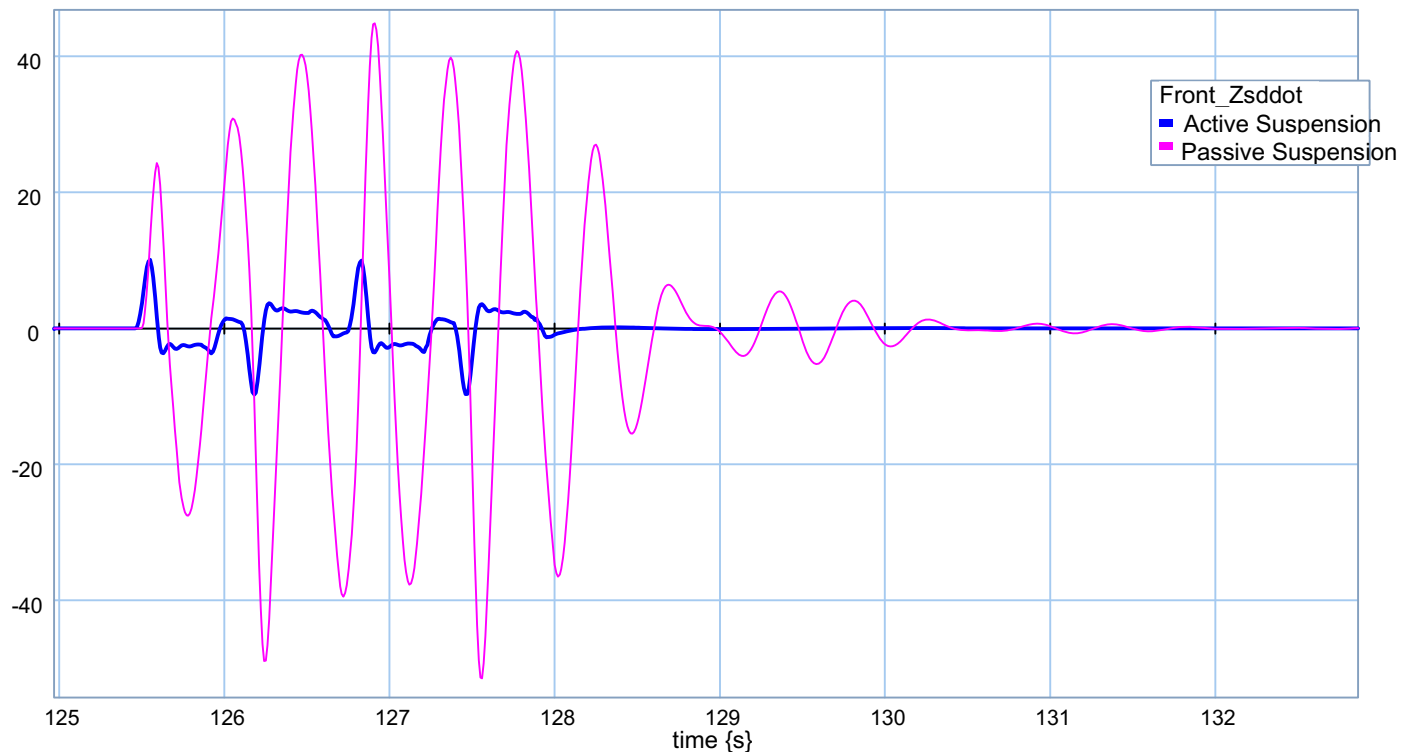


Figure 6.31: Front sprung mass acceleration over 2nd event of custom road profile

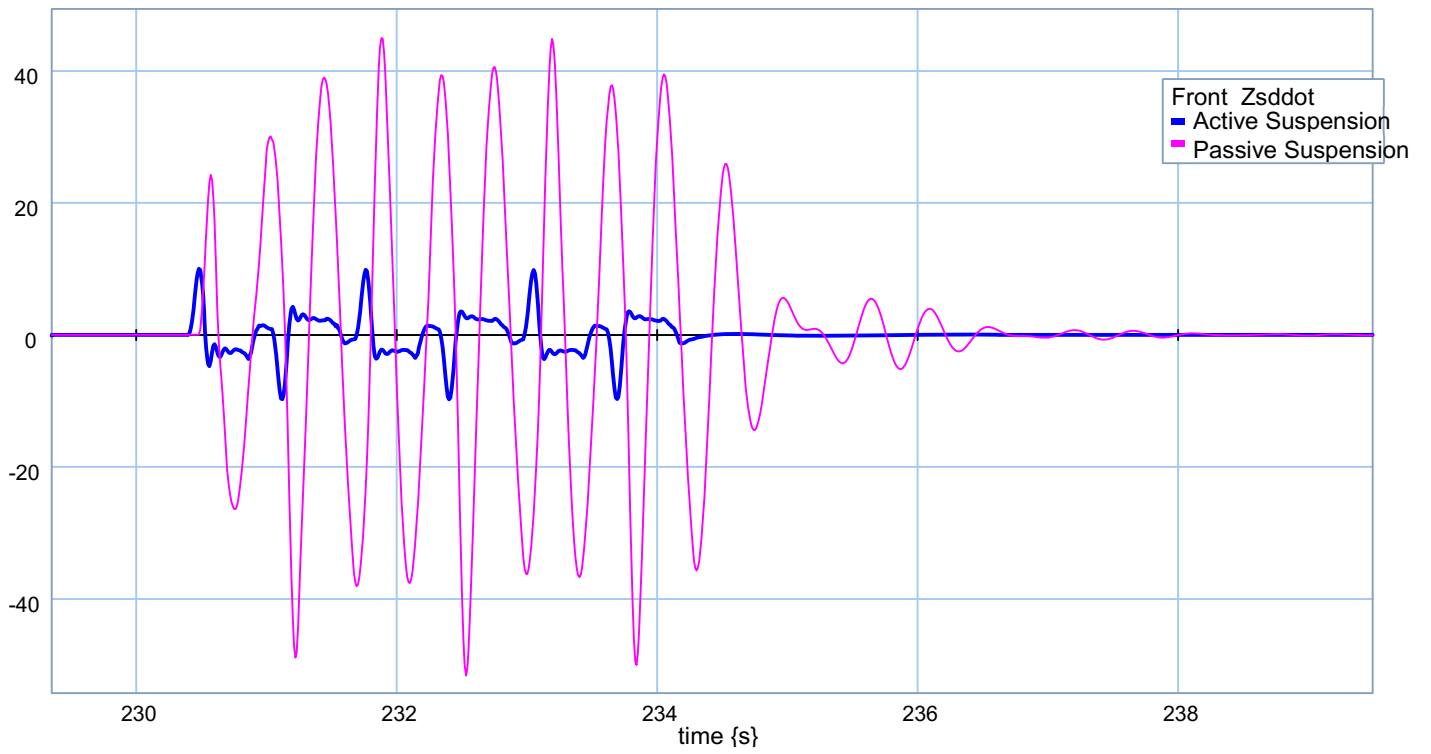


Figure 6.32: Front sprung mass acceleration over 3rd event of custom road profile

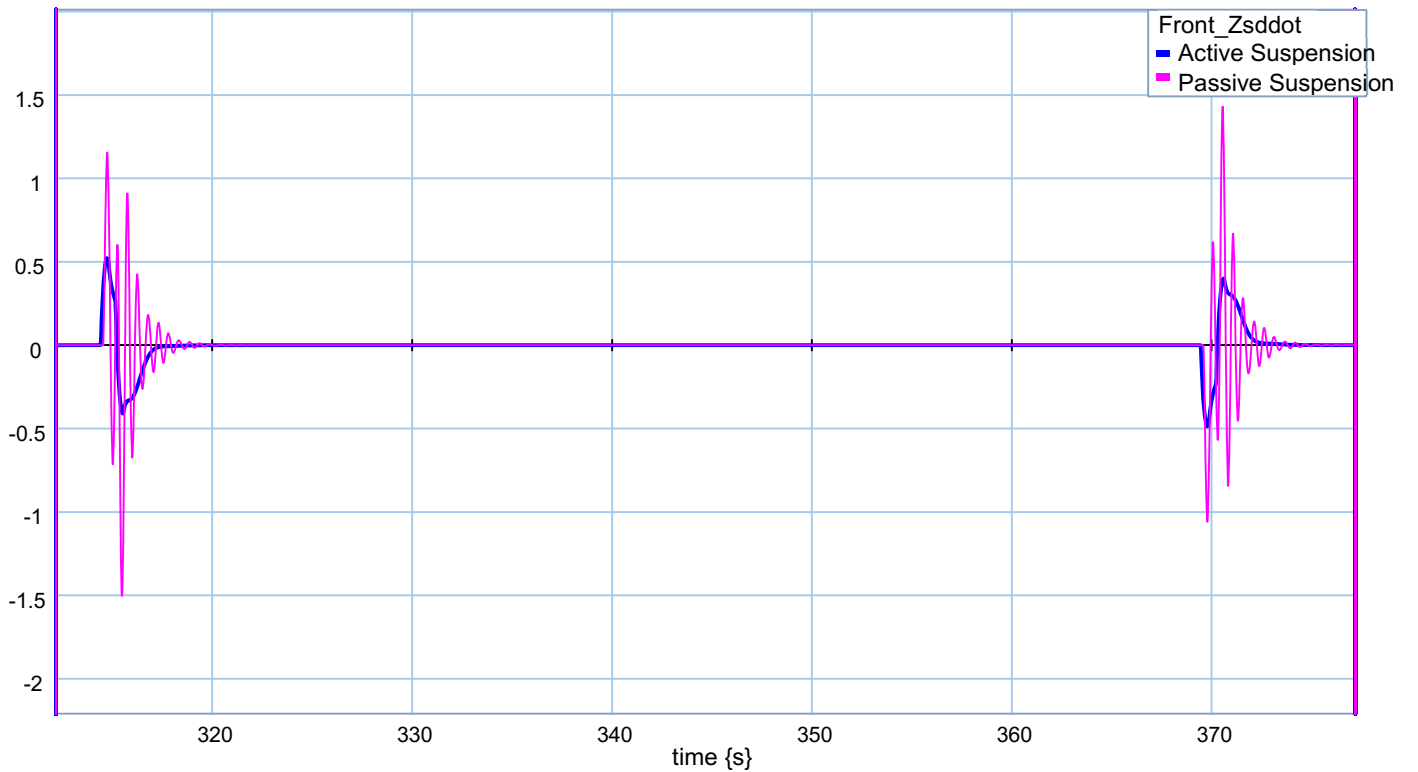


Figure 6.33: Front sprung mass acceleration over 4th event of custom road profile

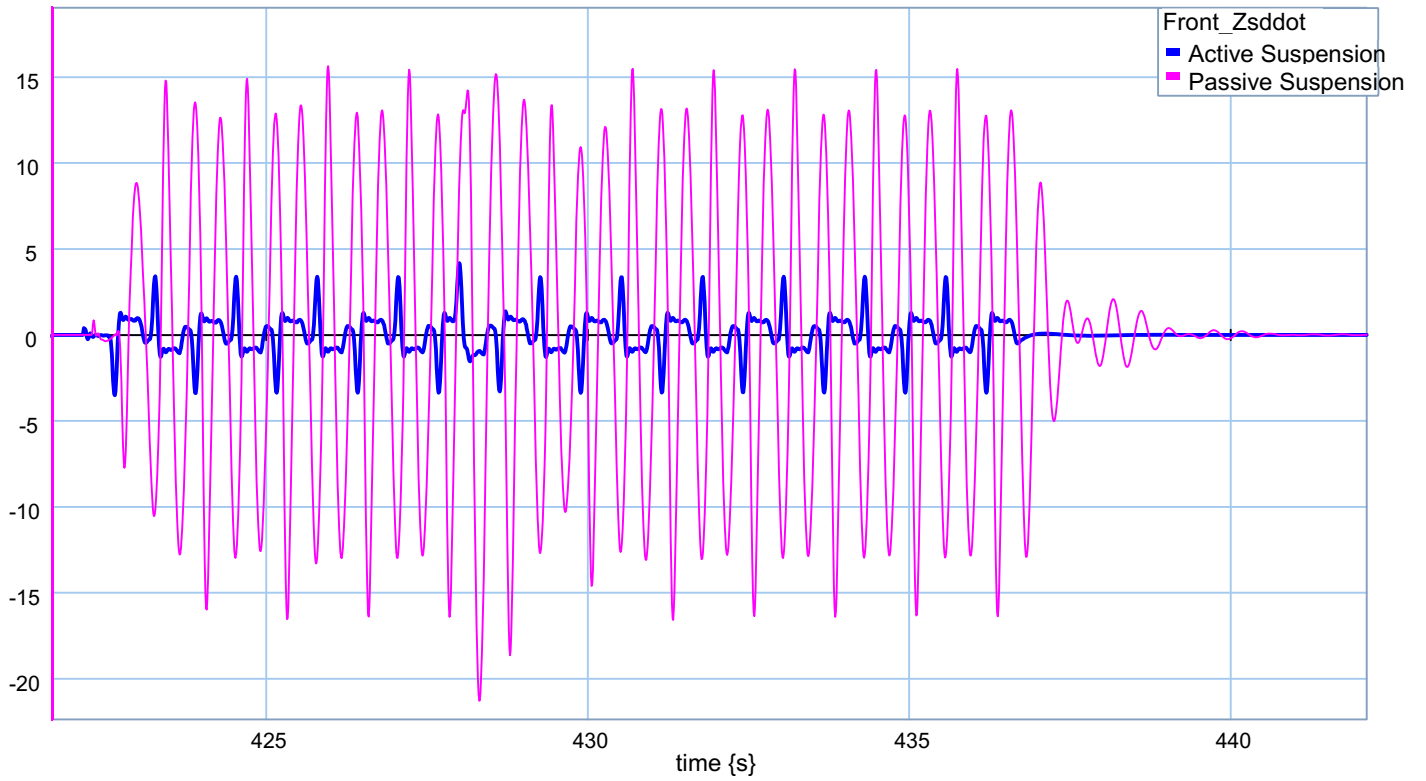


Figure 6.34: Front sprung mass acceleration over 5th event of custom road profile

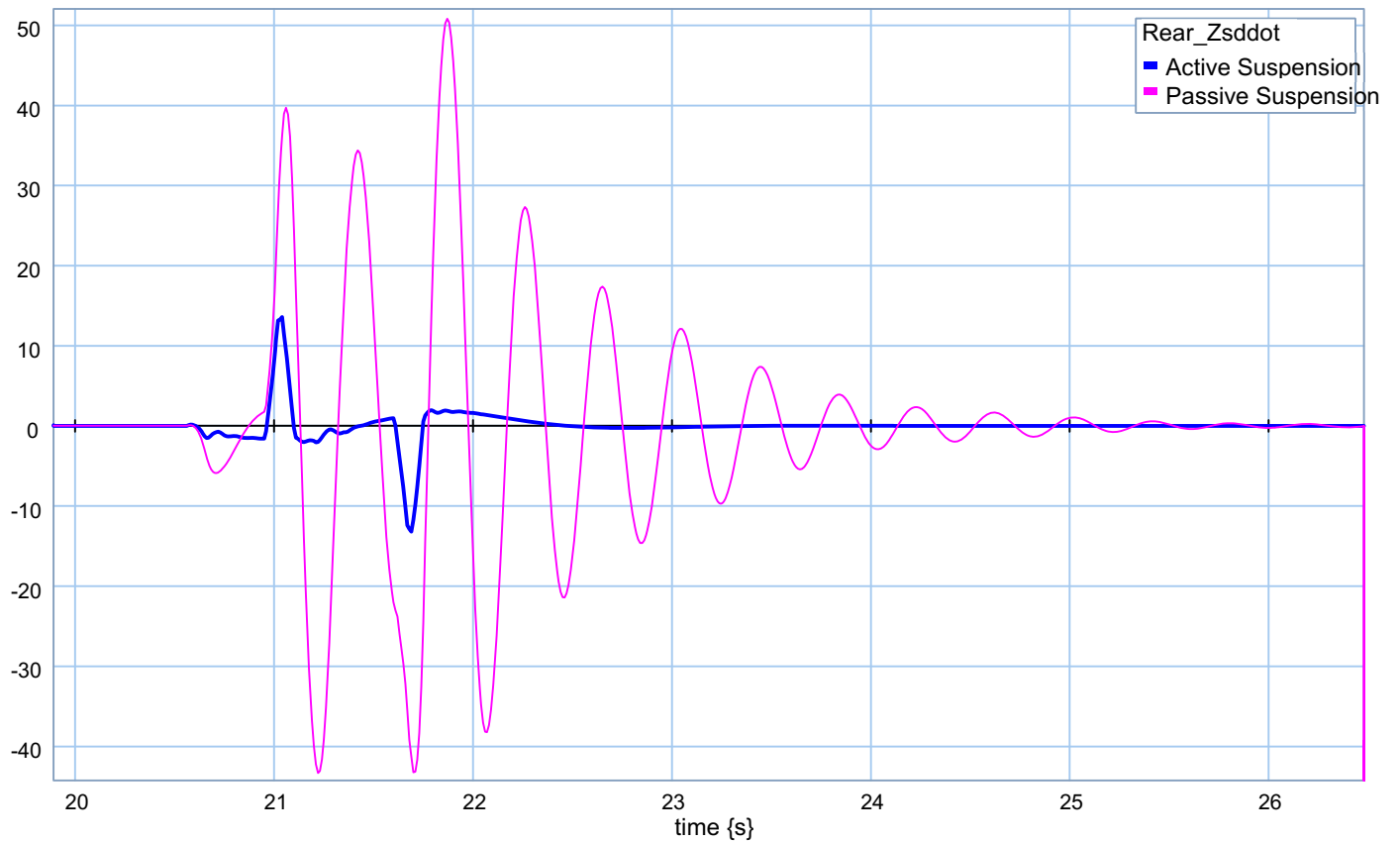


Figure 6.35: Rear sprung mass acceleration over 1st event of custom road profile

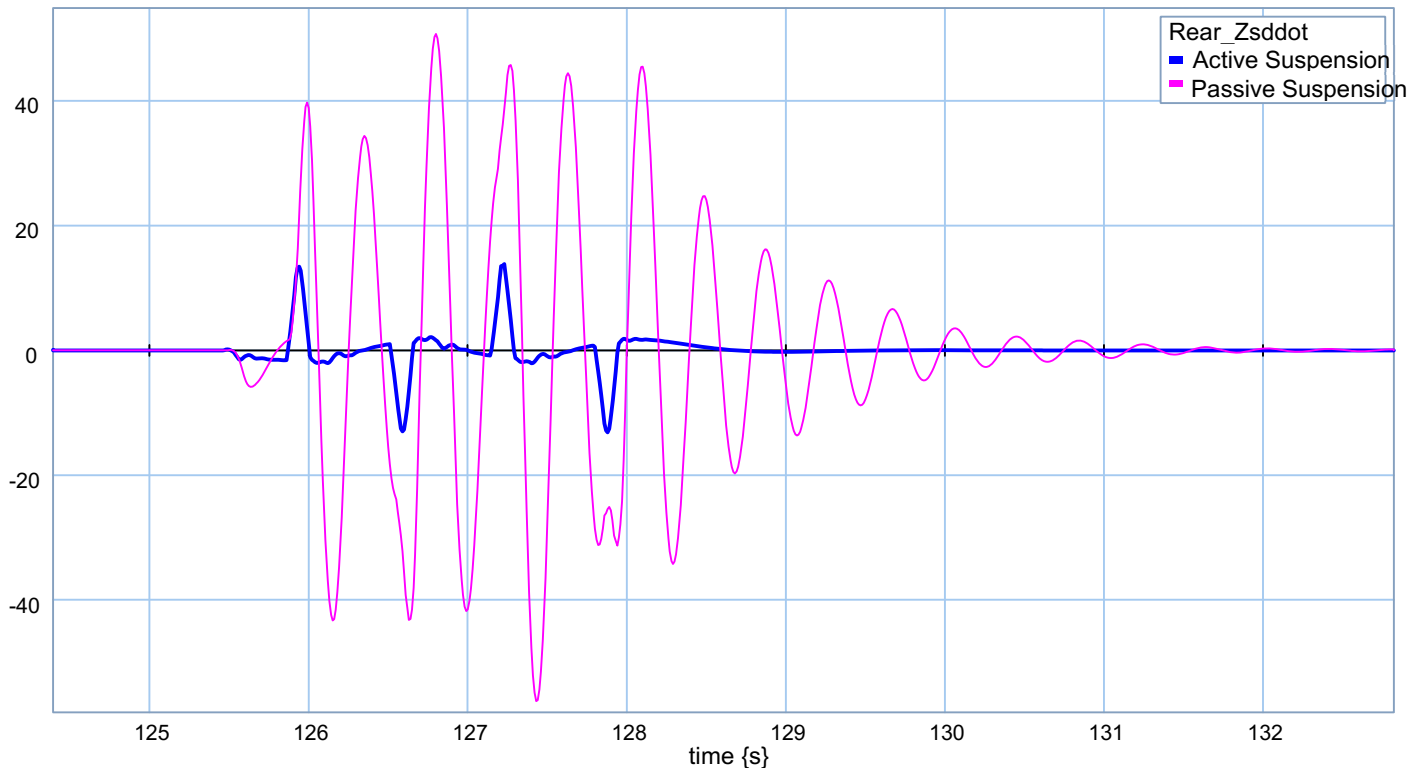


Figure 6.36: Rear sprung mass acceleration over 2nd event of custom road profile

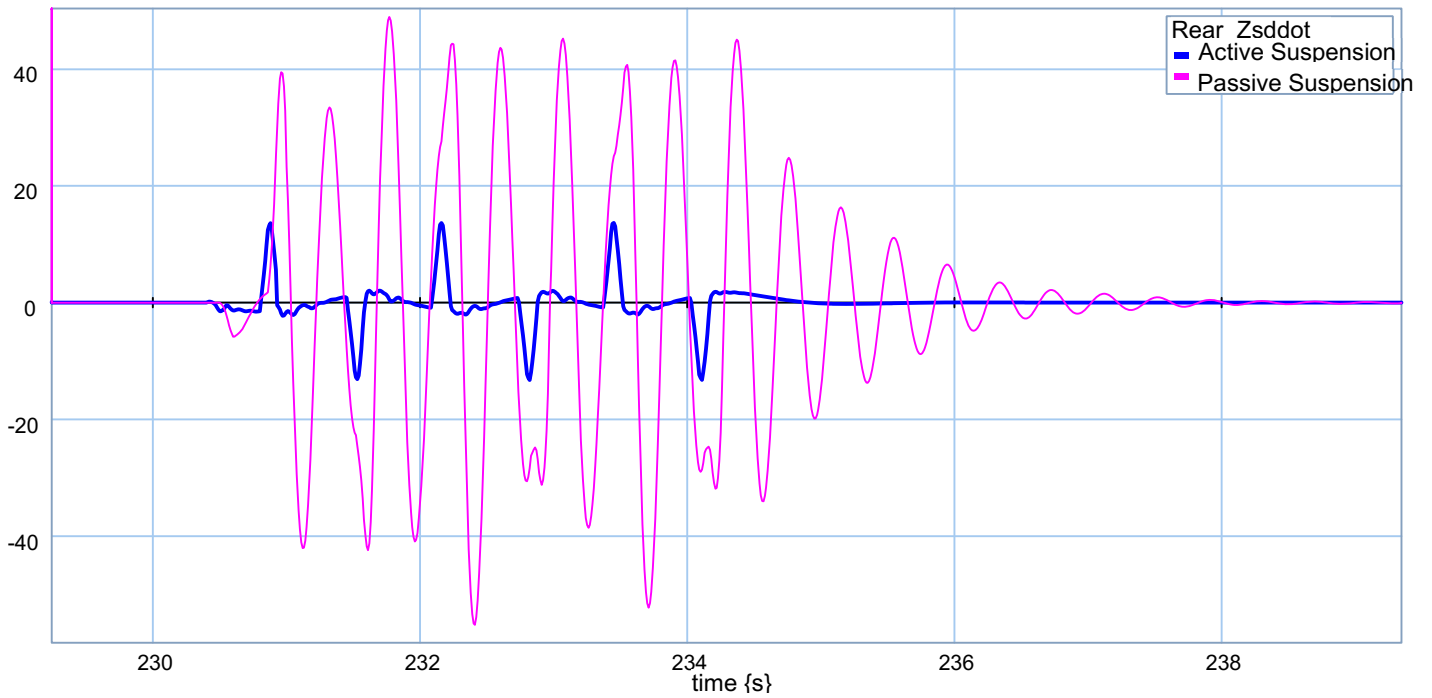


Figure 6.37: Rear sprung mass acceleration over 3rd event of custom road profile

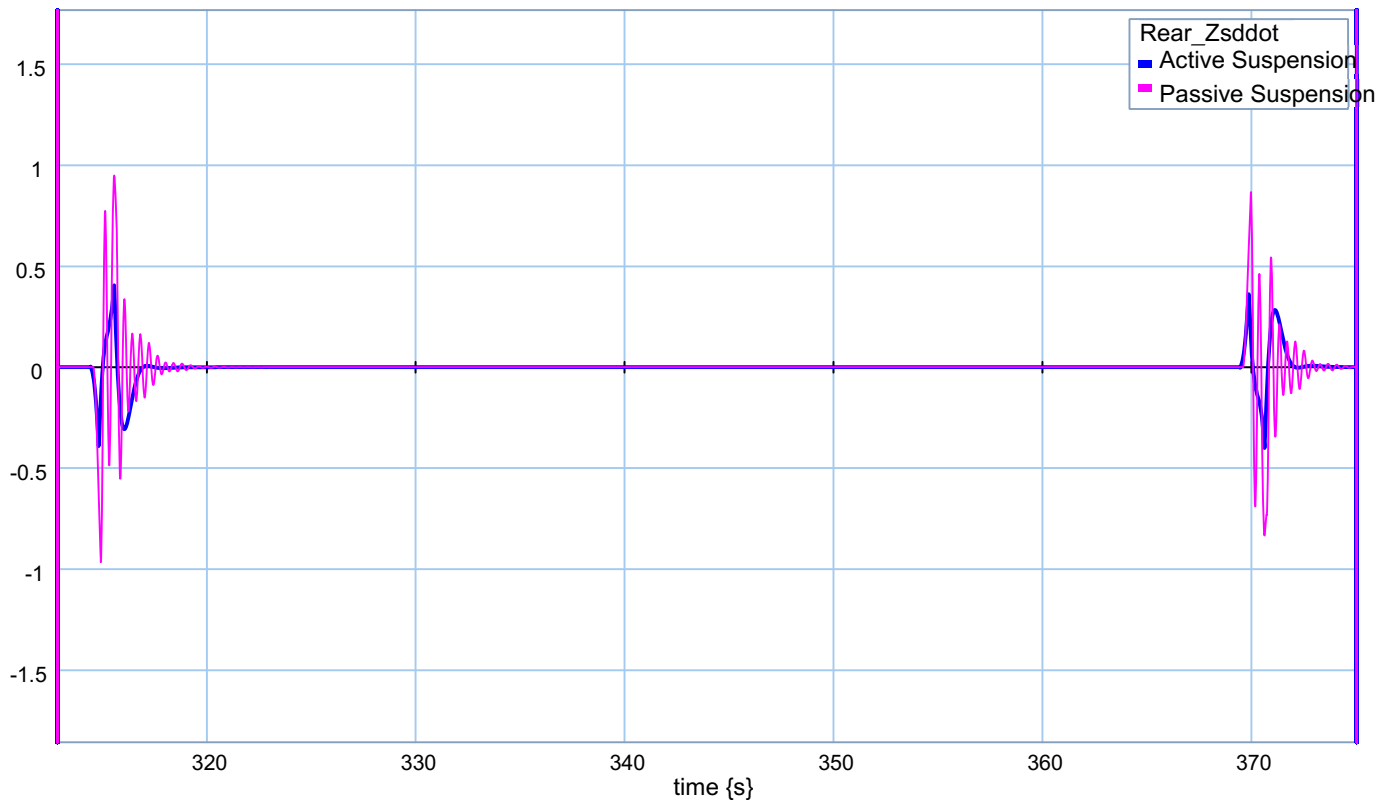


Figure 6.38: Rear sprung mass acceleration over 4th event of custom road profile

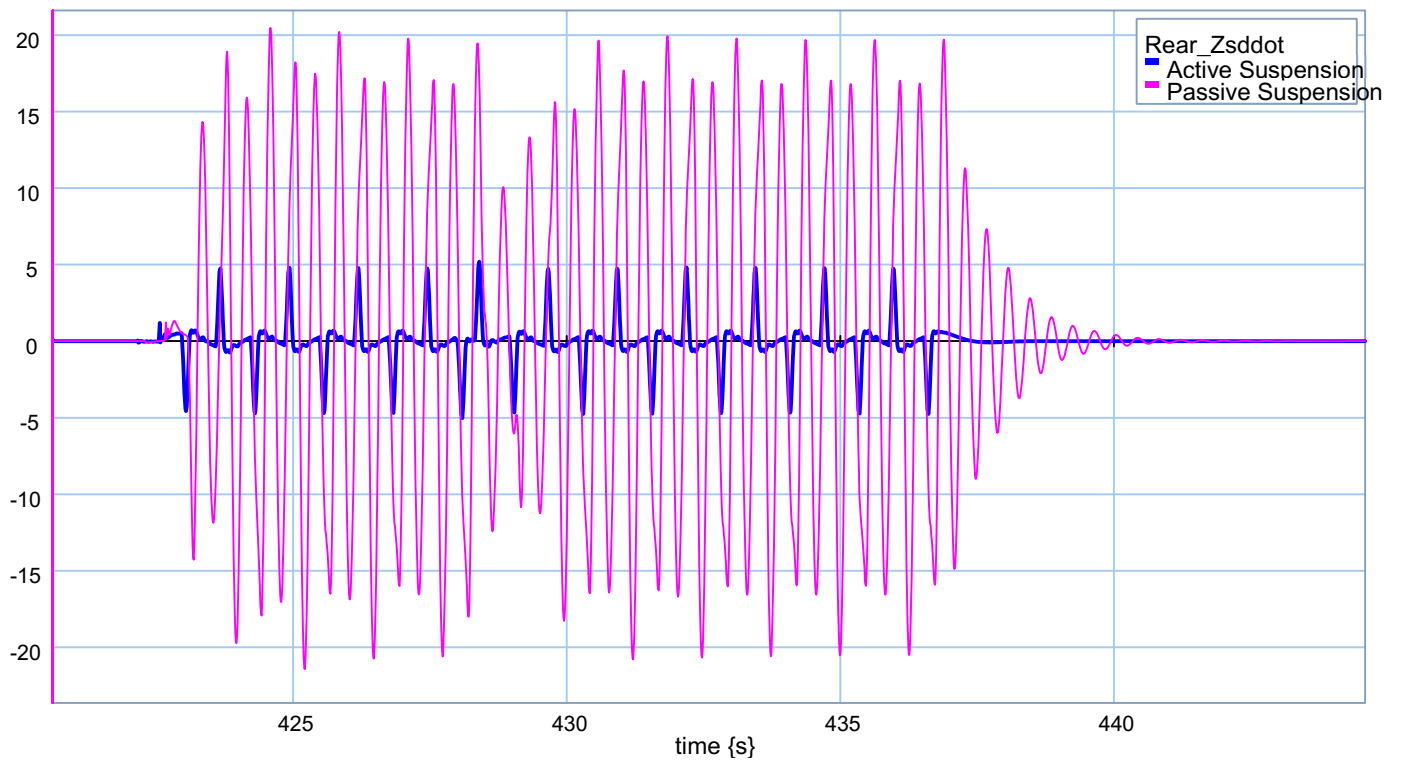


Figure 6.39: Rear sprung mass acceleration over 5th event of custom road profile

In this model, the vertical and pitch acceleration of the vehicle's centre of gravity was also controlled directly. Figure 6.40 to 6.44 demonstrate vertical and pitch acceleration for the vehicle's centre of gravity in passive and active suspension modes.

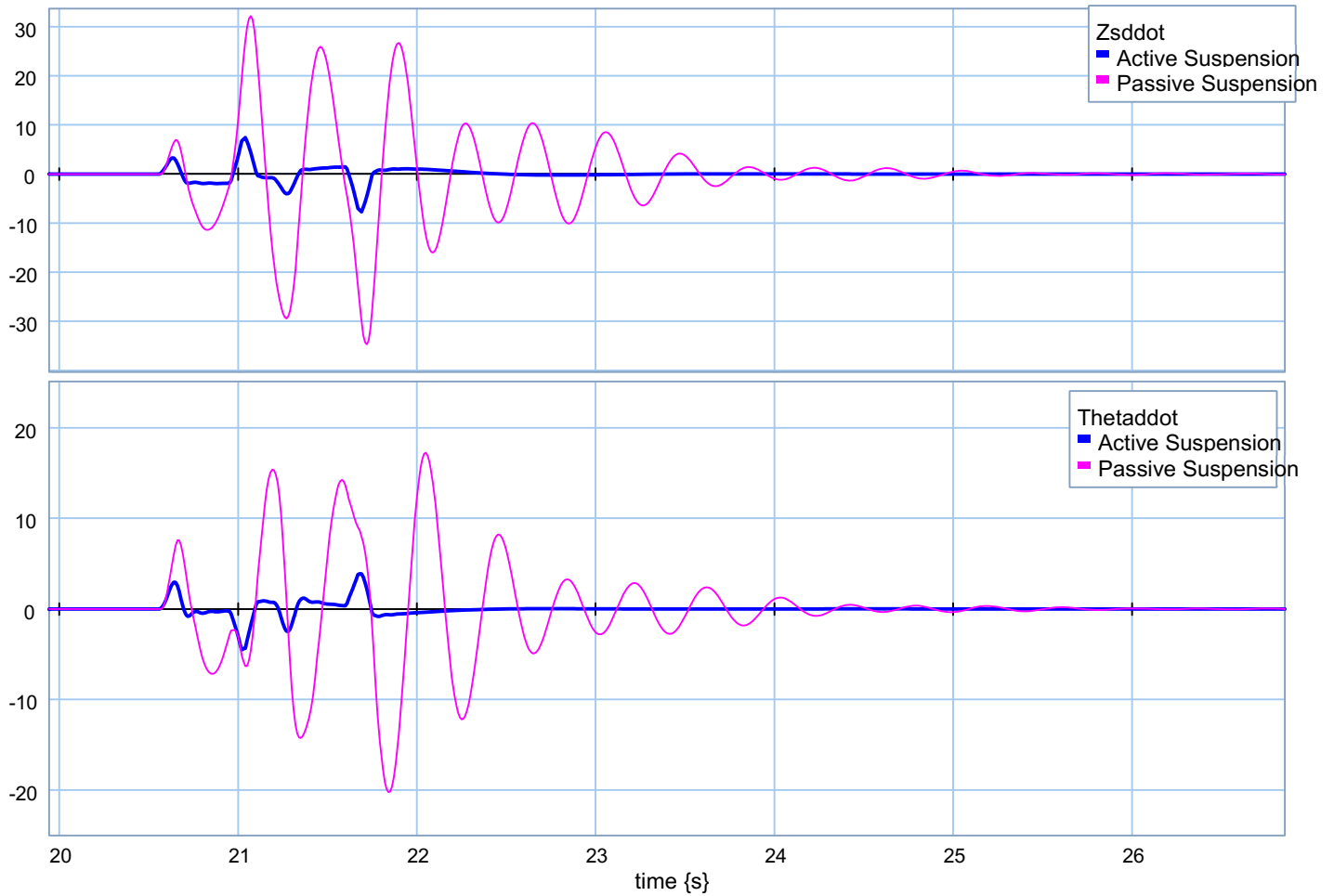


Figure 6.40: Central states over 1st event of custom road profile

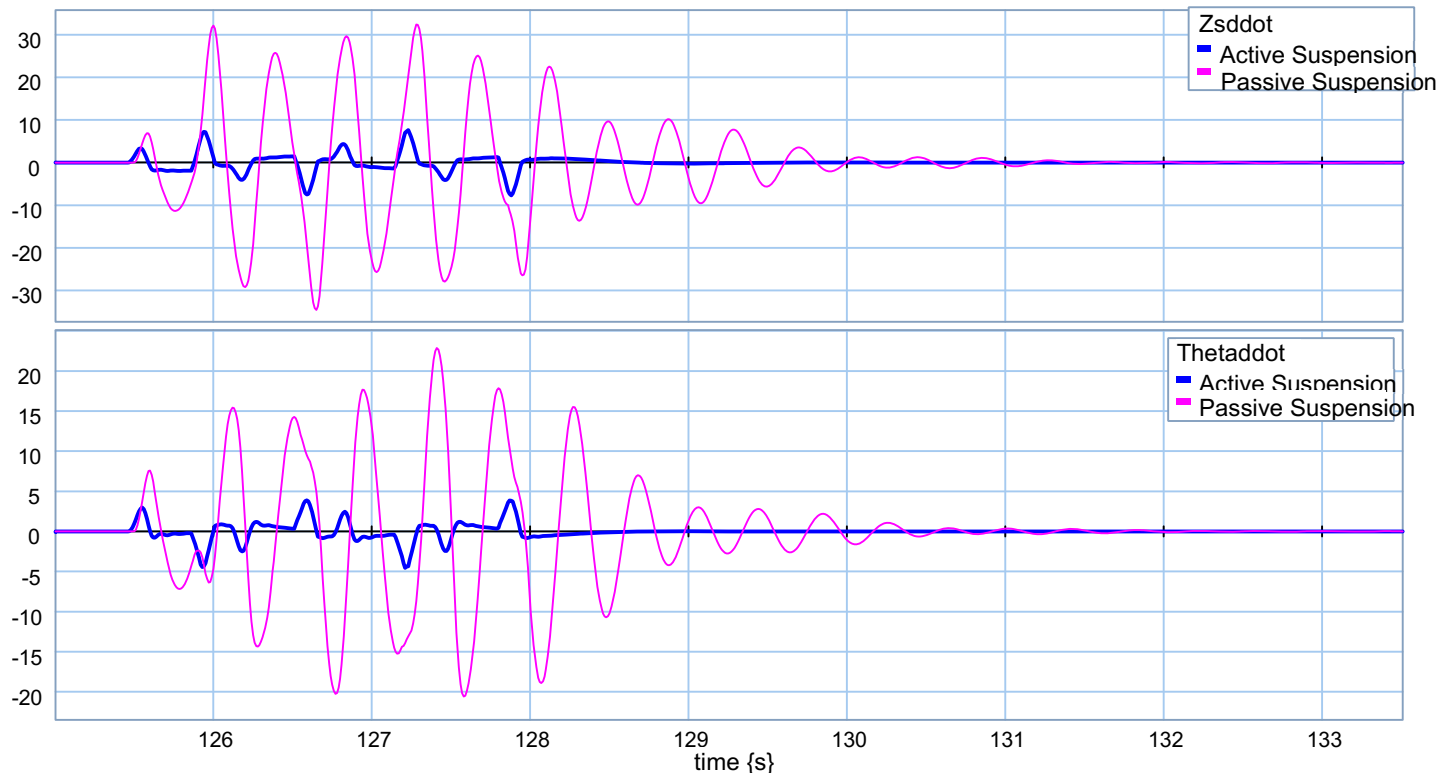


Figure 6.41: Central states over 2nd event of custom road profile

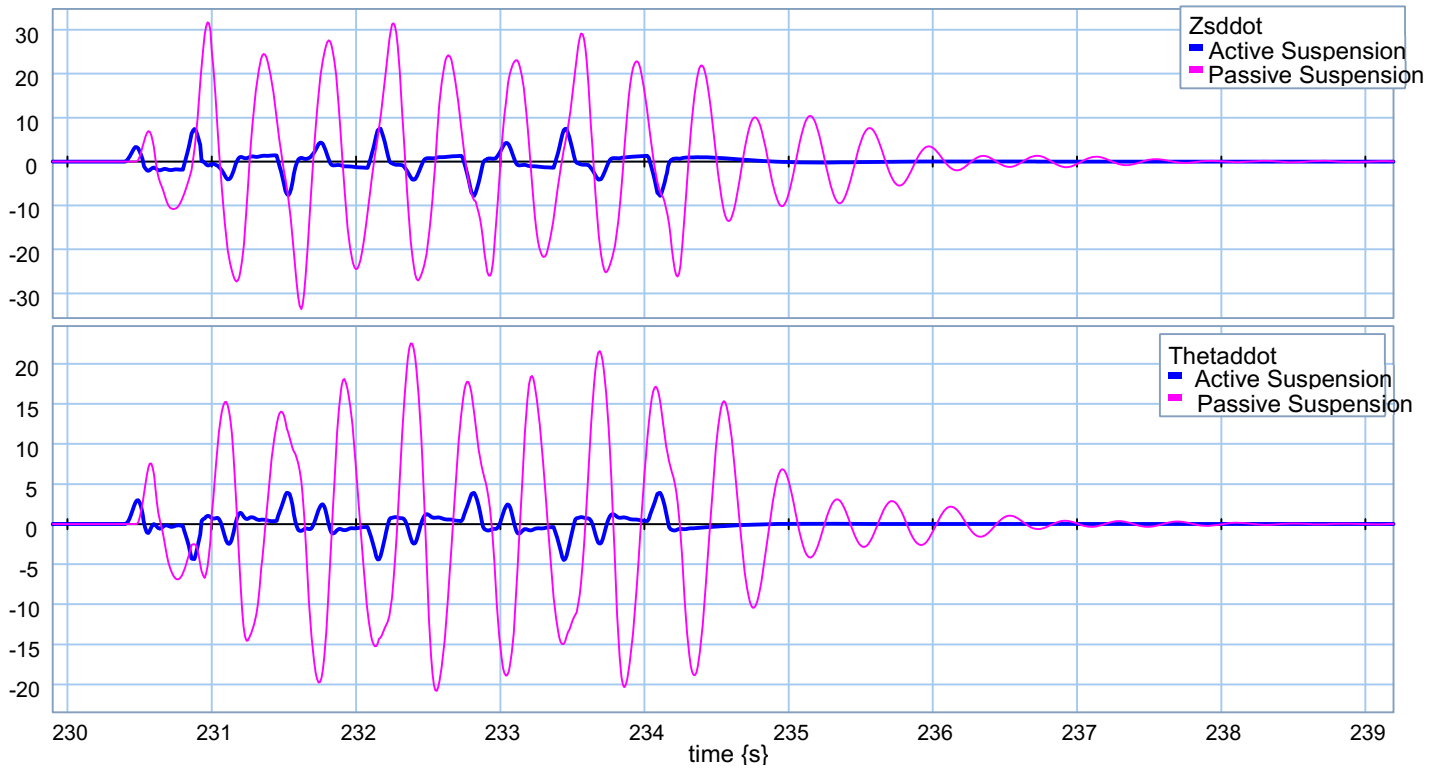


Figure 6.42: Central states over 3rd event of custom road profile

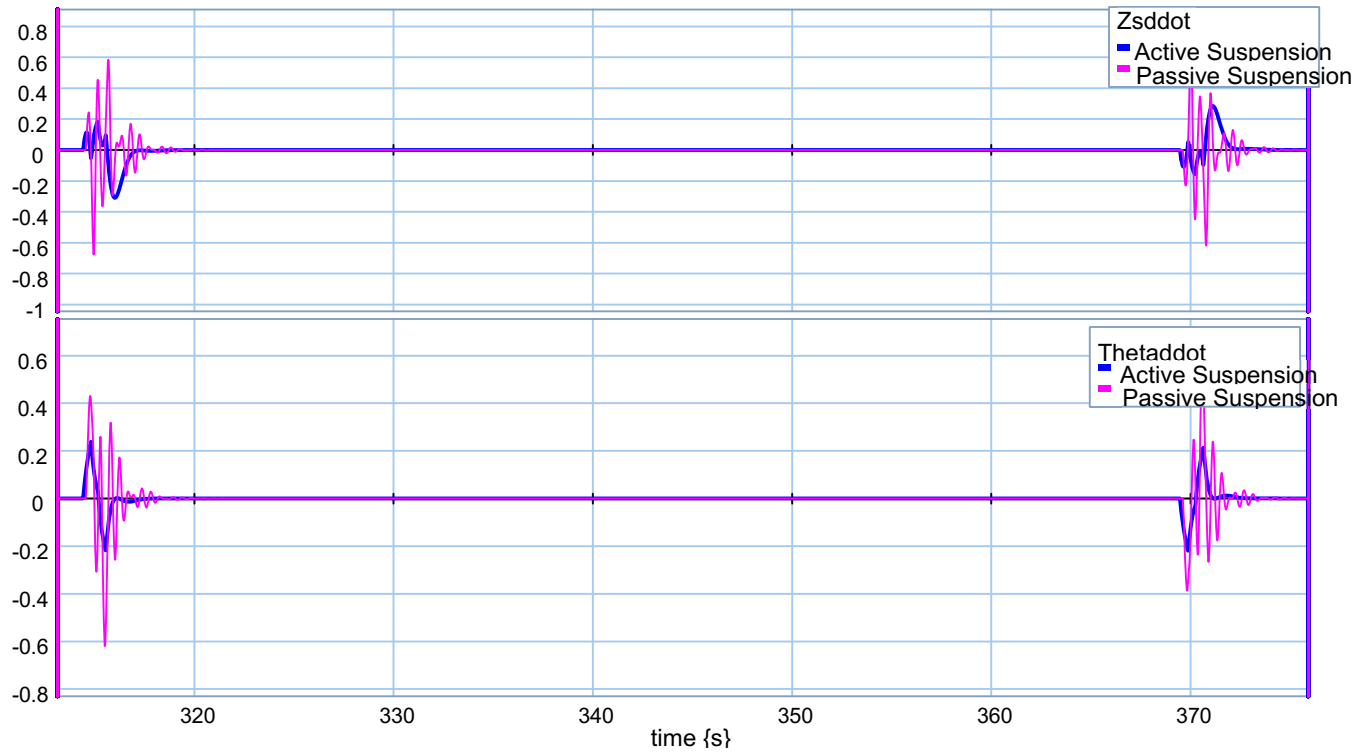


Figure 6.43: Central states over 4th event of custom road profile

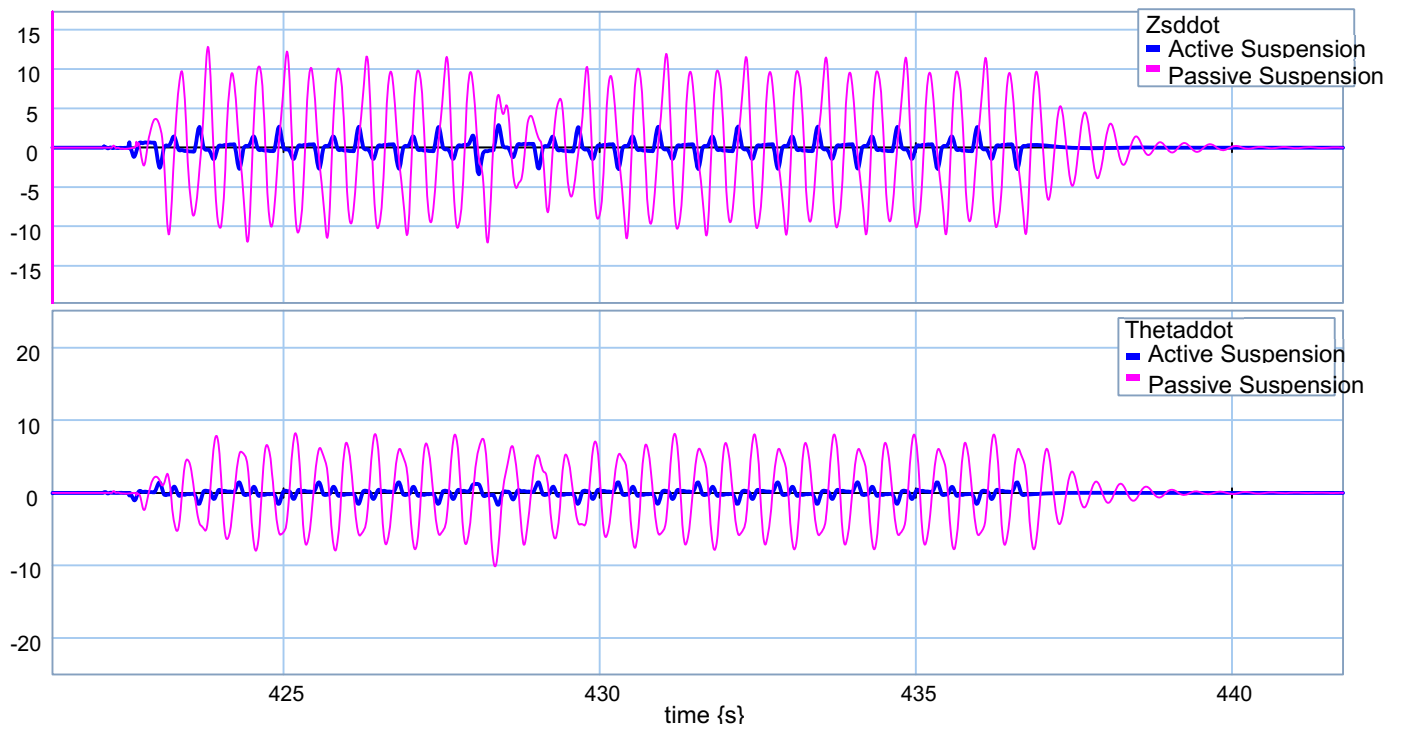


Figure 6.44: Central states over 5th event of custom road profile

6.5.2.1 Ride Quality with Pitch Control

As was discussed in section 6.4, pitch acceleration coefficient ρ_1 was multiplied by “20” in order to have a better improvement on controlling the pitch angle acceleration. Although this factor “20” could improve the pitch acceleration in Wakeham’s work [19], it could not make a significant difference here. The reason could be the huge differences between the vehicle’s parameters in these two works.

6.5.3 Road Holding

Similar to what was done in previous section, five non-linear half-car models were generated corresponding to the five sample cargo masses. The half-car controller with suggested optimum gains outlined in section 6.5.1.2 were used in the front and rear parts of the vehicle and models ran under the same conditions over the custom road profile. The desired results corresponding to the road holding scenario were captured and compared with the situation when there were no actuators used in the vehicle (passive suspension). For instance, results of first model are given in this section. Appendix I covers all graphs for this scenario.

Figures 6.45 and 6.46 demonstrate that the vehicle followed the road profile very well and active suspension could decrease the front and rear performance indices.

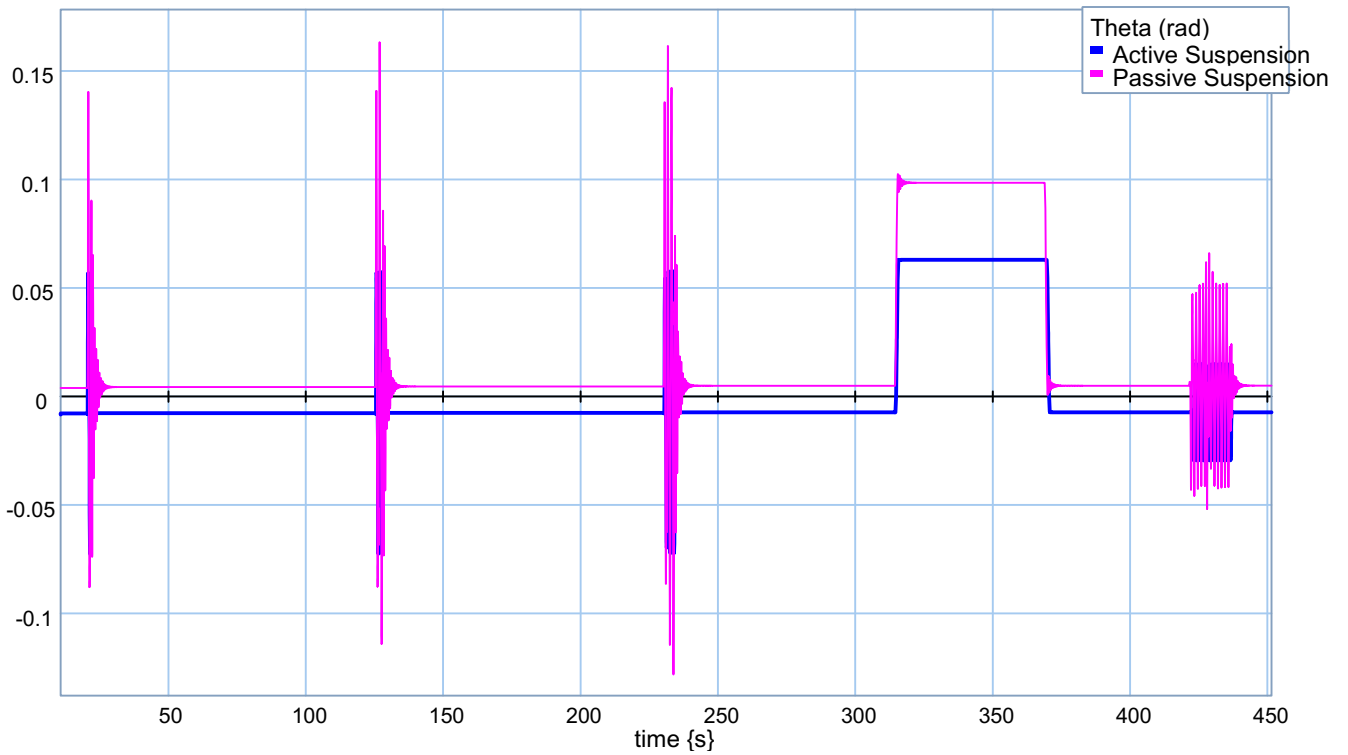


Figure 6.45: Vehicle pitch angle using half-car gains in road holding

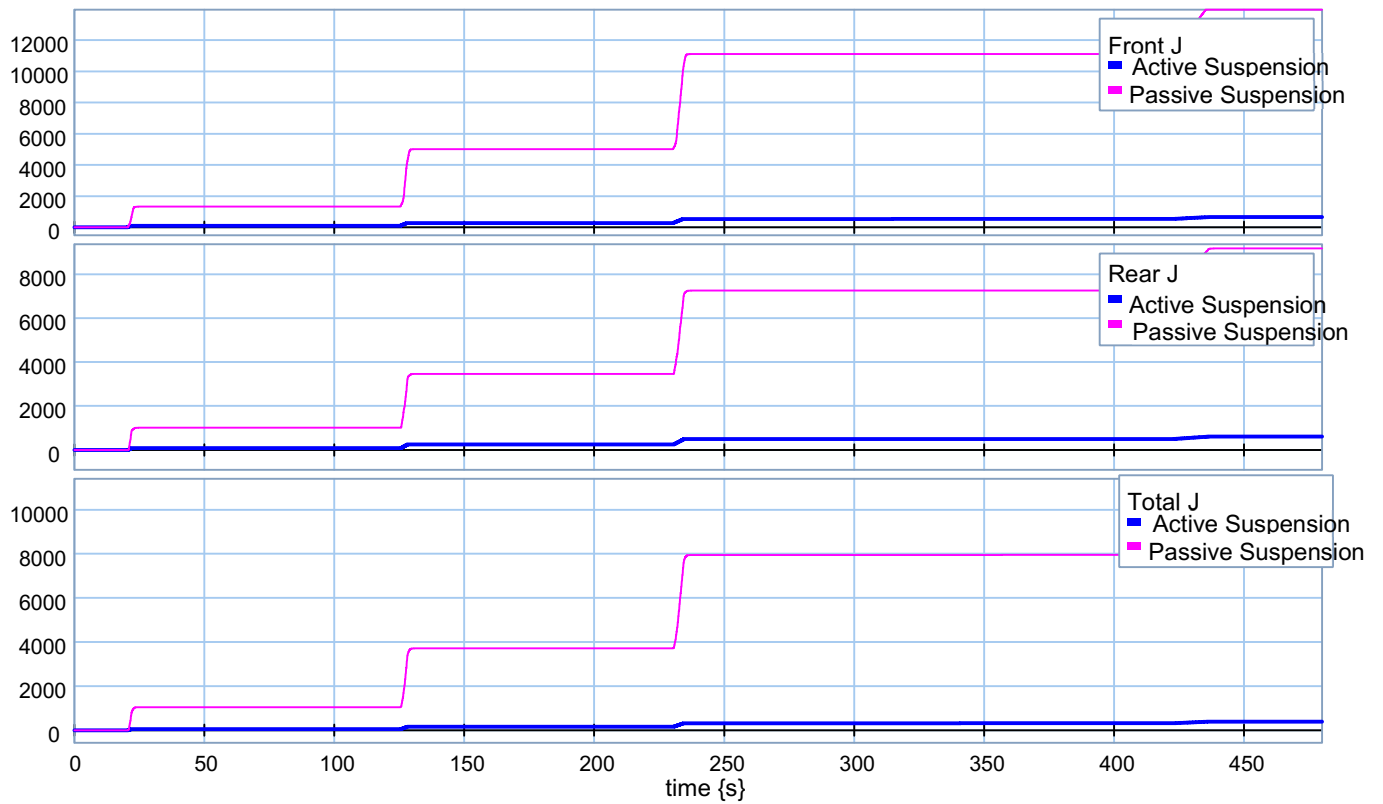


Figure 6.46: Vehicle performance index using half-car gains in road holding

Figures 6.47 and 6.48 represent the effect on having active suspension on tires' vertical velocity and deflection.

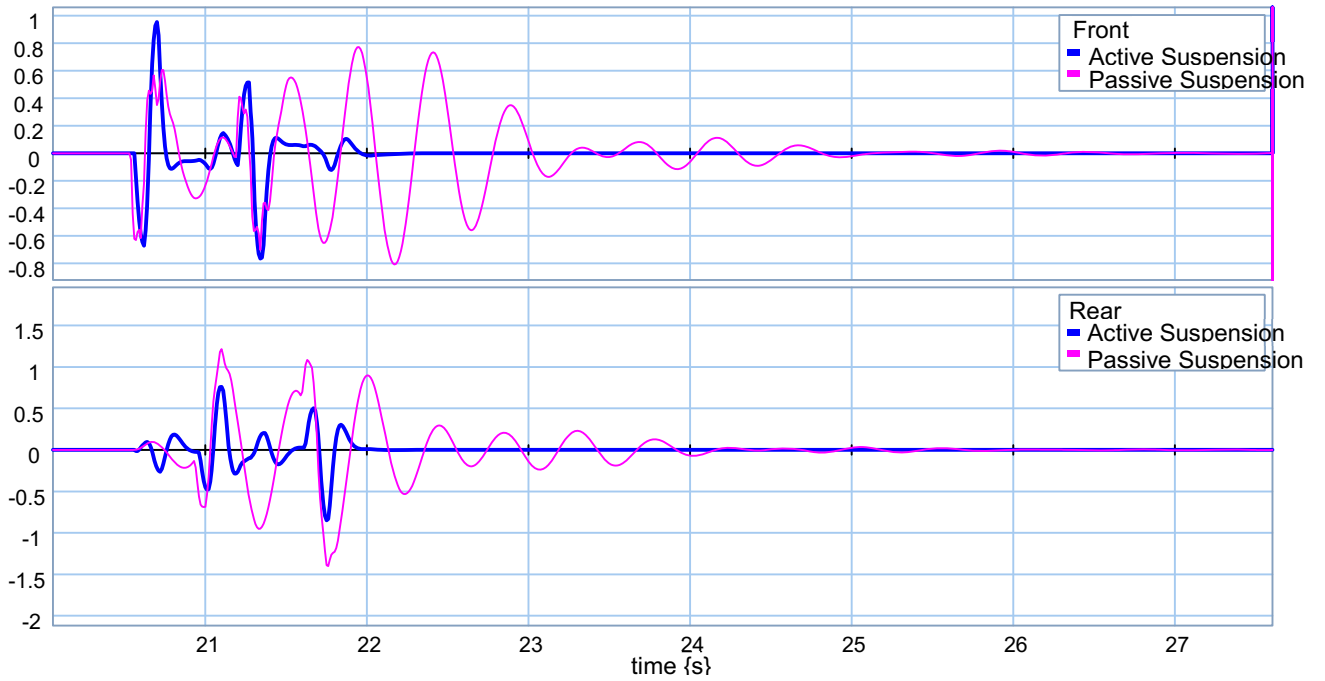


Figure 6.47: Tires' velocities over 1st event of custom road profile in road holding

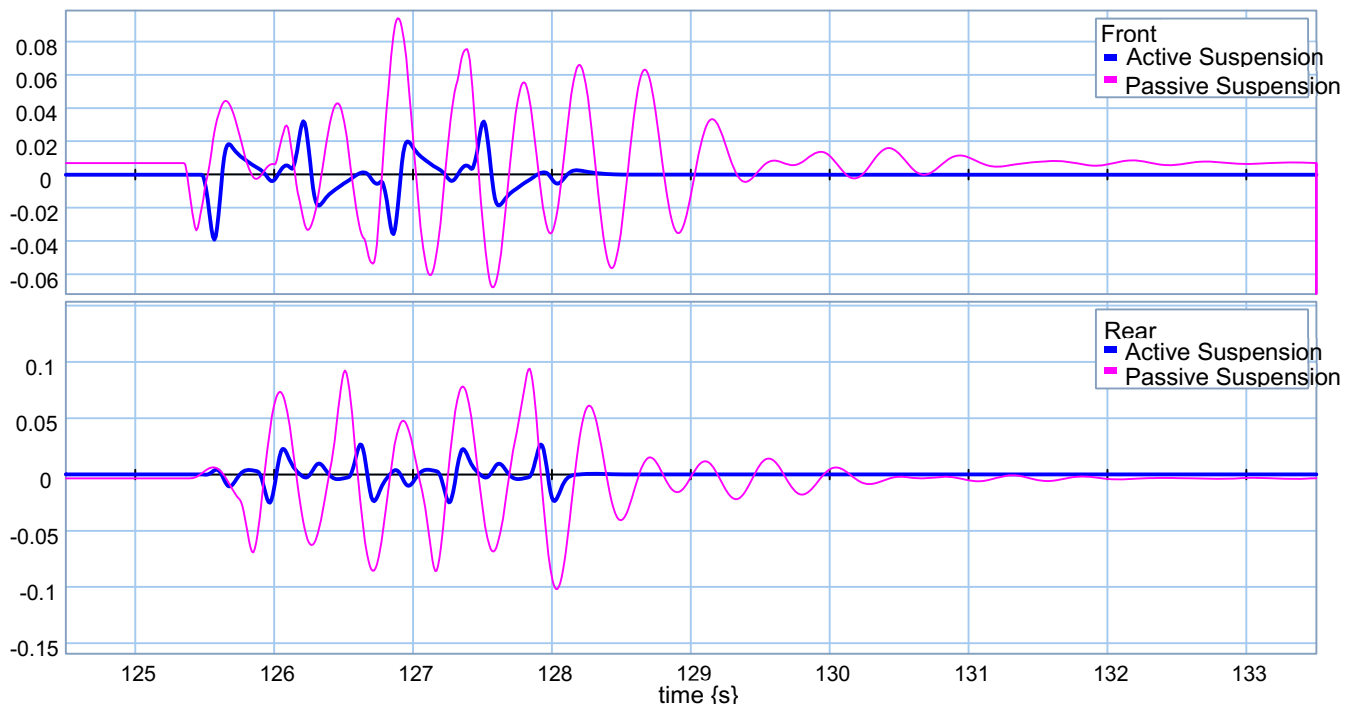


Figure 6.48: Tires' deflections over 2nd event of custom road profile in road holding

6.5.3.1 Heavily Road Holding

In this section, the effects of weighting parameters on road holding performance are studied. In order to control tires' vertical velocities and deflections, first and third coefficients have to be greater than the other ones. As was presented earlier in this chapter, these two coefficients control suspension and tire deflection, respectively. In the heavily road holding scenario, these coefficients are multiplied by "100". The new weighting factors are presented in Table 6.1.

This modification help the vehicle improve its road holding ability. Figure 6.49 compares the new performance index with the passive and previous studied road holding scenario. As it seen, in heavily road holding scenario, the performance index dropped dramatically, which would be result in better performance.

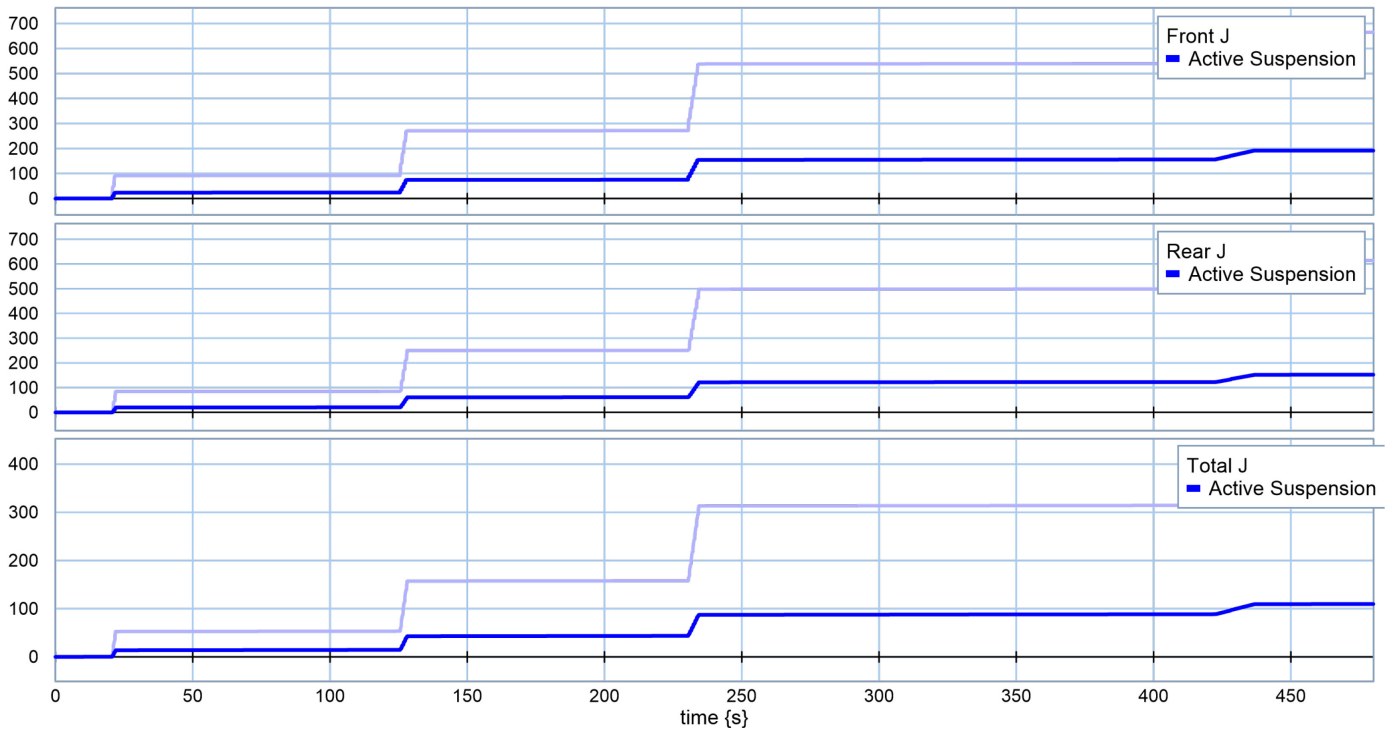


Figure 6.49: Vehicle performance index using half-car gains in road holding

Figures 6.50 and 6.51 demonstrate the advantages of using heavily road holding gains for minimizing tires' vertical velocities and deflections.

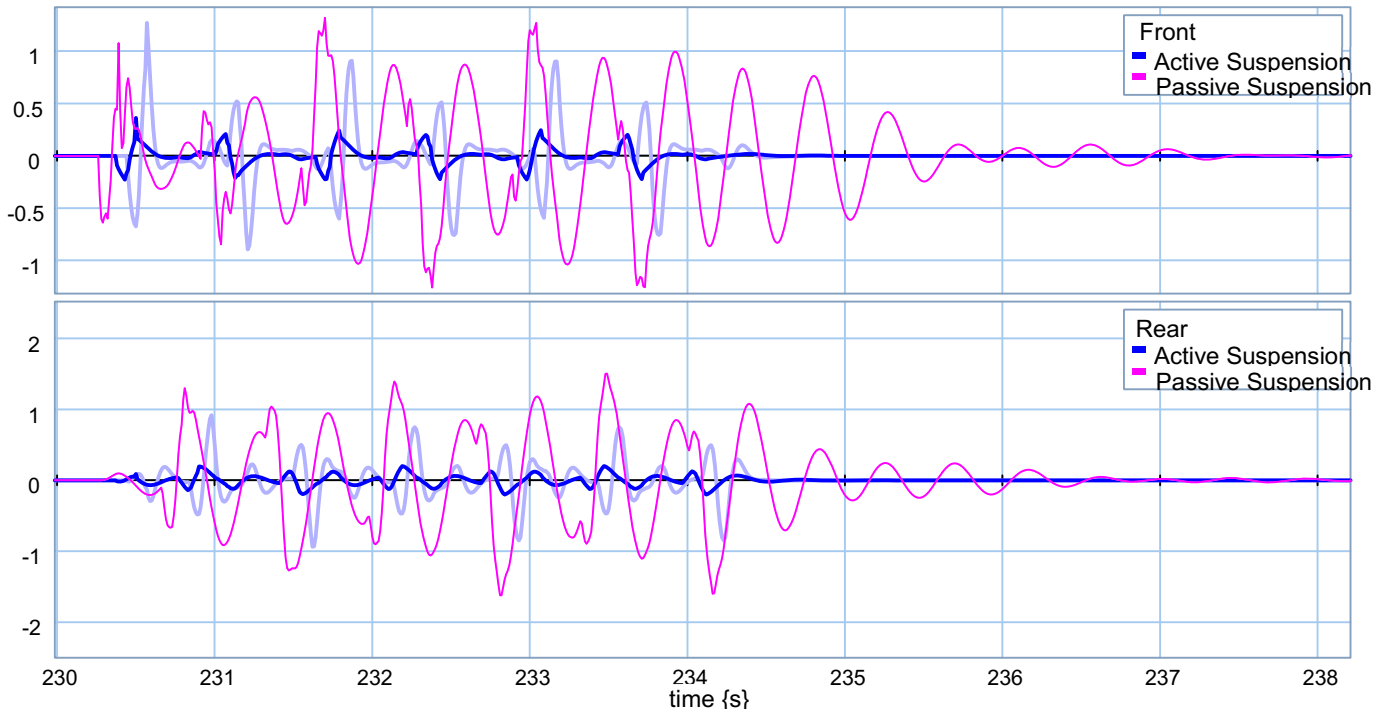


Figure 6.50: Tires' velocities over 3rd event of custom road profile in road holding

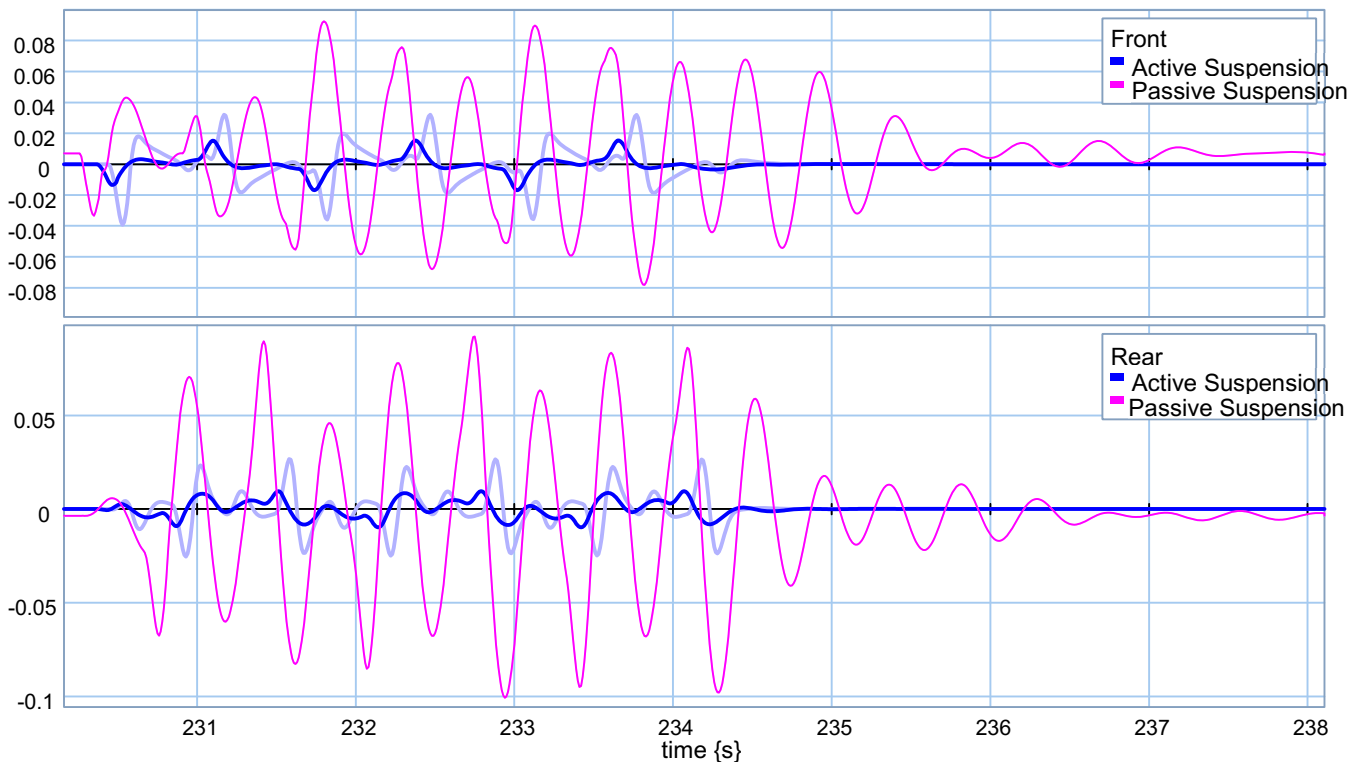


Figure 6.51: Tires' deflections over 3rd event of custom road profile in road holding

6.6.5 Comparison between Quarter-Car Controllers and Half-Car Controller

Both quarter-car and half-car approaches could perfectly meet the purposes they were used for. Appendix J demonstrates data for this comparison in detail. For instance, in this section, the vertical and pitch accelerations for passive and active suspensions are compared. In order to quantify this comparison, two indices are defined as follows:

$$ZI = \int \dot{Z}_s^2 \cdot dt \quad (6-48)$$

$$TI = \int \dot{\theta}^2 \cdot dt \quad (6-49)$$

On a flat road profile, these two indices are zero. Bumps in road profiles make fluctuations in the vertical and pitch acceleration trends, and those indices represent some sort of fluctuations. A better active suspension unit will result in lower indices. Table 6.5 classifies these indices for passive, quarter-car active, and half-car active suspension units for all five studied cases. The vertical acceleration was minimized better while two quarter-car controllers were used. The other index claims that pitch angle acceleration is minimized better with quarter-car controllers when cargo mass is not exceeding almost 9000 kg. Otherwise, half-car approach presents better performance in damping the pitch angle acceleration.

Table 6.5: Ride quality indices comparison

Ride Quality Indices		Mc = 0	Mc = 4500	Mc = 9000	Mc = 13500	Mc = 18000
Thetadot Index	Passive	1546.53	169.20	89.95	101.43	127.62
	Quarter-Car Model	22.53	8.68	7.28	8.60	10.91
	Half-Car Model	23.66	13.82	10.48	8.28	6.63
Zsddot Index	Passive	3446.57	1655.29	649.58	591.42	746.48
	Quarter-Car Model	67.82	27.14	11.33	6.5	5.74
	Half-Car Model	71.36	34.11	24.03	19.51	16.22

6.7 Summary of Conclusions

In the first part, the linear half-car model ran several times over the rough terrain outlined in Chapter 4 while different cargo masses and gain matrices were considered. Having defined the energy indices, an optimum set of gains were presented. These steps were done for both scenarios, i.e., ride quality, and road holding.

$$Energy\ Index = \int Actuator\ HorsePower^2 . dt \quad (6-50)$$

Once the optimum set of gains was presented, the complex non-linear half-car model ran over the severe bumpy road profile outlined in Chapter 4. For every single road events, the results were presented in detail. This procedure was done for each scenarios and the effects of having half-car controllers instead of two quarter-car based actuator units were studied. Results proved that for both scenarios, using active suspension units are superior to the passive ones.

In the last part, the performance of the quarter-car and the half-car based actuators were compared. This comparison was quantified by defining two indices for vertical and pitch accelerations. Table 6.5 demonstrated the results of this comparison, in detail.

Chapter 7

Energy Analysis

7.1 Introduction

Energy has affected everyone's lives and has played an important role everywhere. Meeting the growing demand for saving energy by designing less-wasted systems is a key challenge. Energy is conserved and that means it cannot be either created or be destroyed, but it could be transformed from one form to another. In a simple definition, it can be

explored as an ability of a system to perform work. In classical Mechanics, work is considered as a form of energy and can be presented as follows:

$$Work = \int_A^B \vec{F} \cdot d\vec{s} \quad (7-1)$$

where:

\vec{F} : Force Vector

$d\vec{s}$: Path Element

A : Starting Position

B : Finishing Position

In vehicle dynamics, engine energy is transferred to many other forms while the vehicle is travelling. In a rough terrain lots of energy is converted to heat power in suspension units. Dampers, which are also known as shock absorbers, dissipate the suspension energy in a natural way. The overall energy consumption of the vehicle can be declined if somehow this wasted energy can be reclaimed and re-injected to the system. There are many works done in this area and some mathematically effective ways have been presented in order to reclaim that energy such as modifying the suspension units with hydraulic storage [30], battery coil [31], rack and pinion [32], ball screw [33], linear motion [34], and etc.

Dissipated energy in suspension dampers (shock absorbers) is dependent on which types of suspension is used in the vehicle. In the previous chapters, effects of using active suspension units on ride quality and road holding scenarios were studied. Here, in this chapter, by comparing dissipated energy in shock absorbers for passive and active suspensions, ride quality and road holding are studied again while there is limitation on actuator forces and suspension spring deflections. Results obtained from simulations in this chapter will clarify if it is energy-efficient to replace passive suspension units with either quarter-car or half-car active suspension ones.

7.2 Dissipated Energy in Shock Absorbers

When a vehicle travels on a bumpy road, the road profile cause a shock between the sprung and unsprung masses. A shock absorber, which is a type of dashpot, is a mechanical device designed to damp this shock. In mechanical systems, it is known as a damper which is converting the kinetic energy into the heat power in this case. Dissipated energy in a shock absorber can be evaluated by manipulating the equation 7.1 as follows:

$$W_b = \int F_b \, dx \quad (7-2)$$

$$W_b = \int F_b \frac{dx}{dt} \, dt \quad (7-3)$$

$$W_b = \int F_b \, V \, dt \quad (7-4)$$

Where:

F_b : Damping Force

V : Suspension Vertical Velocity

By substituting the damping force into the equation 7.4, a closed form equation will be derived based on damping coefficient b and suspension velocity V , representing the dissipated energy in a shock absorber.

$$W_b = b \int V(t)^2 dt \quad (7-5)$$

7.3 Active Suspension Actuators

In general, an actuator is defined as a motor which is responsible for controlling a mechanism or system at a desired level. In active suspension designing for a half-car model, actuators raise or lower the chassis height in the front and rear section of the vehicle. By doing this, they could improve ride quality or road holding or any other desired scenario while appropriate weighting factors and cost function had defined. In both quarter-car and half-car active suspension models, actuators do work when states are off their desired levels. For instance, in ride quality scenario, where the purpose is controlling vertical acceleration, actuators don't make any forces when the vehicle is travelling on a flat road. But as soon as

the vehicle hits a bump on its way, actuators generate forces and try to meet the purpose as soon as possible.

In theory, ride quality or road holding can be improved in the best way while appropriate weighting factors are chosen for designing active suspension units. However, in reality, in energy's point of view, it may not be beneficial to install those actuators as they may require much more energy than the amount that the vehicle's engine could produce. Hence, there is a trade-off between having the best performance and spending the least energy.

7.4 Limitation on Actuator Force

As it was pointed out in previous section, in reality, an appropriate limitation on active suspension actuators is needed. In this research, this limitation is applied based on a primitive assumption about the percentage of engine energy going to actuators. However, the input energy for front and rear actuators are not considered equal as the rear actuator needs to generate more energy than the front one due to differences in vehicle's parameters for the front and rear. Table 7.1 classified the assumption considered on actuation units.

Table 7.1: Assigned power from engine for actuating units

Engine Power	Actuators' Power Percentage	Total Actuators' Power Amount	Front Actuator's Power Amount	Rear Actuator's Power Amount
460 hp	25%	115 hp	40 hp	75 hp

In this section, the first model ran on the custom bumpy road profile outlined in chapter 4 while there were two independent quarter-car active suspensions had used in the front and rear part of the vehicle. Figures 7.1 and 7.2 represent required force for the actuators after limitation.

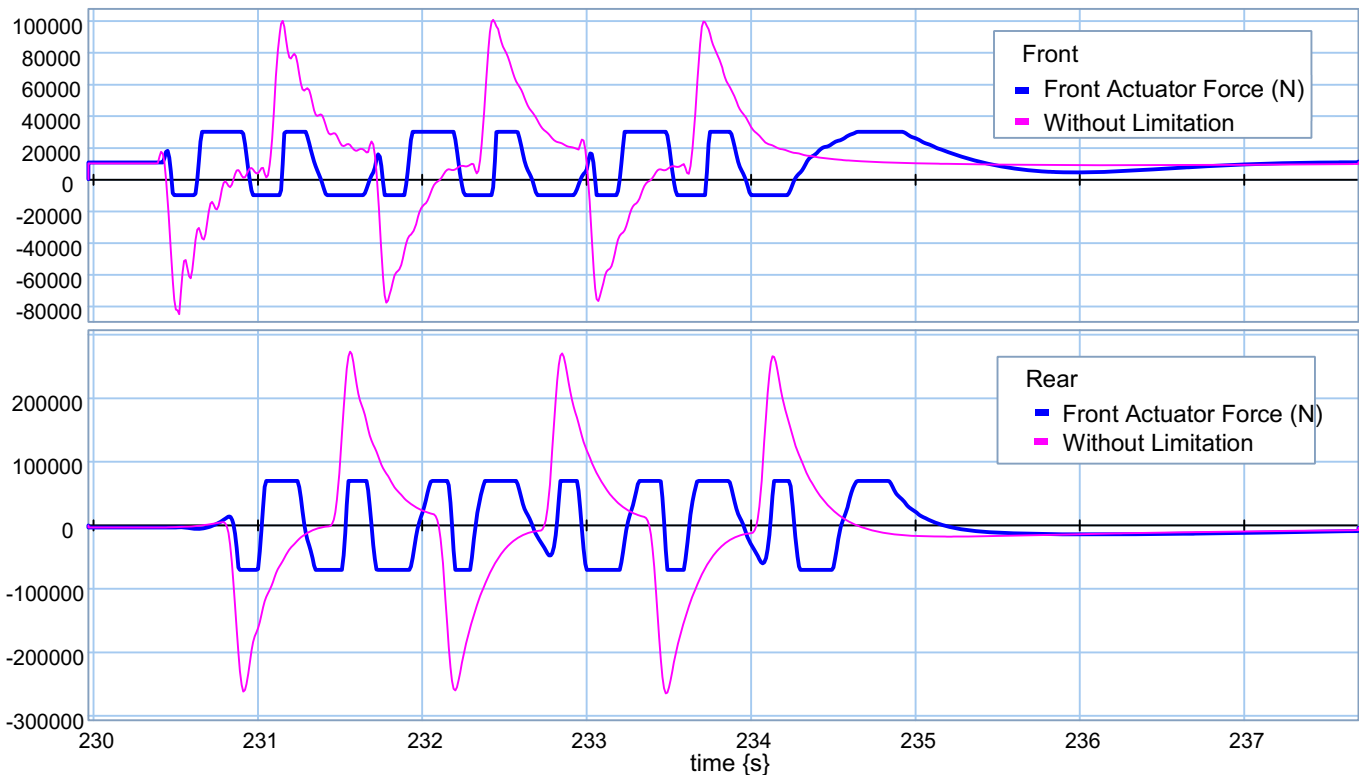


Figure 7.1: Limitation on actuator force for 3rd event on the road profile using quarter-car active suspension units

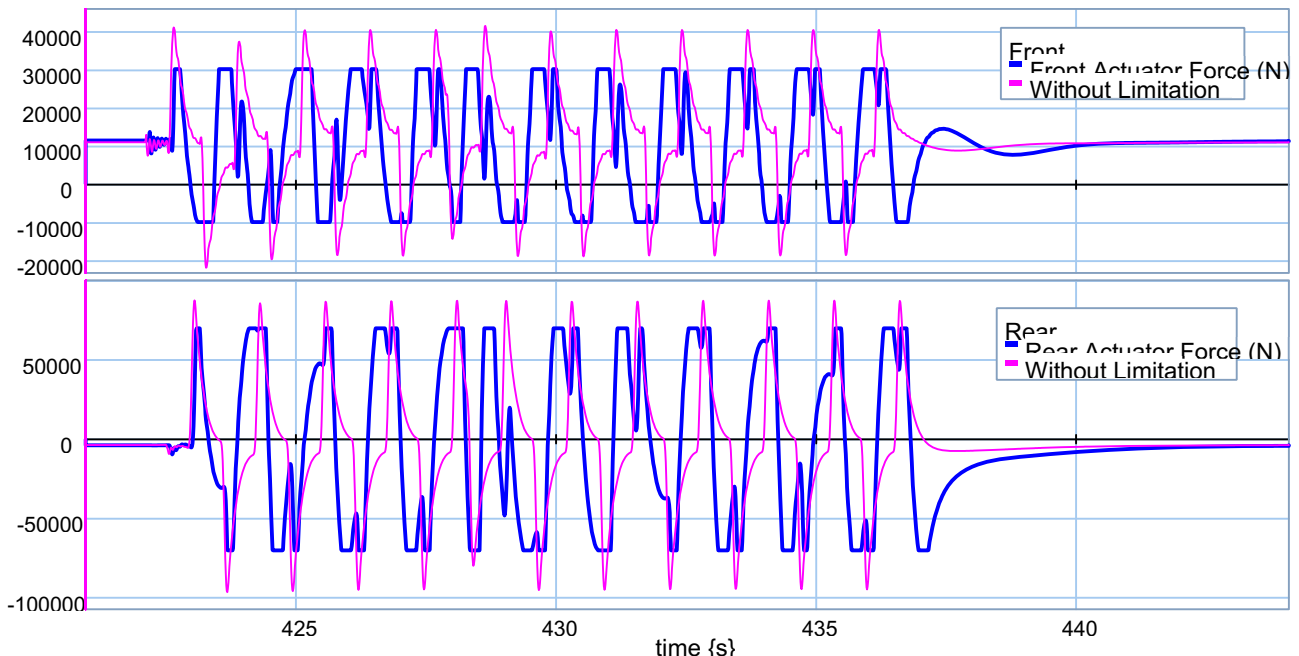


Figure 7.2: Limitation on actuator force for 5th event on the road profile using quarter-car active suspension units

Figures 7.3 and 7.4 compare the required horsepower for the front and rear actuators for the 3rd and 5th events on the studied road profile. The 3rd event contains three severe continuous bumps and the 5th event represents a normal rough terrain.

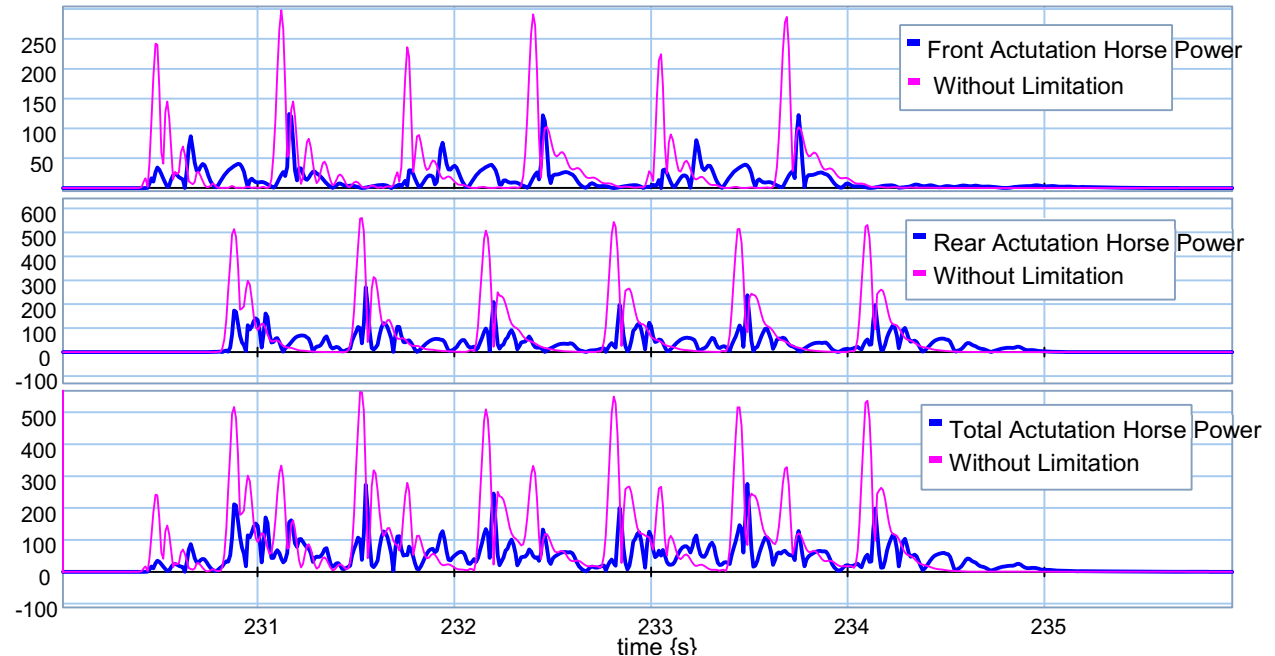


Figure 7.3: Limitation on actuator power for 3rd event on the road profile using quarter-car active suspension units

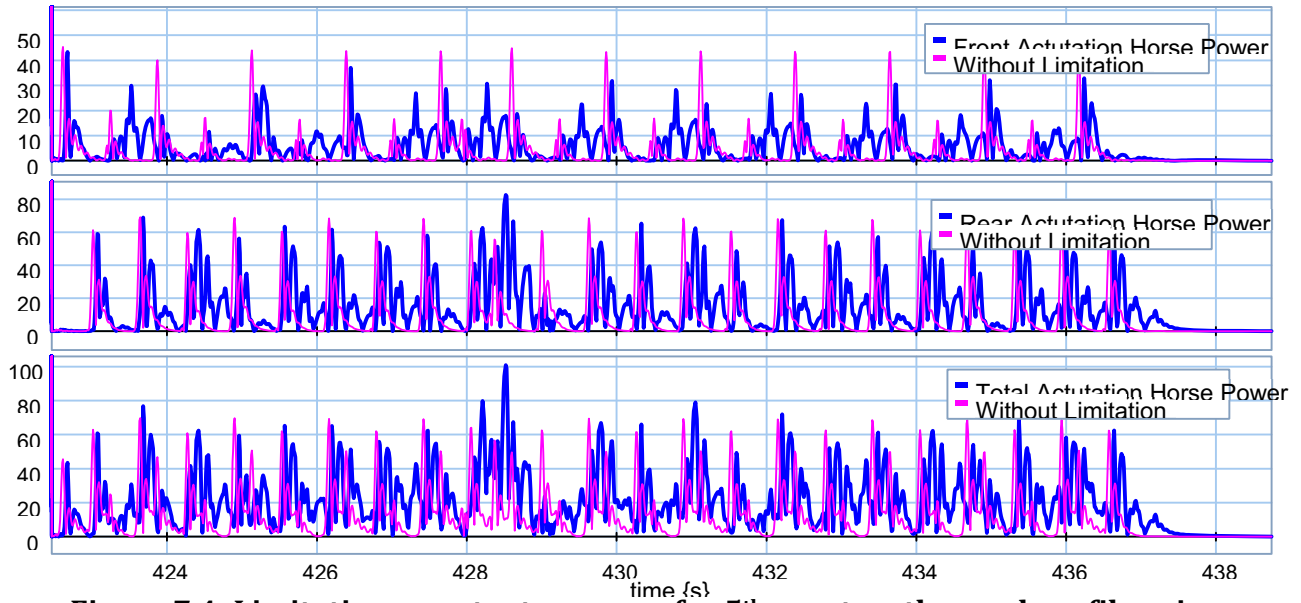


Figure 7.4: Limitation on actuator power for 5th event on the road profile using quarter-car active suspension units

Figures 7.5 to 7.8 compare the same Figures when two quarter-car active suspension has been replaced with half-car active suspension units.

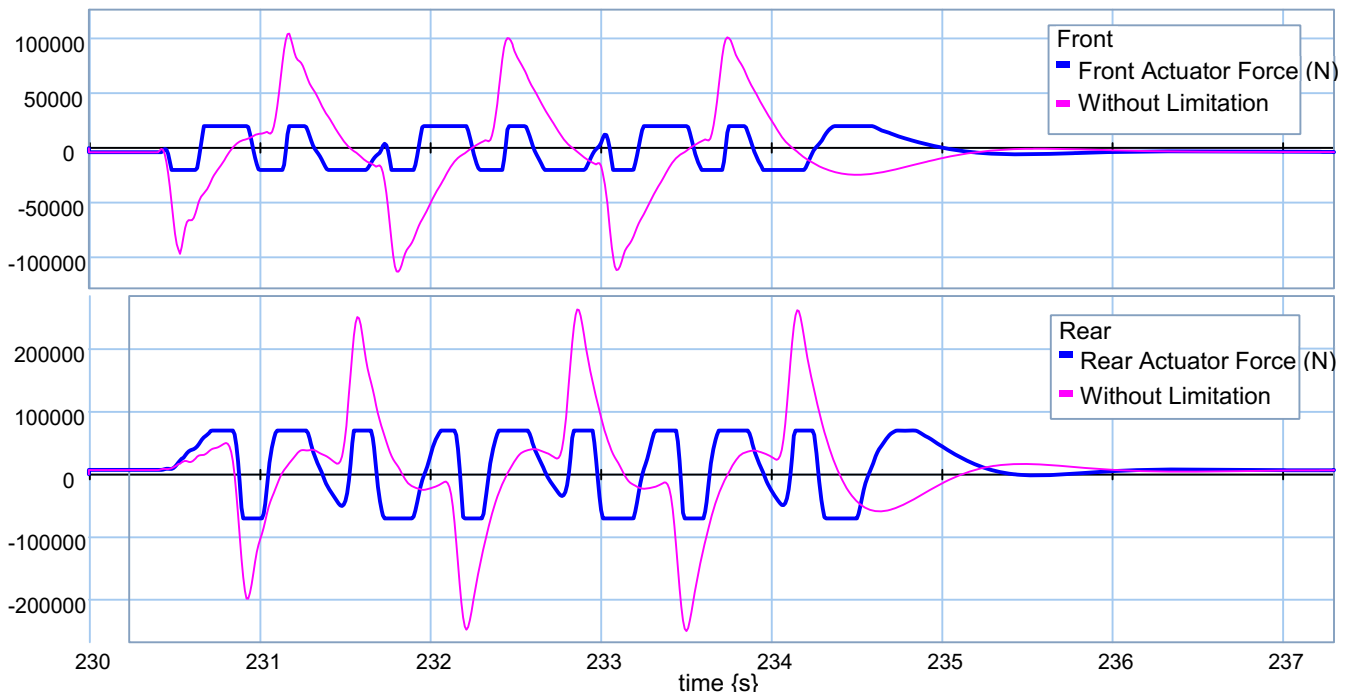


Figure 7.5: Limitation on actuator force for 3rd event on the road profile using half-car active suspension units

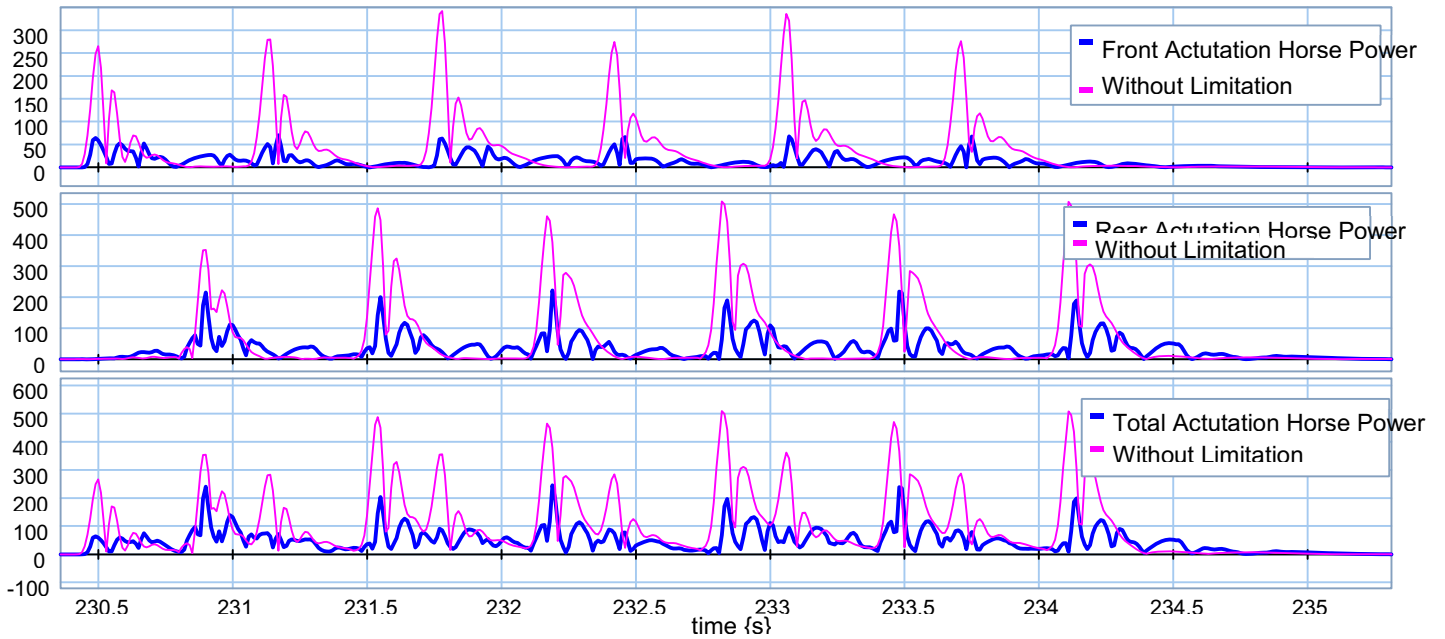


Figure 7.6: Limitation on actuator power for 3rd event on the road profile using half-car active suspension units

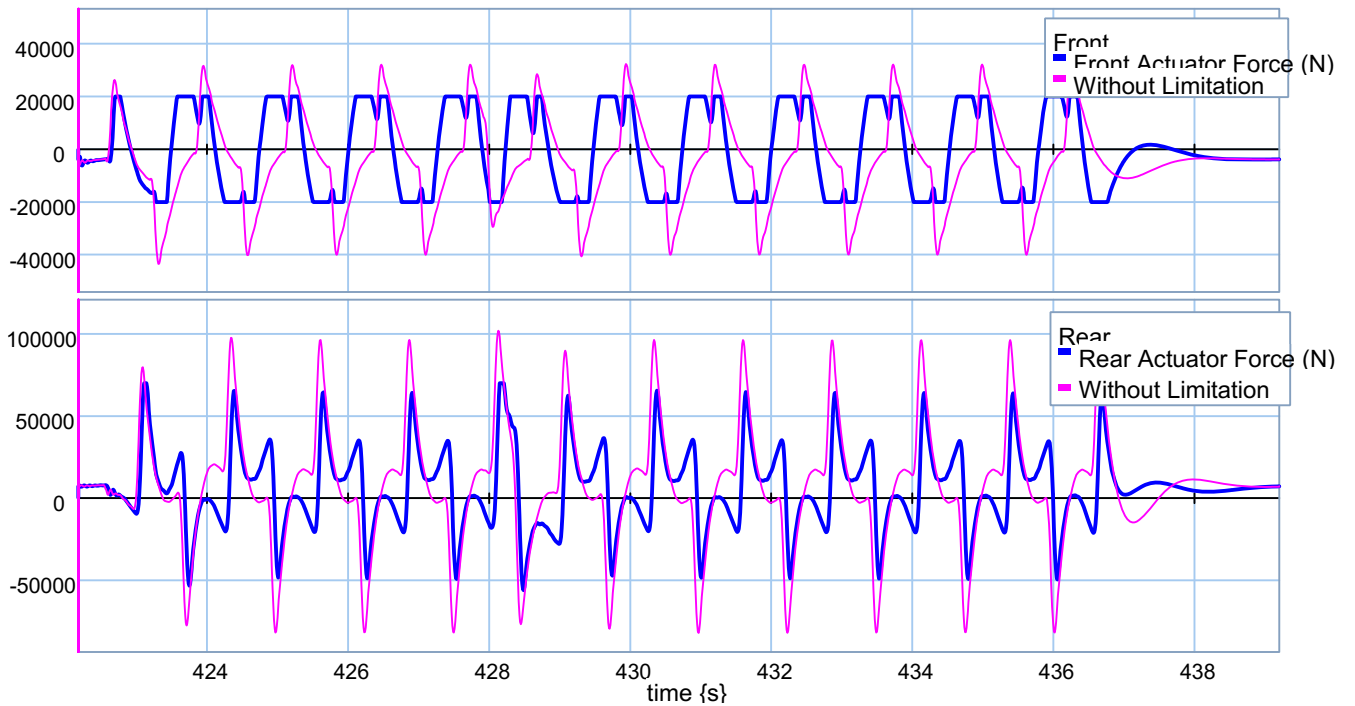


Figure 7.7: Limitation on actuator force for 5th event on the road profile using half-car active suspension units

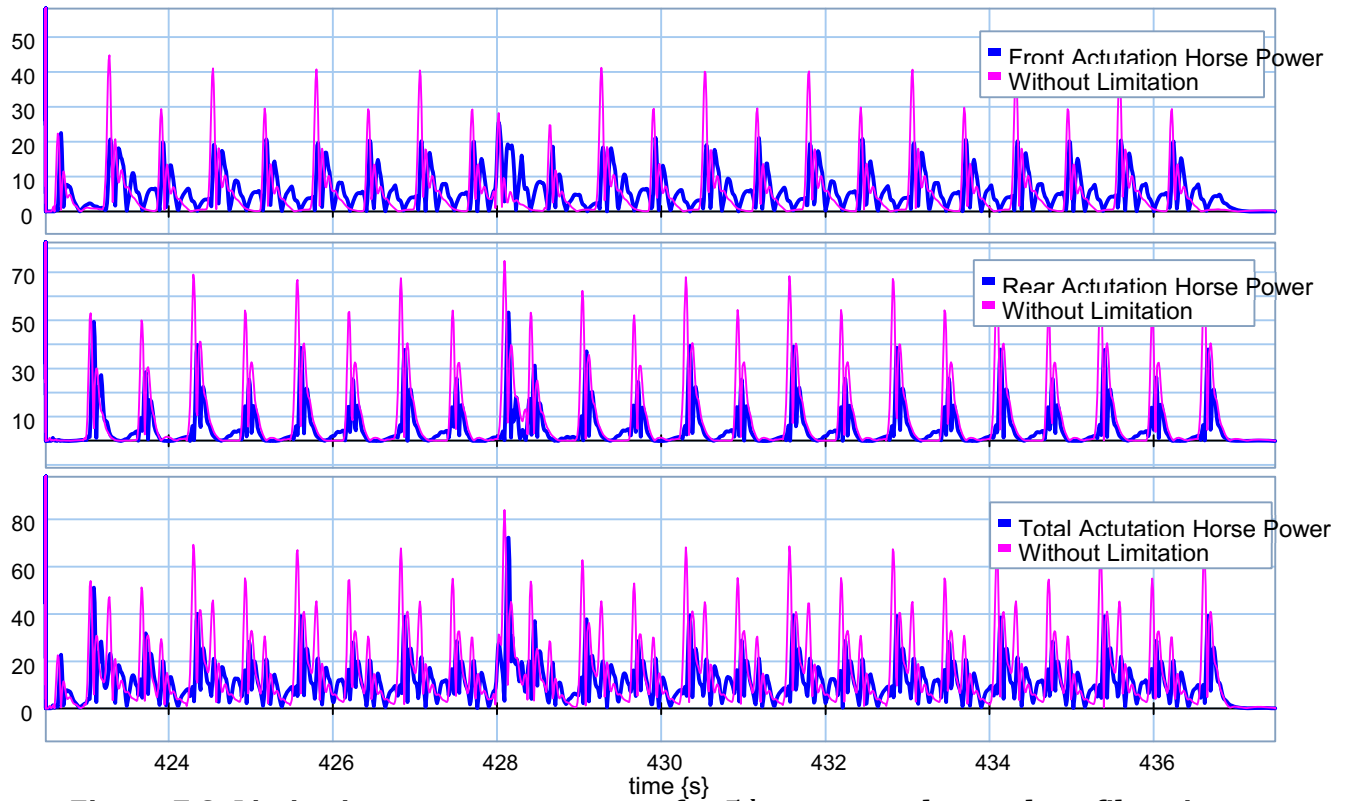


Figure 7.8: Limitation on actuator power for 5th event on the road profile using half-car active suspension units

7.5 Limitation on Spring Deflection

Another limitation which has to be considered in order to make the simulation more realistic is controlling the suspension spring deflection. In reality, force-deflection relationship for a spring force is not linear in all region. Figure 7.9 demonstrate the model which is used in this work for suspension springs.

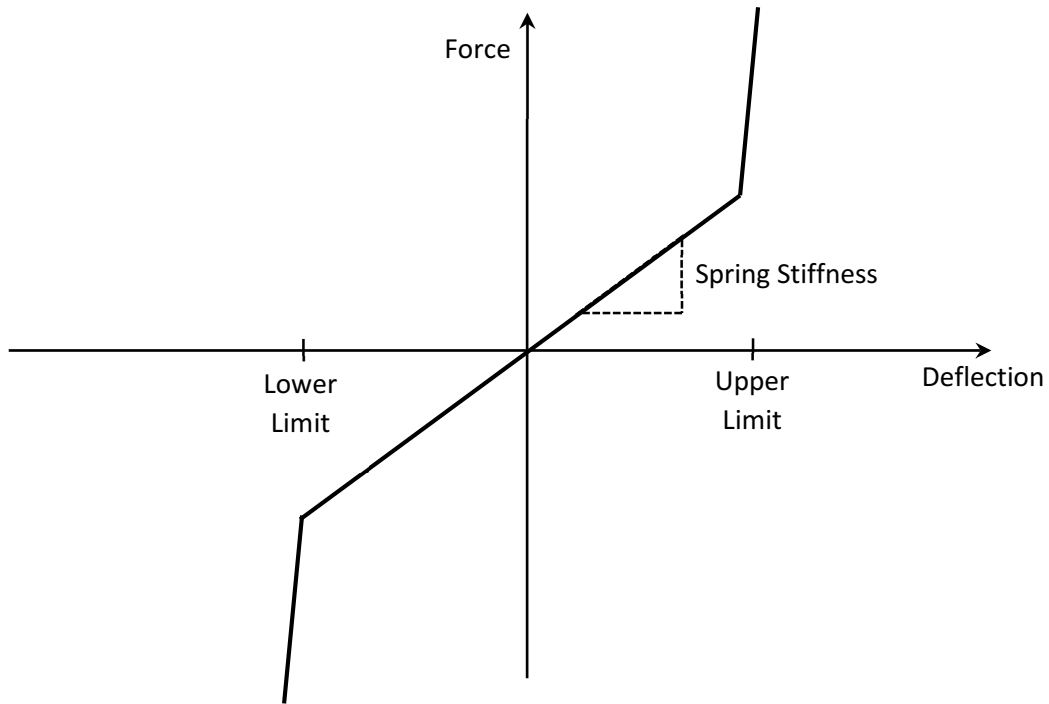


Figure 7.9: Force-deflection relationship for a realistic spring

In this Figure, slope for the middle part represents the spring stiffness, while slopes for the other two regions are bushings' stiffnesses. Figures 7.10 and 7.11 compare the springs' deflections for the following three scenarios for quarter-car and half-car active suspension modes, respectively.

- a. Passive suspension
- b. Active suspension without limitation on required actuations' forces and springs' deflections
- c. Active suspension with limited assigned force to actuators and controlled springs' deflections

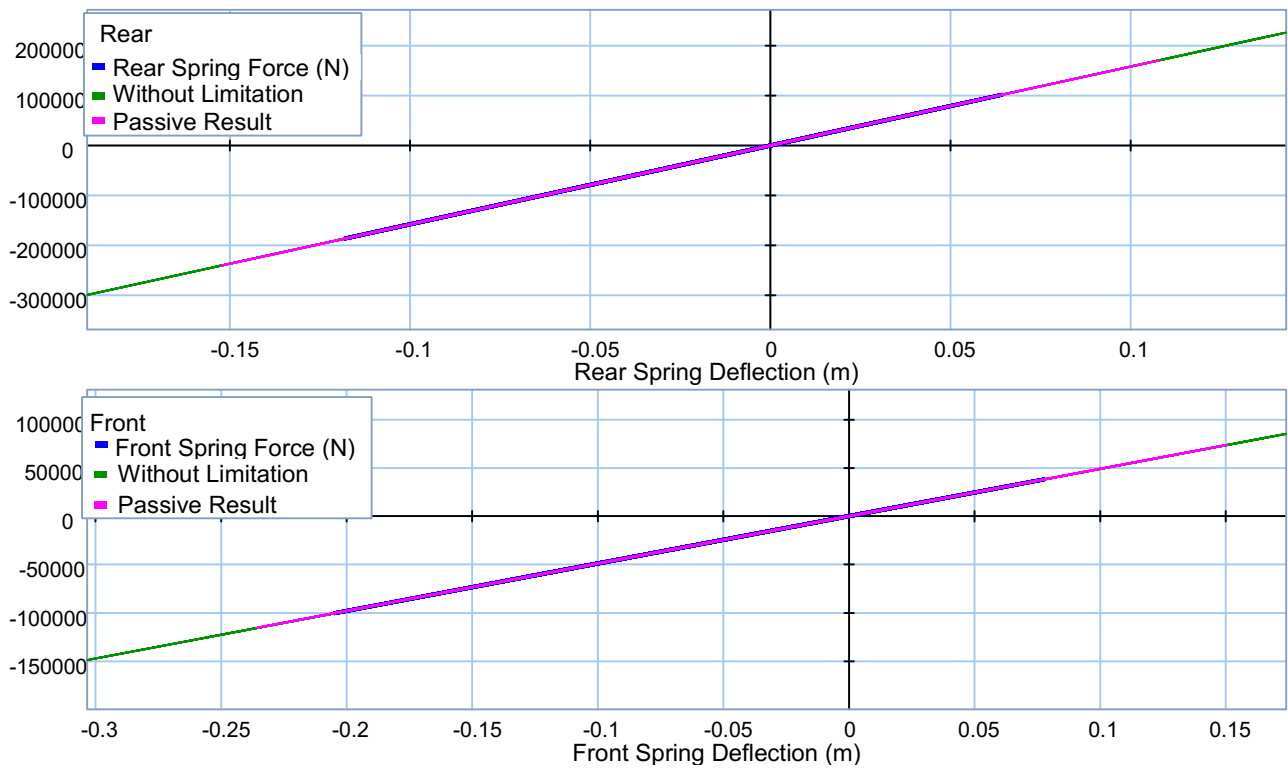


Figure 7.10: Force-deflection relationship for a realistic spring in QCM

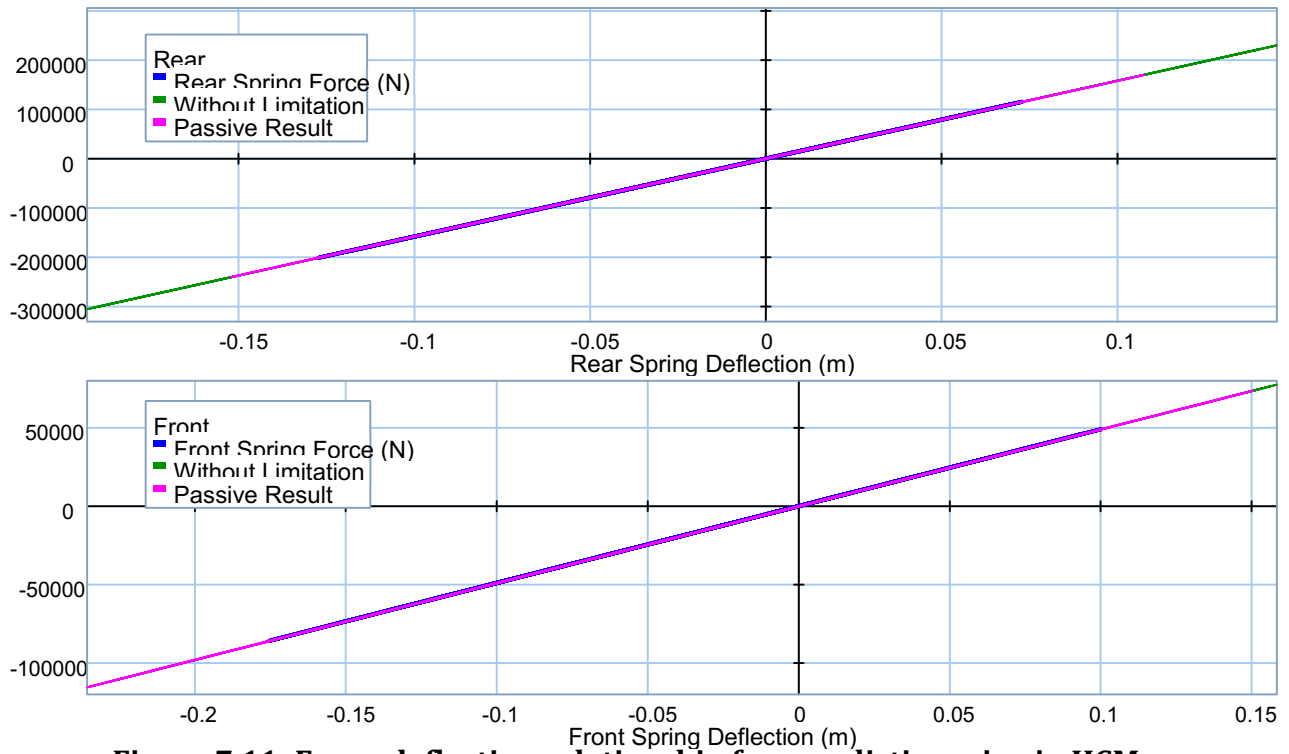


Figure 7.11: Force-deflection relationship for a realistic spring in HCM

7.6 Half-Car Model using Two Quarter-Car Active Suspension Units

As it was outlined in chapters 5 and 6, the proposed actuation units could perfectly control the vehicle vertical and pitch accelerations in ride quality scenario. One of the best way to verify this claim is by comparing the performance indices in passive and active suspensions. As it was expected, limiting the actuator forces and controlling spring deflections move the system from its ideal situation where the performance index was at its minimum value. Figures 7.12 and 7.13 demonstrate the performance index trend when quarter-car and half-car active suspensions were used, respectively. By analyzing these graphs, it could be deduced that even the new model can lower the performance index very well.

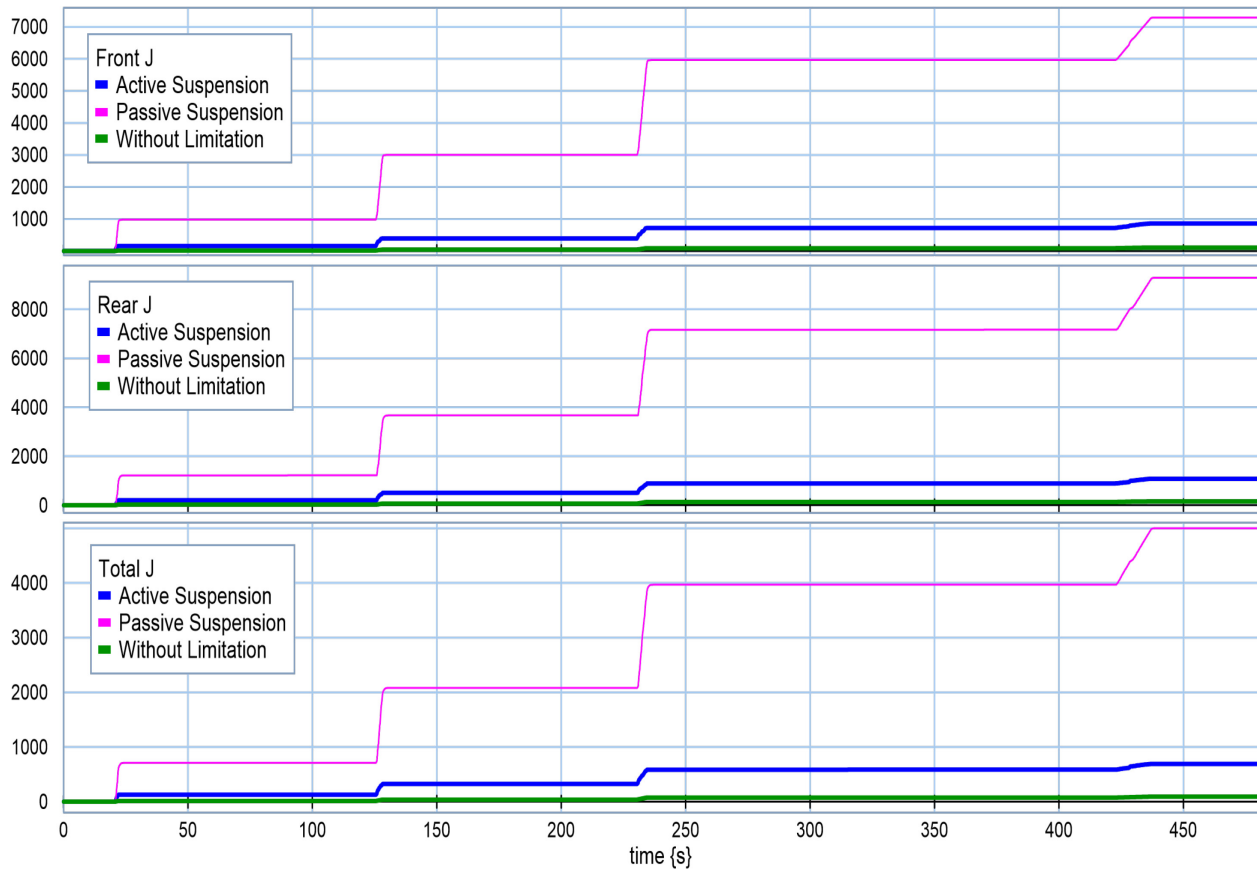


Figure 7.12: Performance indices using quarter-car active suspension units

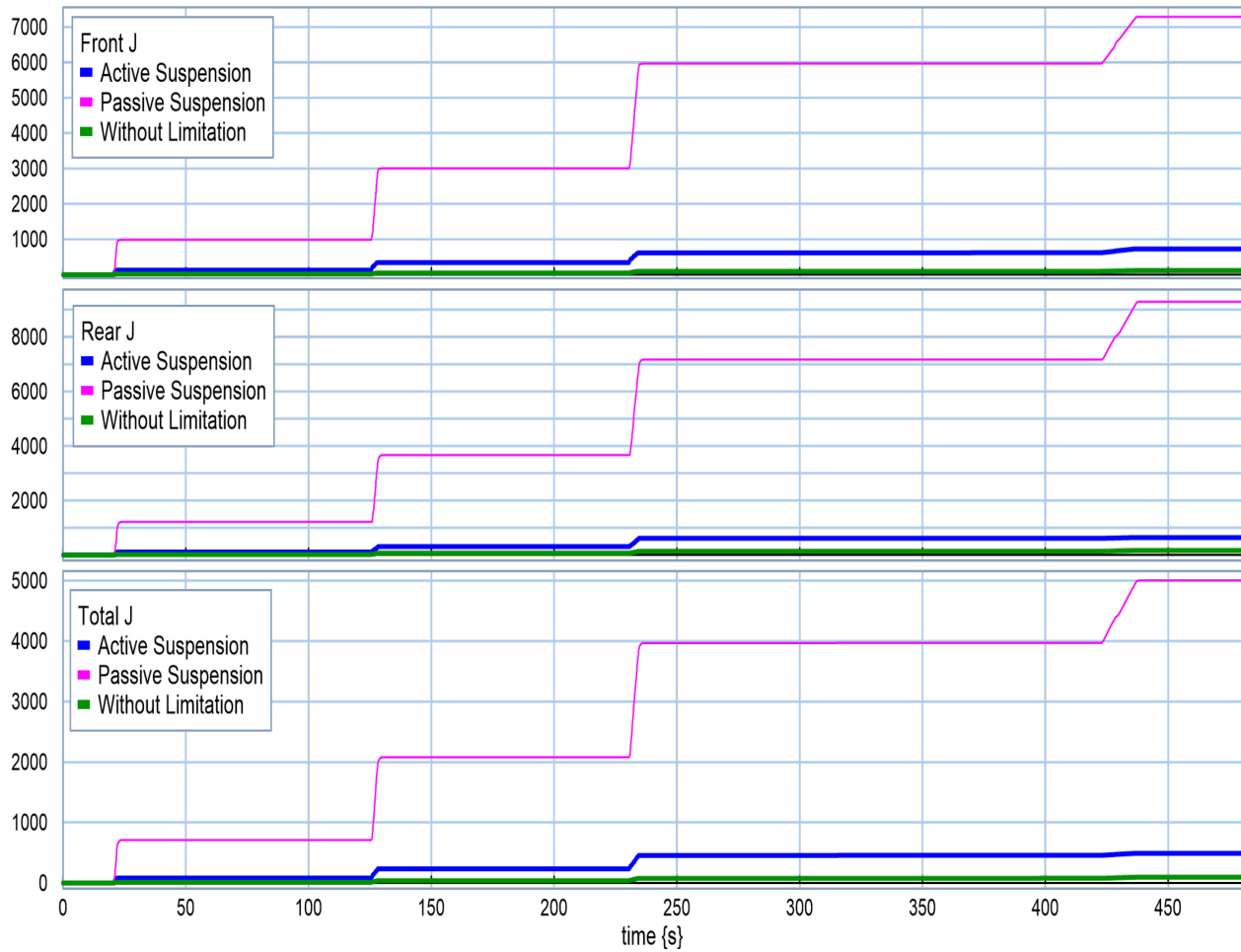


Figure 7.13: Performance indices using half-car active suspension units

On another hand, dissipated energy in shock absorbers was recorded for all three considered cases outlined in previous section. The highest lost energy happened in passive suspension scenario. Graphs 7.14 and 7.15 demonstrate the amount of horsepower which can be saved by using active suspension units.

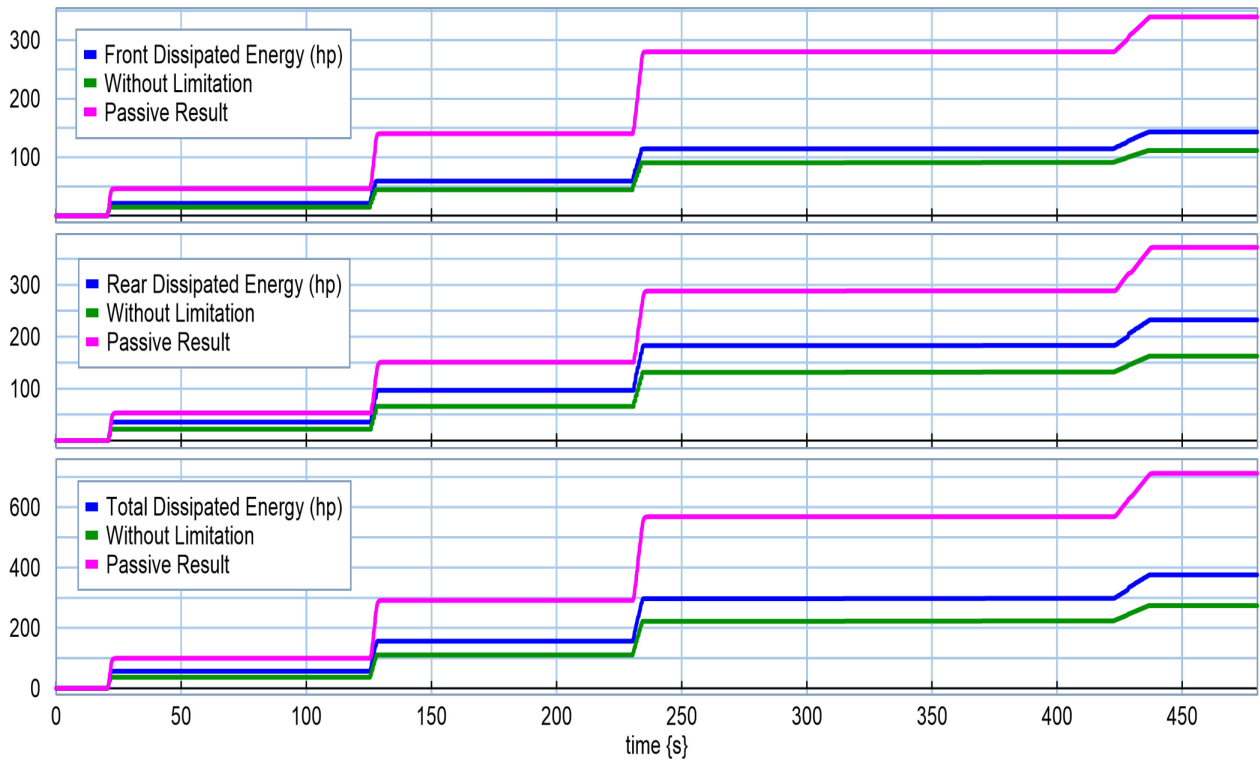


Figure 7.14: Dissipated power in suspension using quarter-car actuation units

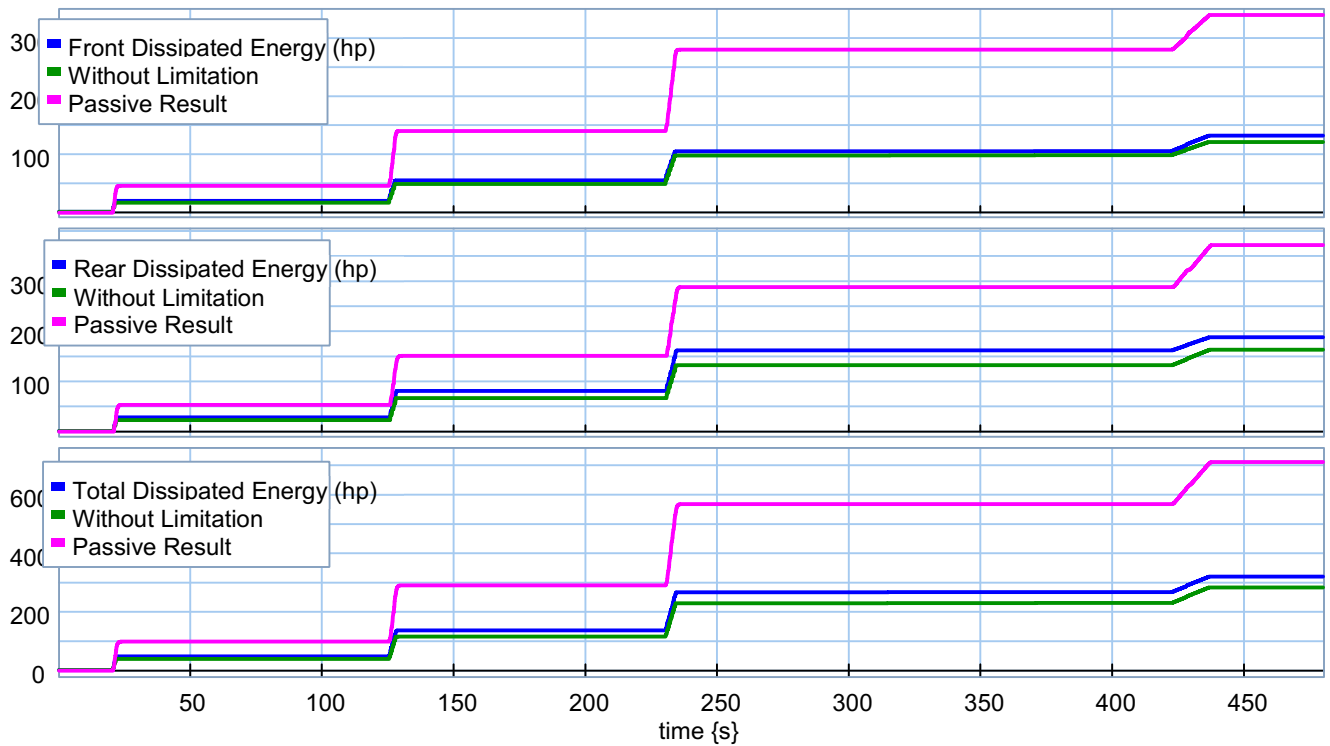


Figure 7.15: Dissipated power in suspension using half-car actuation units

By analyzing these two Figures in detail, the amount of each significant jump in the curves can be evaluated. Using active suspension units can be reasonable if amount of required actuator power does not exceed the summation of amount of saved power in dampers and assigned power for actuation units. Meeting this criteria is a key challenge. Figures 7.16 to 7.19 demonstrate each of these jumps separately. The amount of saved power for each case is evaluated and results can be found in Table 7.2.

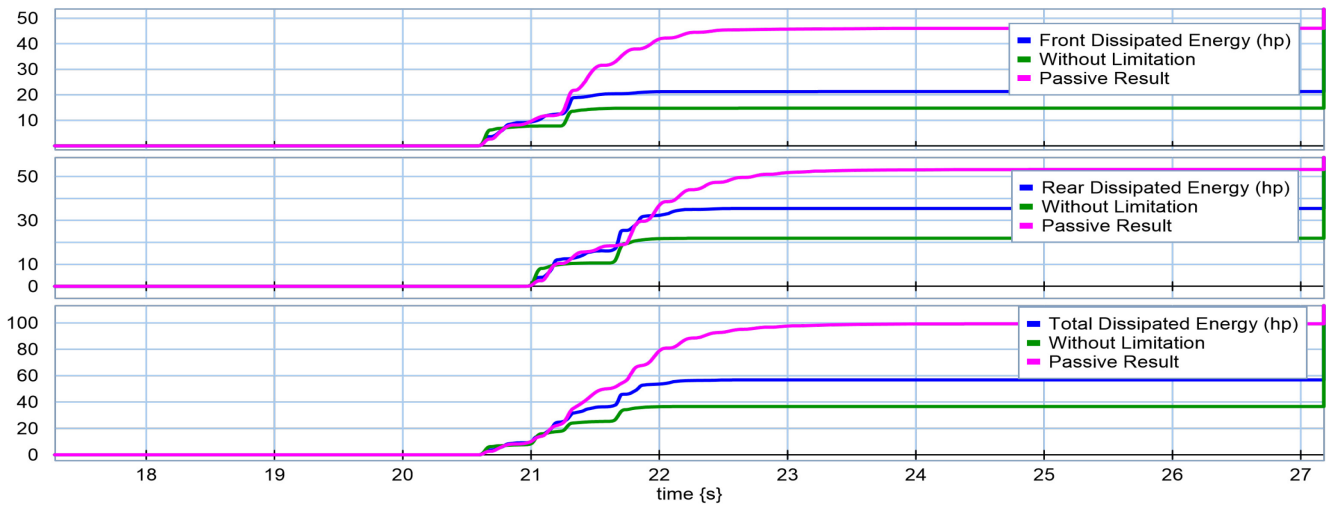


Figure 7.16: Dissipated power comparison in the 1st hike (QCM)

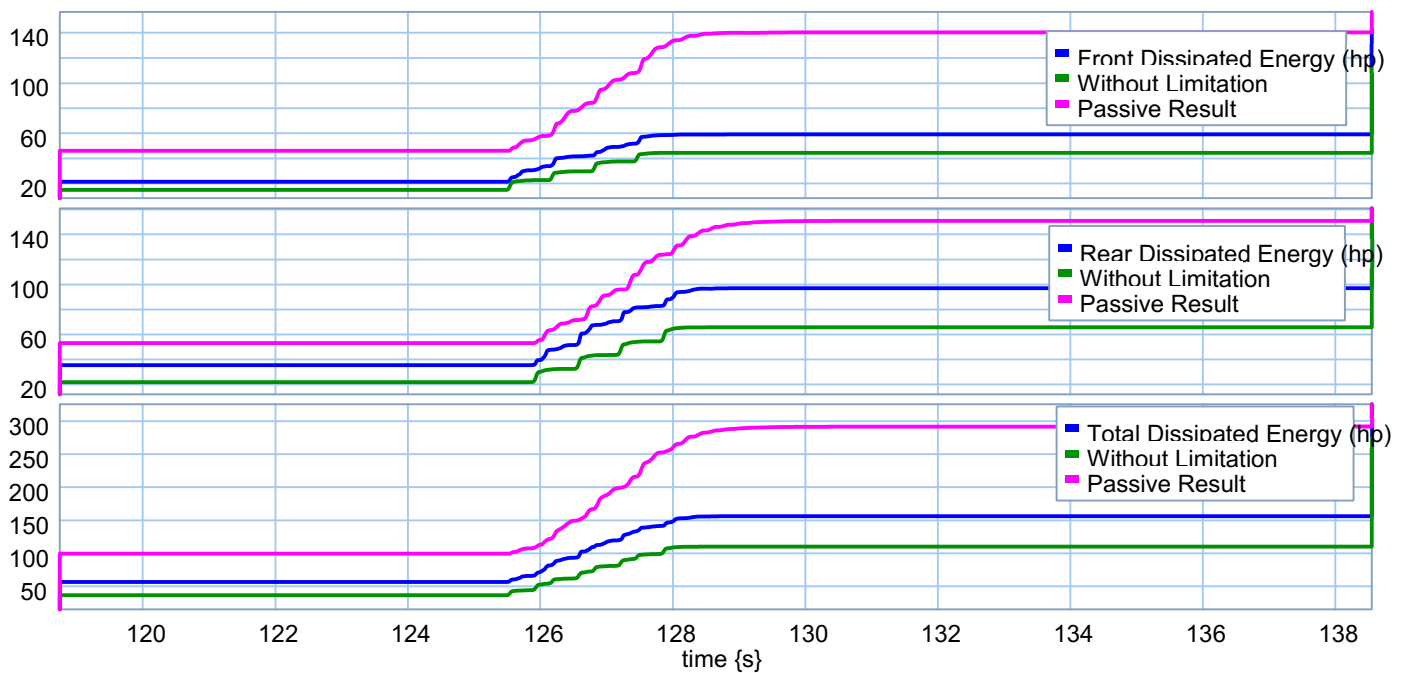


Figure 7.17: Dissipated power comparison in the 2nd hike (QCM)

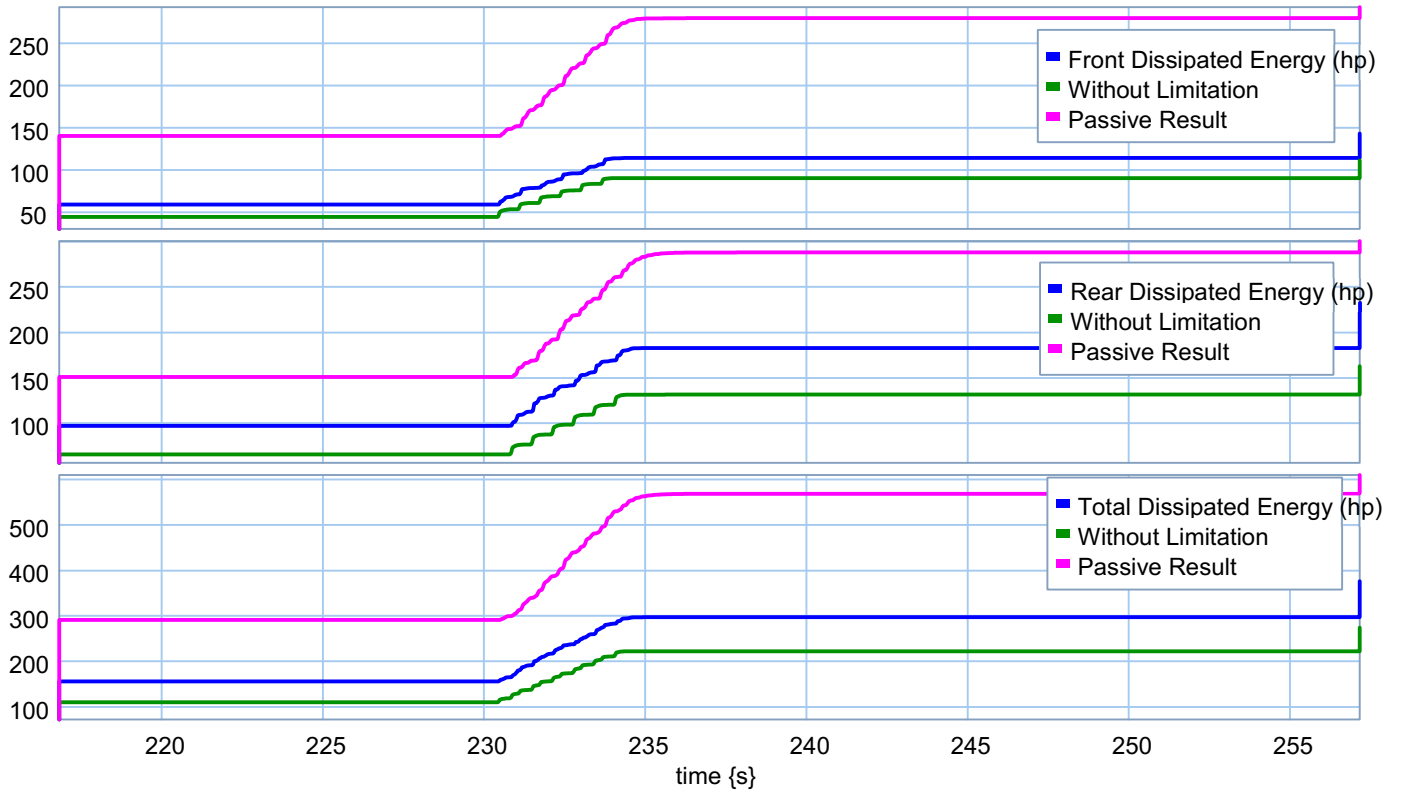


Figure 7.18: Dissipated power comparison in the 3rd hike (QCM)

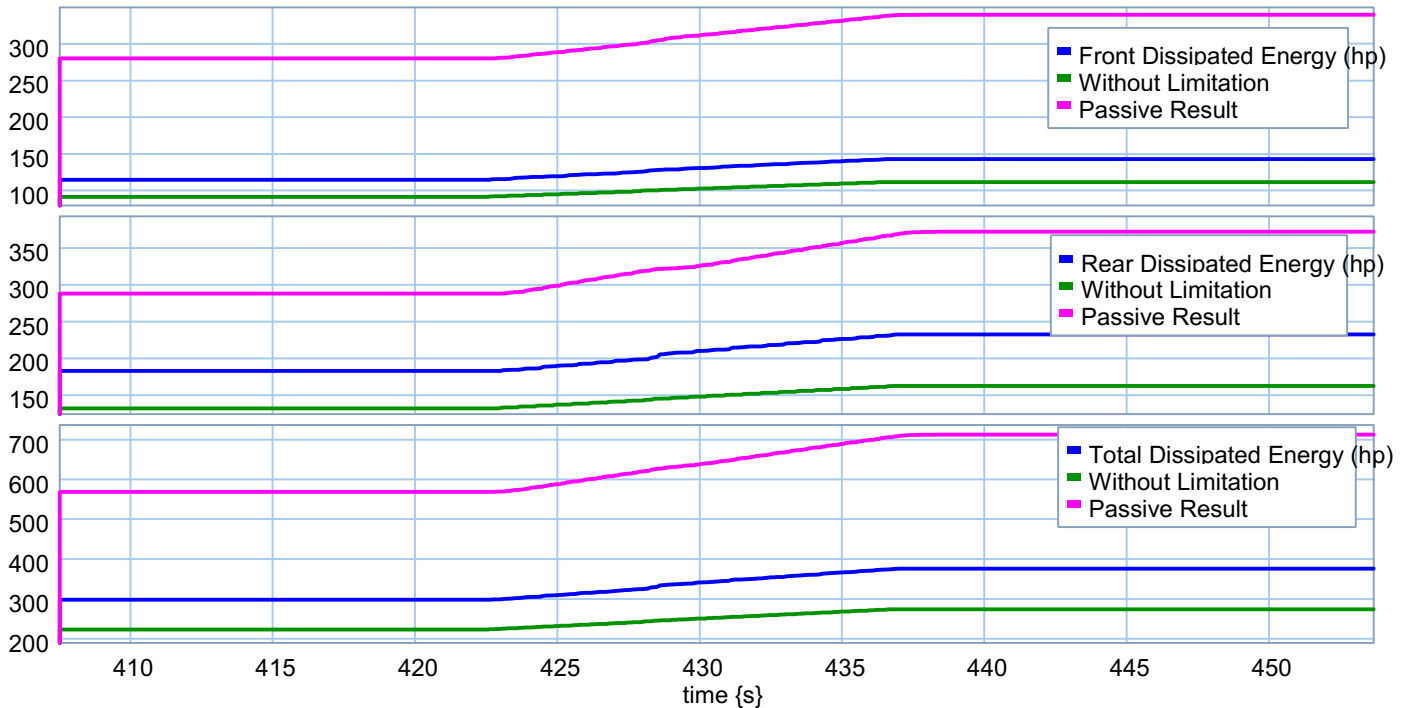


Figure 7.19: Dissipated power comparison in the 4th hike (QCM)

Table 7.2: Dissipated power in suspension spring comparison (QCM)

Mode	1 st Hike		2 nd Hike		3 rd Hike		4 th Hike	
	Front	Rear	Front	Rear	Front	Rear	Front	Rear
Passive (hp)	47	53	92	95	140	135	61	92
Without Limitation (hp)	15	21	29	46	50	63	25	36
After Limitation (hp)	21	36	40	57	55	80	26	55
Saved Energy (hp)	26	17	52	38	85	55	35	37

For instance, one of the rows of Table 7.2 is calculated in the following. Adding the assigned 25% of engine power (Table 7.1) to the saved power in suspension dampers explore how using two quarter-car active suspension units could efficiently improve the ride quality.

For the second hike of the rear part:

- *Passive suspension mode: Dissipated power : $150 - 55 = 95$ (hp)*
- *Ideal active suspension mode: Dissipated power : $66 - 20 = 46$ (hp)*
- *Realistic suspension mode: Dissipated power : $95 - 38 = 57$ (hp)*
- *Saved power = Passive dissipated – Realistic dissipated = $95 - 57 = 38$ (hp)*
- *Assigned power for the actuator = 25% of engine power + Saved power =
= $75 + 38 = 113$ (hp)*

Figures 7.20 and 7.21 represent the improvement in ride quality for the severe bumps and rough terrain events on a road. As it is seen, for the regular unevenness road profile, the realistic model perfectly matches the ideal model where the actuation force and spring stiffness are not limited. The reason can be easily obtained by re-looking at Figure 7.2. As it is seen there, the amount of required horsepower for minimizing the vehicle vertical acceleration is not that high and is in the range of limited allowable actuation power. However, when the vehicle hits severe bump series, the amount of required actuation force for controlling the vertical acceleration is much greater than the amount of allowable actuating force. Hence, the active suspension performance is not that great in improving the ride quality for severe bumpy road profile.

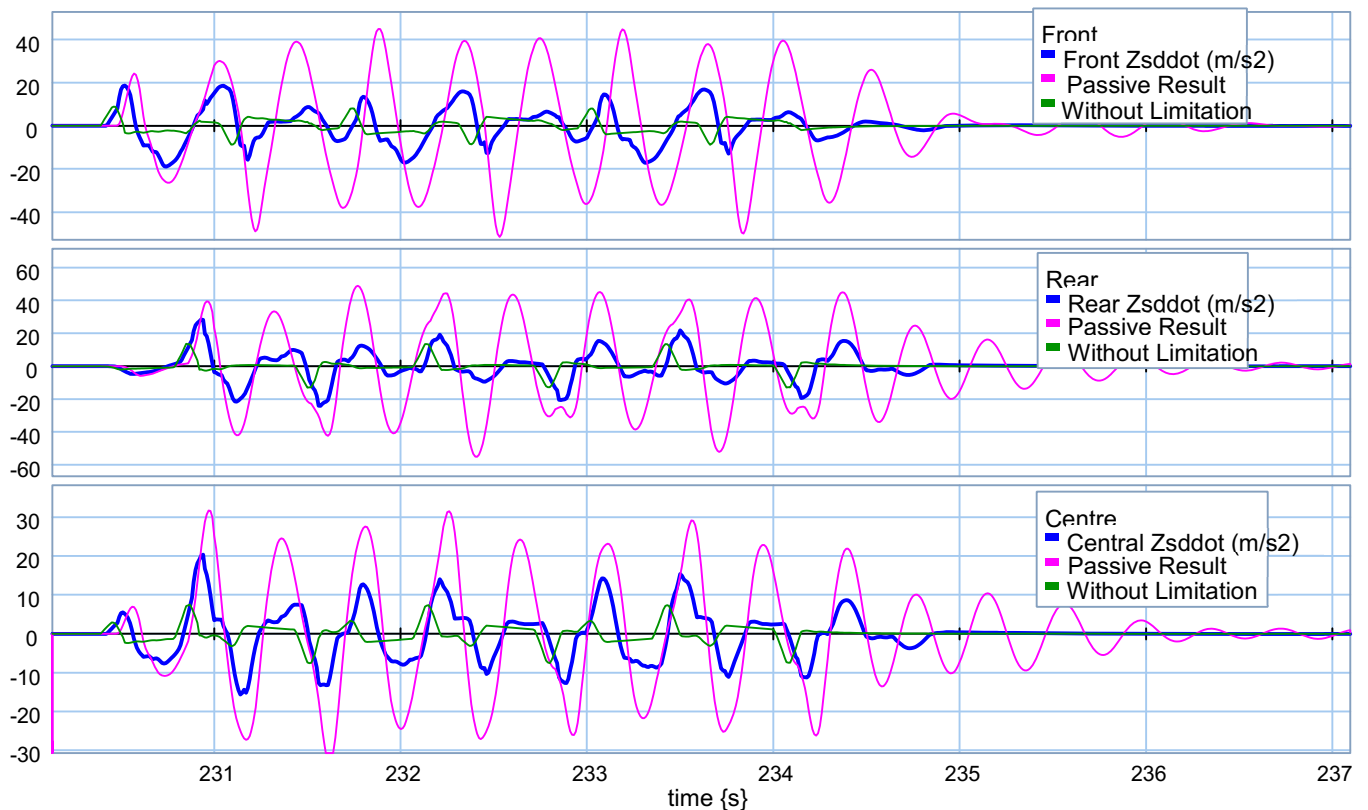


Figure 7.20: Ride quality performance for 3rd event of the road profile (QCM)

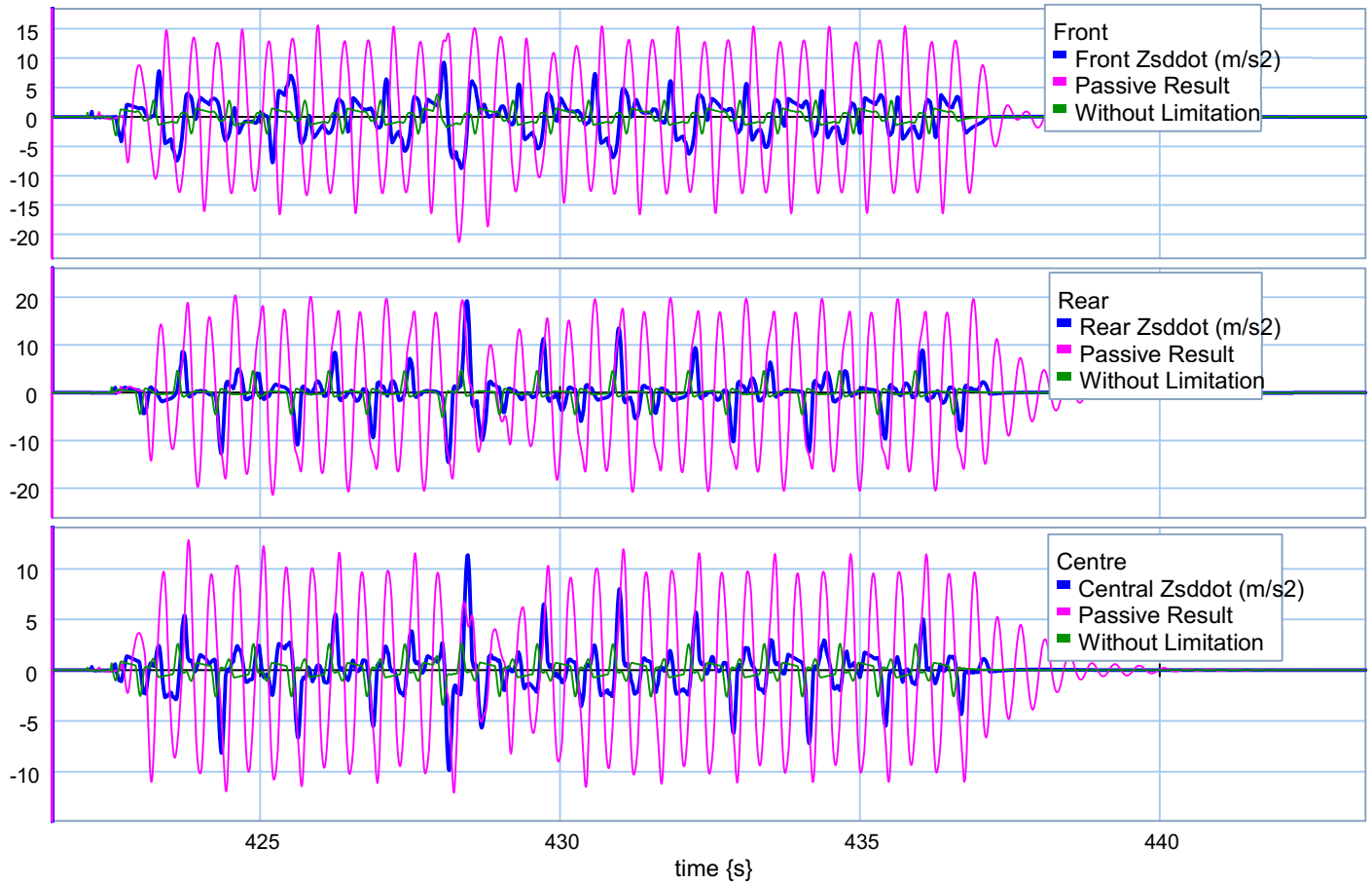


Figure 7.21: Ride quality performance for 5th event of the road profile (QCM)

7.7 Half-Car Model using Half-Car Active Suspension Units

In this section, quarter-car active suspension units had replaced with half-car active suspension units and then the model ran over the same road profile under the same condition. Figure 7.15 represent dissipated power in shock absorbers. The four significant jumps are demonstrated separately in Figures 7.22 to 7.25.

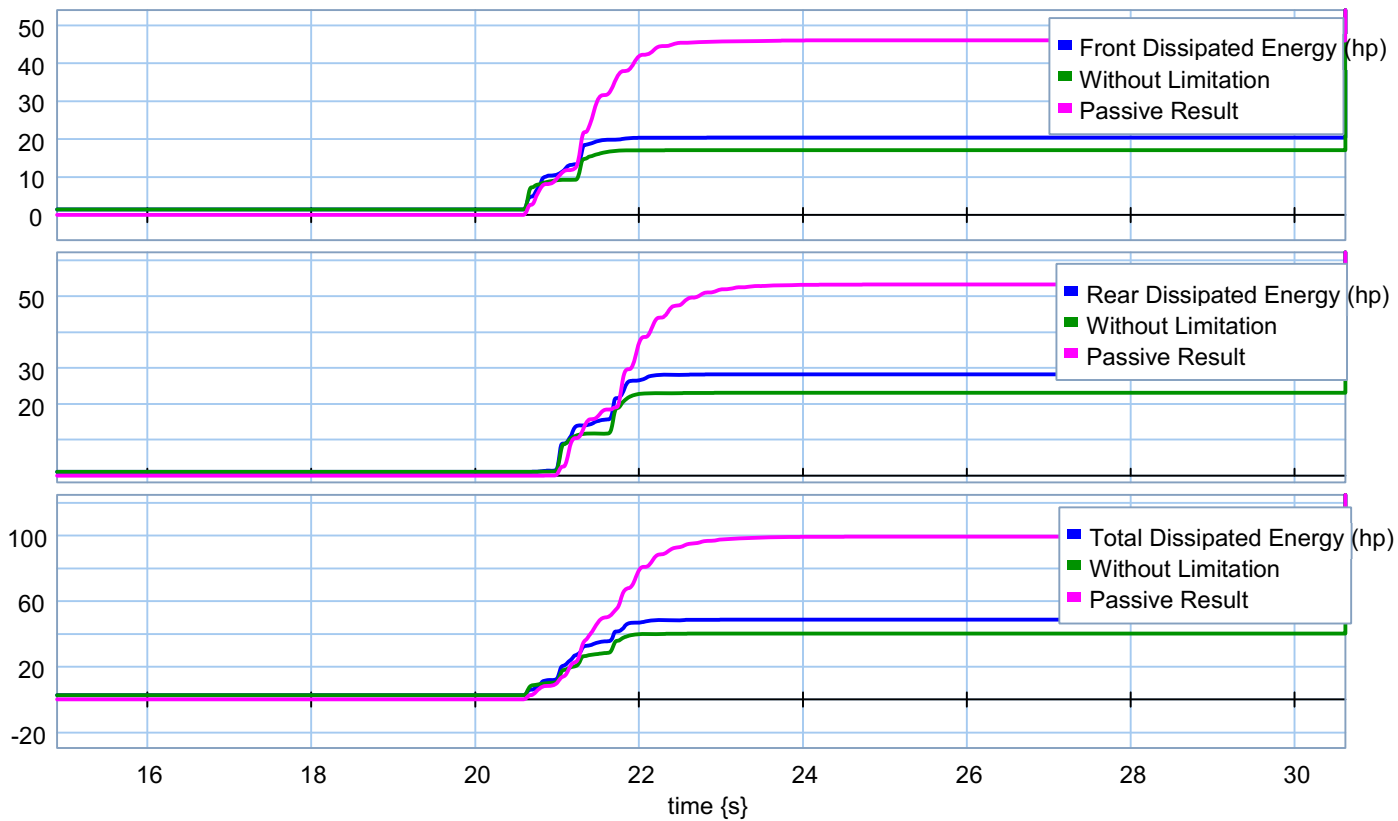


Figure 7.22: Dissipated power comparison in the 1st hike (HCM)

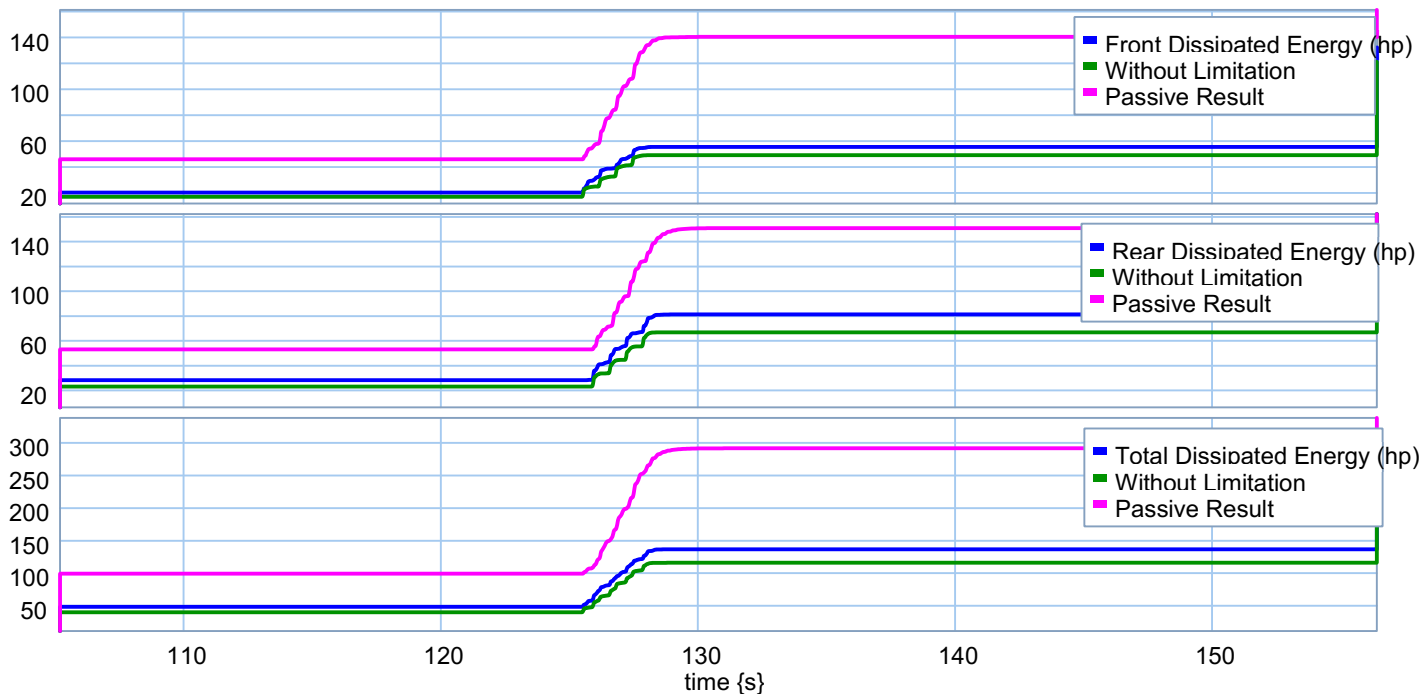


Figure 7.23: Dissipated power comparison in the 2nd hike (HCM)

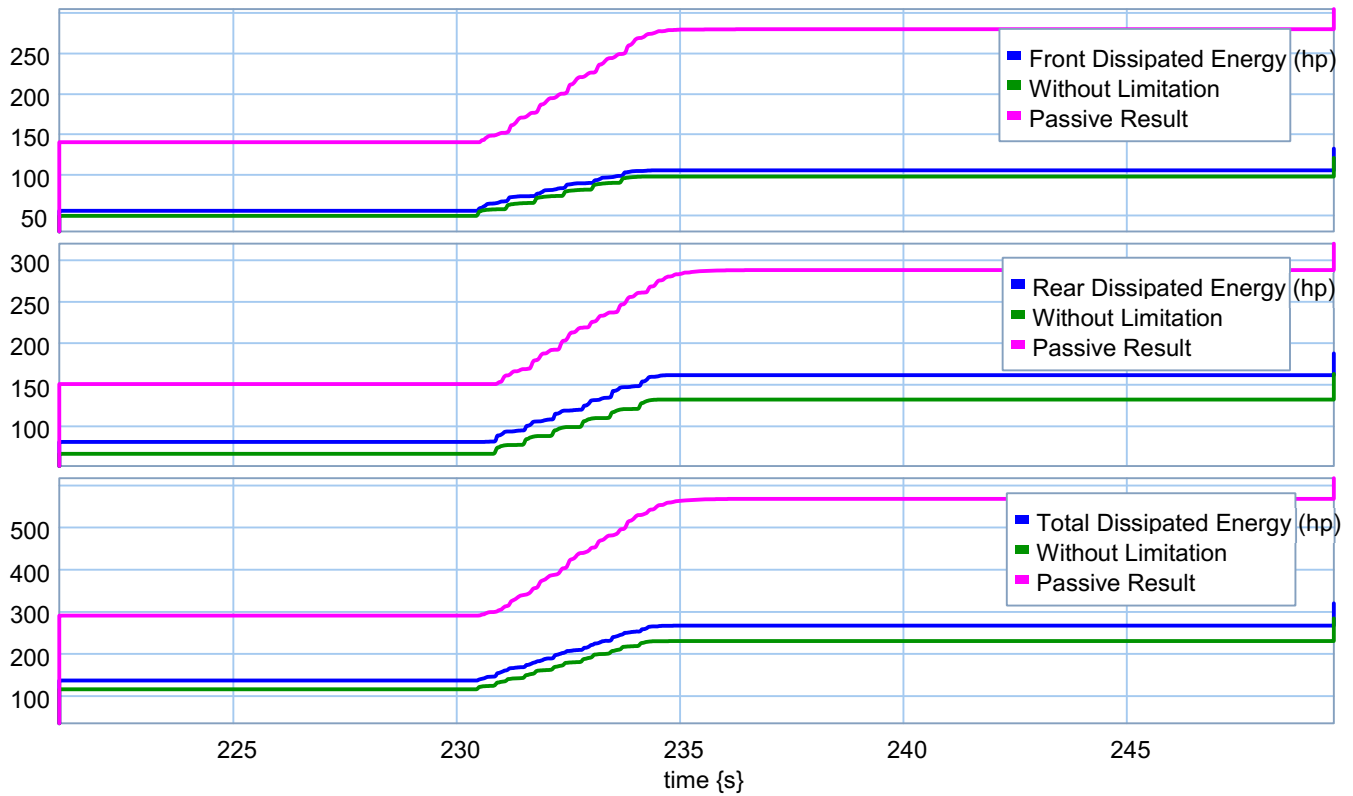


Figure 7.24: Dissipated power comparison in the 3rd hike (HCM)

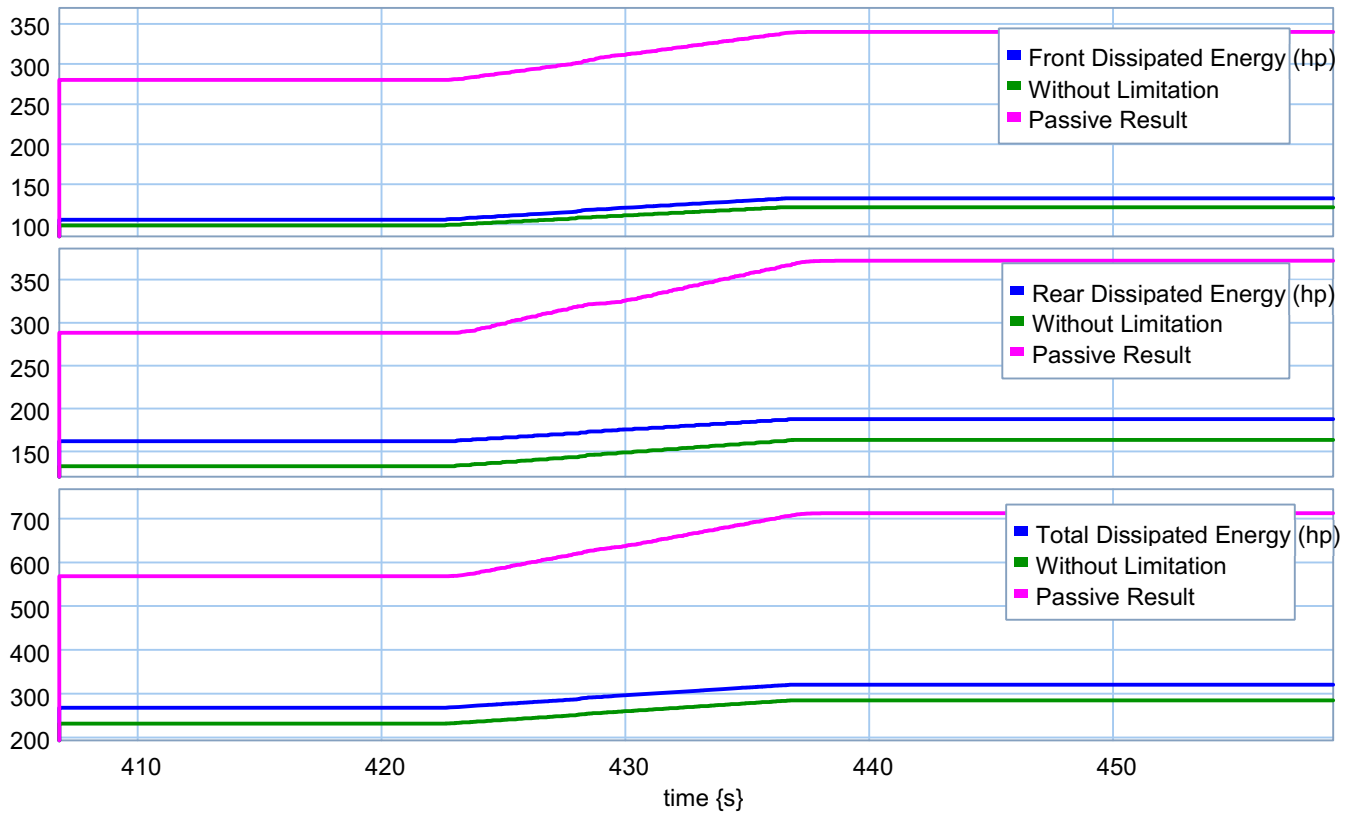


Figure 7.25: Dissipated power comparison in the 4th hike (HCM)

Table 7.3 categorizes the saved power in the suspension dampers while half-car active suspension units have used in the half-car vehicle model.

Table 7.3: Dissipated power in suspension spring comparison (HCM)

Mode	1 st Hike		2 nd Hike		3 rd Hike		4 th Hike	
	Front	Rear	Front	Rear	Front	Rear	Front	Rear
Passive (hp)	47	53	92	95	140	135	61	92
Without Limitation (hp)	18	22	32	43	33	65	37	26
After Limitation (hp)	20	29	37	51	43	79	40	31
Saved Energy (hp)	27	24	55	44	97	56	21	61

Required limited force and power for the front and rear actuators are demonstrated in Figures 7.5 and 7.8 for the 3rd and 5th event of the studied road profile. Figures 7.26 and 7.27 represent vehicle vertical acceleration for the corresponding road events. As it is seen, using half-car active suspension units could greatly improve the ride quality for a regular rough road profile. It could also decrease the fluctuation and damp the vertical acceleration faster on severe bumpy road profile.

The same improvement has seen in road holding scenario as well. Appendix K provide recorded graphs for this scenario approved that it is energy-efficient to use active suspension units in the vehicle instead of passive one.

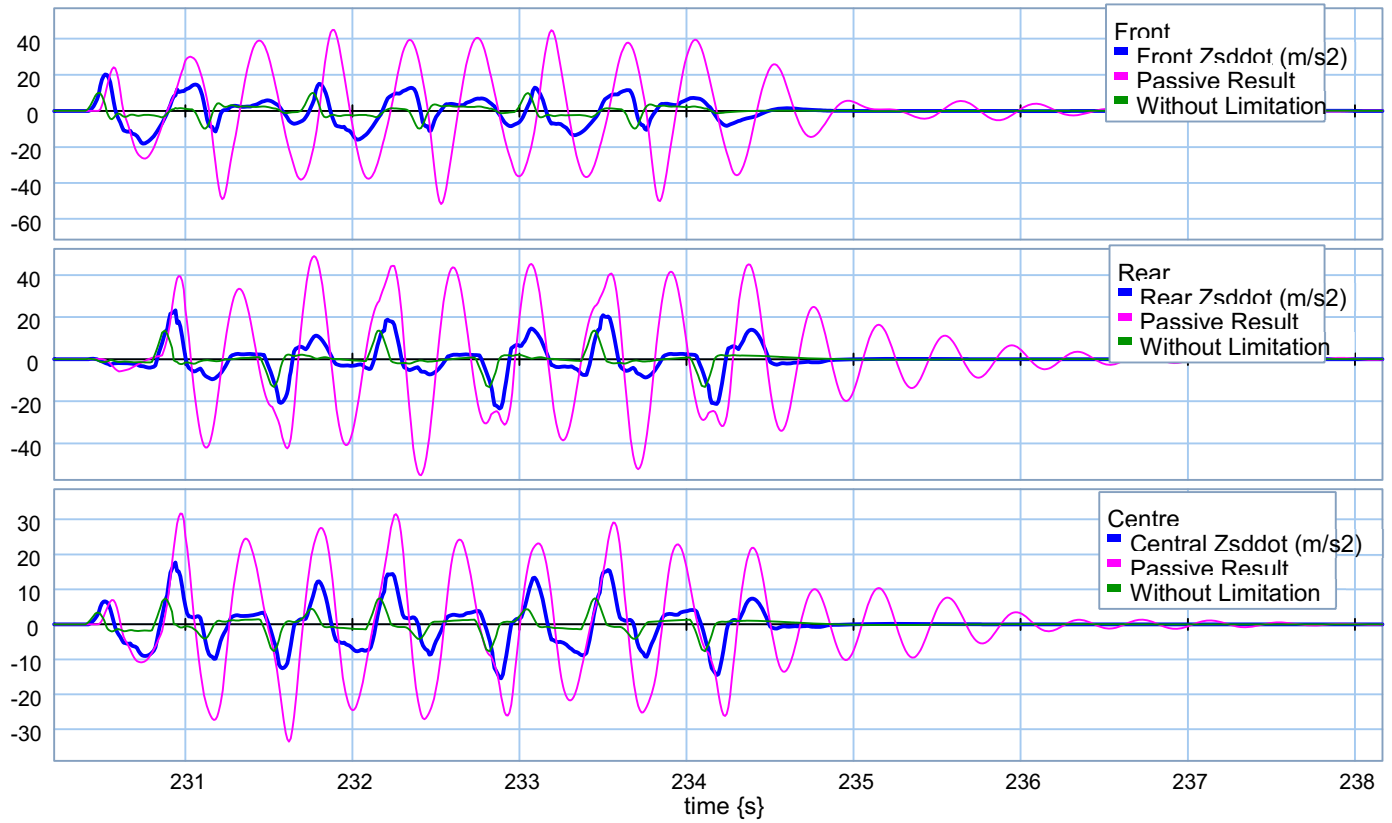


Figure 7.26: : Ride quality performance for 3rd event of the road profile (HCM)

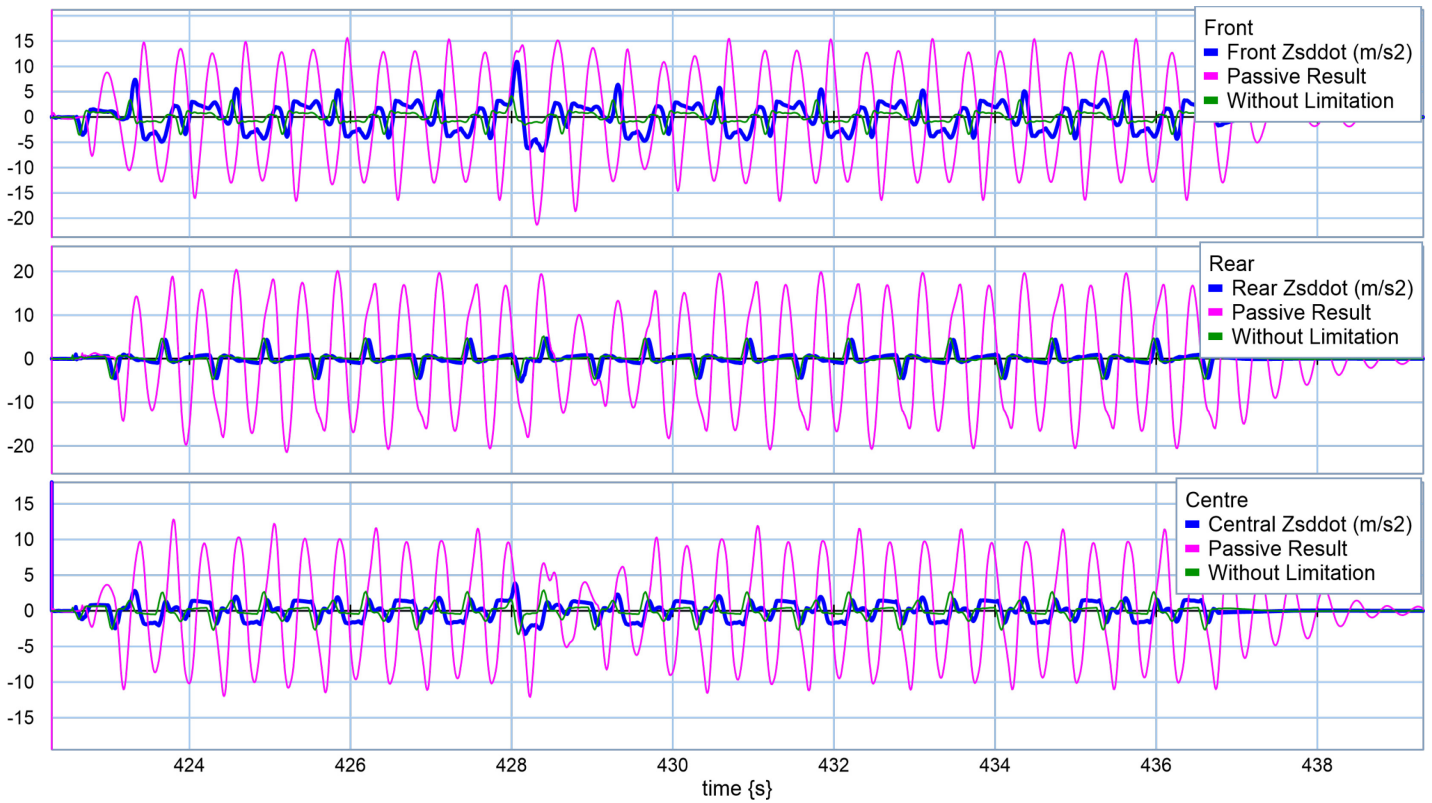


Figure 7.27: Ride quality performance for 5th event of the road profile (HCM)

Having looked at Tables 7.2 and 7.3, the amount of saved energy can be compared. Results demonstrate that half-car active suspension units are more energy-efficient than quarter-car ones as more amount of energy can be saved. This may not make any noticeable differences in the ride quality improvement on a normal rough terrain. But when the vehicle hits severe bumps on the road, half-car active suspension actuators can better improve the ride quality since they could save more energy. Hence, more power can be assigned to the actuators and it results in having better performance over bumpy roads.

Chapter 8

Conclusions and Recommendations for Future Work

8.1 Summary of Conclusions

This research tried to present a renewed exploration into active suspension. For this reason, a non-linear half-car model was developed in order to study heave and pitch motions. The purpose of this work can be defined as presenting a good force actuator system which can improve vehicle ride quality and road holding while the required actuator force and

energy remain physically reasonable. In order to have more realistic results, besides the non-linear terms in the model, deflections of shock absorbers are also controlled.

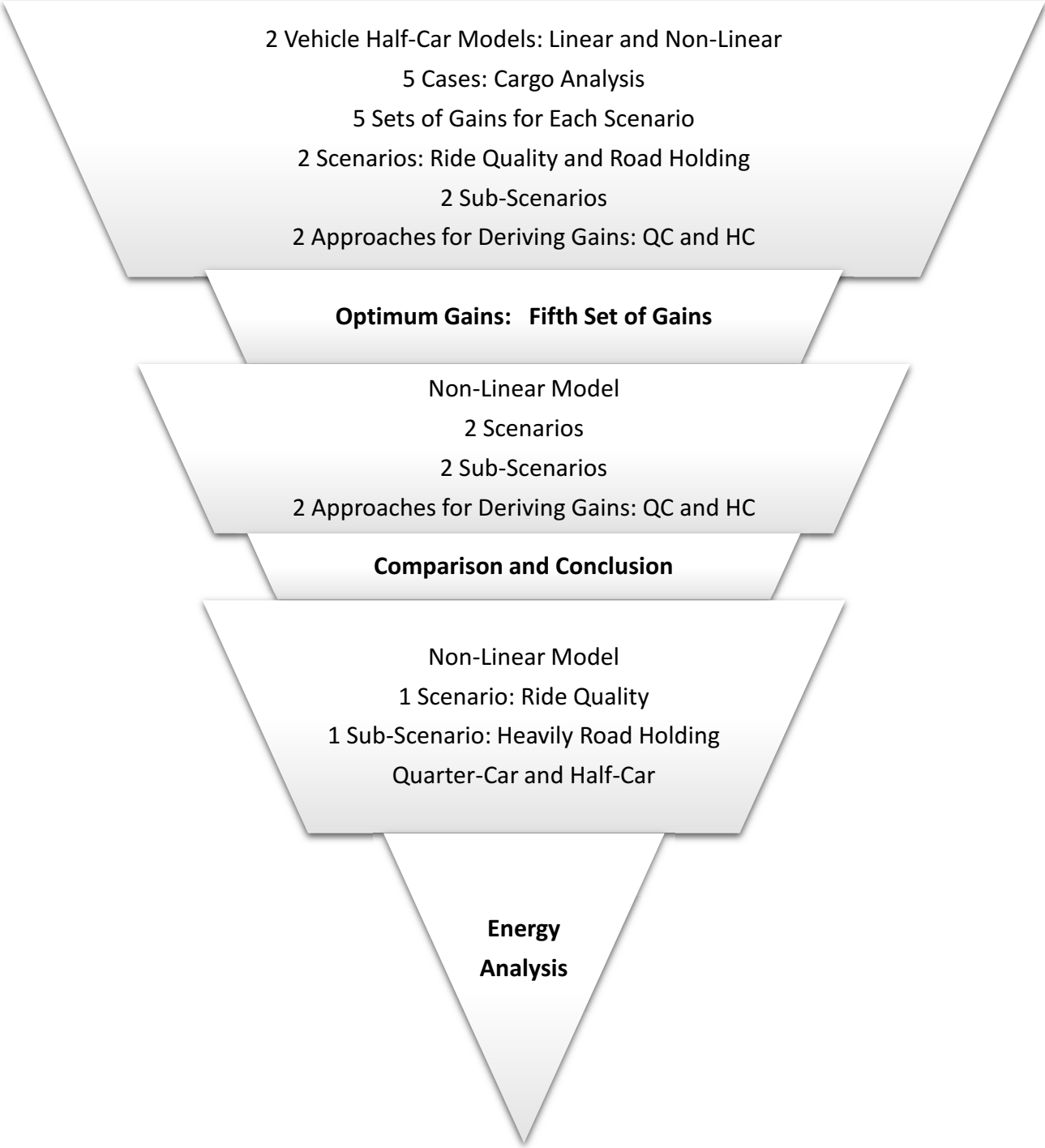


Figure 8.1: Work summary

In dynamical systems, it is sometimes desired for a system to work at the minimum cost. This goal can be achieved through optimal control theory. The value of the cost function, which has set to be minimum, can be minimized by a proportional feedback control law, i.e., $u = -G \cdot x$ where G is the system gain matrix. In this work, after solving the LQR problem, the gain matrix G was derived. Active suspension gains for the half-car model obtained by using two approaches, i.e., quarter-car and half-car. Corresponding system equations for each approach were derived using LQR method, and the proper feedback gains were obtained for both scenarios. The obtained gains for each studied scenario were dependant on vehicle parameters. Cargo mass is one of these important factors. The effects of having varying cargo masses are also studied in this research and an optimum set of gains is introduced which can be efficient for all possible cargo masses. Finally, net energy cost of active suspension was evaluated by subtracting passive damper power savings from the required actuator power. Hence, the efficiency of substituting passive suspension with active one was declared. This paper aimed to study the energy efficiency of using quarter car and half car states by designing optimal controllers for the half car vehicle model.

Results showed that active suspension, whether quarter-car or half-car controller, can improve both ride quality and road holding. Ride quality which can be defined as a vehicle's responses to a road surface can be improved by minimizing the effects of road improprieties on the vehicle occupants. The quarter-car controllers showed better performance than the half-car based controller in minimizing the vehicle vertical acceleration. This point was true for all various cargo masses. However, when pitch angle

acceleration were required to be minimized, the half-car controller performed better for cargo masses less than almost 9000 kg and quarter car controllers could not differentiate the vertical heaving from the pitching and the half car controller was superior. However, when the cargo mass exceeded 9000 kg, the quarter-car controller did a better job.

Although ride quality or road holding can be improved in the best way in theory, it may not be energy efficient to use active suspension as they may require more energy than the amount that the vehicle's engine could produce. In this work, in order to have a feasible model, actuator force and deflection in shock absorbers were limited. Energy analysis showed less energy was dissipated in shock absorbers when either quarter-car or half-car controllers were used instead of passive suspension. This research deduces that not only does active suspension improve ride quality and road holding, but also it is more energy efficient than one might expect simply based on actuator energy output. Results demonstrated that more energy could be saved by using half-car active controllers than the quarter-car ones. However, for a regular rough road, both types of controllers did a great job. That extra saved energy in half-car controllers could help the vehicle perform better if there was any severe bump placed in the path.

8.2 Future Work

It was briefly demonstrated in this work that how modifying the weighting factors in the cost function could improve the desired purposes in road holding scenario. It seems there is an abundance of research on exploring some methods in order to present the optimum weighting factors based on important factors such as vehicle parameters. Another area suggested for doing more researches in the future is mainly about the efficiency of variant methods in order to reclaim the dissipated energy in shock absorbers to the system again.

Bibliography

- [1] Ward's Auto results, "http://wardsauto.com/ar/world_vehicle_population_110815", 2011.
- [2] Controllab Products B.V., "20-sim v4.1.05." www.20sim.com, 2009.
- [3] K. Huibert, and S. Raphael, "*Linear Optimal Control Systems*", Wiley Interscience, 1st edition, ISBN 0-471-51110-2, 1972.
- [4] Xubin Song, "*Cost-Effective Skyhook Control for Semiactive Vehicle Suspension Applications*", *The Open Mechanical Journal*, pp 17-15, 2009.
- [5] G. Rideout, L. Stein, and S. Louca, "*Extension and Application of An Algorithm for Systematic Identification of Weak Coupling and Partitions in Dynamic System Models*", *Simulation Modelling Practice and Theory* 17 p271-292, 2009.
- [6] www.mathworks.com/help/control/ref/care.html.
- [7] K. Efatpanah, H. Beno, and P. Nichols, "*Energy Requirements of a Passive and an Electromechanical Active Suspension System*", *Vehicle System Dynamics* 34, p437-458, 2000.
- [8] Hubbard M., Karnopp D., "*Modelling and Simulating and Simulation of Vehicle Bump and Skid Response Using Bond Graphs*", *International journal of Vehicle Design*, 1983.

- [9] Hrovat D., "*Applications of Optimal Control to Advanced Automotive Suspension Design*", Journal of Dynamic Systems, Measurements, and Control, 1993.
- [10] Margolis D., Shim T., "*A Bond Graph Model Incorporating Sensors, Actuators, and Vehicle Dynamics for Developing Controllers for Vehicle Safety*", Journal of Franklyn Institute, 2000.
- [11] ACSL, Simulation software, www.aegistg.com.
- [12] Barak P., Ng X., Gadde K., "*State space formulation by bond graph models for vehicle system dynamics*", SAE Technical Papers, 2008.
- [13] The MathWorks, "*Matlab v2009b.*" www.mathworks.com, 2009.
- [14] M. S. Kumar, and S. Vijayarangan, "*Design of LQR controller for active suspension system*", Indian Journal of Engineering and Materials Sciences, pp 173-179, June 2006.
- [15] G. Filippini, N. Nigro, and S. Junco, "*Vehicle dynamics simulation using bond graphs*", Universidad National de Rosario, Argentina, 2010.
- [16] Chantranuwathana and H. Peng, "*Force tracking control for active suspensions-theory and experiments*", in Control Applications, Proceedings of the 1999 IEEE International Conference on, vol. 1, pp. 442 - 447, 1999.
- [17] G. Rideout, L. Stein, and S. Louca, "*Extension and Application of An Algorithm for Systematic Identification of Weak Coupling and Partitions in Dynamic System Models*", Simulation Modelling Practice and Theory 17 p271-292, 2009.

- [18] H. Adibi-asl and G. Rideout, "*Bond graph modeling and simulation of a full car model with active suspension*," in Proceedings of the 20th IASTED International Conference on Modelling and Simulation, 2009.
- [19] K. J. Wakeham and G. Rideout, "*Model Complexity Requirements in Design of Half-Car Active Suspension Controllers*", ASME Dynamic System and Controls Conference, Arlington, 2011.
- [20] R. Krtolica and D. Hrovat, "*Optimal Active Suspension Control based on a Half-Car Model: An Analytical Solution*", Automatic Control, IEEE Transactions on, vol. 37, pp. 528 – 532, April 1992.
- [21] Thomas D. Gillespie, "*Fundamentals of Vehicle Dynamics*", Published by Society of Automotive Engineers, 1992, pp. 178-180.
- [22] P. S. Fancher, R. D. Ervin, C. B. Winkler, and T. D. Gillespie, "A Factbook of the Mechanical Properties of the Components for Single-Unit and Articulated Heavy Trucks", The university of Michigan, Transportation Research Institute, Ann Arbor, Michigan 48109, 1986.
- [23] Henry M. Paynter, "Analysis and Design of Engineering Systems", MIT Press, Cambridge MA, 1961.
- [24] Karnopp D.C, Margolis D.L., and Rosenberg R.C., "*System Dynamics, A Unified Approach*", J Wiley, NY, 1990.
- [25] Breedveld P.C., "*Physical Systems Theory in Terms of Bond Graphs*", PhD Thesis, University of Twente, Enschede, Netherlands, 1984.
- [26] Breedveld P.C., "*Multibond-Graph Elements in Physical Systems Theory*", Journal of the Franklin Institute, vol 319 pp. 1-36, 1985.

- [27] T. Butsuen, "*The design of semi-active suspensions for automotive vehicles*", PhD thesis, Massachusetts Institute of Technology, 1989.
- [28] MAPLE, mathematical and analytical software, www.maplesoft.com.
- [29] www.internationaltrucks.com.
- [30] C. Shian, H. Ren, and L. Senlin, "*New Reclaiming Energy Suspension and its Working Principle*", Chinese Journal of Mechanical Engineering, pp. 177-182, 2007.
- [31] H. Ren, C. Shian, and L. Senlin, "*A Permanent Magnetic Energy Regenerative Suspension*", ZL 200520072480.9, 2005.
- [32] C. Shian, H. Ren, and L. Senlin, "*Operation Theory and Structure Evaluation of Reclaiming Energy Suspension*", Transactions of the Chinese Society for Agricultural Machinery, pp. 5-9, 2006.
- [33] Z. Yong-chao, "*Isolation and Energy Regenerative Performance Experimental Verification of Automotive Electrical Suspension*", Journal of Shanghai Jiaotong University, pp. 874-877, 2008.
- [34] W. Zhengquan, and C. Yu, "*Brief Introduction to Structure and Principle of Electromagnetic Shock Absorber*", Motor Technology, pp. 56-59, 2007.

Appendices

Appendix A: Cargo Mass Analysis

Mc	J	b=xG	a	L	DR	DI
0	20,010.630	1.420	2.310	3.730	0.61472	0.840580628
4500	30,729.123	0.999	2.731	3.730	0.36579	0.957976476
9000	39,586.991	0.811	2.919	3.730	0.27786	1.028557208
13500	47,794.328	0.705	3.025	3.730	0.23289	1.080143662
18000	55,698.842	0.636	3.094	3.730	0.20559	1.120576238

Ms	-Ms . g	Msr	Msf	Mur	Muf
7,257.40	-71,195.0940	4,494.5292	2,762.8708	449.4529	276.2871
11,757.40	-115,340.0940	8,608.4702	3,148.9298	449.4529	276.2871
16,257.40	-159,485.0940	12,722.4113	3,534.9887	449.4529	276.2871
20,757.40	-203,630.0940	16,836.3523	3,921.0477	449.4529	276.2871
25,257.40	-247,775.0940	20,950.2933	4,307.1067	449.4529	276.2871

Mc (kg)	Total xG	Mc . (xG-x1)^2	M . (b-xG)^2	Total Inertia
0	1.42	0	3.57817E-28	20010.63
500	1.349099956	529.5233599	36.481616	21394.13498
1000	1.286786155	934.6754704	128.7893006	22709.09477
1500	1.231587914	1246.488788	257.6312704	23967.25006
2000	1.18235228	1487.302911	409.8721059	25177.80502
2500	1.138162625	1673.475204	576.472016	26348.07722
3000	1.098281046	1817.164159	751.1632923	27483.95745
3500	1.062106829	1927.528909	929.5823822	28590.24129
4000	1.029145984	2011.552106	1108.690223	29670.87233
4500	0.998988552	2074.614541	1286.378791	30729.12333
5000	0.971291465	2120.90286	1461.200196	31767.73306

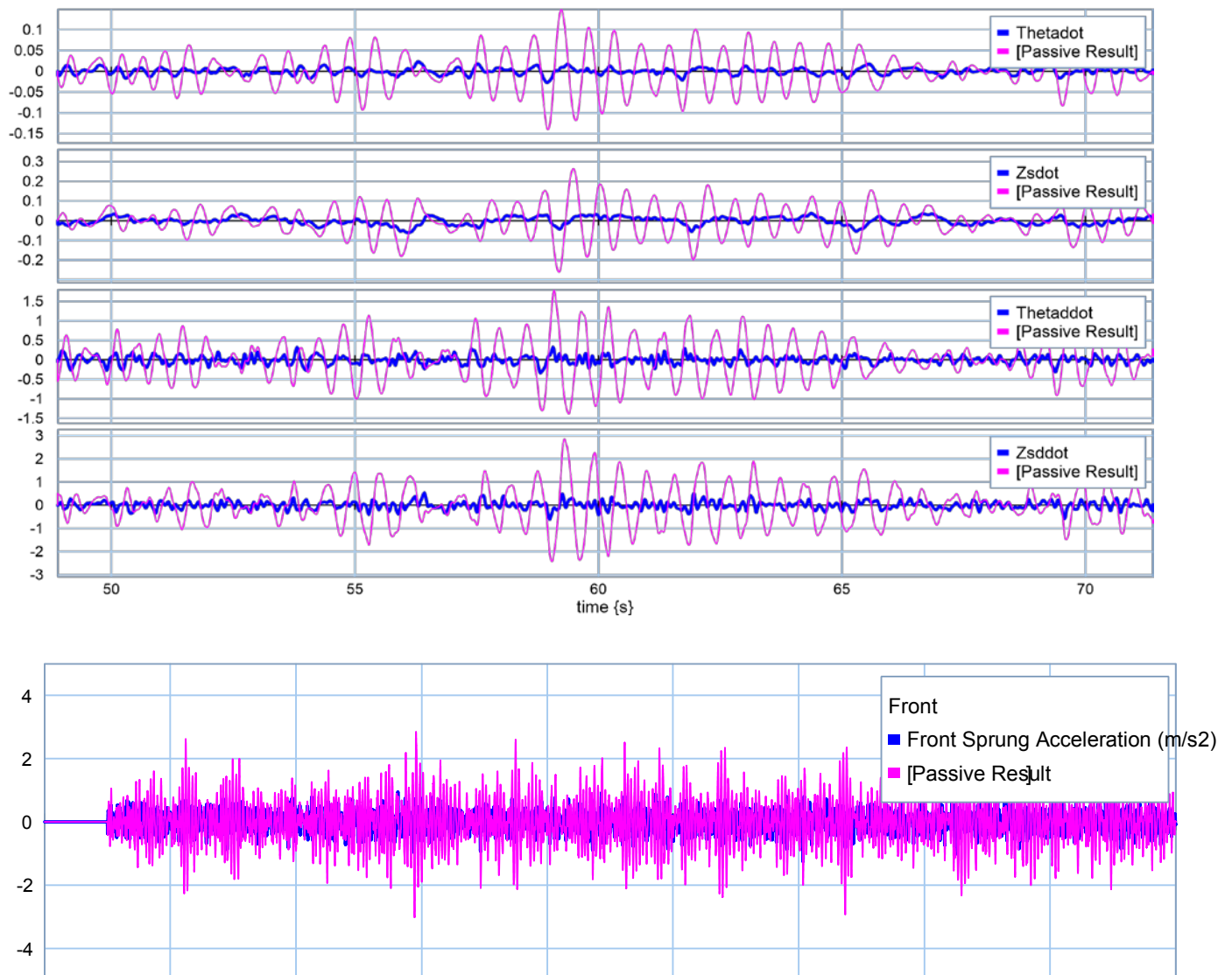
5500	0.945765438	2153.703109	1632.177791	32789.0109
6000	0.922164829	2175.614886	1798.672984	33794.91787
6500	0.900279704	2188.709477	1960.290407	34787.12988
7000	0.87992958	2194.647945	2116.809824	35767.08777
7500	0.860958434	2194.770208	2268.136876	36736.03708
8000	0.843230695	2190.162878	2414.267234	37695.06011
8500	0.826627997	2181.711382	2555.26039	38645.10177
9000	0.811046539	2170.140329	2691.220405	39586.99073
9500	0.796394906	2156.045013	2822.281756	40521.45677
10000	0.782592279	2139.916168	2948.598904	41449.14507
10500	0.769566941	2122.159563	3070.338607	42370.62817
11000	0.757255031	2103.111582	3187.674291	43286.41587
11500	0.745599497	2083.051714	3300.78192	44196.96363
12000	0.734549212	2062.212593	3409.837009	45102.6796
12500	0.724058226	2040.788128	3515.012484	46003.93061
13000	0.714085124	2018.940109	3616.477171	46901.04728
13500	0.704592483	1996.803599	3714.394768	47794.32837
14000	0.695546398	1974.491358	3808.92317	48684.04453
14500	0.686916084	1952.097481	3900.214054	49570.44154
15000	0.67867352	1929.700407	3988.41267	50453.74308
15500	0.670793149	1907.365413	4073.657771	51334.15318
16000	0.66325161	1885.146687	4156.081653	52211.85834
16500	0.656027511	1863.089059	4235.810273	53087.02933
17000	0.649101223	1841.229452	4312.963413	53959.82286
17500	0.6424547	1819.598092	4387.654891	54830.38298
18000	0.63607133	1798.219537	4459.992789	55698.84233

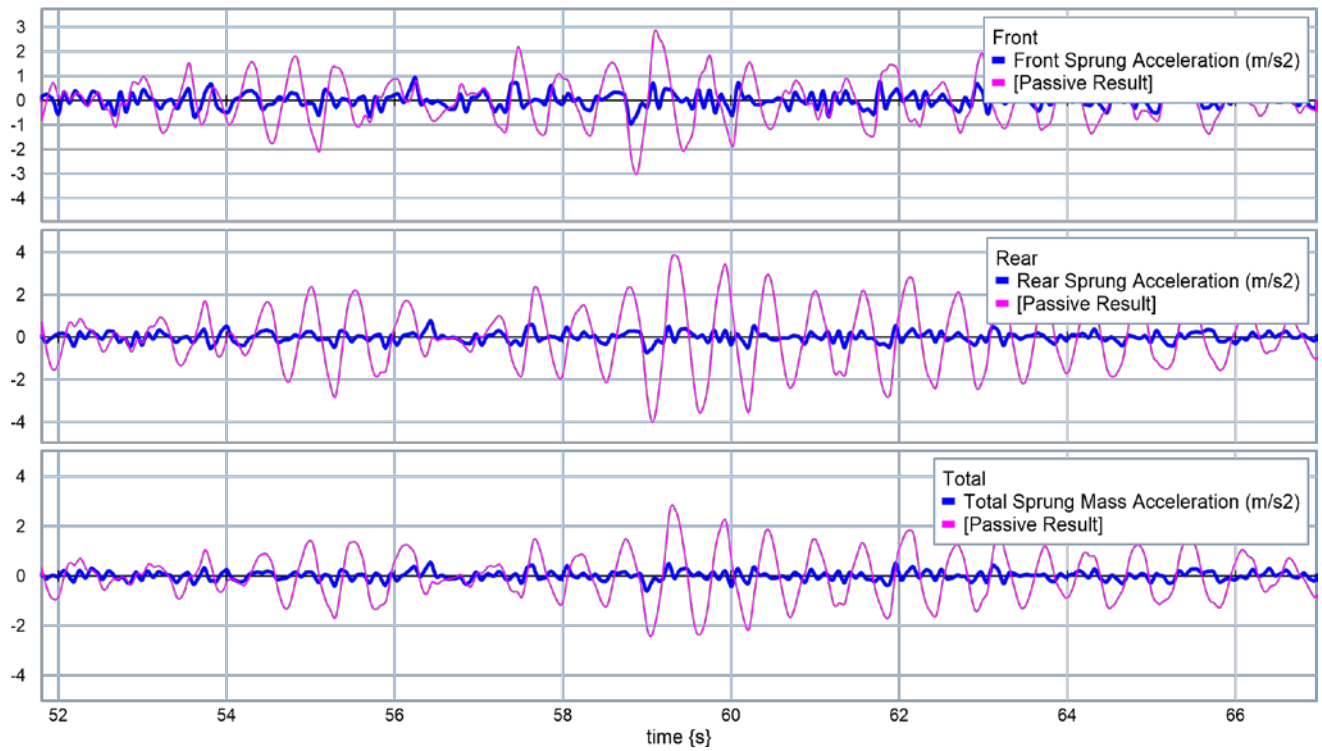
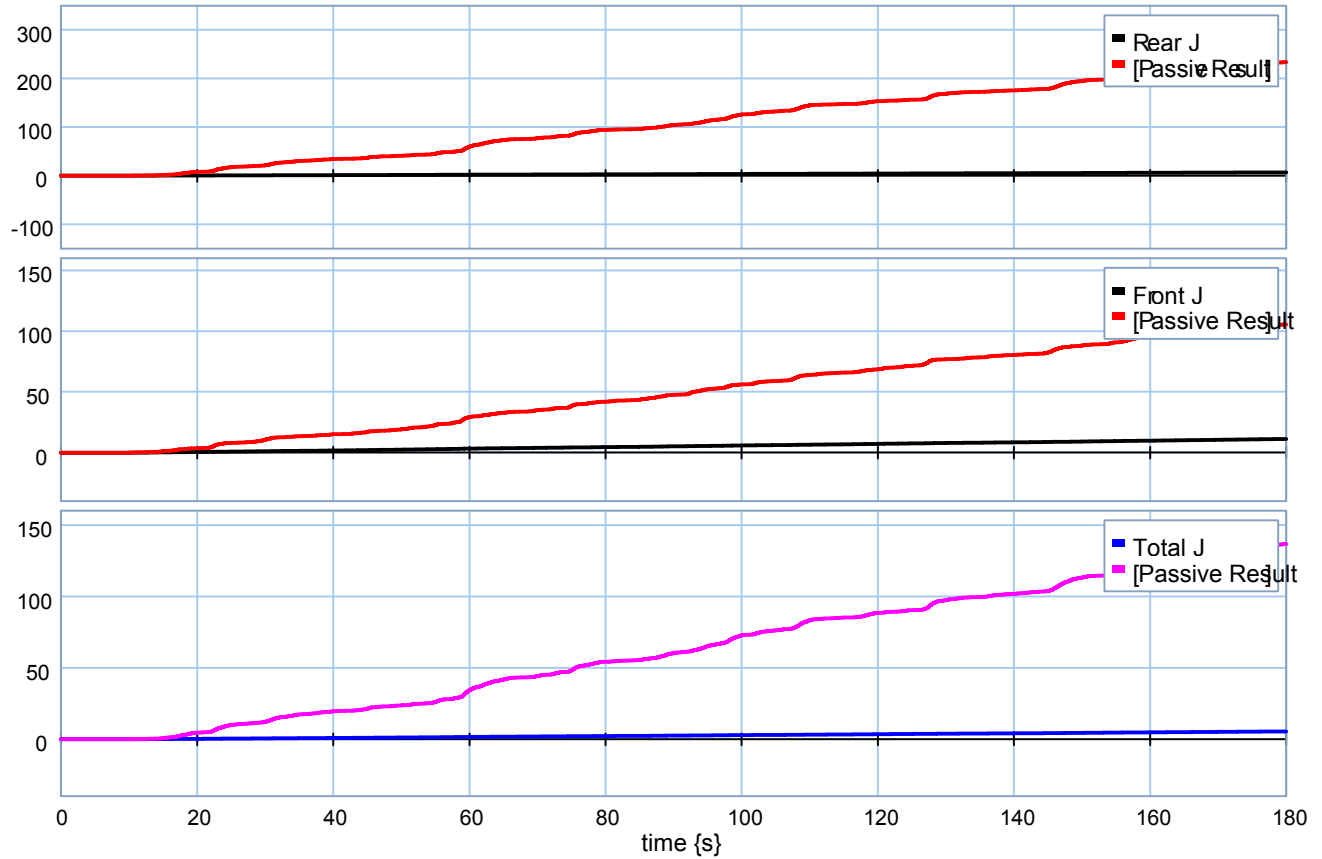
$k = \sqrt{J/M}$	$xG . (a+b-xG)$	DI	Status
1.660503712	3.2802	0.840580628	Coupled
1.660692685	3.212072145	0.858604686	Coupled
1.658357846	3.14389375	0.874759443	Coupled
1.65432758	3.07701413	0.889433596	Coupled
1.649166173	3.012217091	0.902906061	Coupled
1.643264258	2.949932431	0.915382805	Coupled
1.636895625	2.890367045	0.927019733	Coupled
1.630253914	2.833587556	0.937937428	Coupled
1.623476881	2.779573064	0.948230942	Coupled
1.616662775	2.728249172	0.957976476	Coupled
1.609881586	2.679510054	0.96723605	Coupled
1.603182899	2.63323282	0.976060829	Coupled

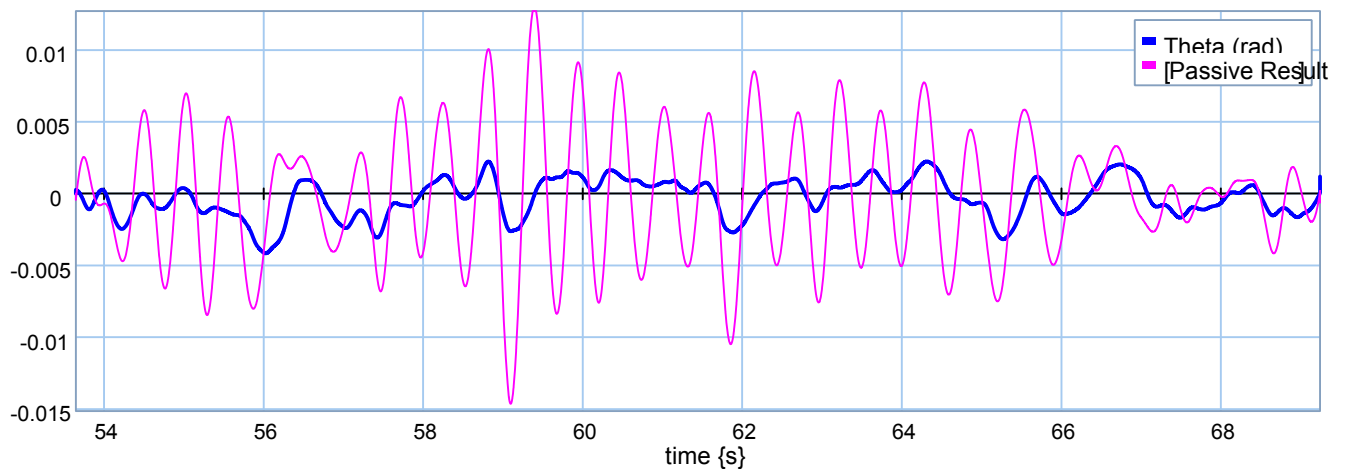
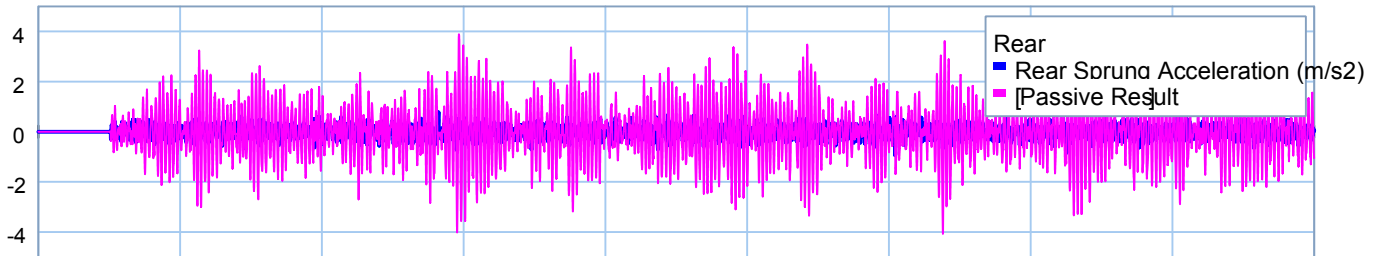
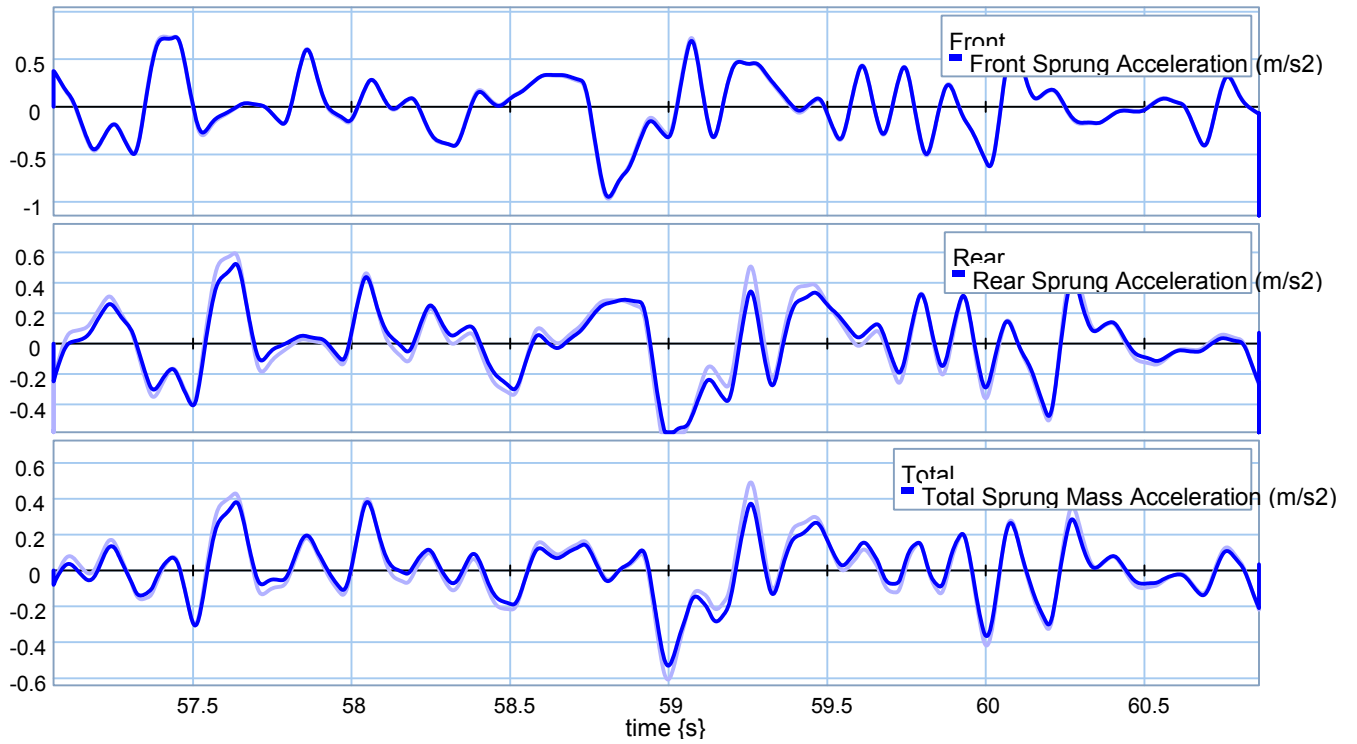
1.596601444	2.58928684	0.984493541	Coupled
1.59016107	2.547539751	0.992570274	Decoupled
1.583877623	2.507861268	1.00032181	Decoupled
1.577761041	2.470125535	1.007774652	Decoupled
1.5718169	2.434212487	1.014951809	Coupled
1.566047562	2.400008583	1.021873415	Coupled
1.560453024	2.367407102	1.028557208	Coupled
1.555031557	2.336308153	1.035018921	Coupled
1.549780192	2.306618526	1.041272589	Coupled
1.544695077	2.278251413	1.047330803	Coupled
1.539771754	2.251126083	1.053204914	Coupled
1.535005363	2.225167513	1.058905206	Coupled
1.530390801	2.200306016	1.064441031	Coupled
1.52592284	2.176476869	1.069820933	Coupled
1.521596212	2.153619949	1.075052742	Coupled
1.517405676	2.131679394	1.080143662	Coupled
1.513346069	2.110603273	1.085100339	Coupled
1.509412338	2.090343286	1.089928923	Coupled
1.505599564	2.070854482	1.094635121	Coupled
1.501902982	2.052094996	1.099224242	Coupled
1.498317991	2.034025808	1.103701238	Coupled
1.49484016	2.016610522	1.108070735	Coupled
1.491465228	1.999815163	1.112337064	Coupled
1.488189112	1.98360799	1.116504292	Coupled
1.485007897	1.967959323	1.120576238	Coupled

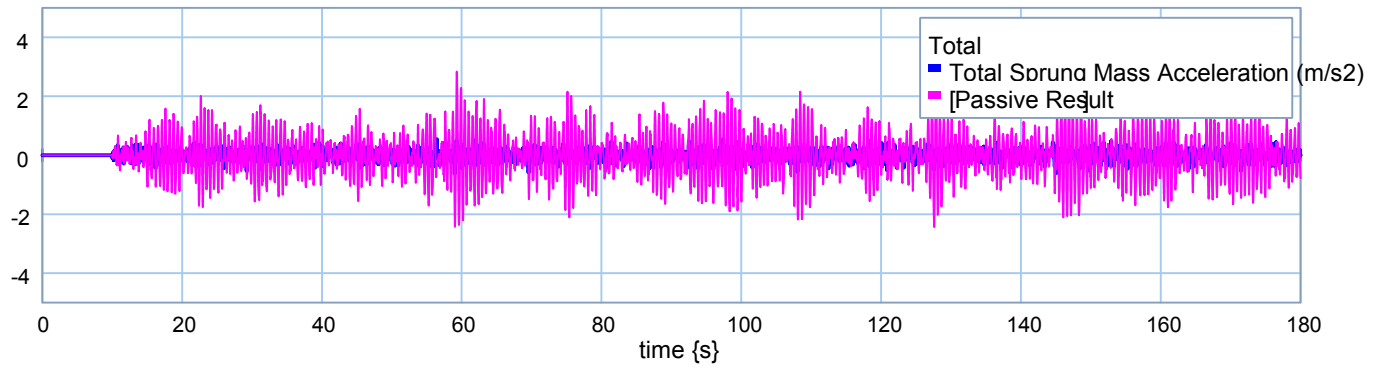
Appendix B: Linear HalfCar Model, Ride Quality Scenario, QuarterCar Active Suspensions.

❖ $M_c = 4500 \text{ kg.}$

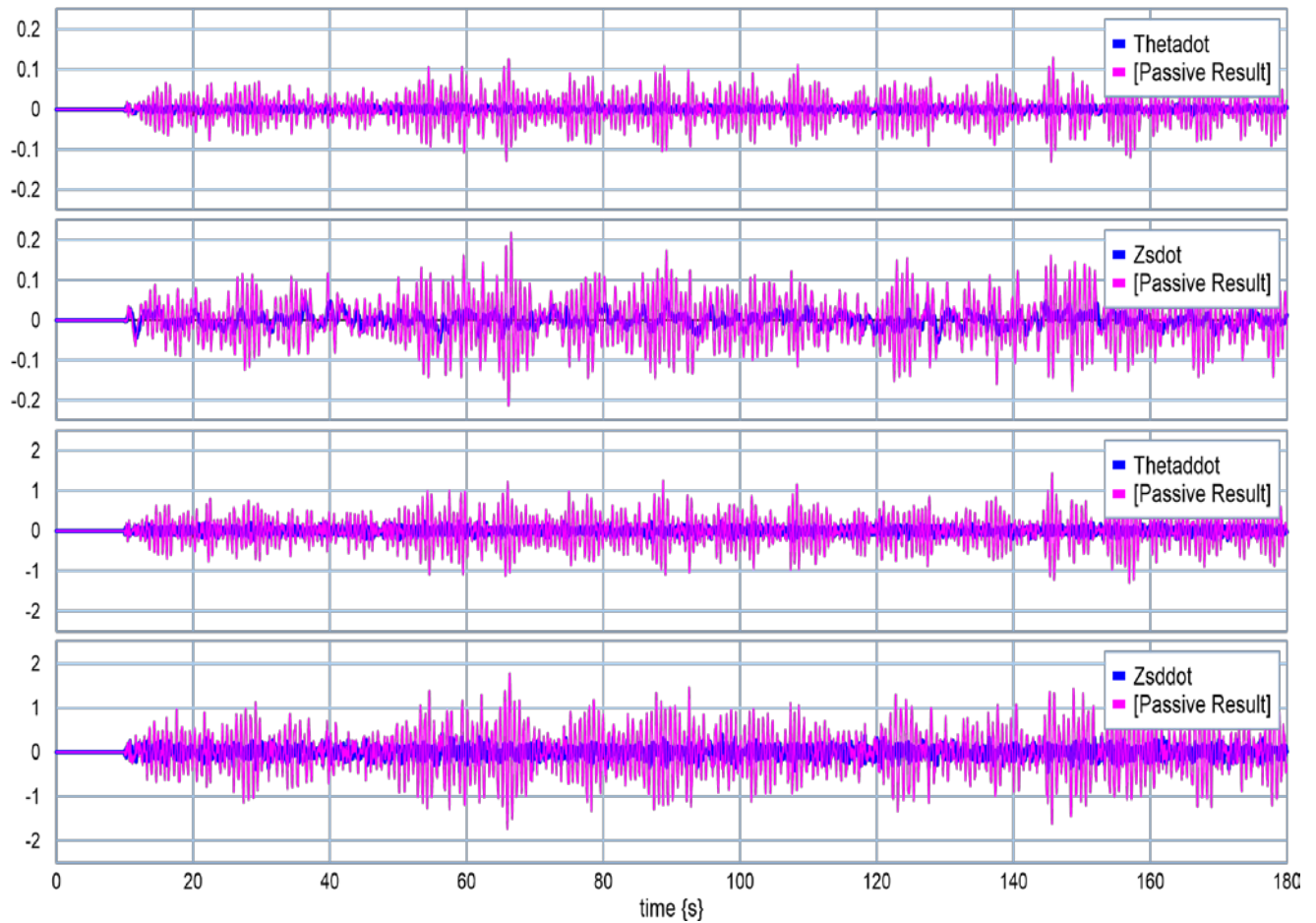


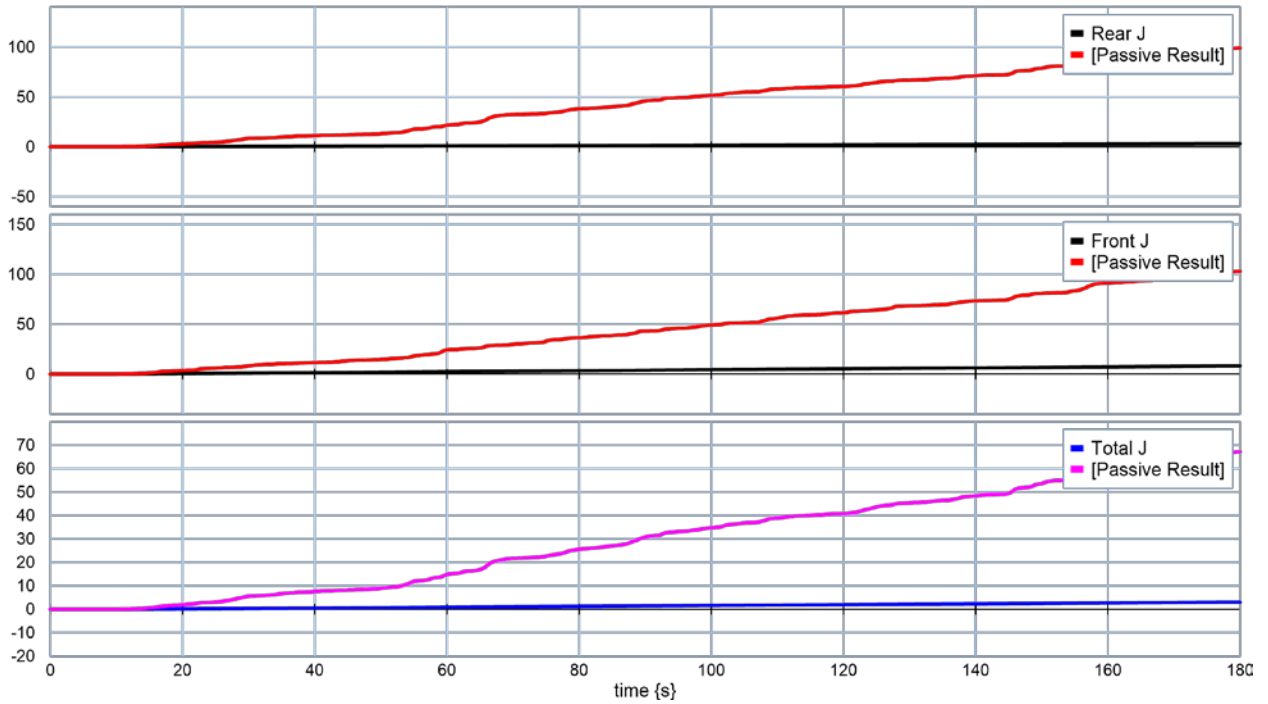
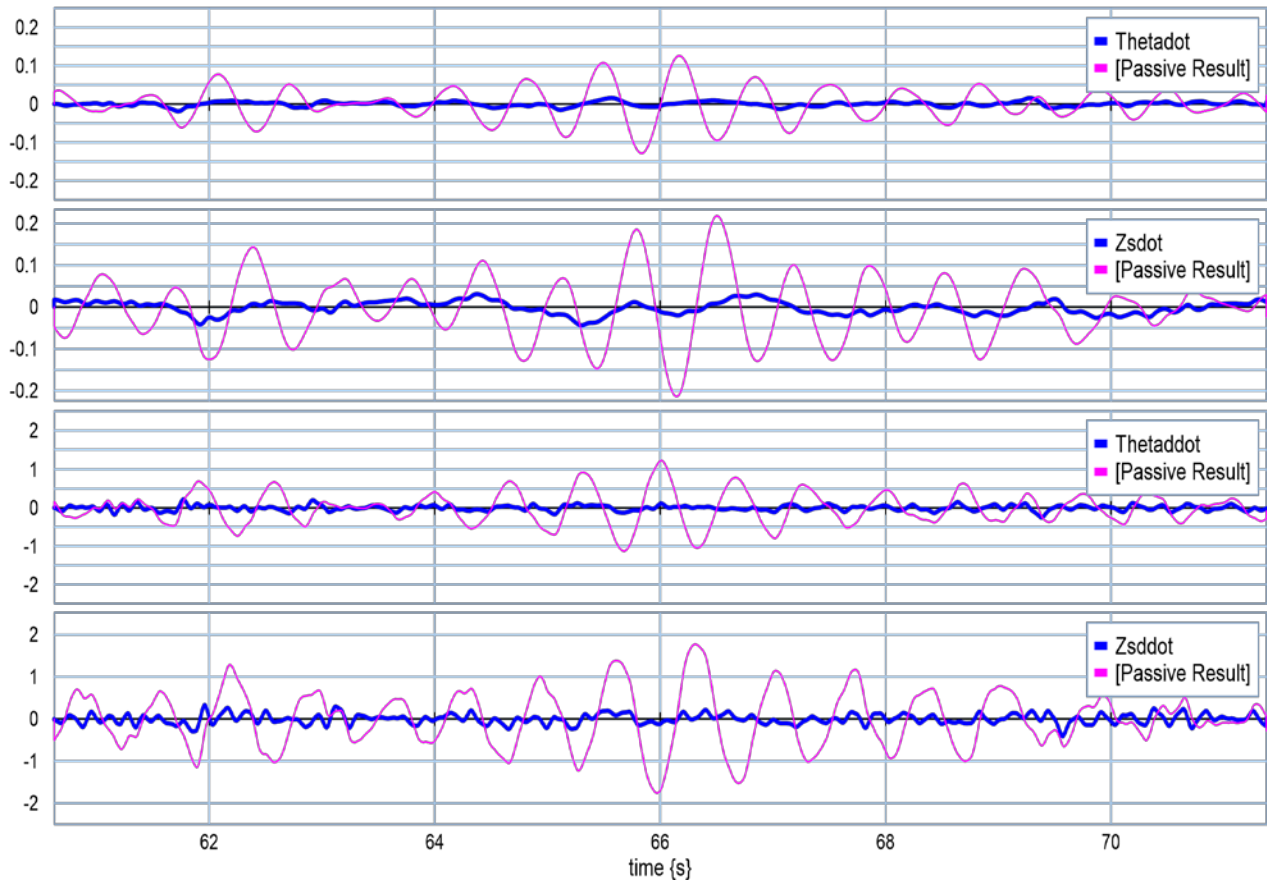


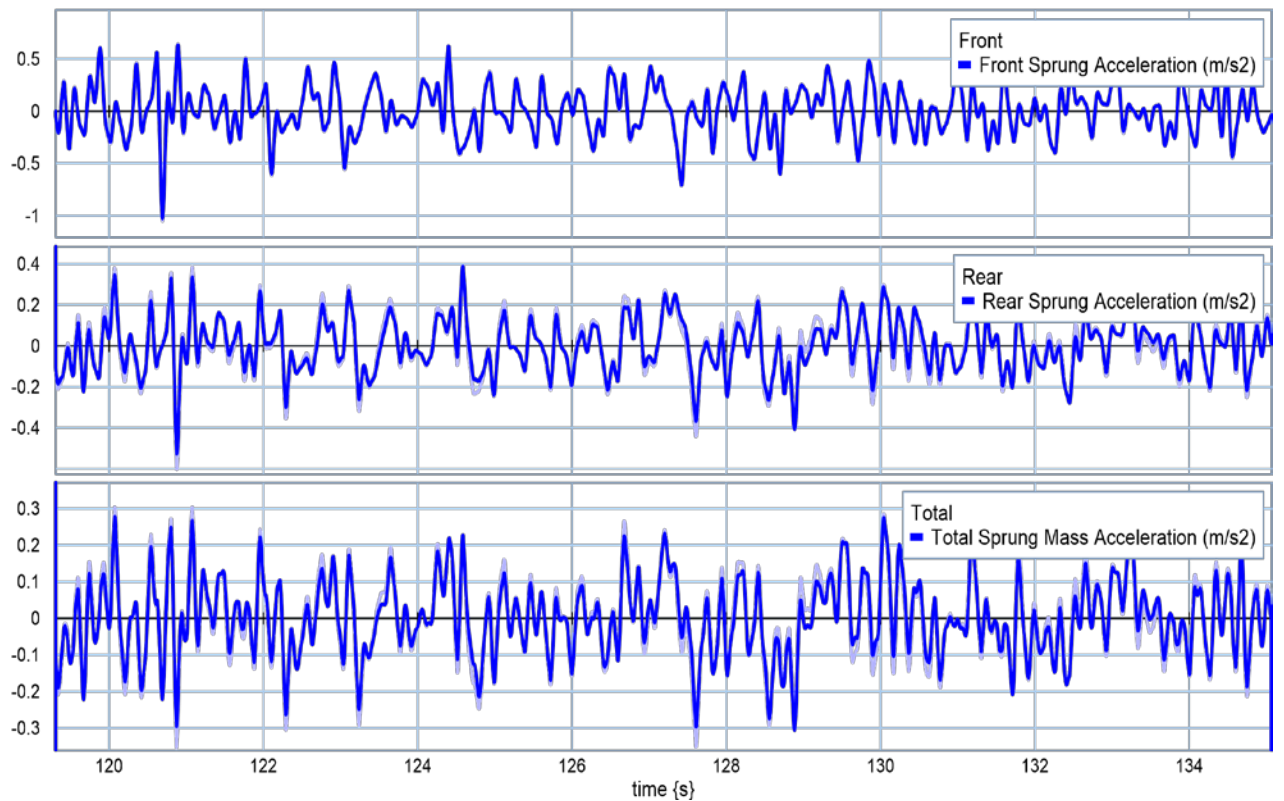
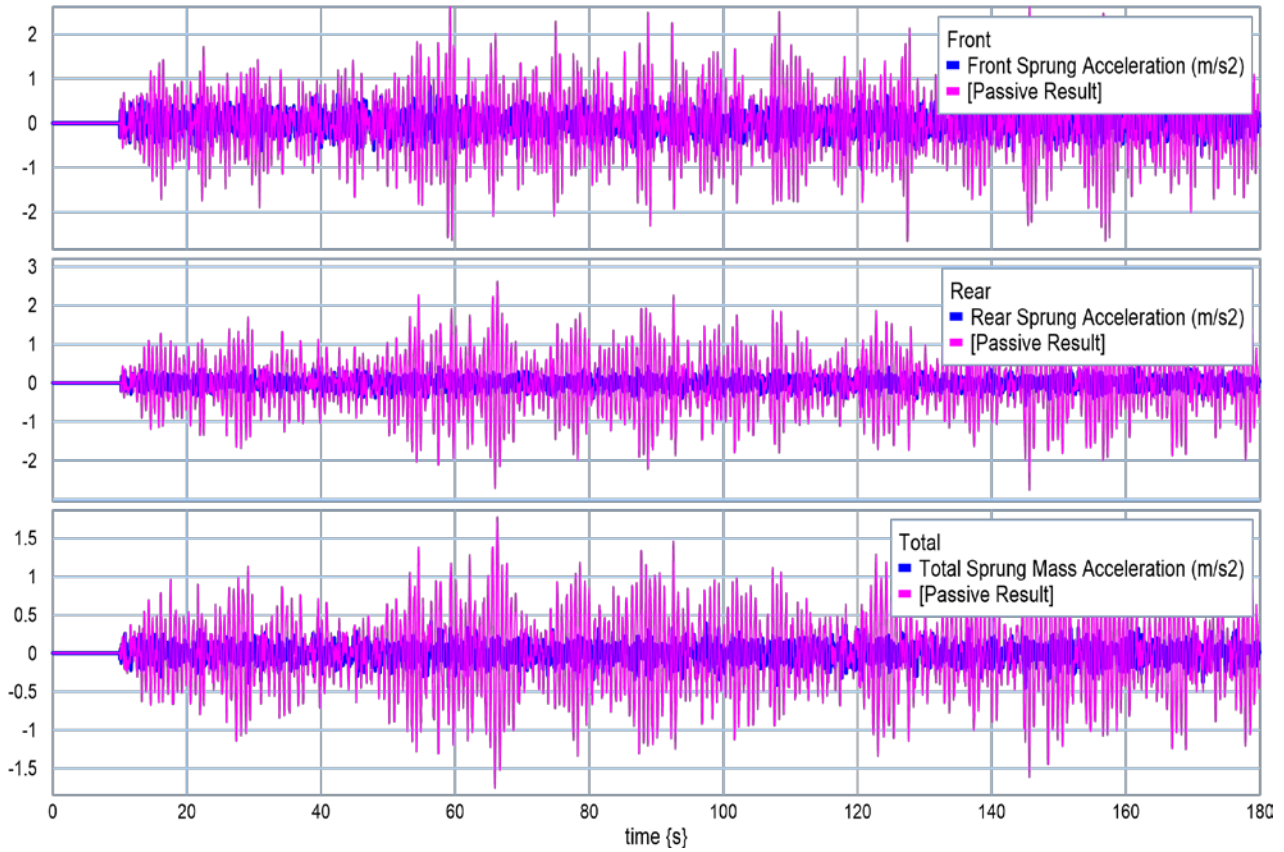


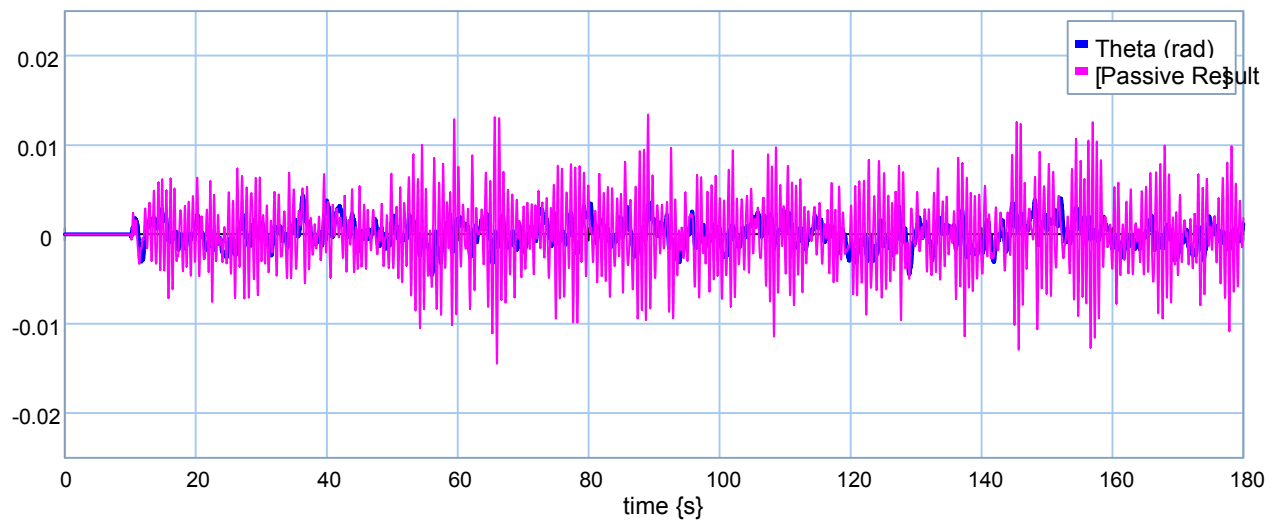
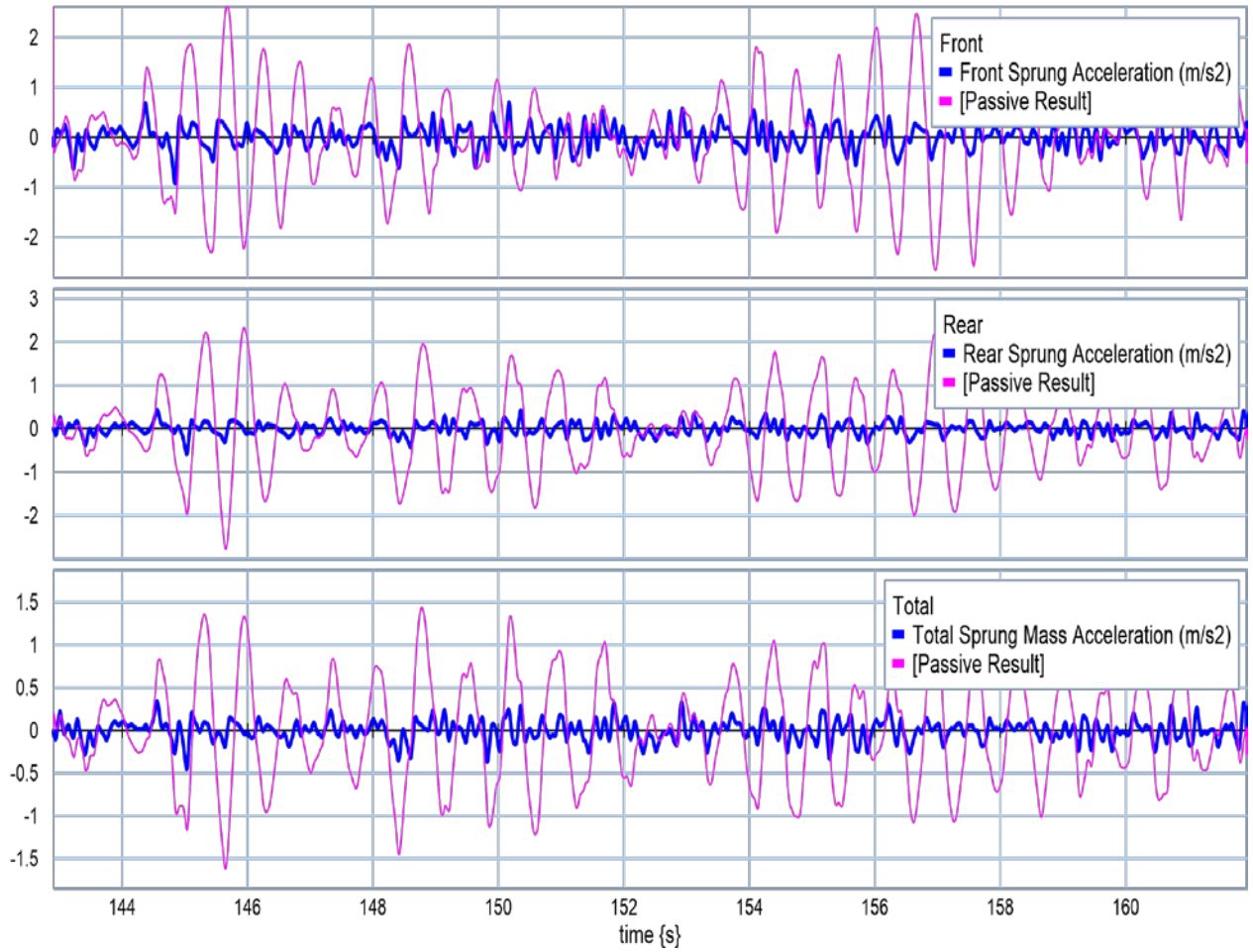


❖ **$M_c = 9000 \text{ kg.}$**

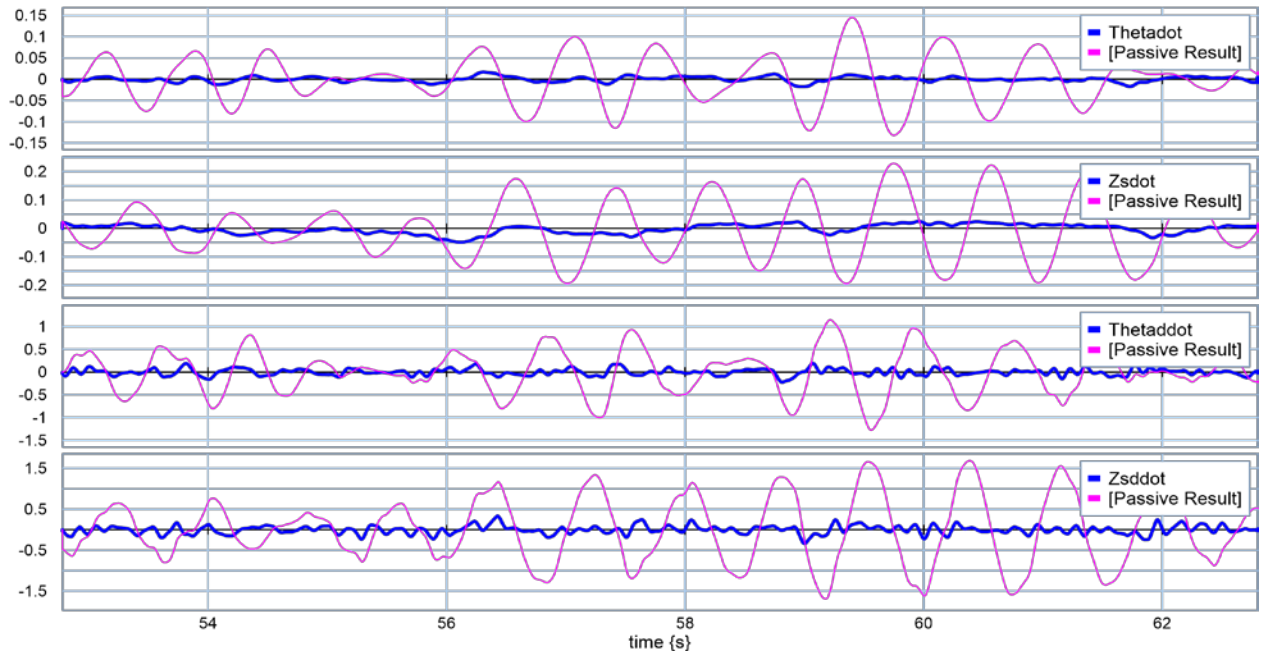
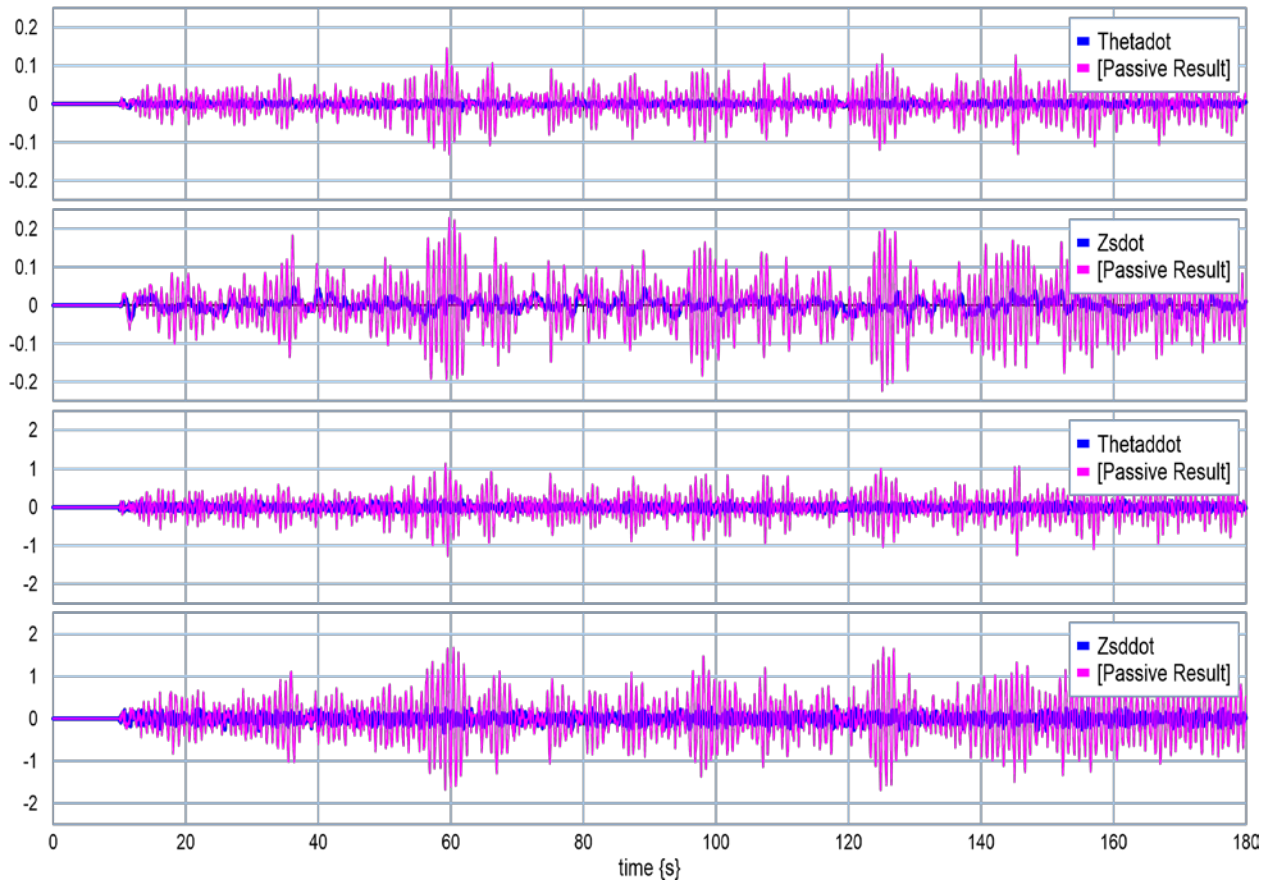


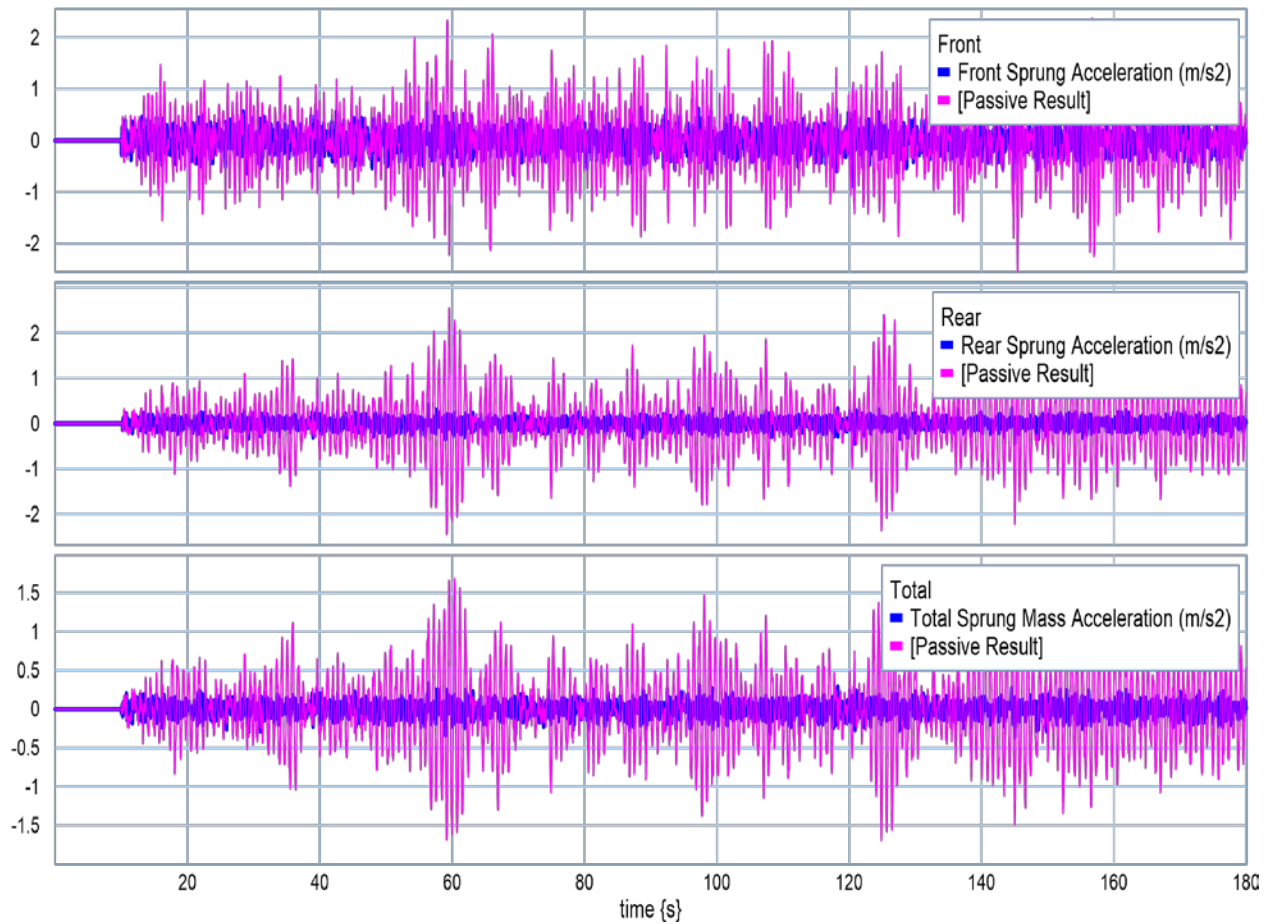
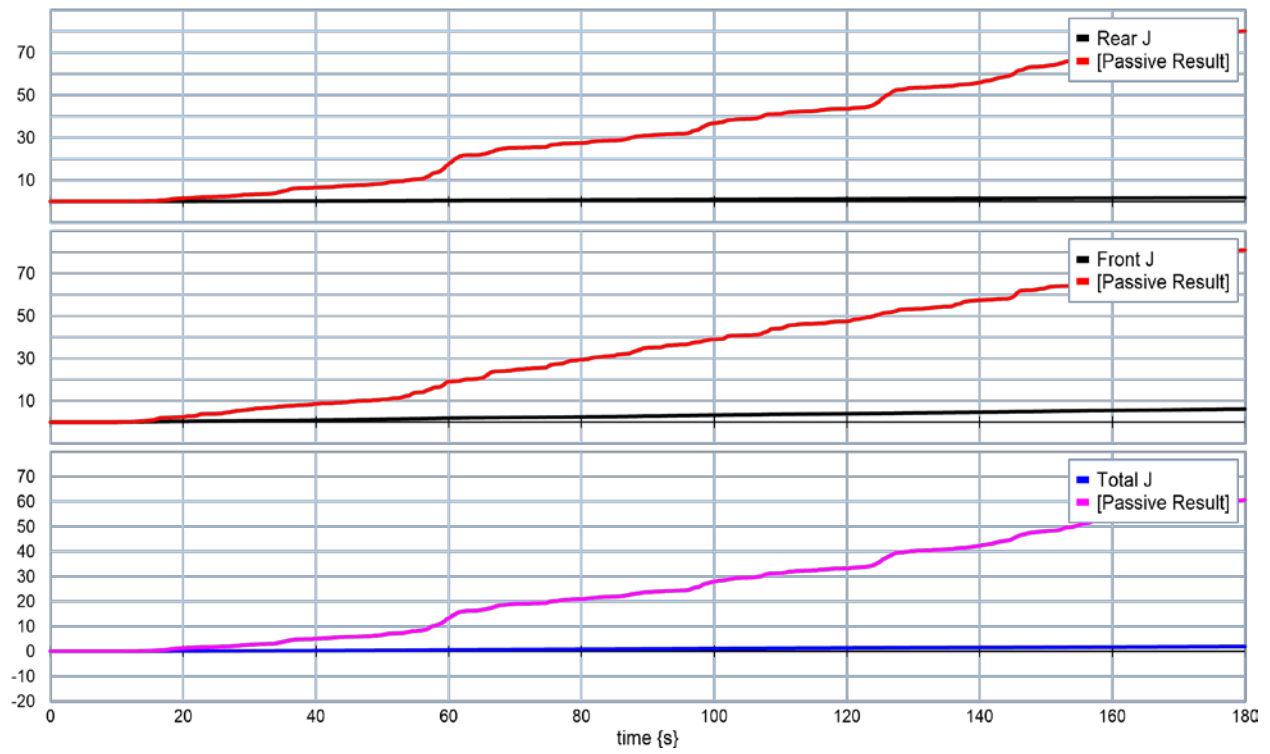


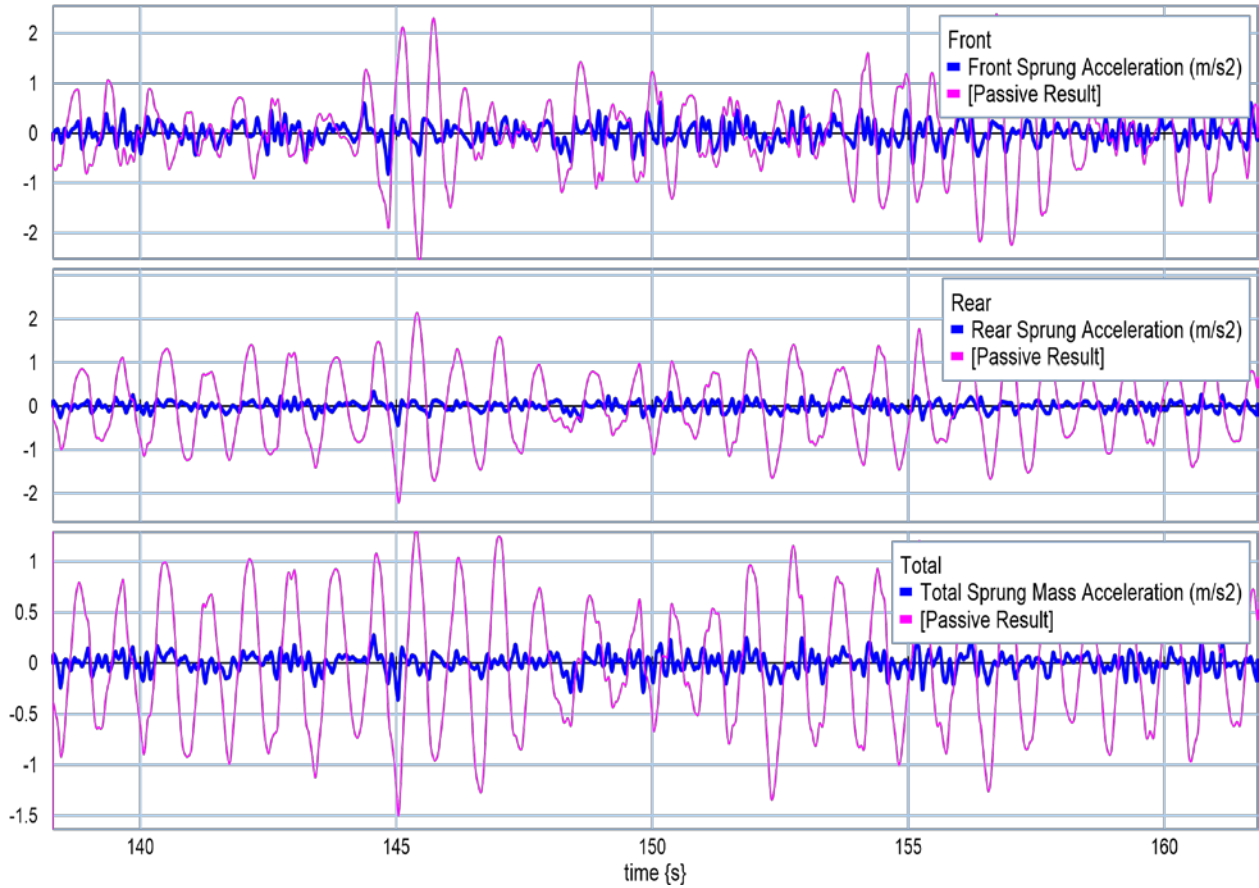
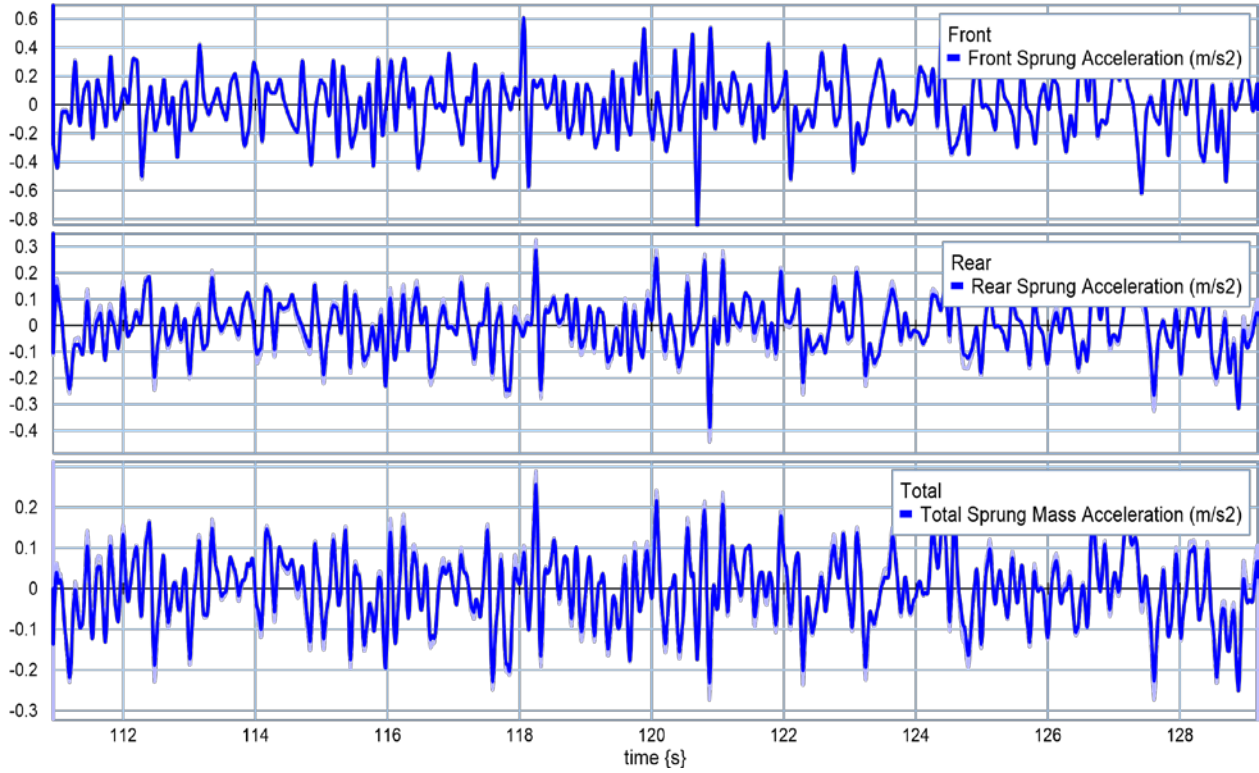


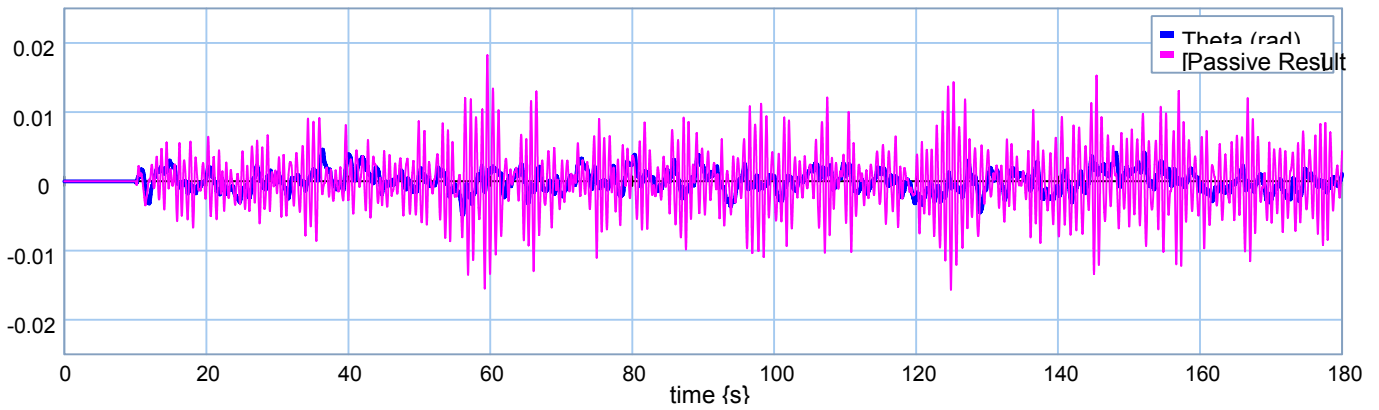


❖ $M_c = 13500 \text{ kg.}$

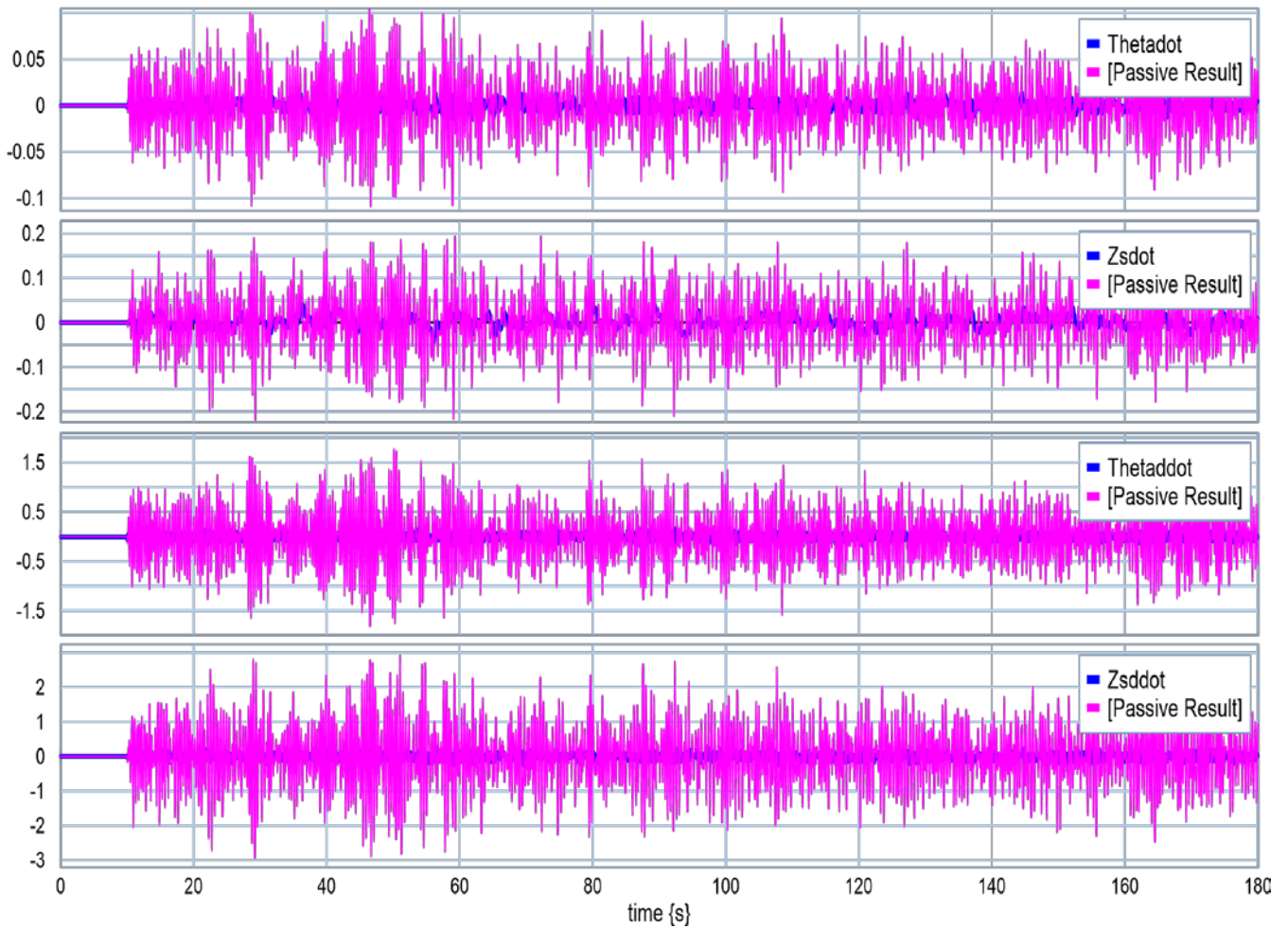


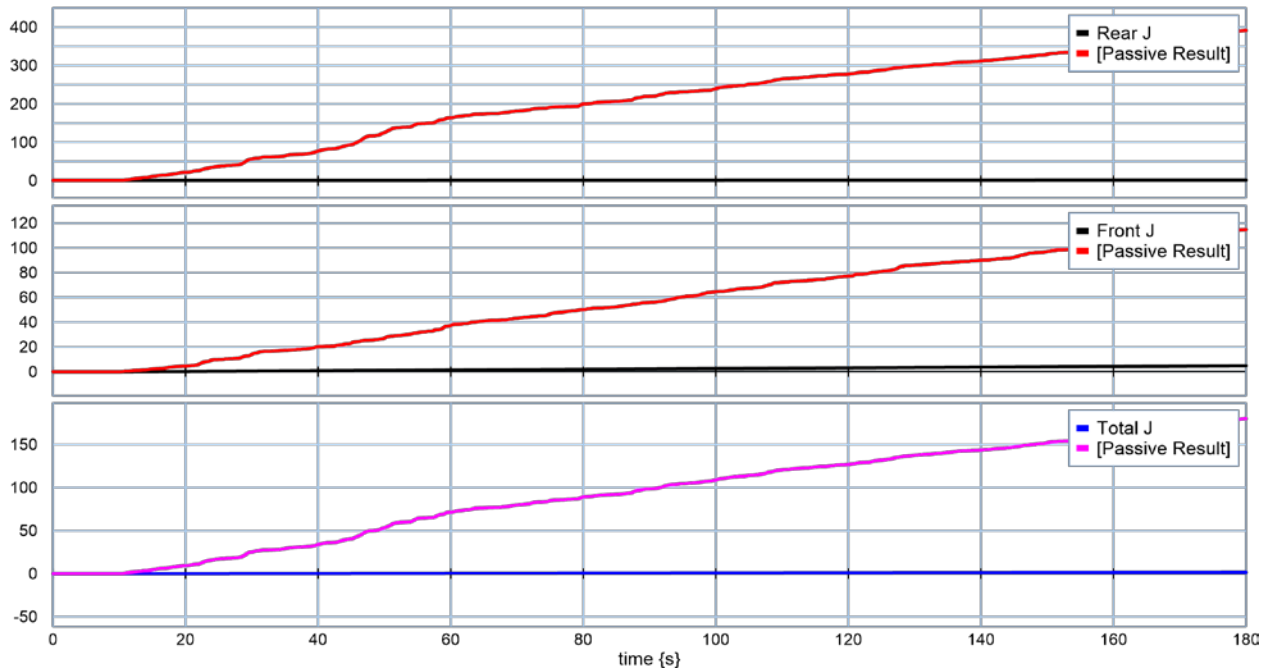
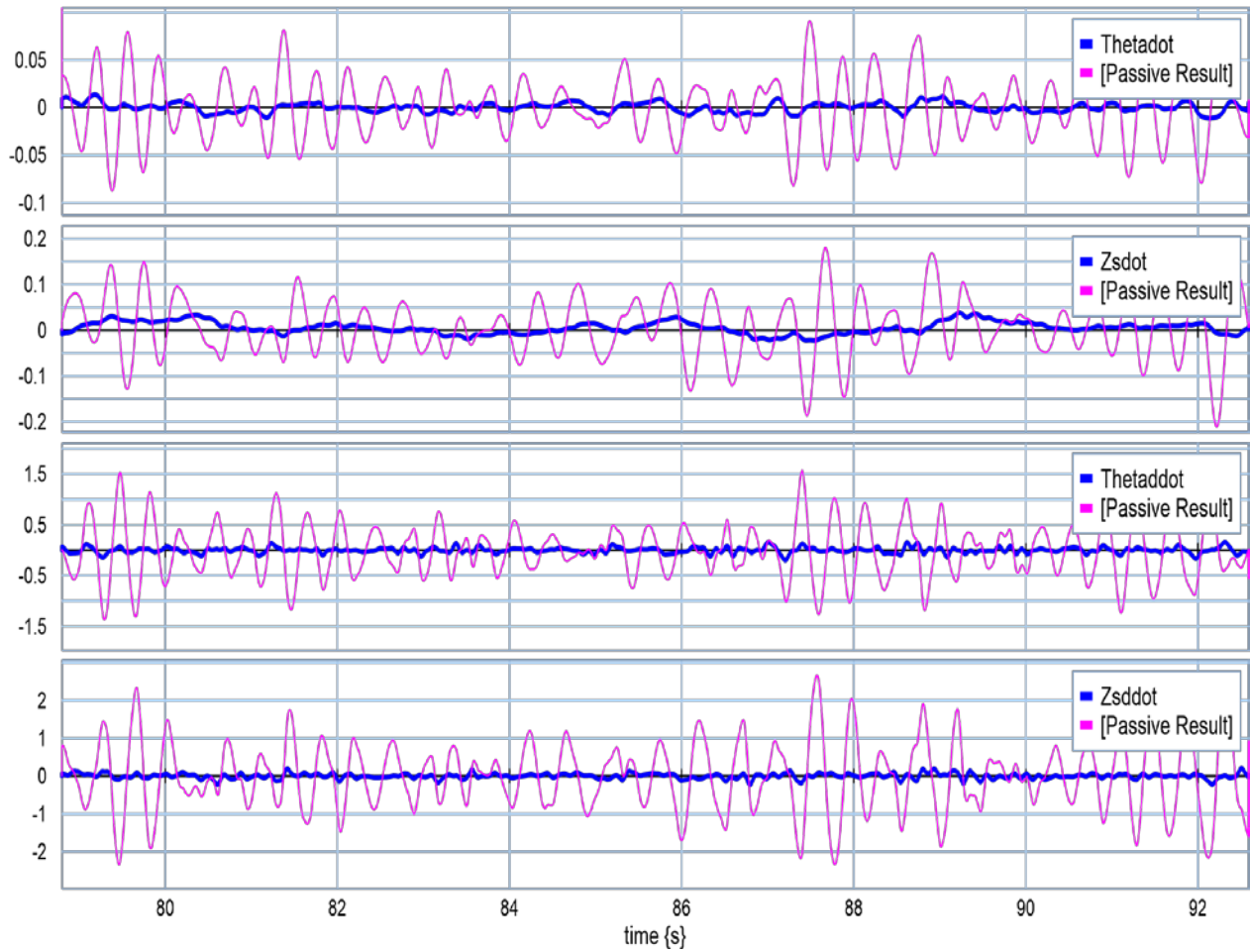


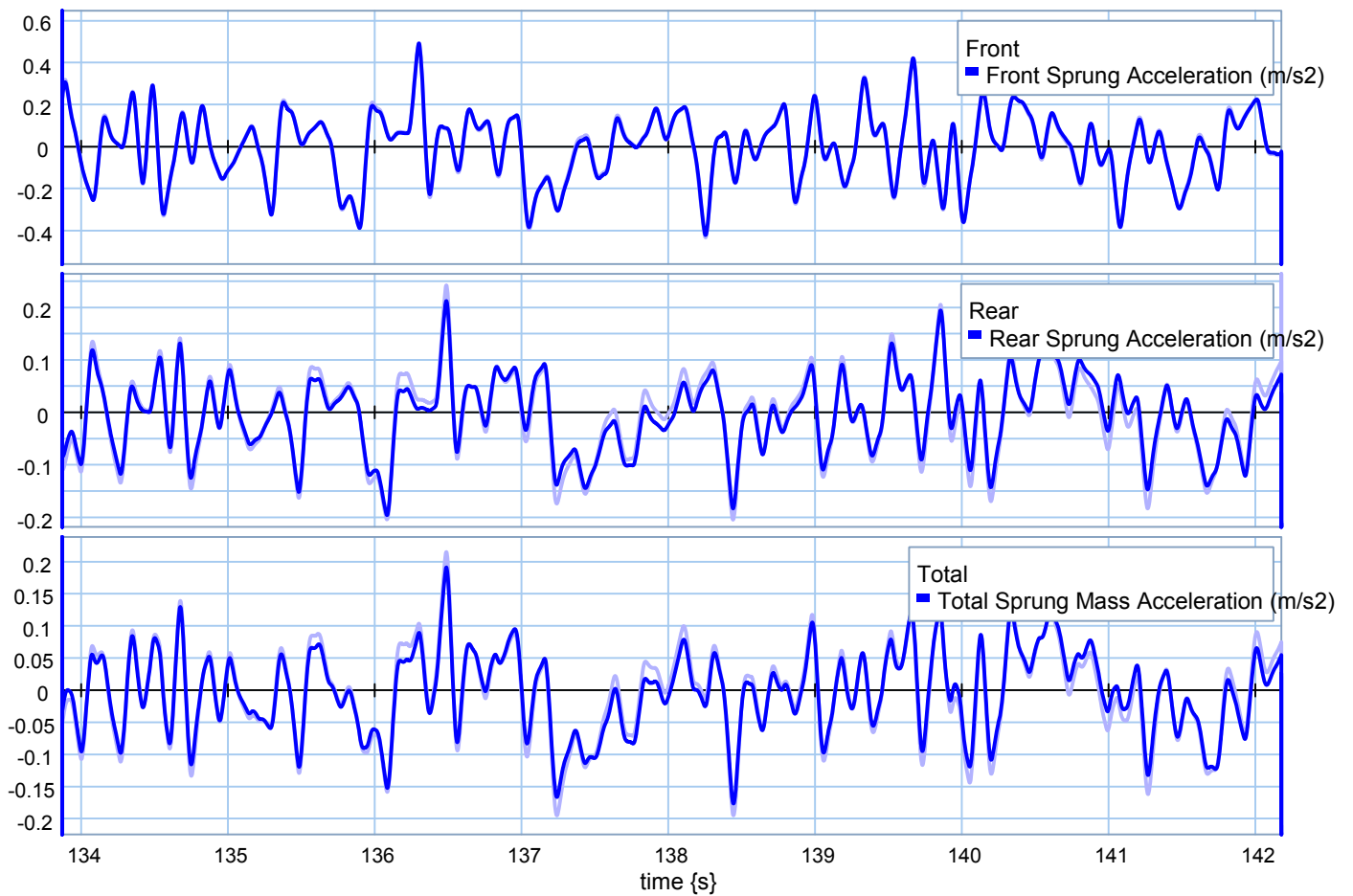
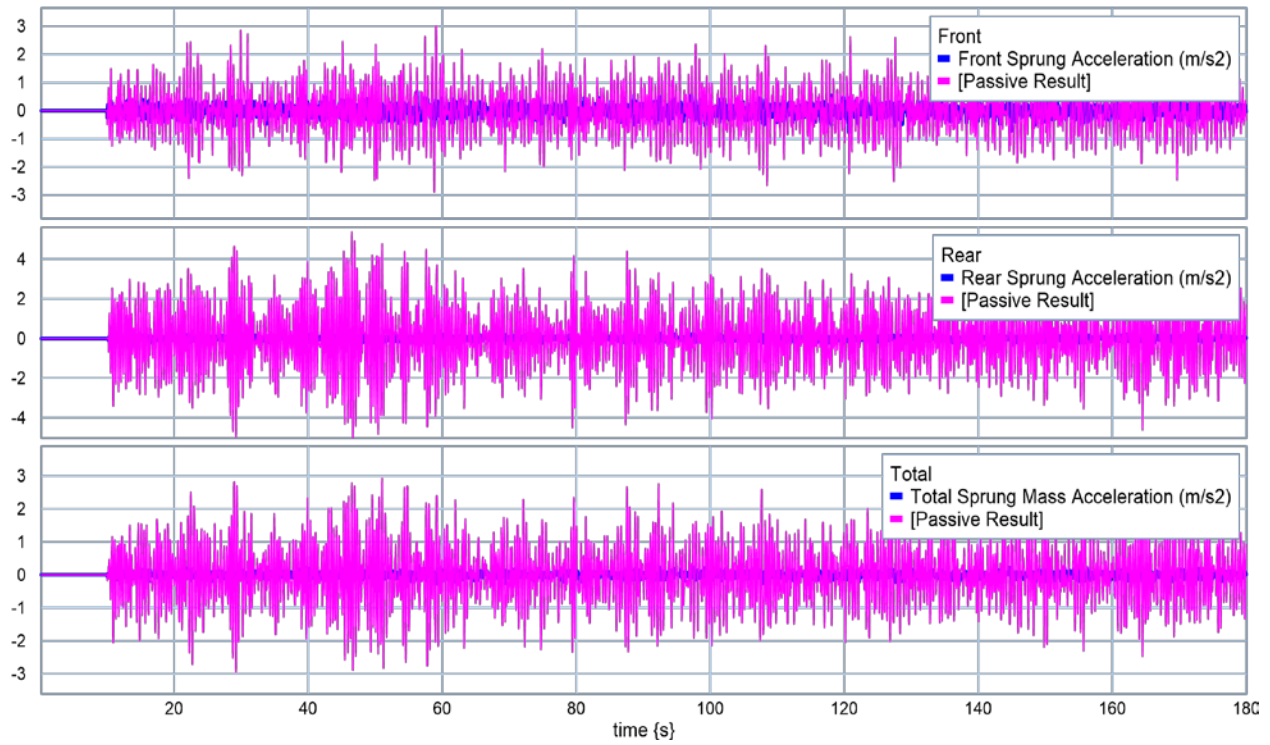


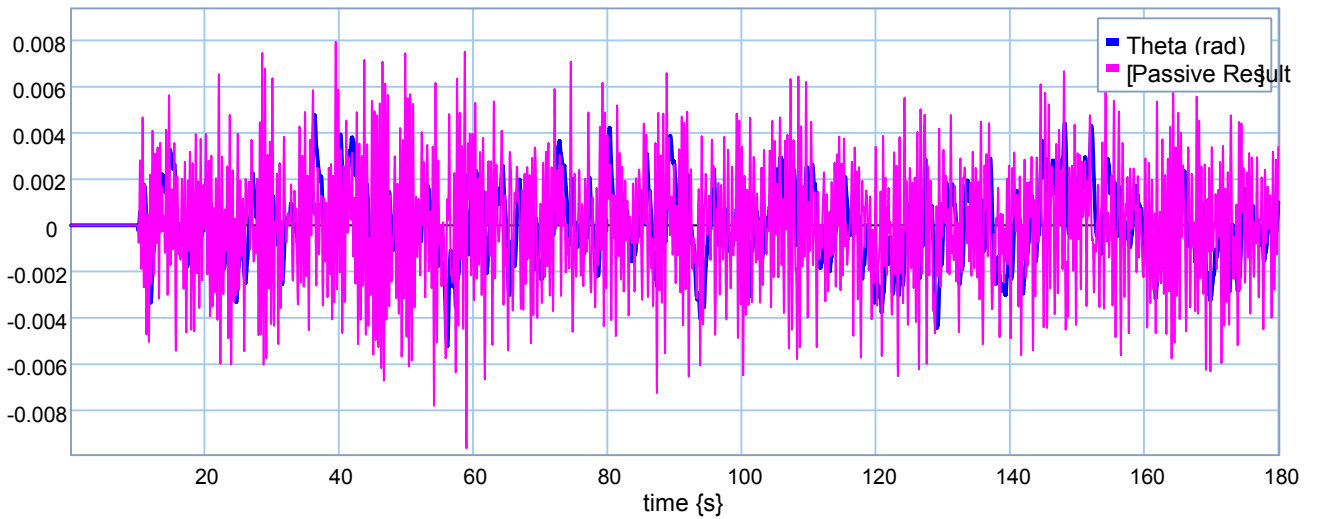
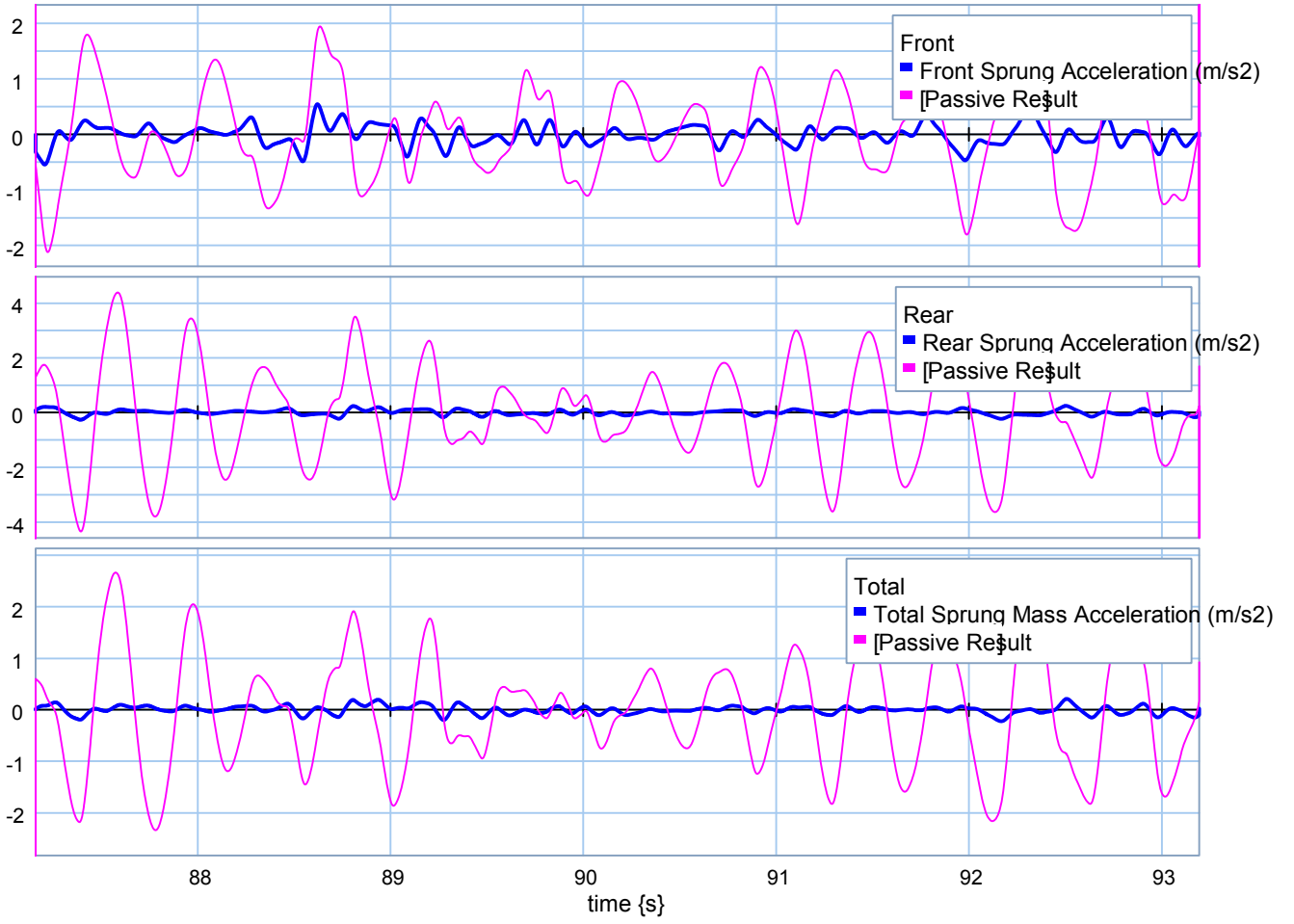


❖ **Mc = 18000 kg.**



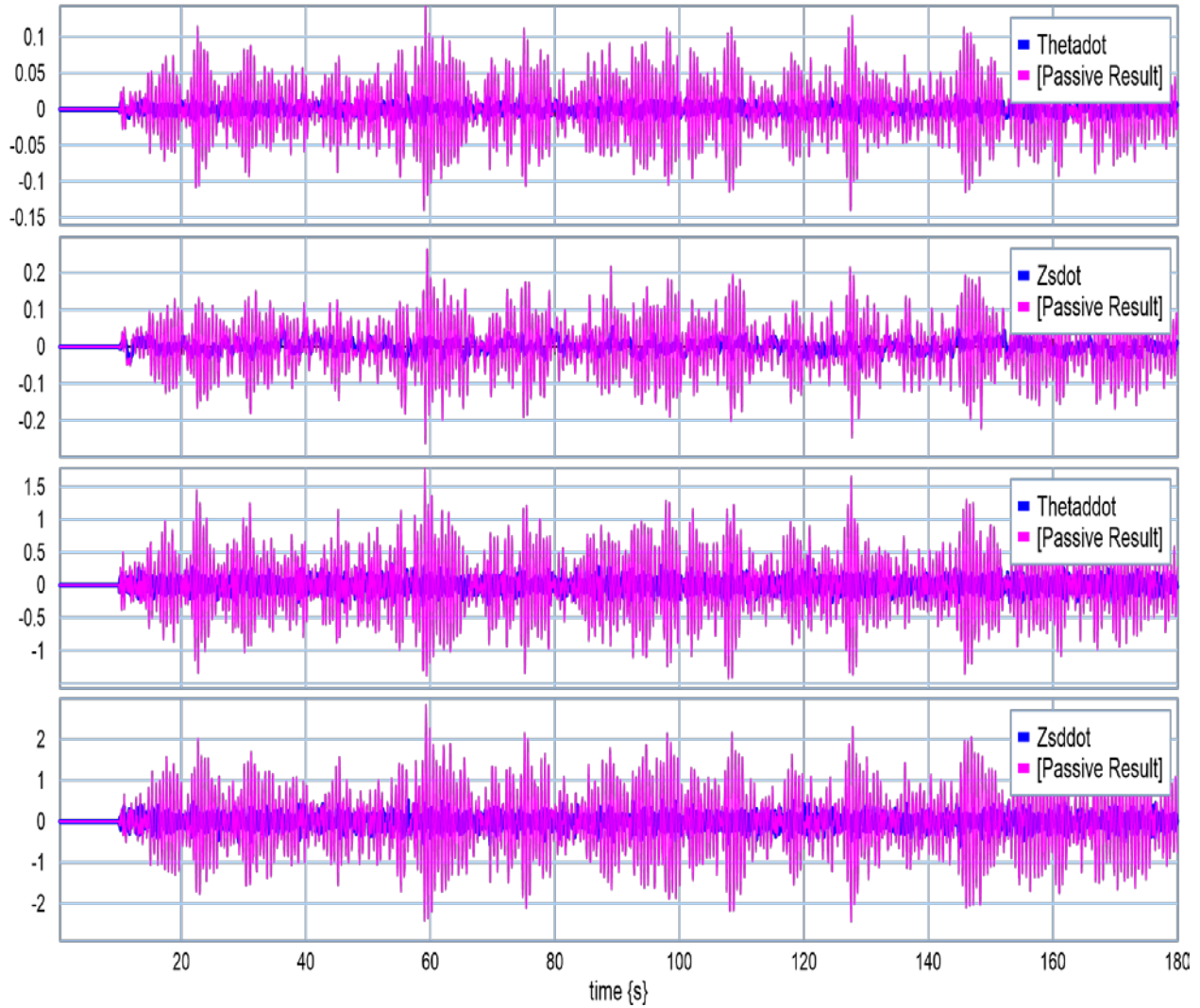


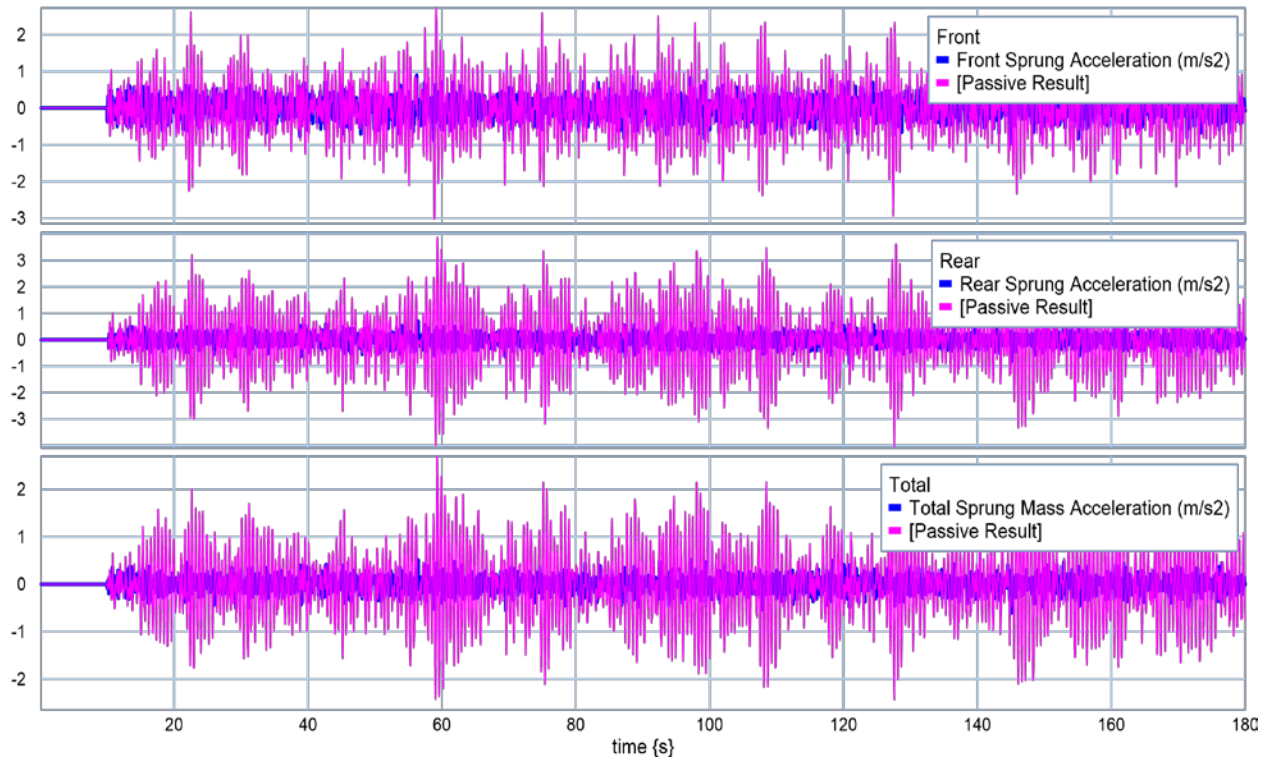
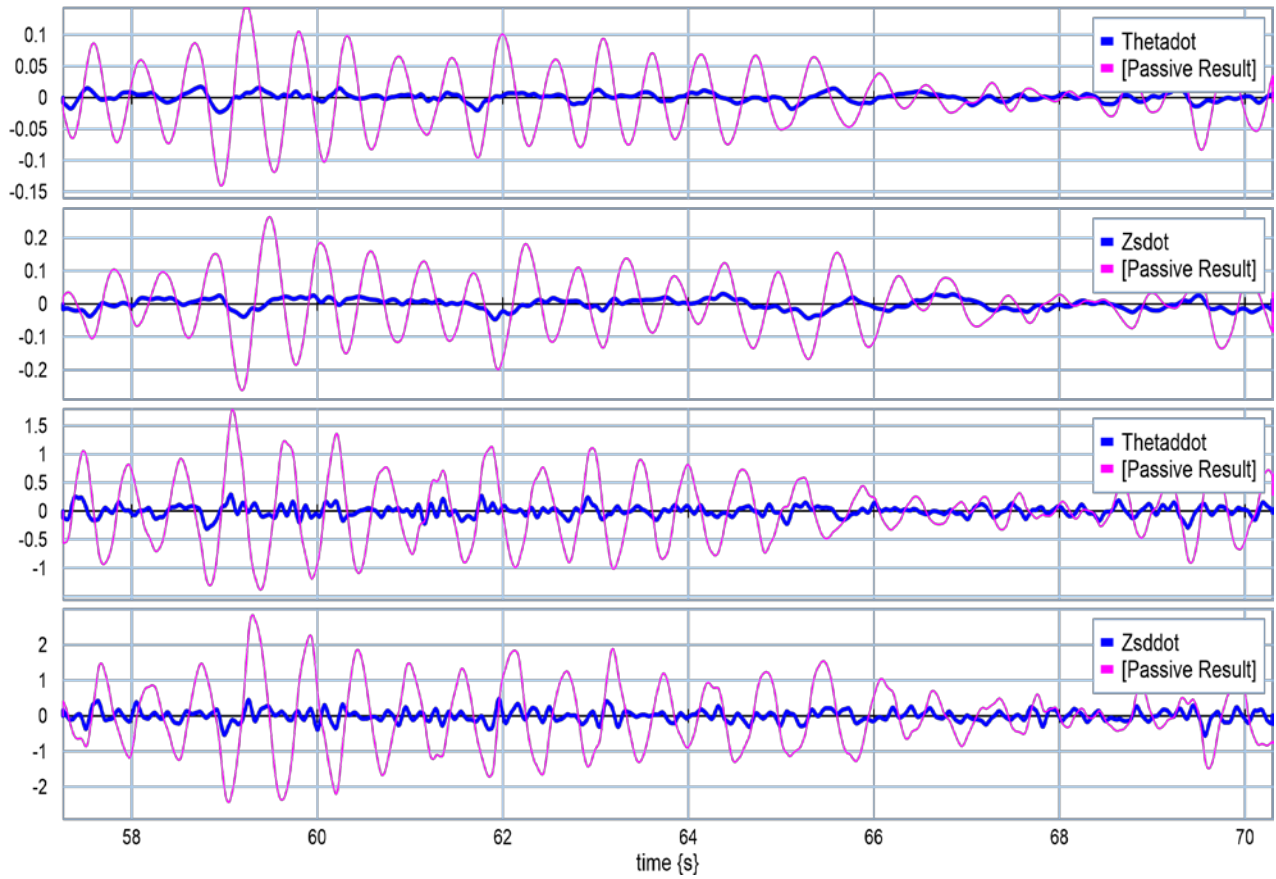


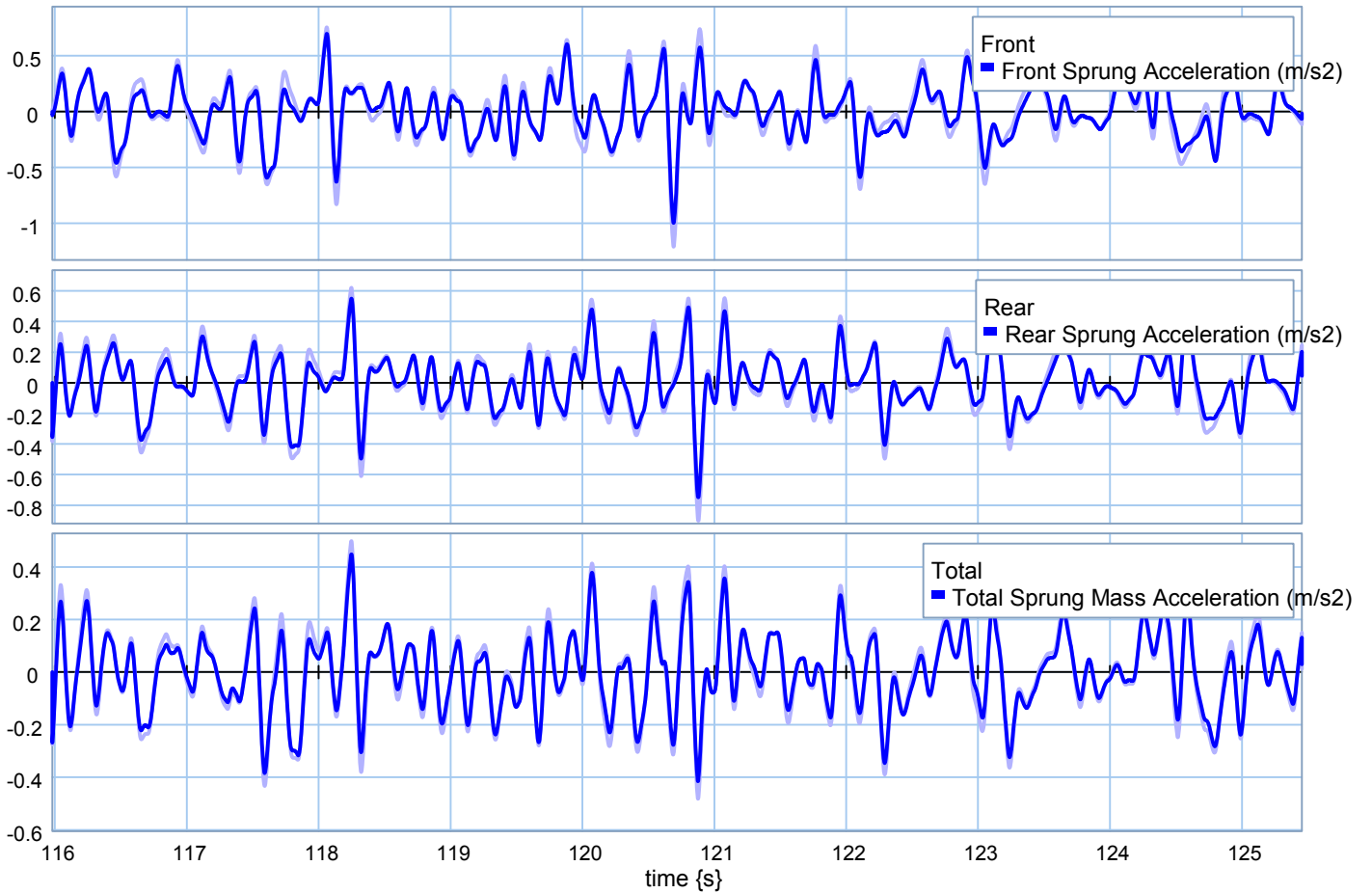
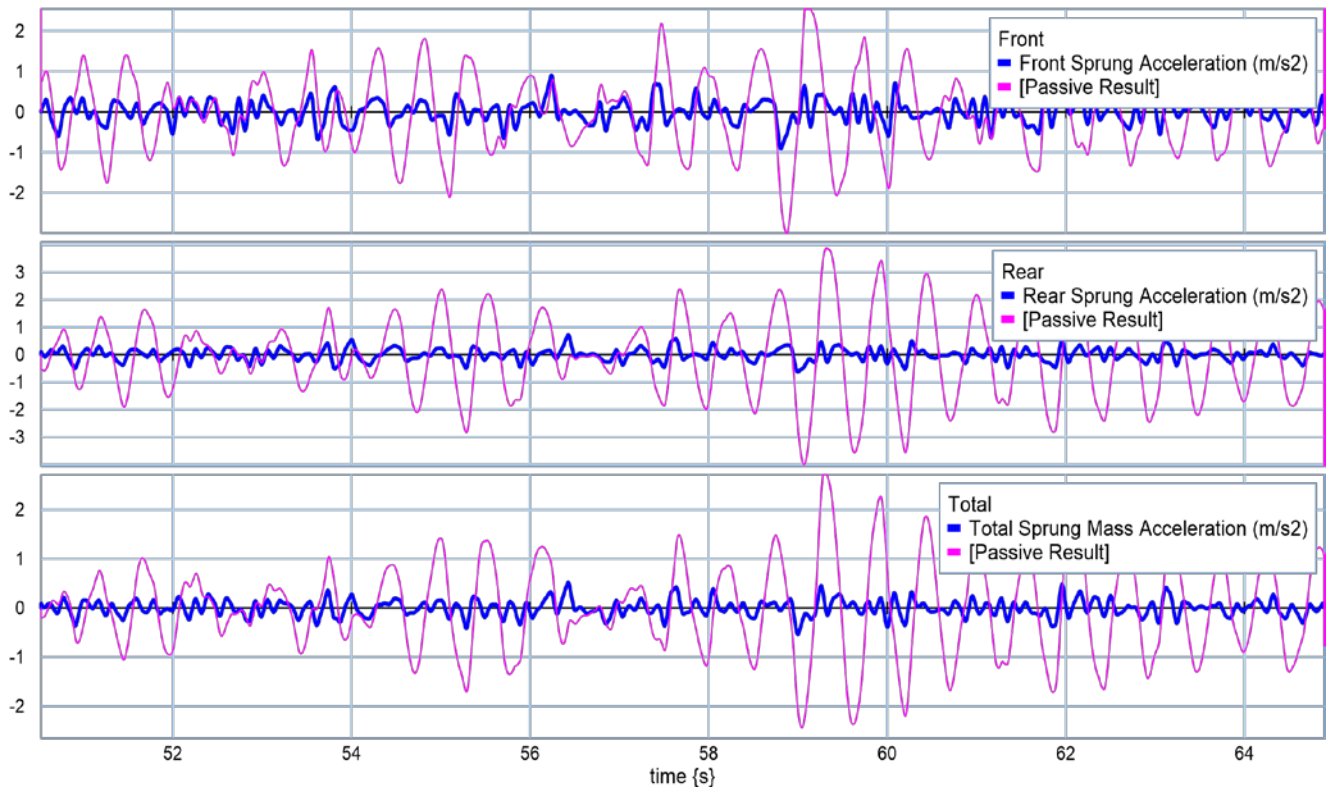


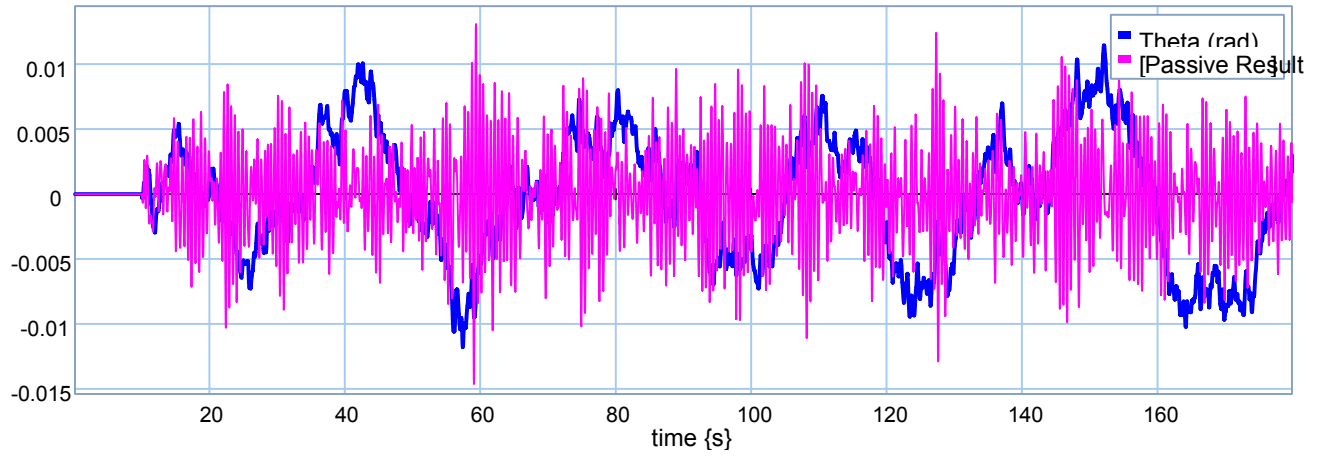
Appendix C: Linear Half-Car Model, Ride Quality Scenario, Half-Car Active Suspensions.

❖ $M_c = 4500 \text{ kg}$.

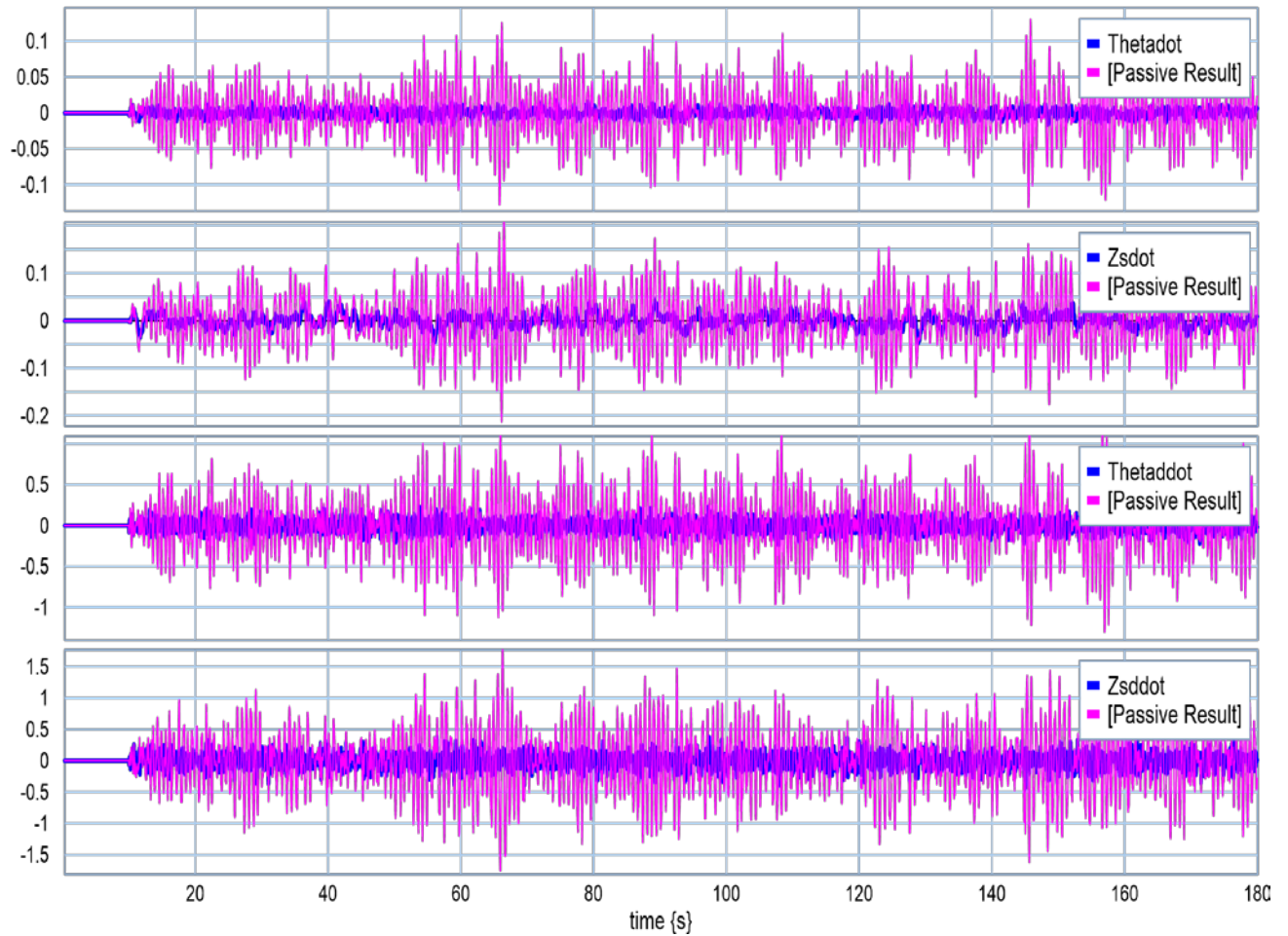


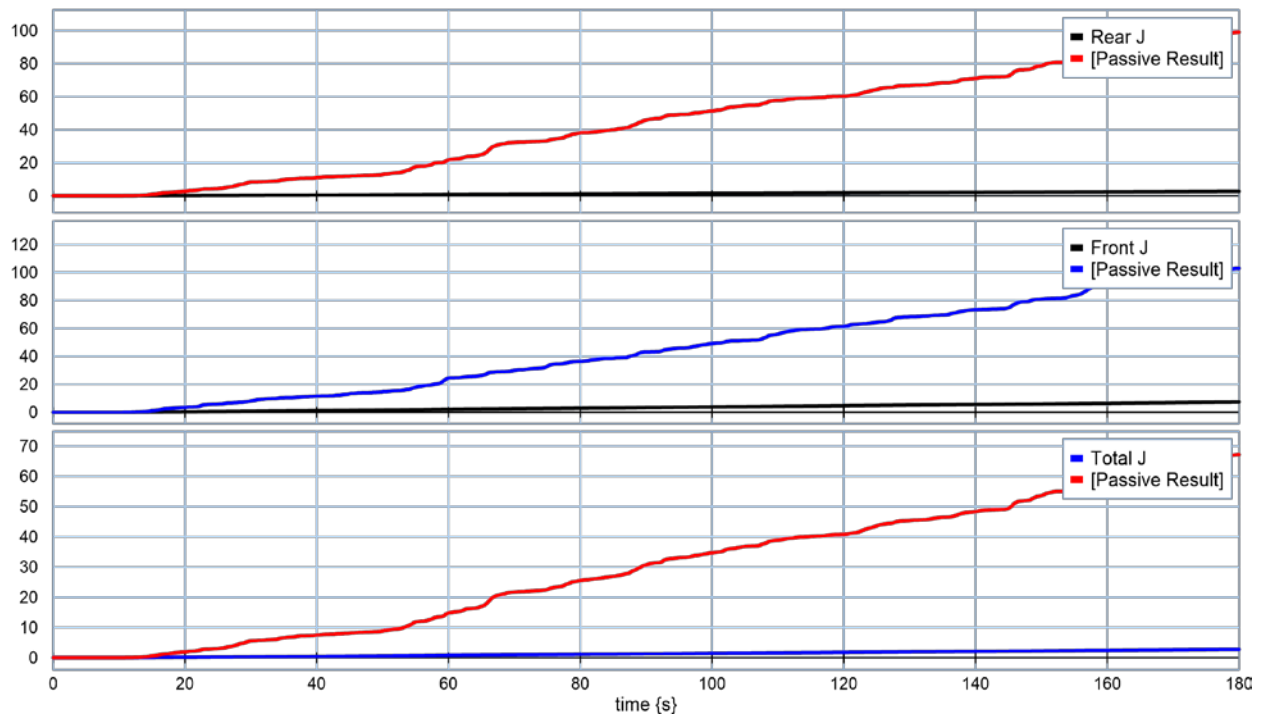
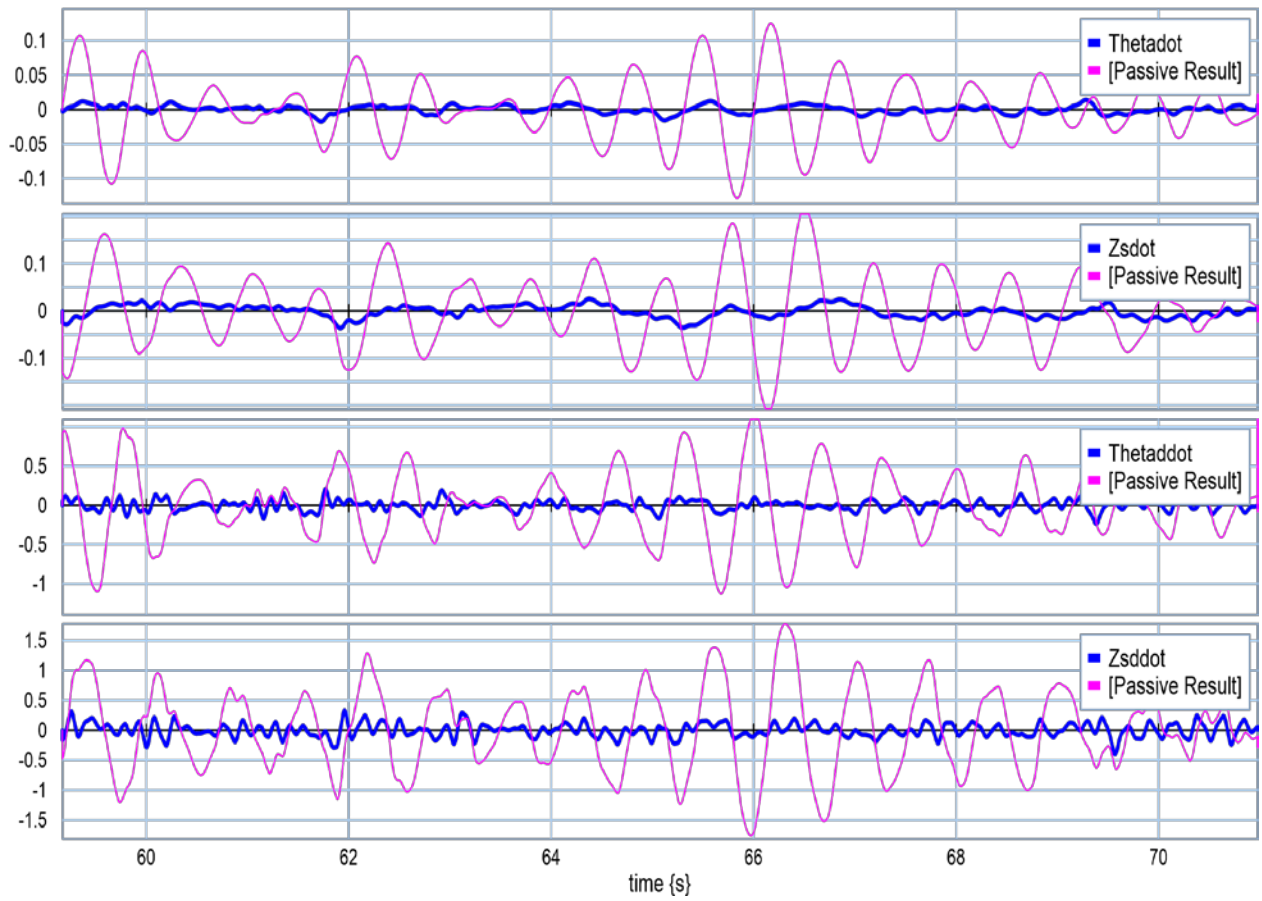


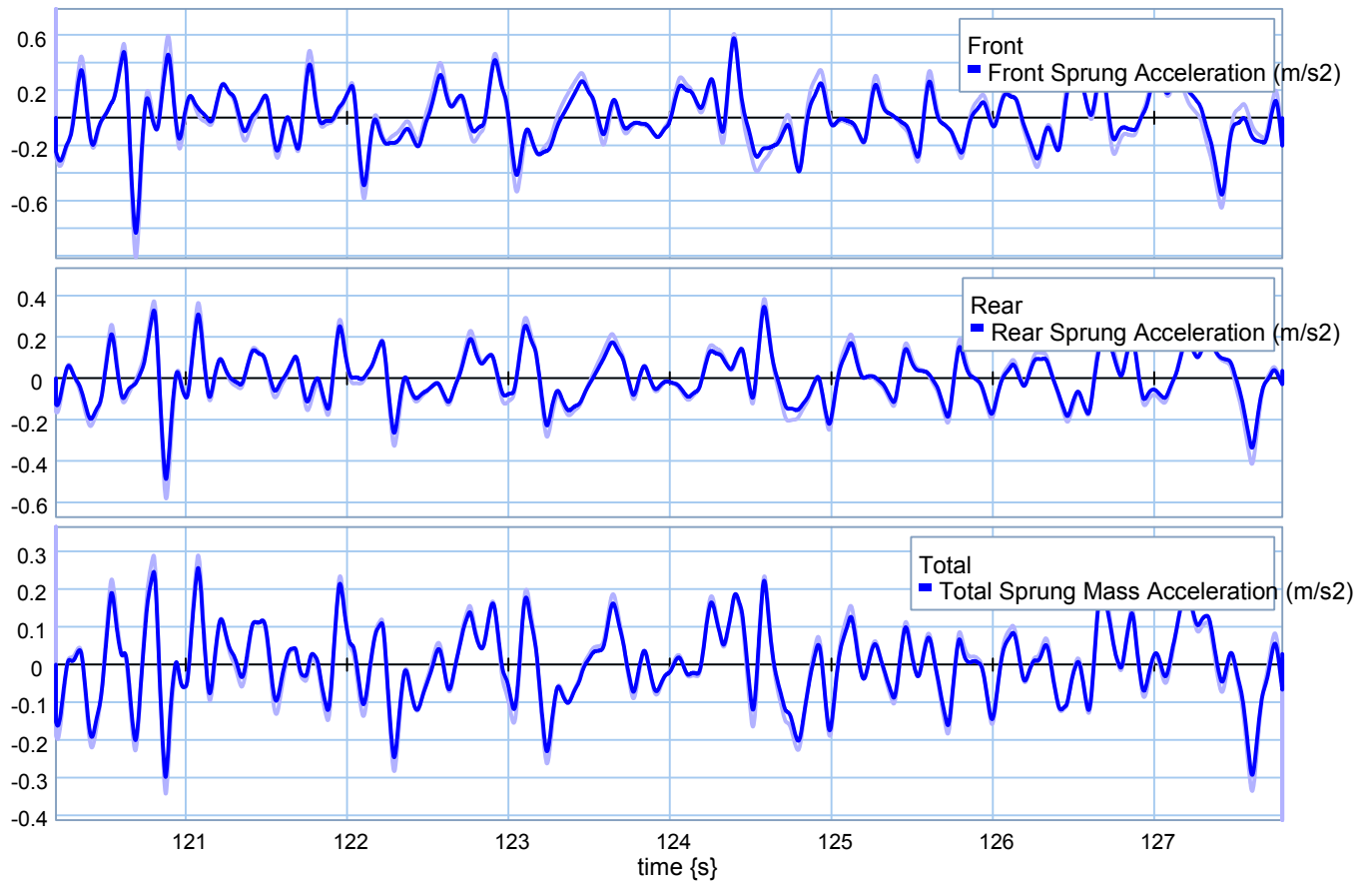
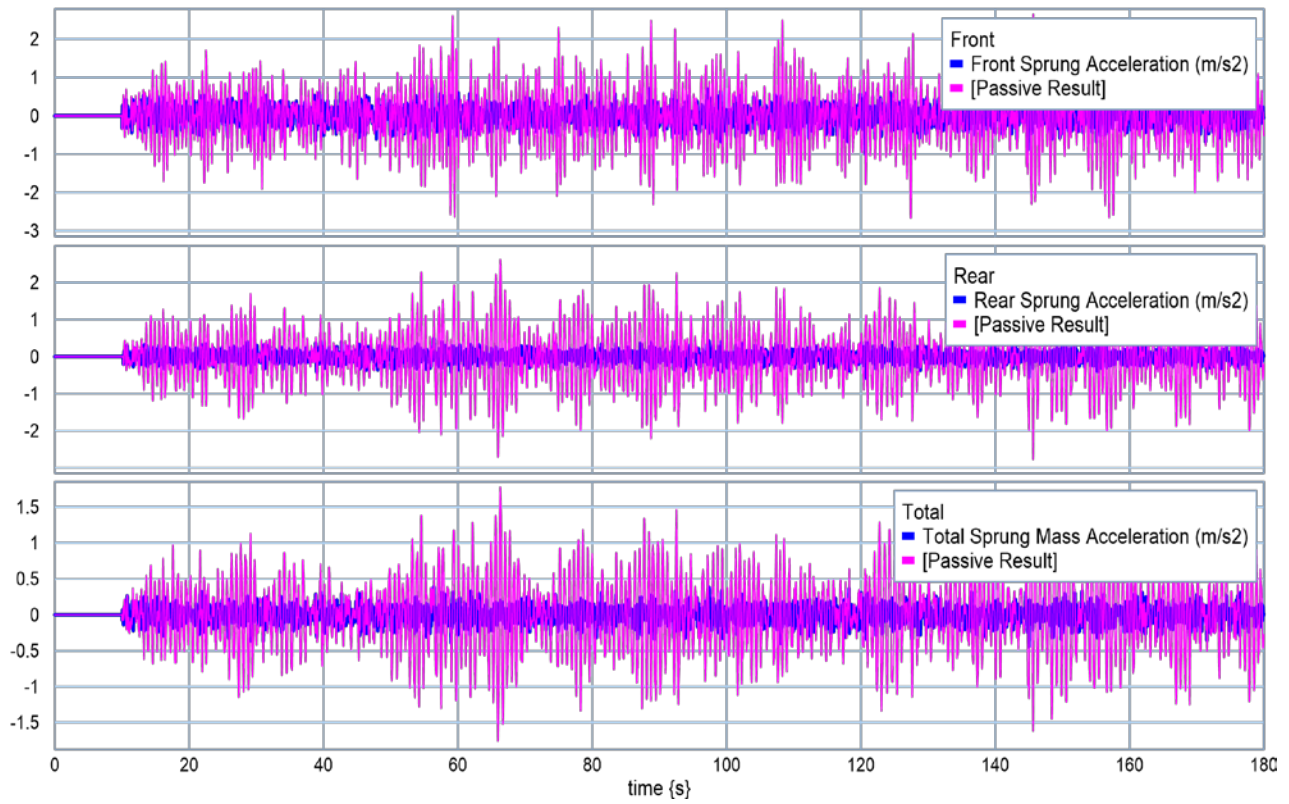


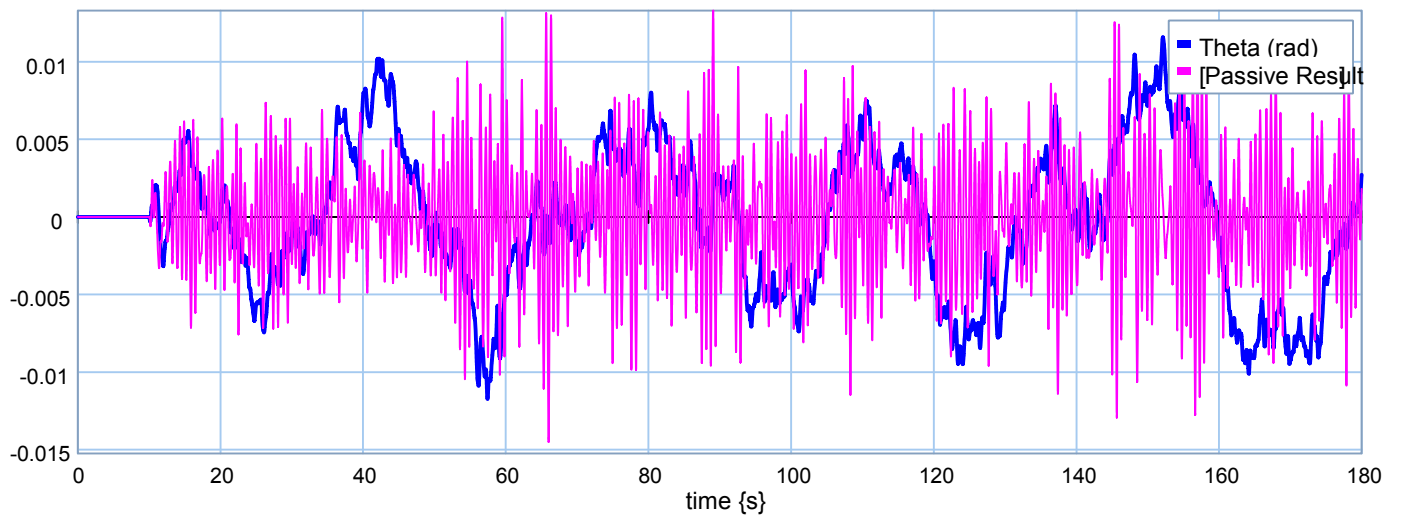
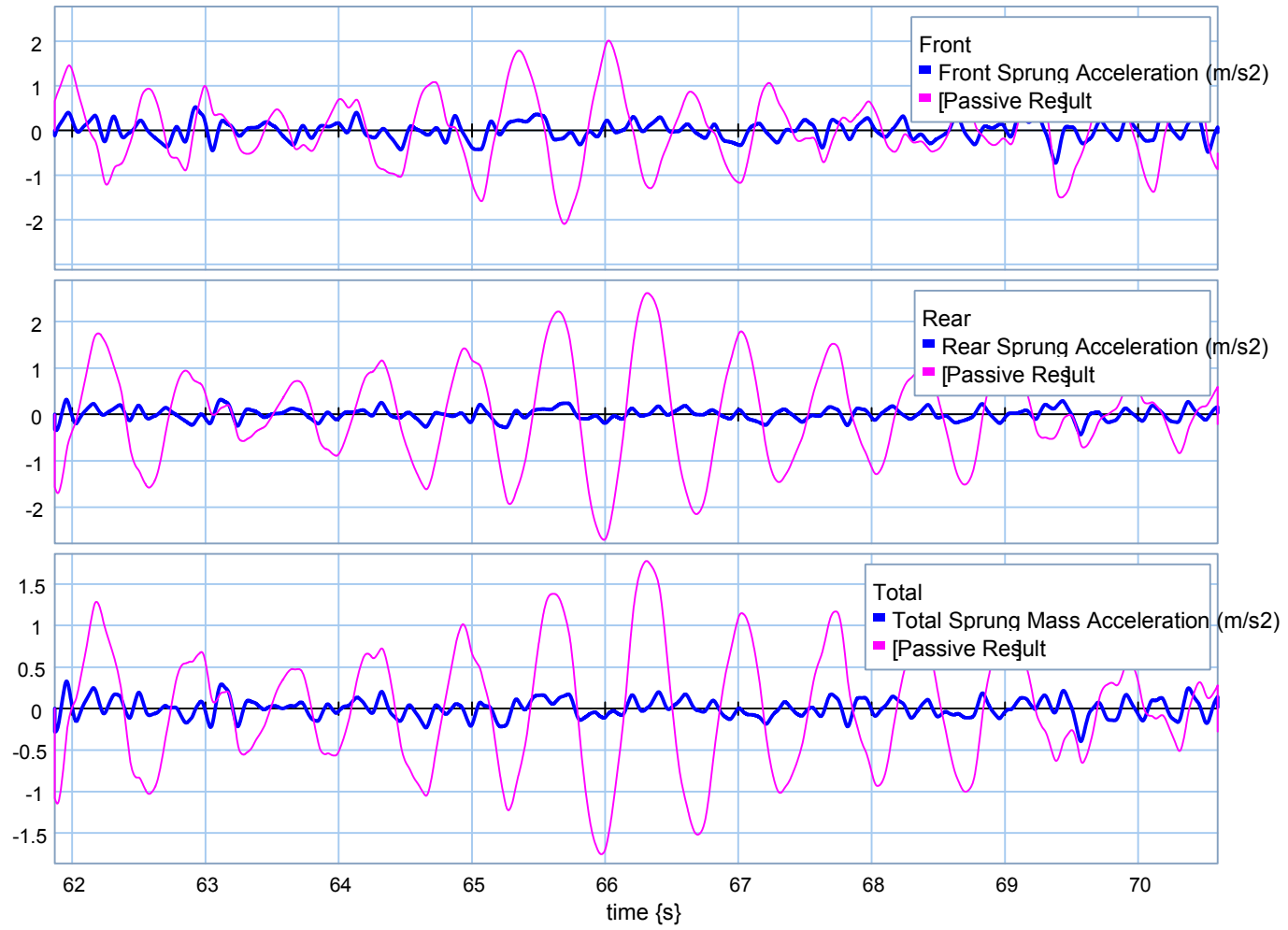


❖ **$M_c = 9000 \text{ kg.}$**

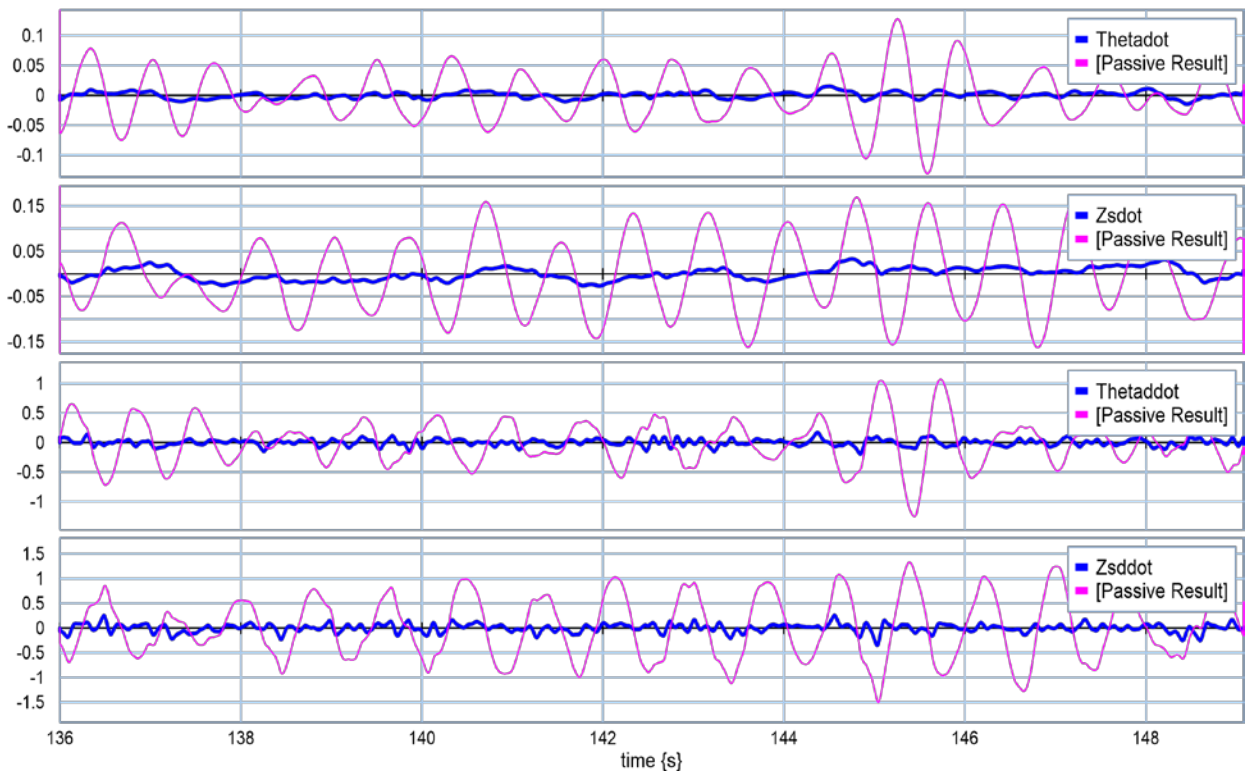
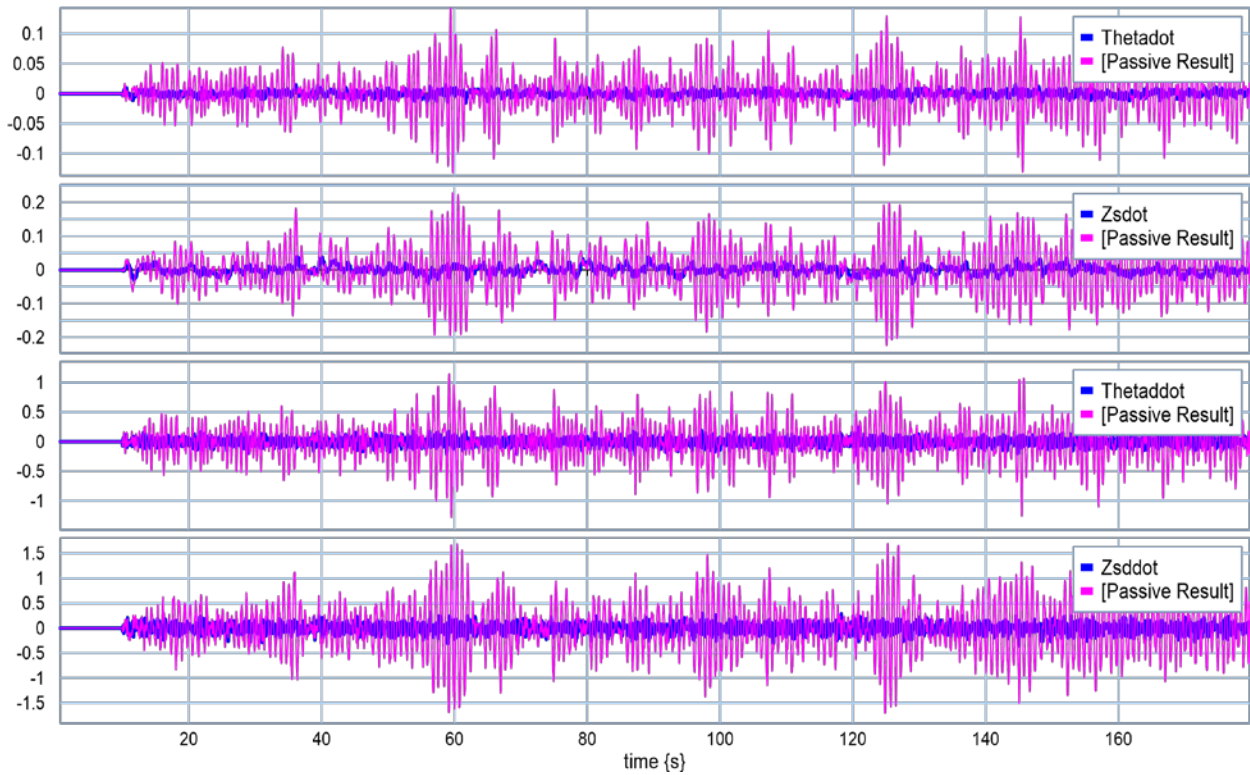


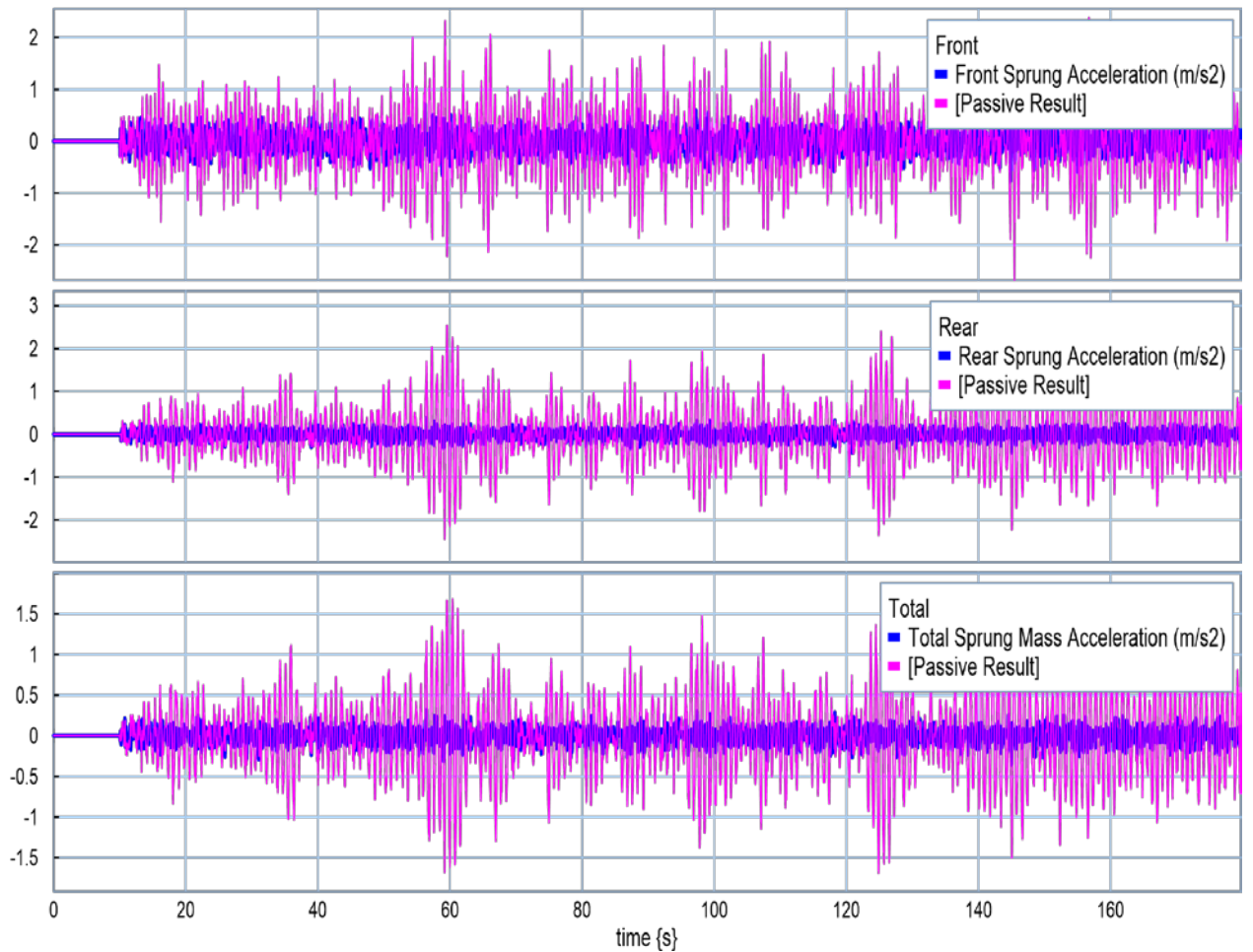
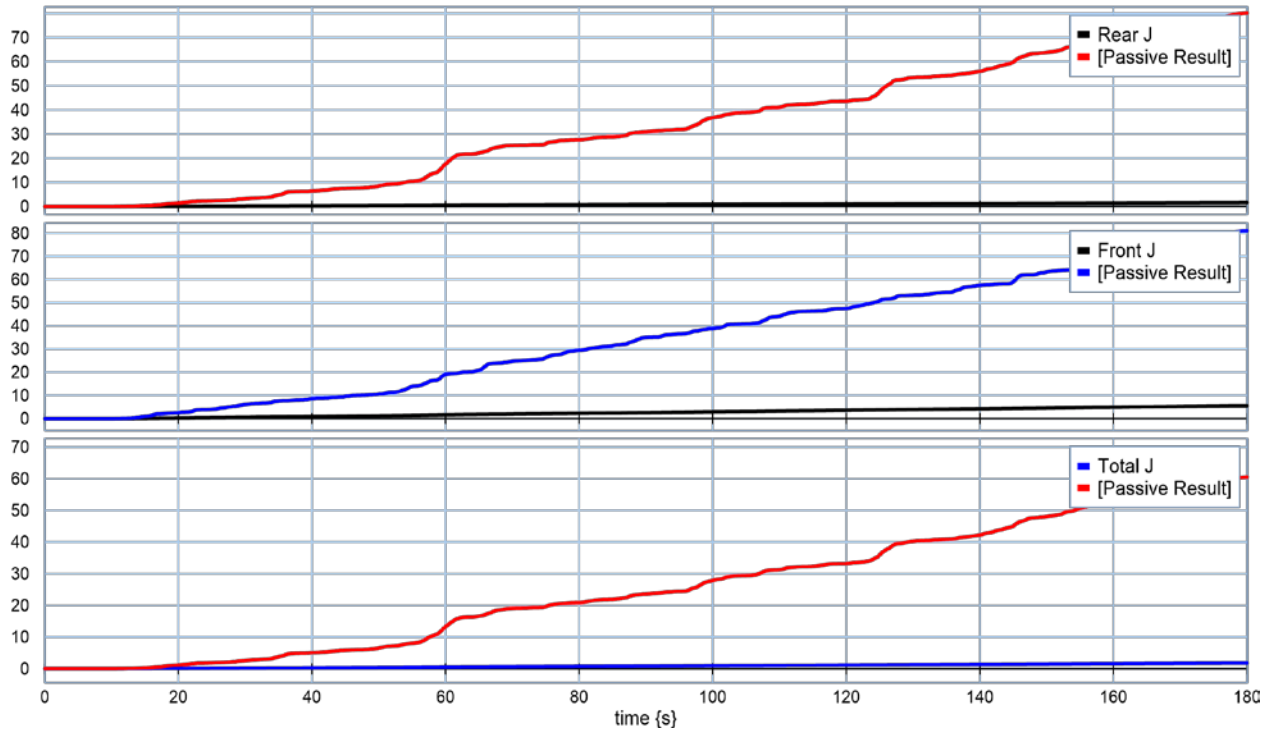


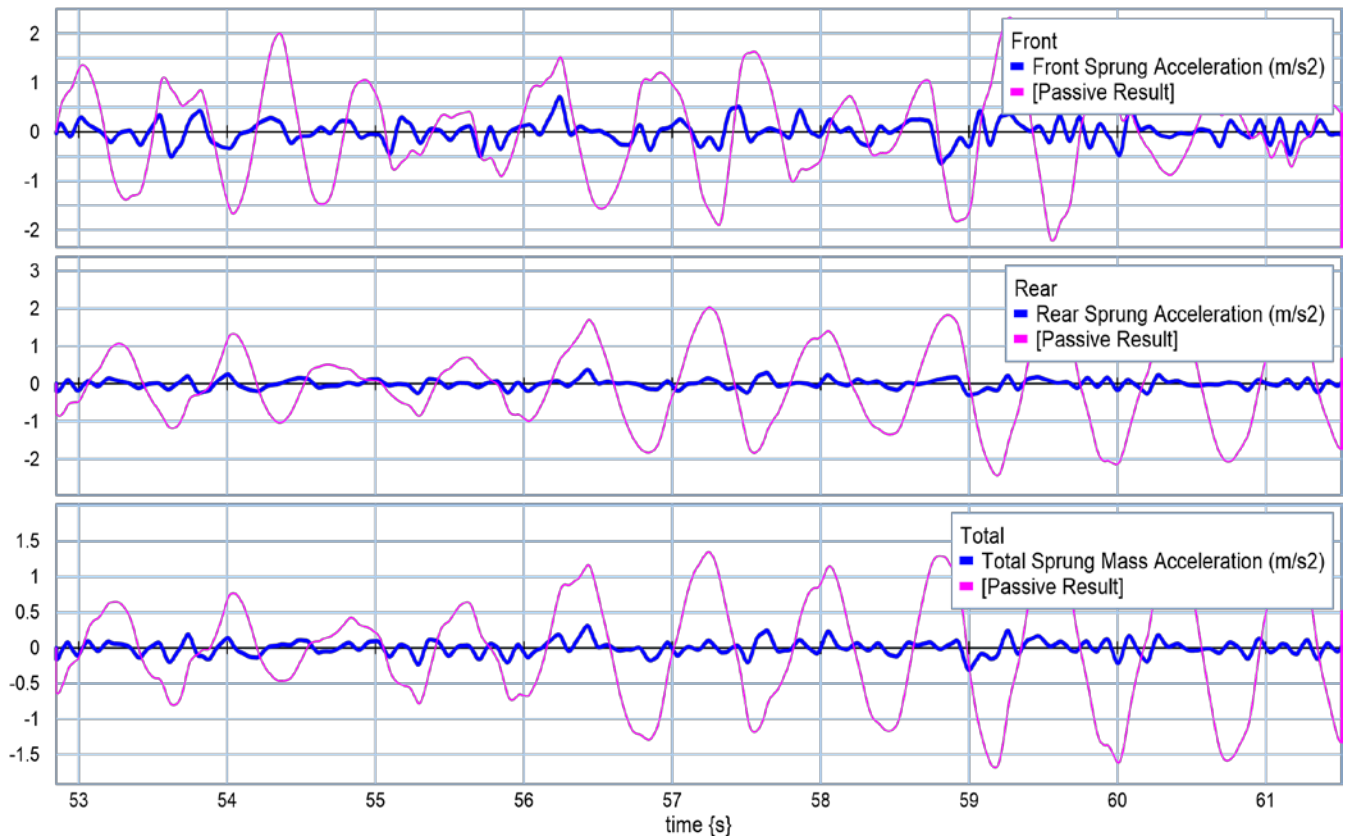
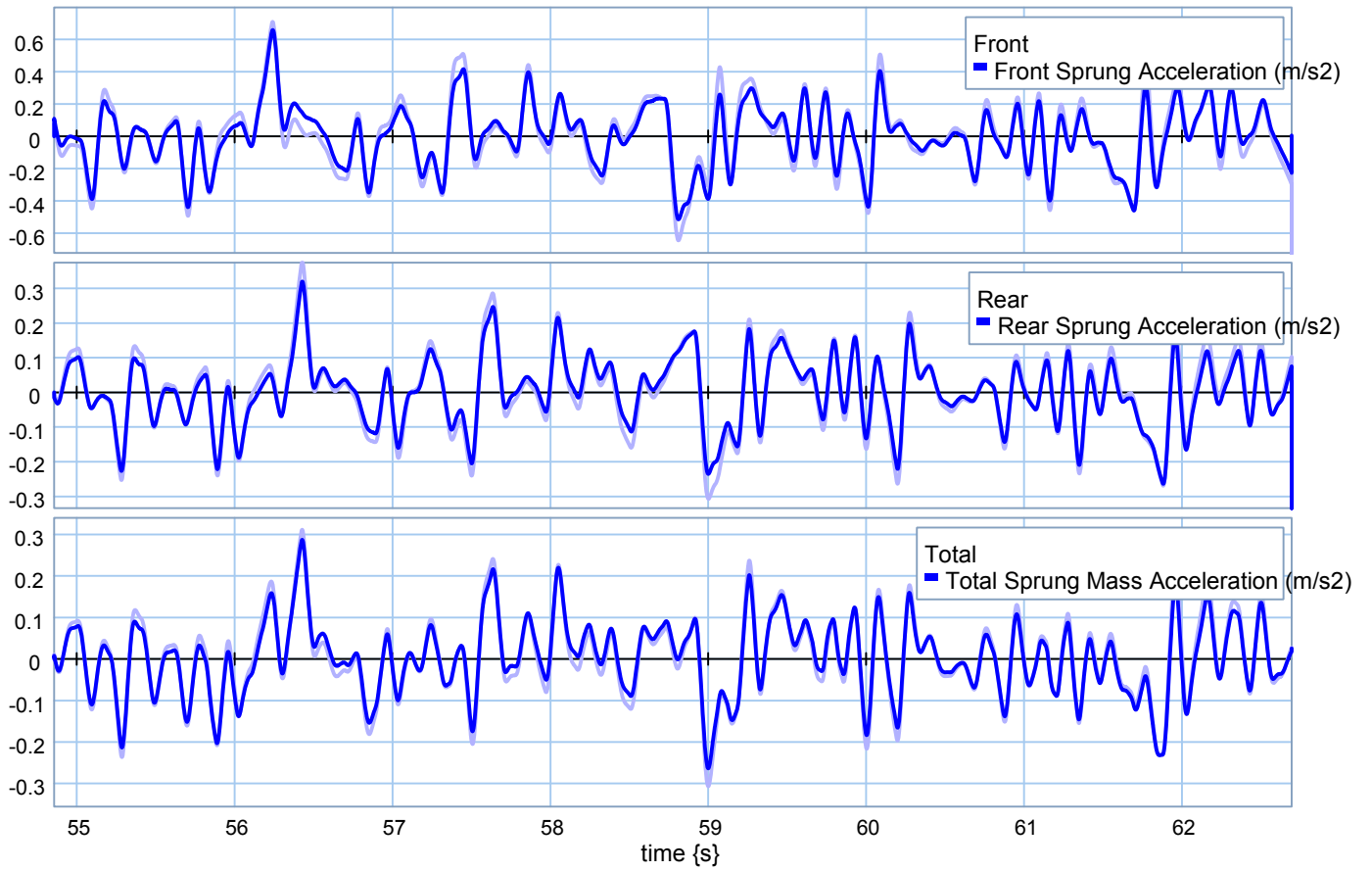


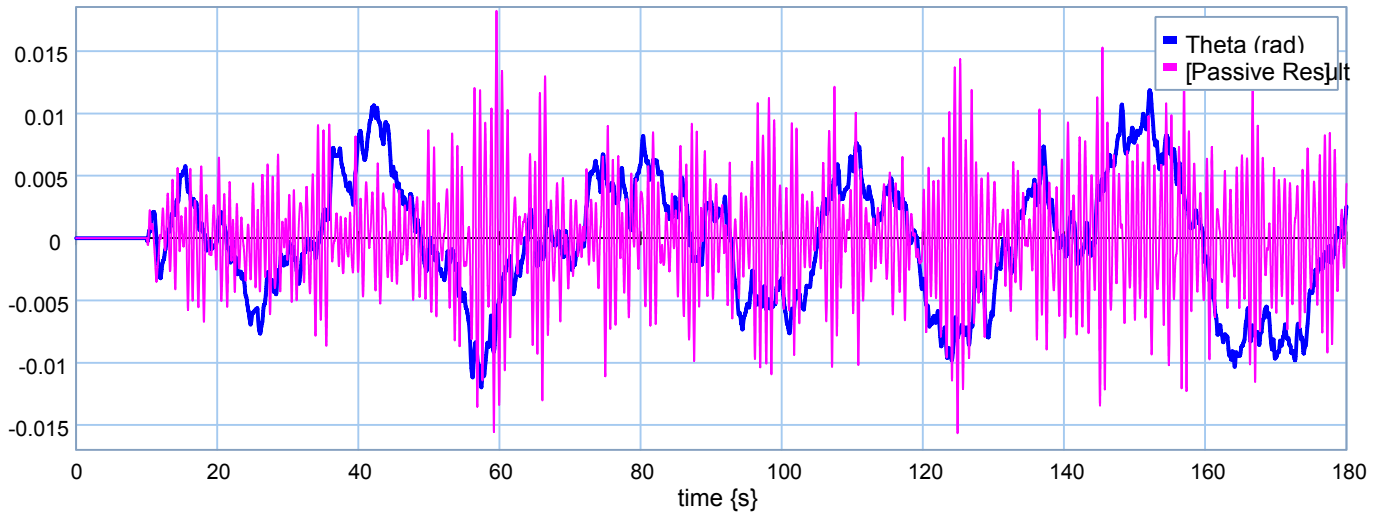


❖ $M_c = 13500 \text{ kg.}$

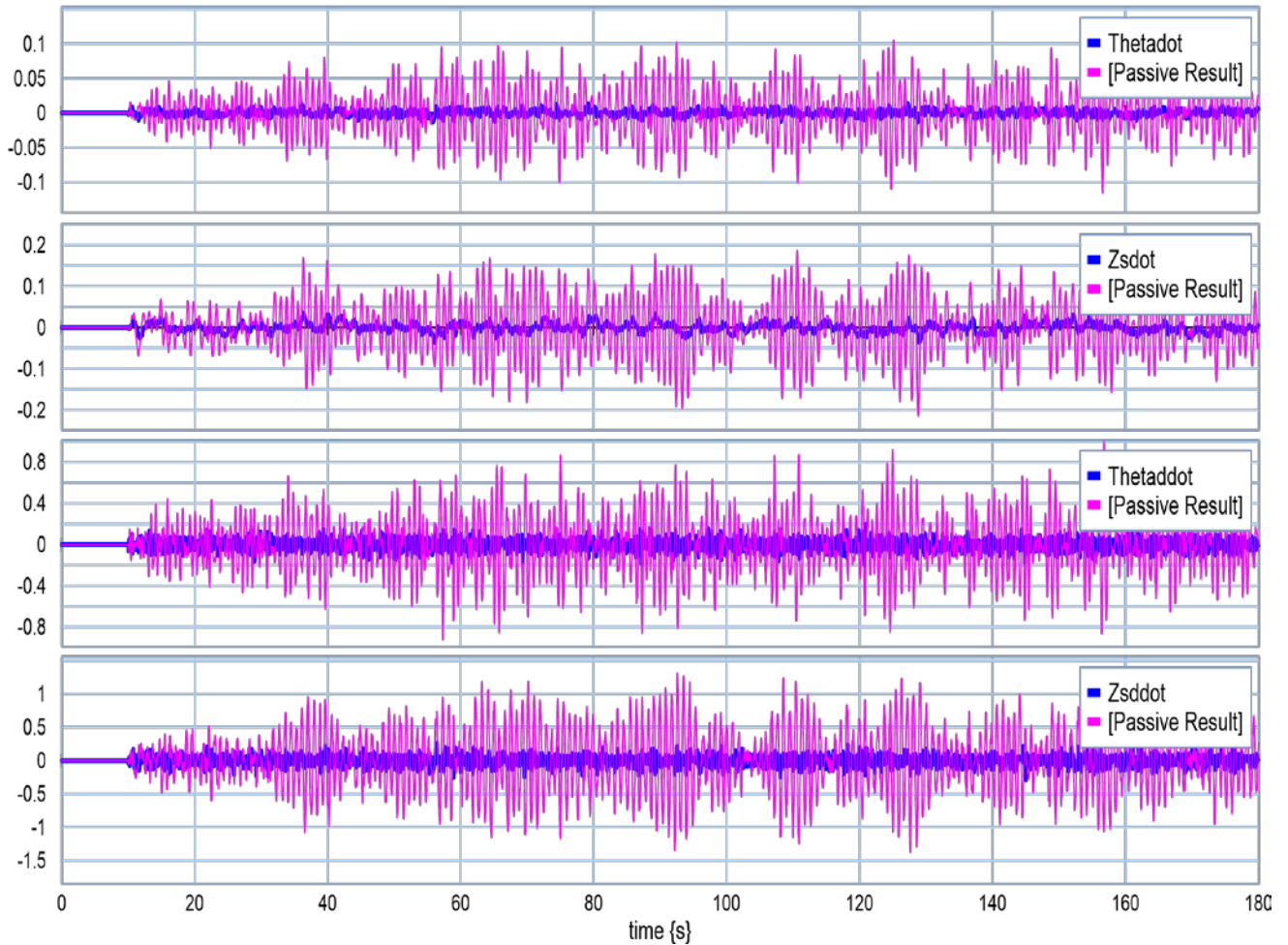


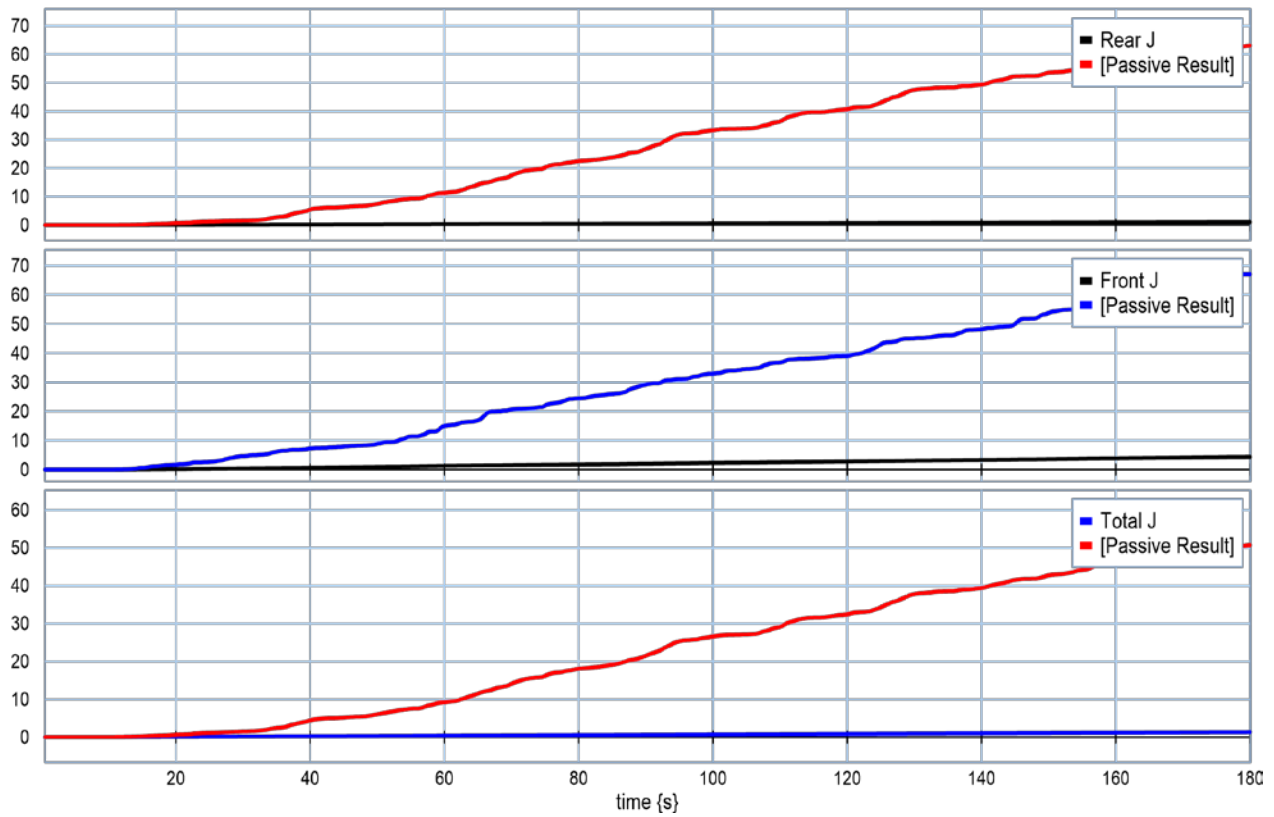
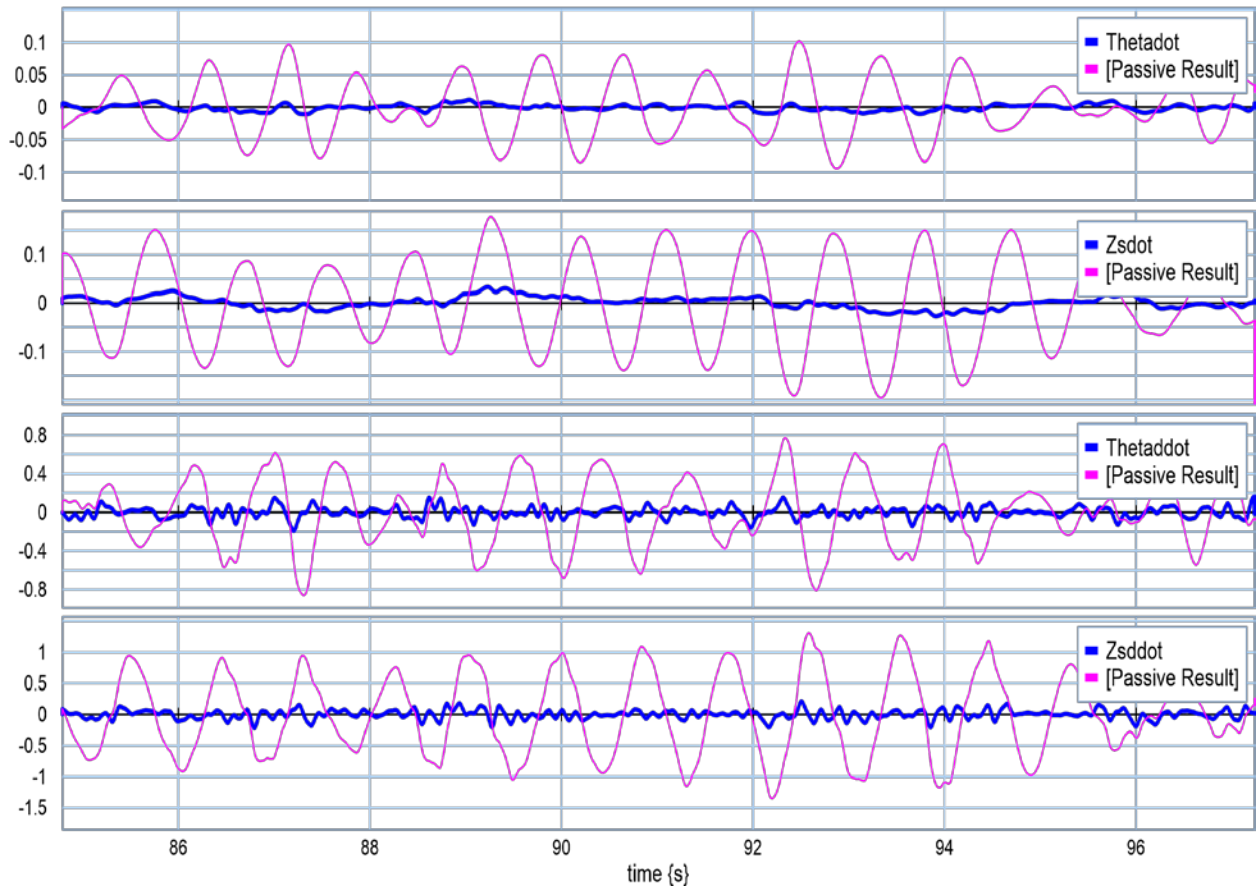


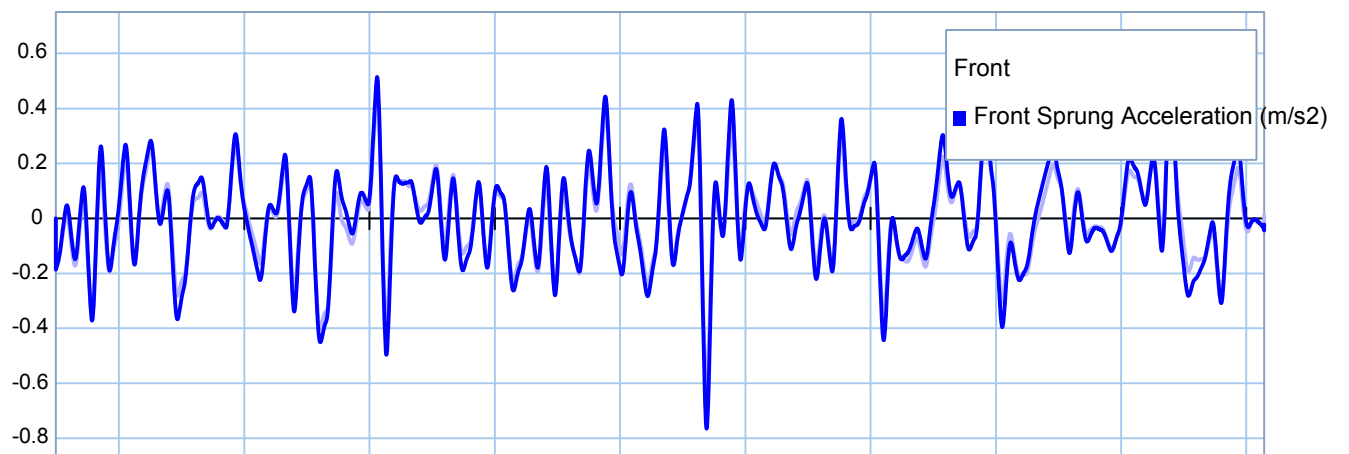
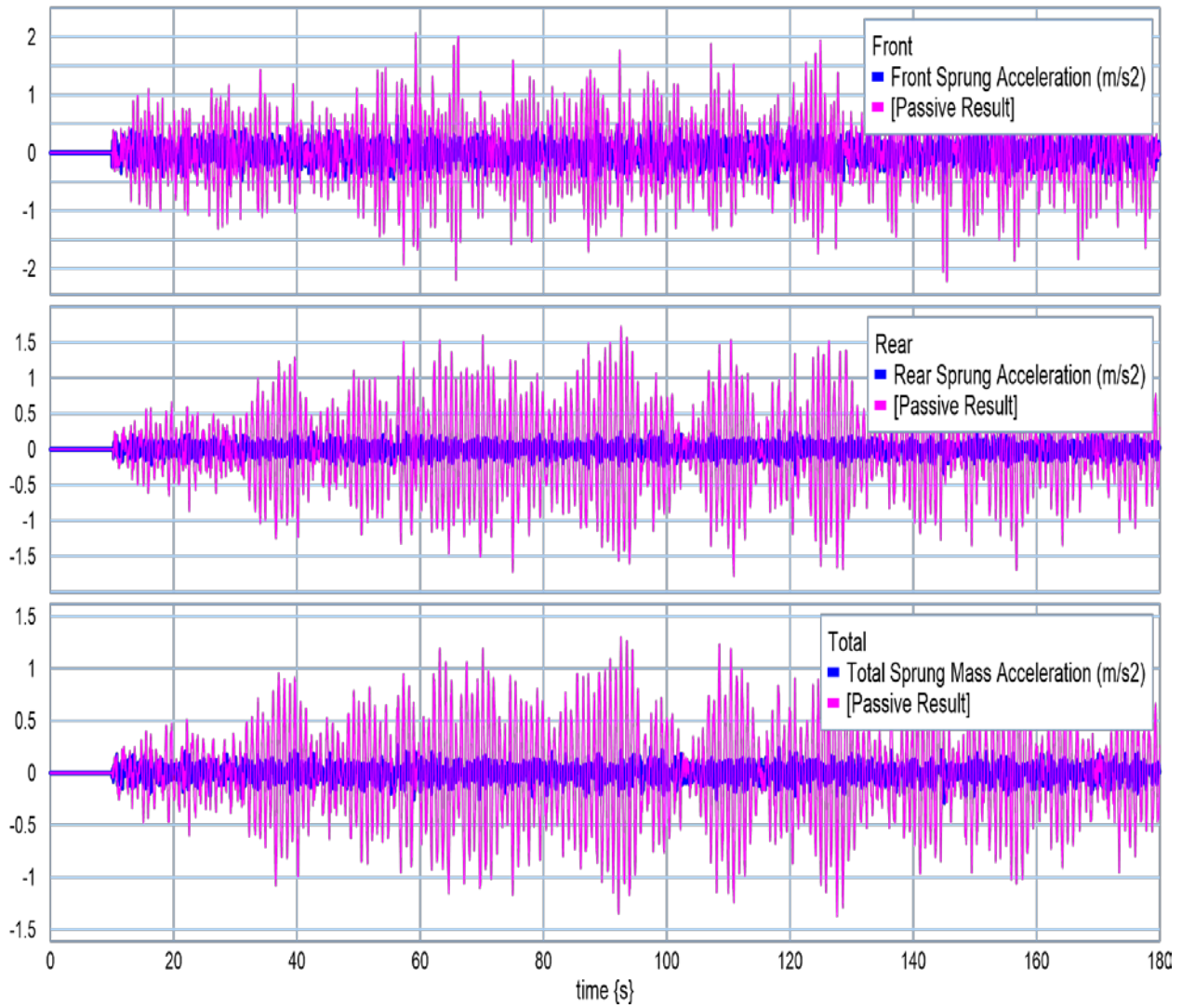


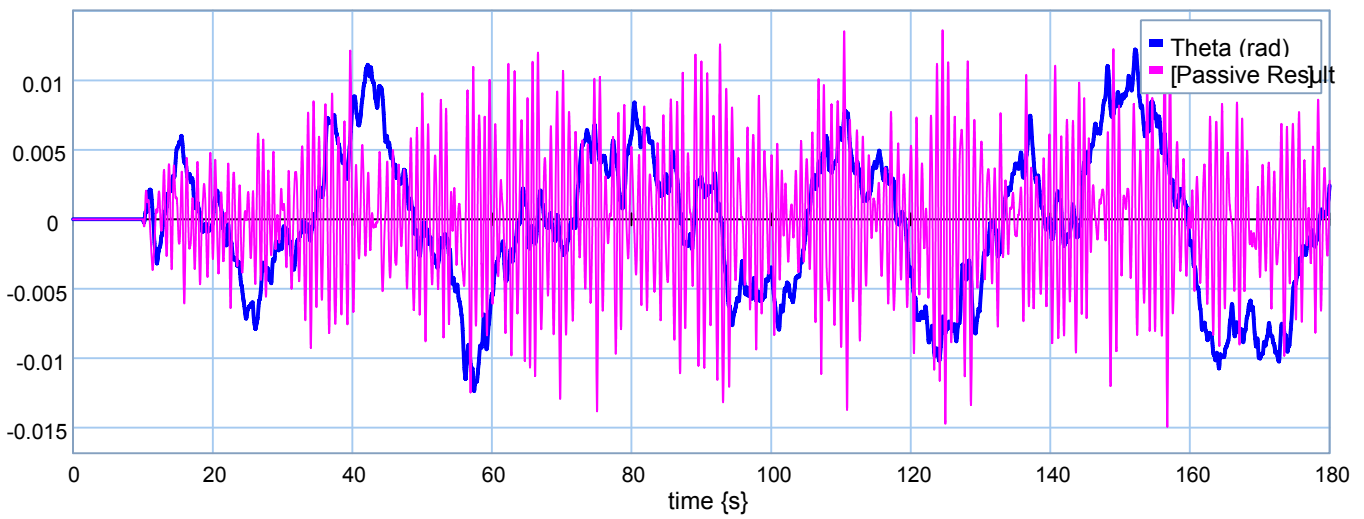
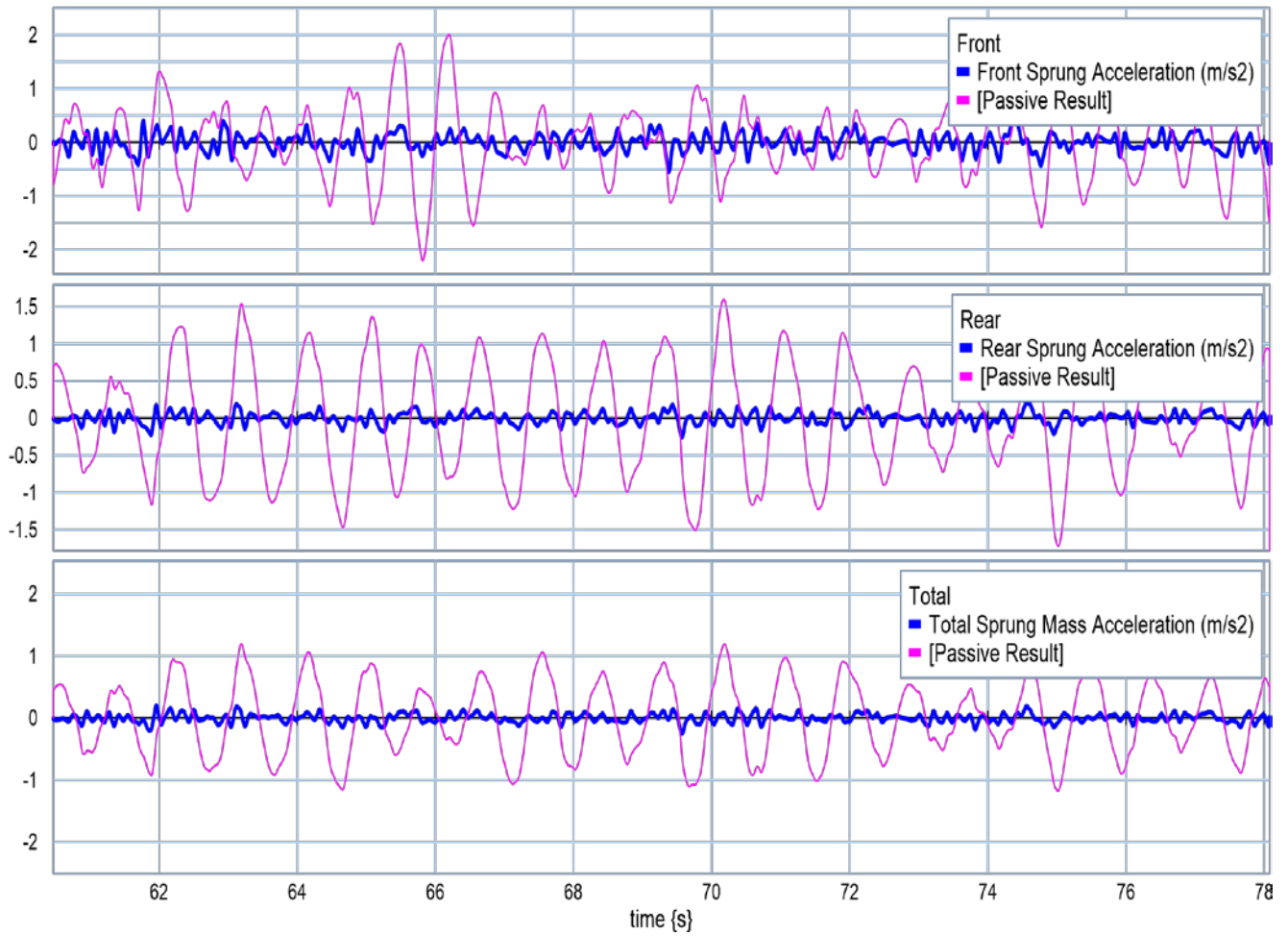


❖ **$M_c = 18000$ kg.**



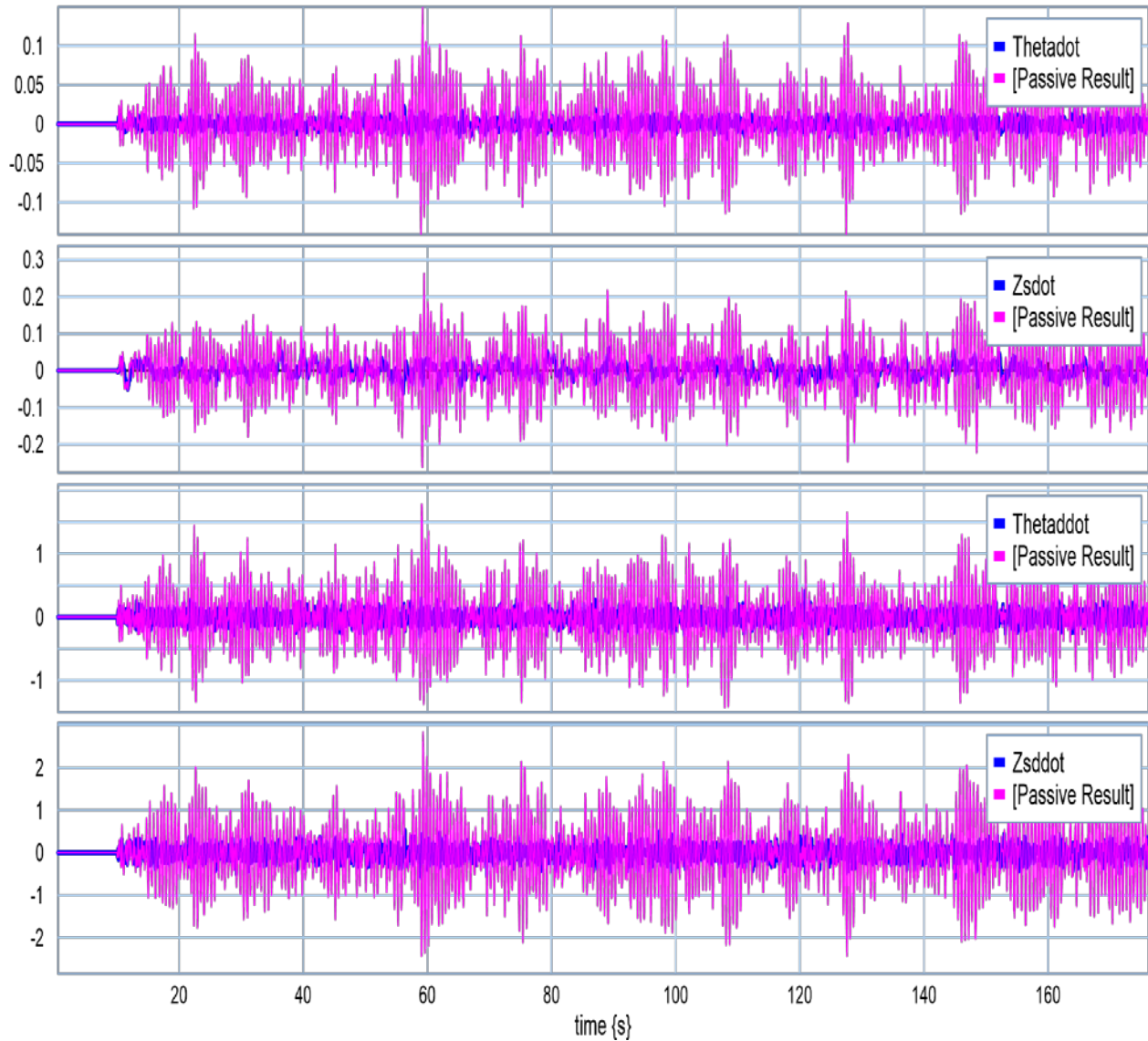


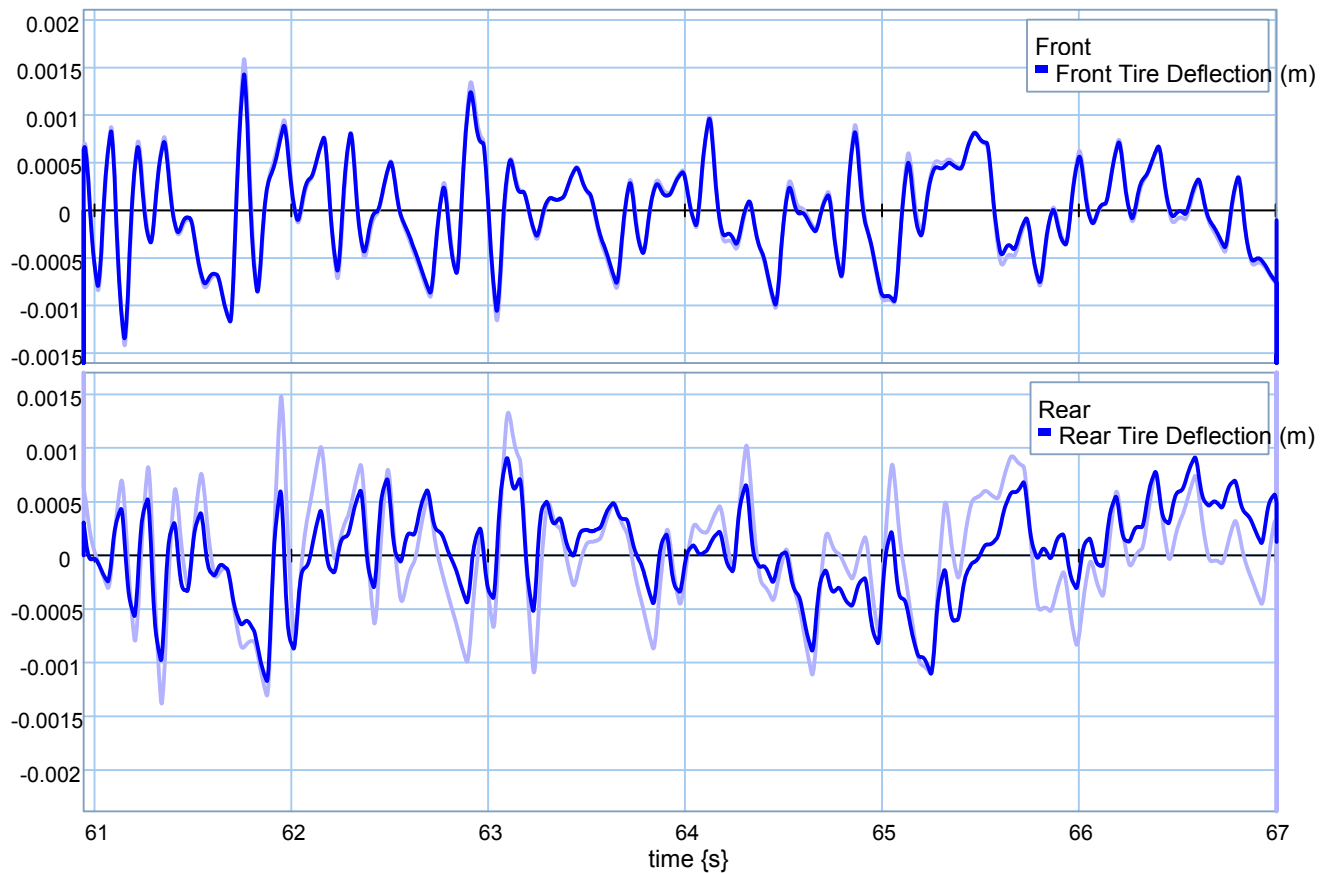
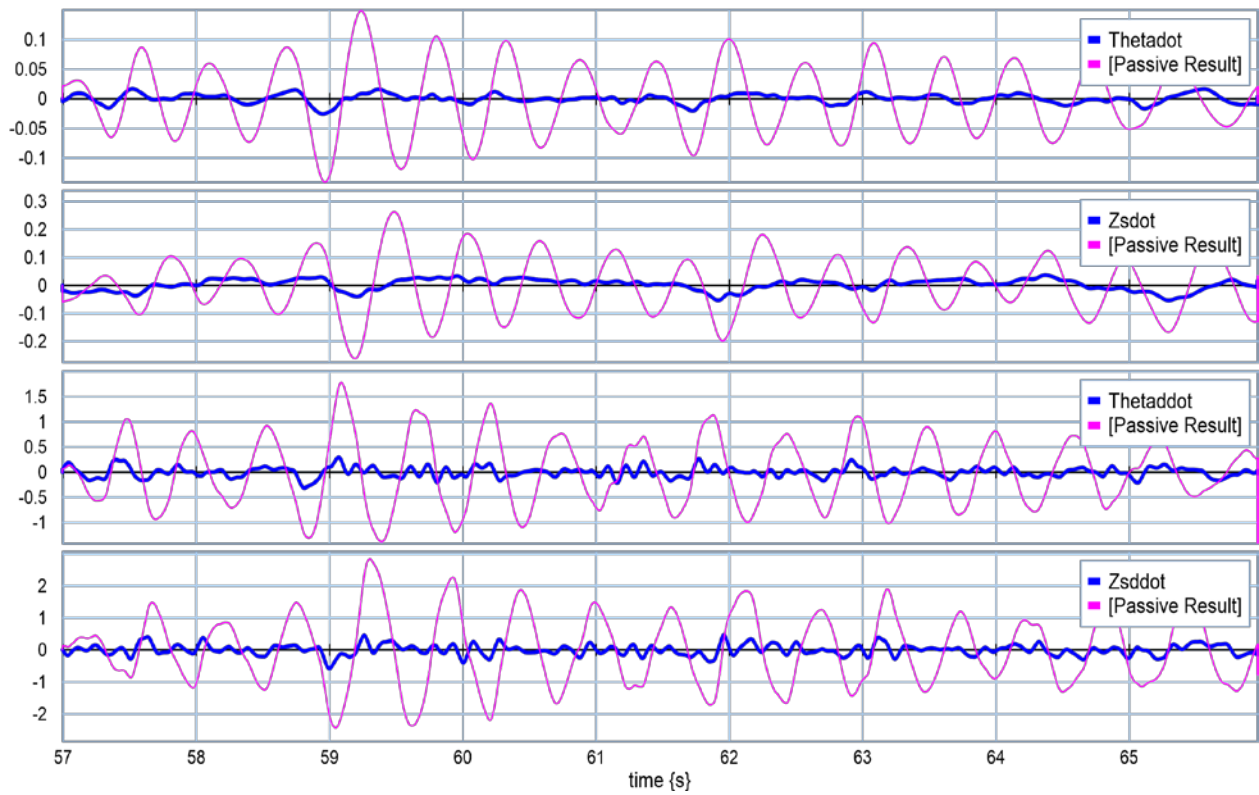


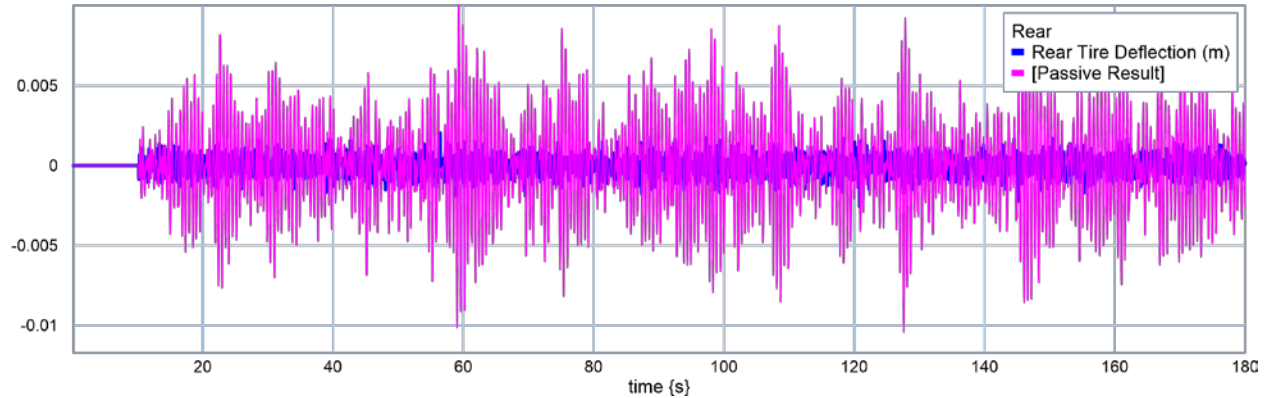
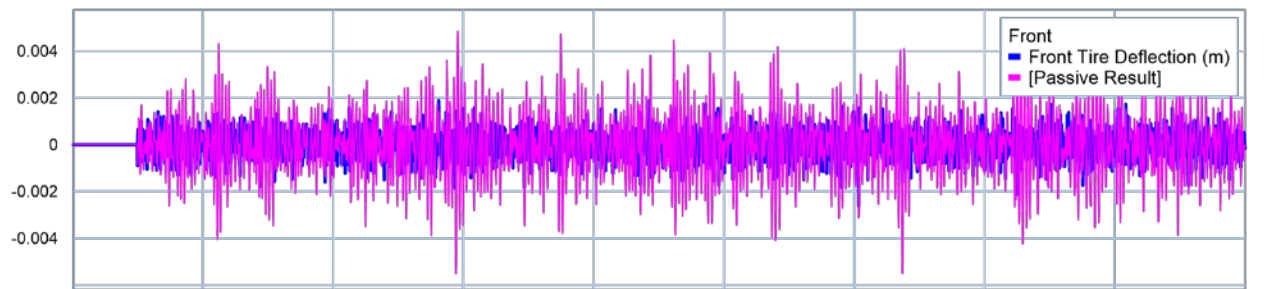
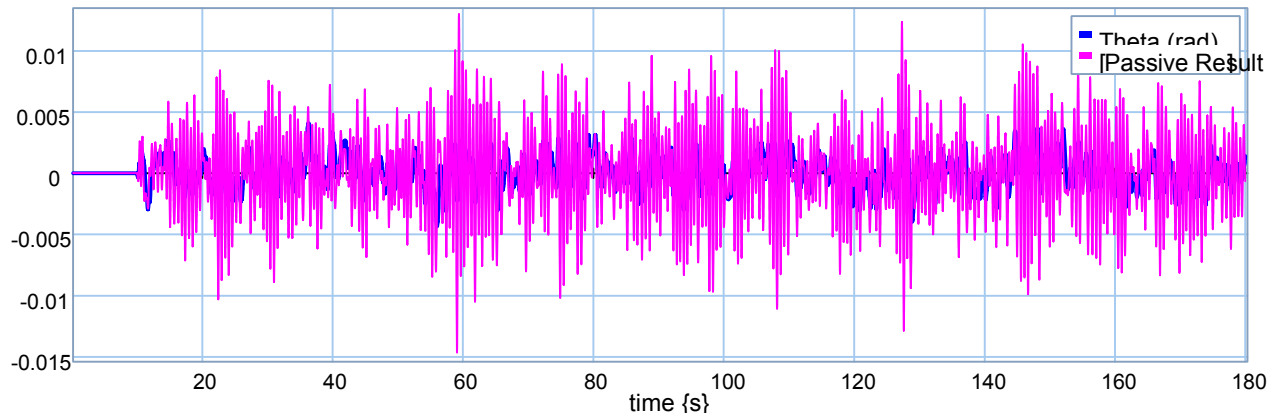
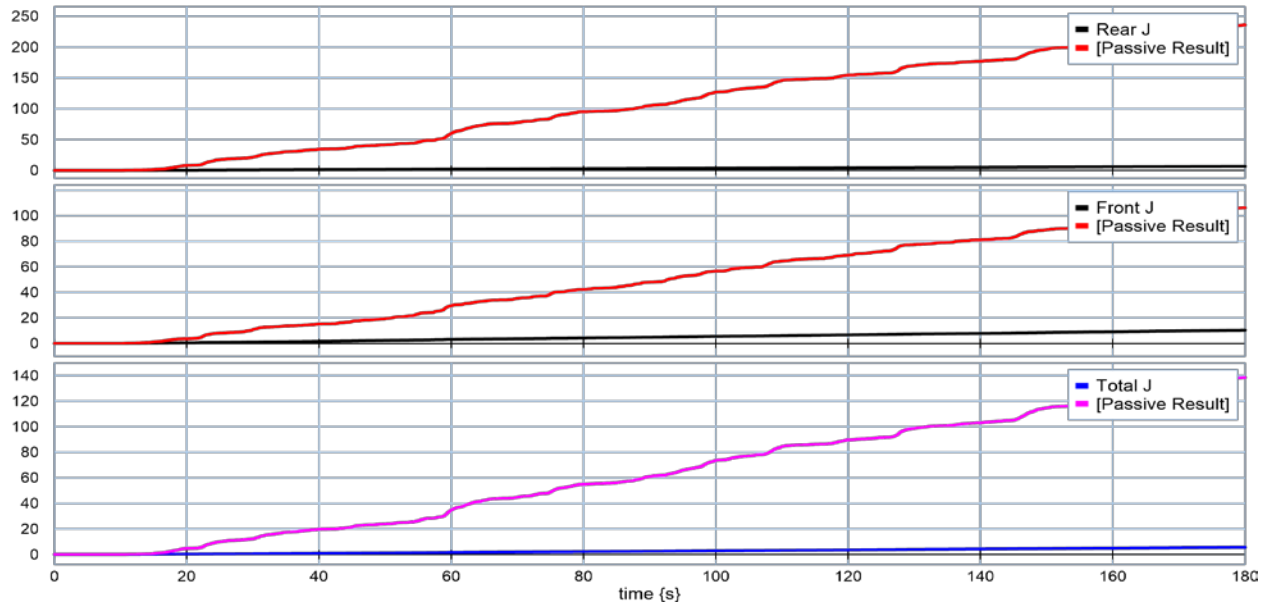


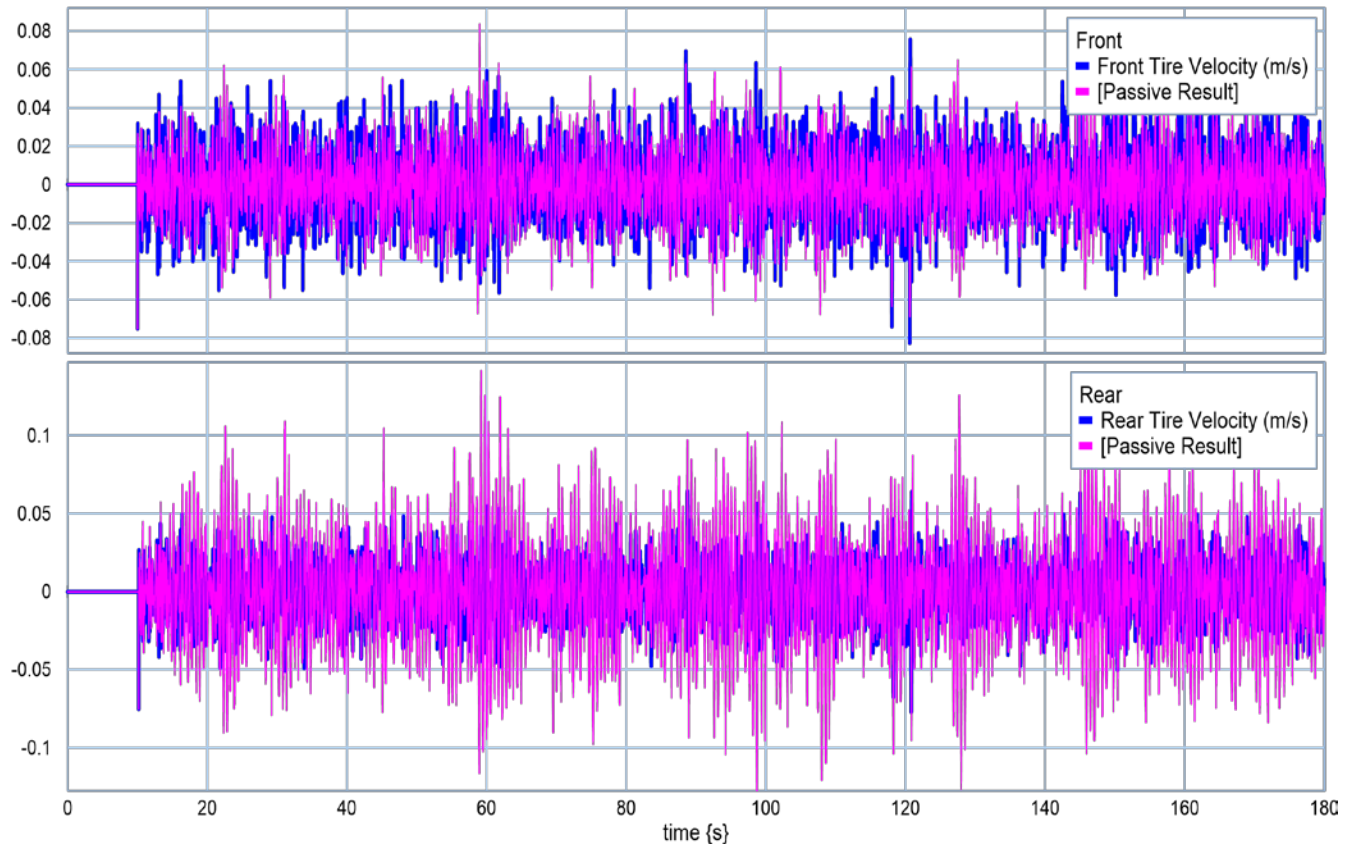
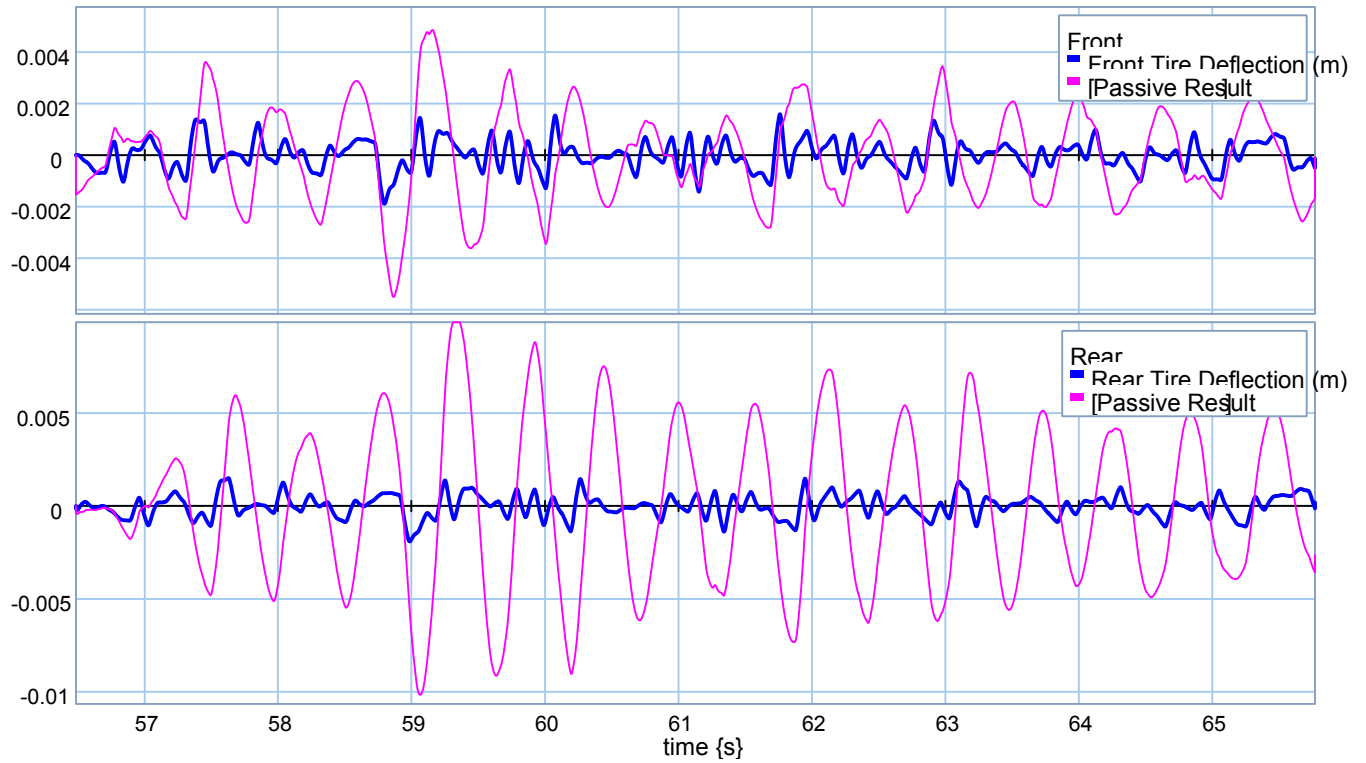
AppendixD: Linear HalfCar Model, Road Holding Scenario, QuarterCar Active Suspensions.

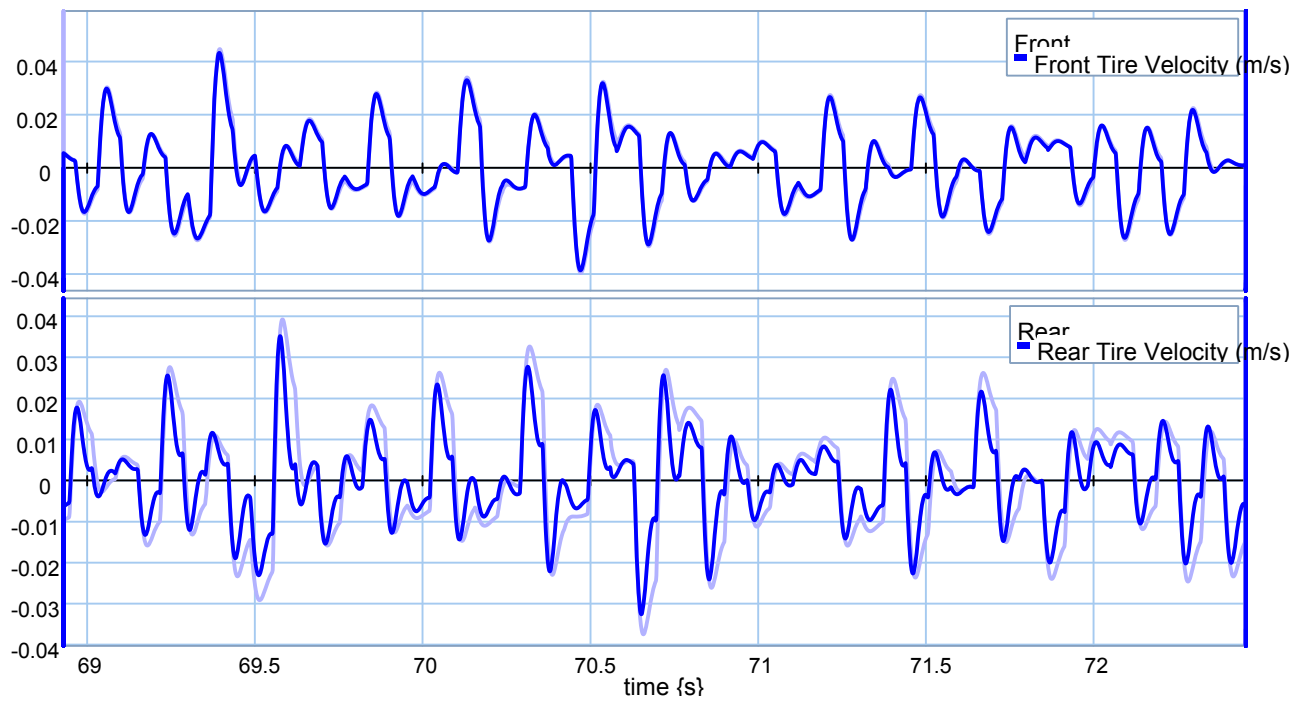
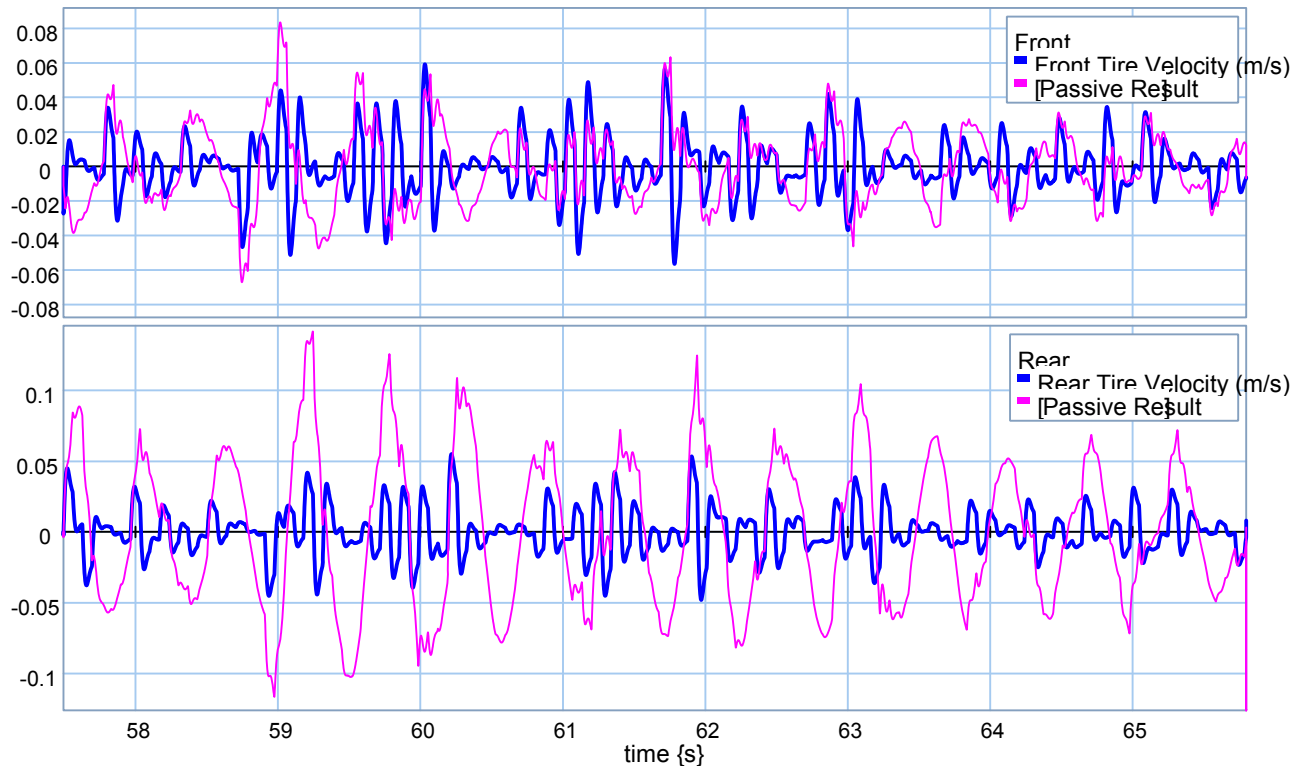
❖ $M_c = 4500 \text{ kg}$.



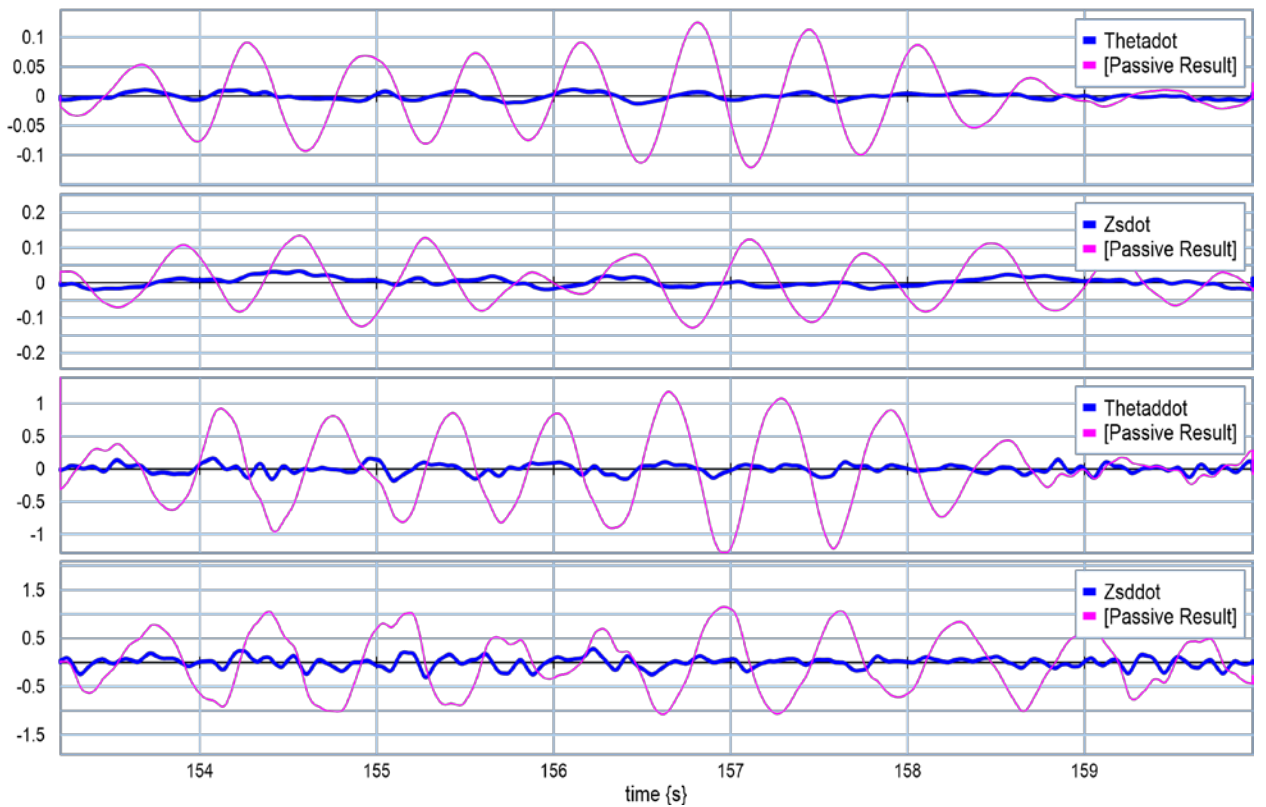
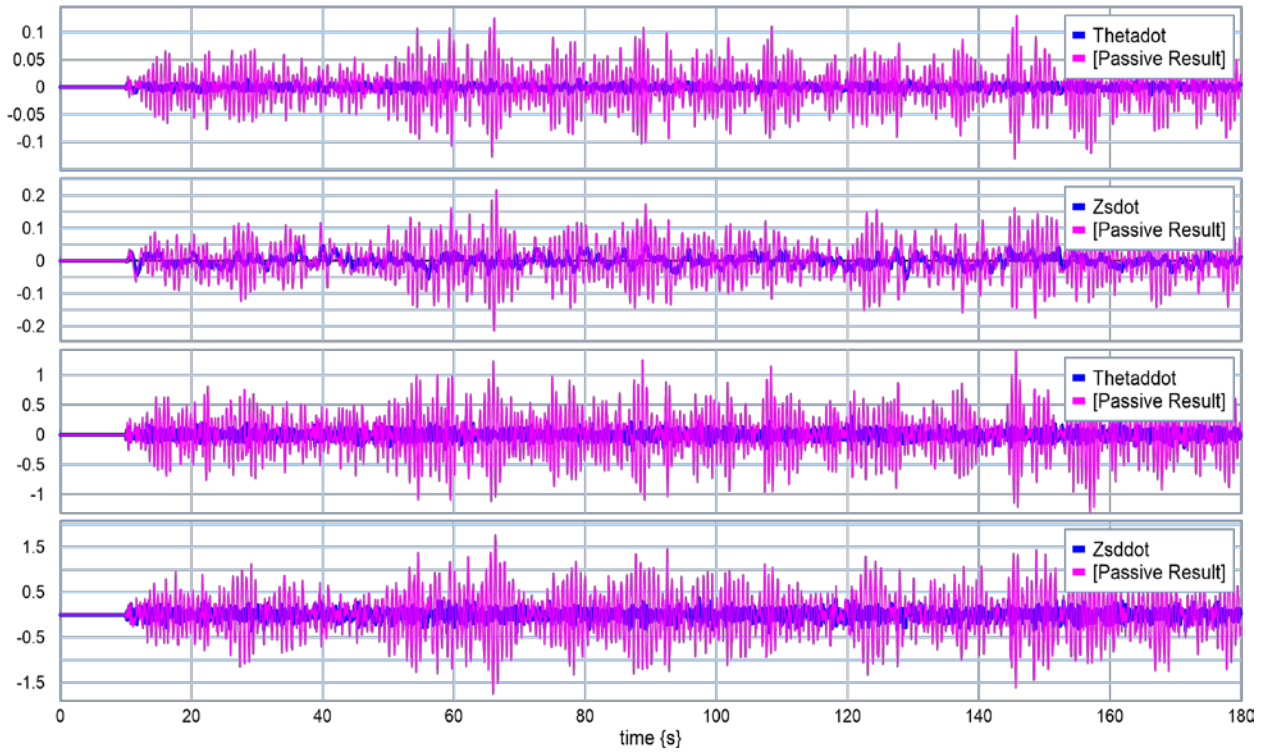


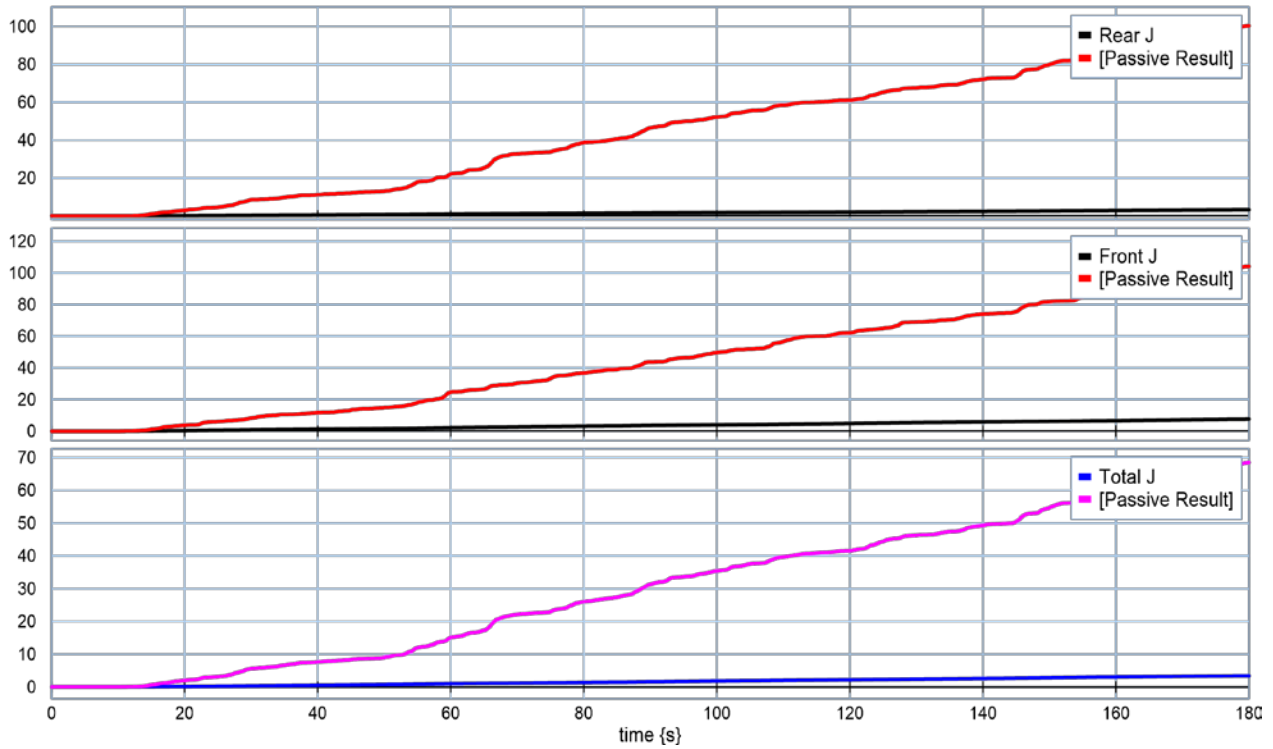
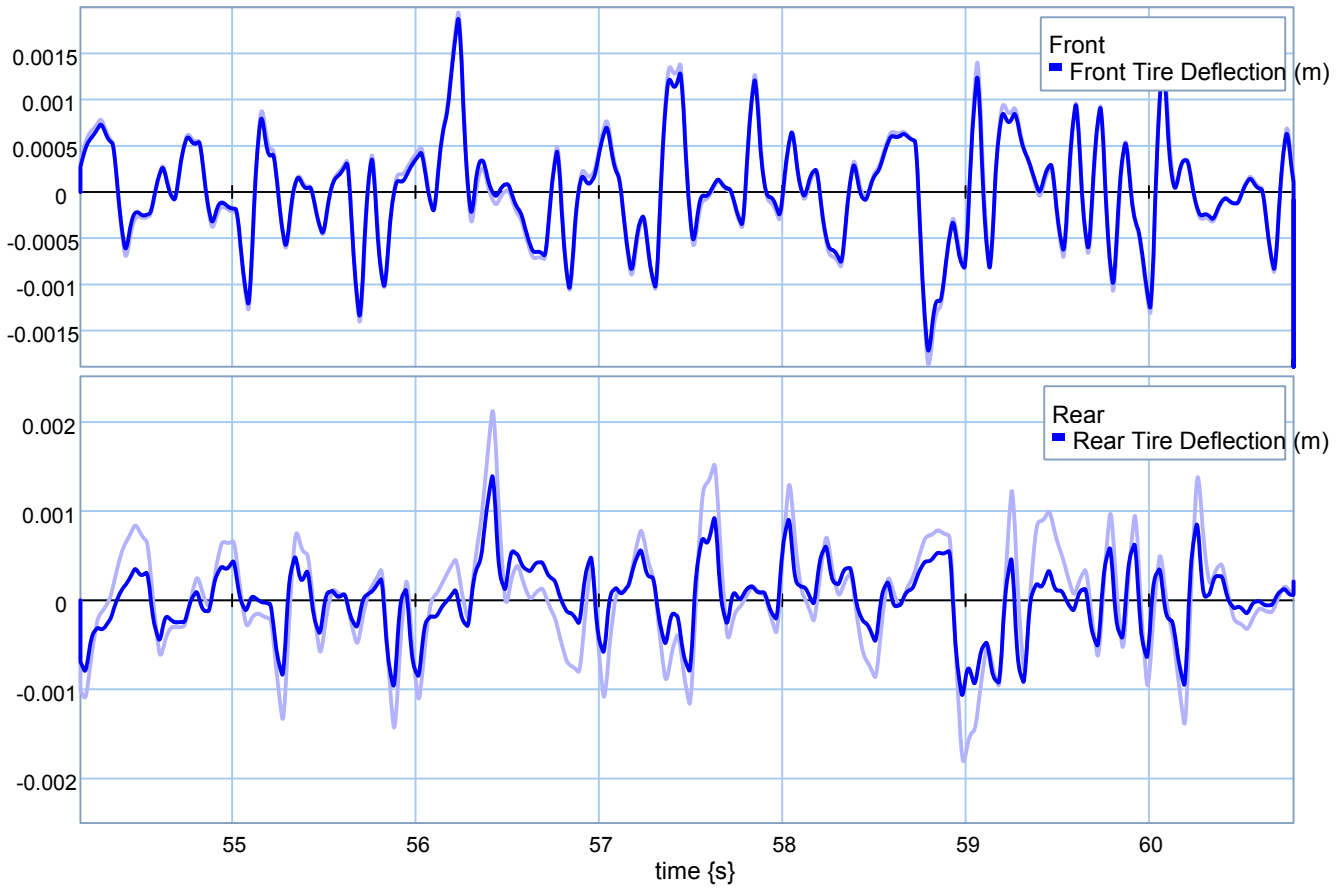


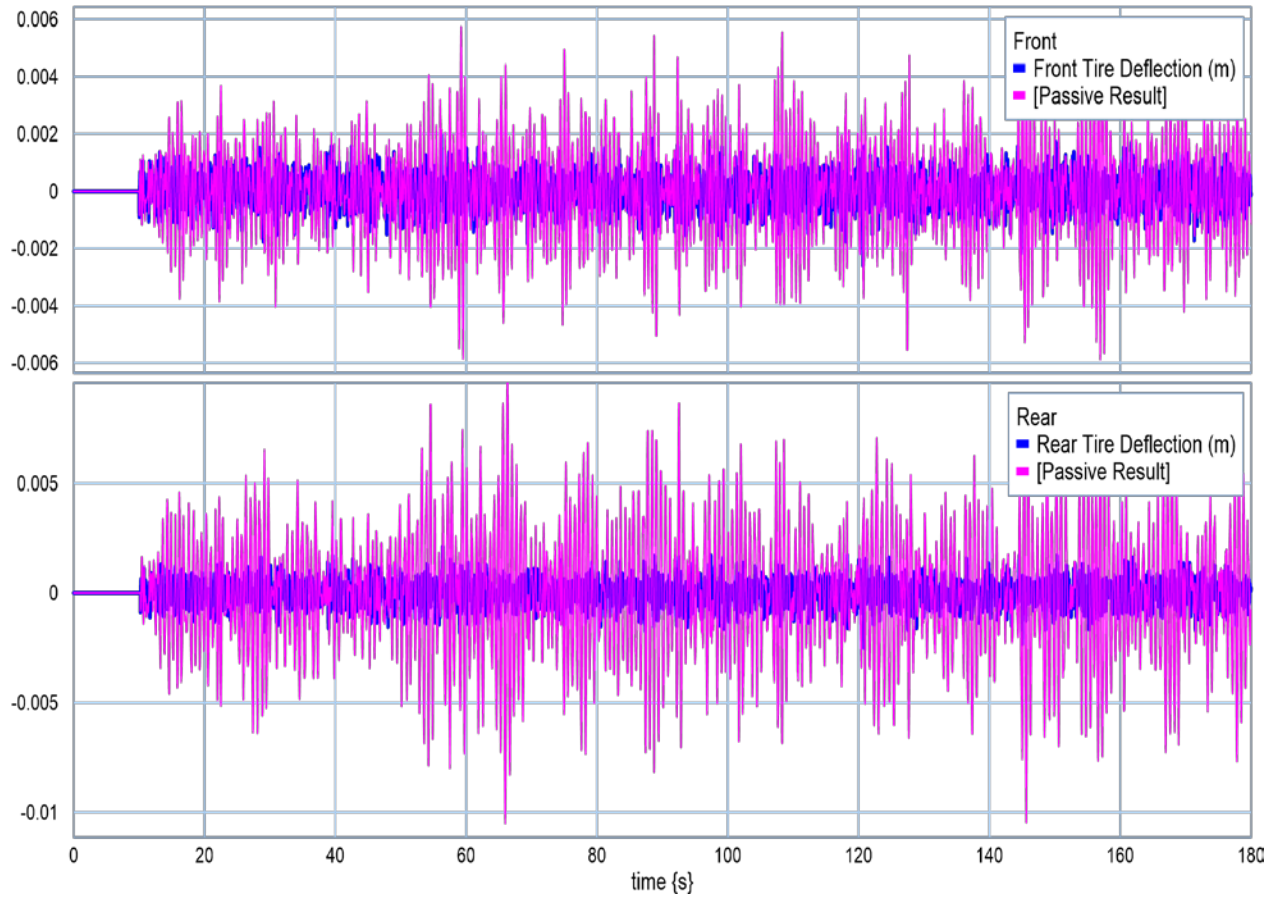
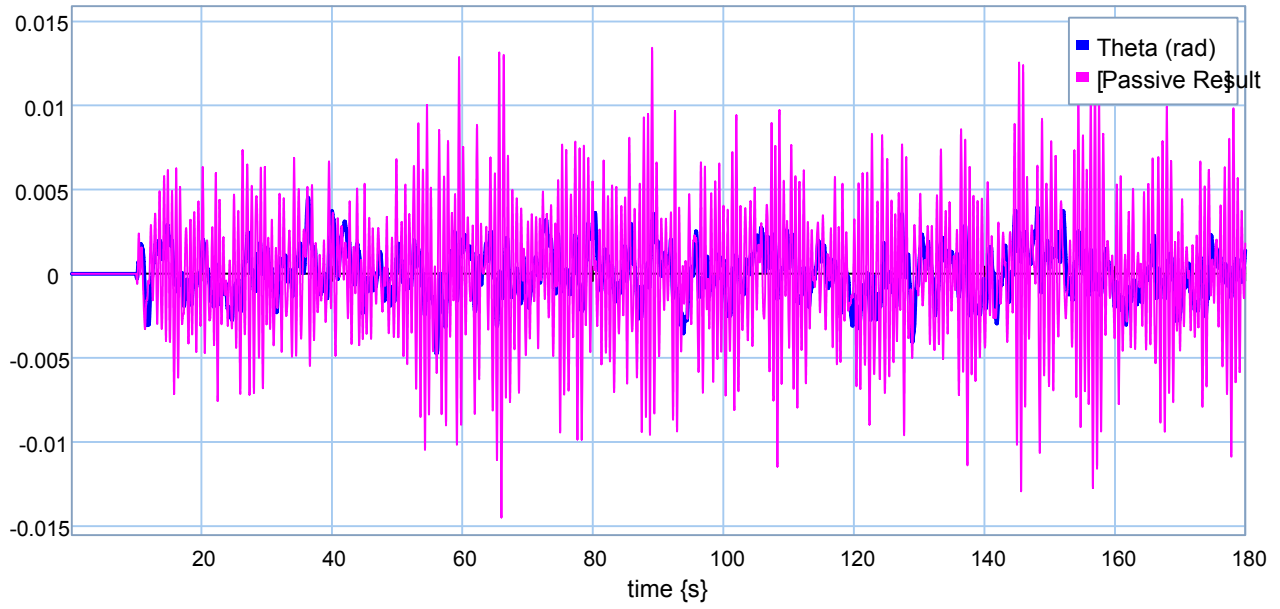


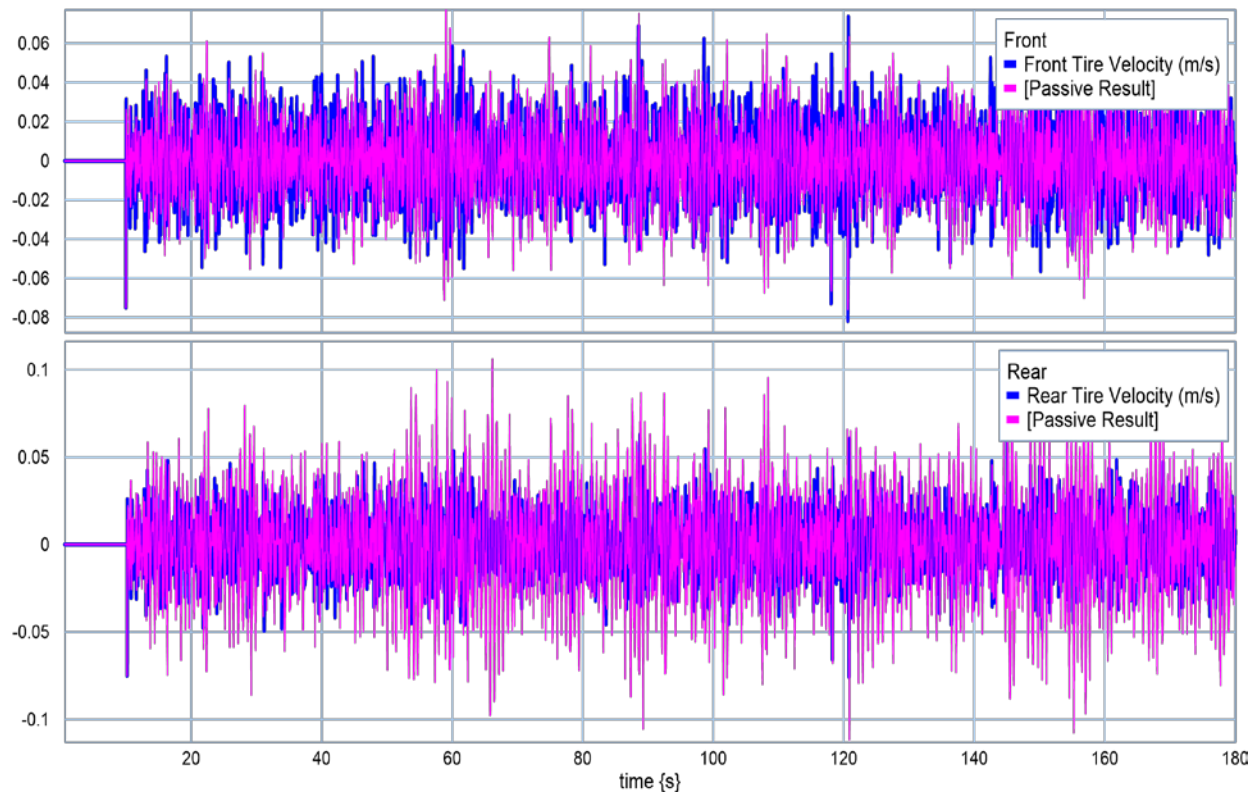
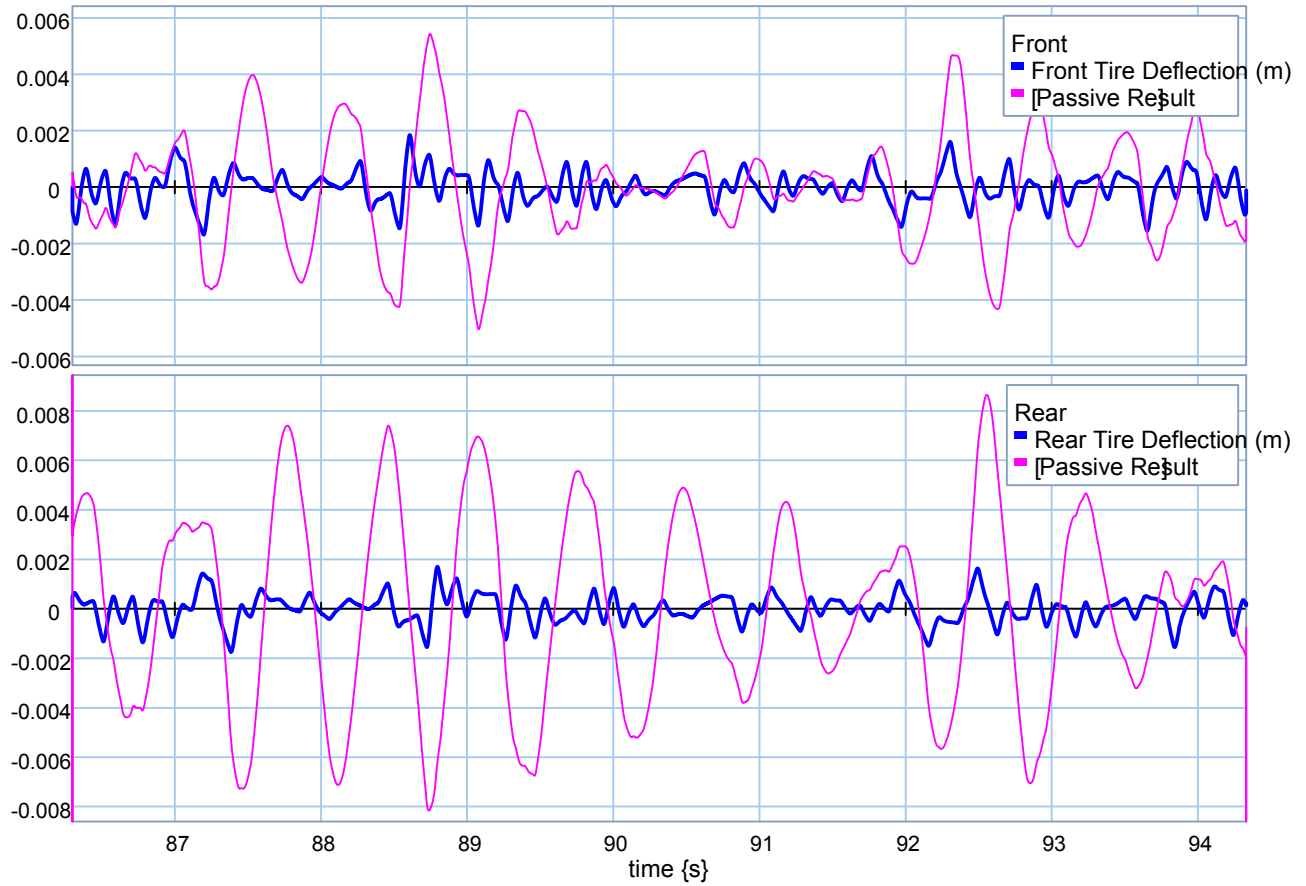


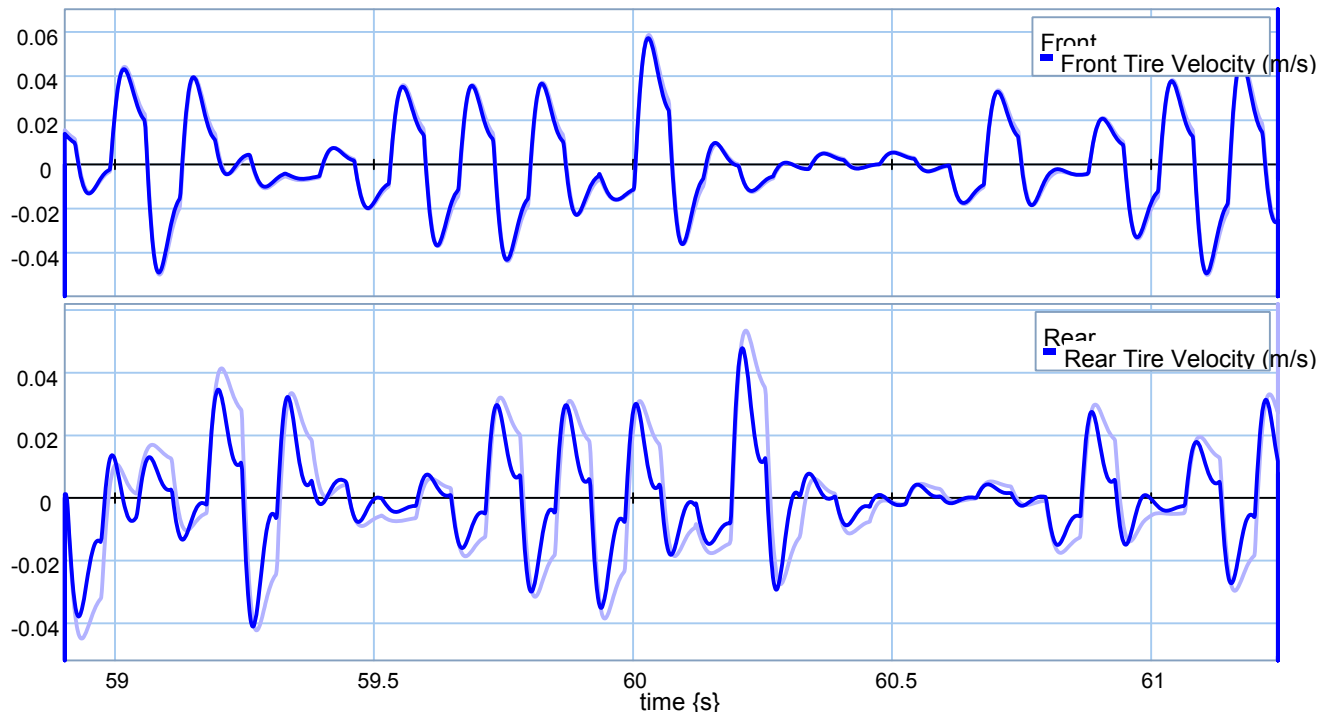
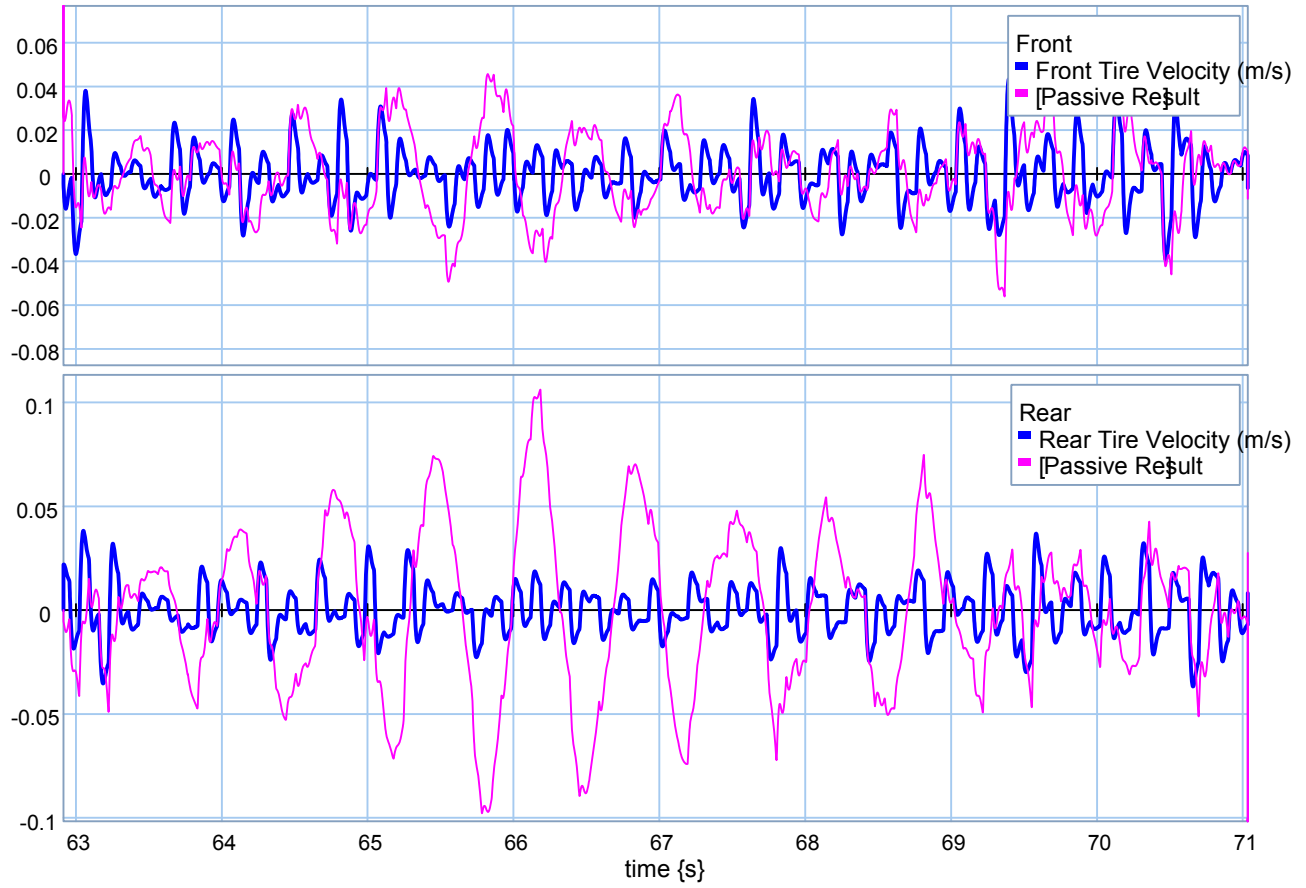
❖ $M_c = 9000 \text{ kg.}$



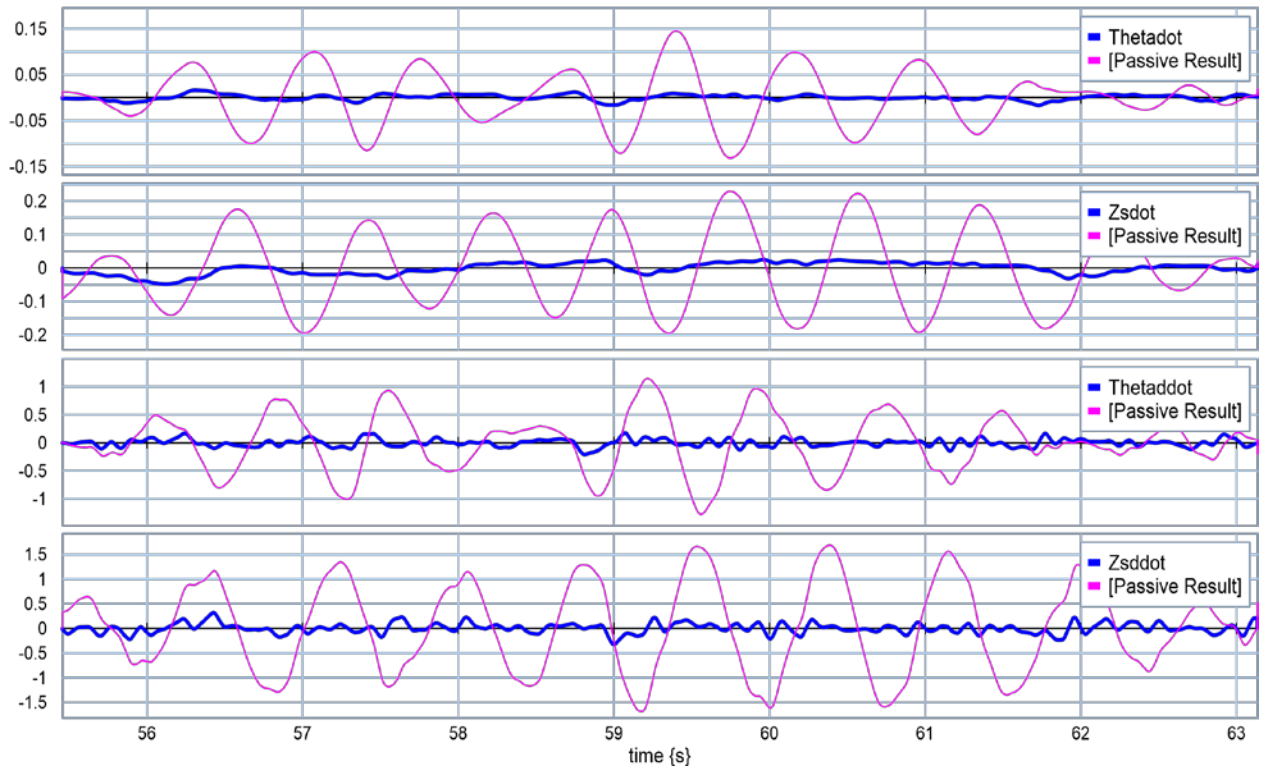
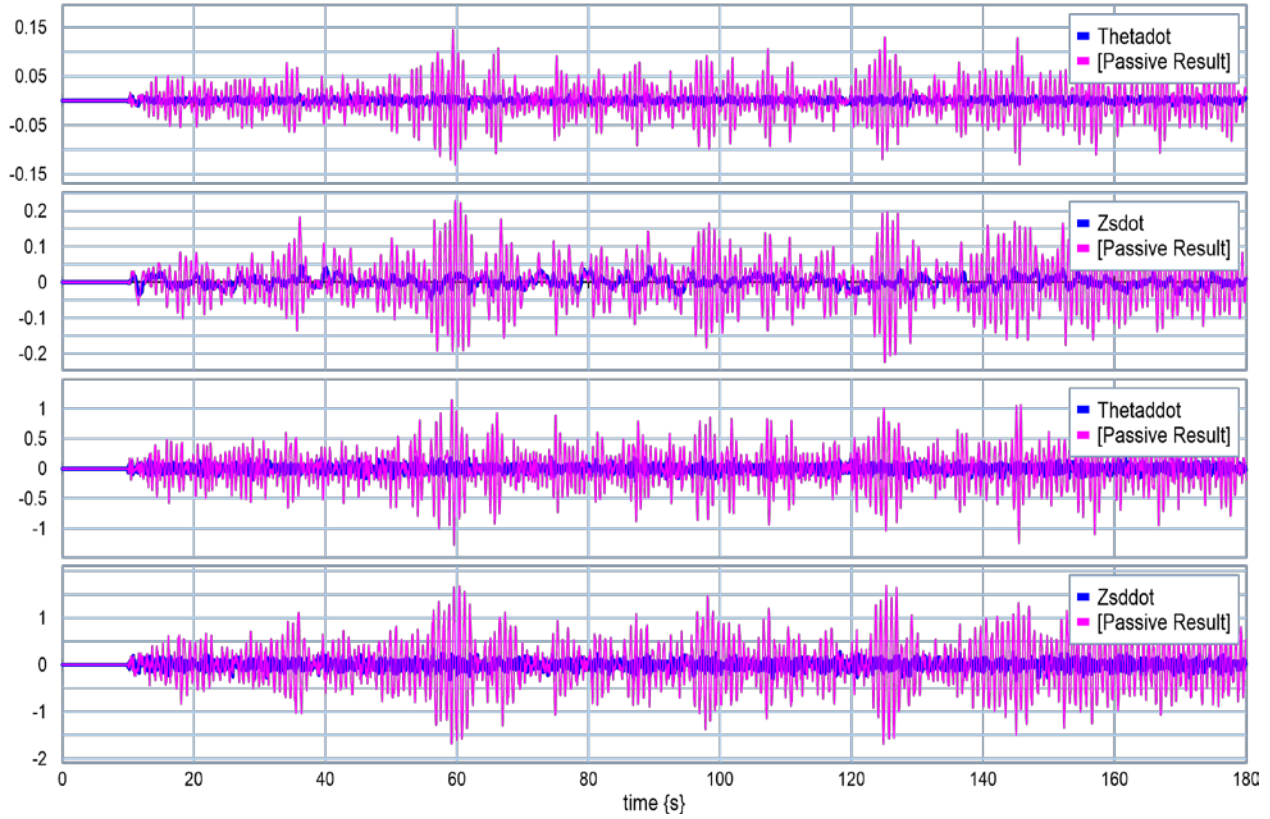


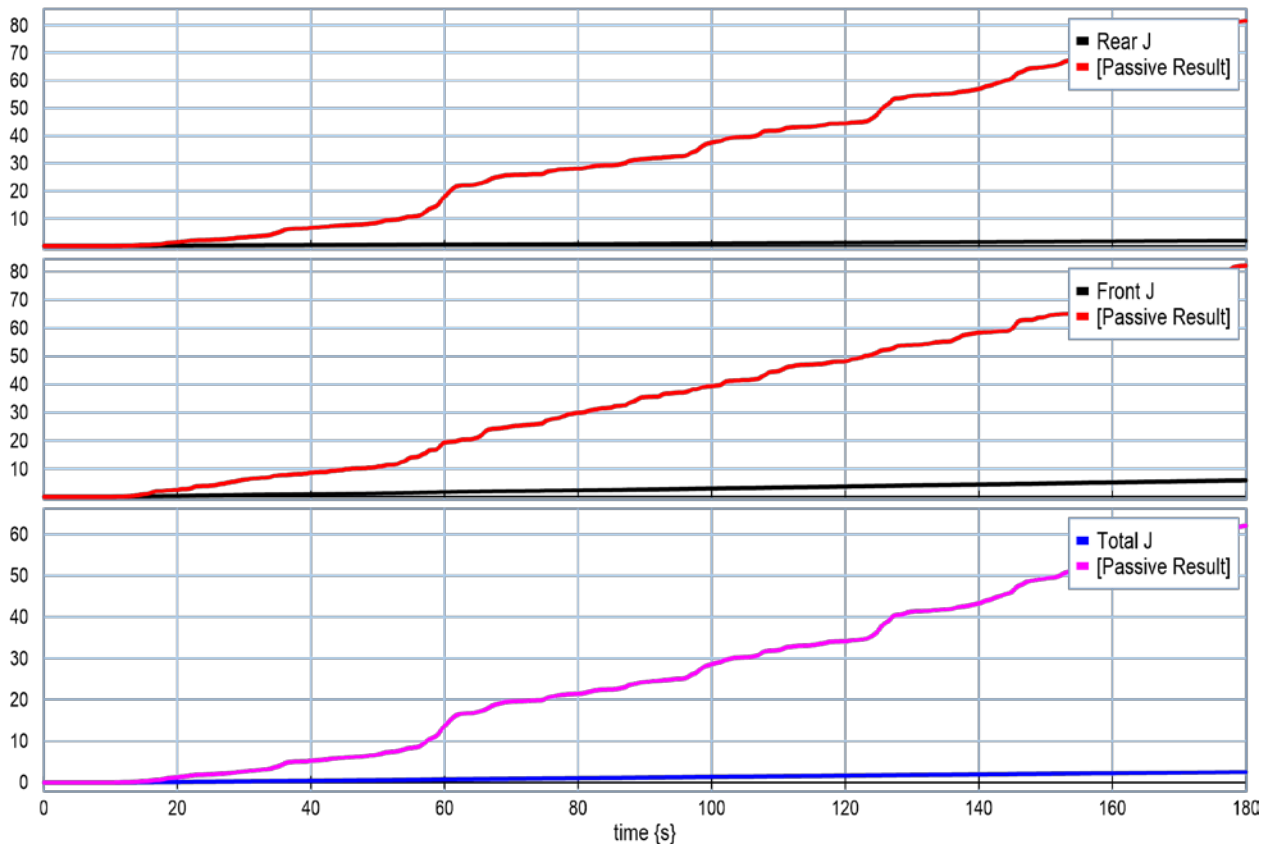
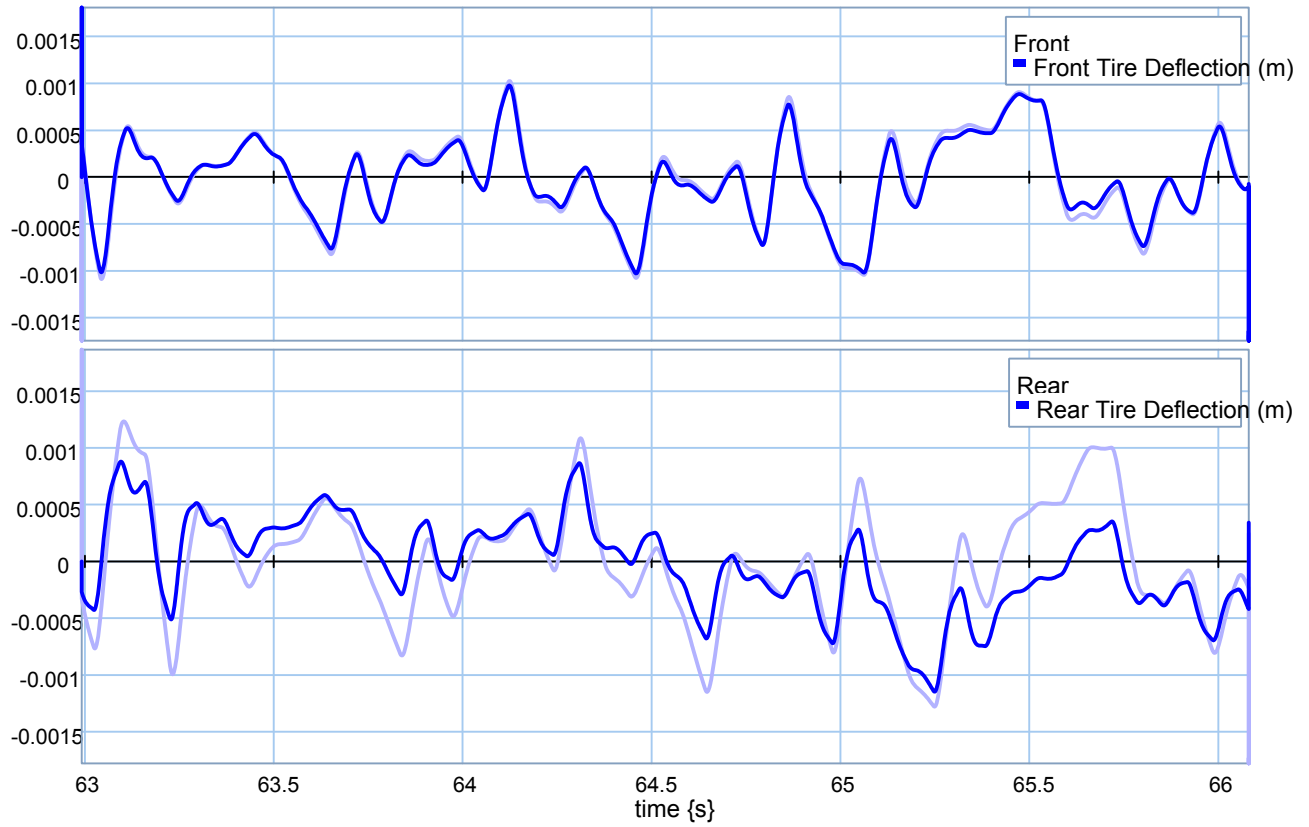


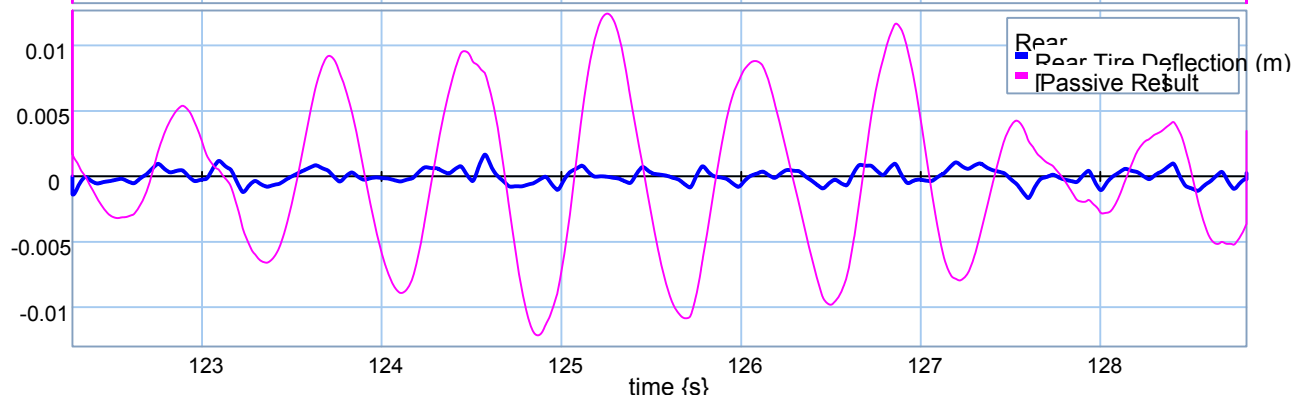
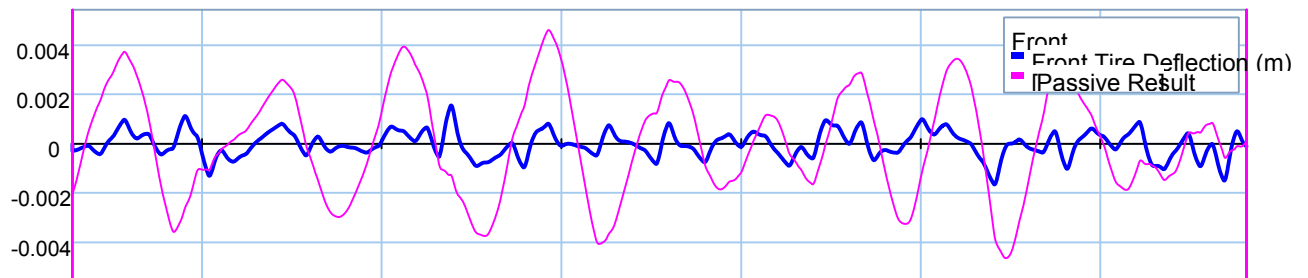
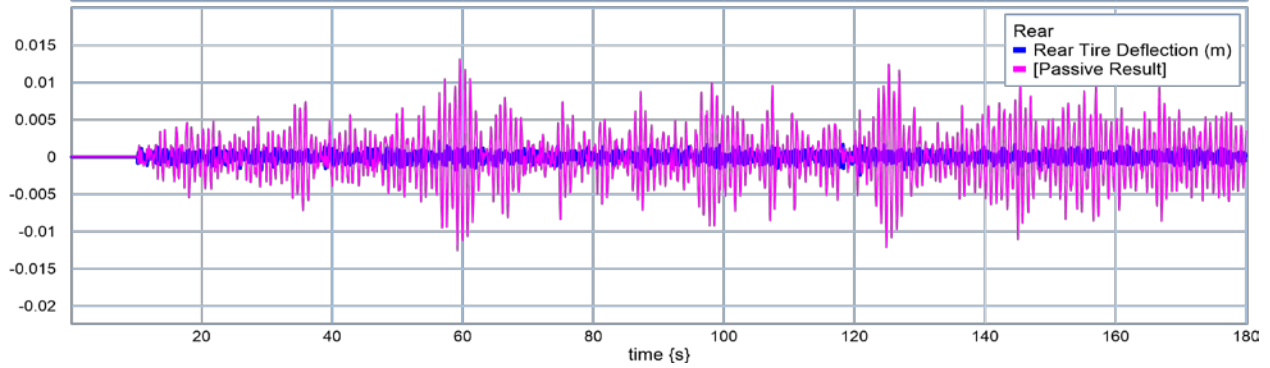
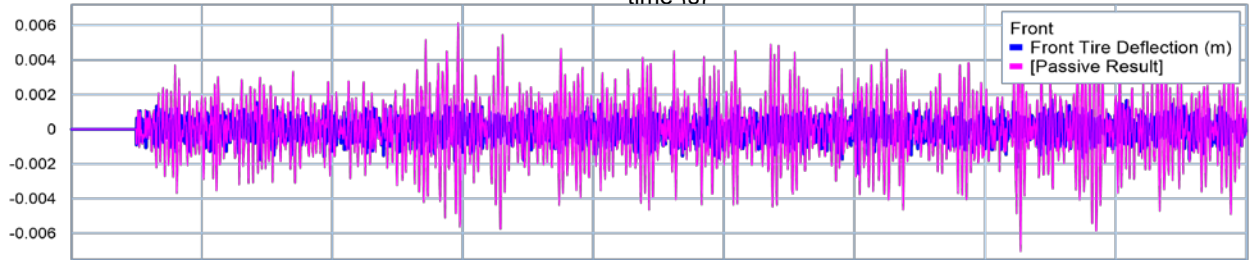
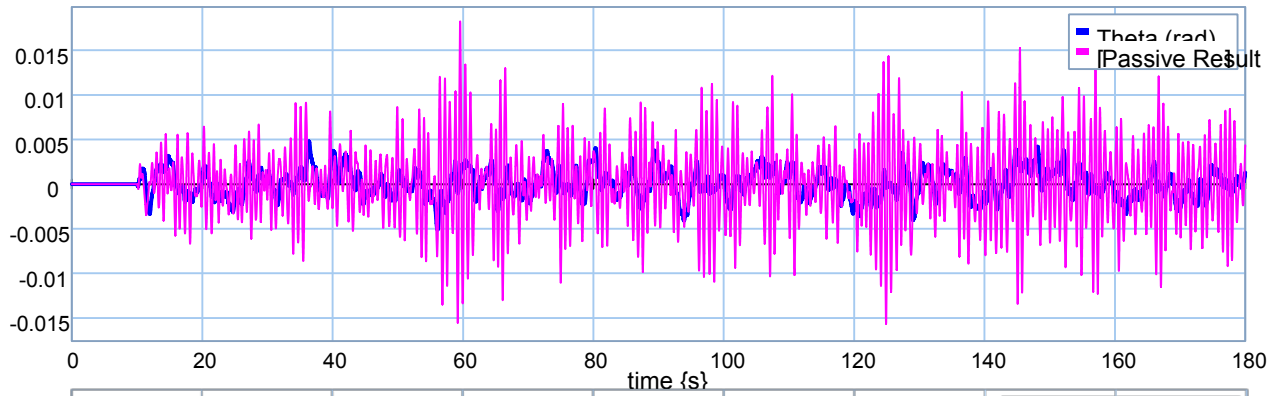


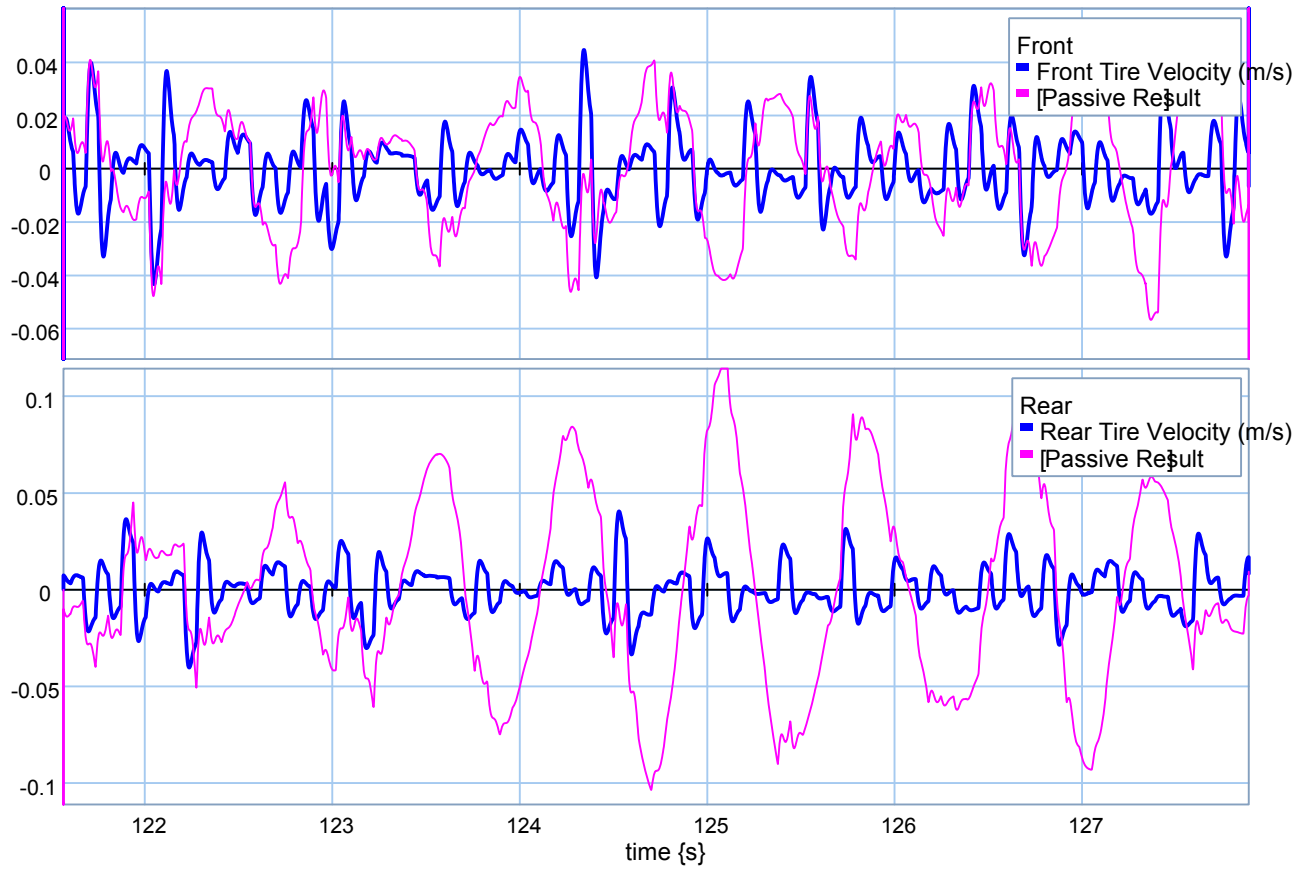
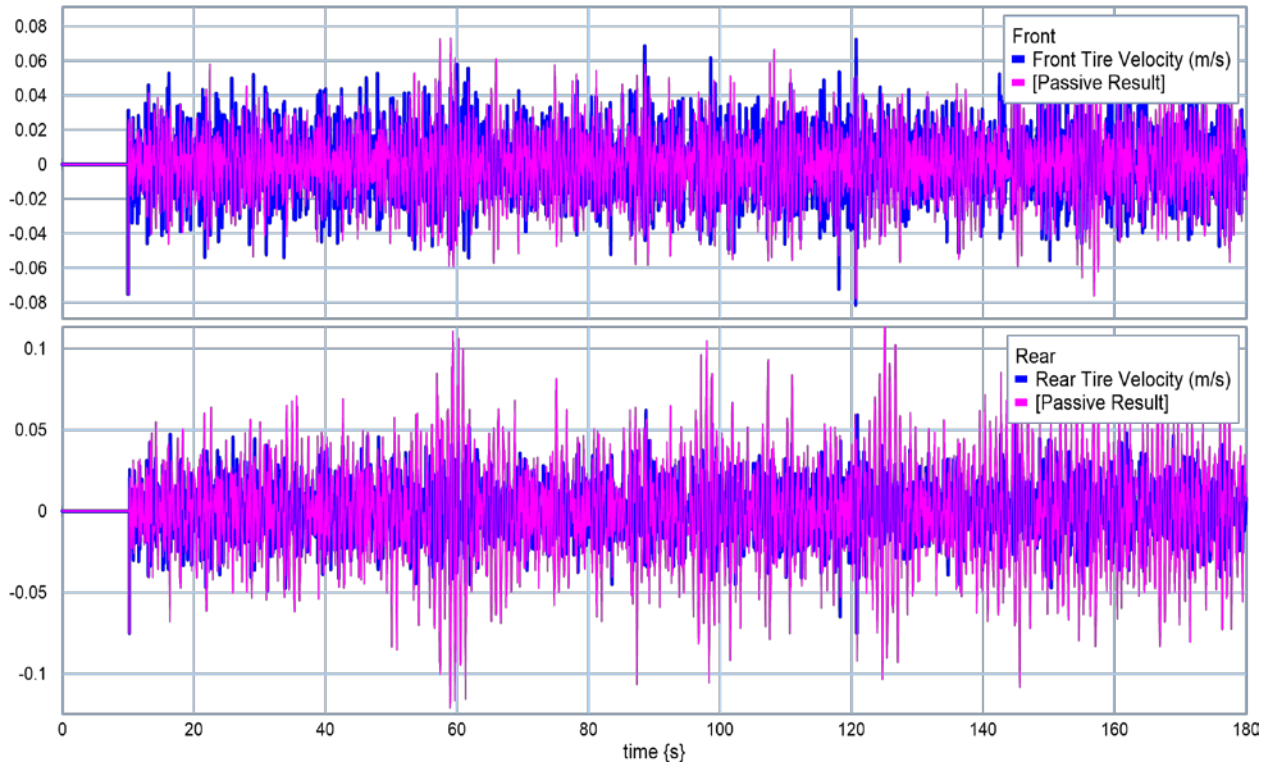


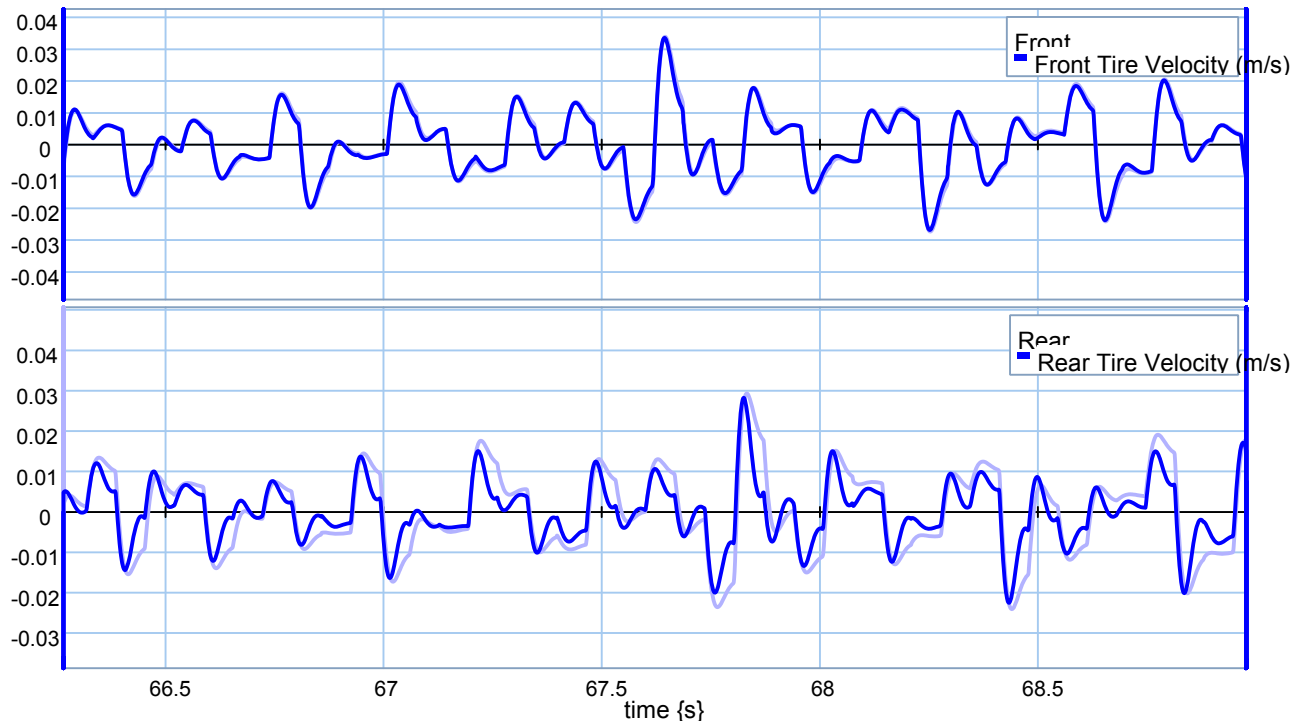
❖ **Mc = 13500 kg.**



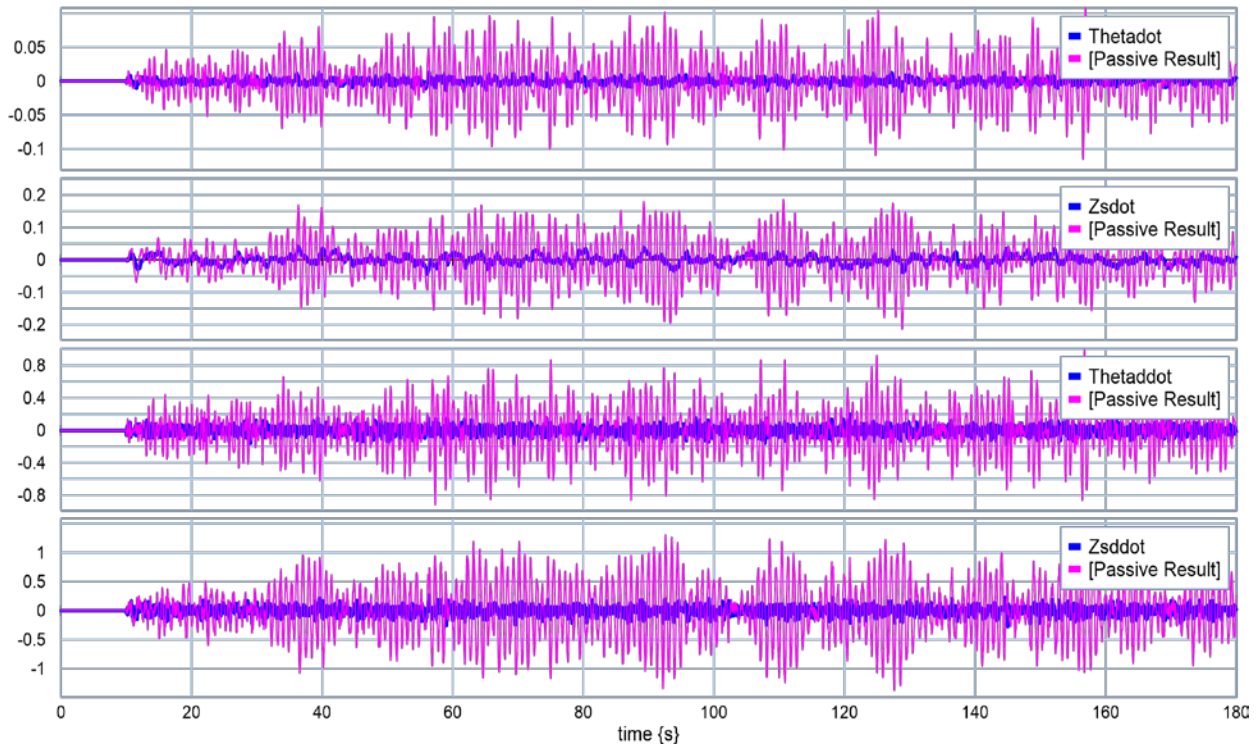


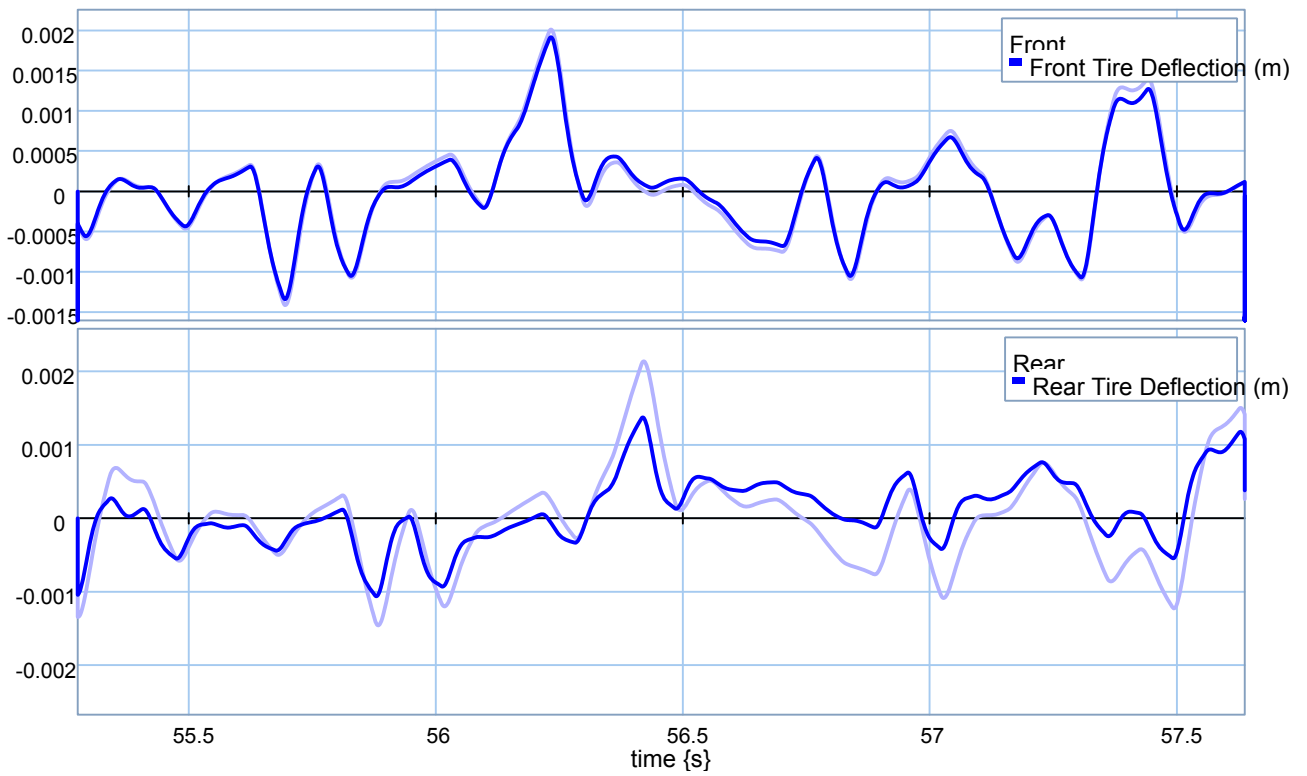
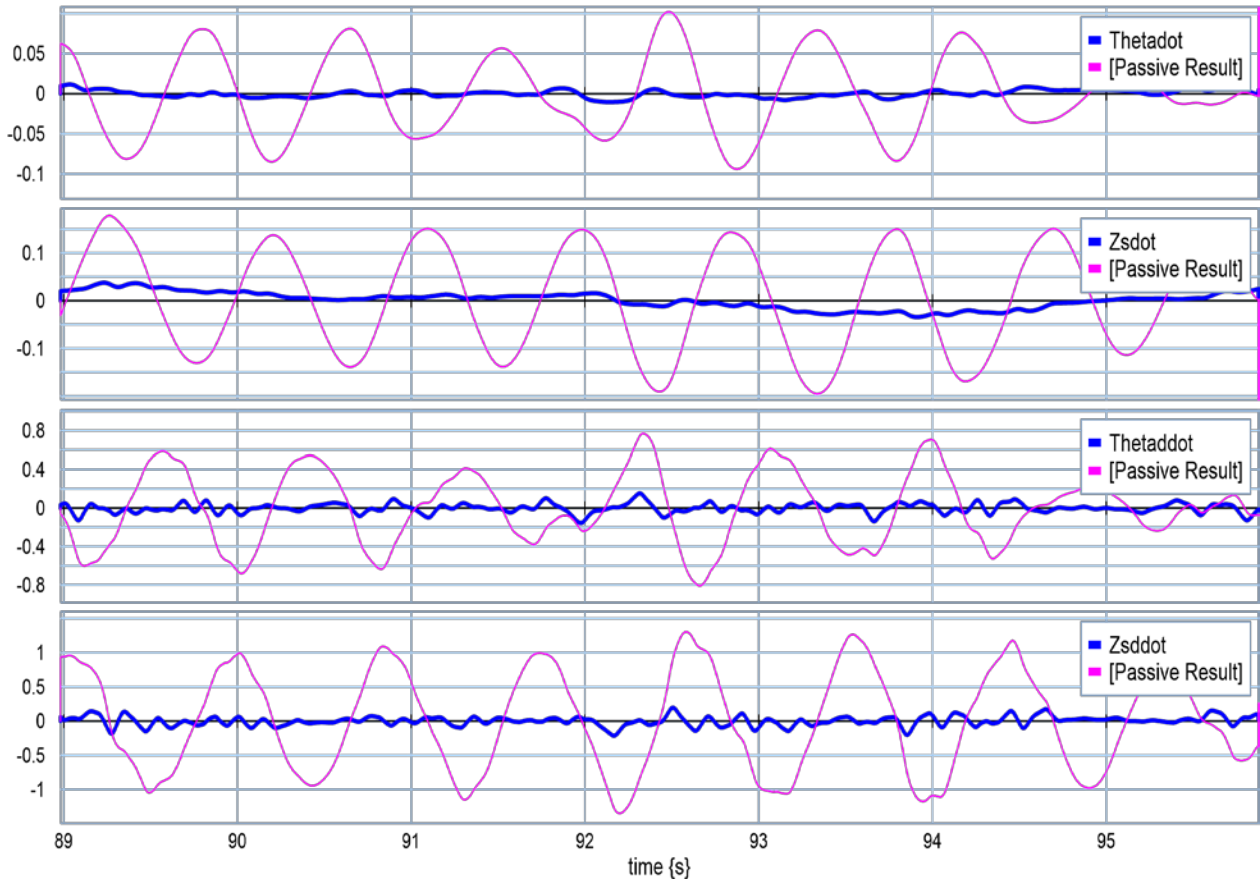


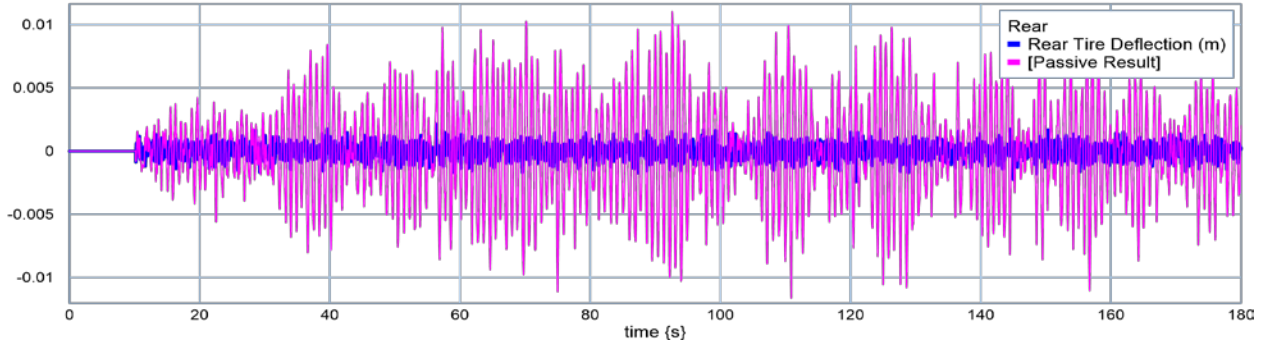
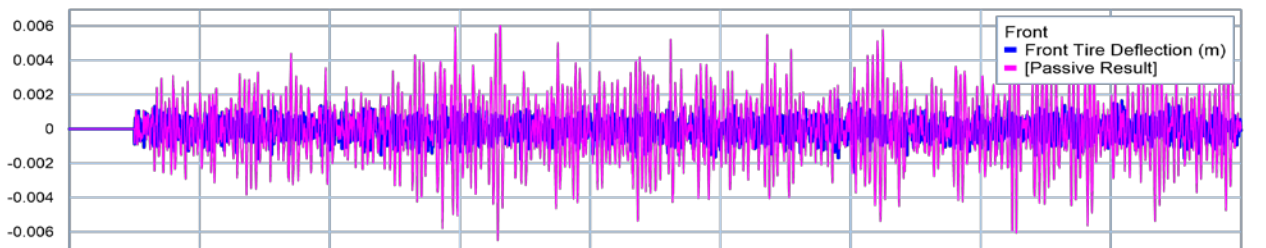
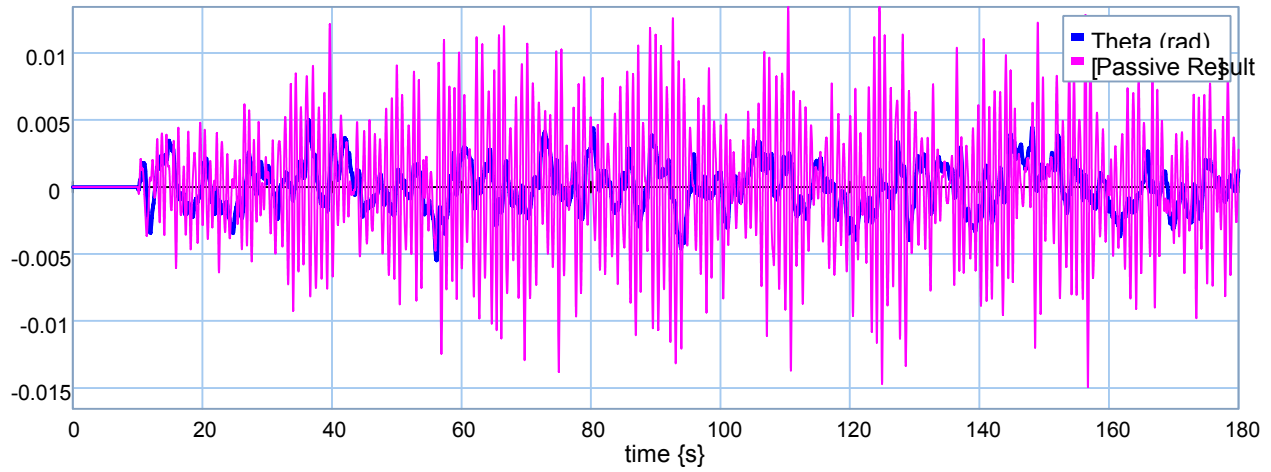
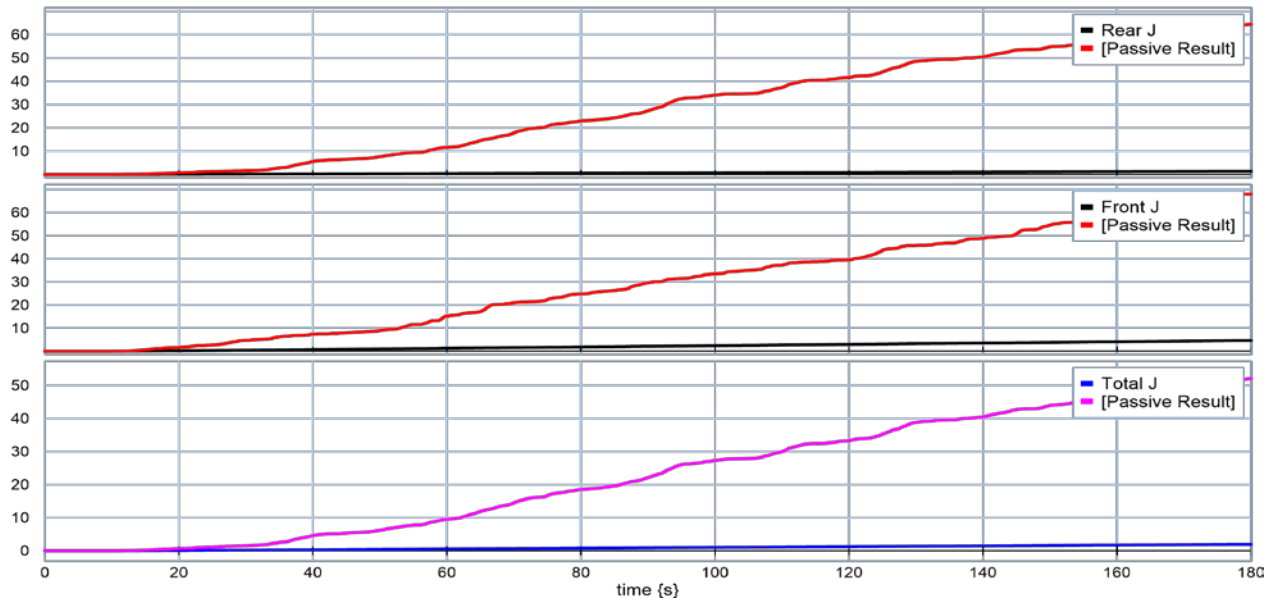


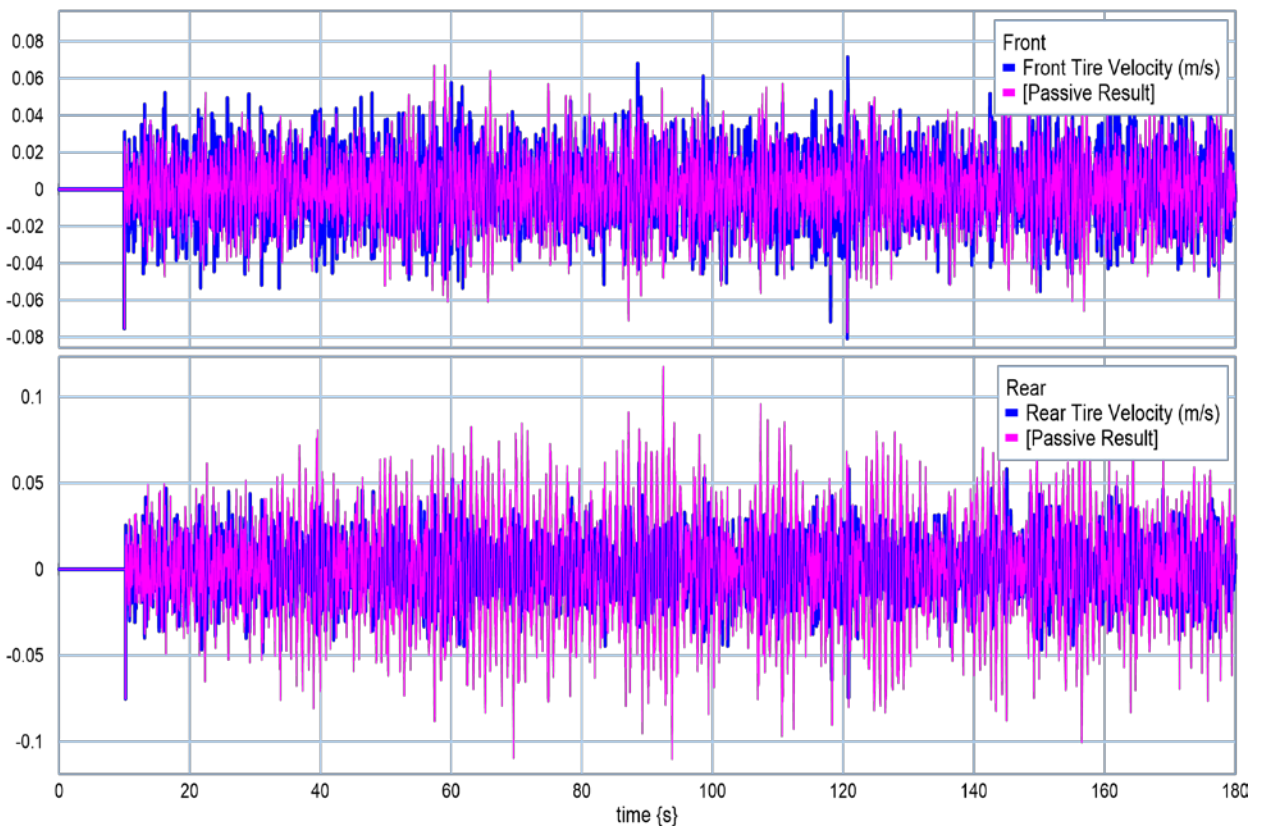
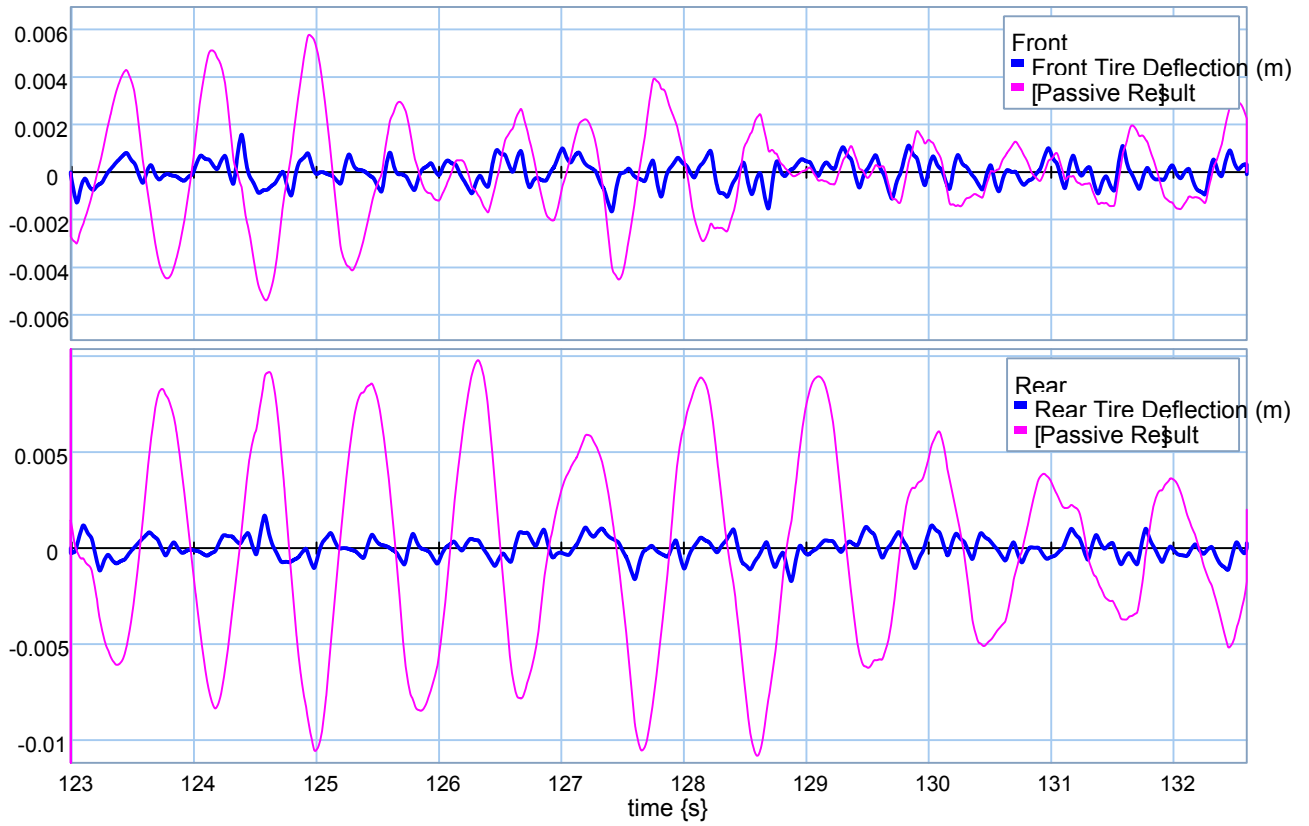


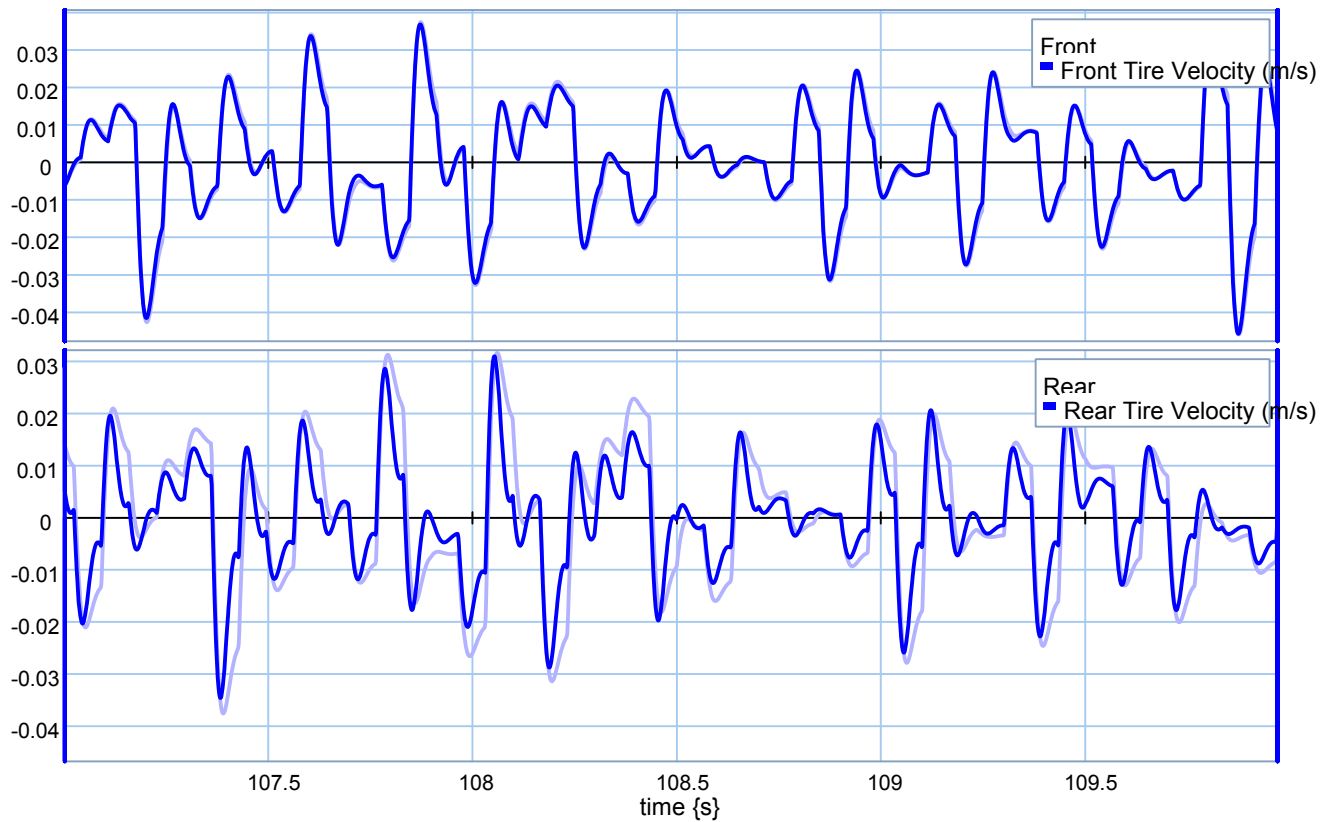
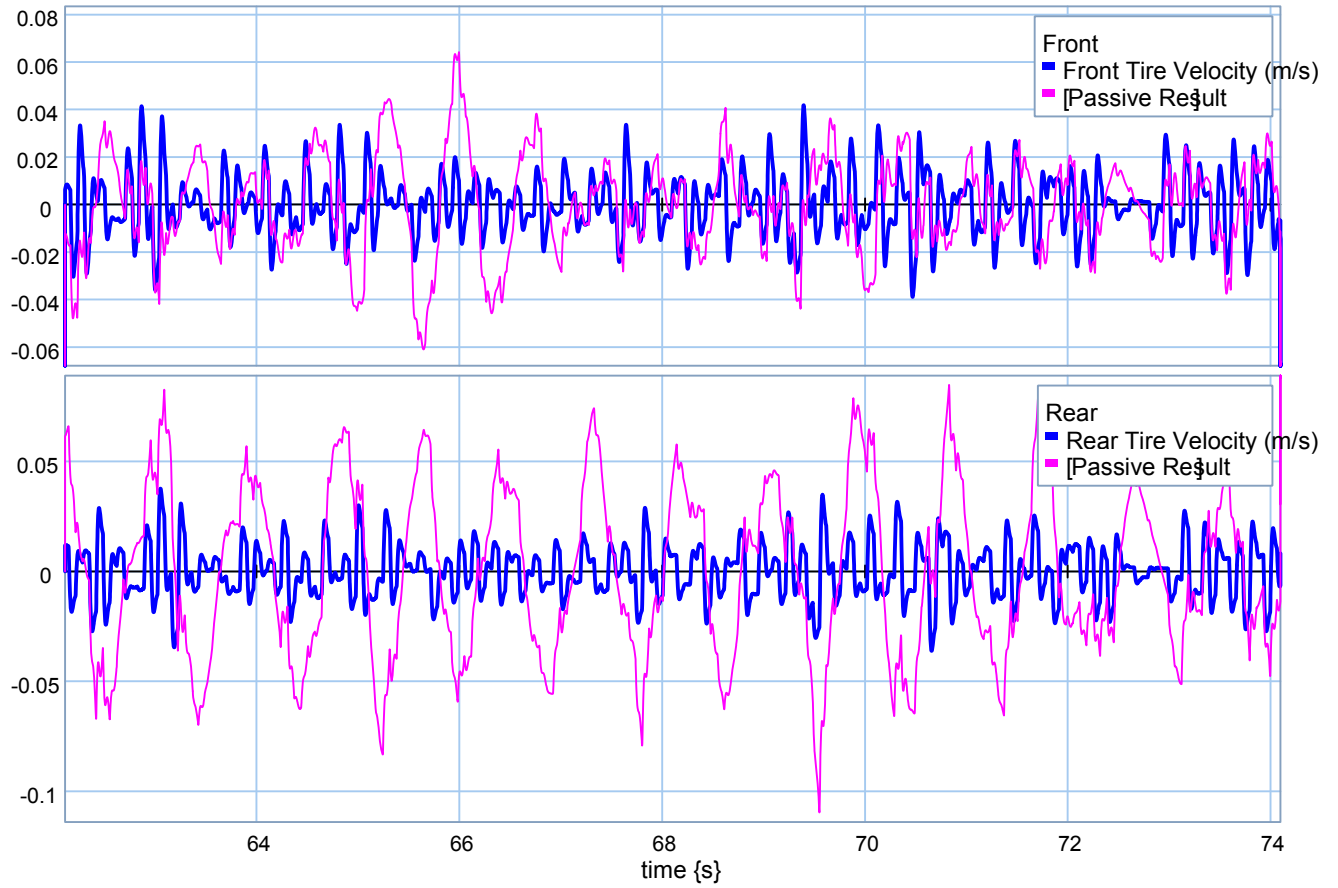
❖ **$M_c = 18000 \text{ kg.}$**





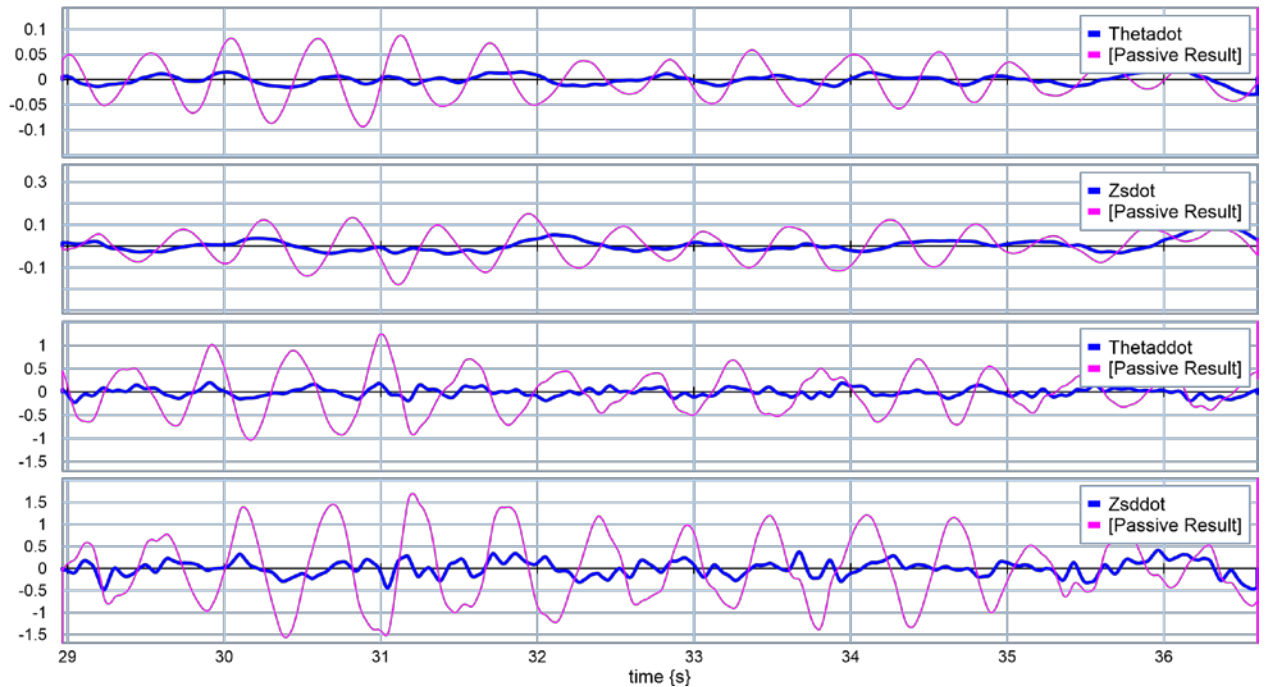
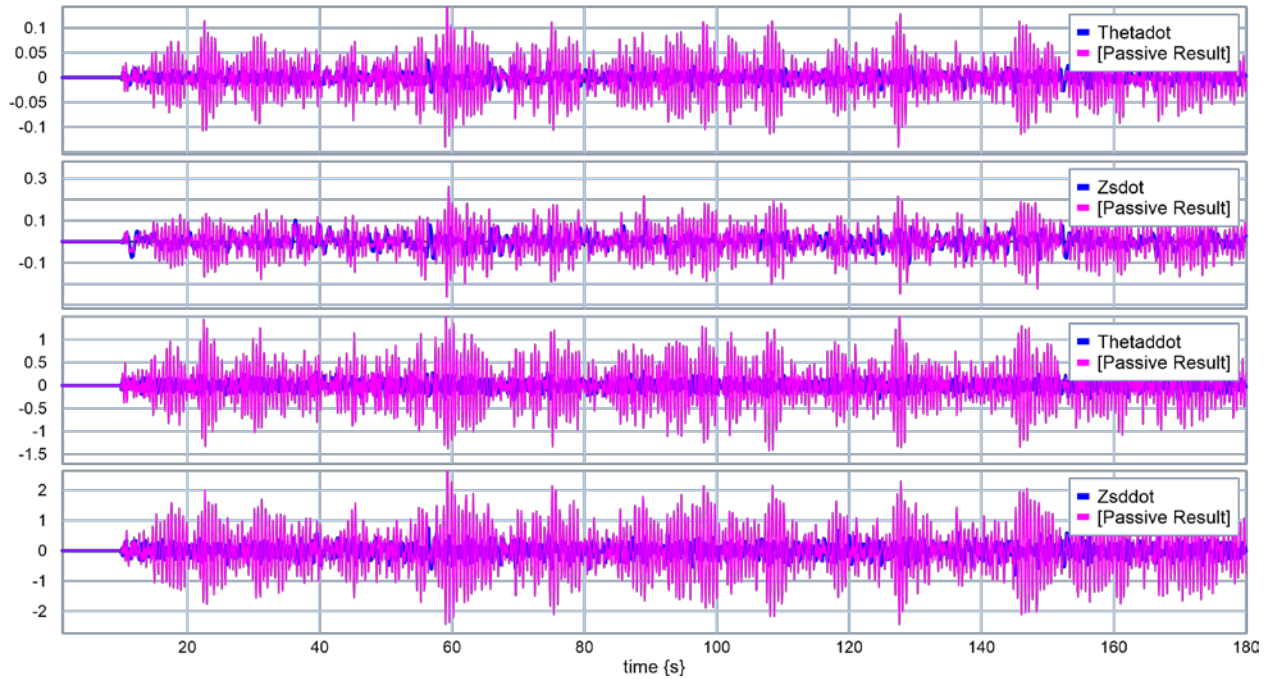


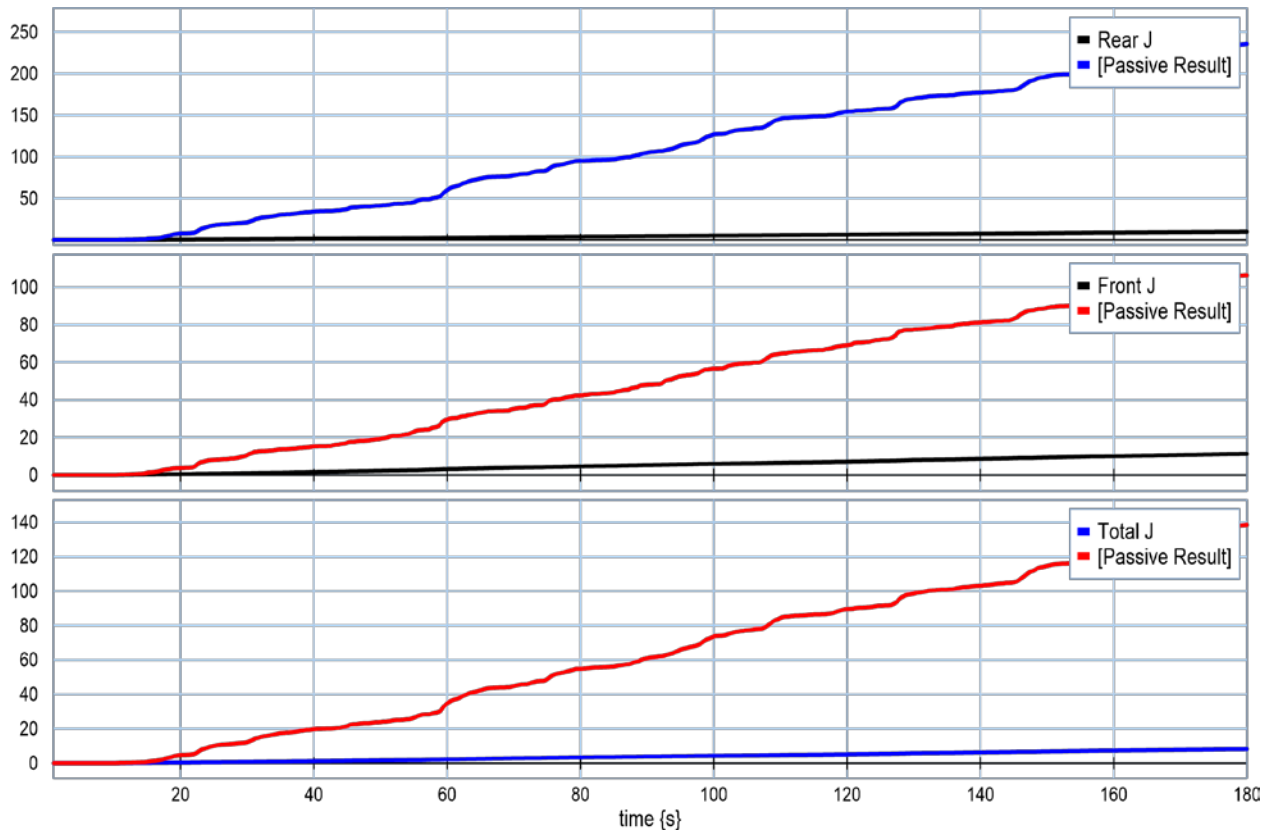
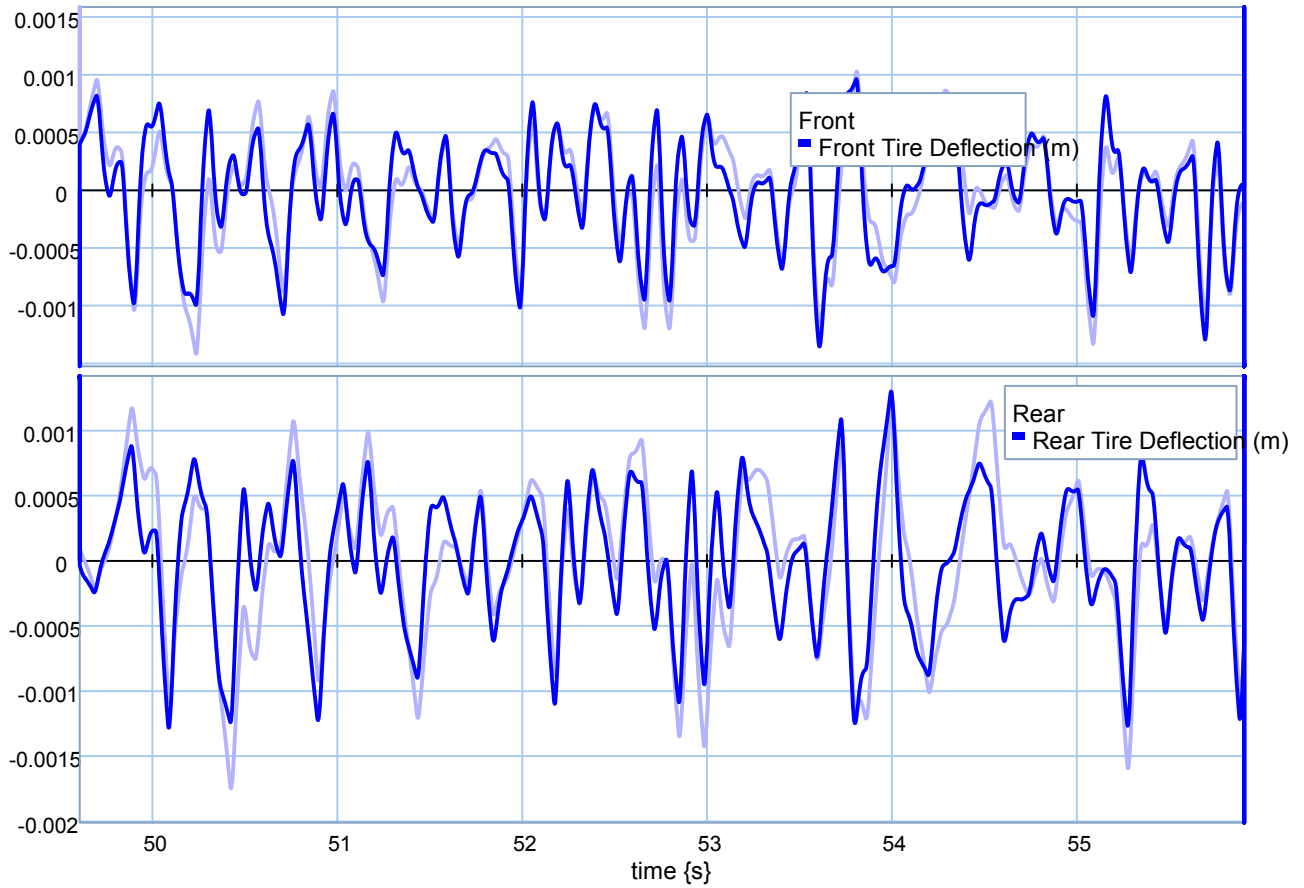


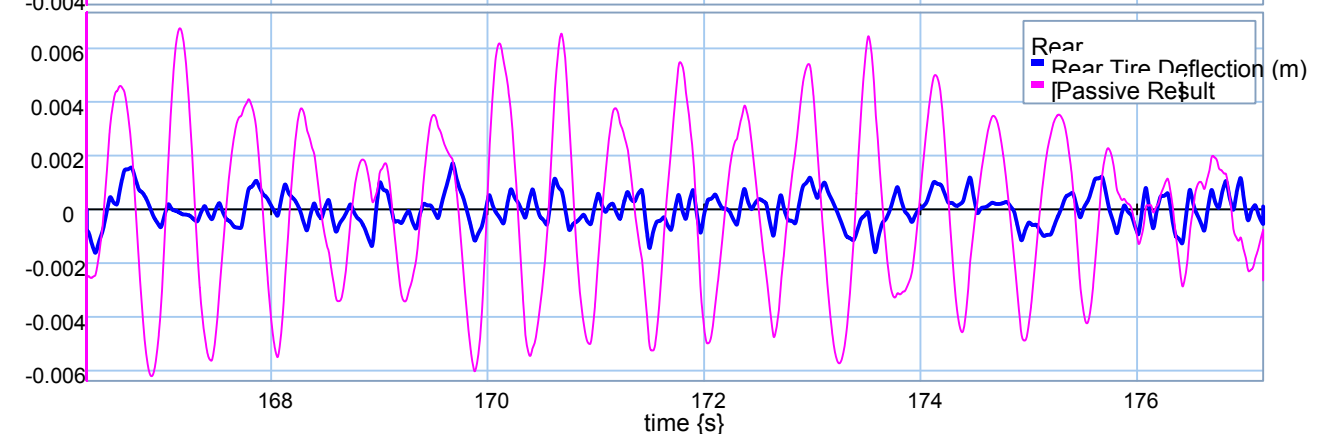
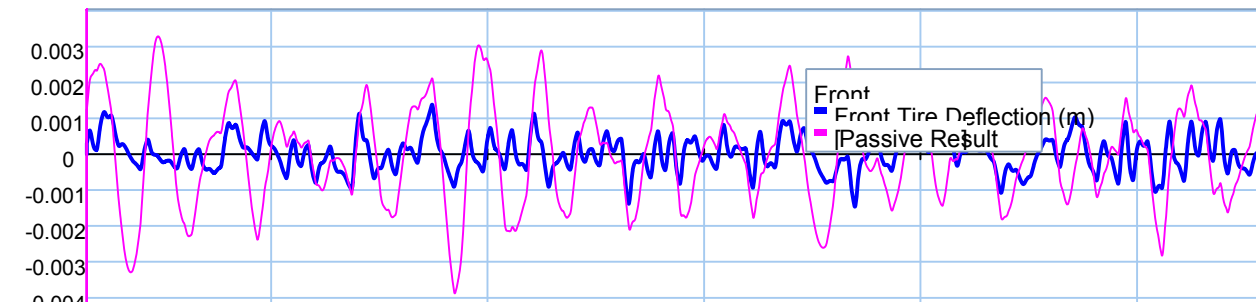
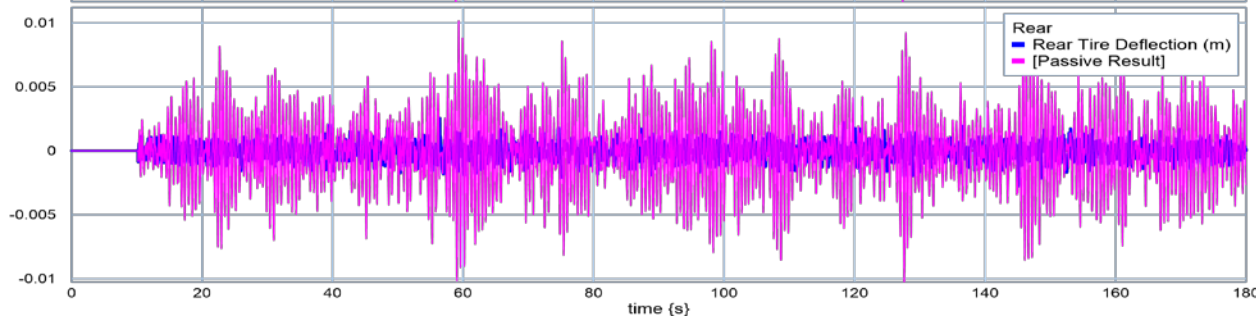
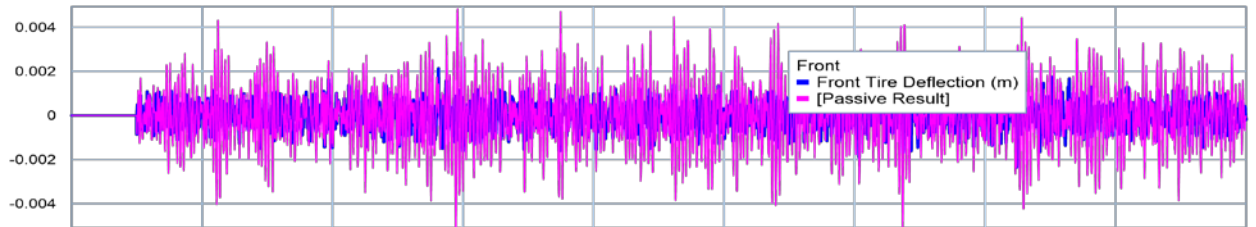
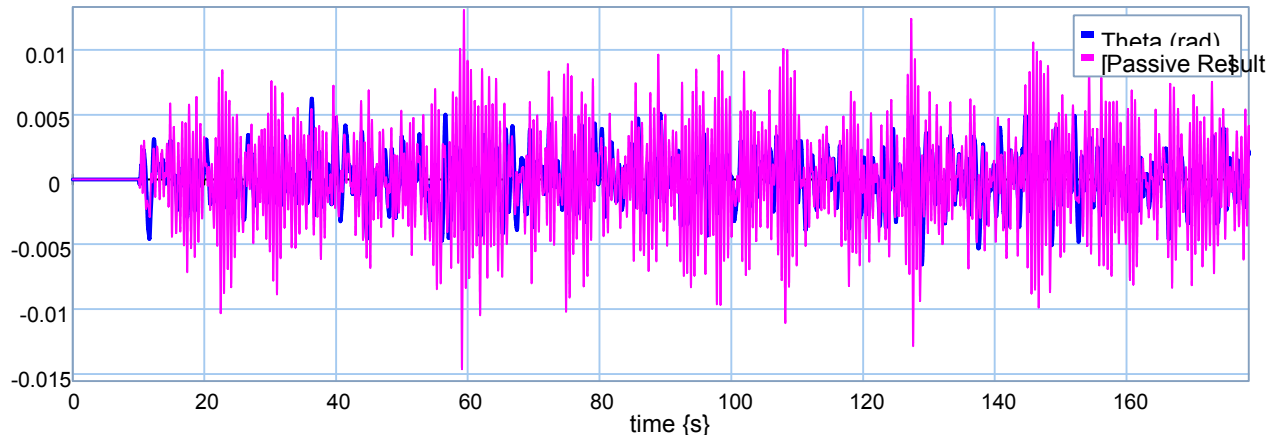


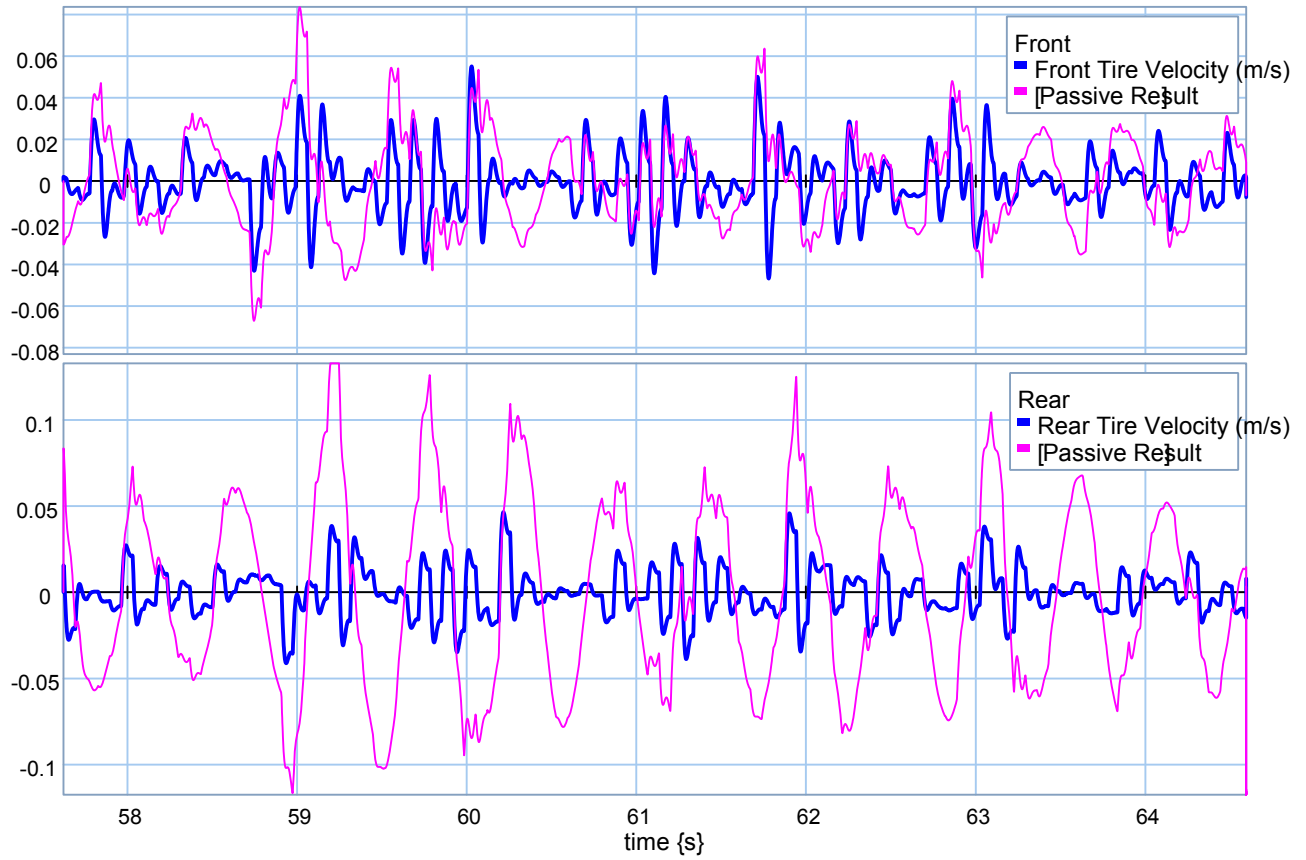
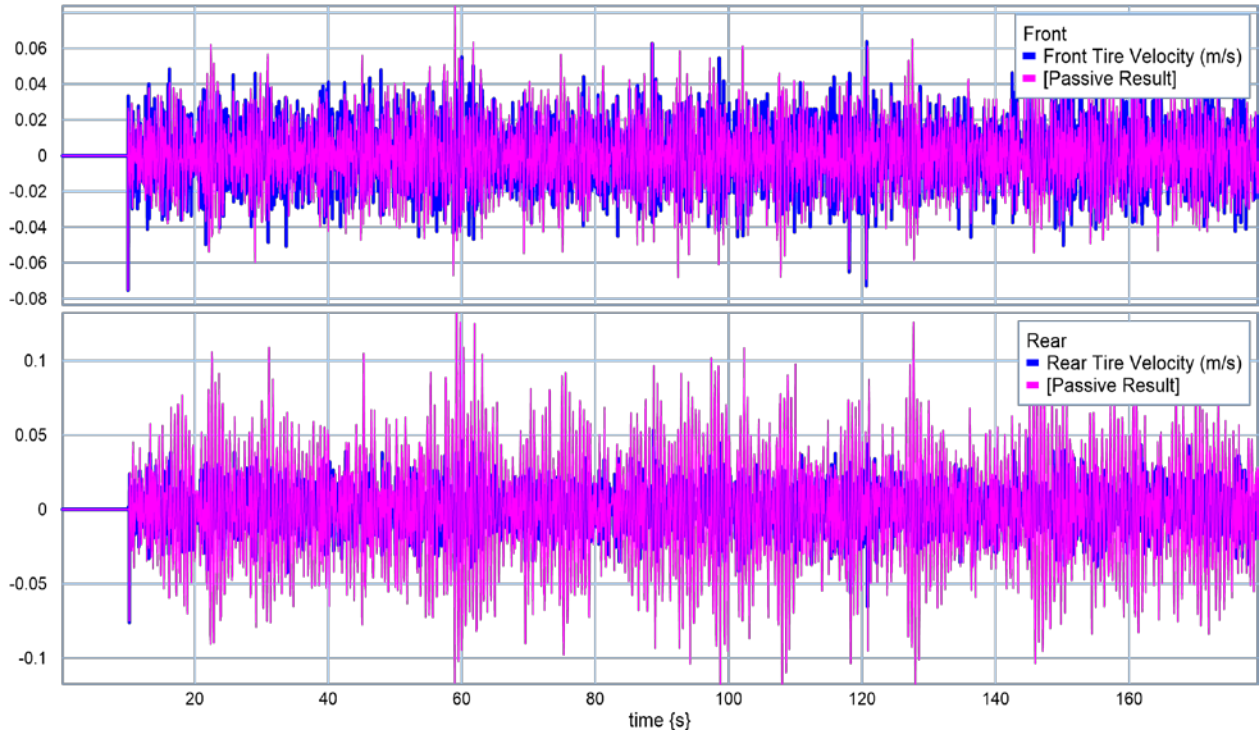
AppendixE: Linear HalfCar Model, Road Holding Scenario, HalfCar Active Suspensions.

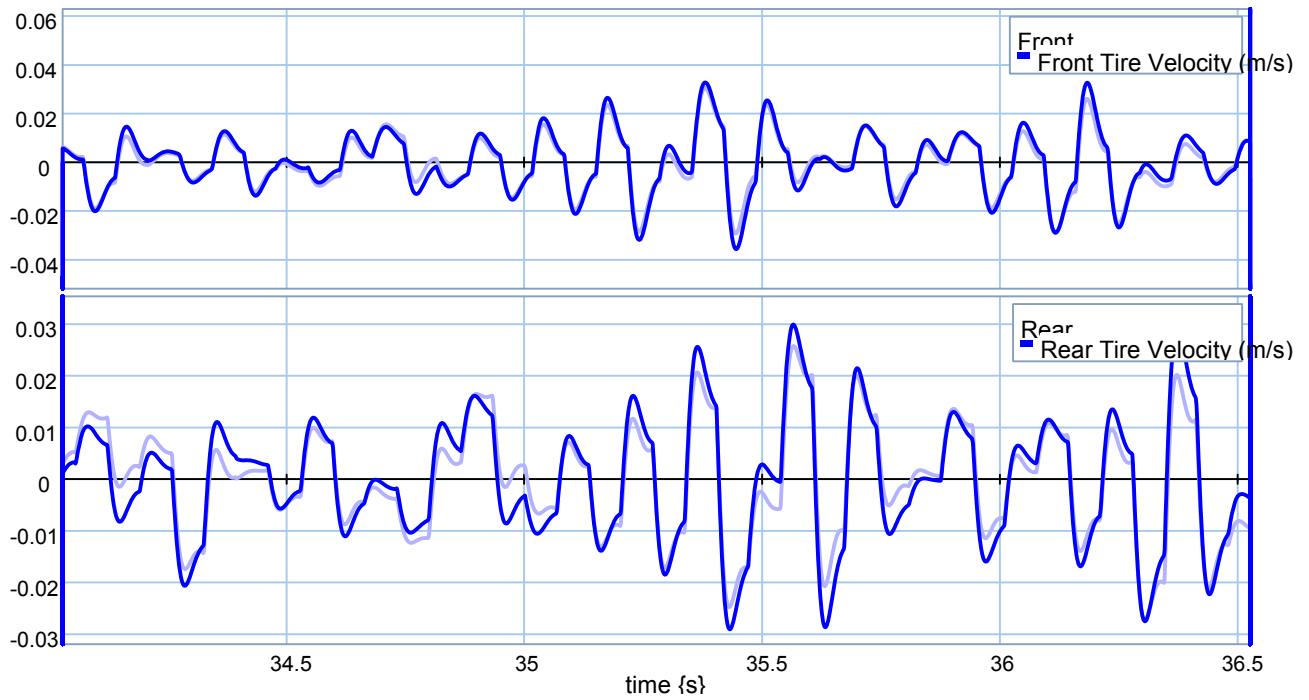
❖ $M_c = 4500 \text{ kg.}$



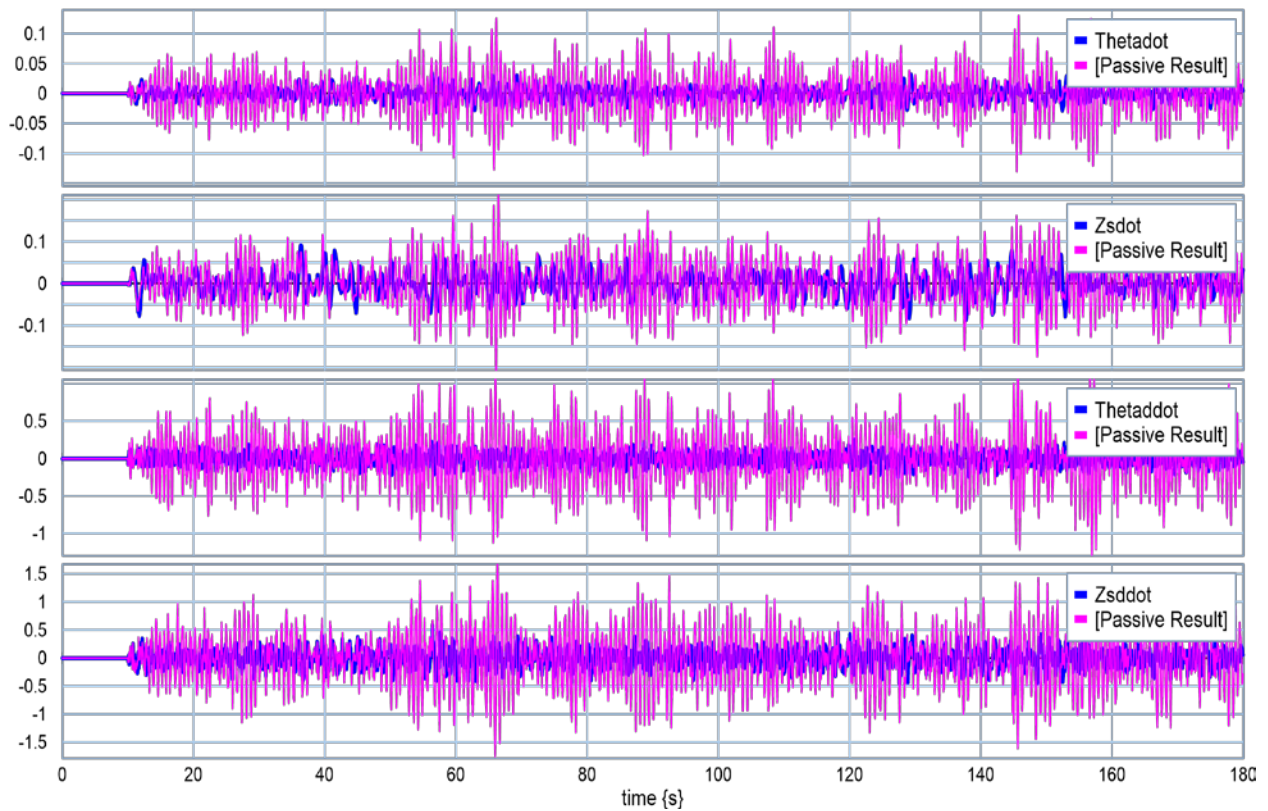


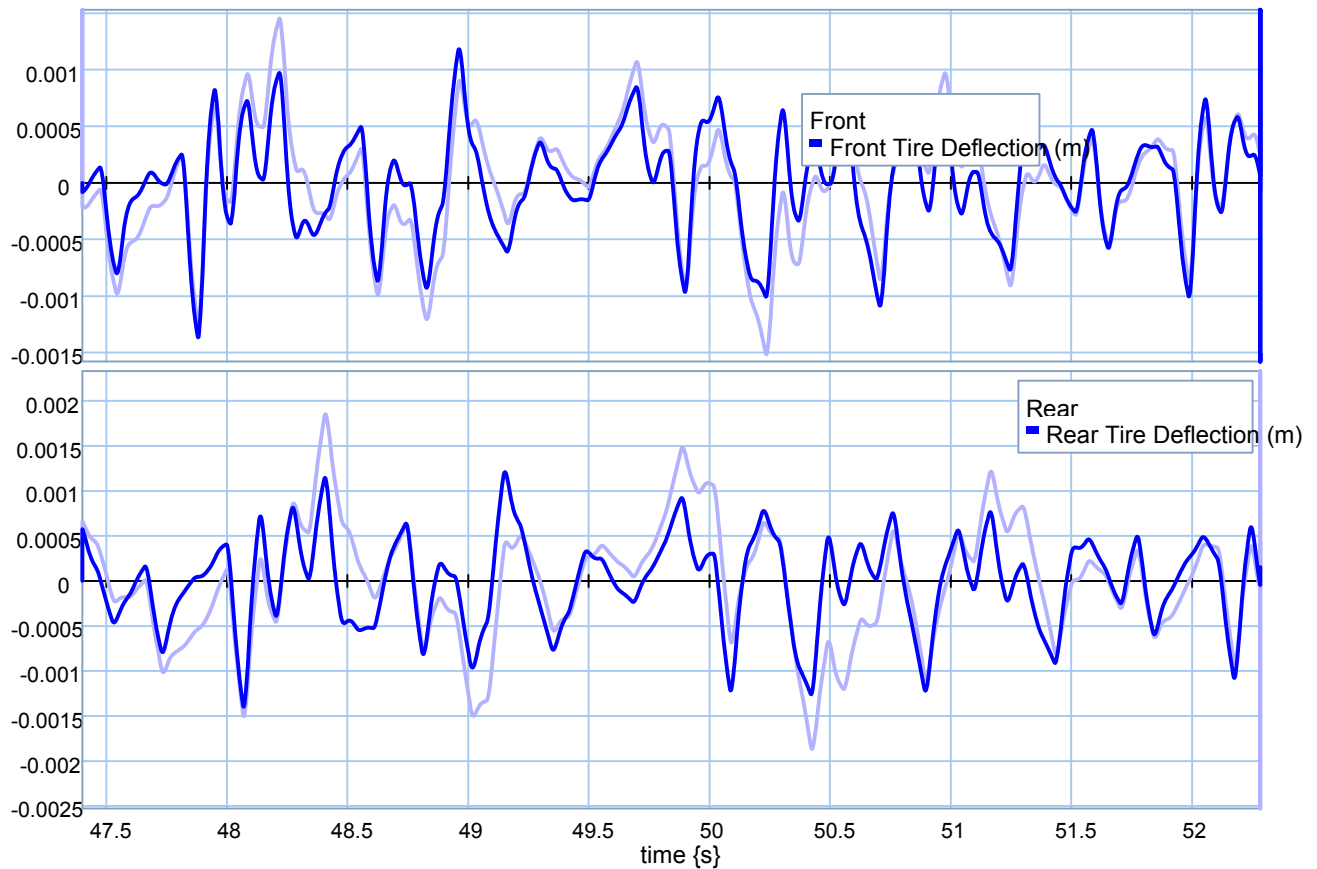
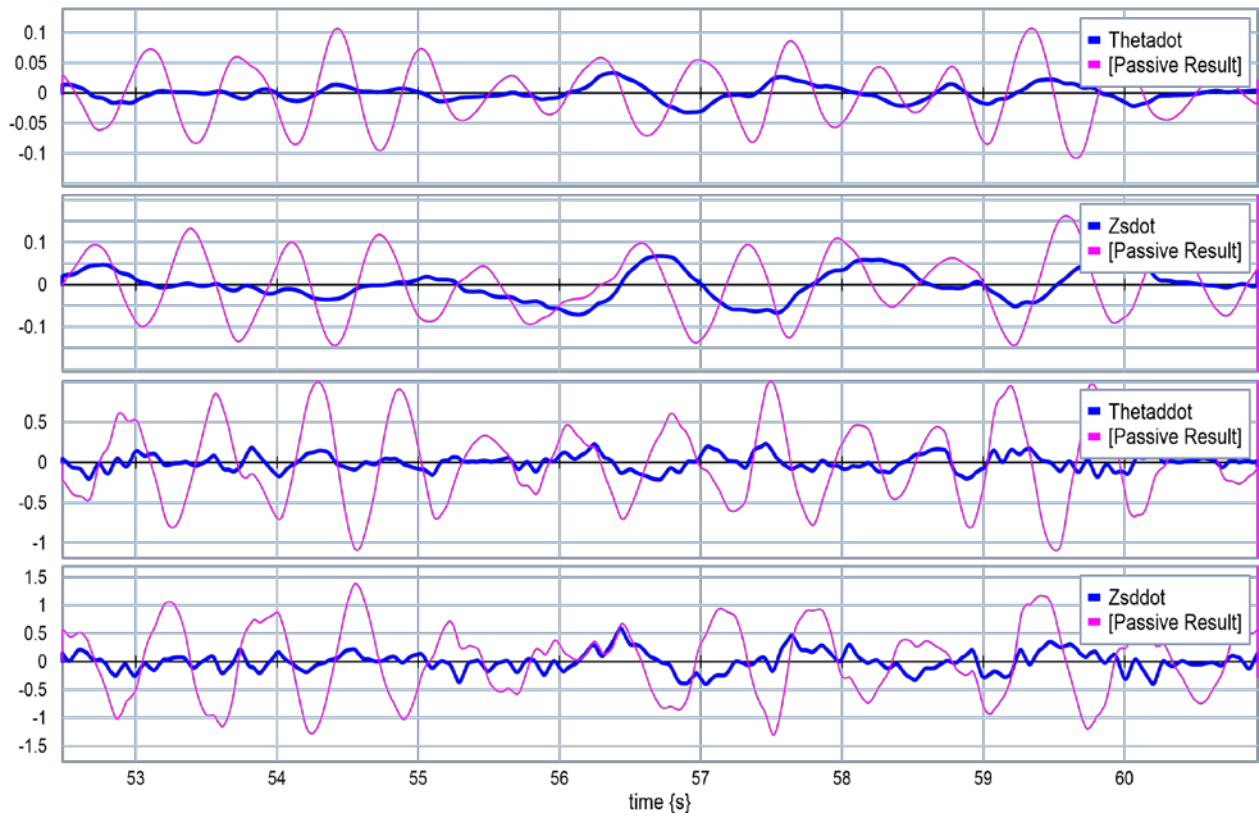


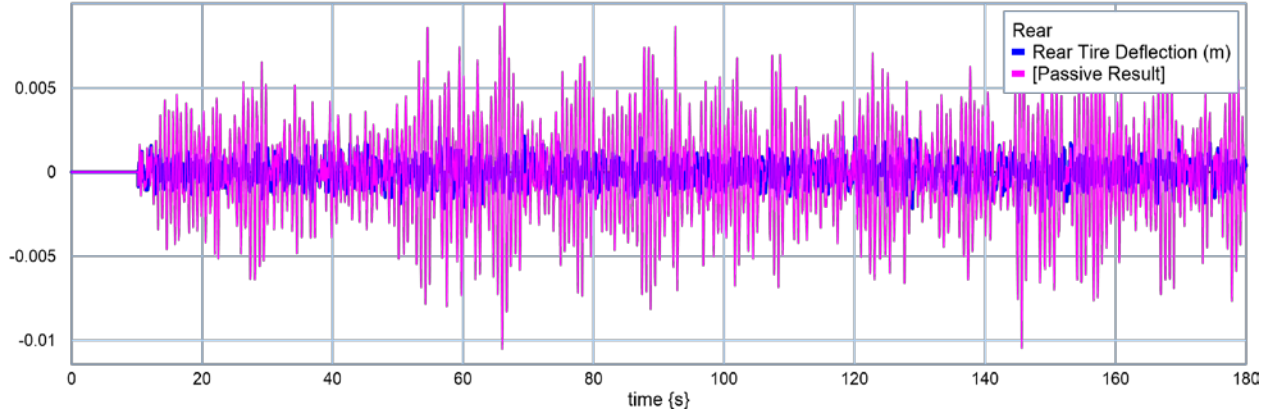
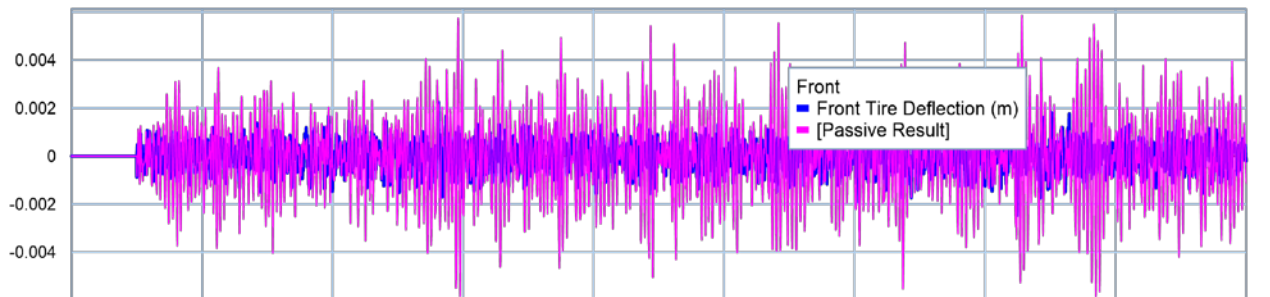
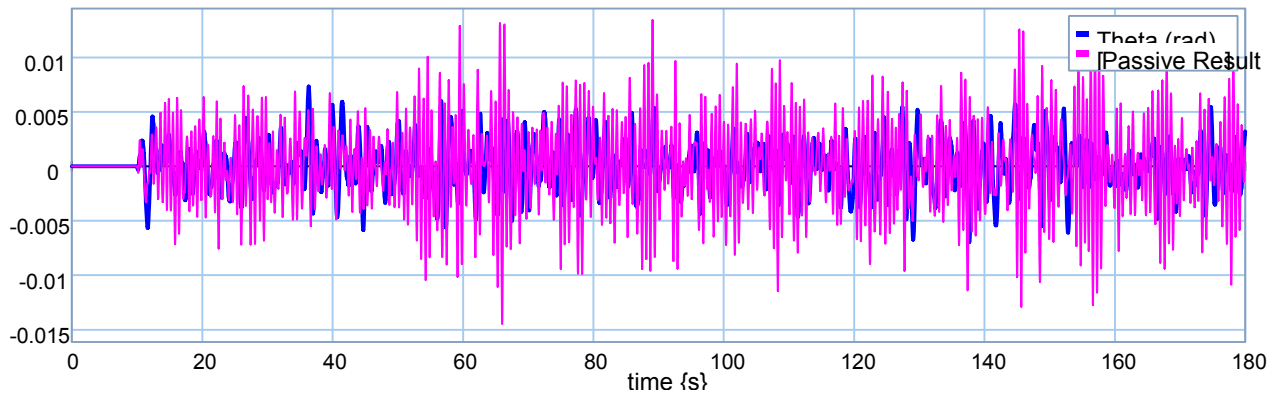
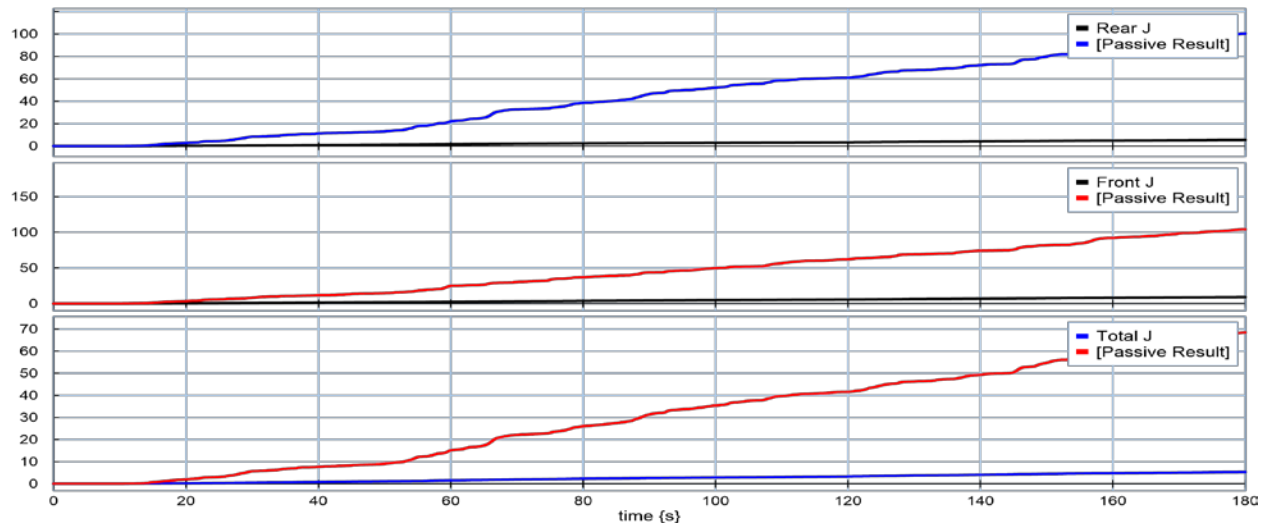


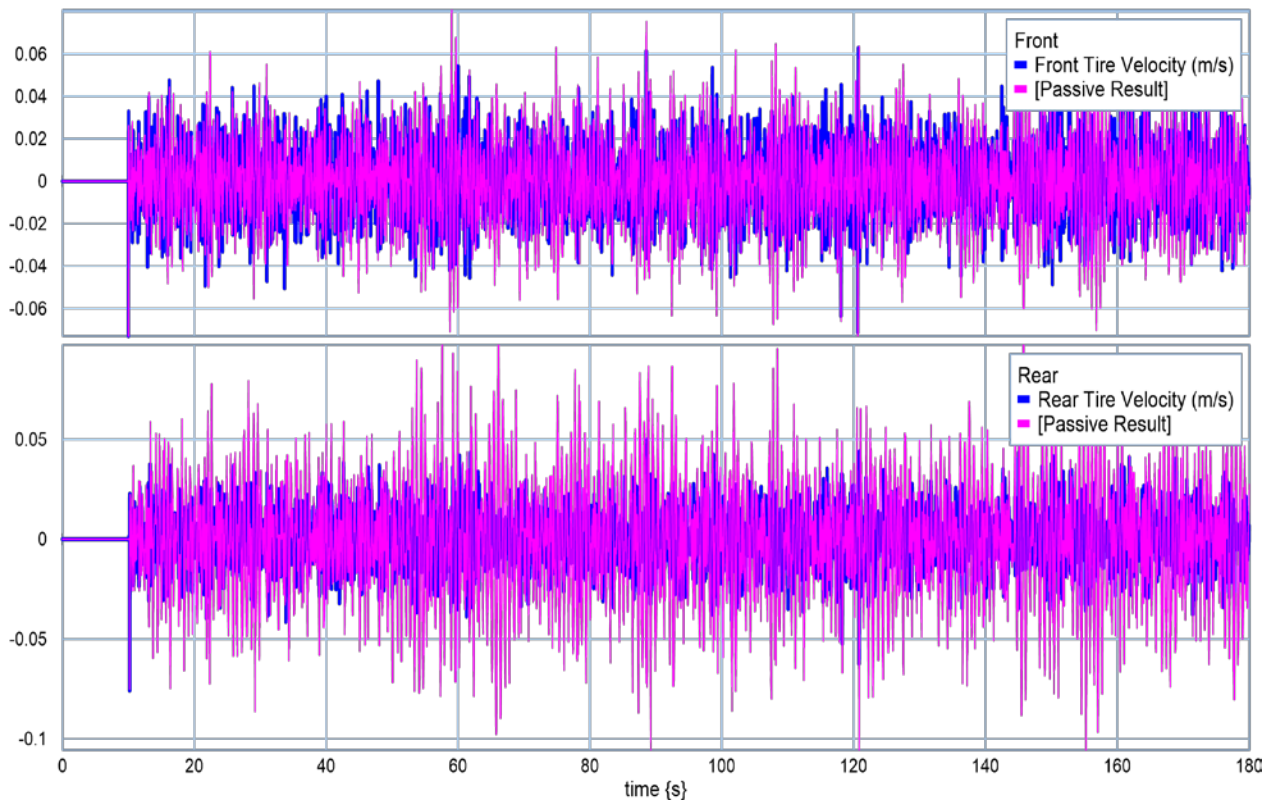
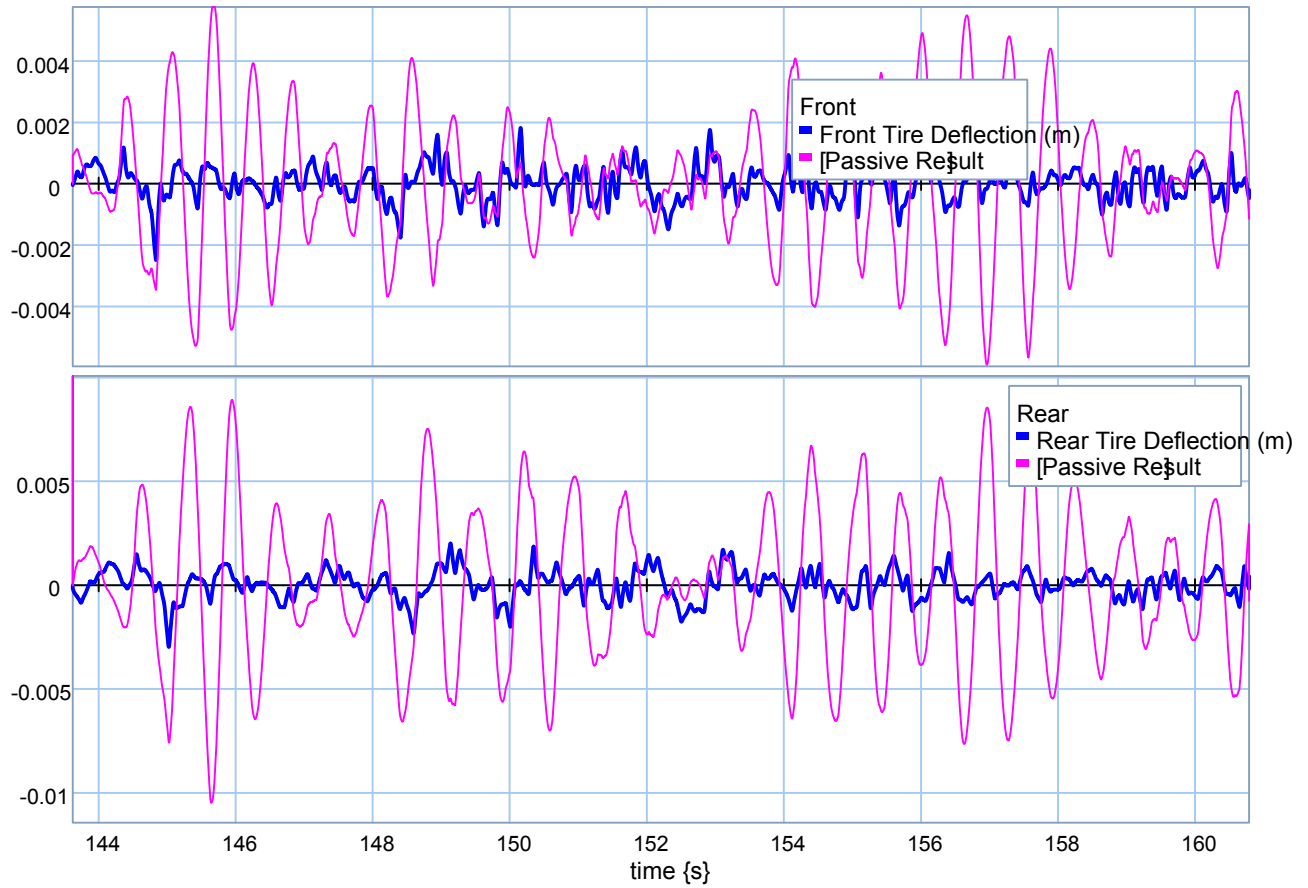


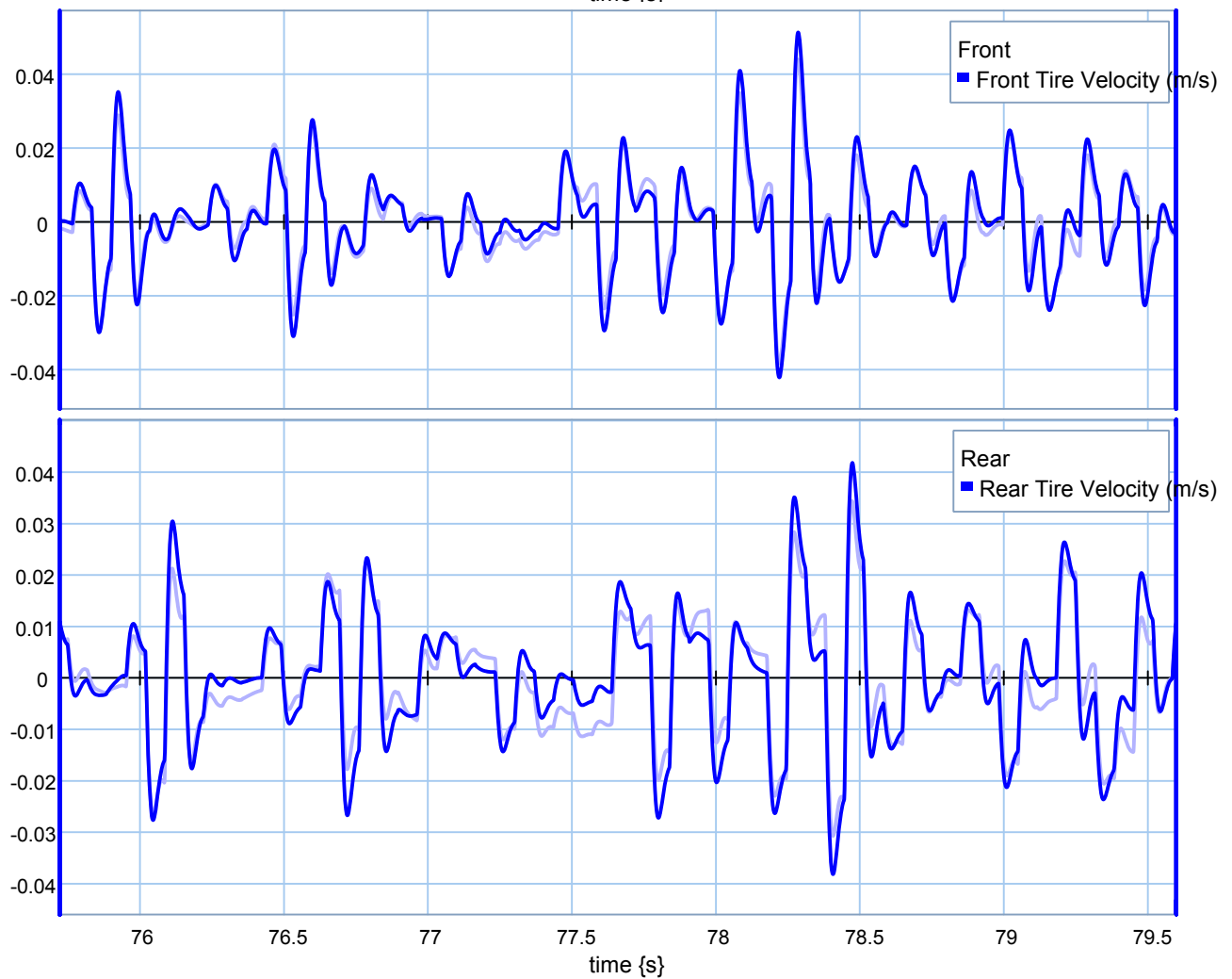
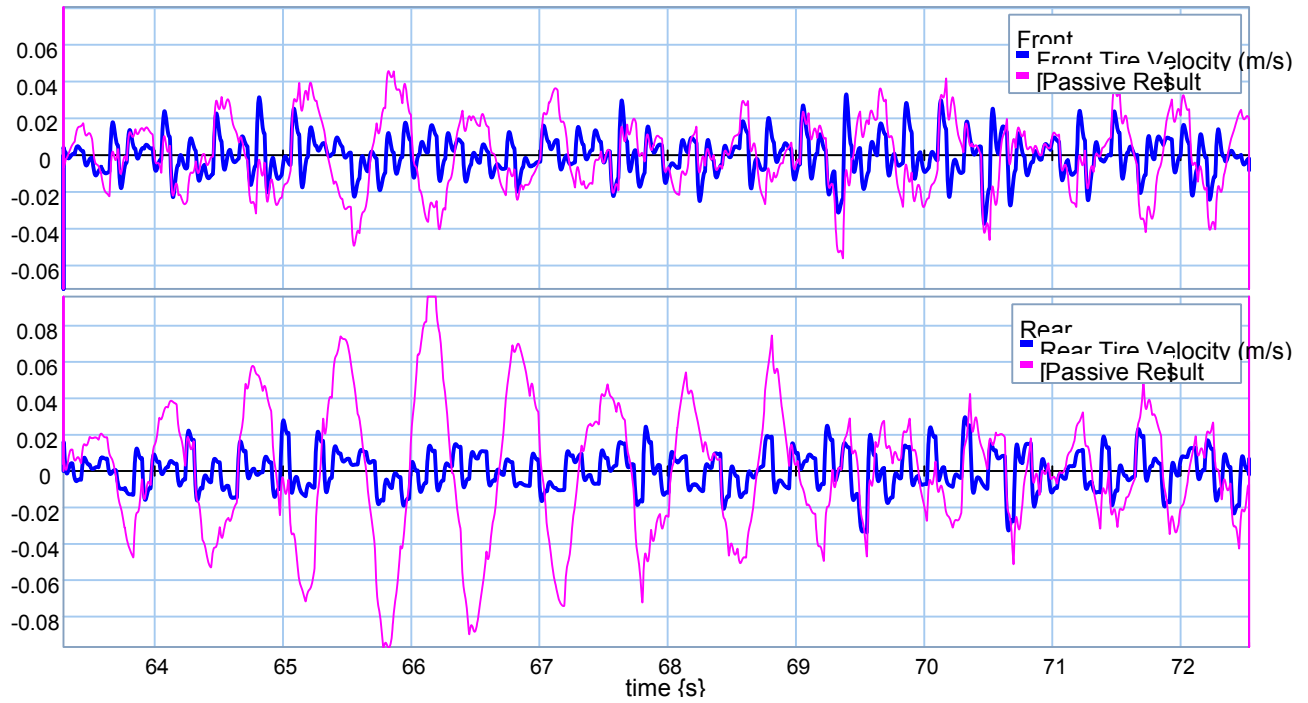
❖ **Mc = 9000 kg.**



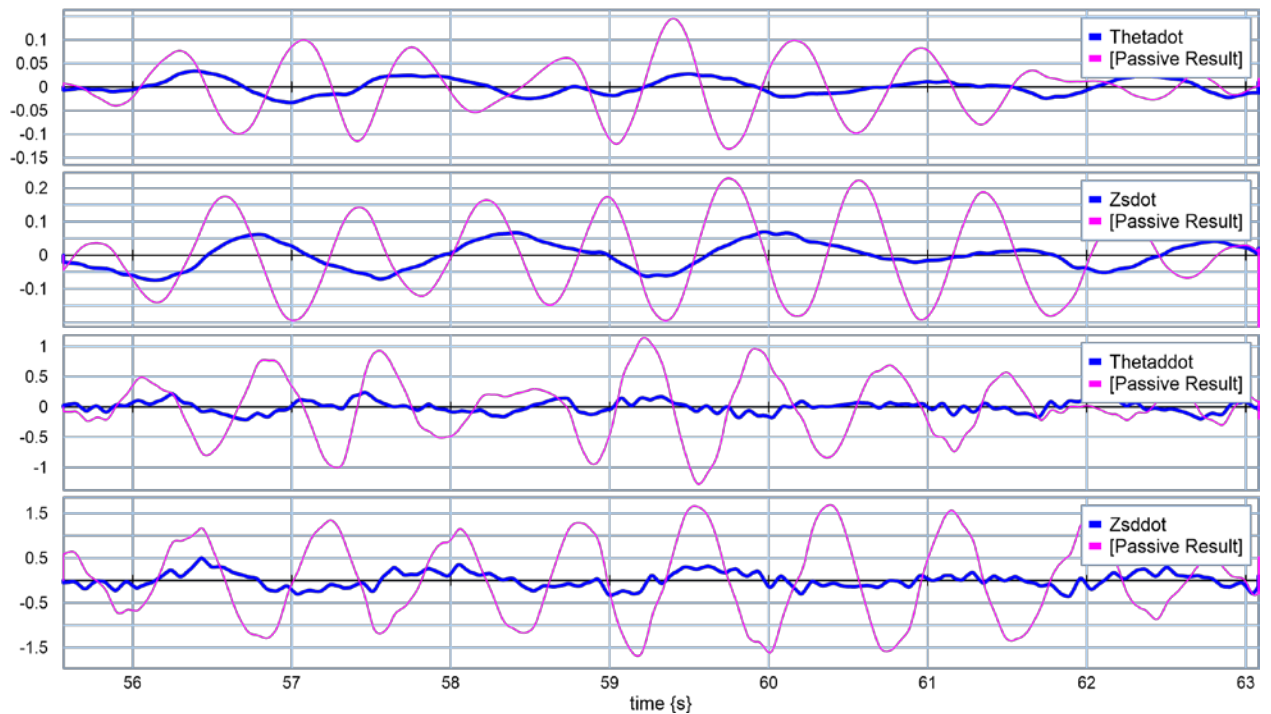
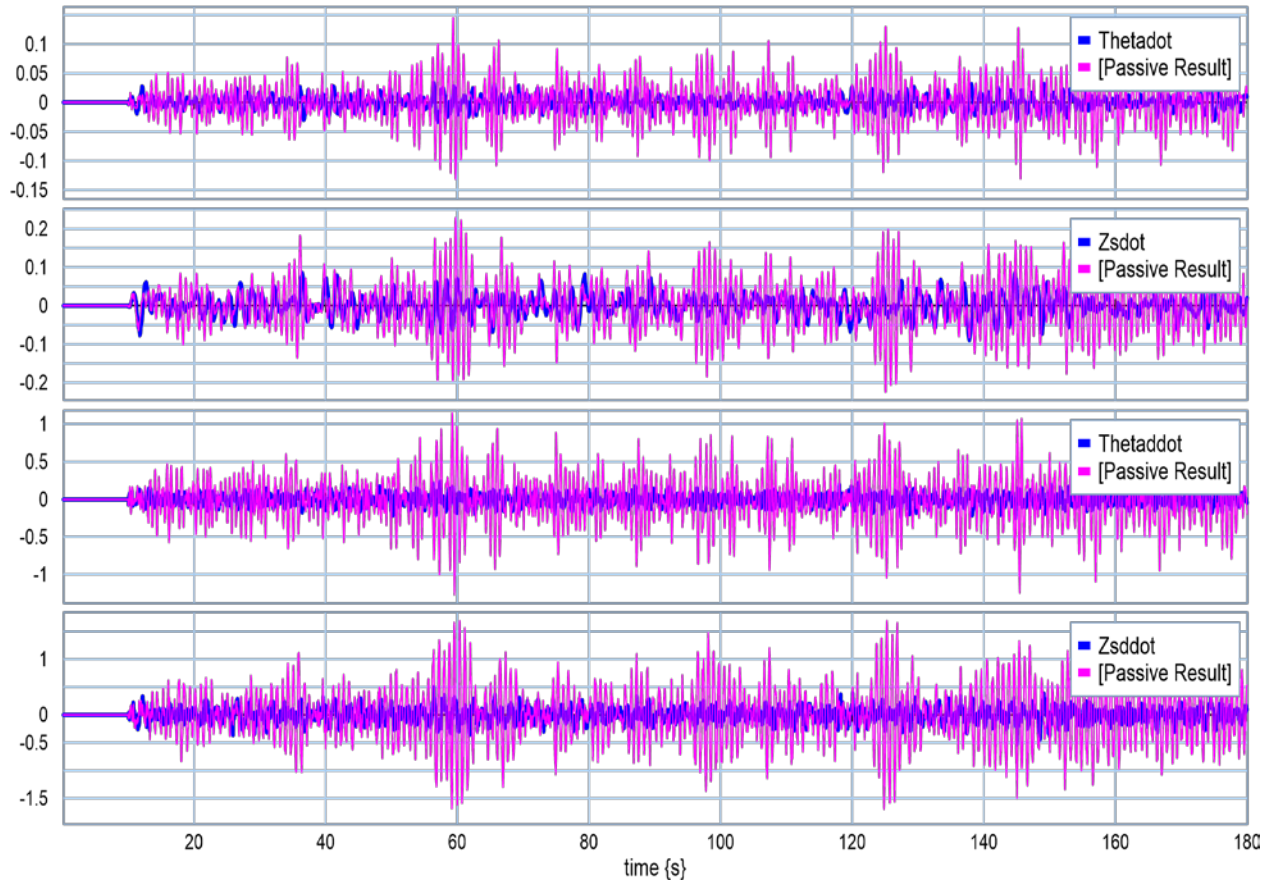


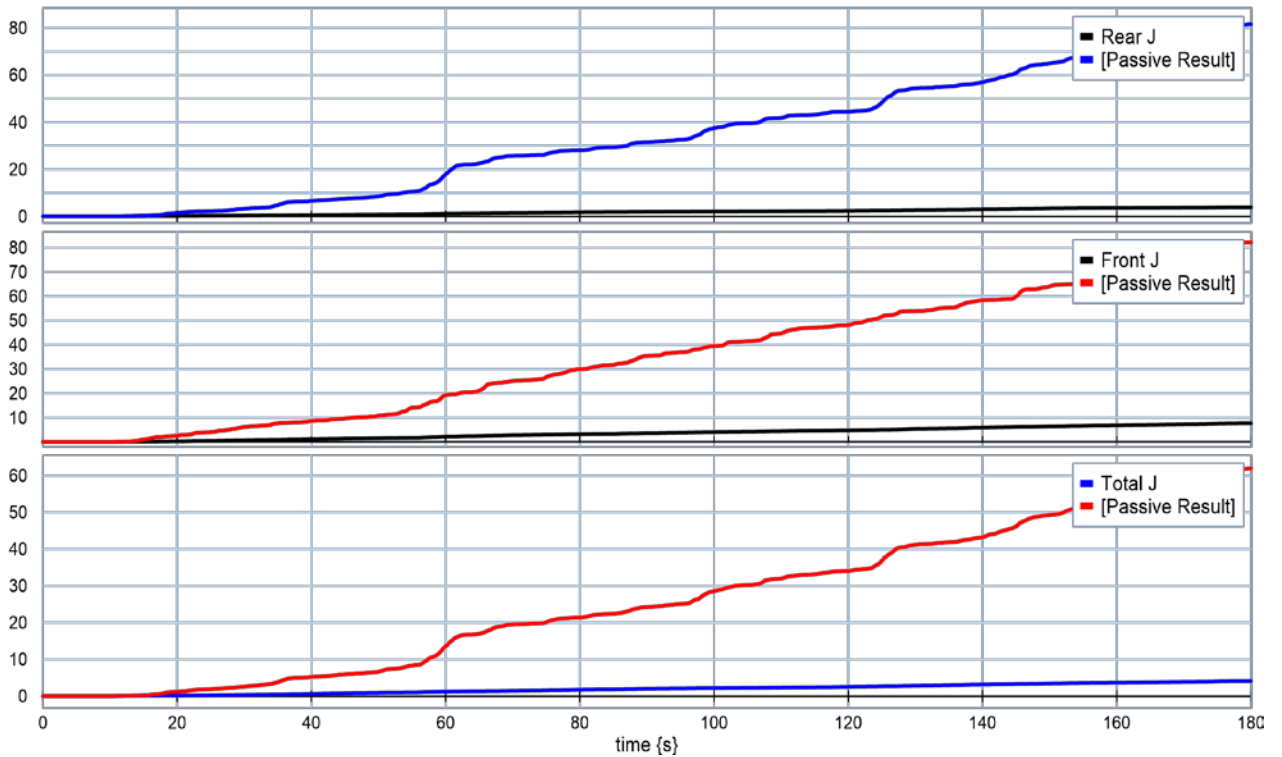
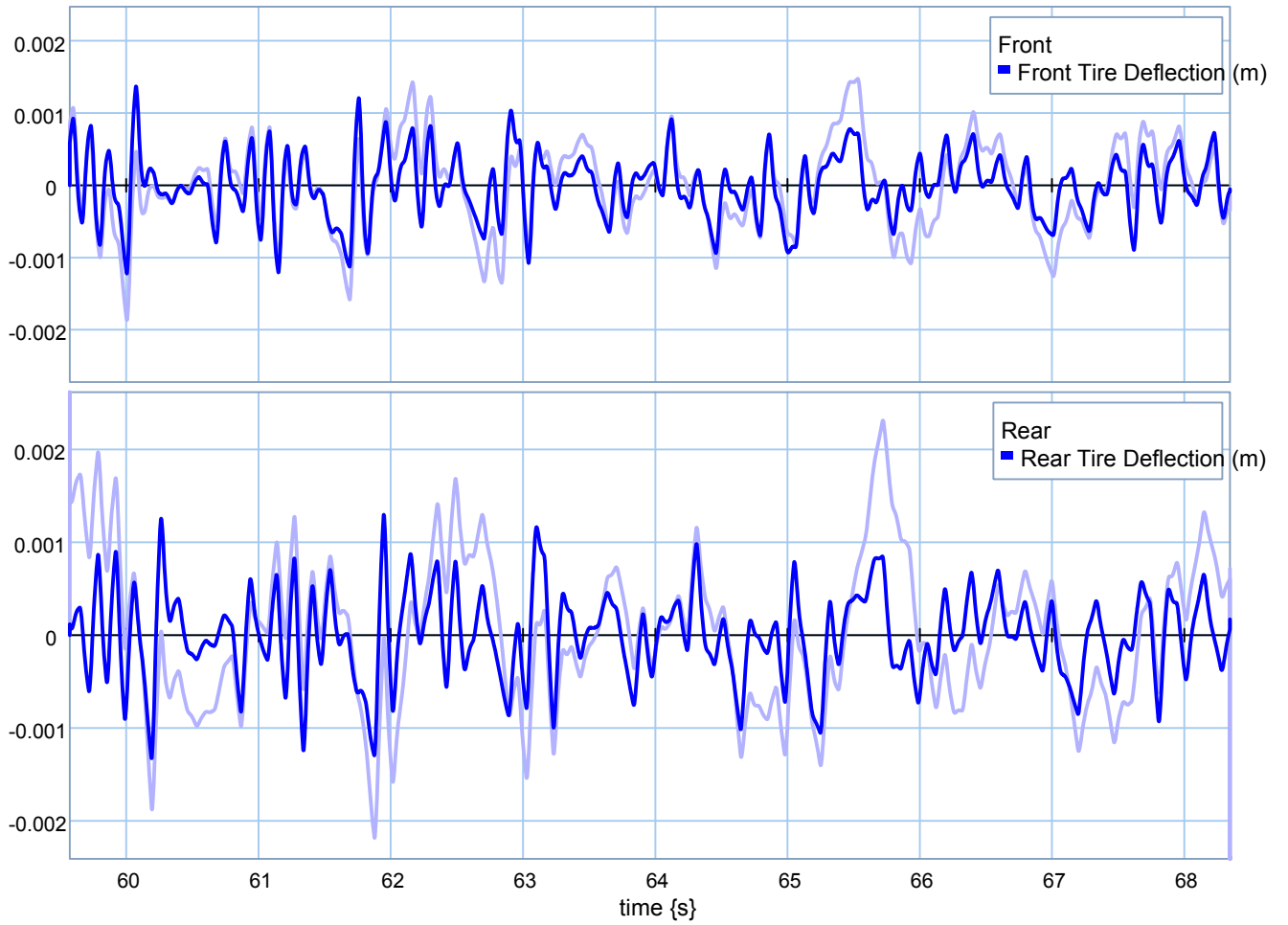


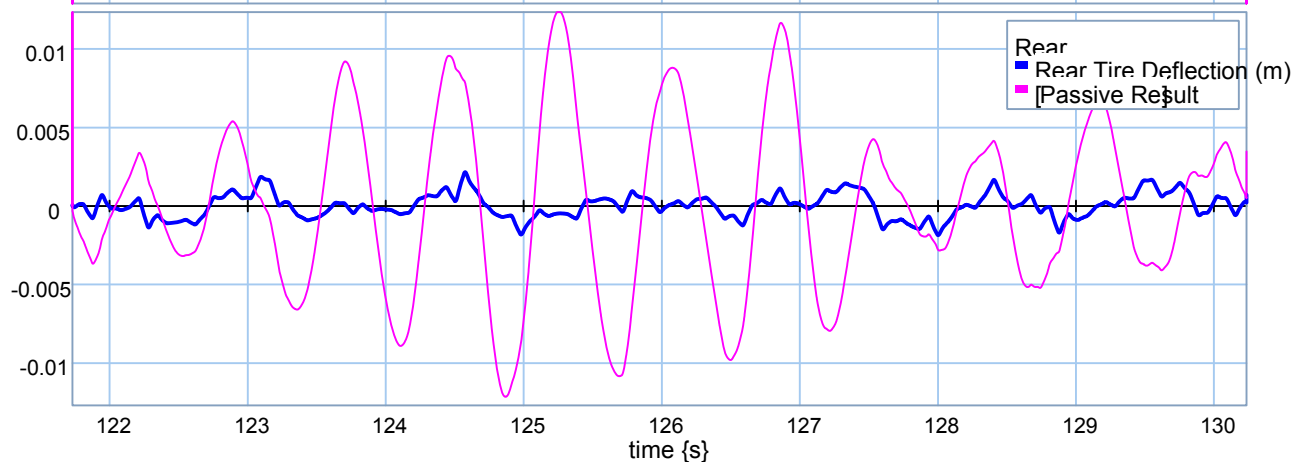
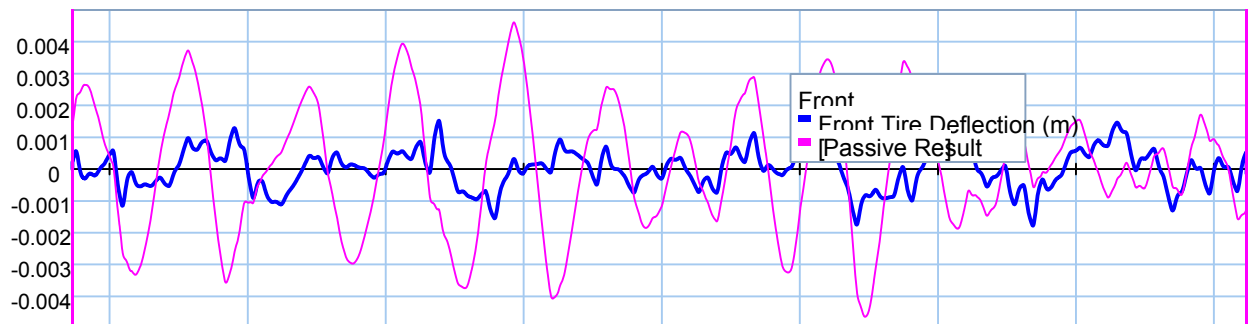
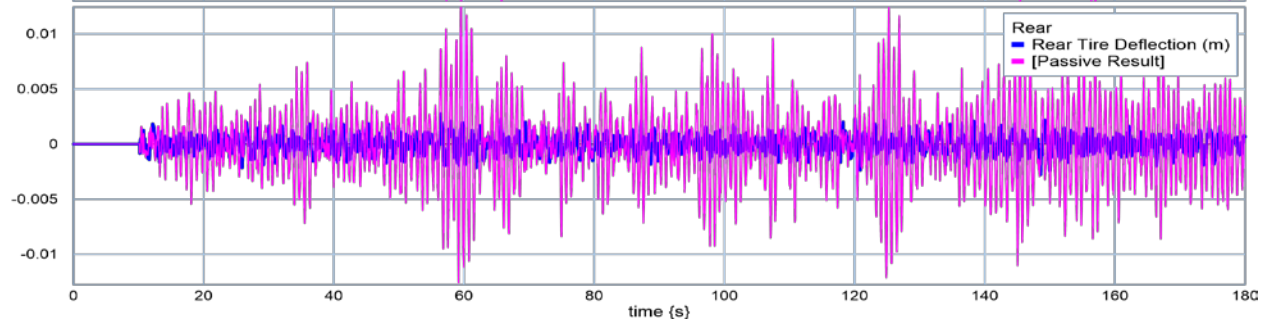
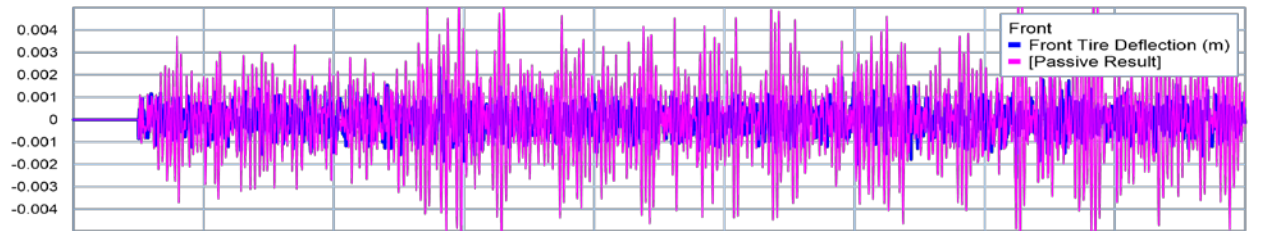
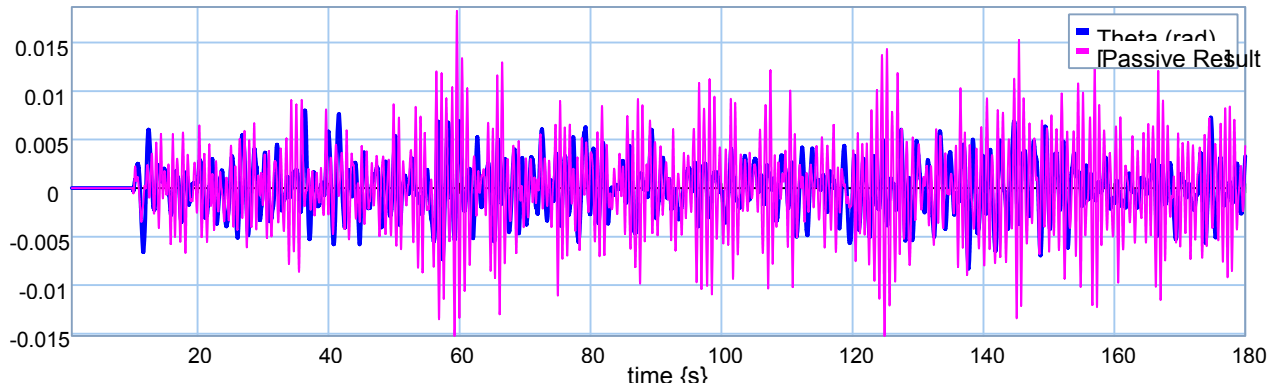


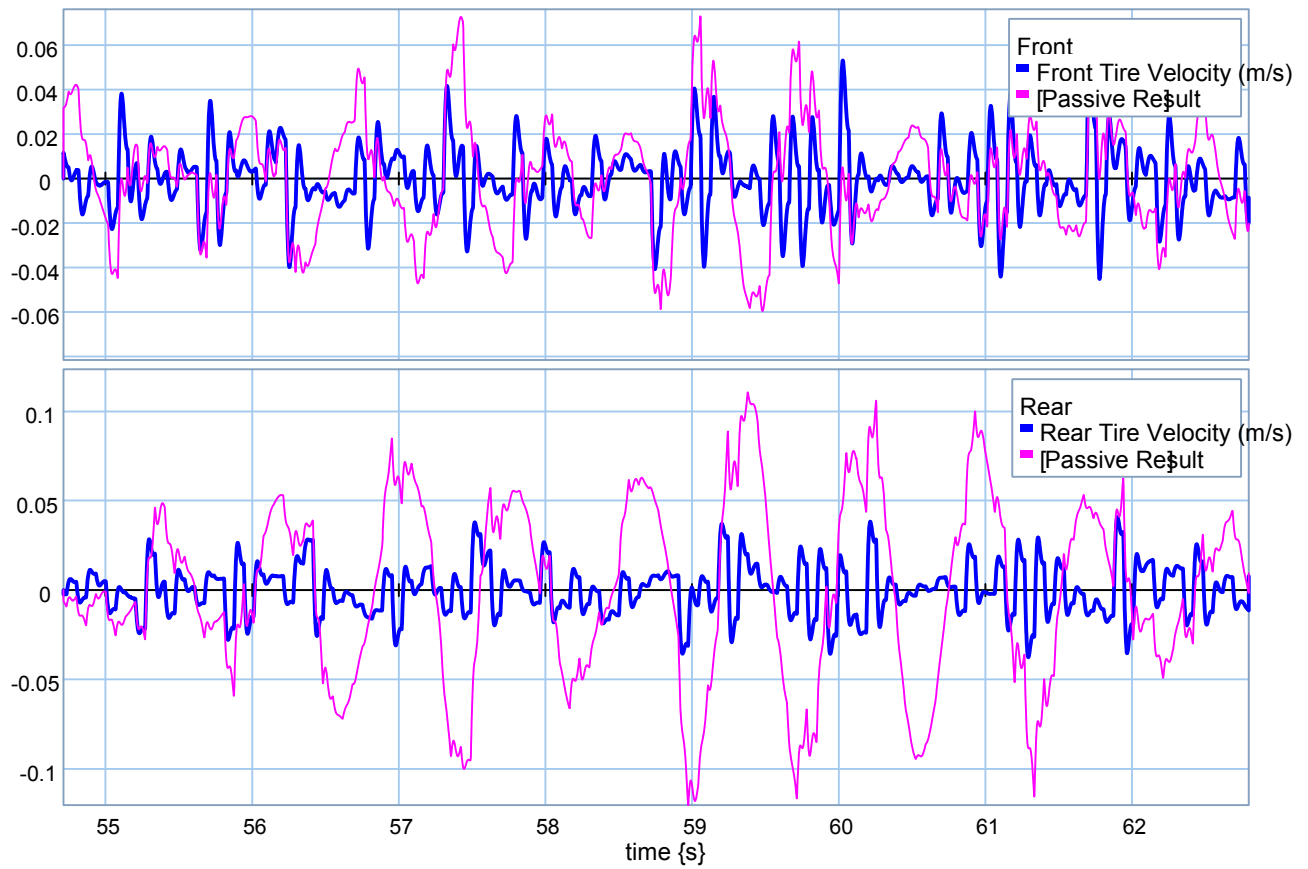
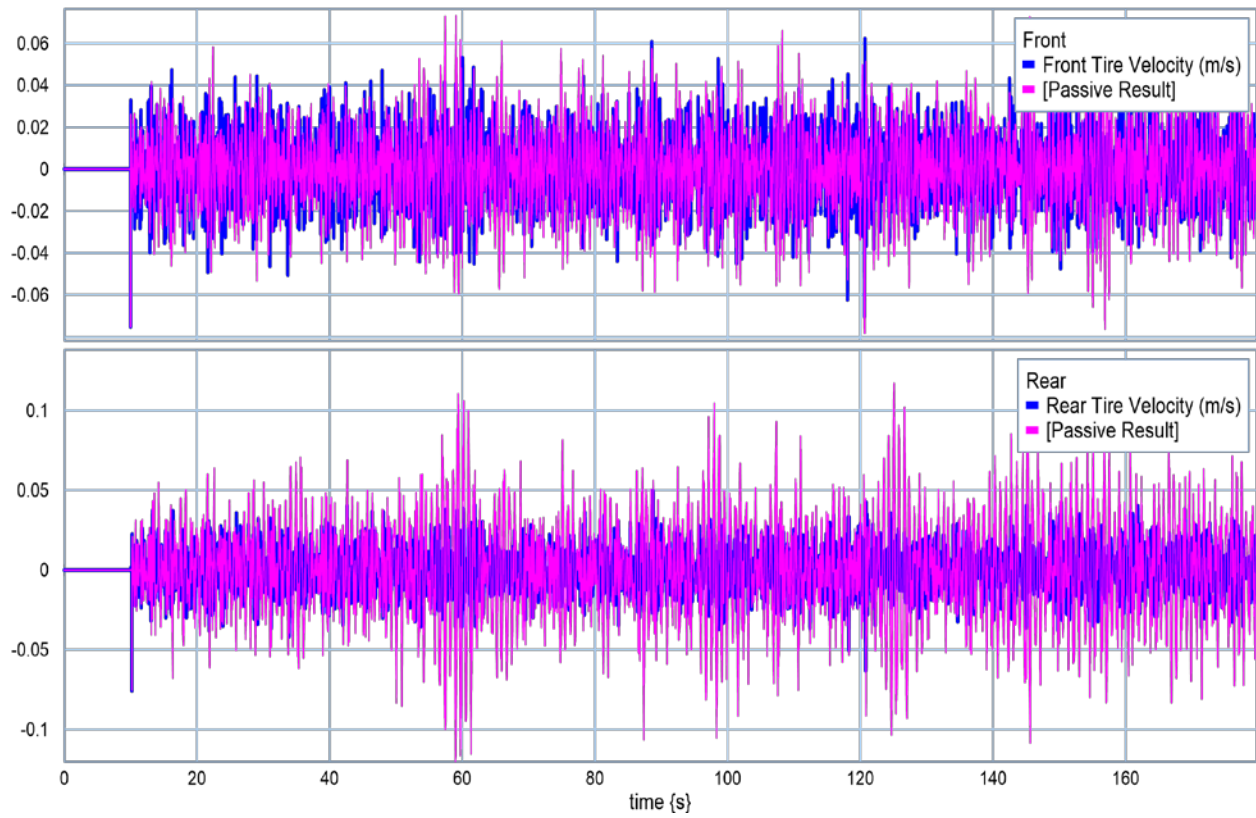


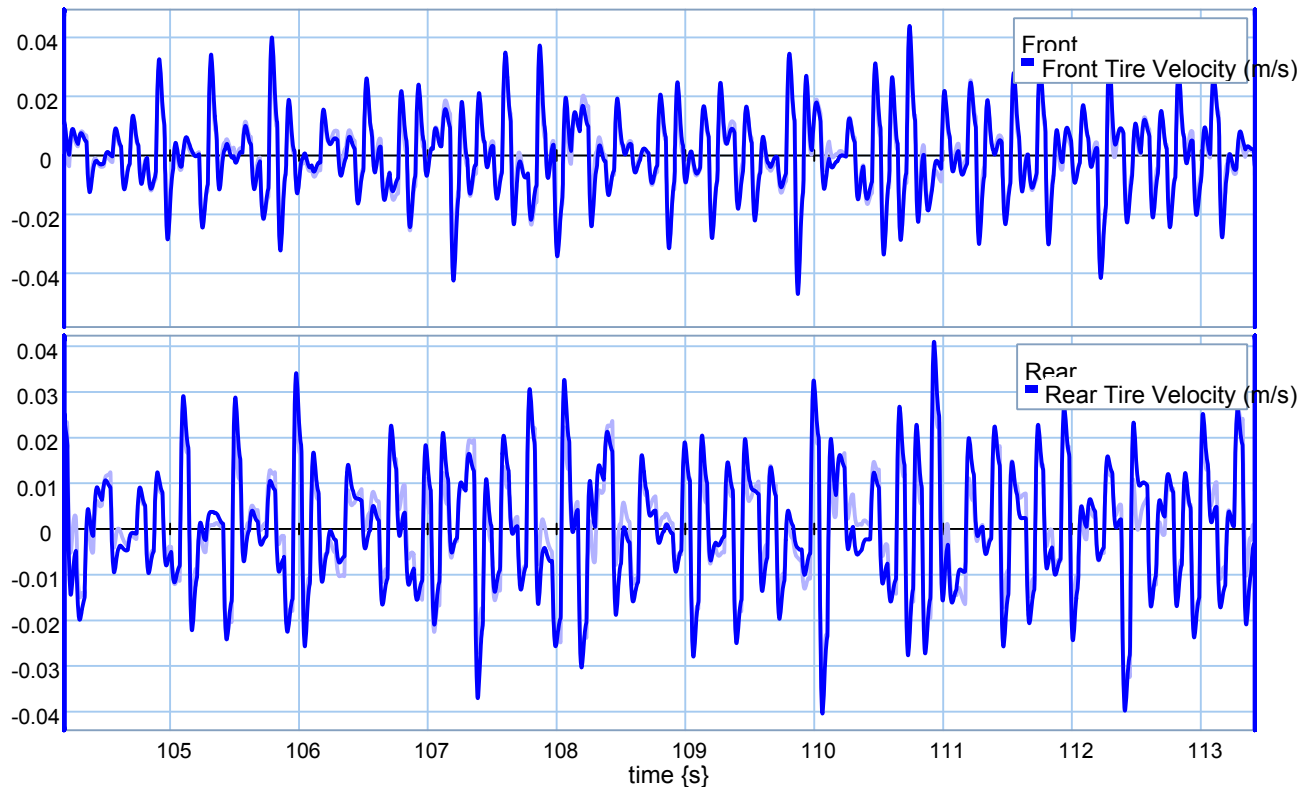
❖ $M_c = 13500 \text{ kg.}$



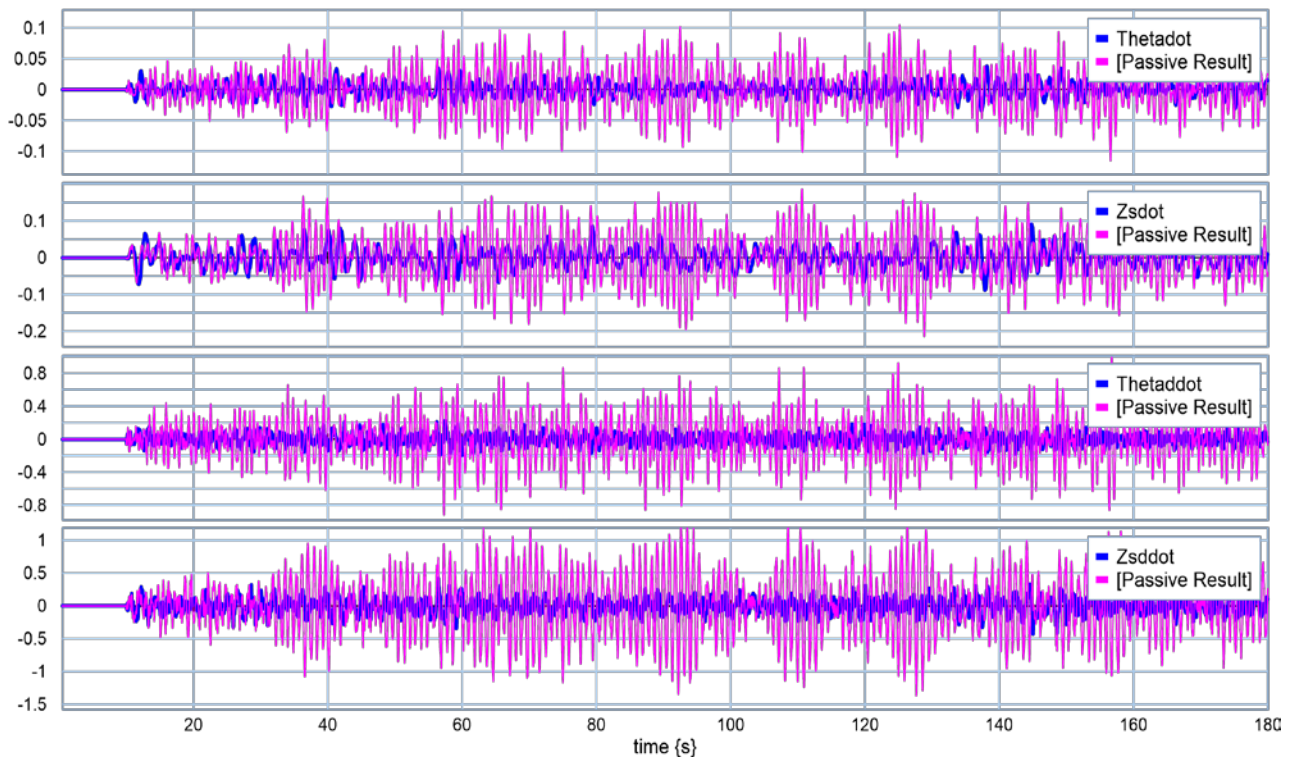


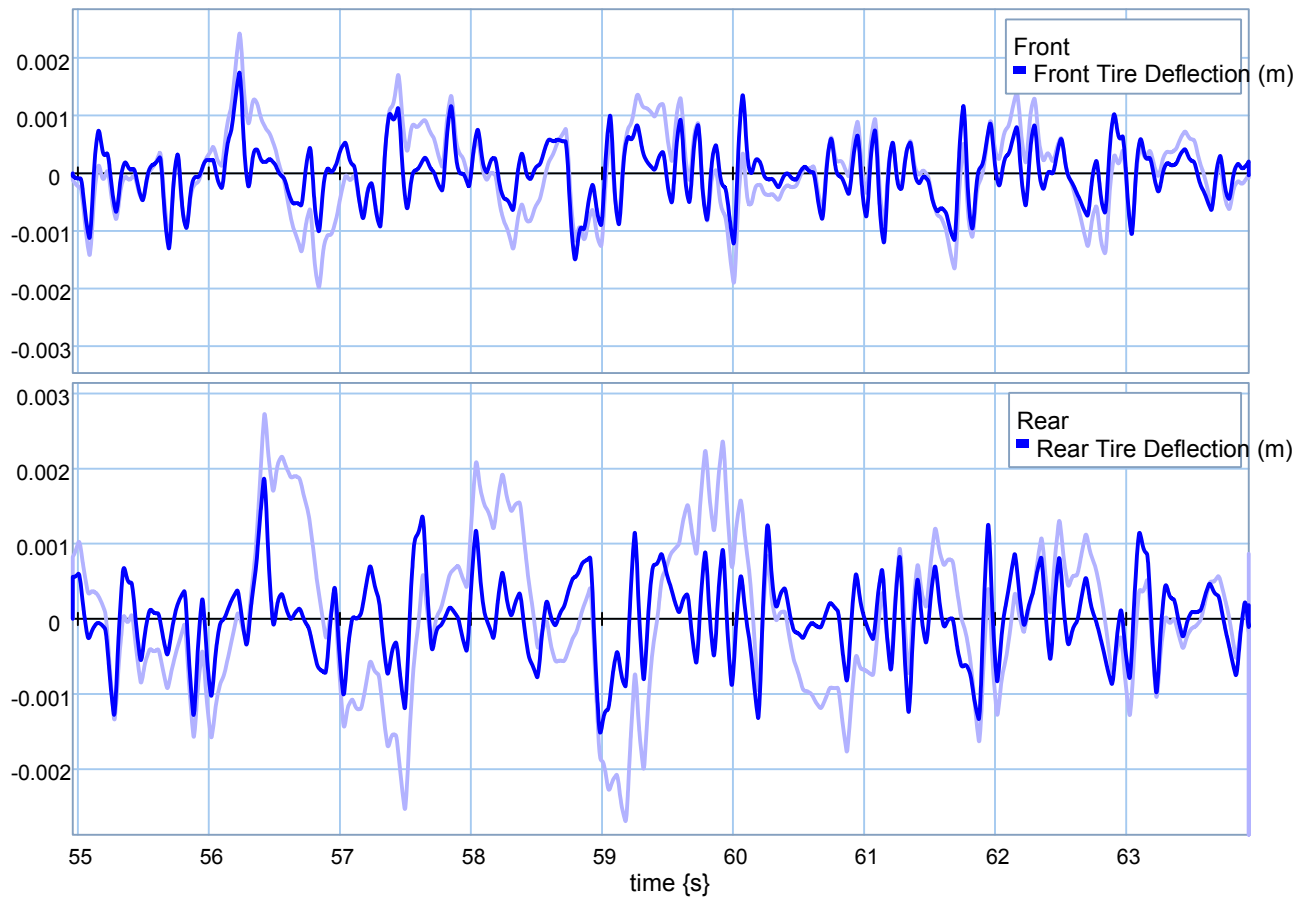
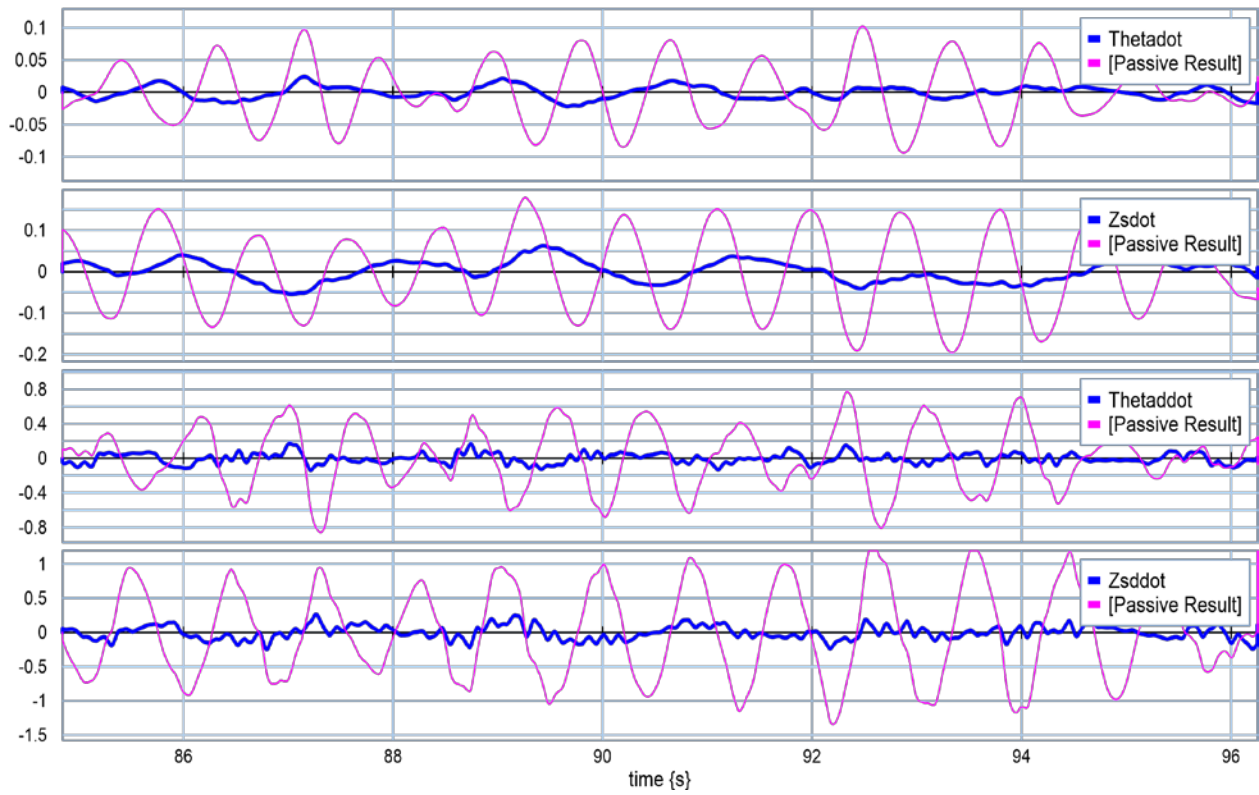


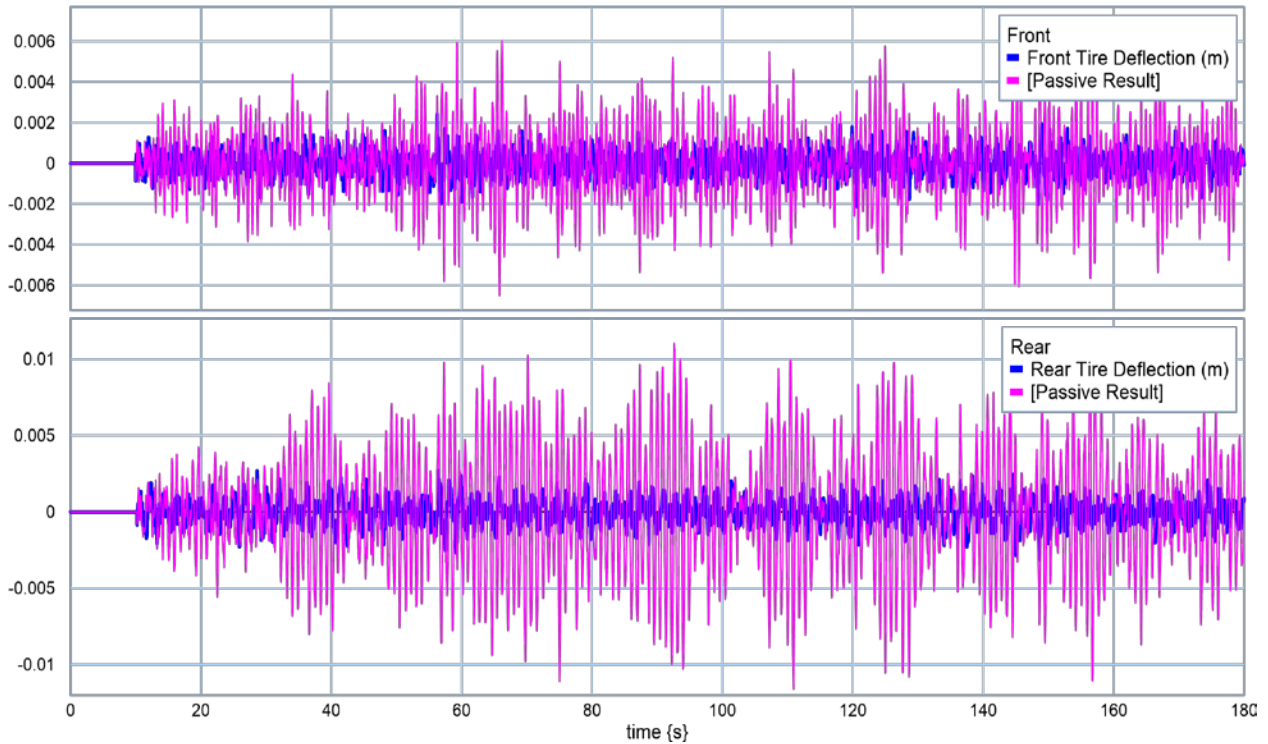
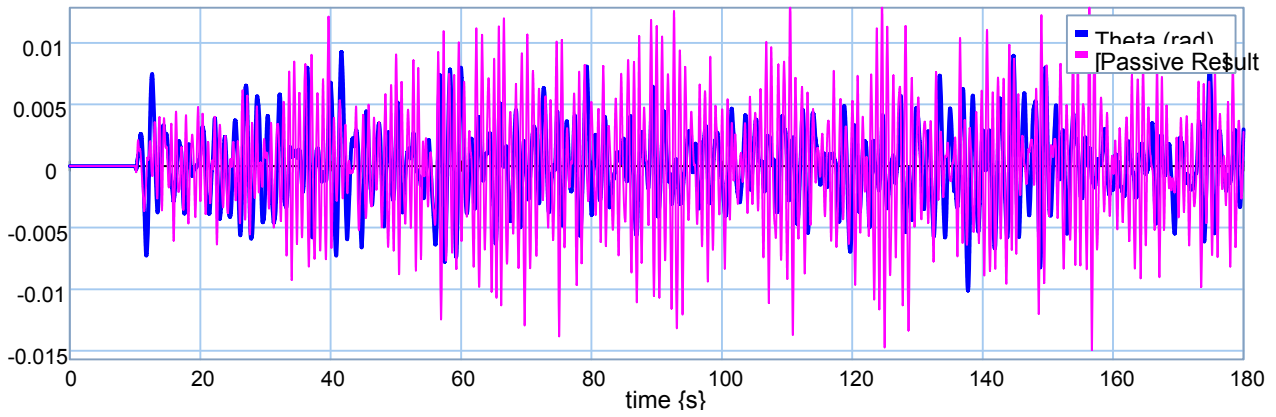
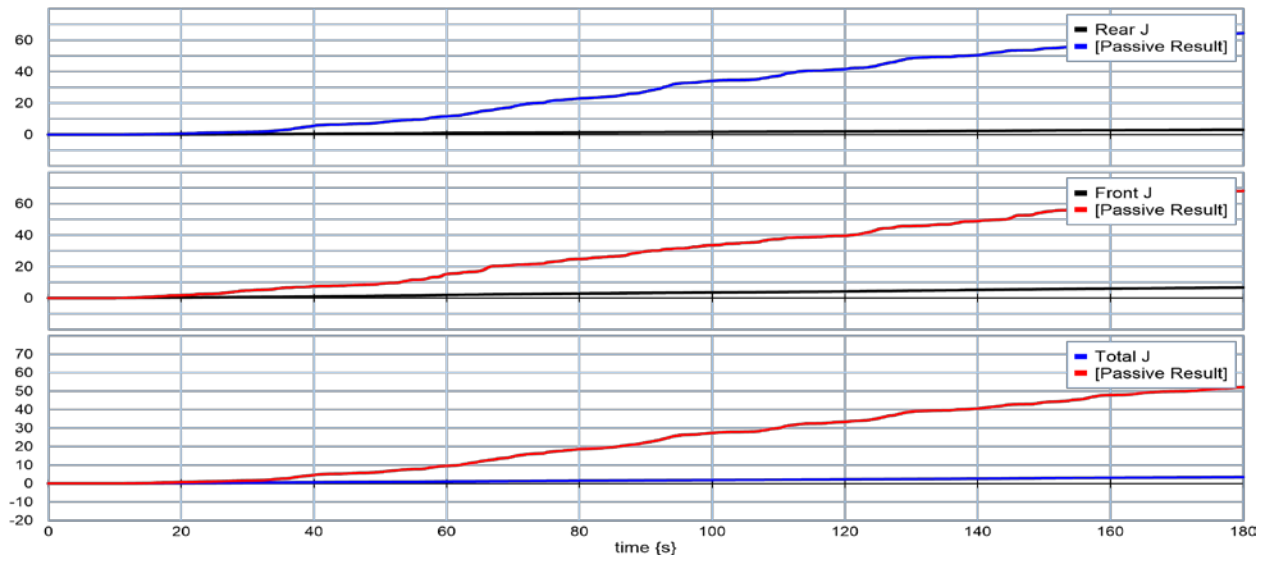


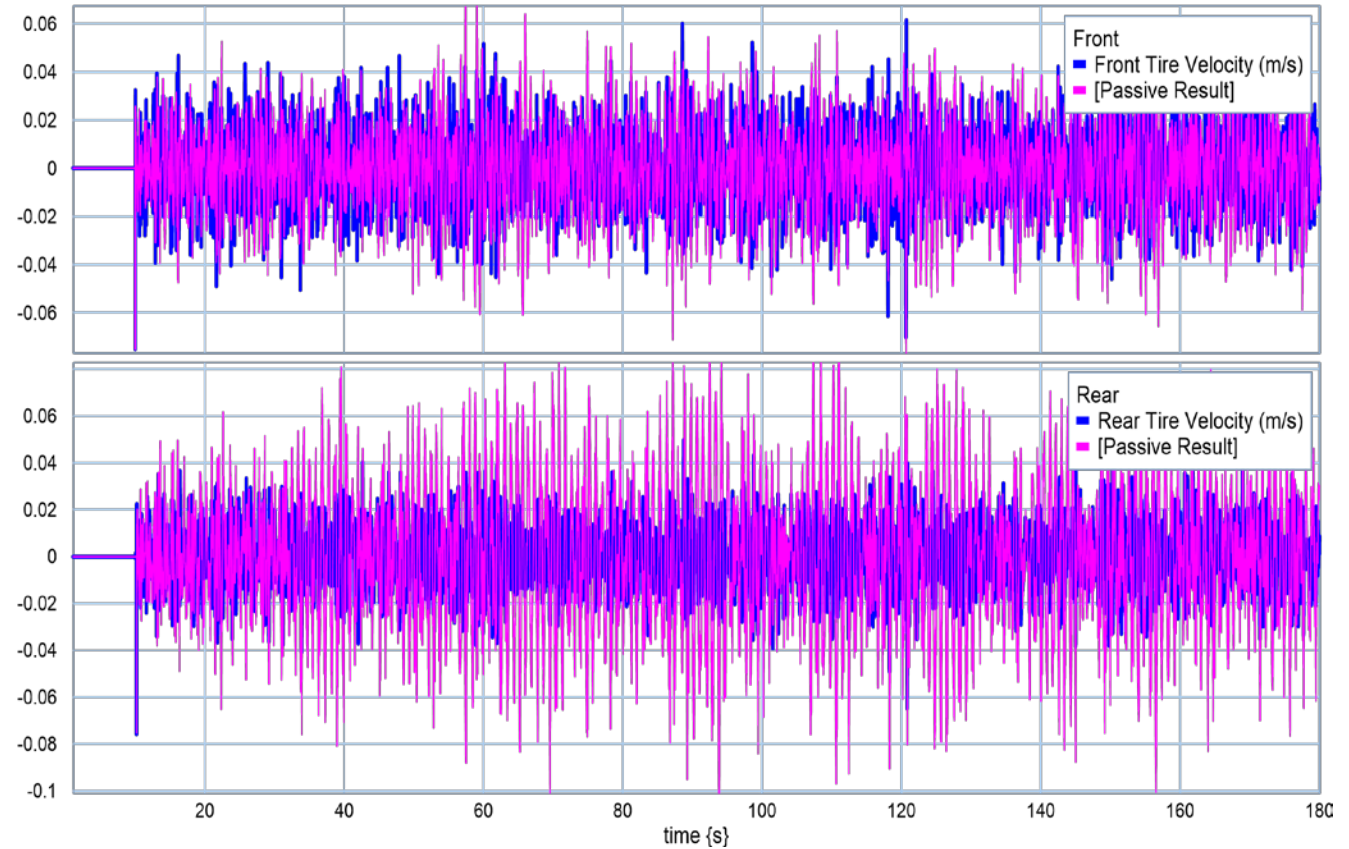
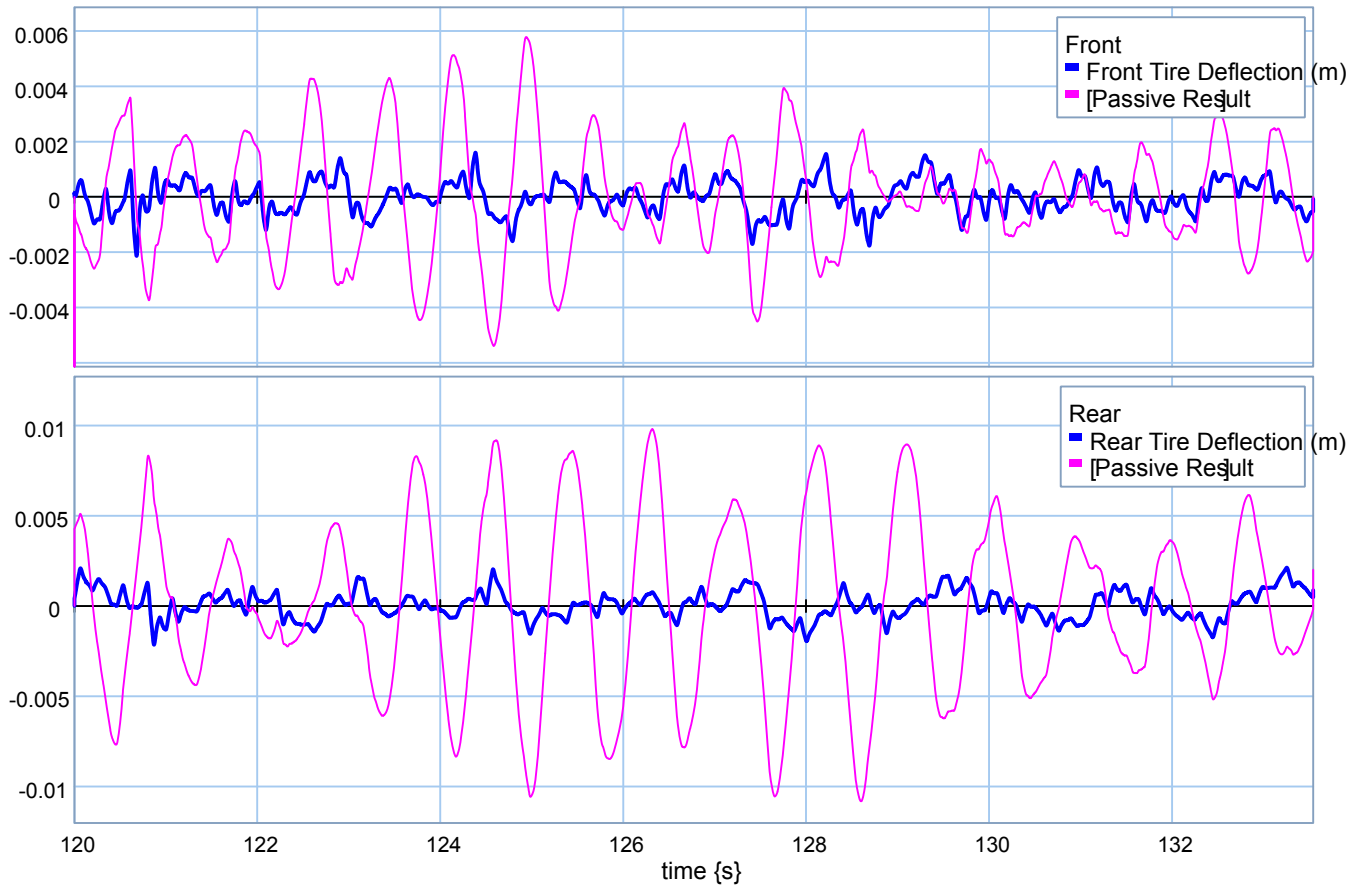


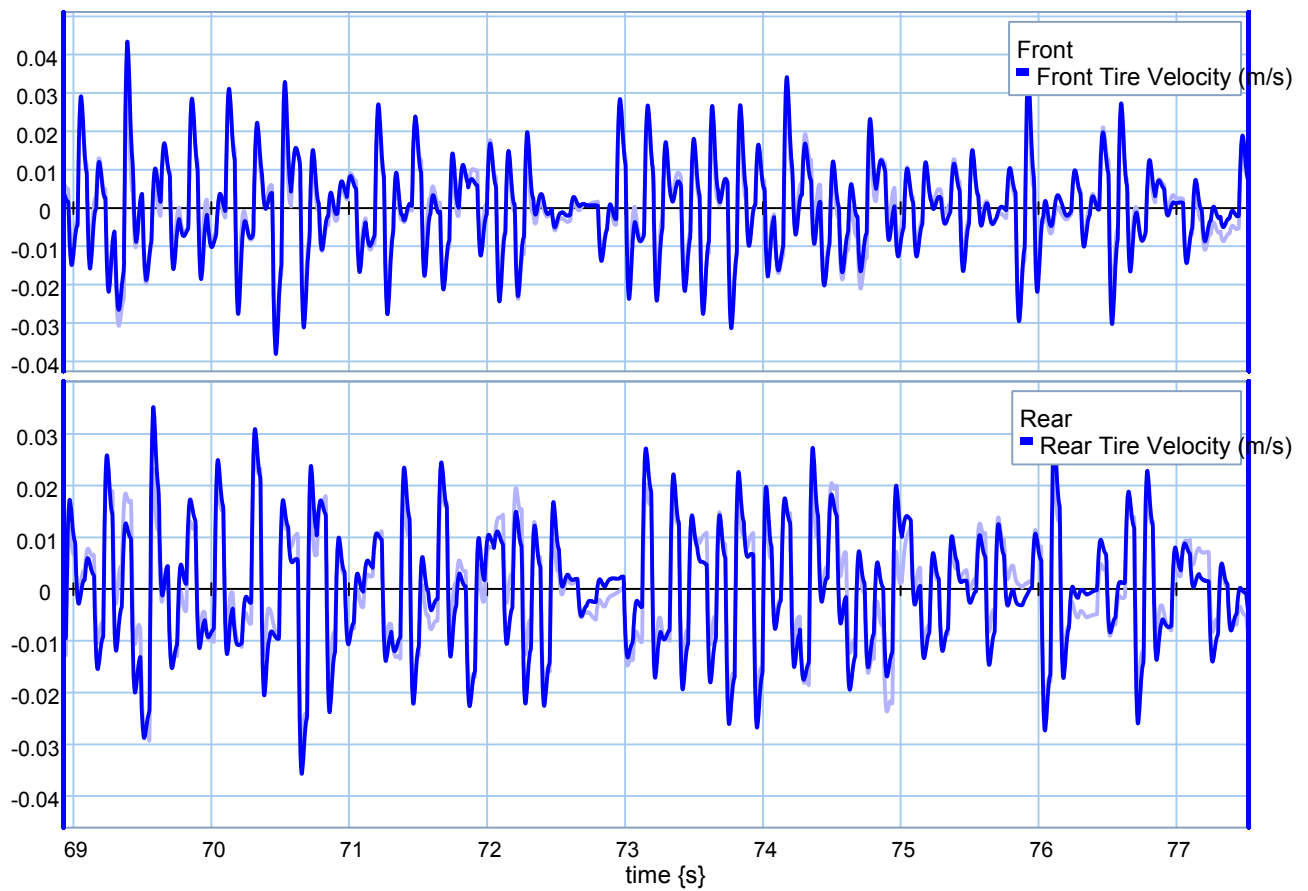
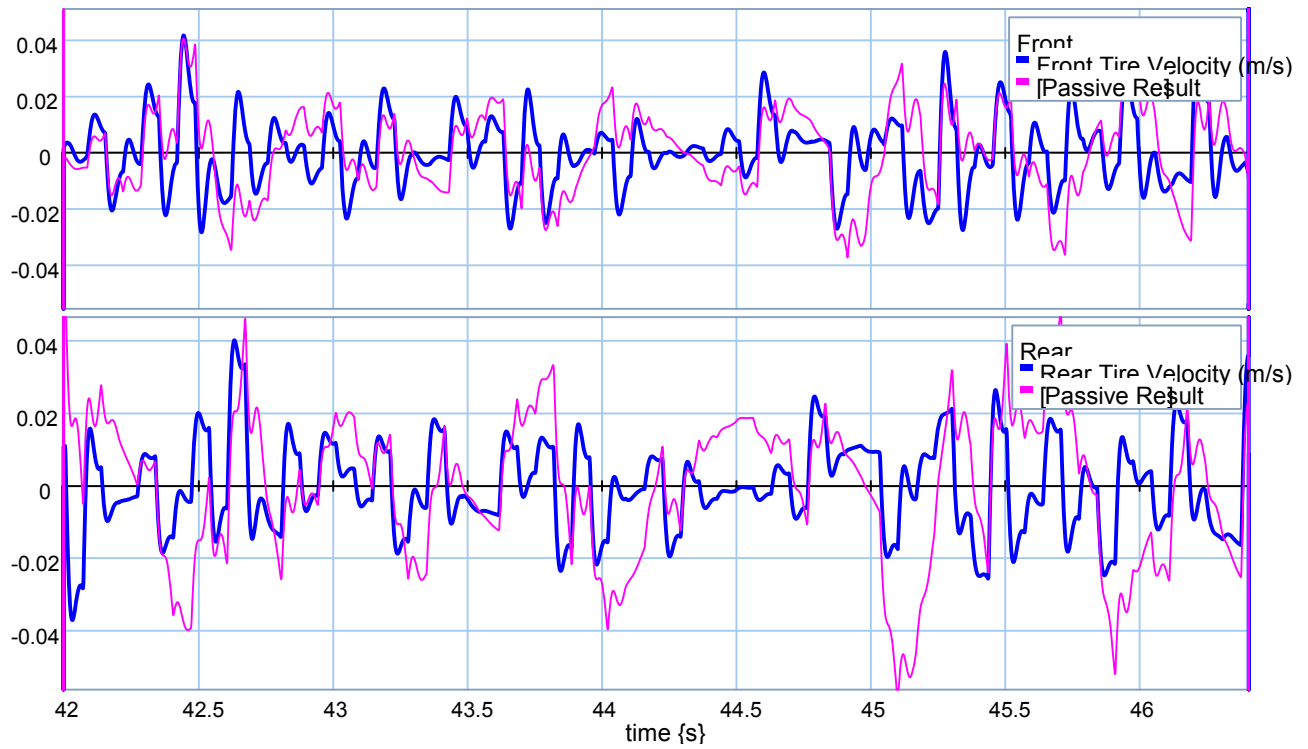
❖ **$M_c = 18000 \text{ kg.}$**





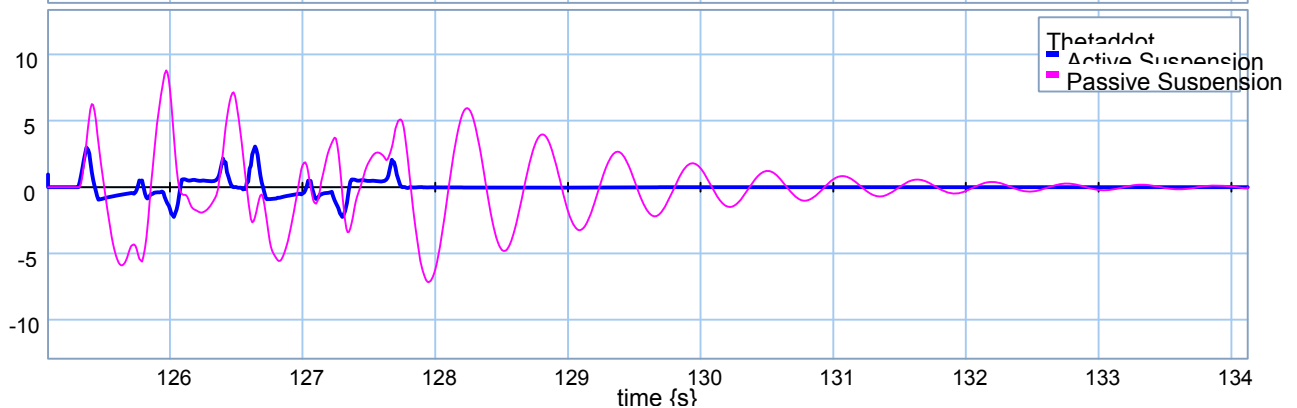
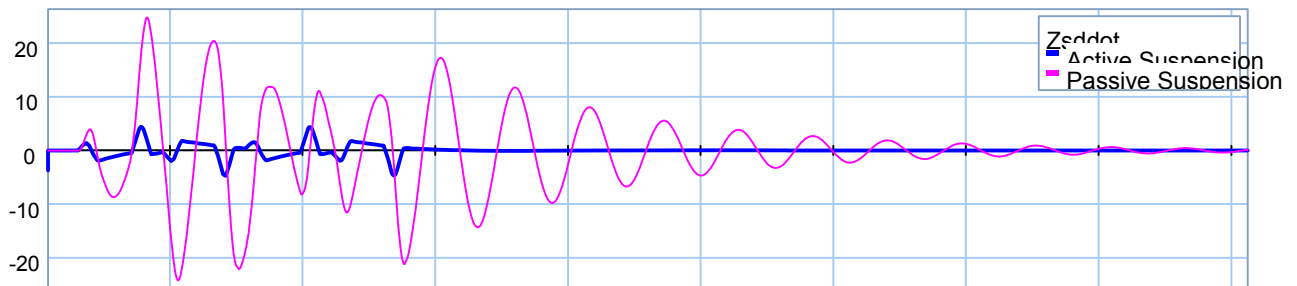
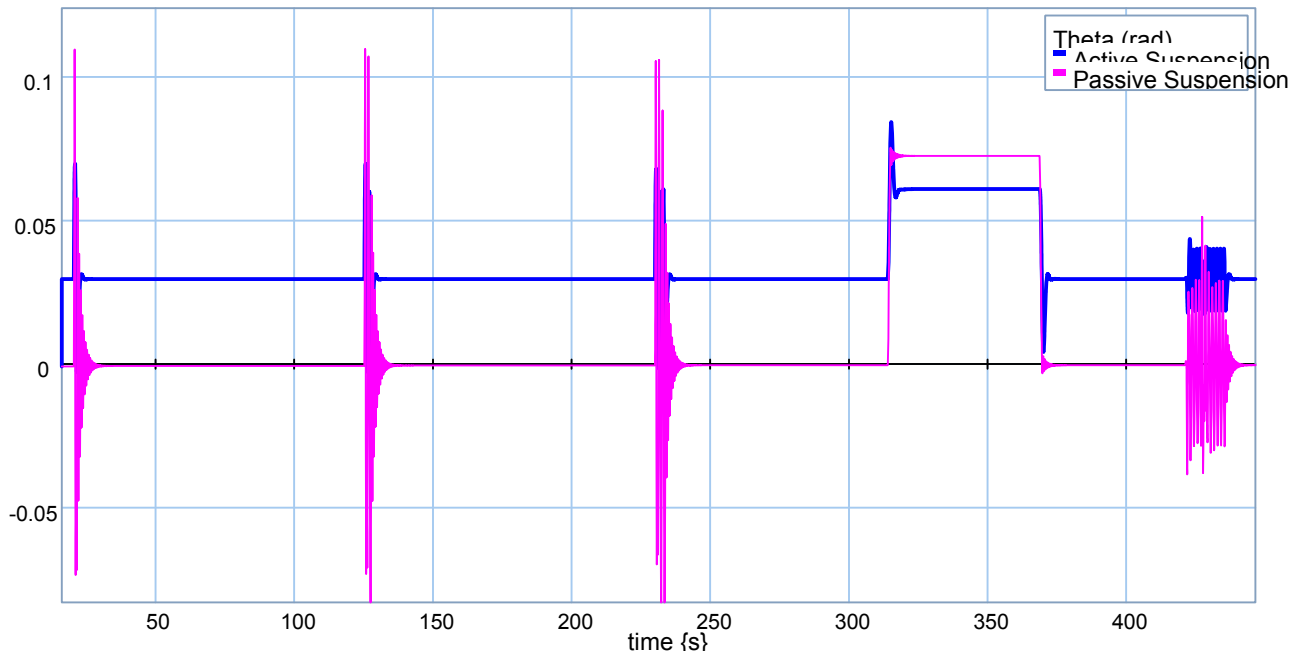


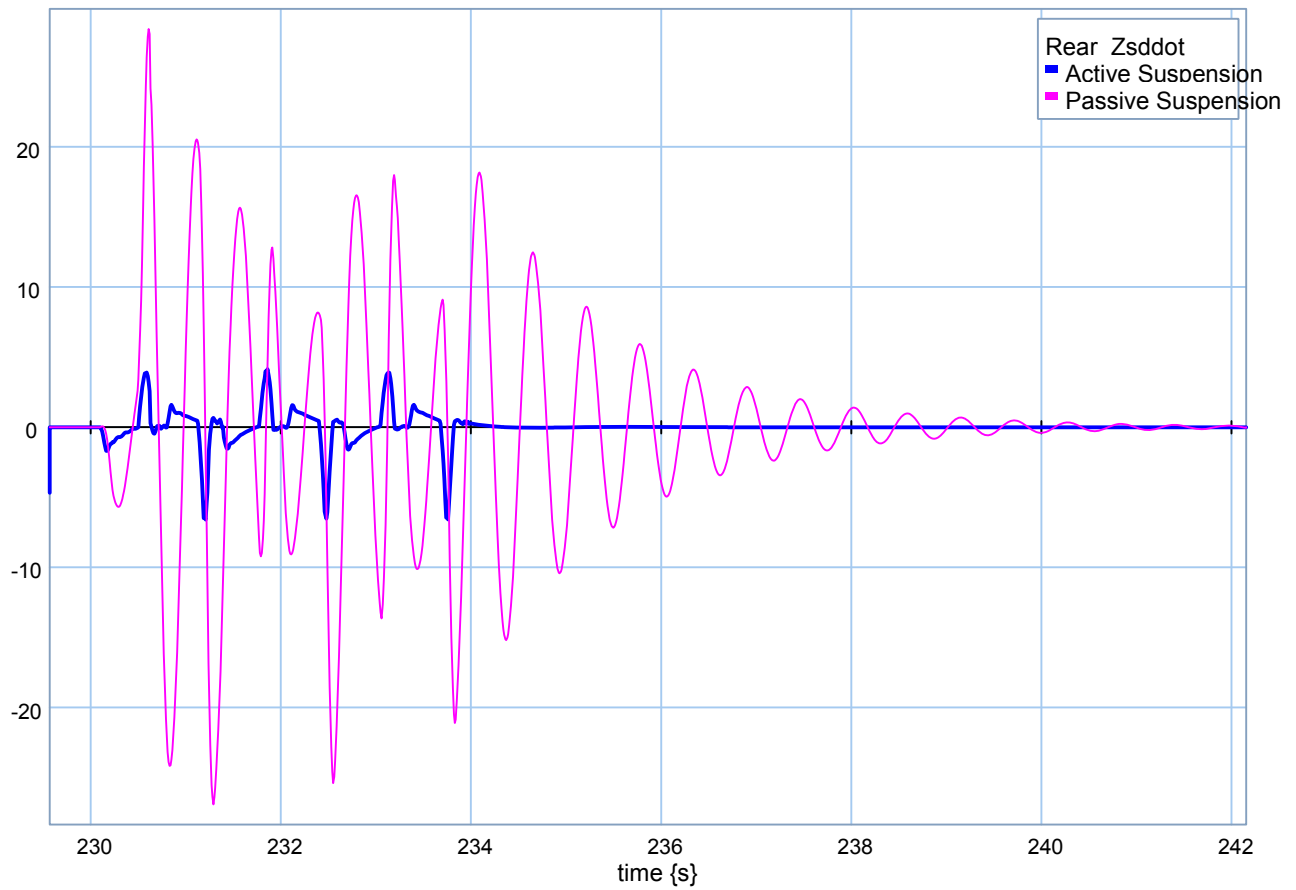
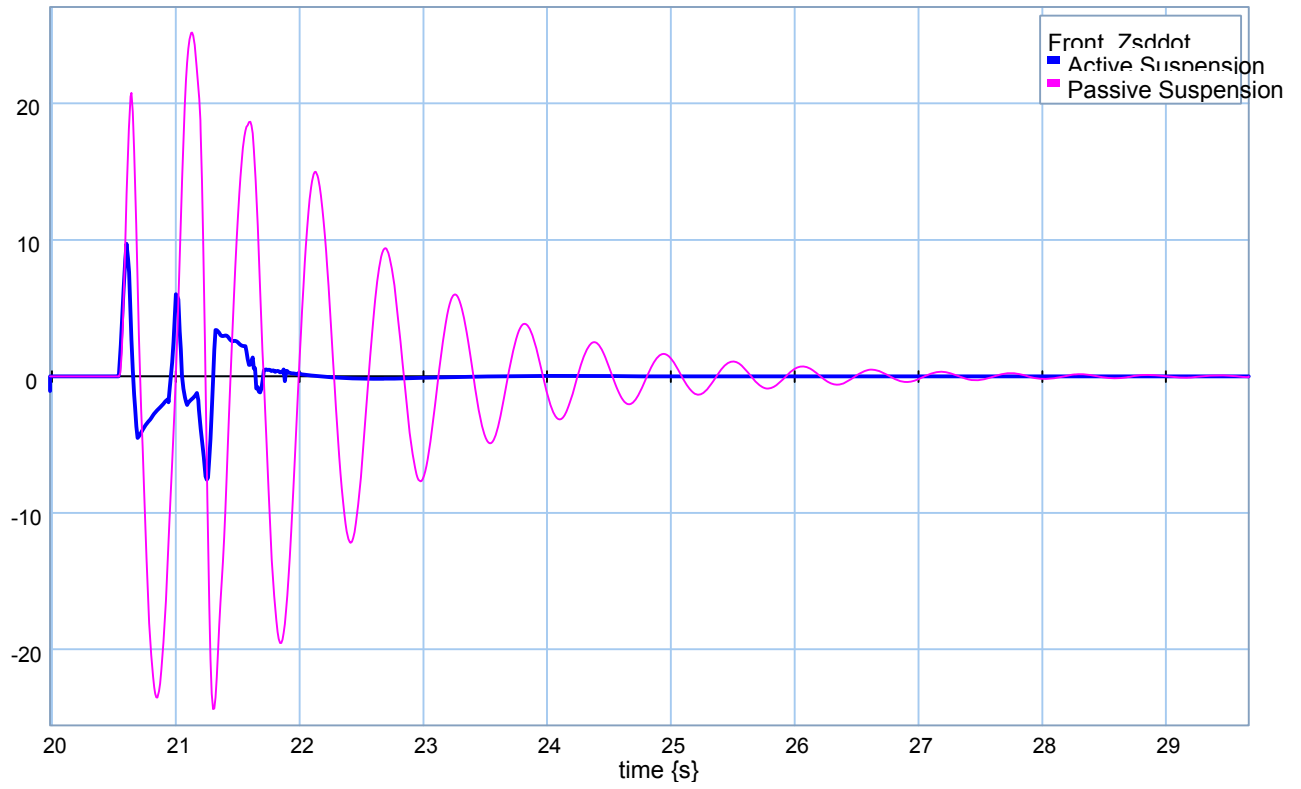




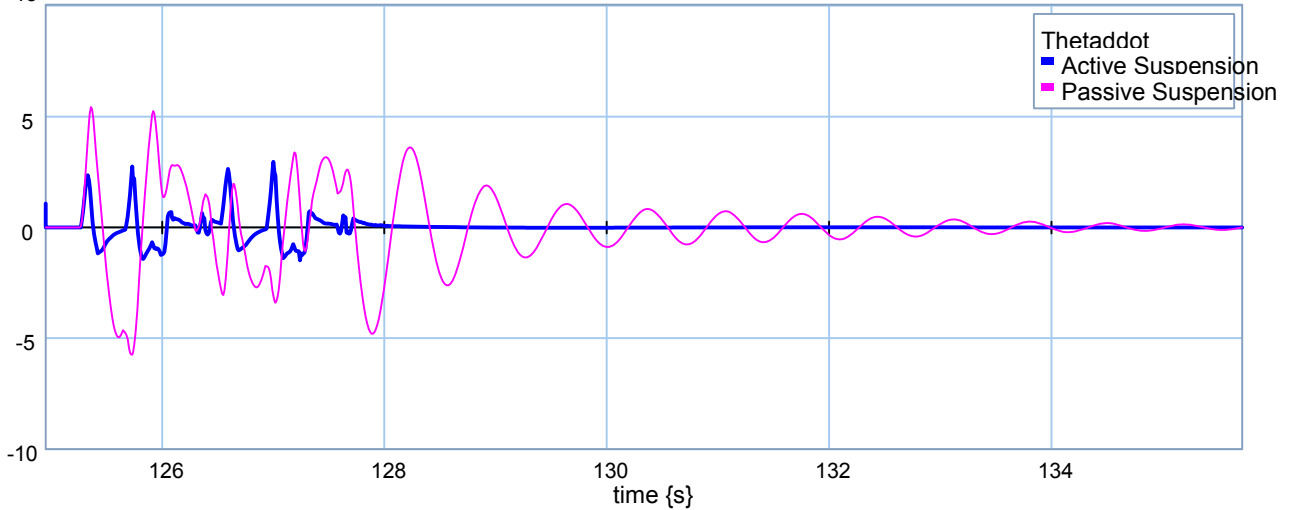
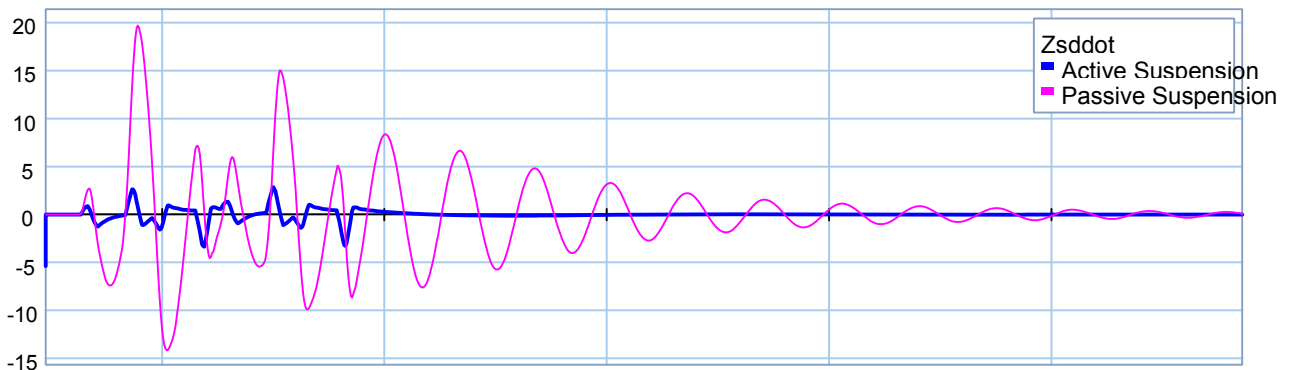
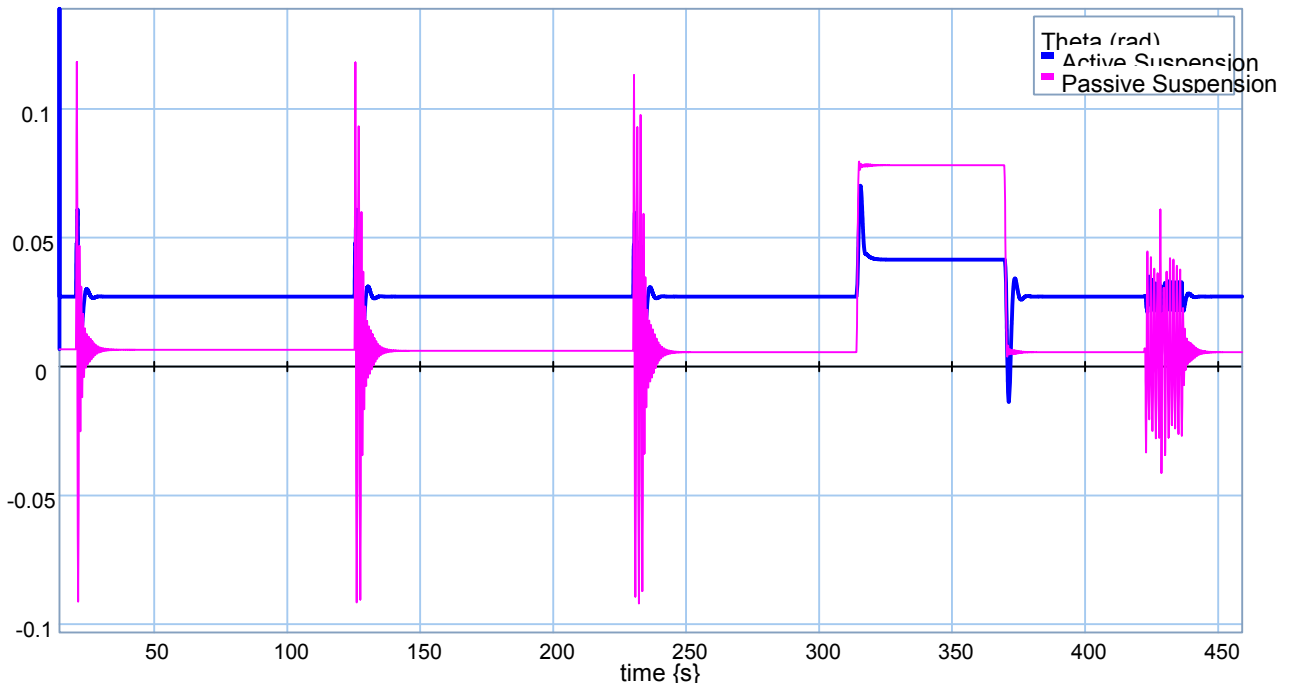
Appendix F: Non-Linear Half-Car Model, Ride Quality Scenario, Quarter-Car Active Suspensions.

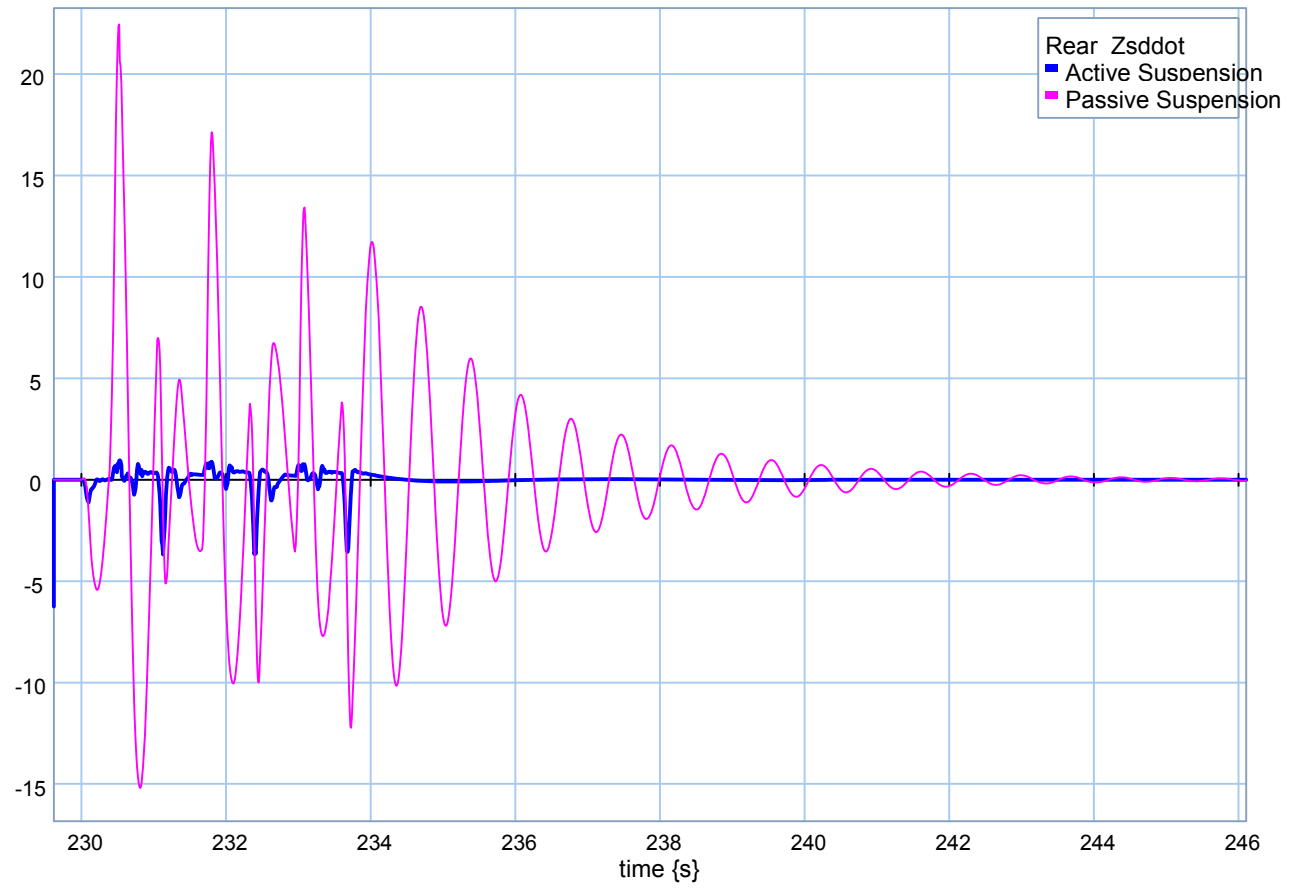
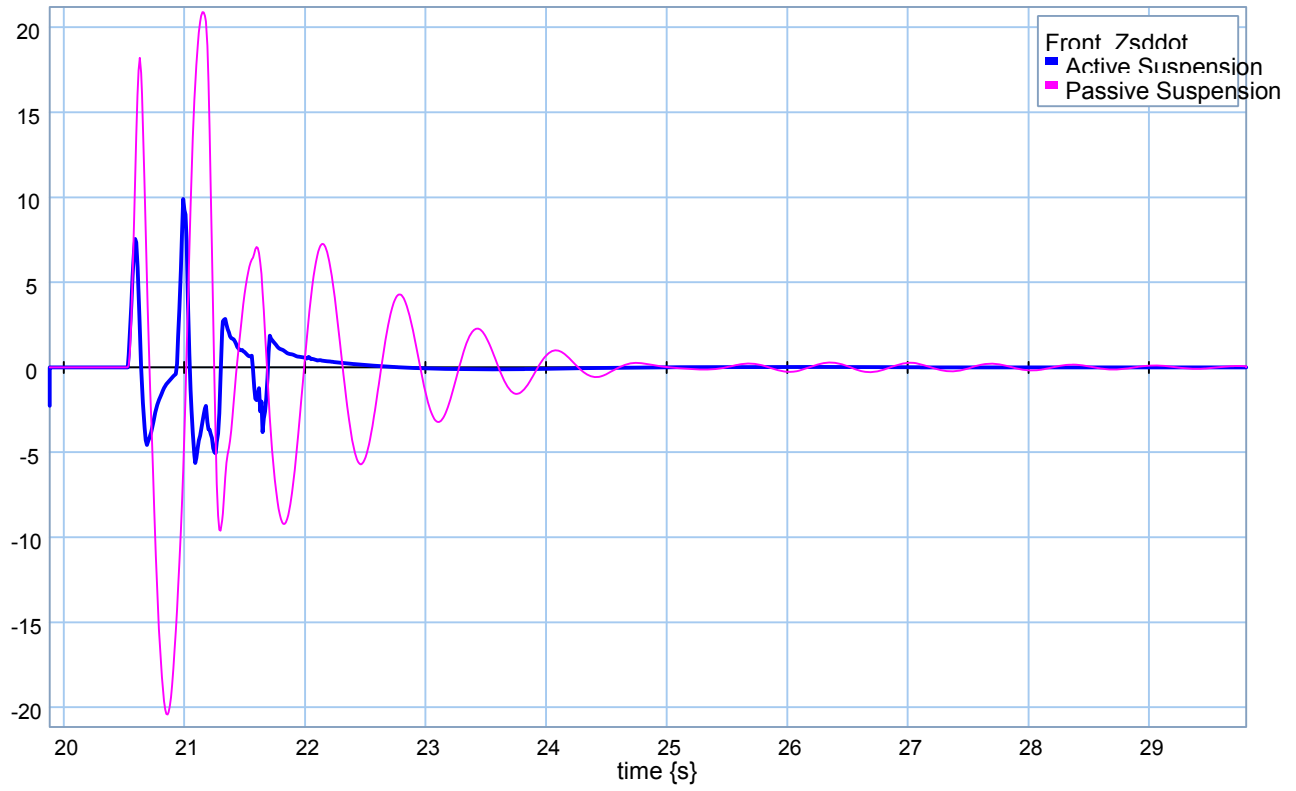
❖ $M_c = 4500 \text{ kg}$.



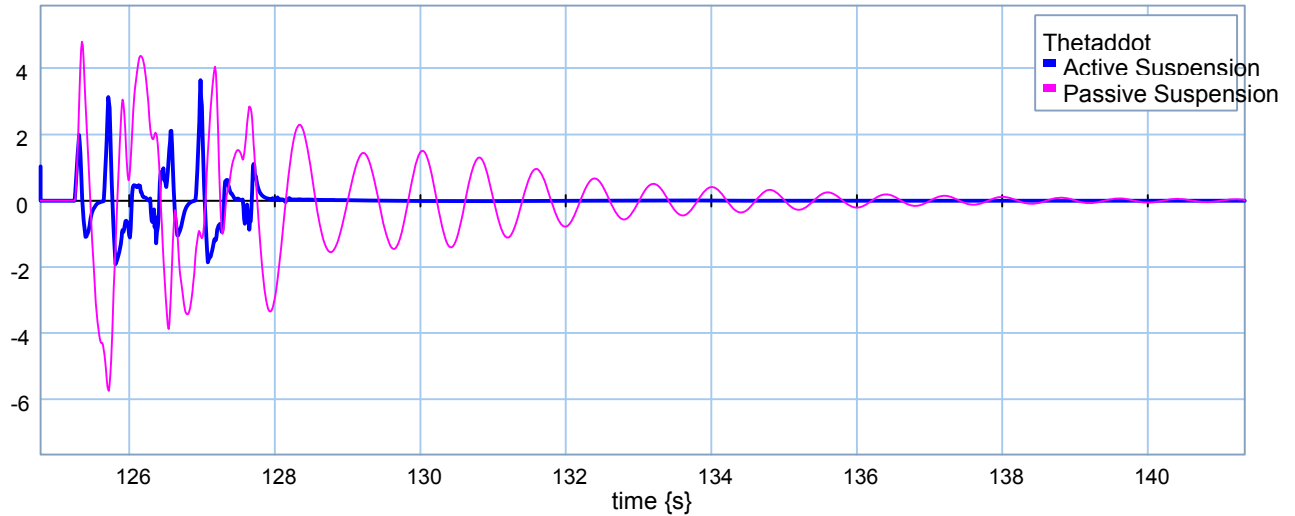
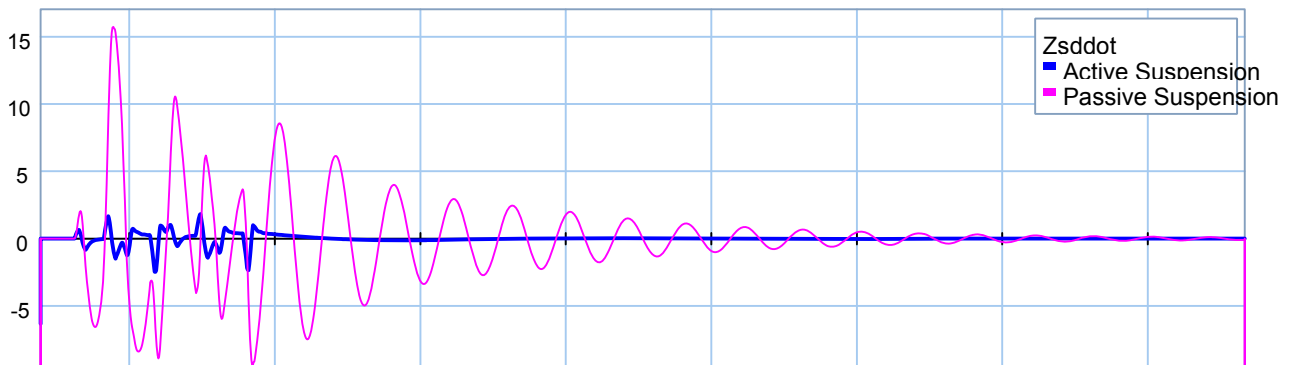
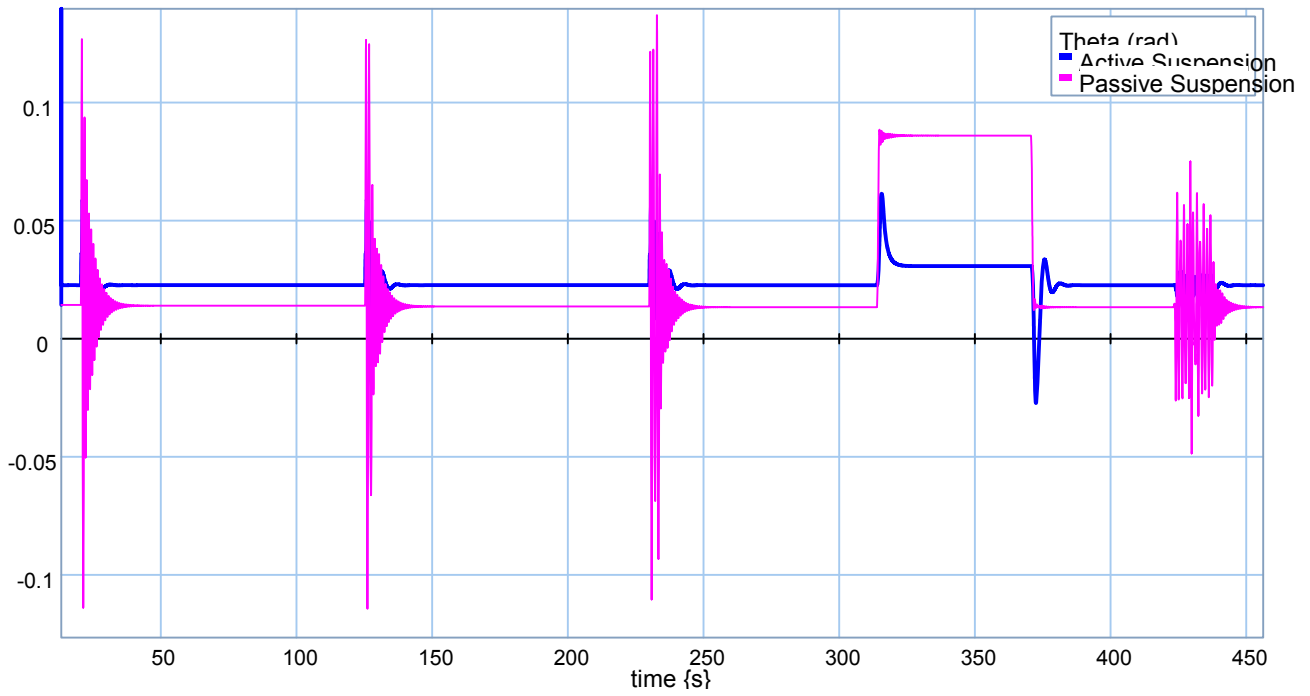


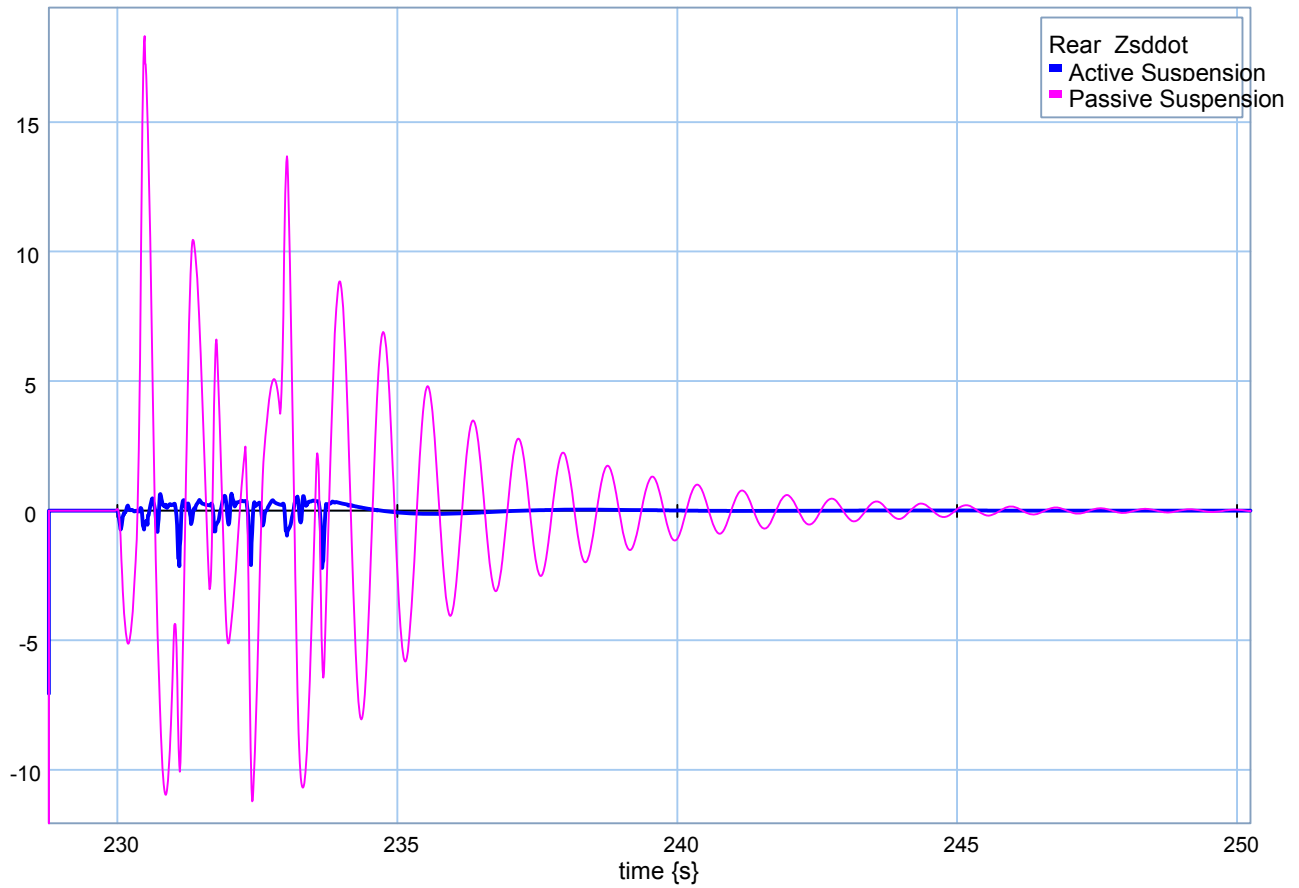
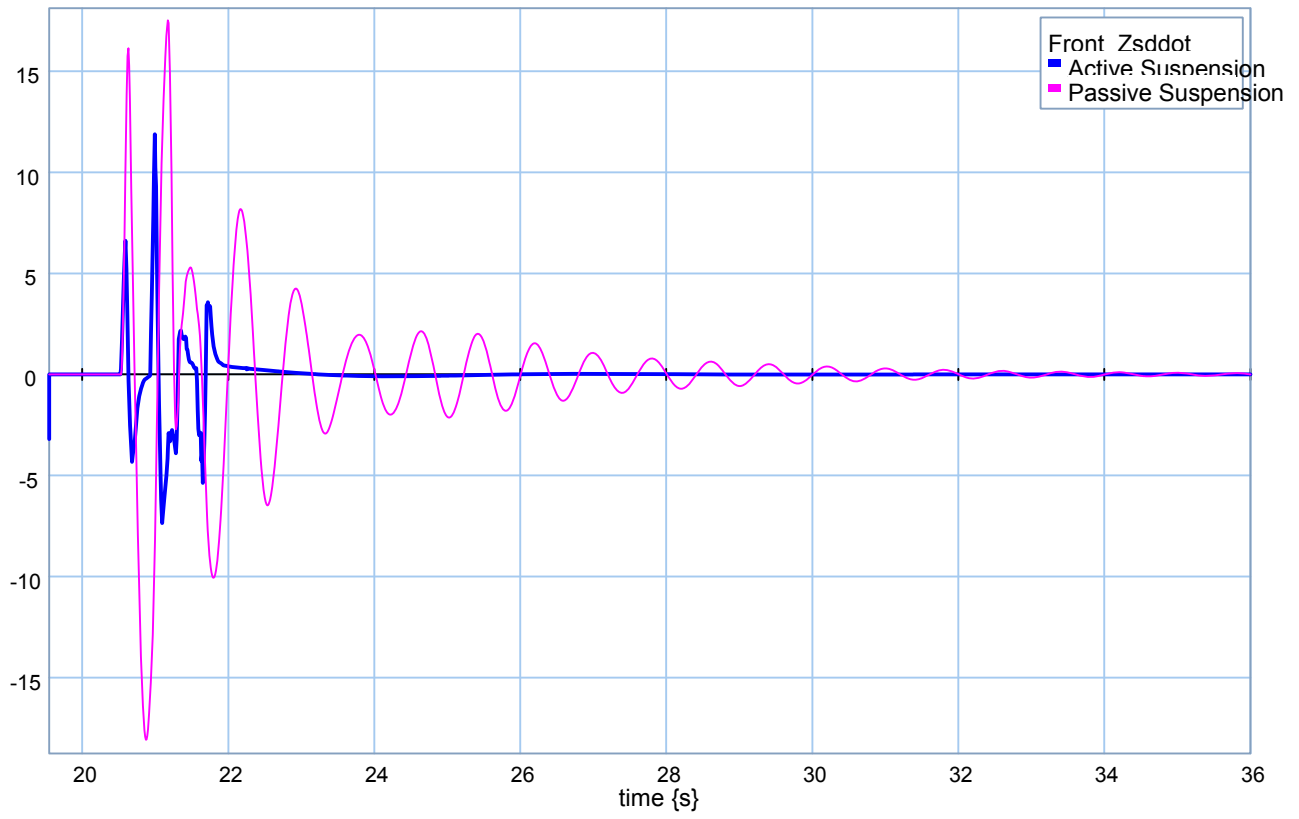
❖ **$M_c = 9000 \text{ kg.}$**



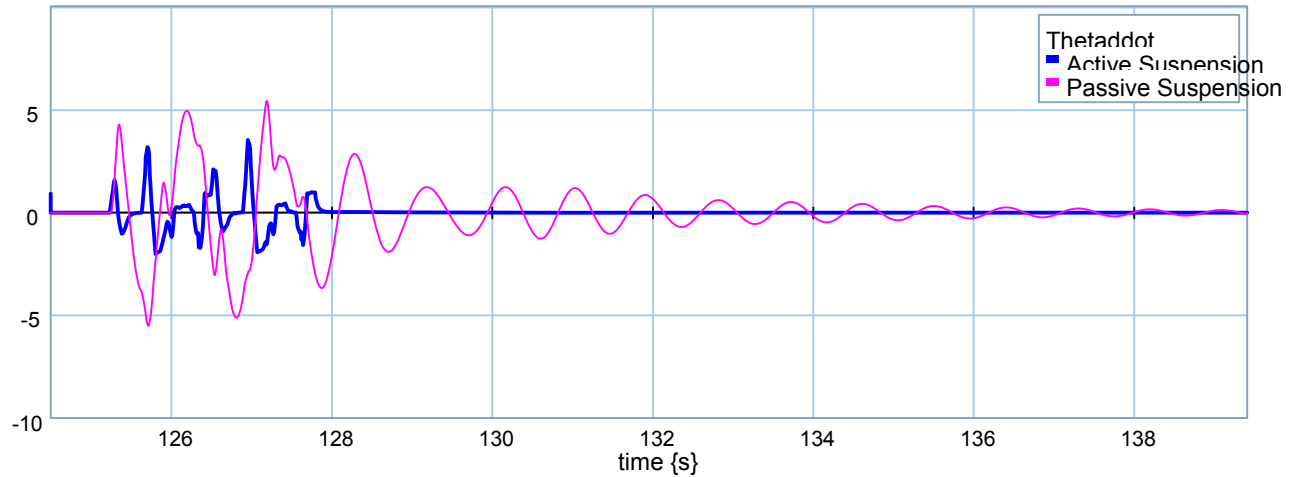
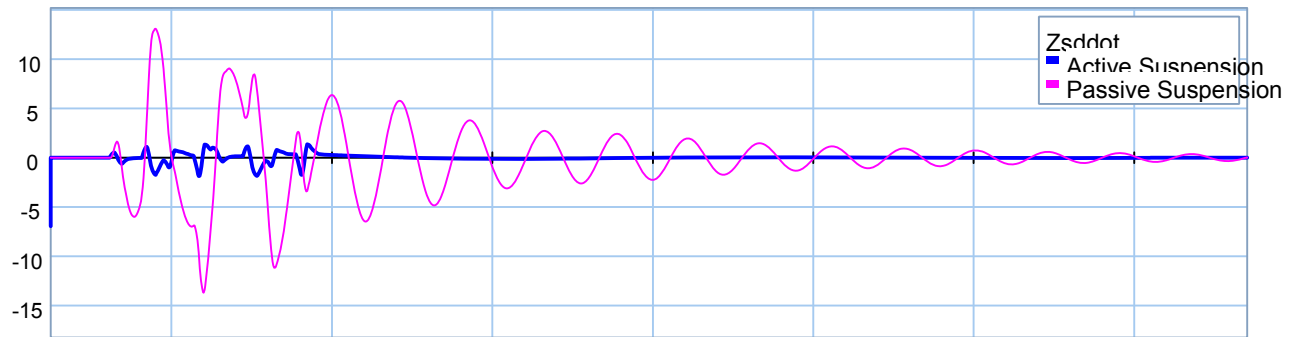
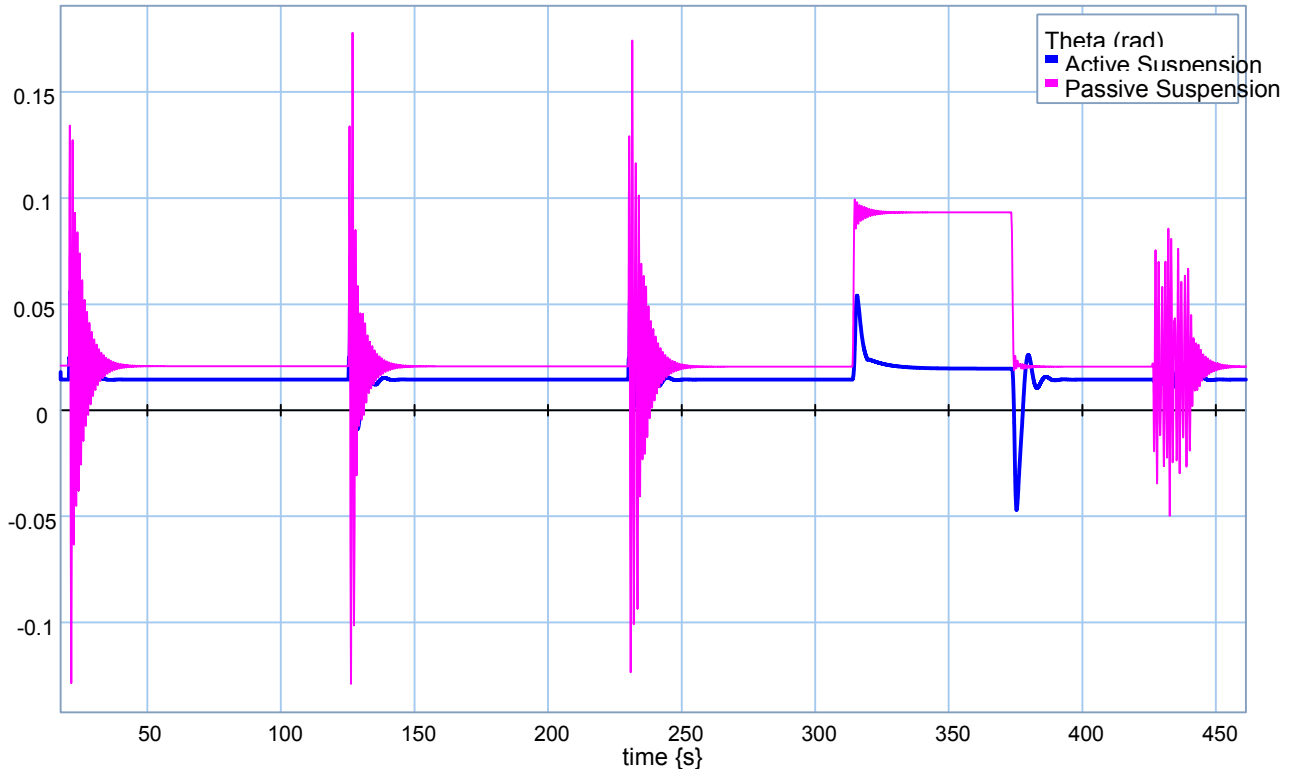


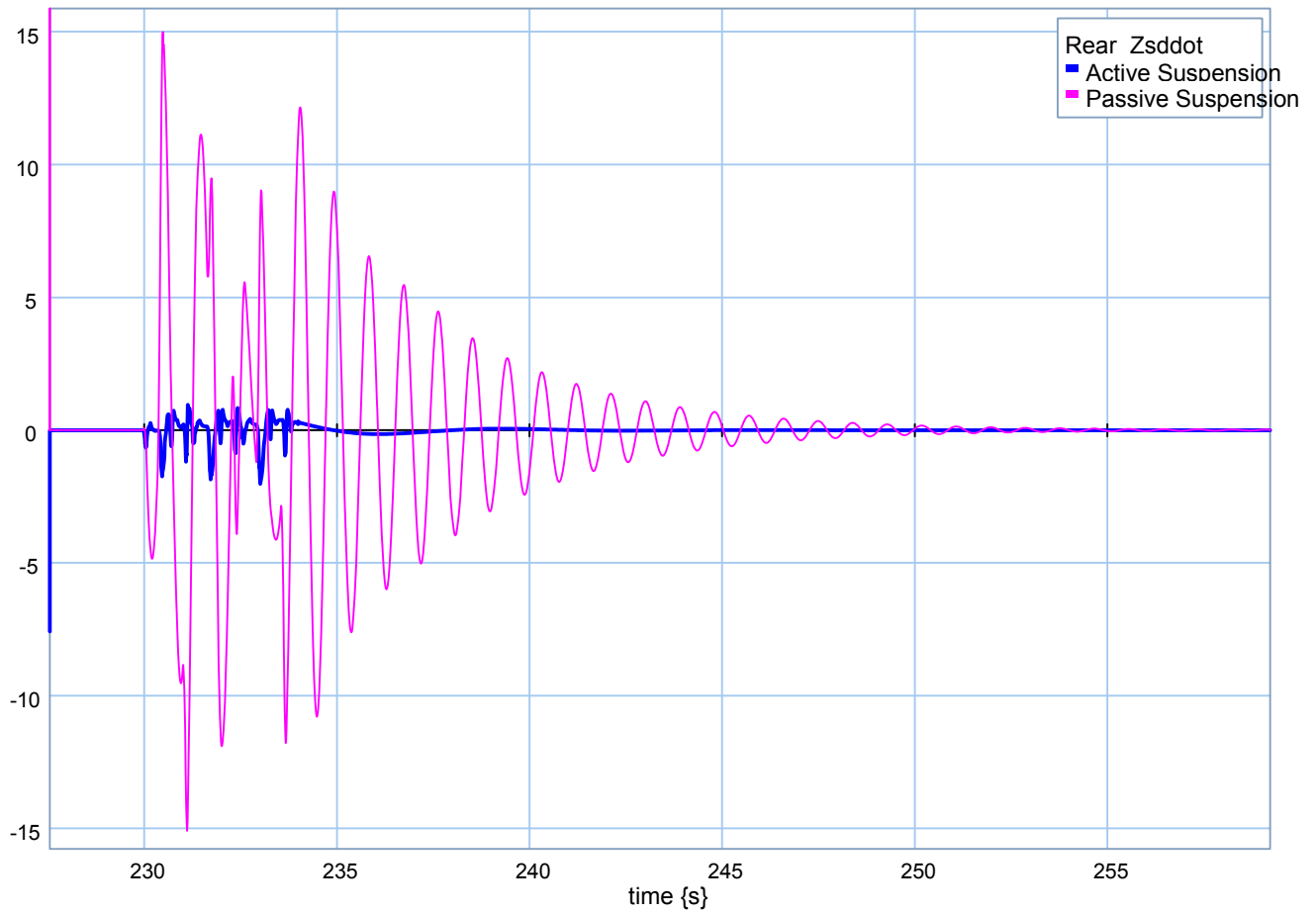
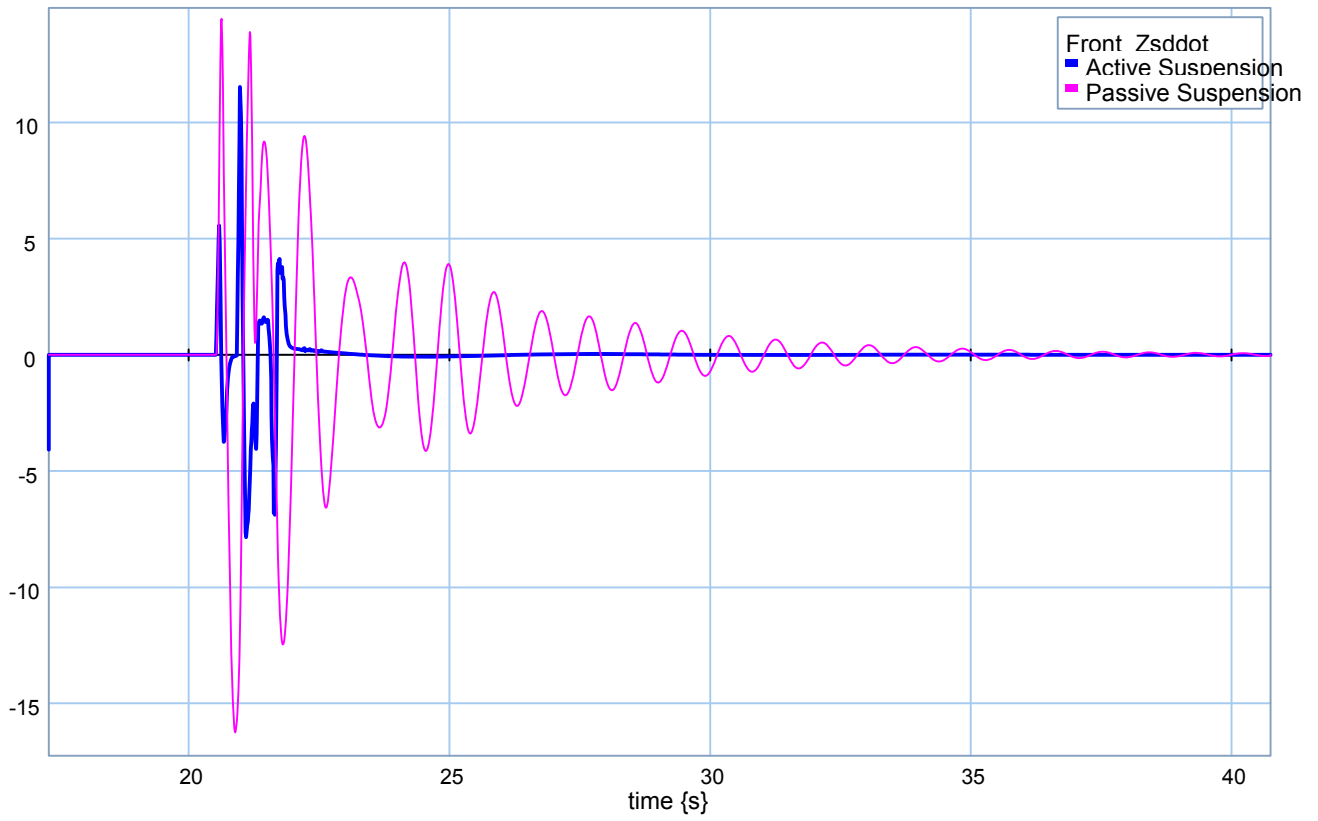
❖ **$M_c = 13500 \text{ kg.}$**





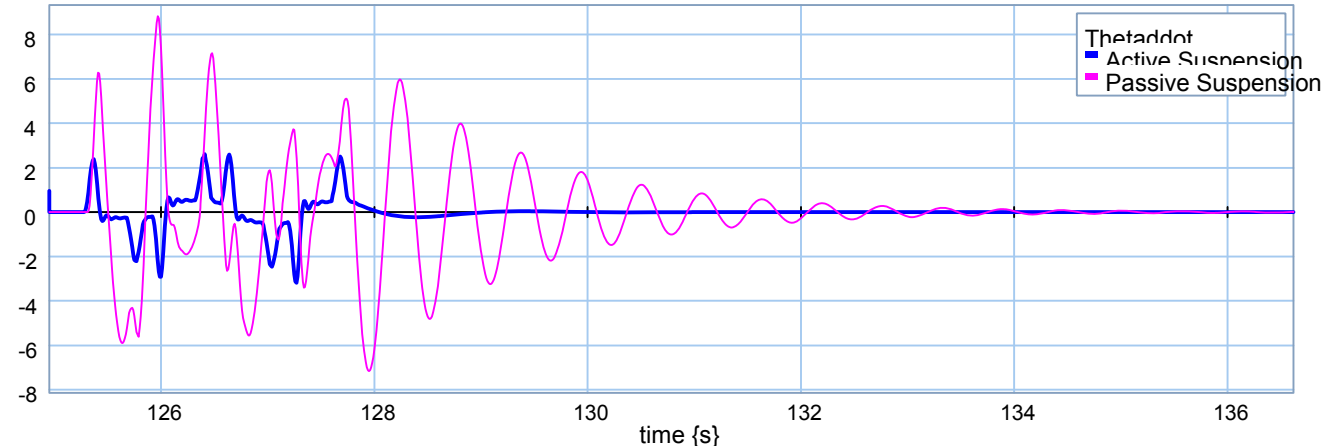
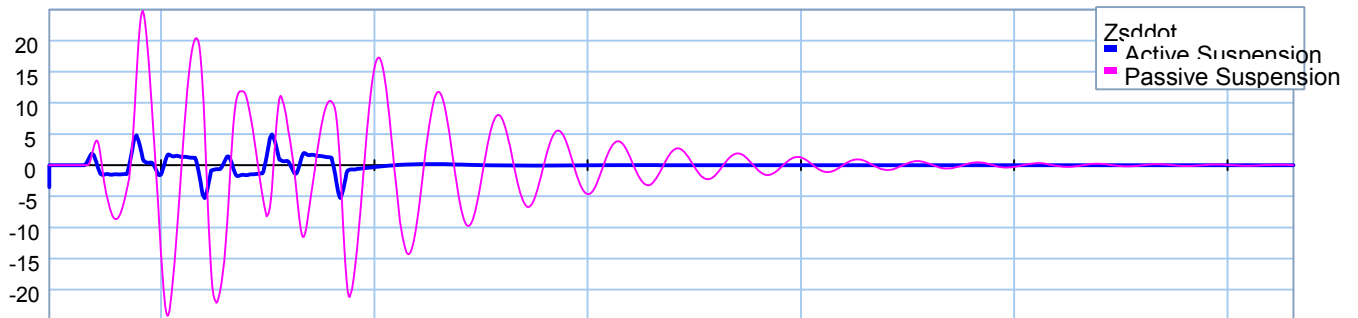
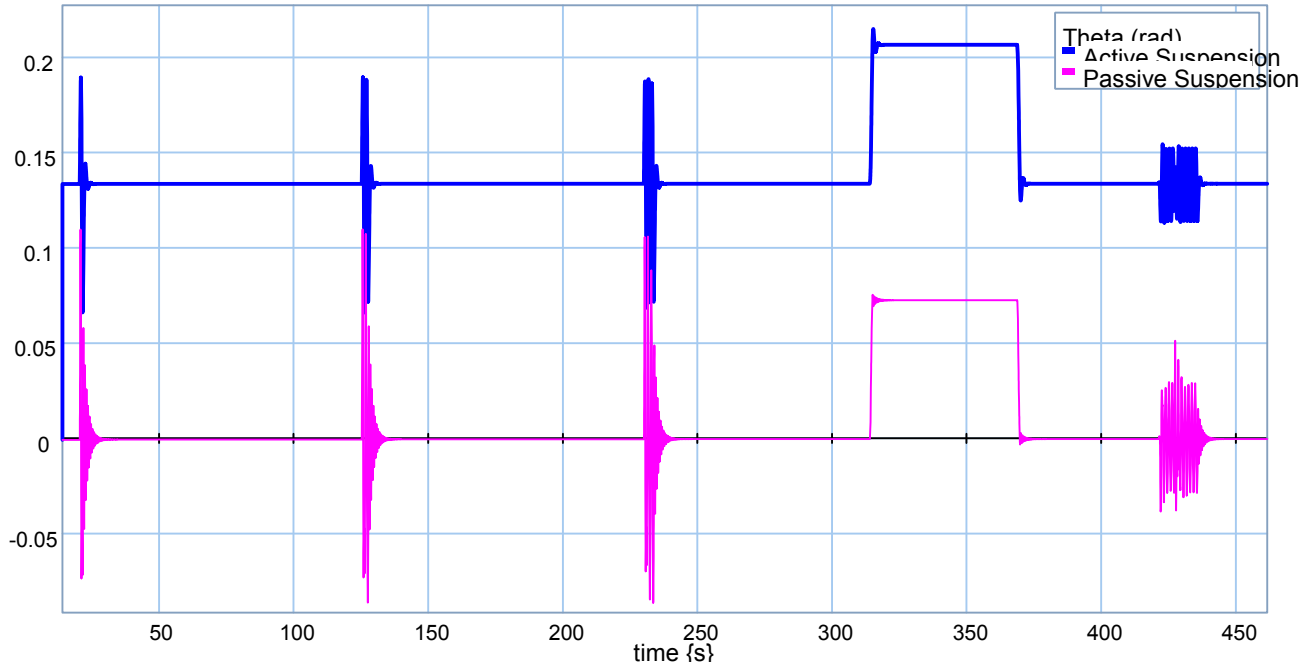
❖ **$M_c = 18000 \text{ kg.}$**

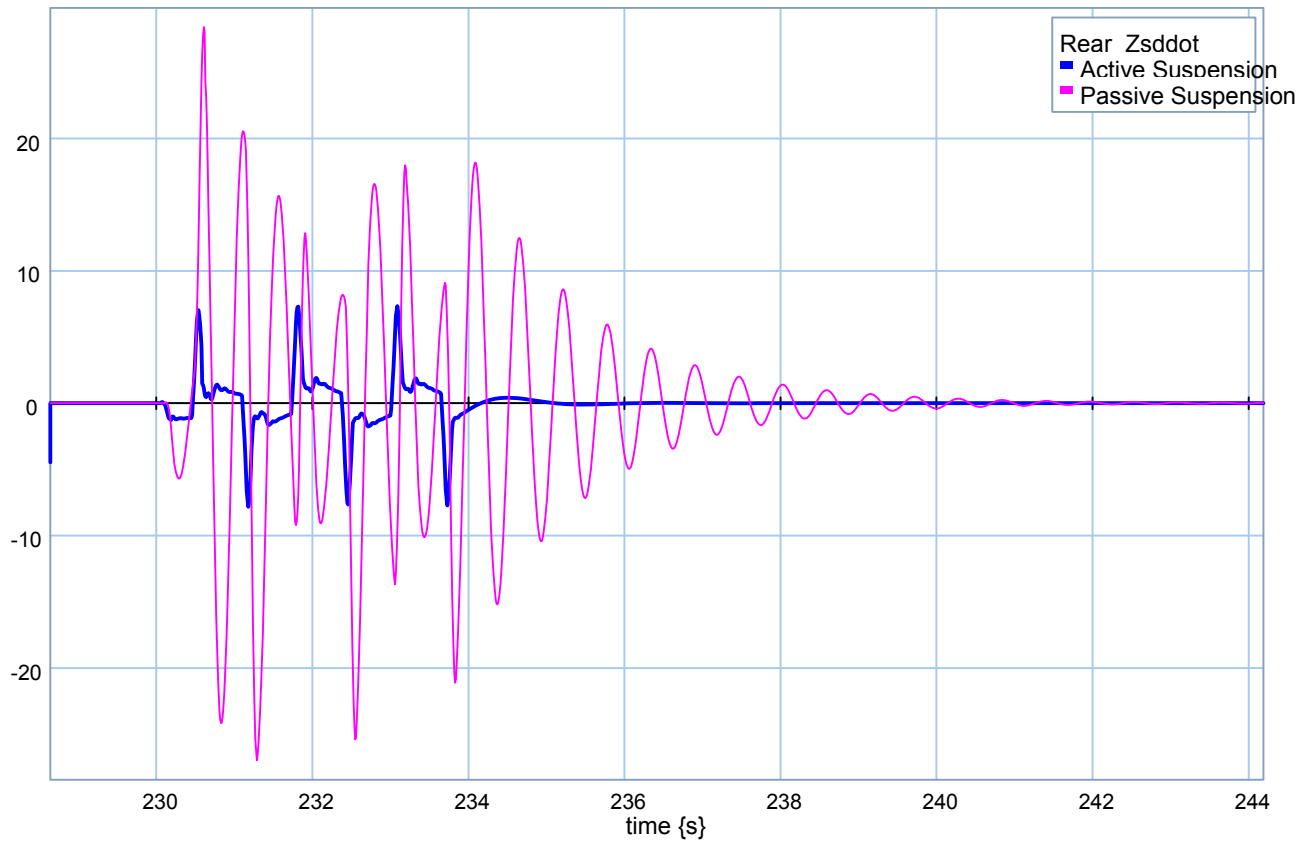
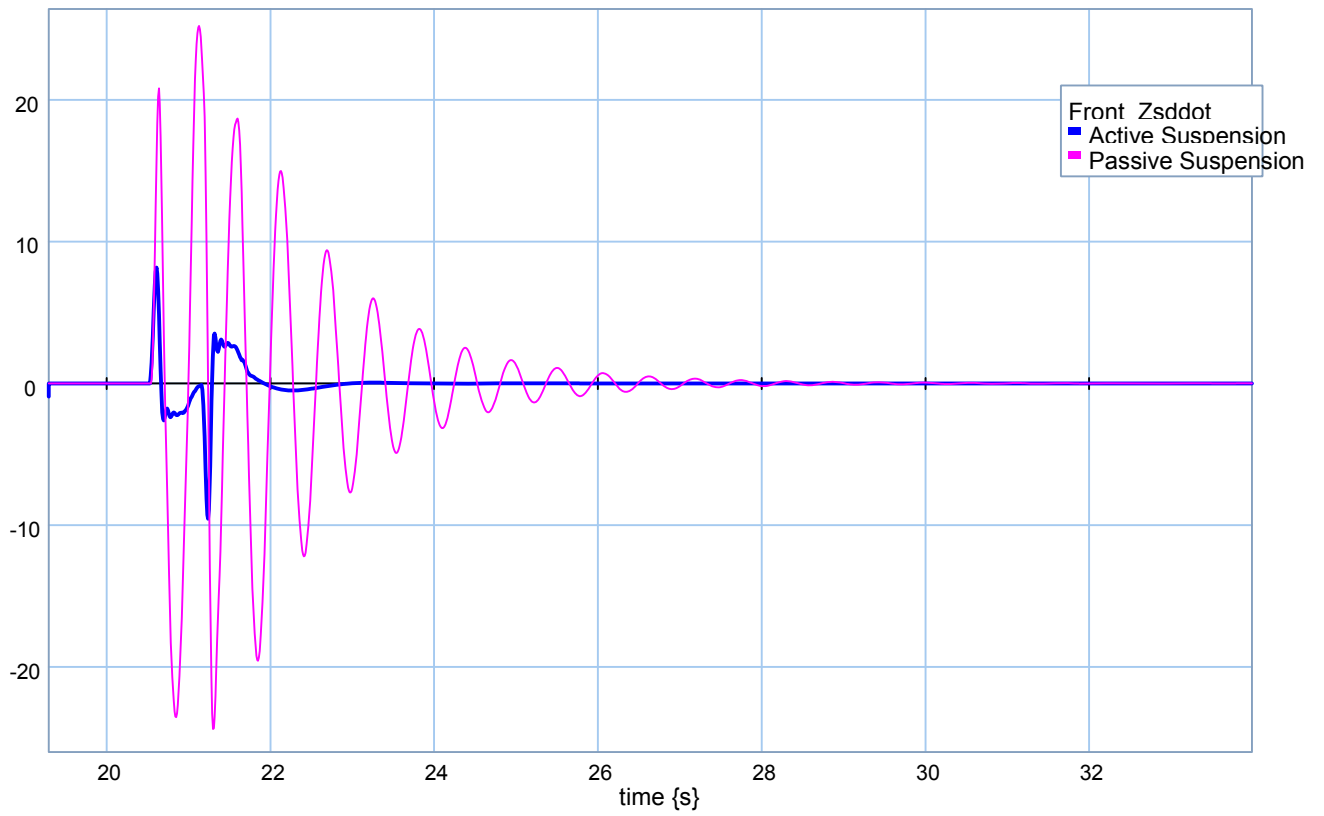




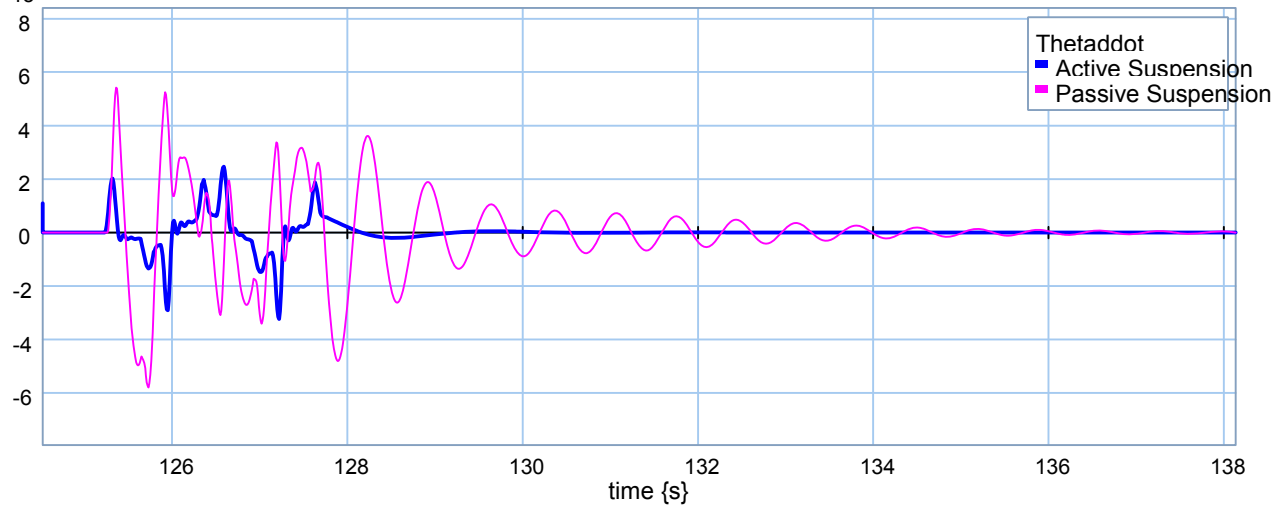
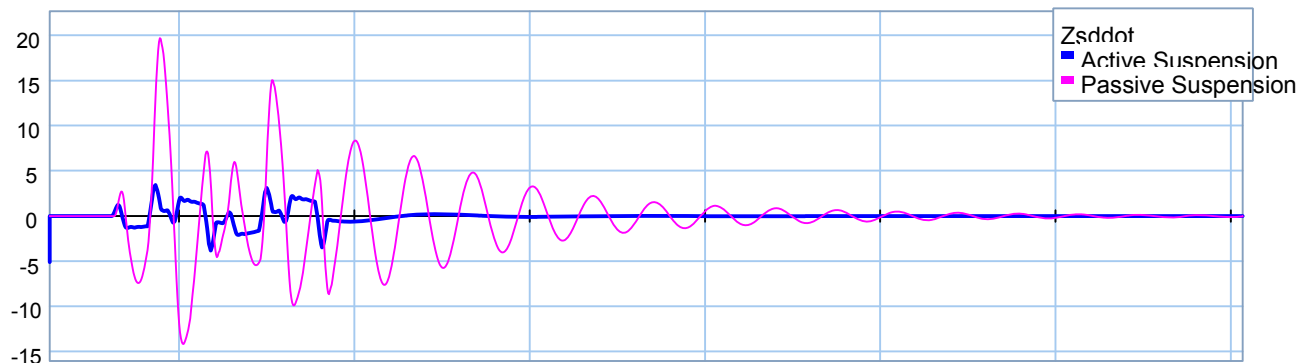
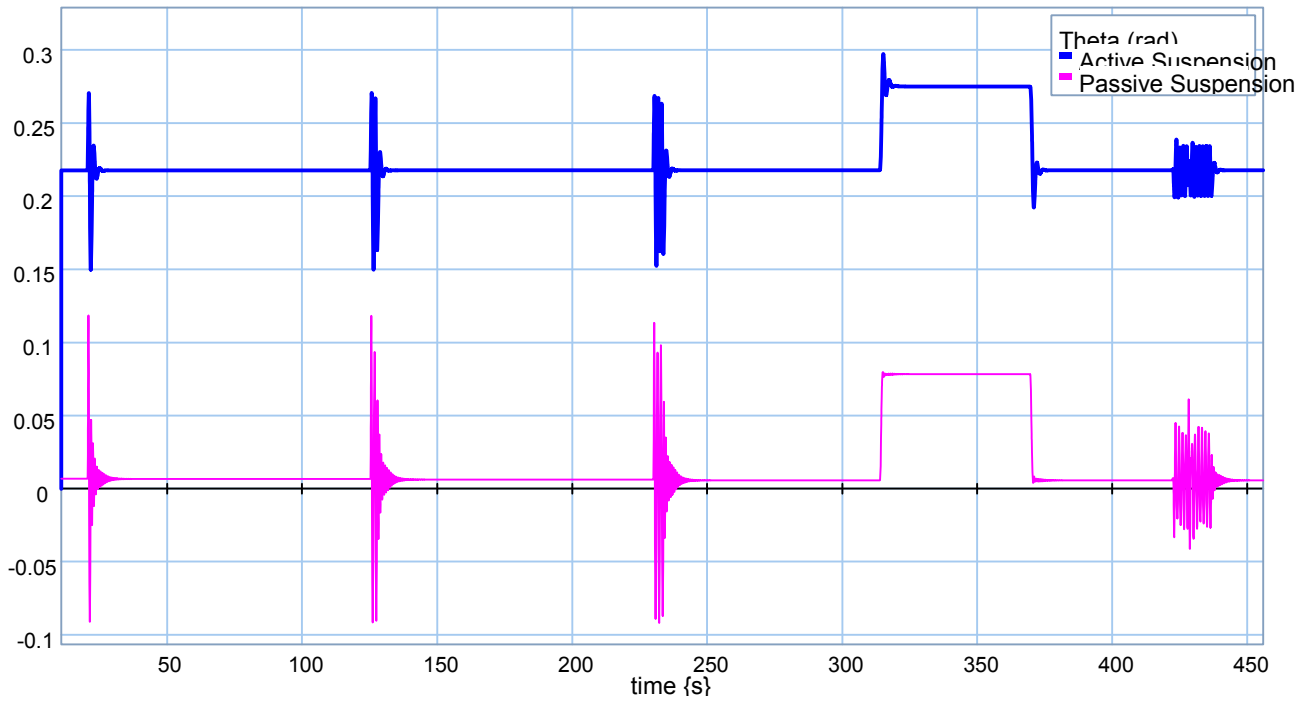
Appendix G: Non-Linear Half-Car Model, Ride Quality Scenario, Half-Car Active Suspensions.

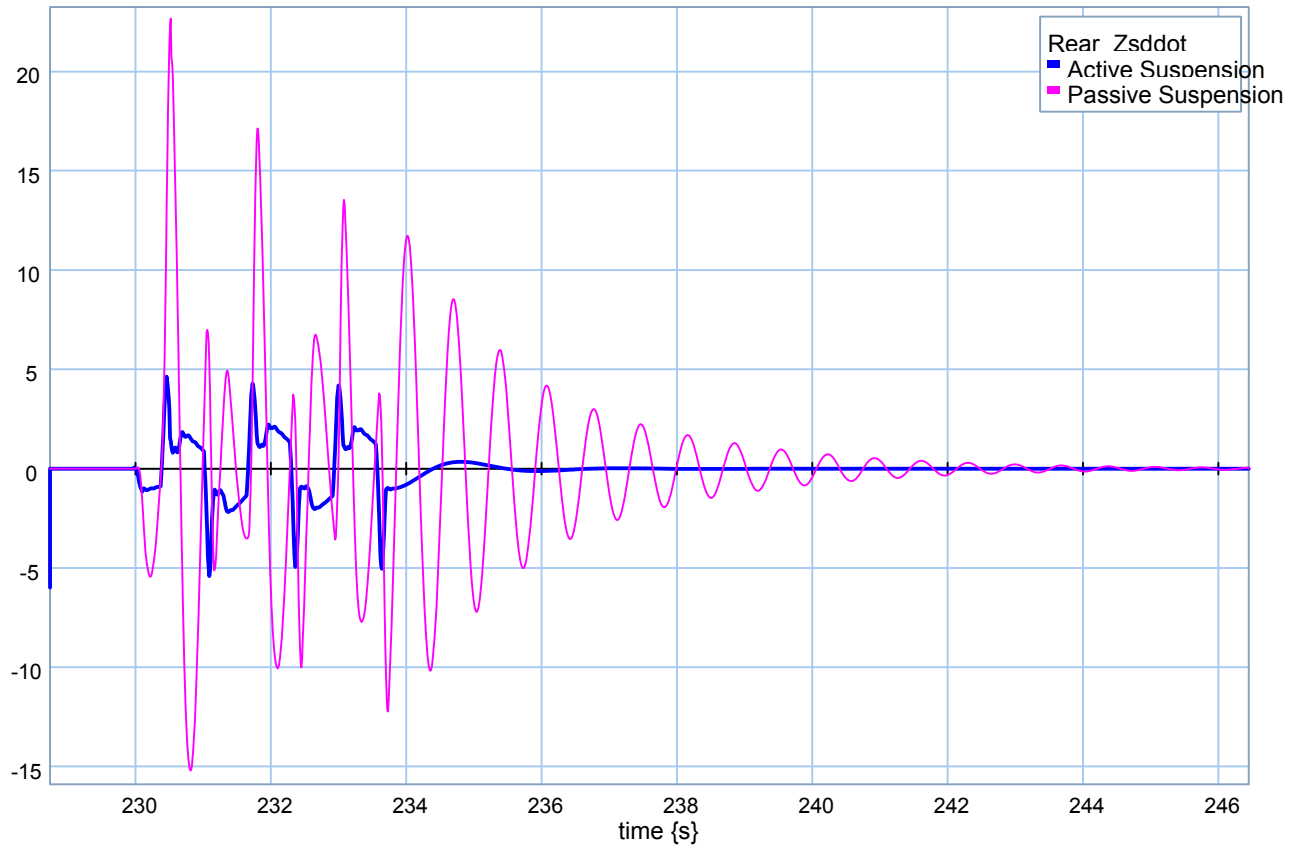
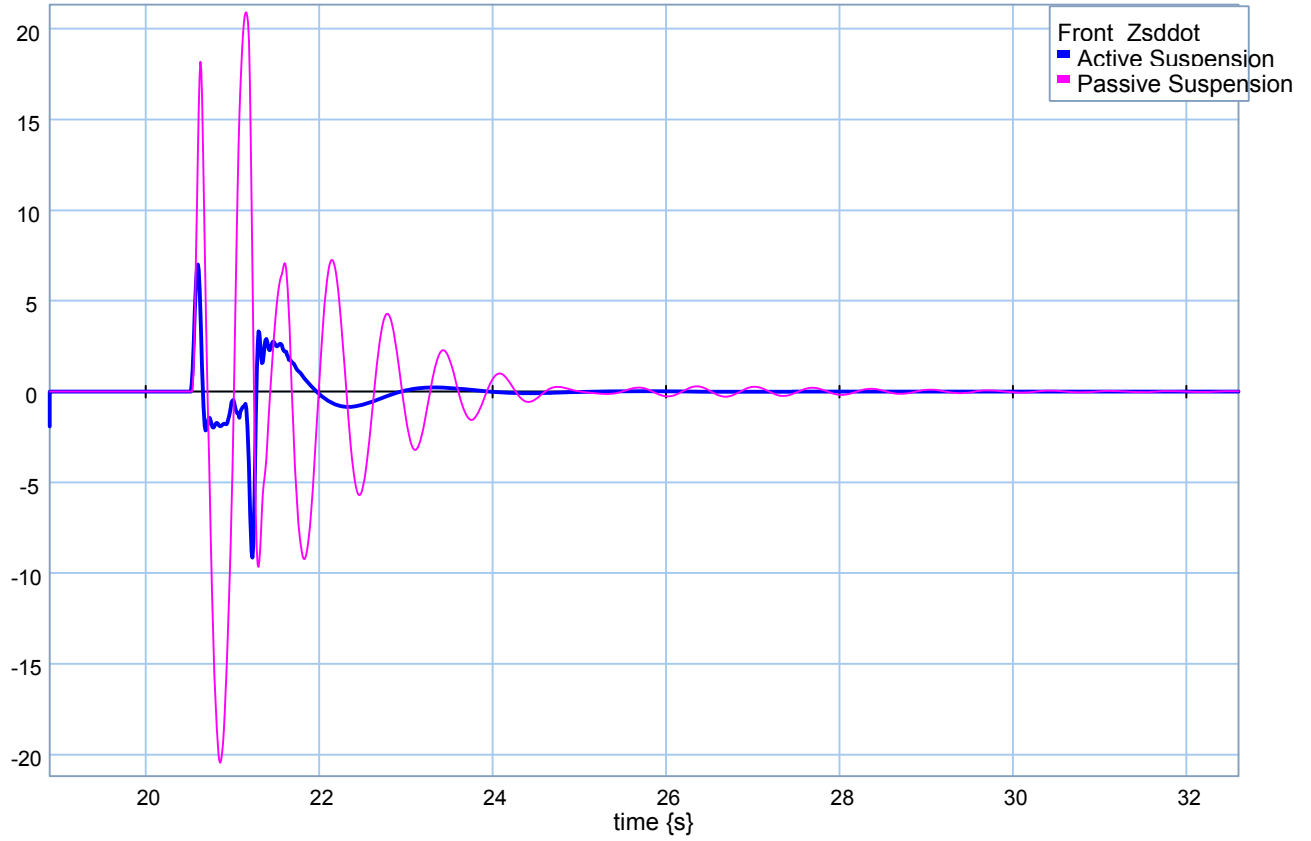
❖ $M_c = 4500 \text{ kg}$.



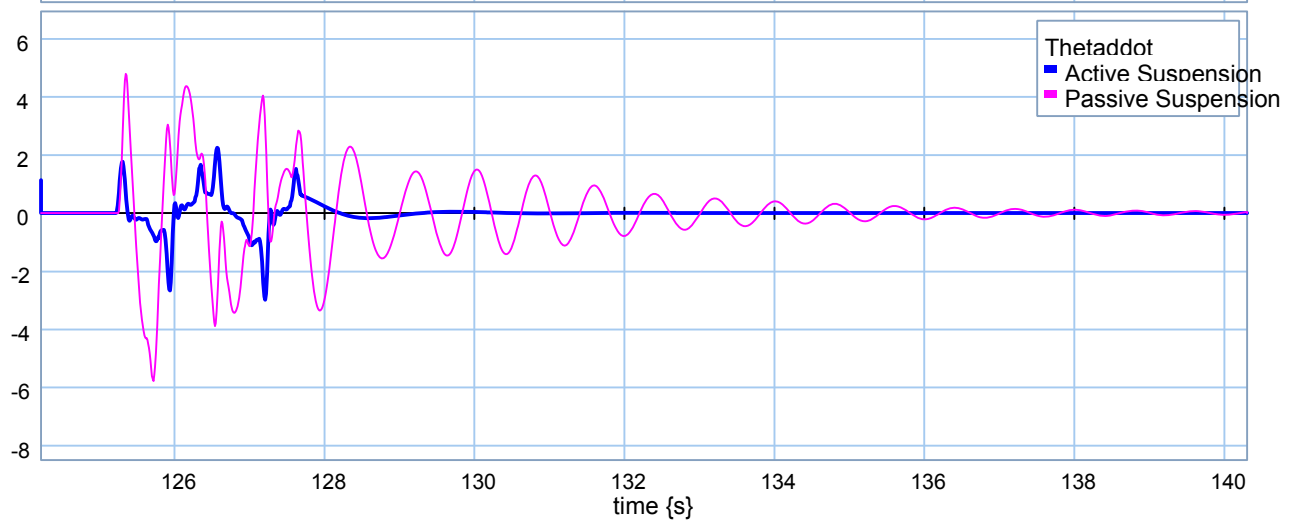
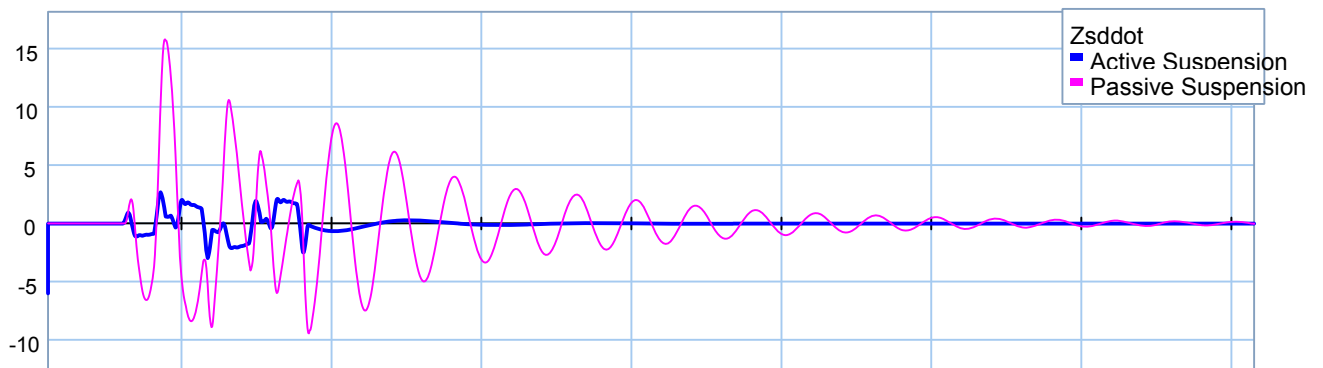
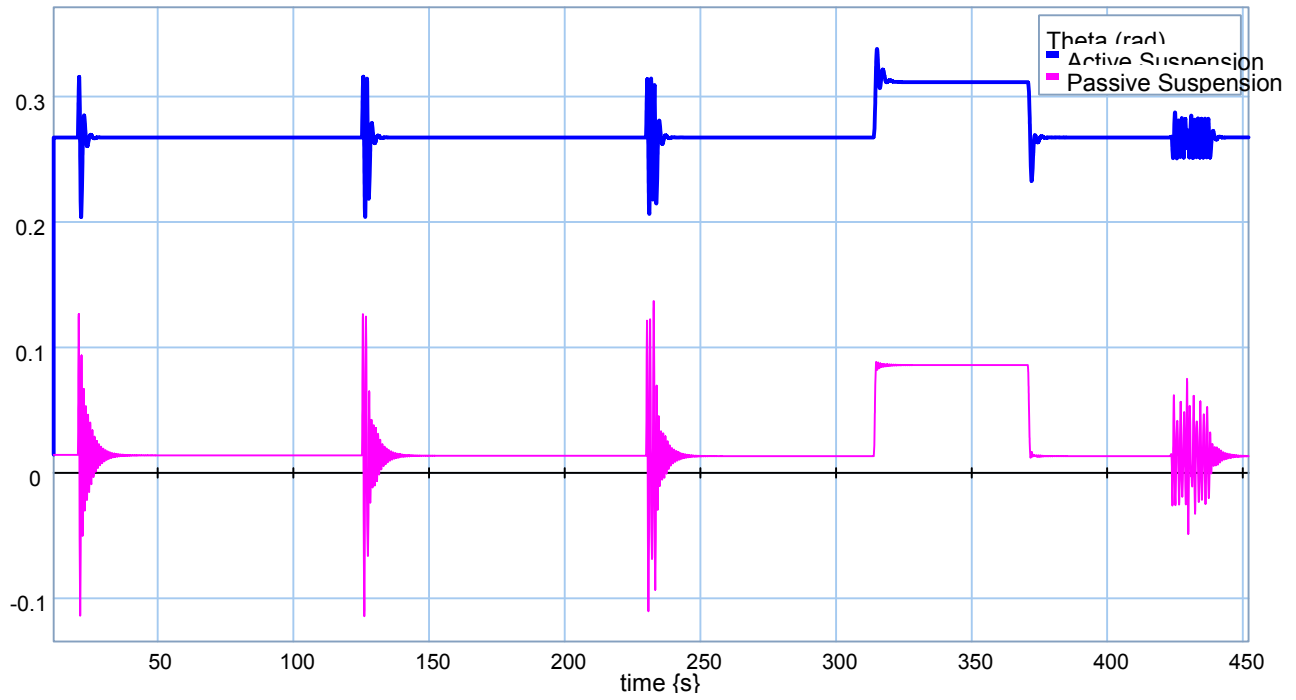


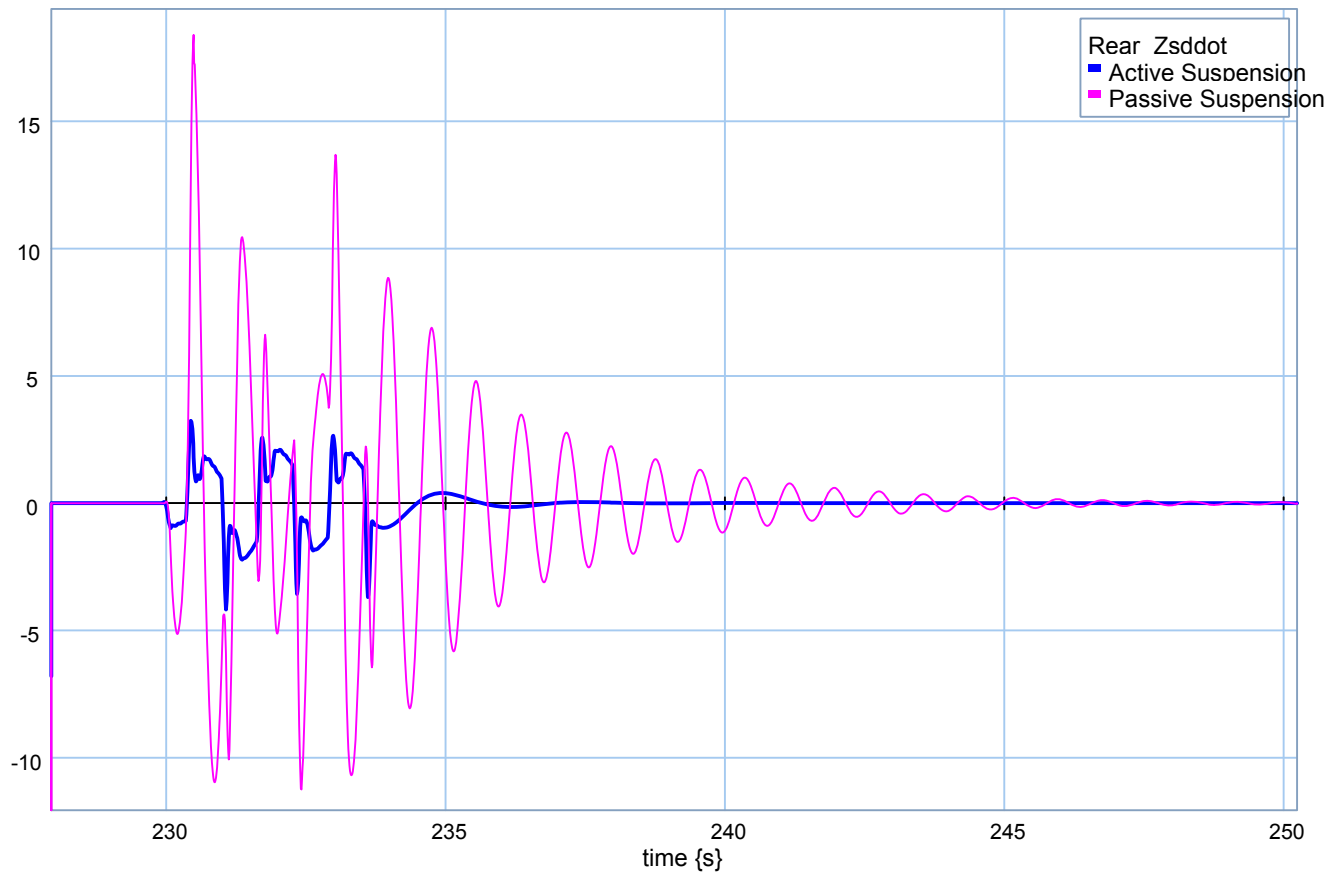
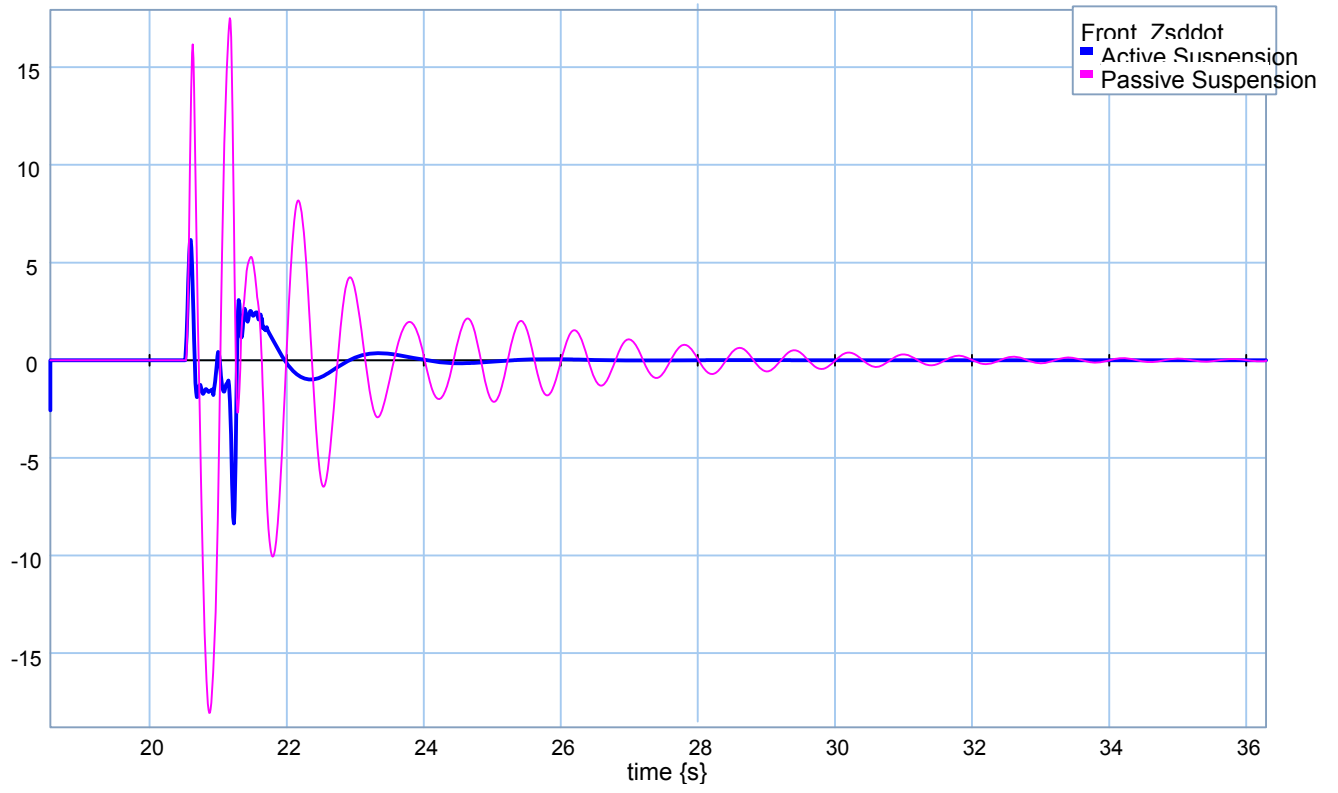
❖ **Mc = 9000 kg.**



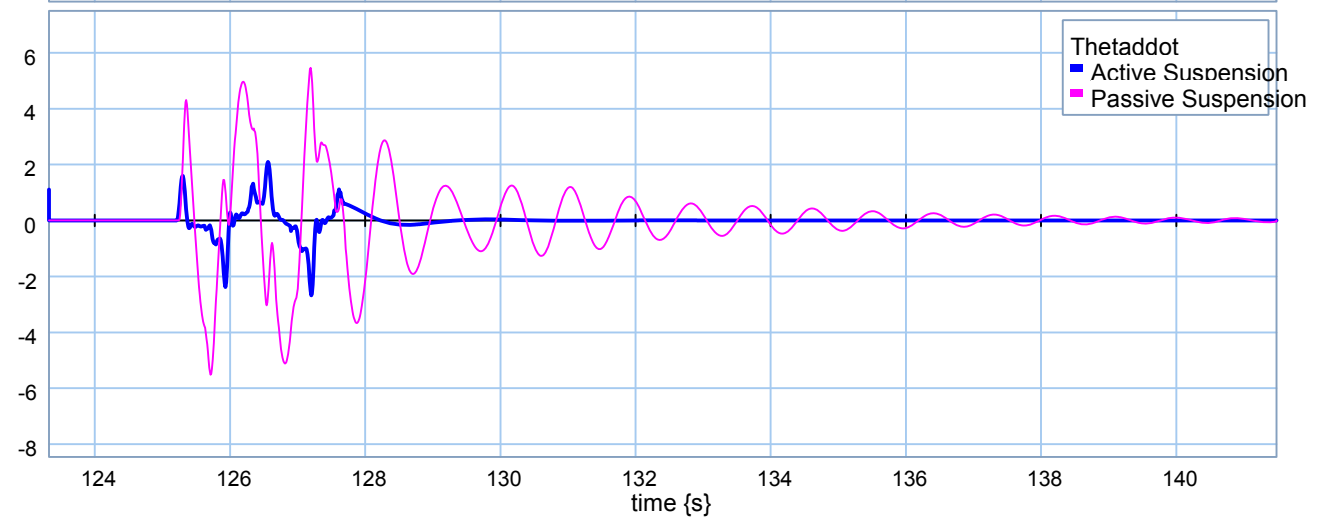
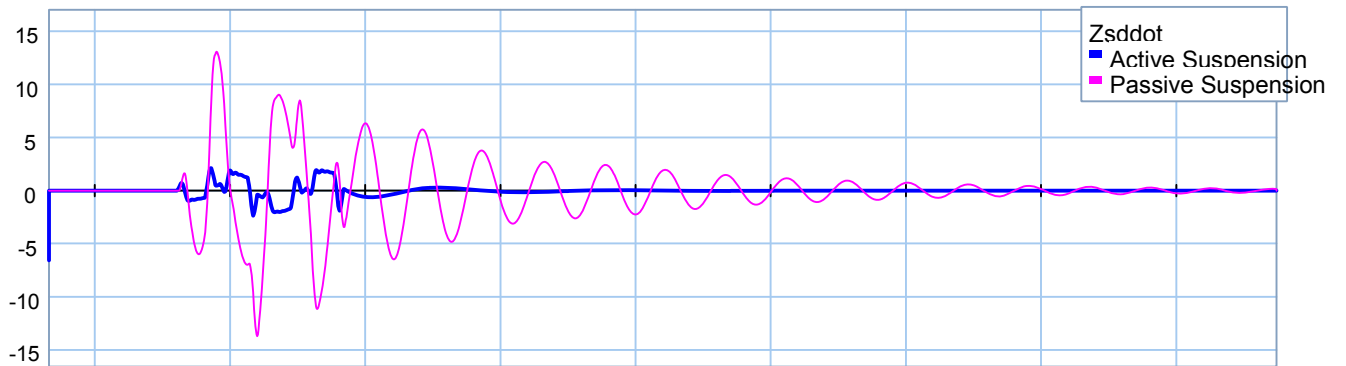
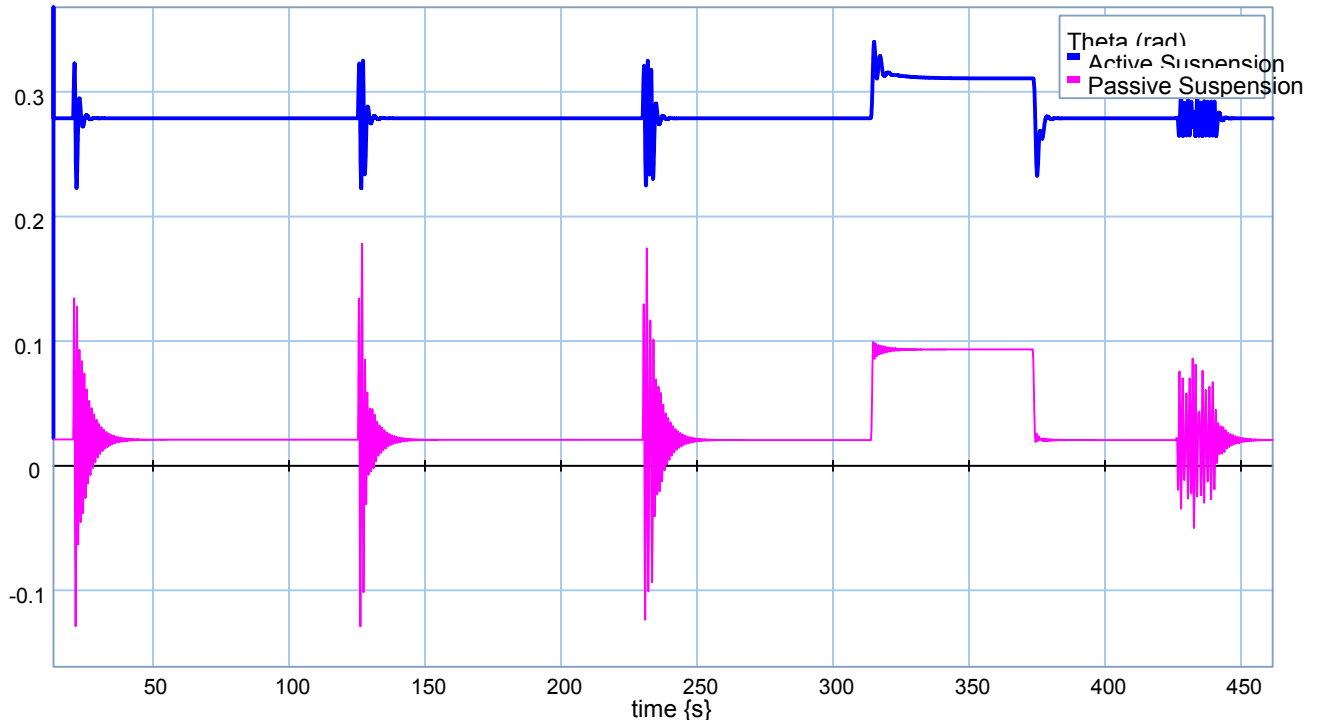


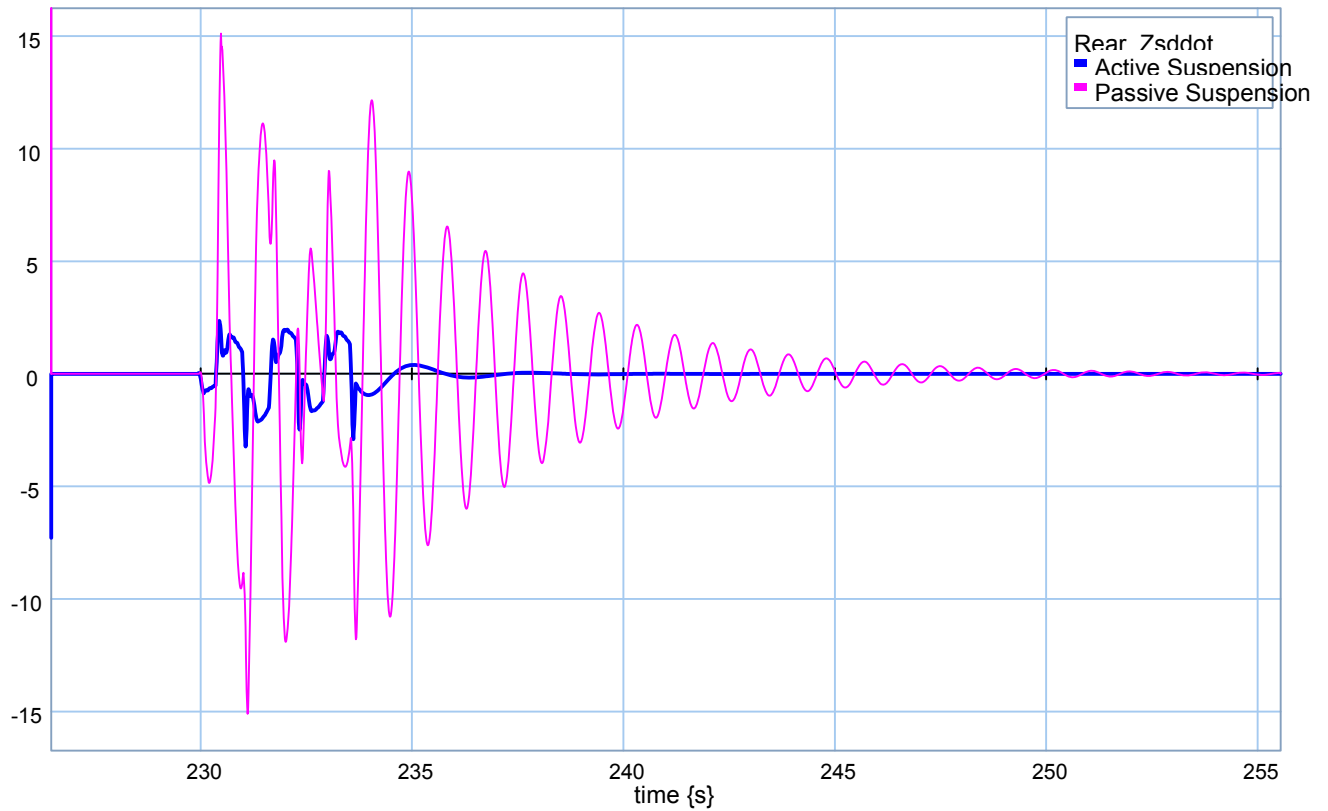
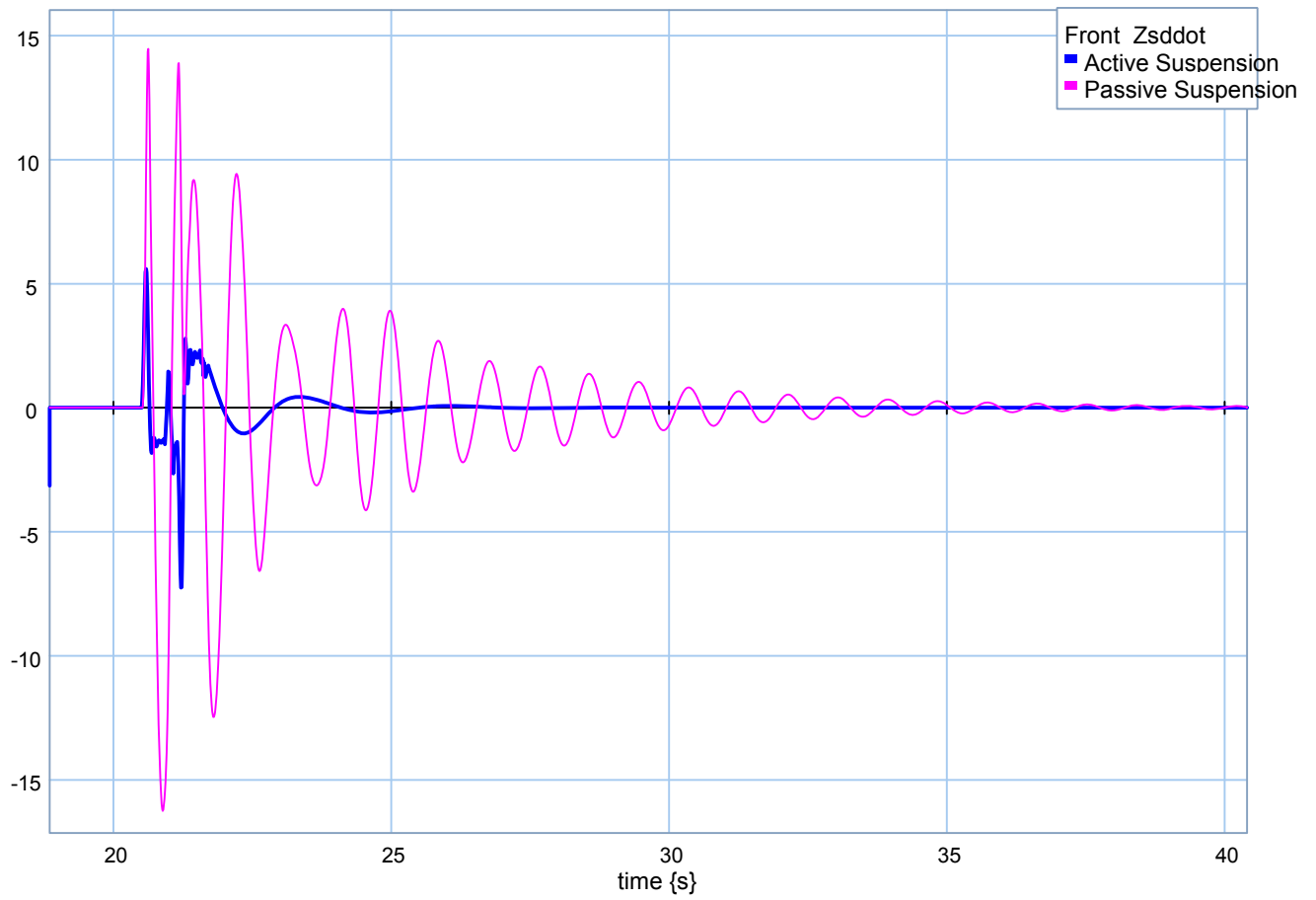
❖ **Mc = 13500 kg.**





❖ **Mc = 18000 kg.**

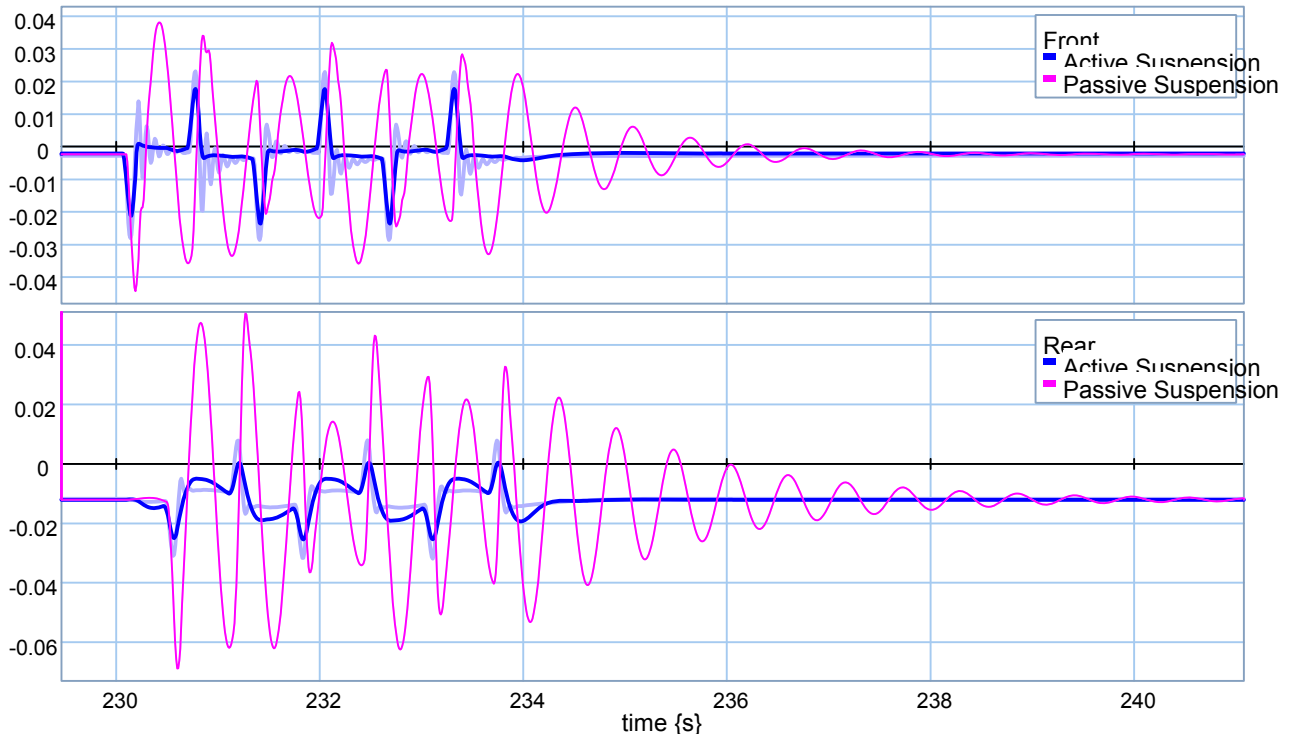
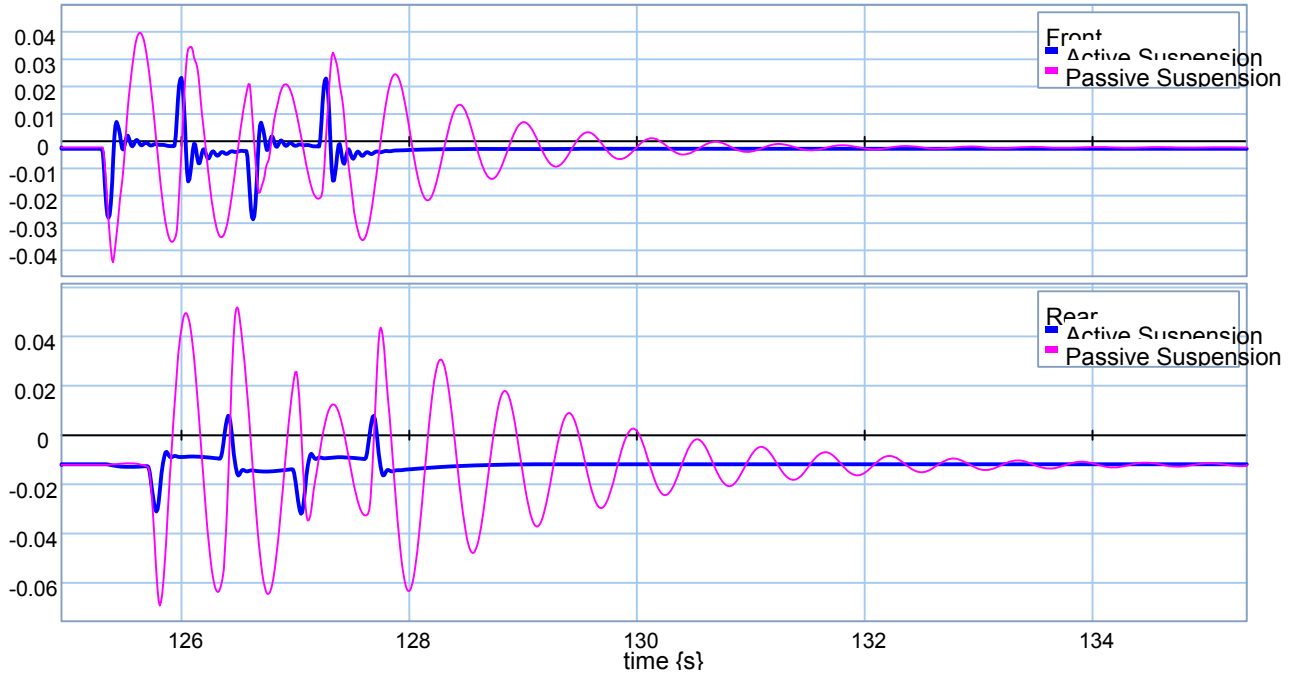


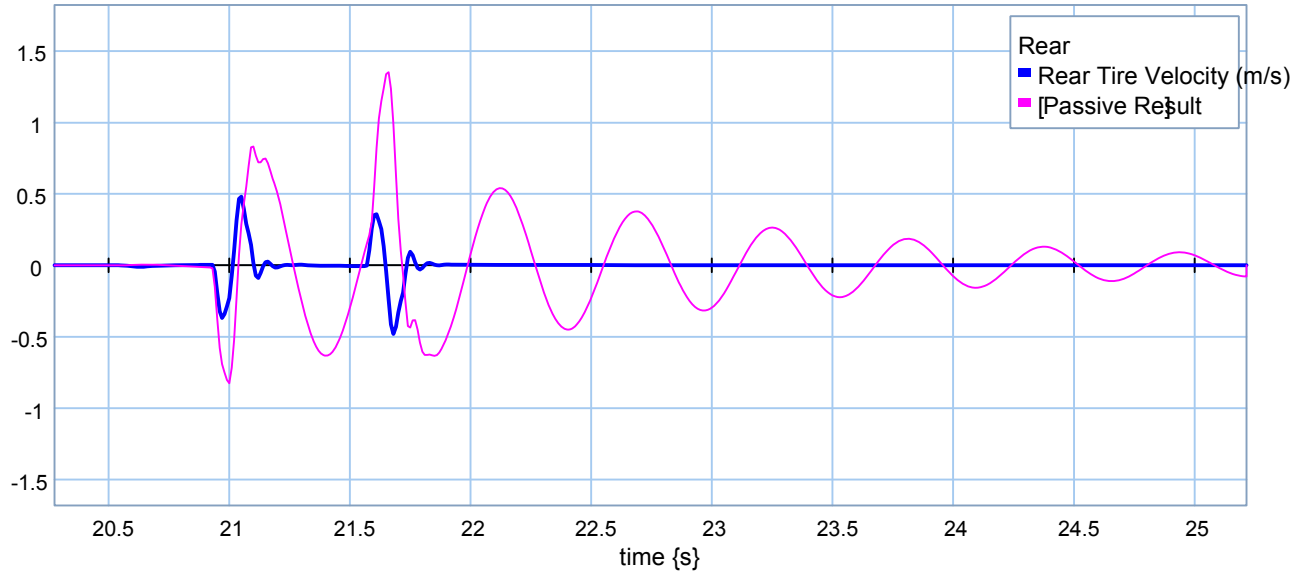
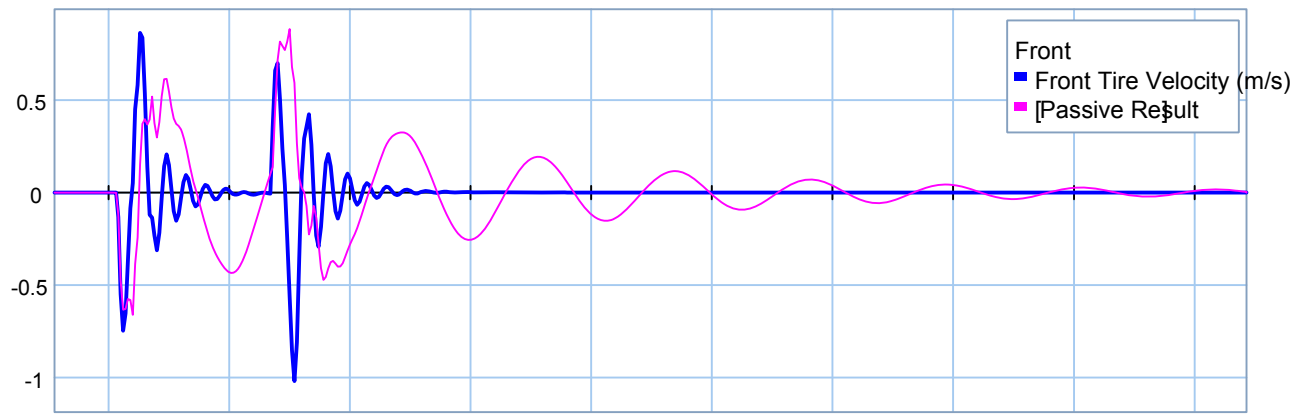
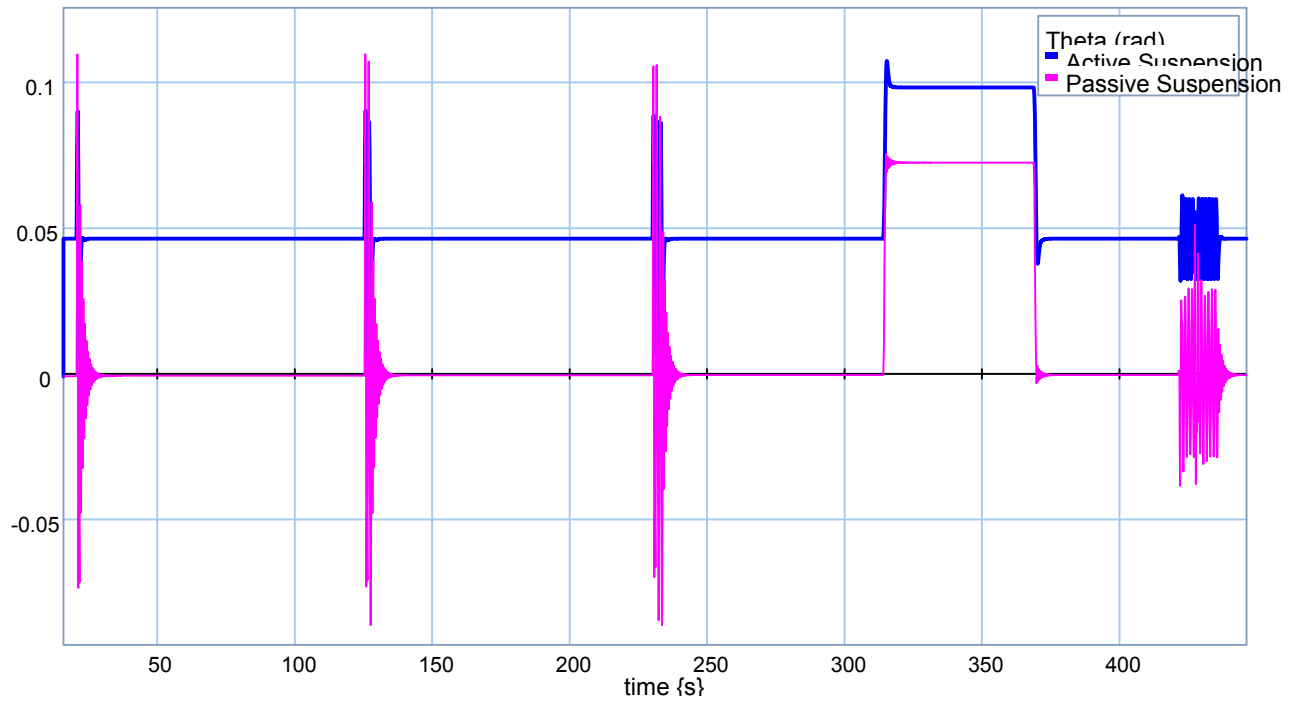


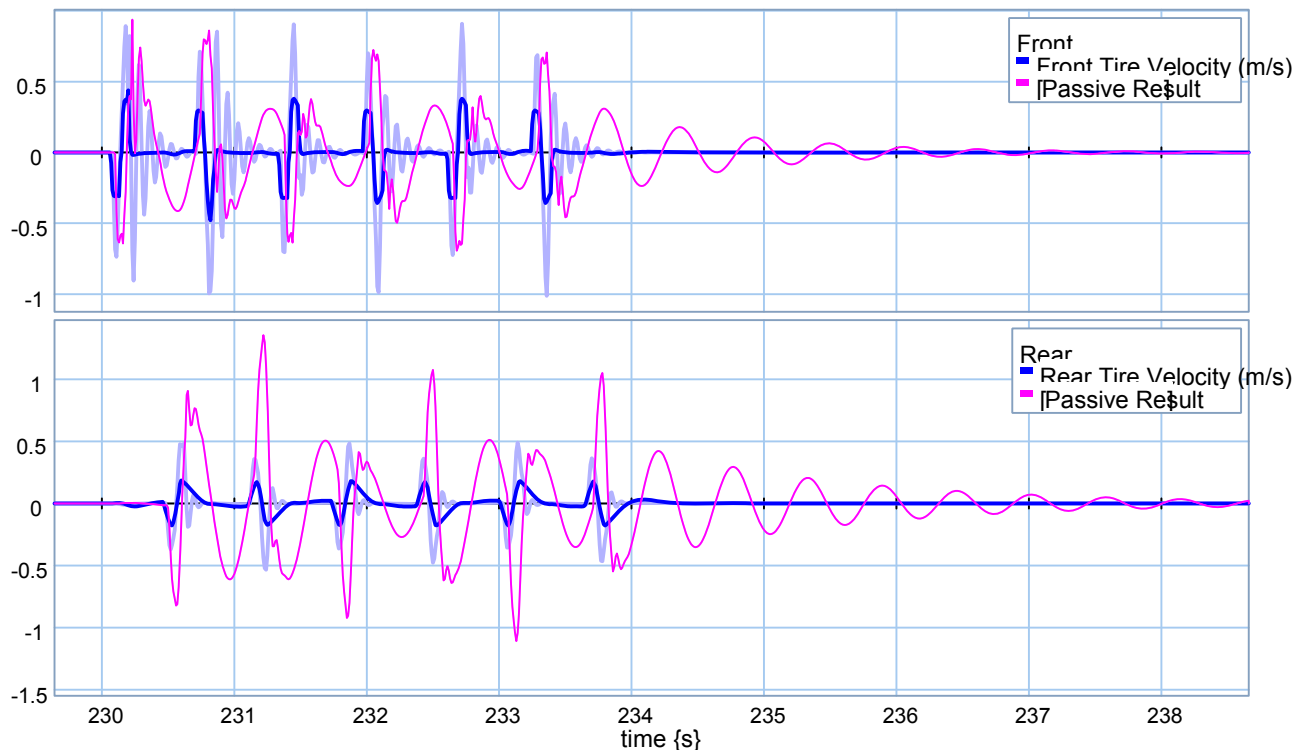
Appendix H: Non-Linear Half-Car Model, Road Holding Scenario

Quarter-Car Active Suspensions.

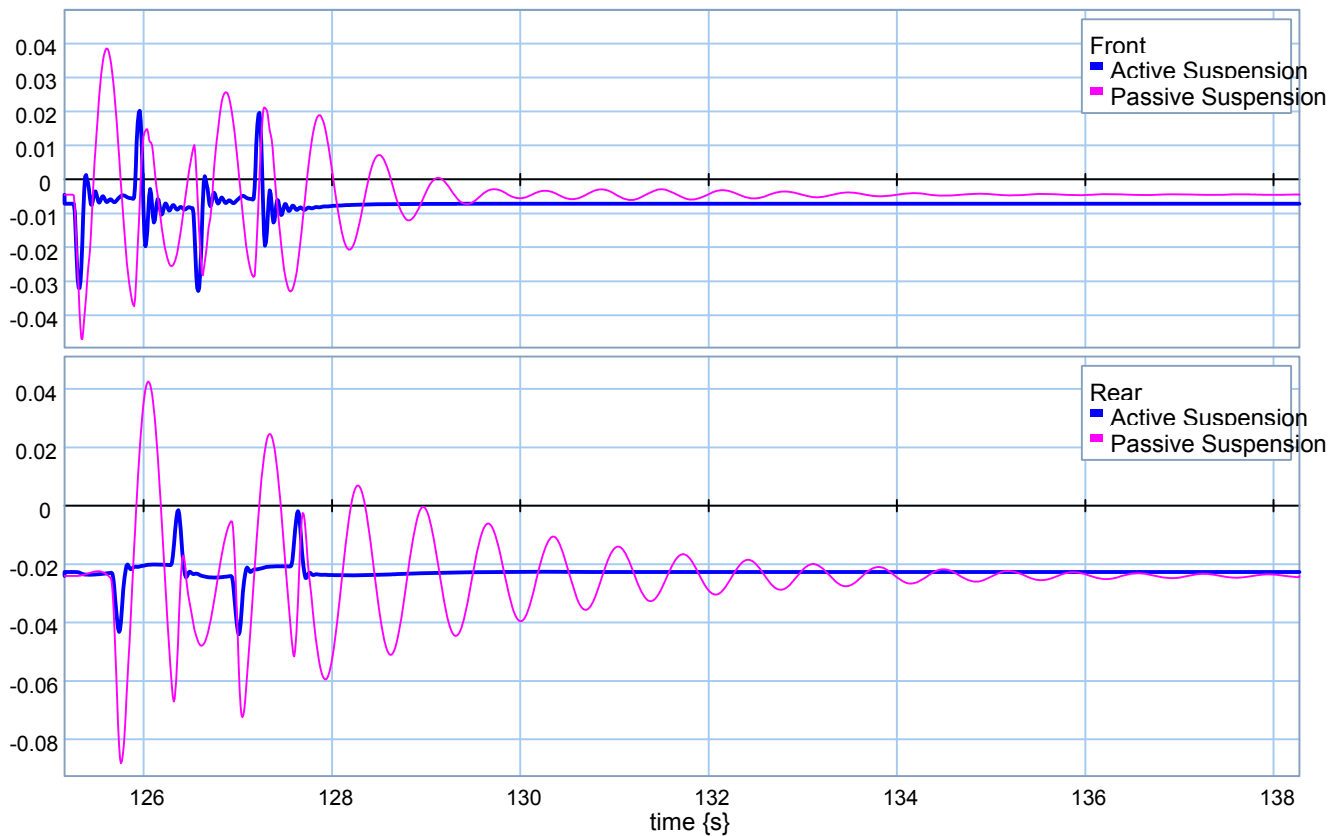
❖ $M_c = 4500 \text{ kg}$.

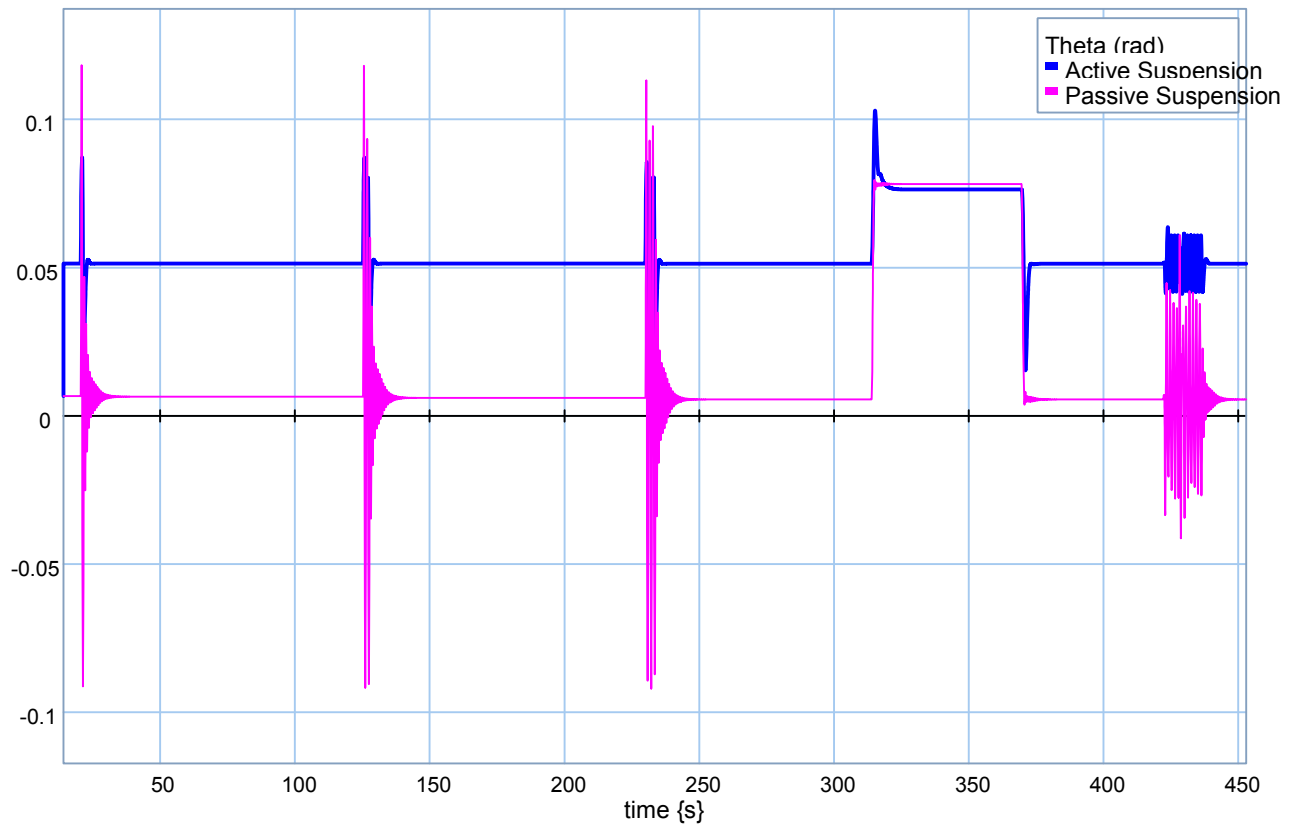
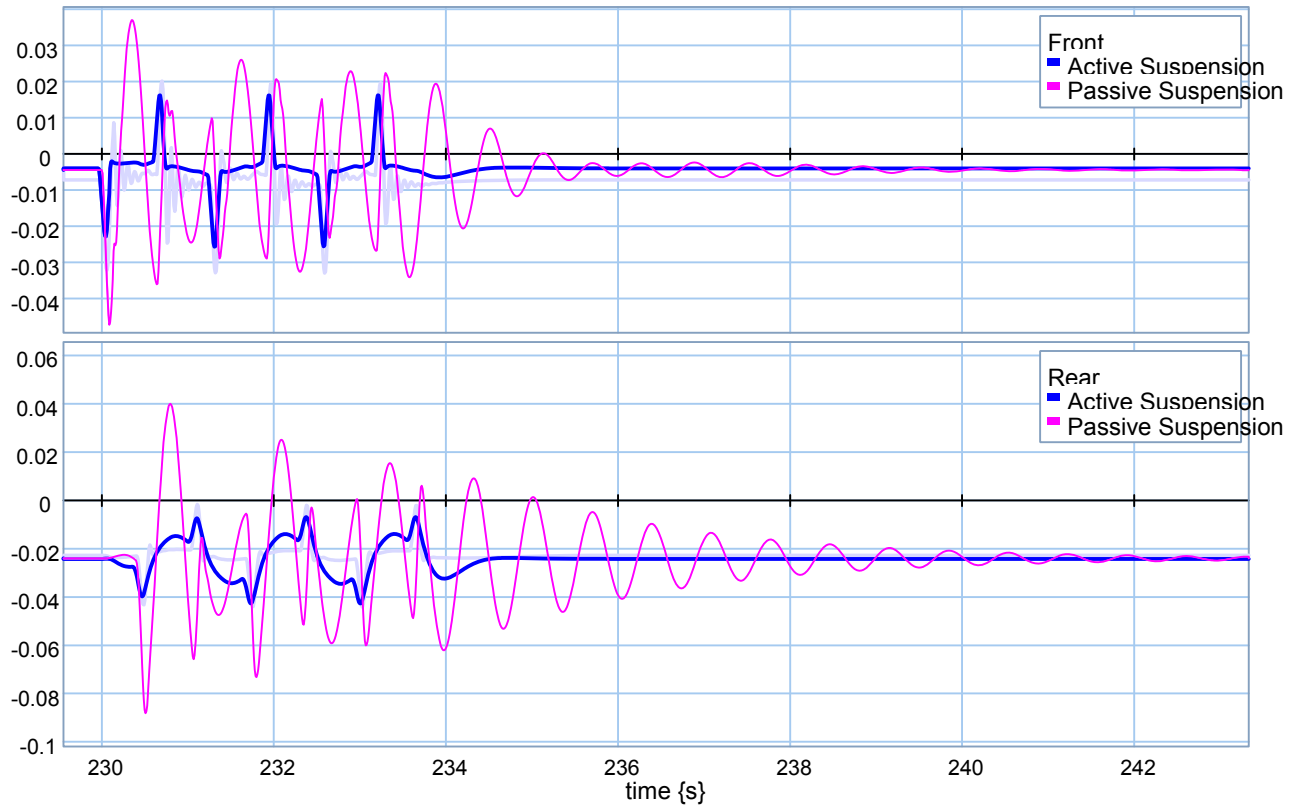


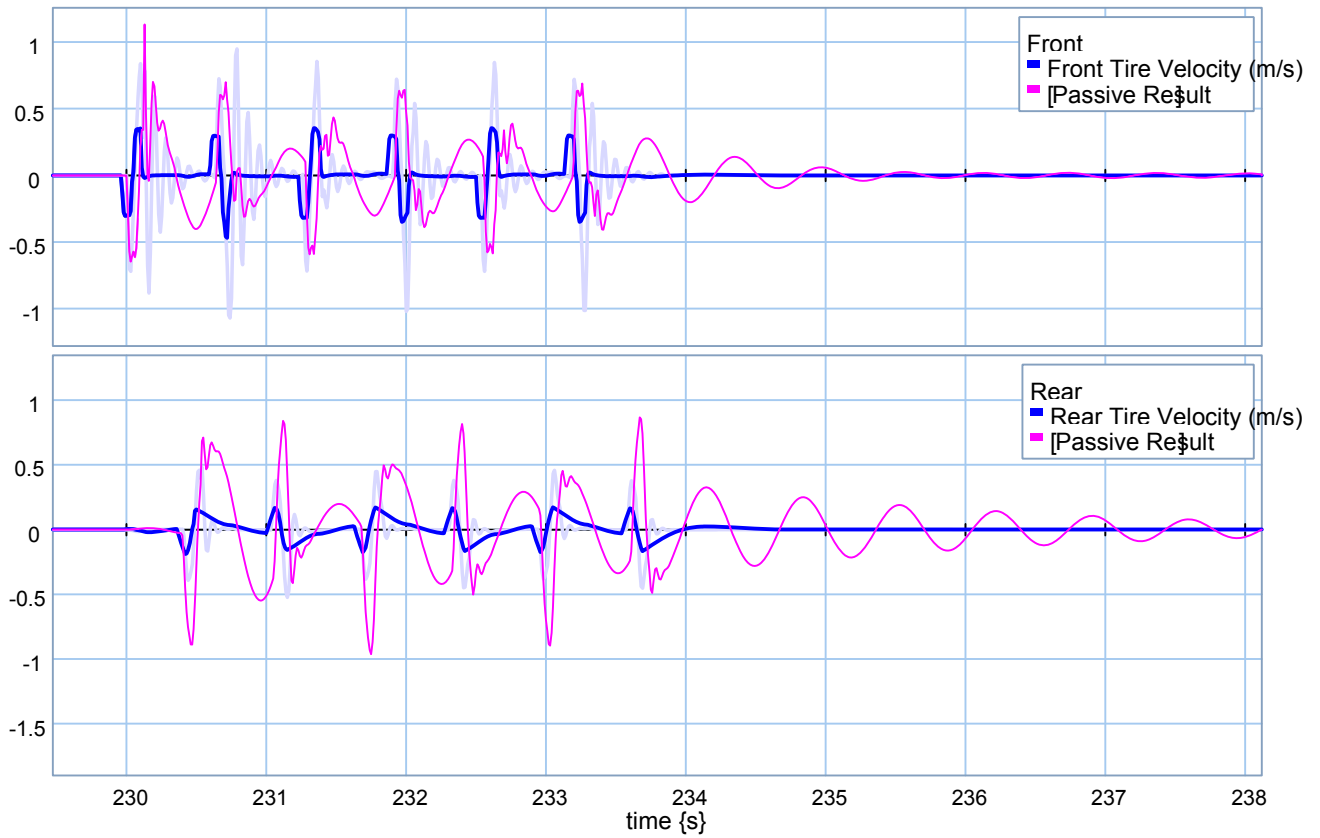
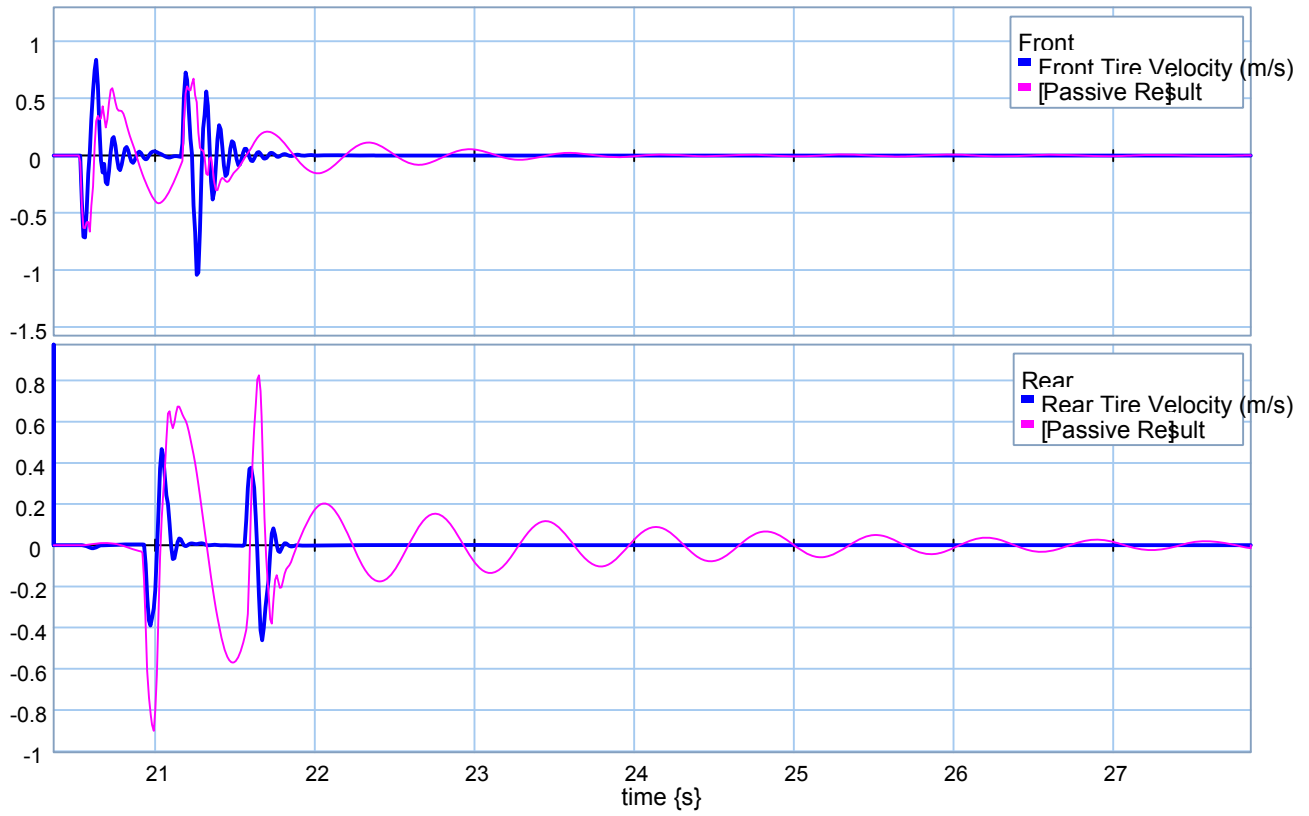




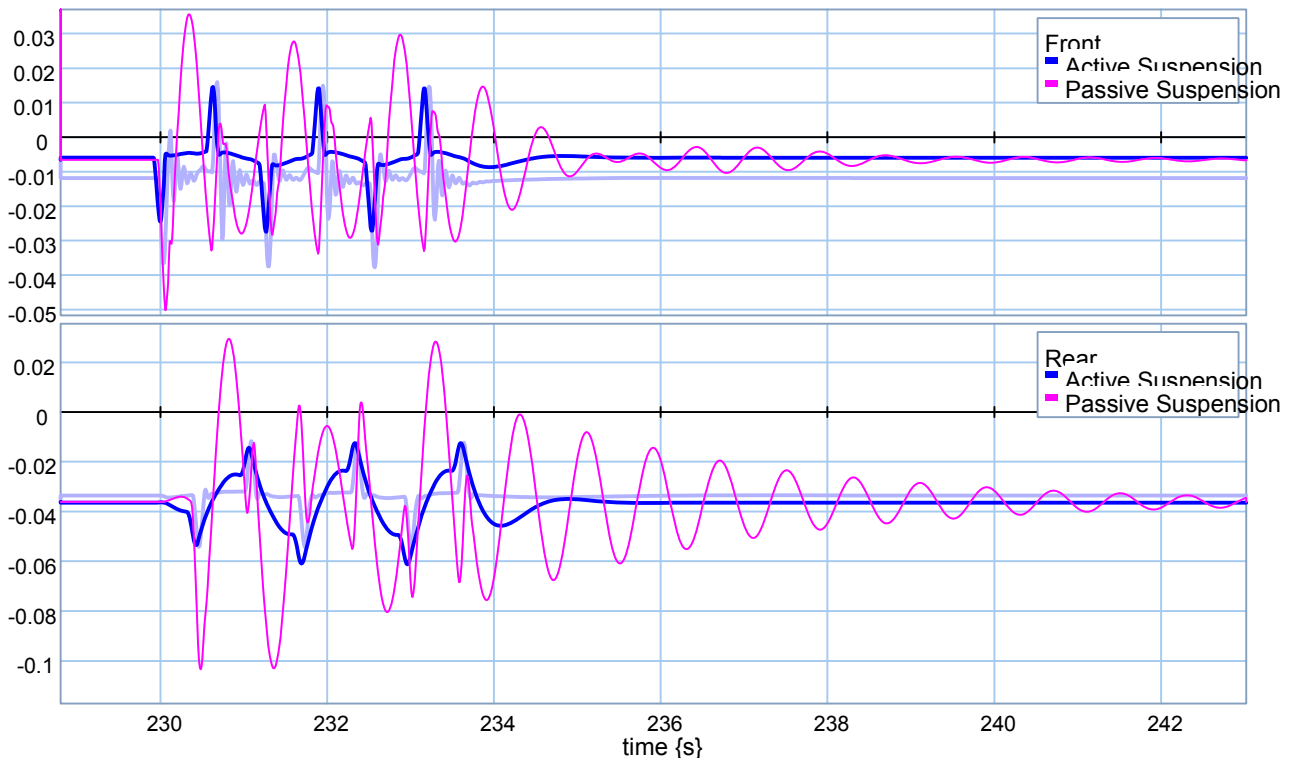
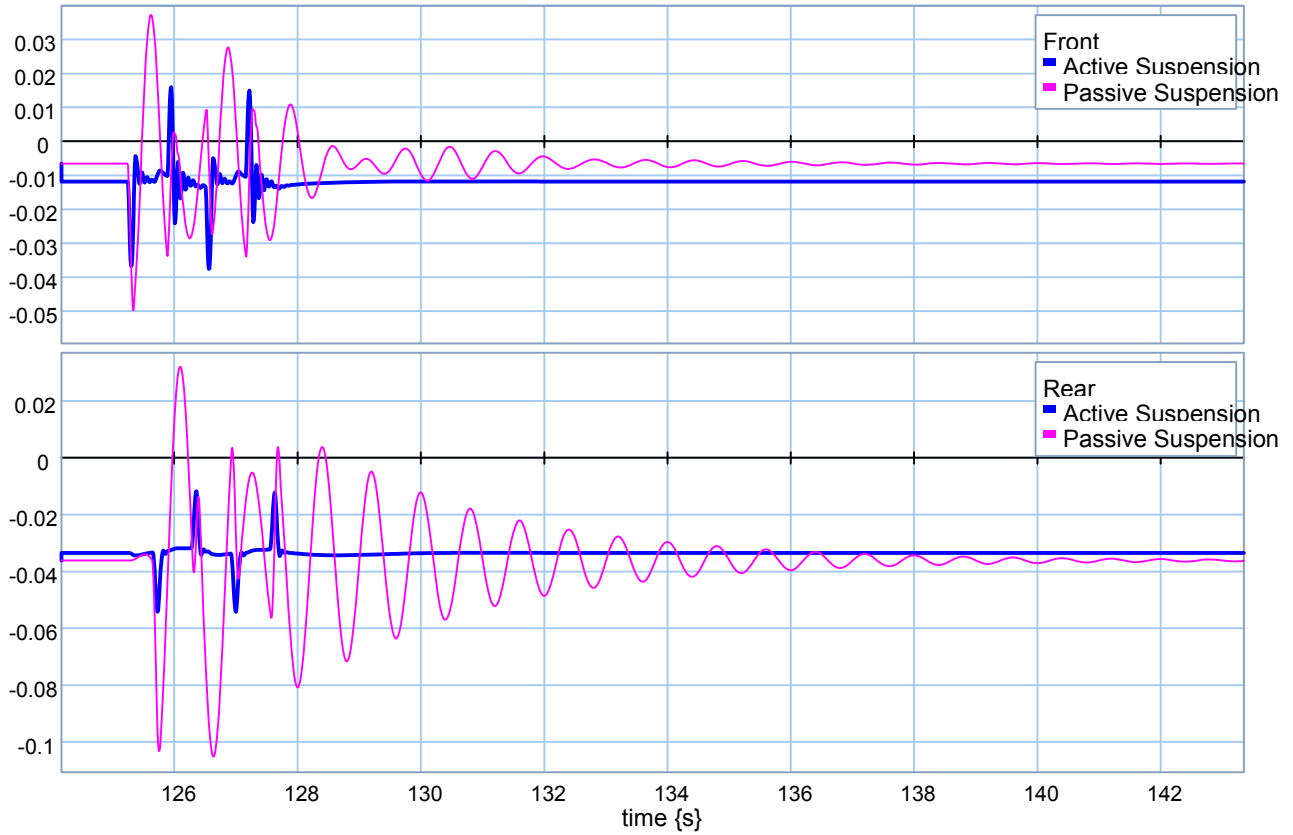
❖ **$M_c = 9000 \text{ kg.}$**

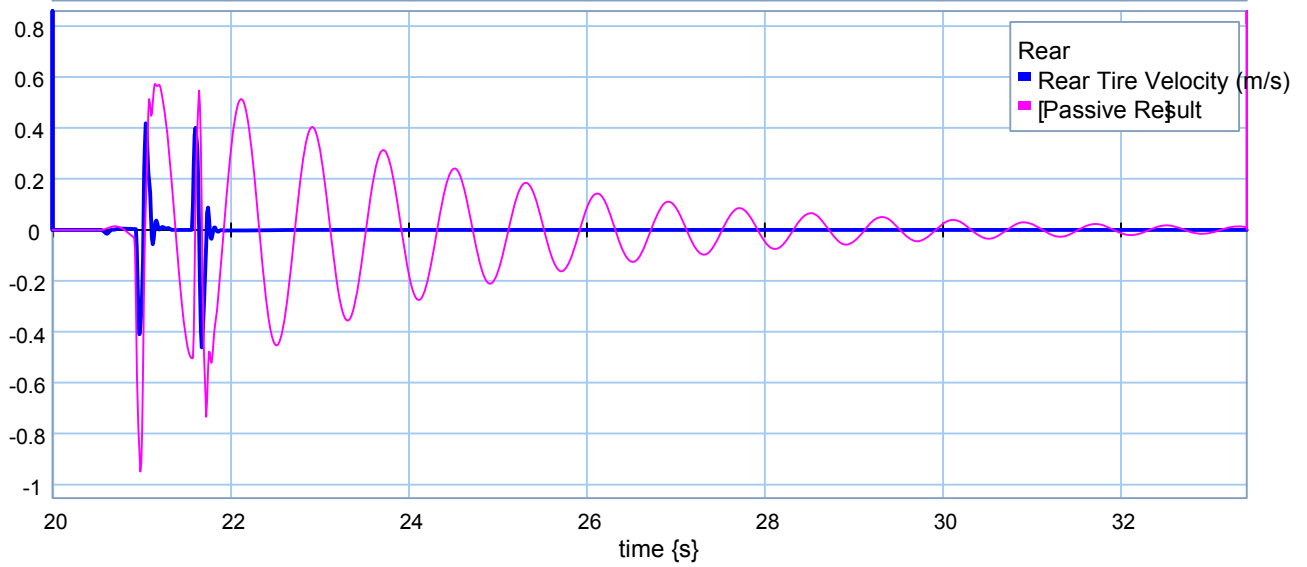
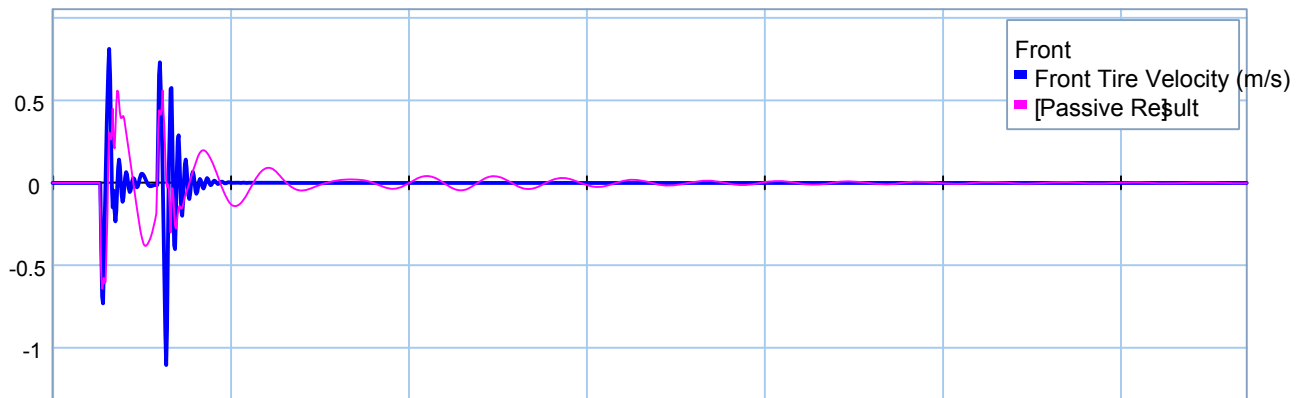
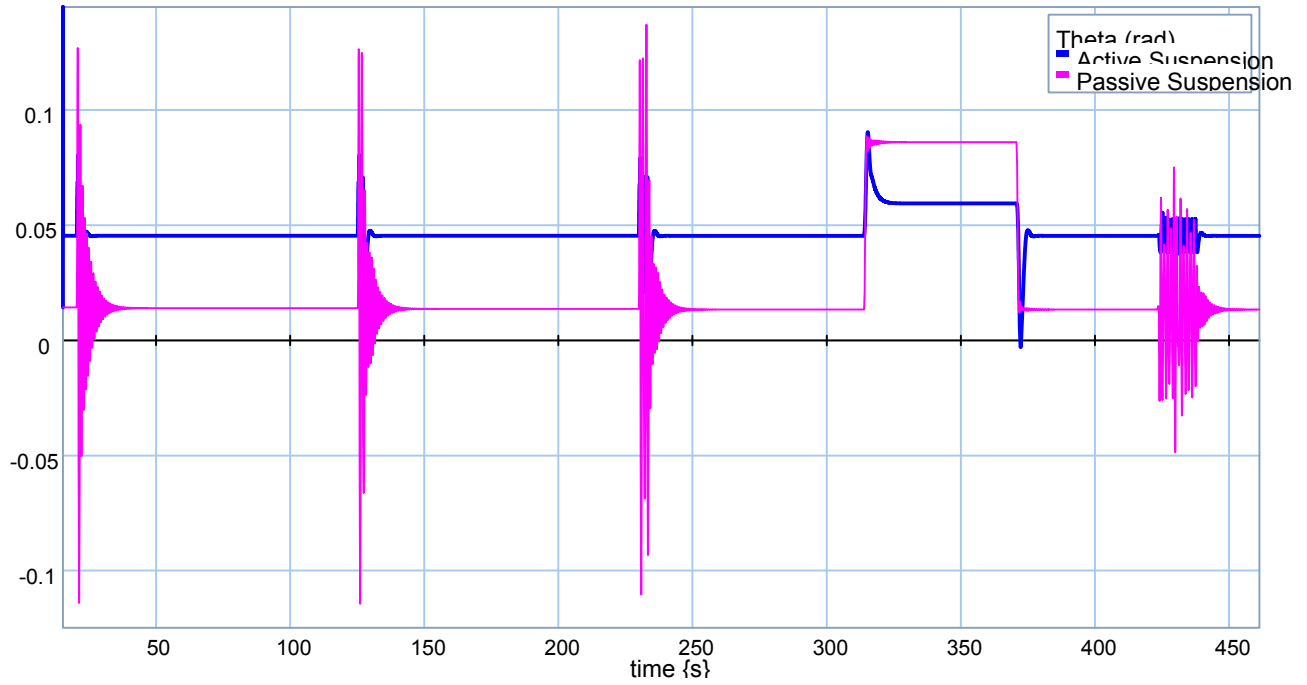


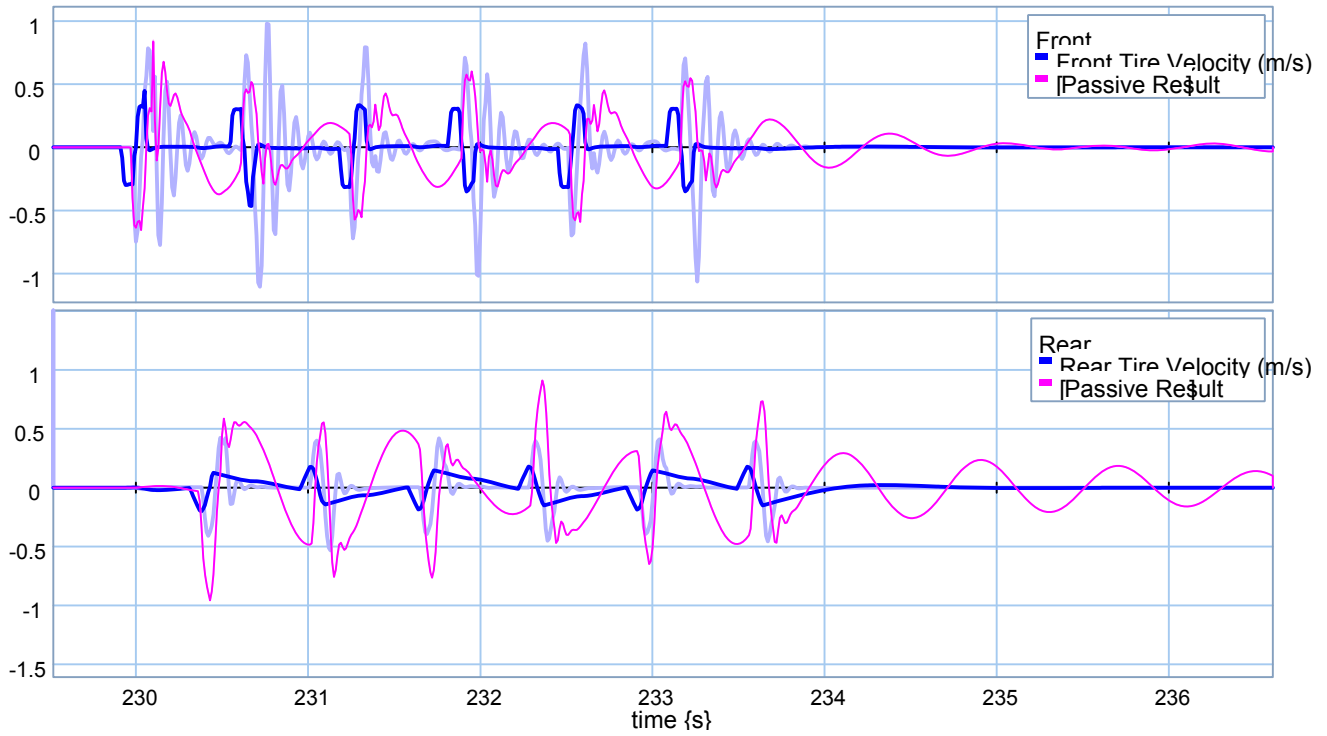




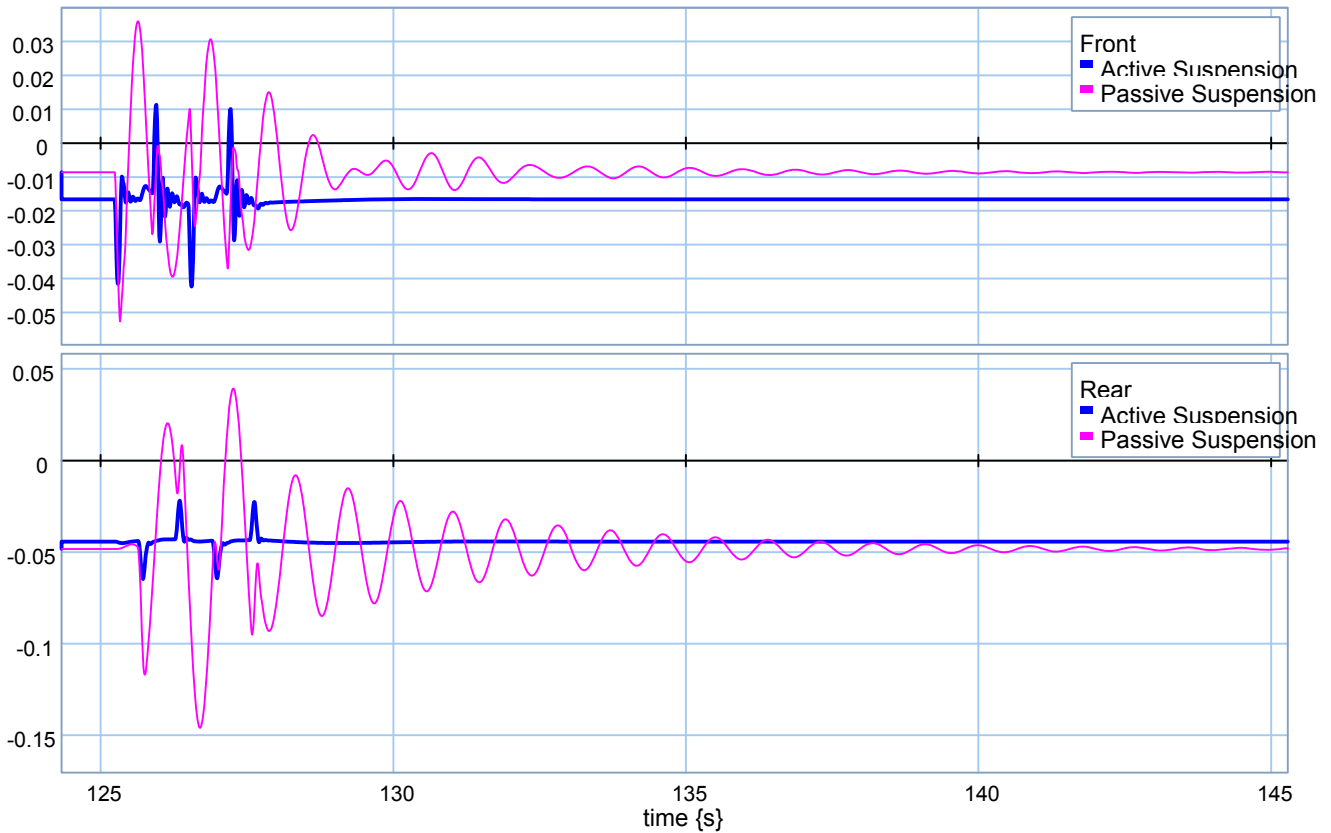
❖ **$M_c = 13500 \text{ kg.}$**

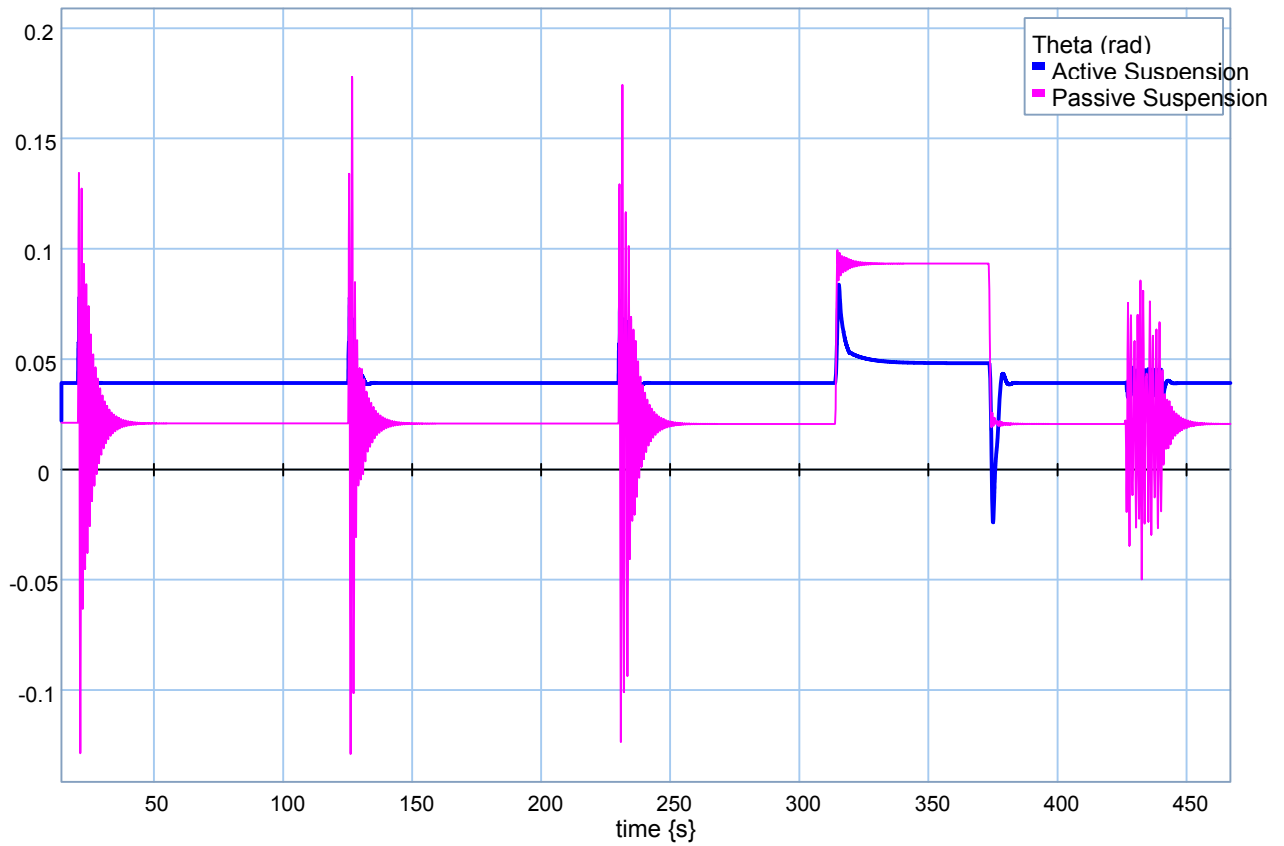
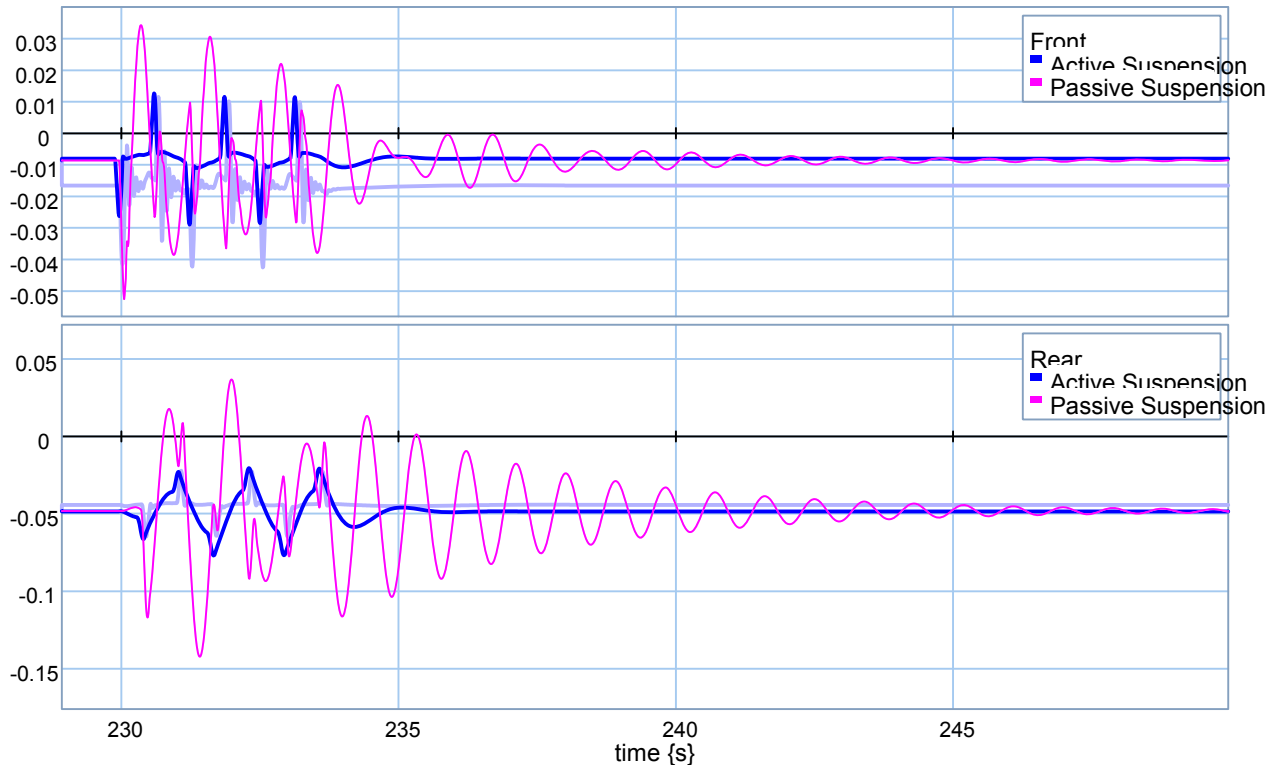


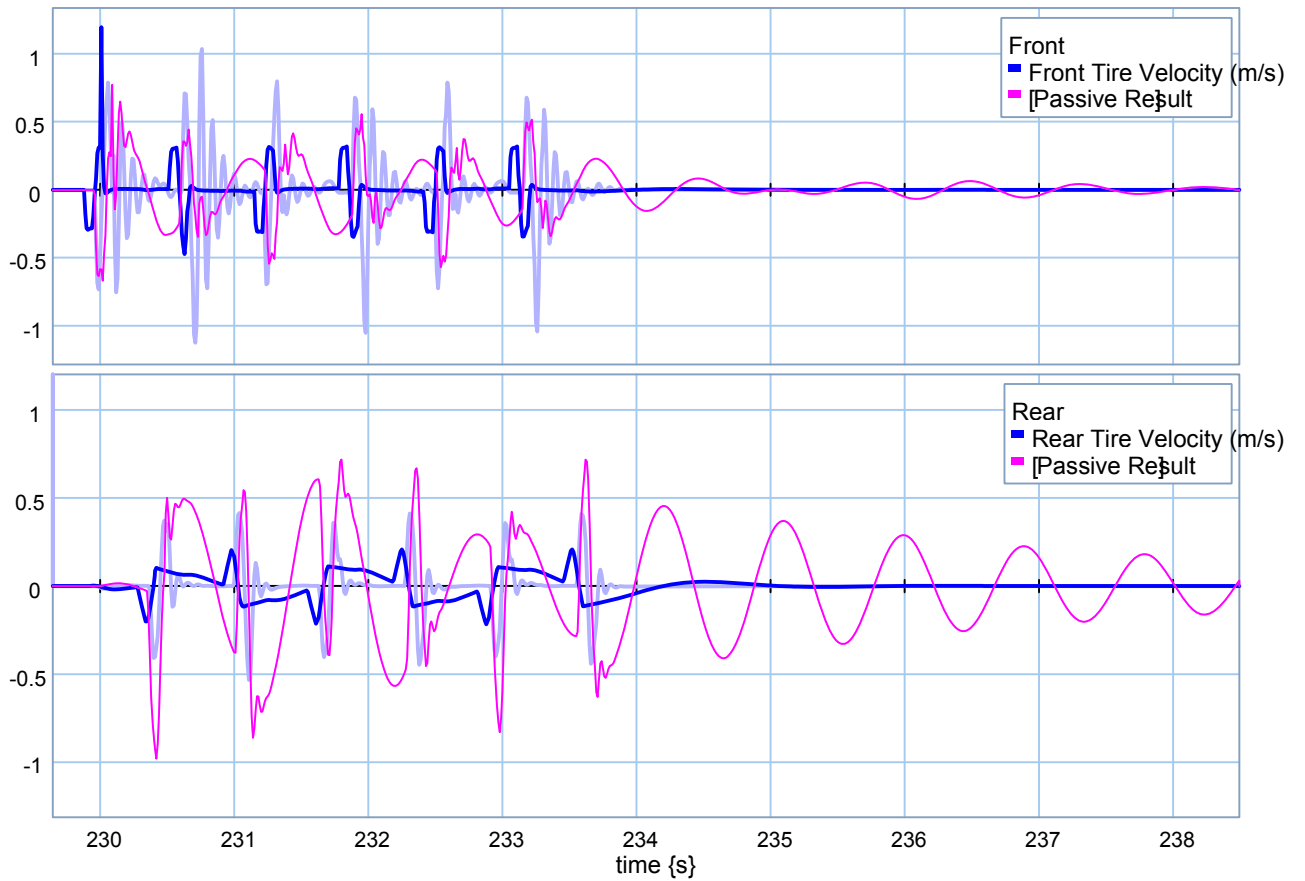
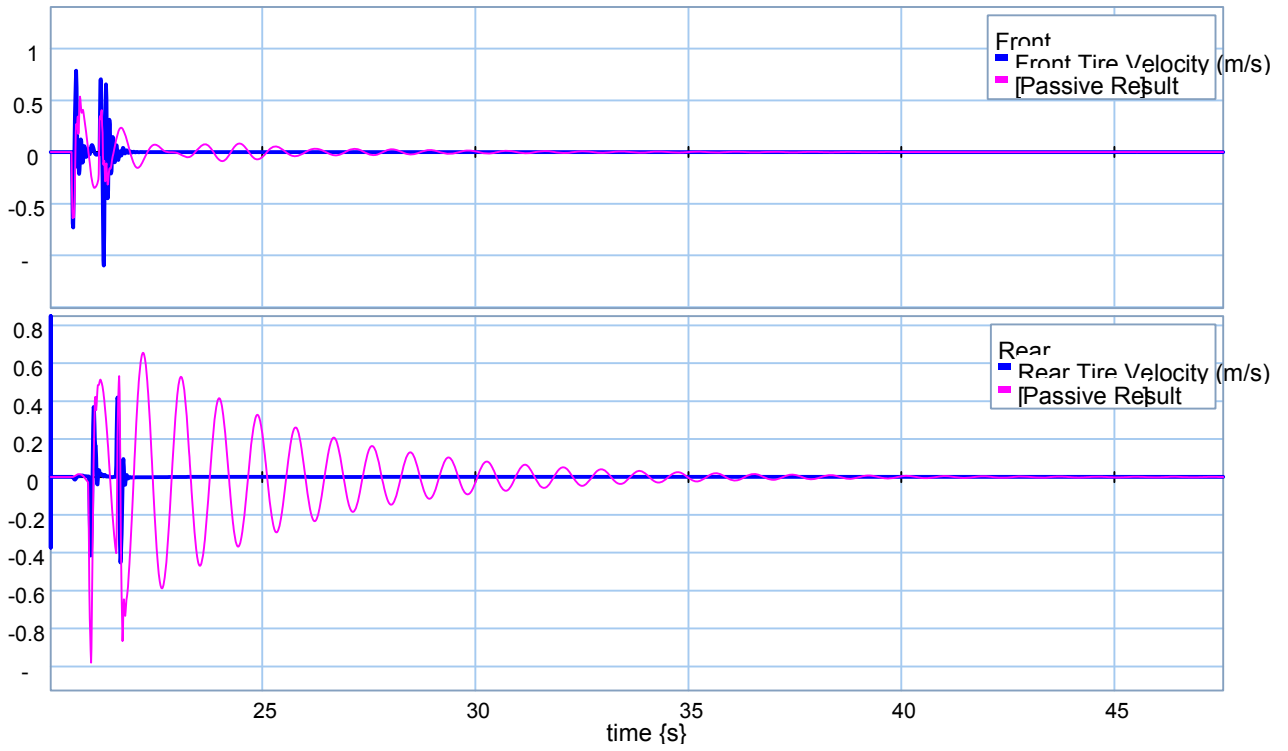




❖ **$M_c = 18000 \text{ kg.}$**

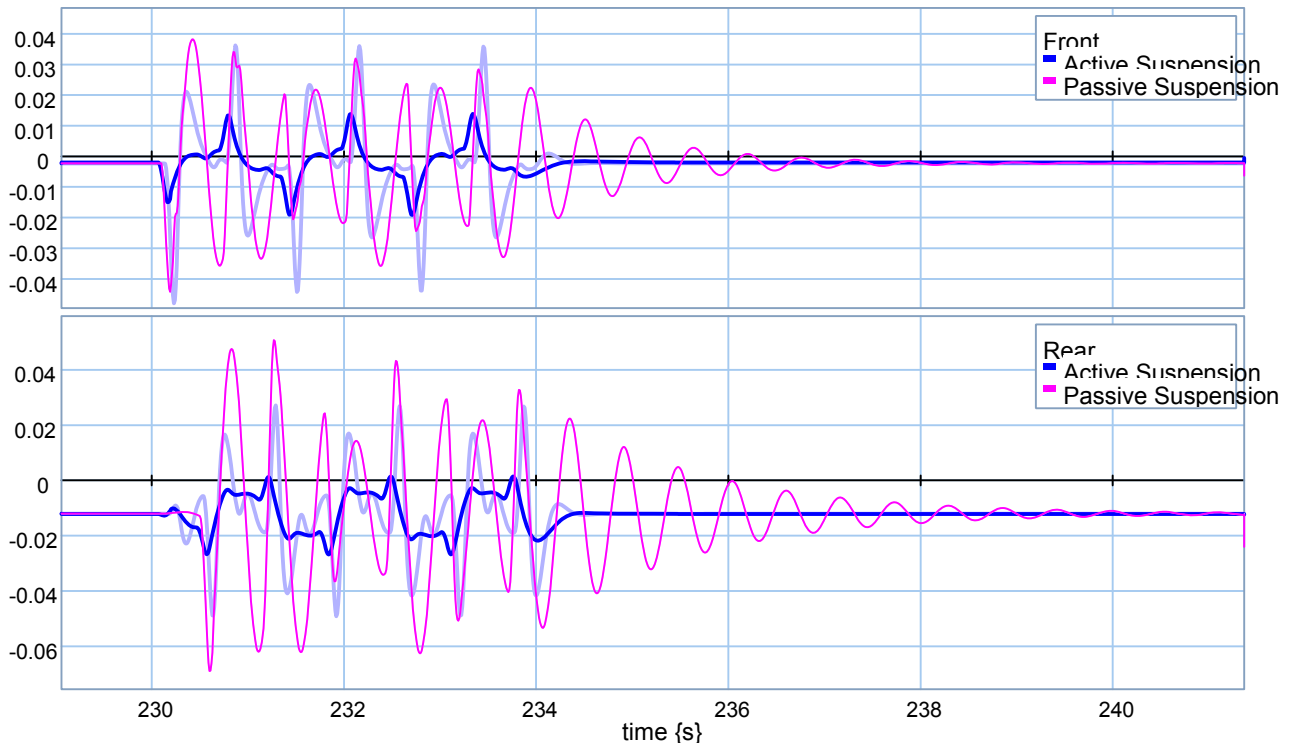
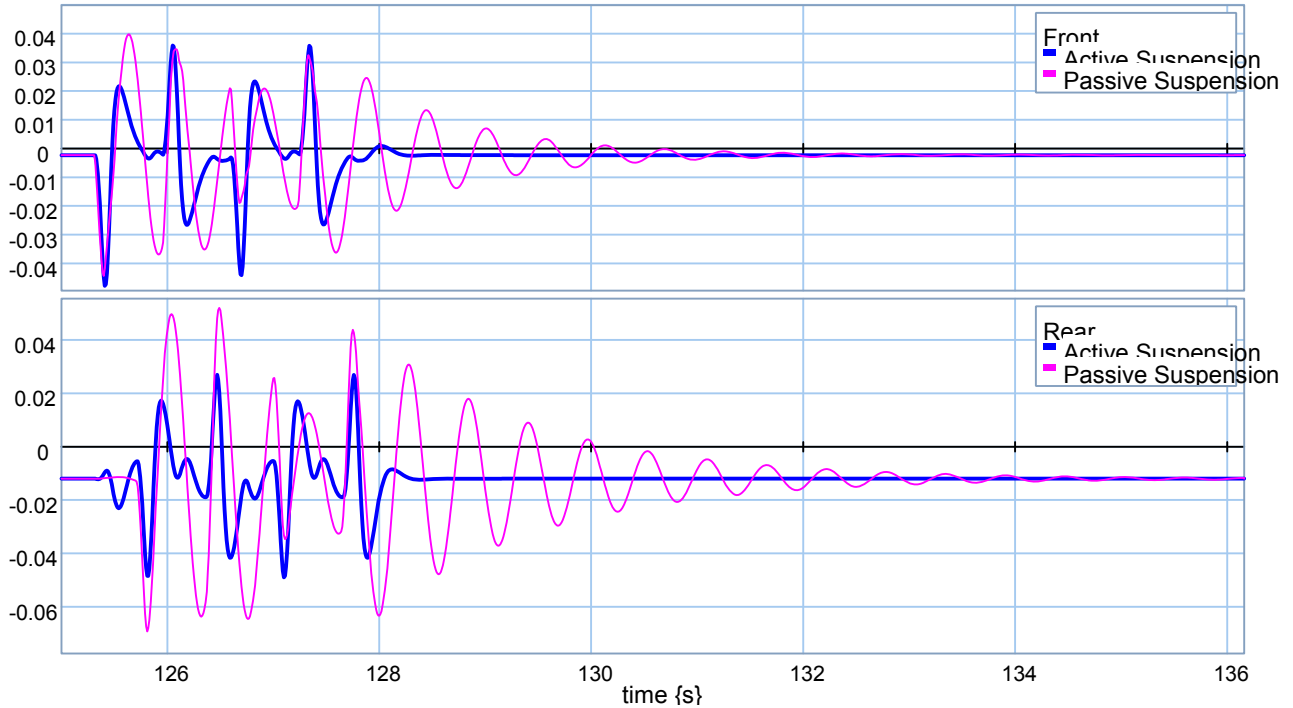


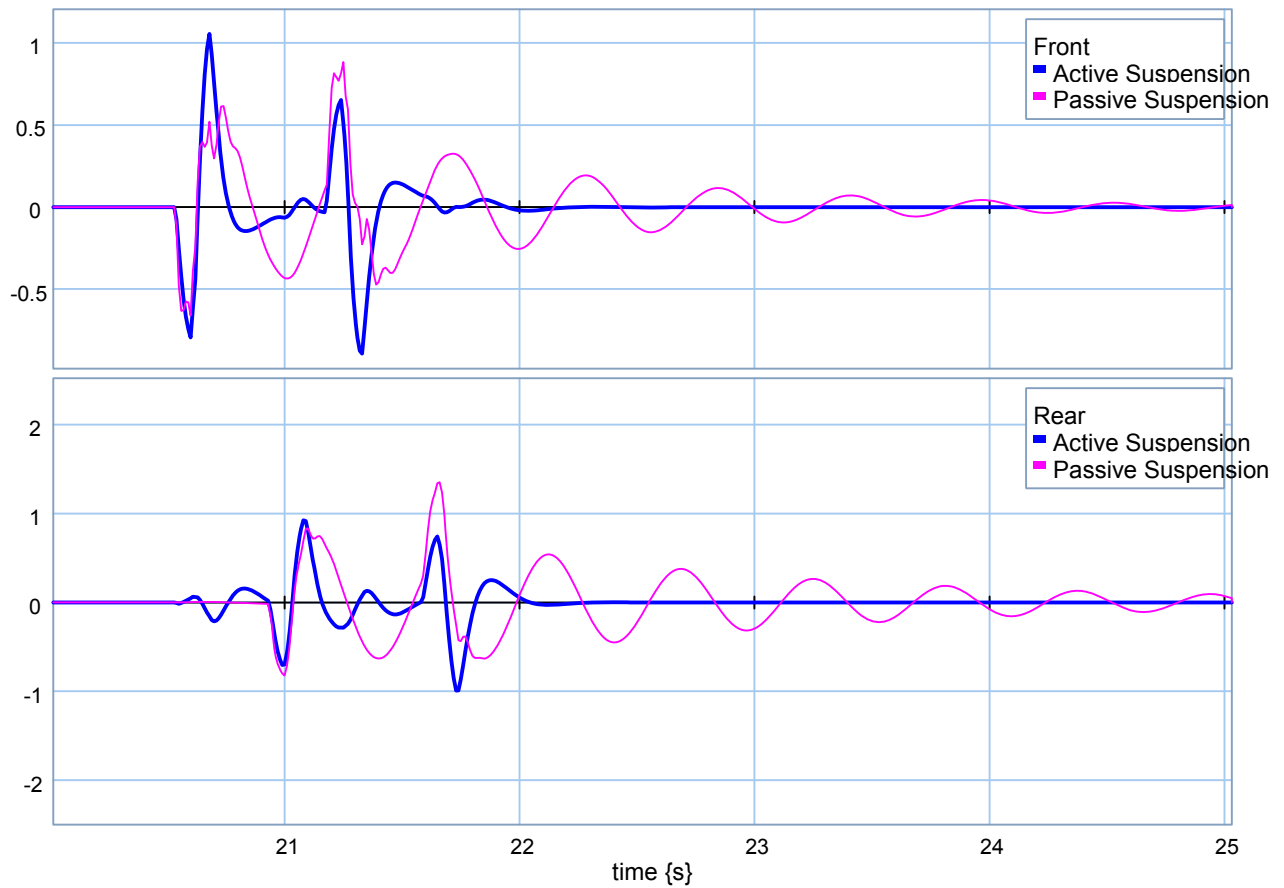
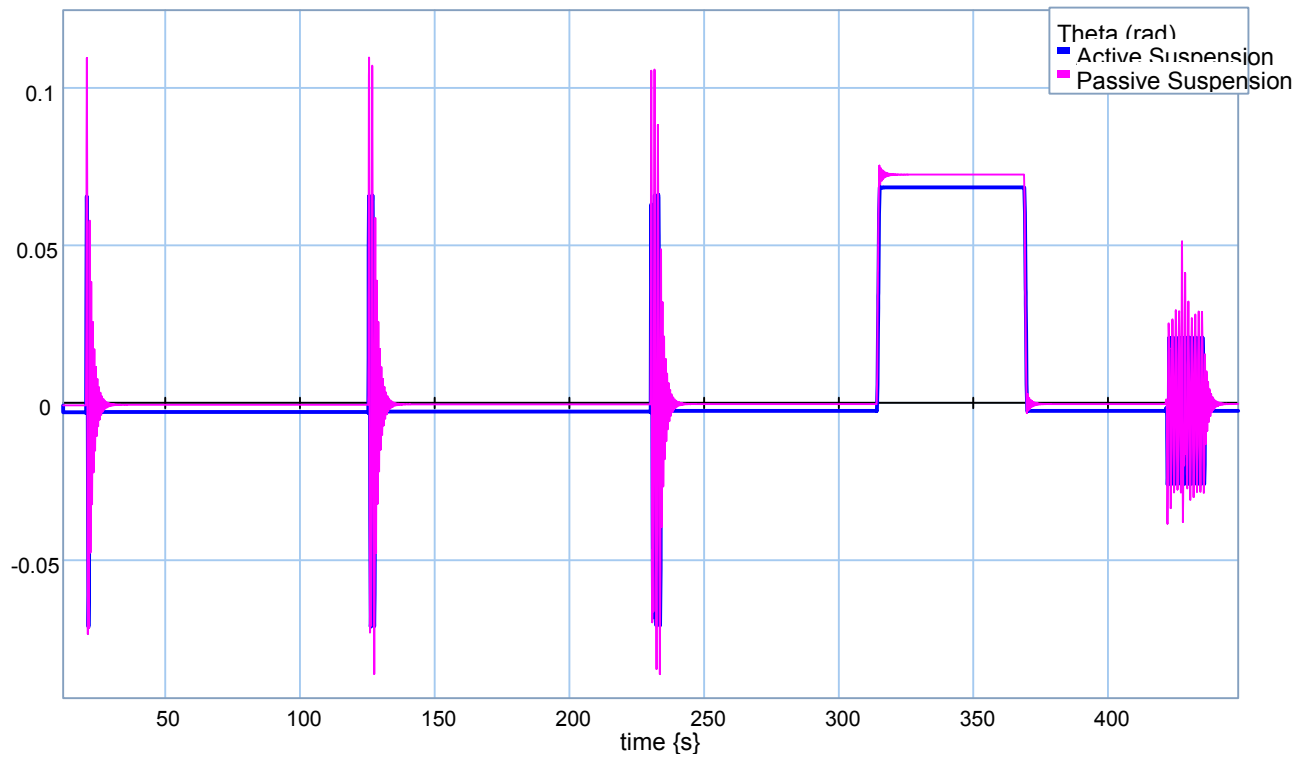


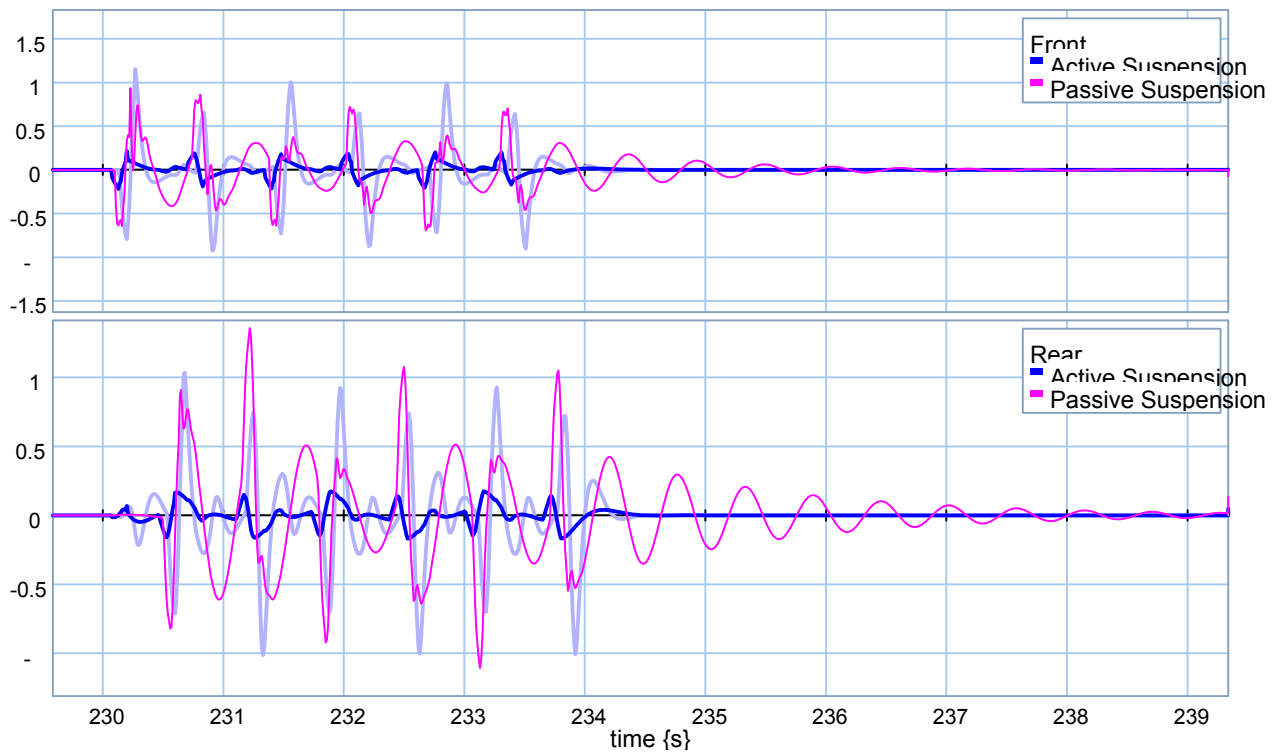


Appendix I: Non-Linear Half-Car Model, Road HoldingScenario, HalfCar Active Suspensions.

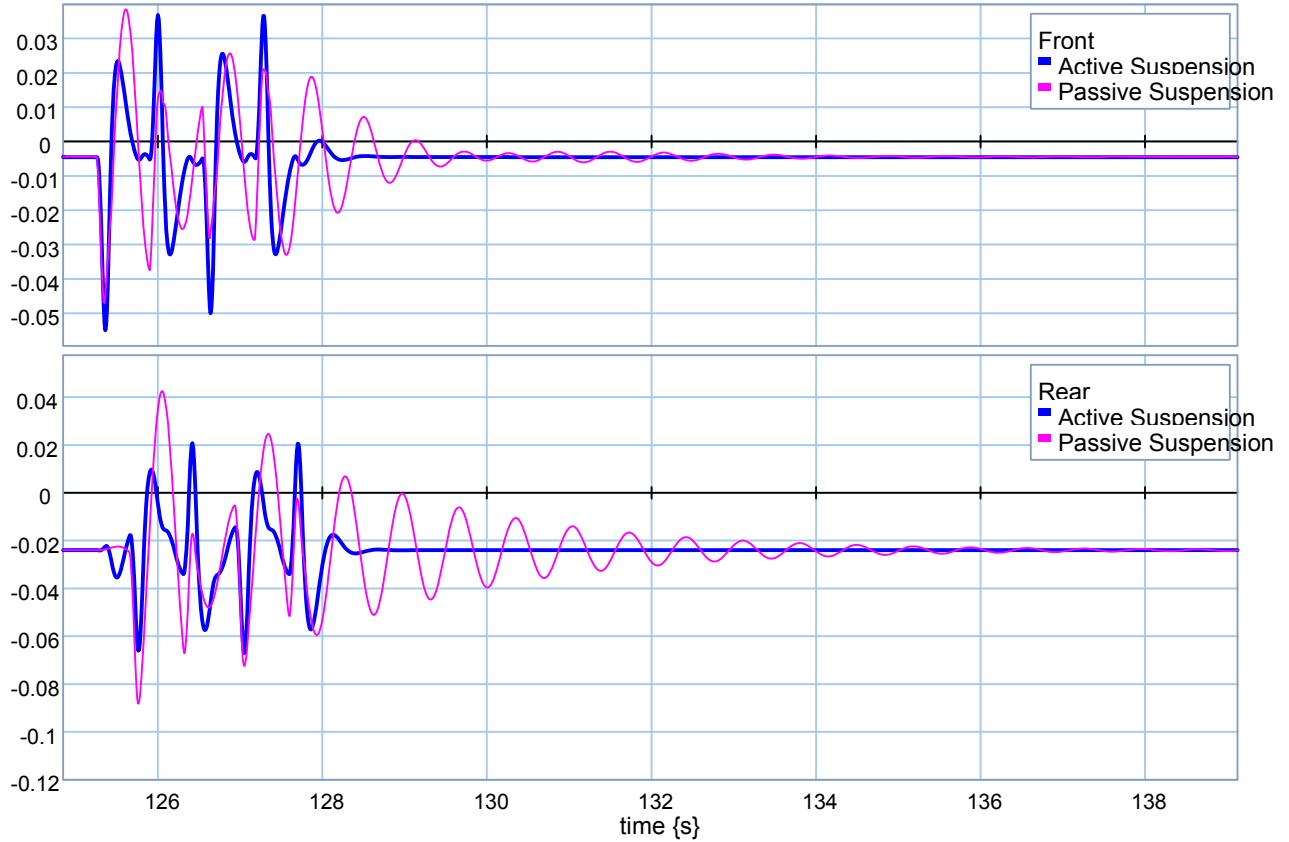
❖ $M_c = 4500 \text{ kg}$.

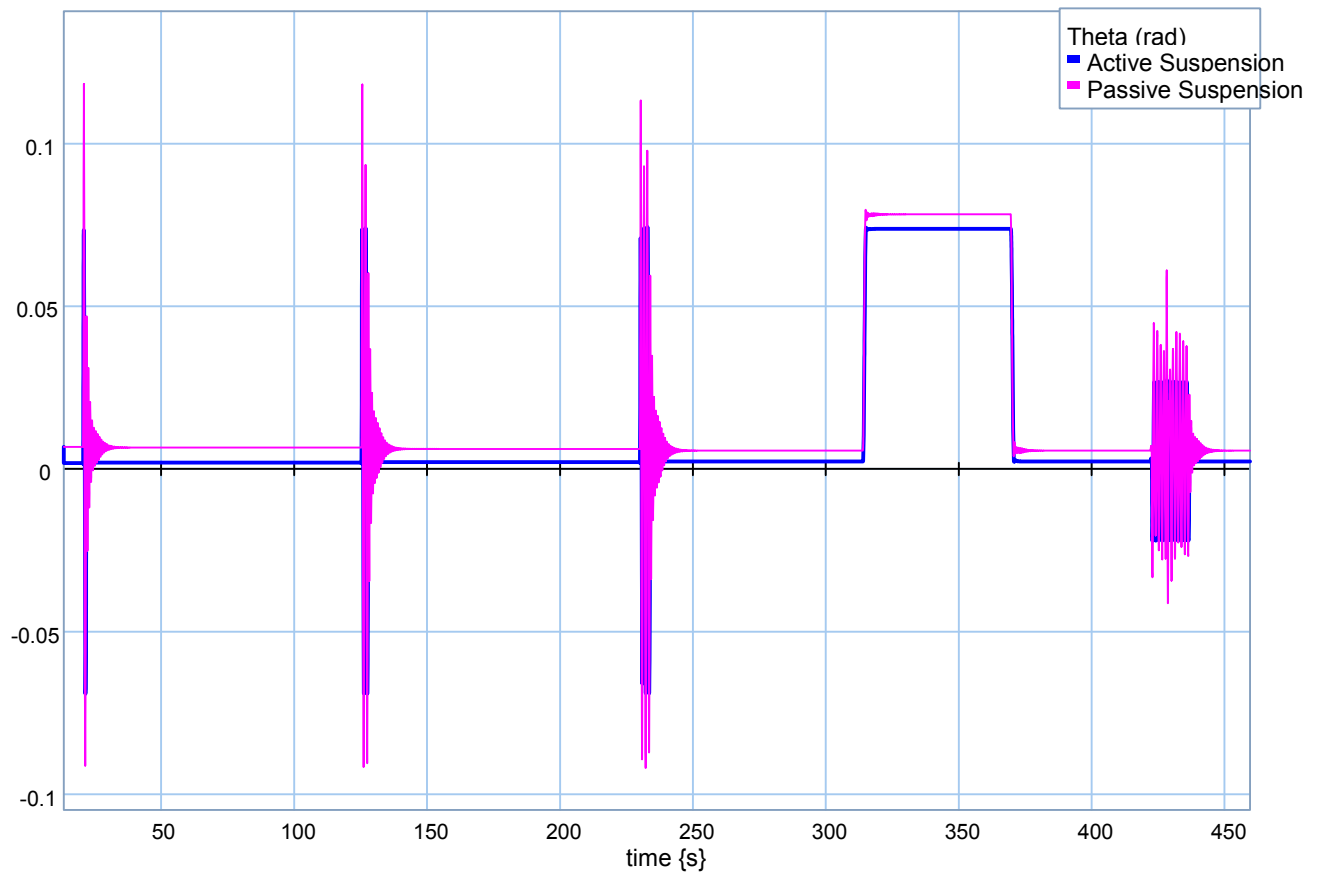
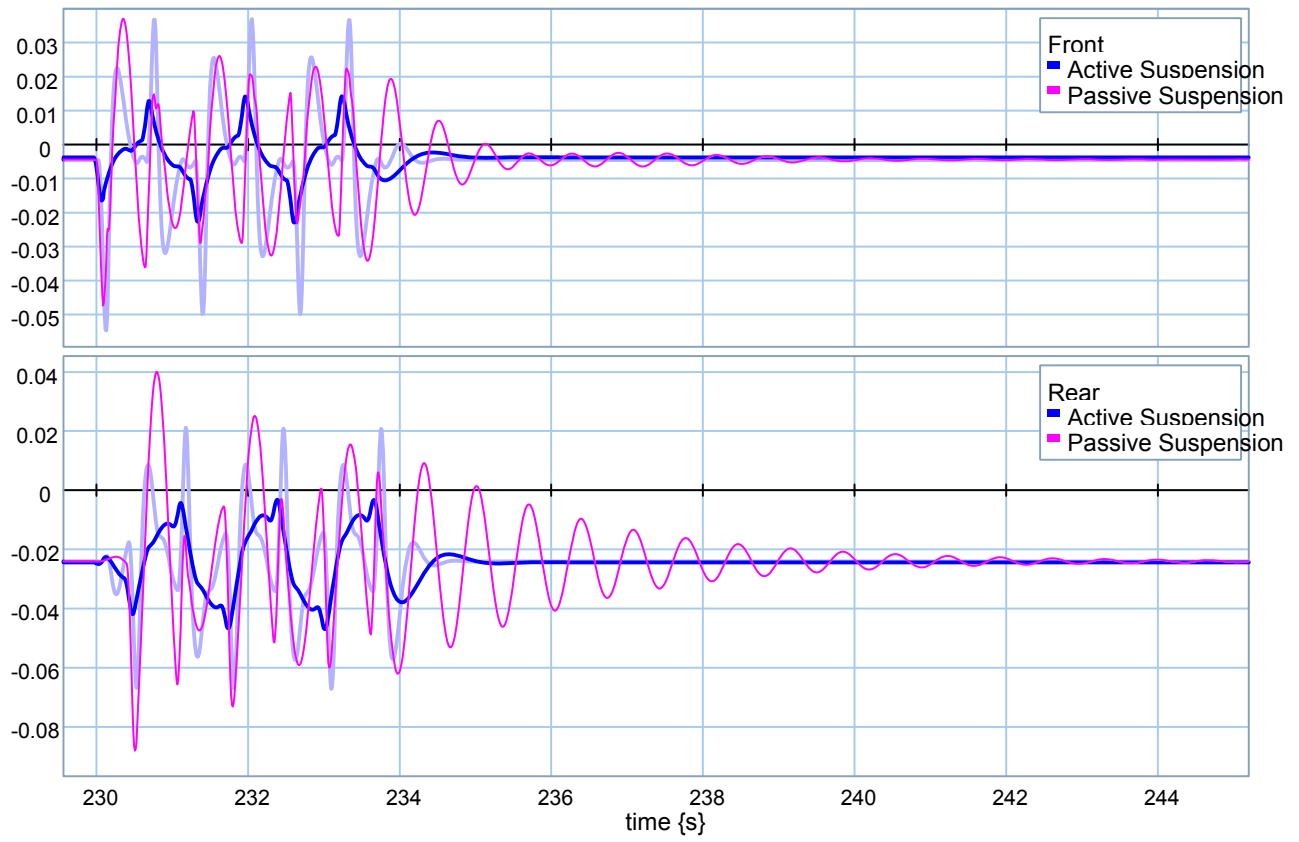


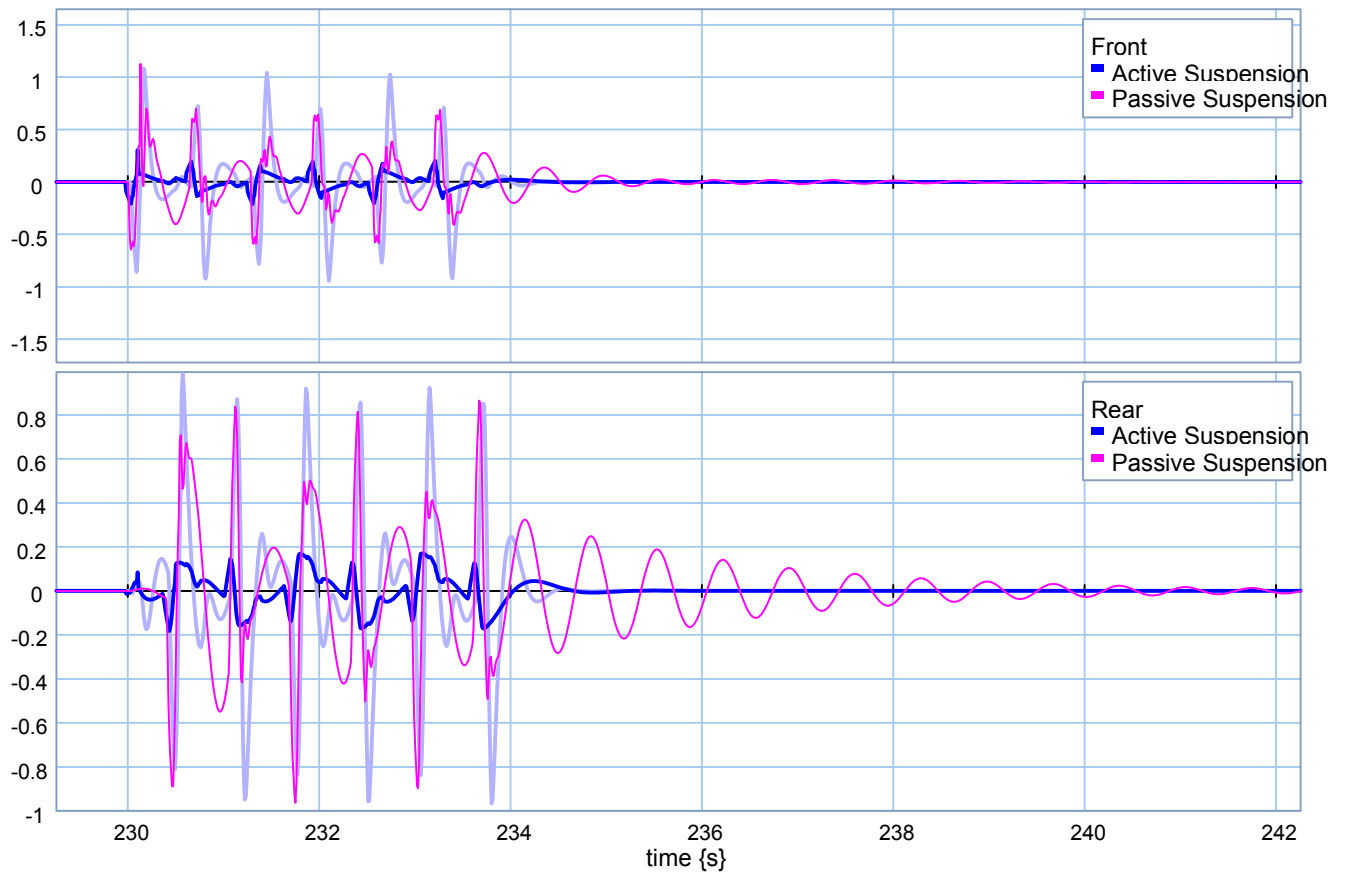
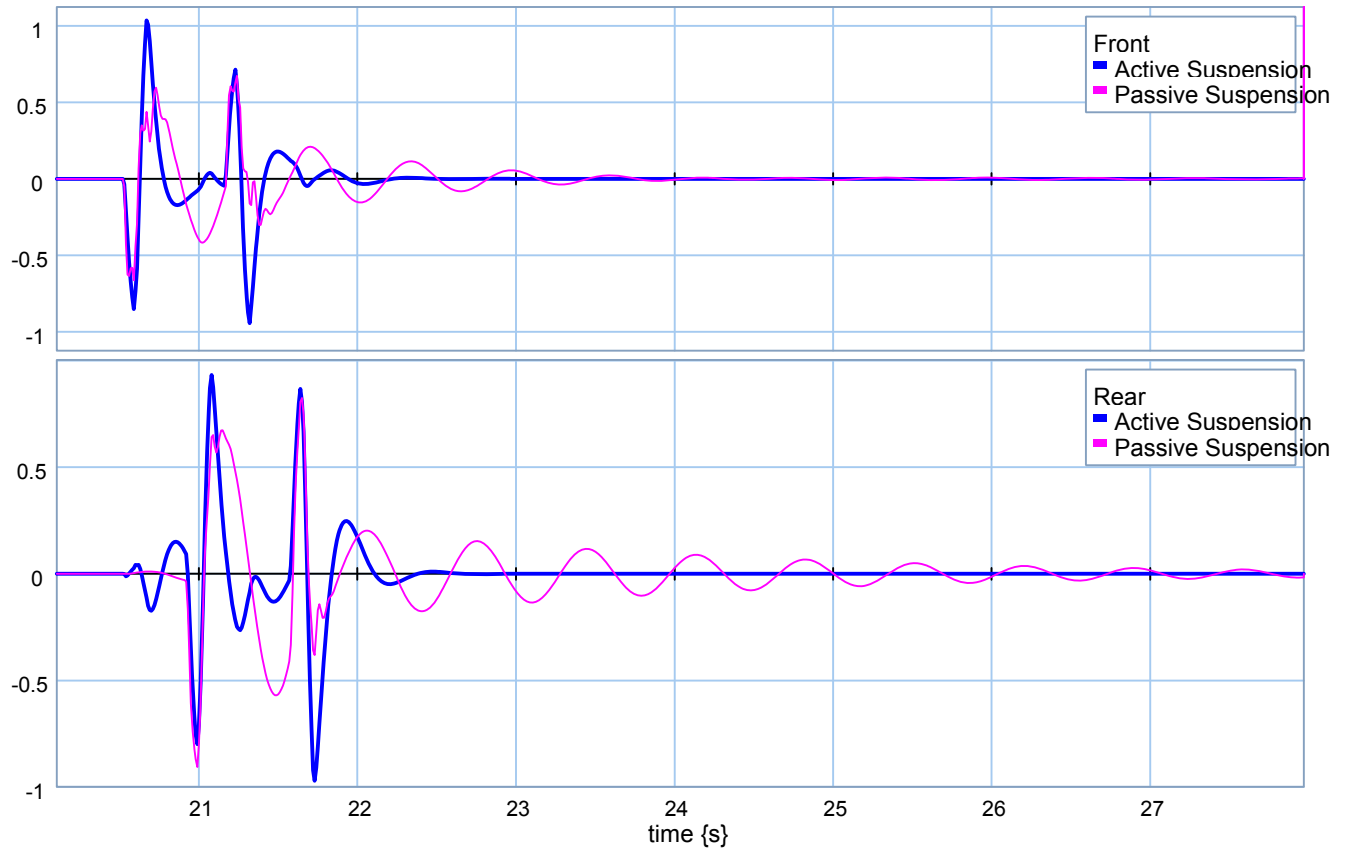




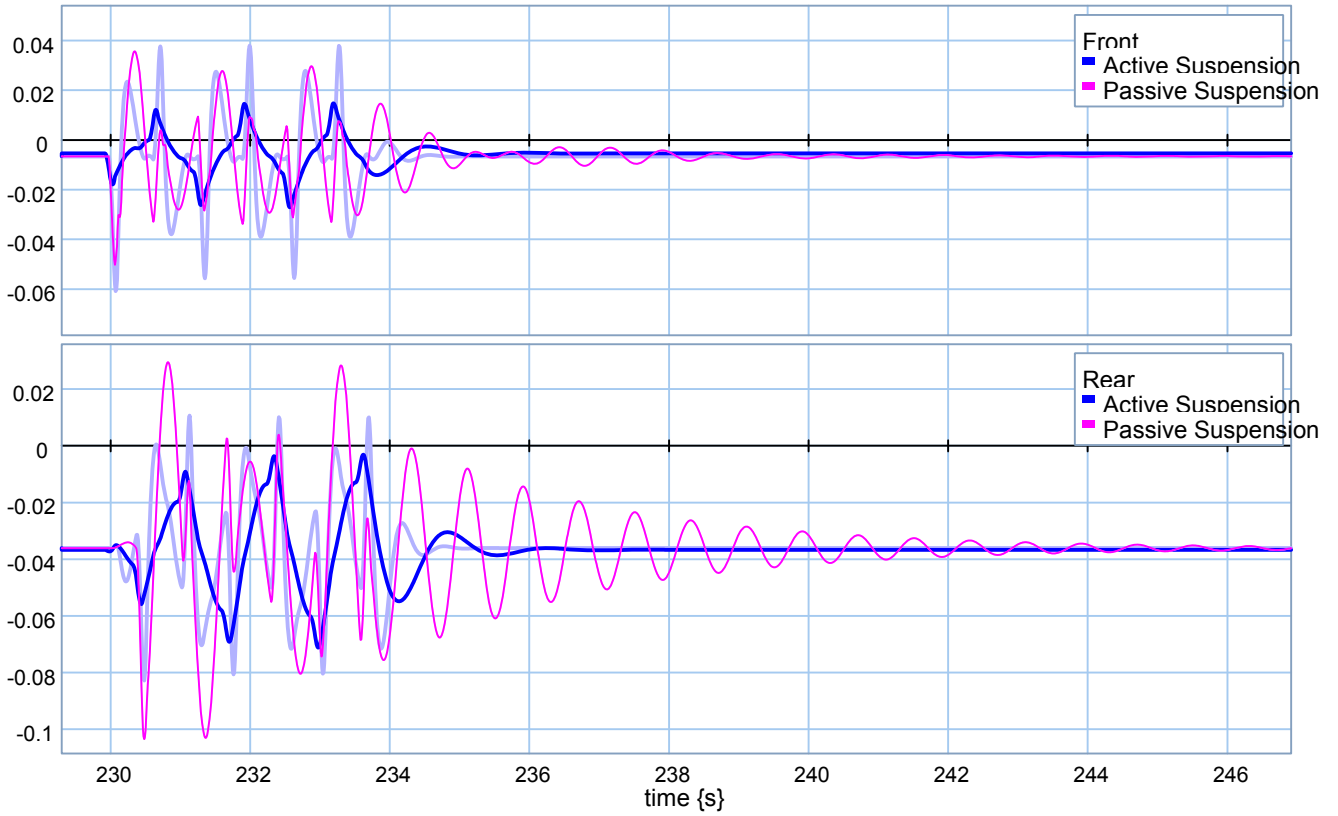
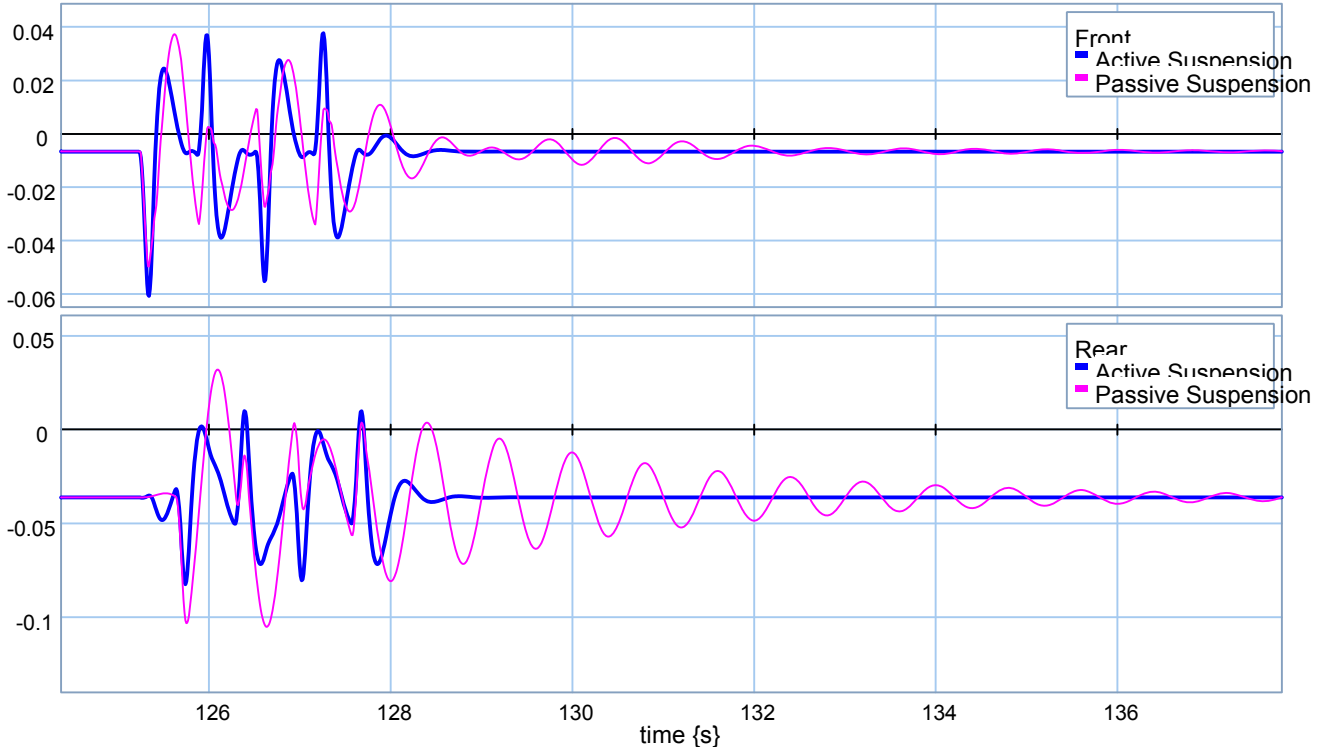
❖ **$M_c = 9000 \text{ kg.}$**

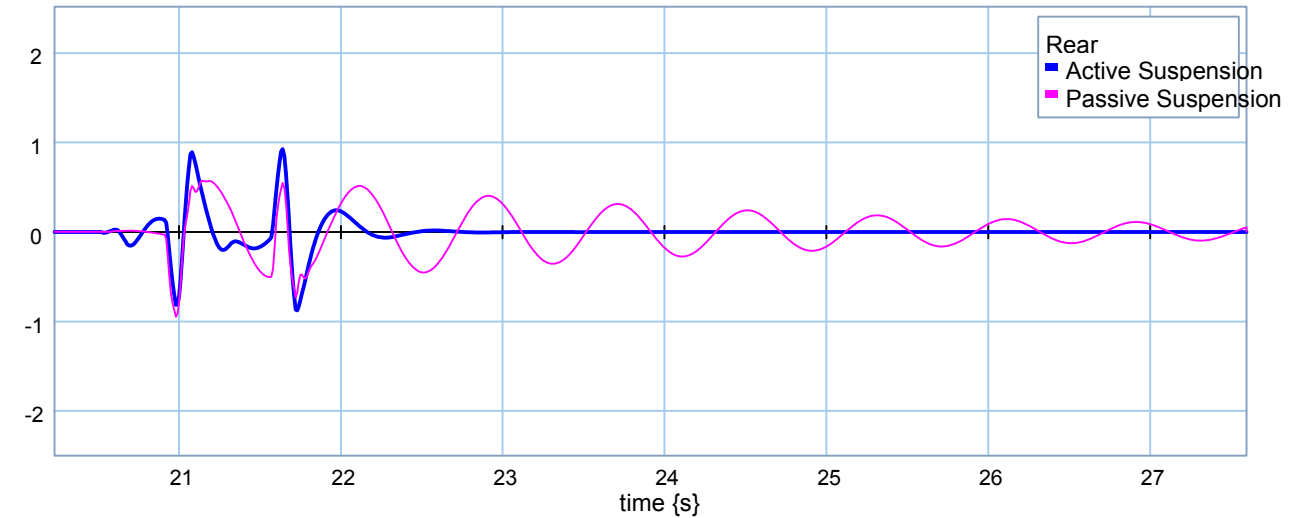
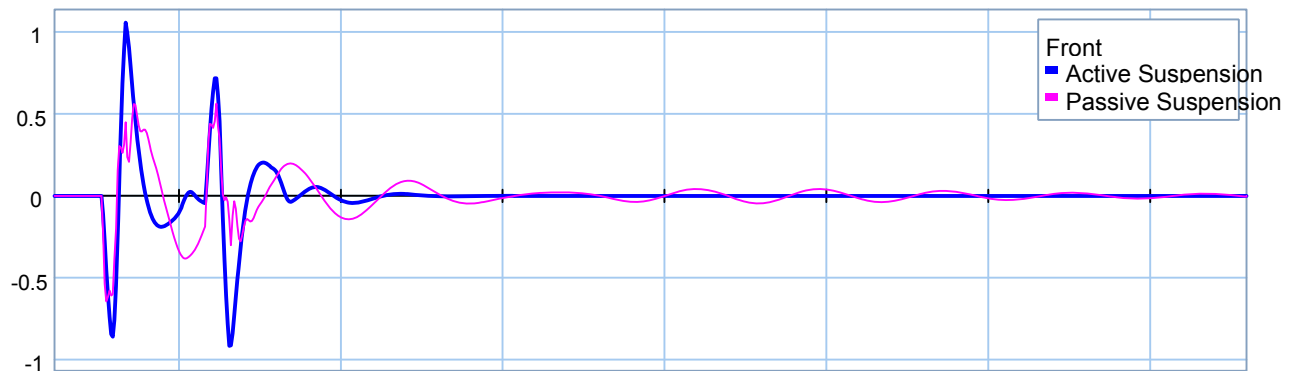
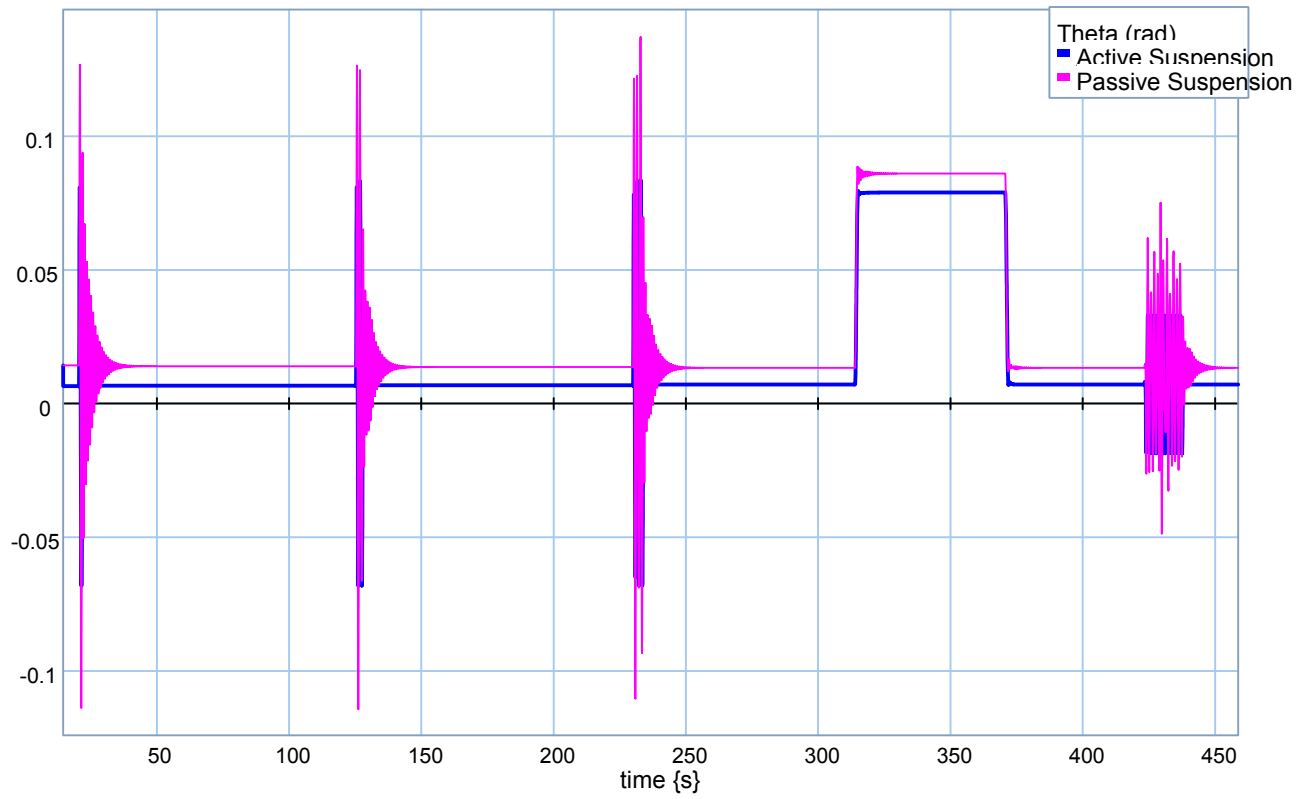


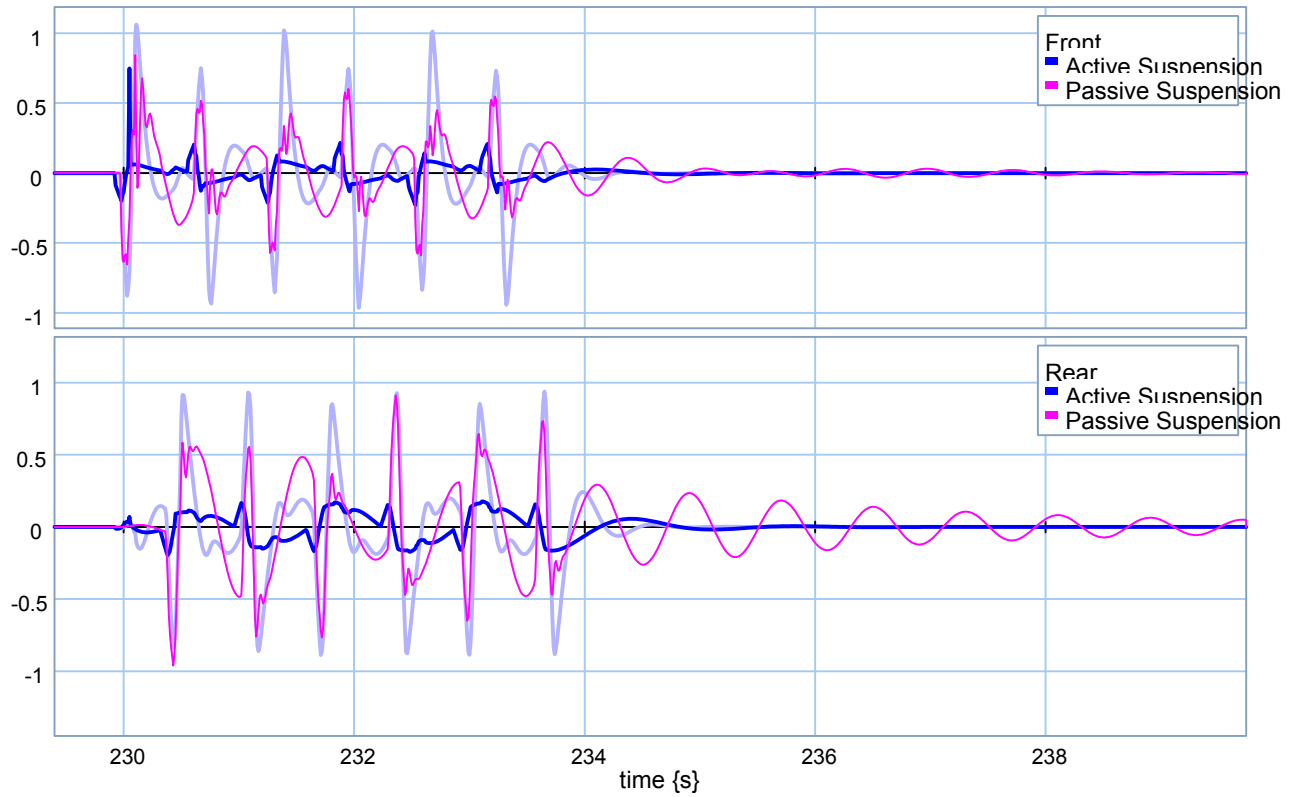




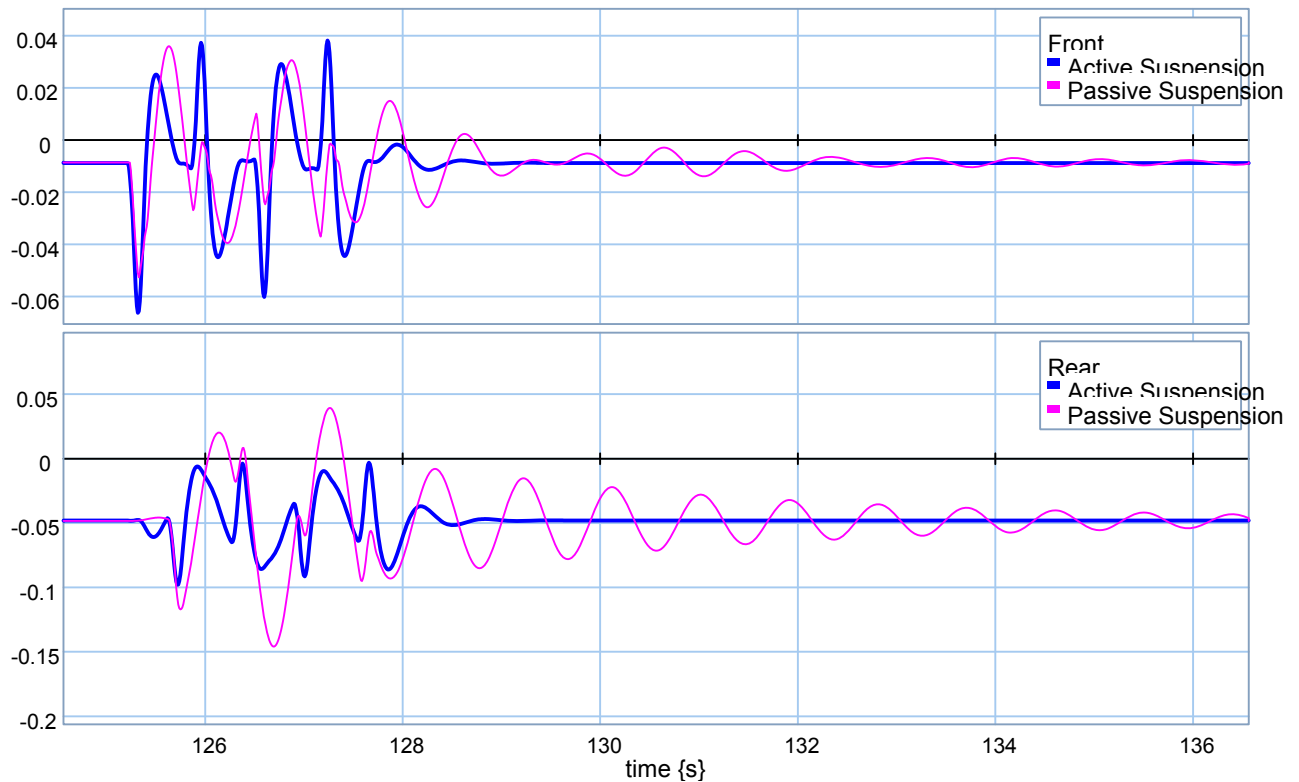
❖ **Mc = 13500 kg.**

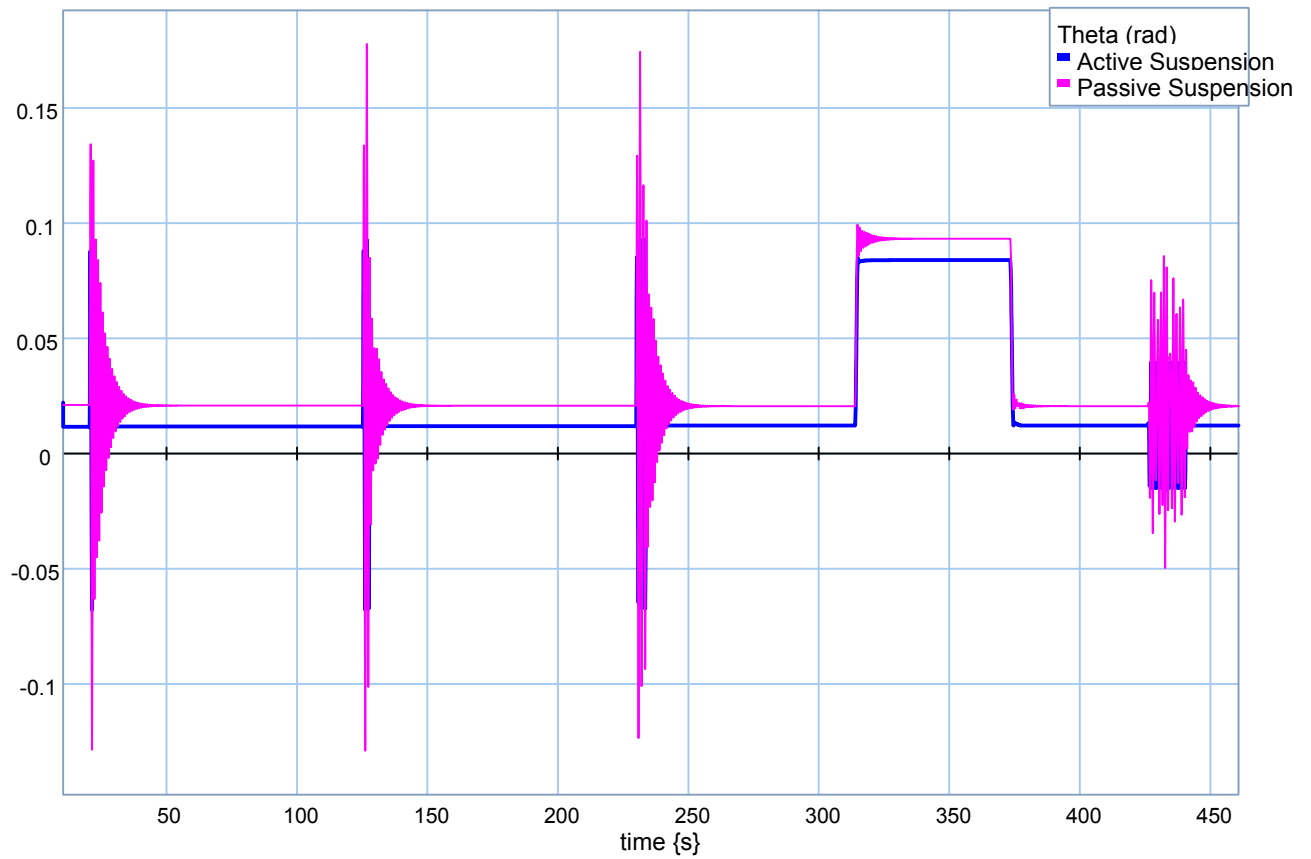
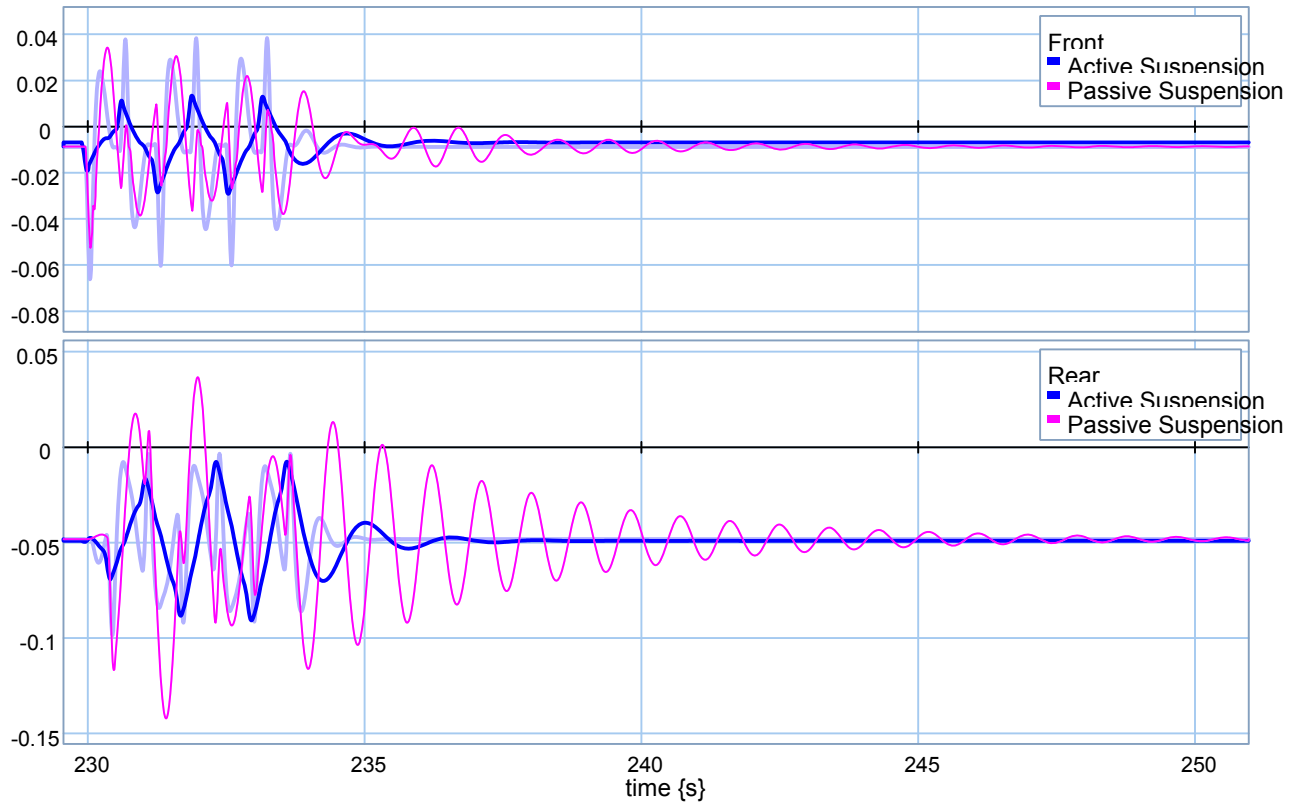


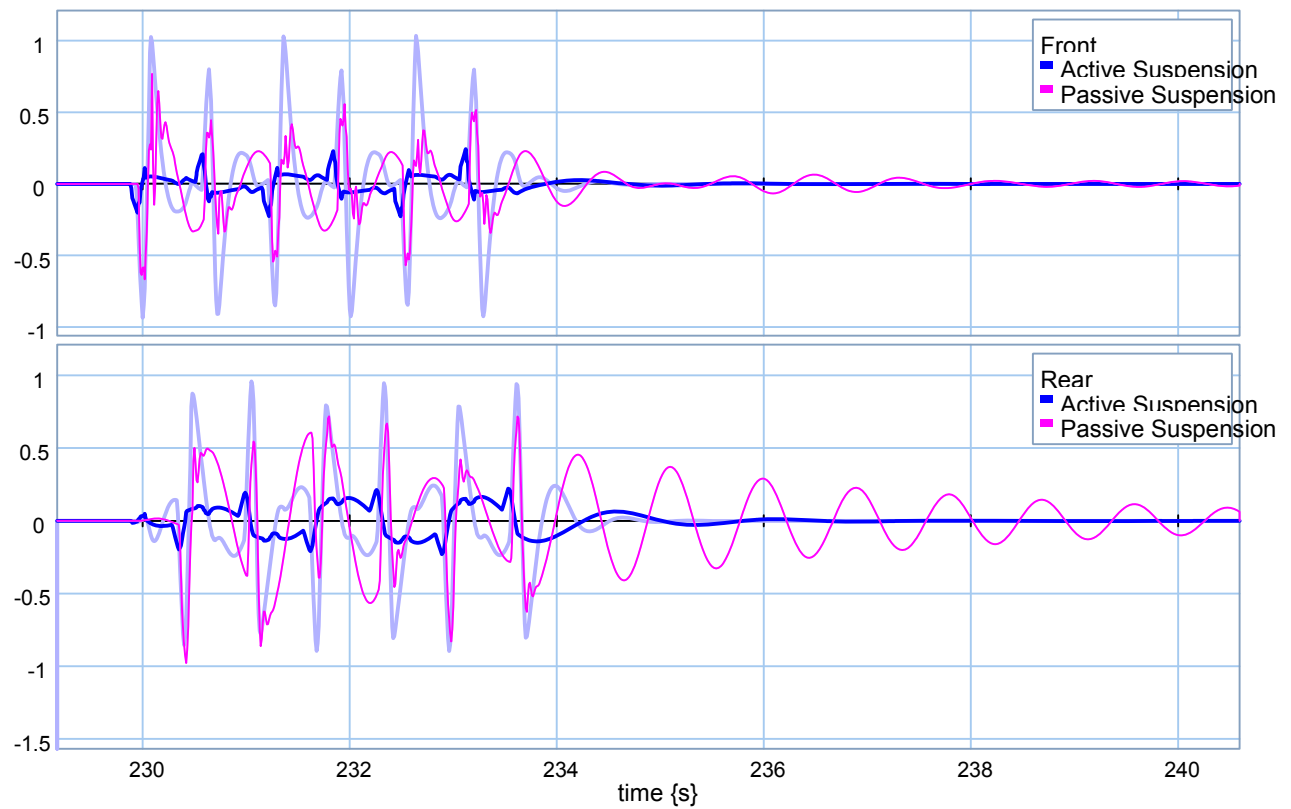
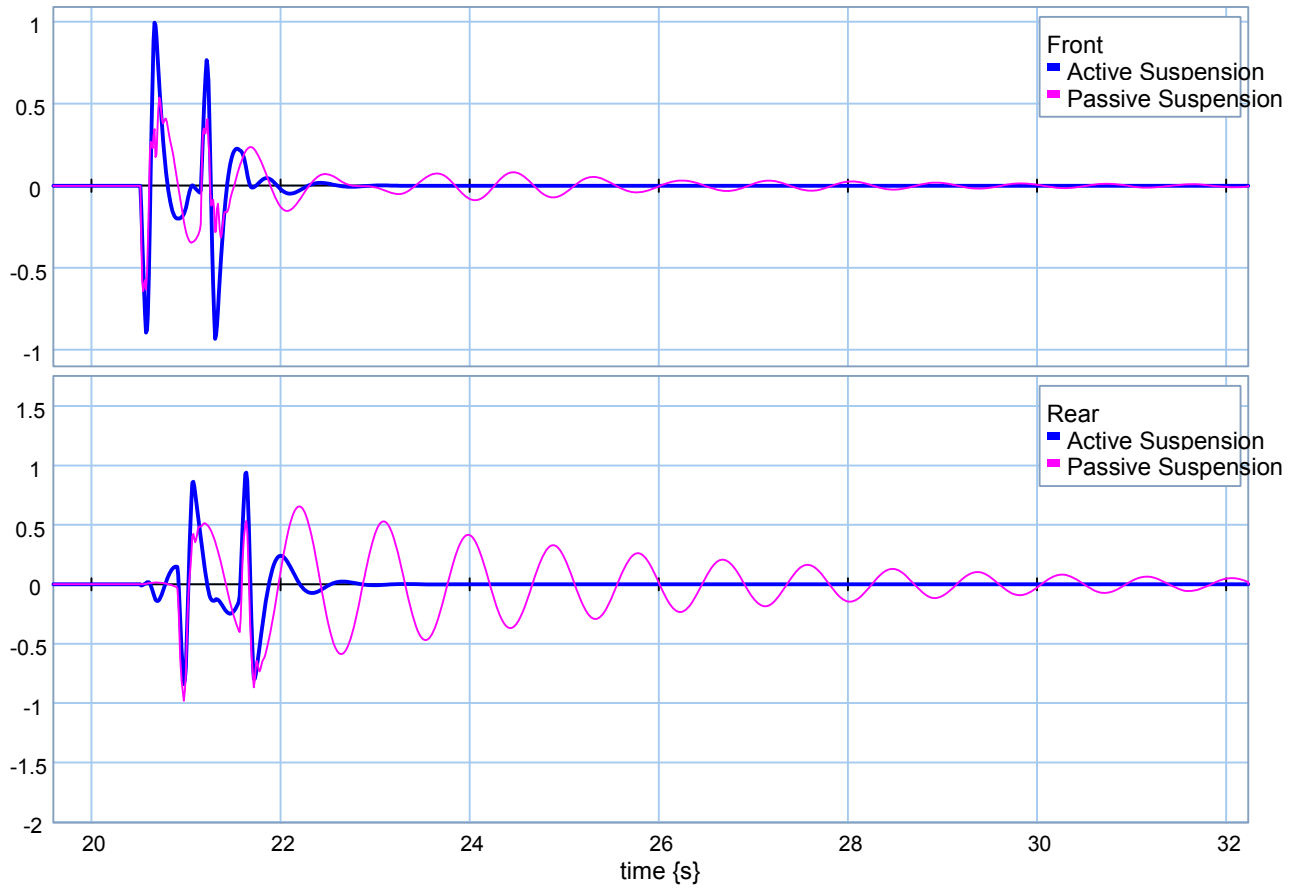




❖ **$M_c = 18000 \text{ kg.}$**







Appendix J: Non-Linear HalfCar Model, Quarter Car and Half-Car Approaches Comparison.

❖ Road Holding

Time	Passive Suspension		QuarterCar Approach		HalfCar Approach	
	Vtf	Vtr	Vtf	Vtr	Vtf	Vtr
0	1.04E-15	-1.82E-15	6.12E-16	1.99E-15	1.07E-15	-5.83E-16
0.5002	6.2E-17	-1.65E-16	0.00199551	0.01256801	0.00065889	-0.0012638
1.000006	-1.39E-17	1.35E-16	0.00032449	0.0003514	0.0000683	0.0000349
1.500076	-3.39E-17	1.42E-16	-0.0000425	0.000021	0.0000152	0.0000296
2.000147	4.61E-17	-7.75E-17	-0.0000578	-0.0000416	-8.74E-07	0.00000177
2.500218	7.53E-17	1.64E-16	-0.000021	-0.000021	-1.54E-06	-7.37E-07
3.000023	-2.32E-17	9.24E-17	-3.32E-06	-4.37E-06	-0.0000005	-3.21E-07
3.500094	3.94E-17	-6.1E-17	6.23E-07	4.31E-07	-8.59E-08	-6.3E-08
4.000164	3.47E-17	3.18E-17	5.69E-07	0.00000071	-2.69E-09	2.04E-09
4.500235	4.16E-17	3.52E-17	1.65E-07	2.99E-07	2.33E-09	6.77E-09
5.000041	4.16E-17	-7.63E-17	5.96E-09	7.31E-08	-1.6E-10	3.22E-09
5.500111	3.62E-17	1.45E-16	-1.76E-08	8.72E-09	-7.96E-10	1.17E-09
6.000182	3.25E-17	-2.48E-18	-9.68E-09	-2.03E-10	-5.66E-10	4.38E-10
6.500253	6.94E-17	-8.29E-17	-3.07E-09	6.02E-10	-2.96E-10	1.94E-10
7.000058	-2.08E-17	1.41E-16	-6.52E-10	9.95E-10	-1.41E-10	9.8E-11
7.500129	9.44E-18	-1.61E-16	-1.12E-10	6.92E-10	-6.7E-11	5.08E-11
8.000199	-1.47E-16	8.35E-17	-4.68E-11	3.45E-10	-3.27E-11	2.59E-11
8.500005	-4.63E-17	1.61E-16	-3.83E-11	1.45E-10	-1.62E-11	1.3E-11
9.000076	-3.24E-17	-9.5E-17	-2.52E-11	5.8E-11	-8.11E-12	6.47E-12
9.500146	3.25E-17	4.78E-18	-1.3E-11	2.41E-11	-4.05E-12	3.21E-12
10.00022	2.73E-17	-7.38E-18	-5.82E-12	1.08E-11	-2.02E-12	1.6E-12
10.50002	6.94E-18	-3.1E-17	-2.44E-12	5.07E-12	-1E-12	7.94E-13
11.00009	-1.18E-17	1.38E-17	-1.03E-12	2.39E-12	-5E-13	3.98E-13
11.50016	-3.28E-17	2.65E-17	-4.54E-13	1.11E-12	-2.7E-13	2.02E-13
12.00023	0	3.03E-17	-2.23E-13	5.04E-13	-1.51E-13	1.11E-13
12.50004	0	4.88E-18	-1E-13	2.53E-13	-4.51E-14	4.41E-14
13.00011	6.94E-18	4.2E-18	-5.93E-14	1E-13	-4.45E-14	2.22E-14
13.50018	2.78E-17	2.09E-17	-2.19E-14	5.27E-14	-1.51E-14	7.42E-15
14.00025	4.16E-17	6.43E-17	-1.98E-14	6E-14	-1.48E-14	7.3E-15

14.50006	4.16E-17	-7.21E-17	-1.78E-14	2.22E-14	-3.21E-15	-7.47E-15
15.00013	6.25E-17	-1.77E-16	2.01E-14	8.24E-15	1.32E-14	7.44E-15
15.5002	2.52E-17	1.24E-16	2.01E-14	2.01E-14	1.49E-14	7.43E-15
1.600249	3.63E-17	2.1E-16	-0.0000615	-0.0000103	0.0000118	0.0000148
16.50008	5.05E-17	3.39E-17	2.01E-14	1.99E-14	1.37E-14	3.28E-15
17.00015	-5.55E-17	1.14E-16	2.01E-14	1.99E-14	1.44E-14	4.95E-15
17.50022	-6.94E-17	8.82E-17	2.01E-14	1.99E-14	1.45E-14	7.46E-15
18.00002	-1.39E-17	1.43E-16	2.01E-14	1.99E-14	1.14E-14	5.59E-15
18.50009	-1.3E-16	-1.64E-16	2.01E-14	1.99E-14	-1.48E-14	1.11E-15
19.00016	4.38E-17	-7.68E-17	2.01E-14	1.99E-14	-1.13E-14	1.45E-15
19.50023	1.39E-17	5.57E-17	2.01E-14	1.99E-14	-1.48E-14	-7.25E-15
20.00004	-2.07E-17	2.92E-19	2.01E-14	1.99E-14	-1.49E-14	-5.1E-15
20.50011	0	5.75E-18	2.01E-14	1.99E-14	-1.05E-14	2.08E-15
21.00014	-0.2343412	-0.6845875	-0.0130951	-0.1702281	-0.0214175	-0.0903573
21.50006	0.4940121	0.46060222	-0.0028886	-0.0256552	0.00979989	0.02982509
22.00062	0.54397691	0.89944986	0.00474177	0.03123636	0.01783672	0.04849511
22.50043	0.3020493	0.2052385	0.00111658	0.00063071	0.00187483	-0.0010733
23.00024	0.08759579	-0.1371606	-0.0000212	0.00016788	-0.0002197	-0.0002389
23.50005	-0.0262312	-0.1624969	-0.0001427	-0.0000894	-0.0001242	-0.0000396
24.00048	-0.0607969	-0.0687214	-0.0000601	-0.0000575	-0.0000324	-0.0000185
24.50029	-0.048951	0.00515446	-0.0000118	-0.0000144	-5.04E-06	-2.96E-06
25.0001	-0.0206983	0.02591015	8.16E-07	9.06E-08	-1.94E-07	7.25E-07
25.50054	0.00225096	0.01597351	0.00000146	0.00000171	6.24E-09	6.59E-07
26.00035	0.01132405	0.00180555	5.01E-07	8.25E-07	-1.15E-07	0.00000029
26.50015	0.00921776	-0.0044671	4.87E-08	2.24E-07	-1.06E-07	1.12E-07
27.00059	0.00317792	-0.00373	-3.87E-08	3.27E-08	-6.28E-08	4.64E-08
27.5004	-0.0012478	-0.0008611	-2.55E-08	2.97E-10	-3.16E-08	2.2E-08
28.00021	-0.0024495	0.00086663	-8.85E-09	9.24E-10	-1.52E-08	1.11E-08
28.50002	-0.001535	0.00097215	-2.04E-09	2.23E-09	-7.35E-09	5.7E-09
29.00045	-0.0002391	0.00035766	-3.49E-10	1.72E-09	-3.62E-09	2.88E-09
29.50026	0.0004592	-0.0001463	-1.13E-10	8.97E-10	-1.8E-09	1.44E-09
30.00007	0.00048099	-0.000265	-9.02E-11	3.87E-10	-9E-10	7.16E-10
30.50051	0.0001998	-0.0001423	-6.23E-11	1.55E-10	-4.49E-10	3.56E-10
31.00031	-0.0000414	0.0000042	-3.36E-11	6.37E-11	-2.24E-10	1.77E-10
31.50012	-0.0001187	0.0000653	-1.54E-11	2.81E-11	-1.12E-10	8.82E-11
32.00056	-0.0000787	0.0000501	-6.49E-12	1.31E-11	-5.56E-11	4.39E-11
32.50037	-0.0000133	0.0000115	-2.73E-12	6.2E-12	-2.77E-11	2.19E-11
33.00018	0.0000227	-0.0000126	-1.19E-12	2.88E-12	-1.38E-11	1.09E-11
33.50061	0.0000239	-0.0000151	-5.46E-13	1.31E-12	-6.87E-12	5.43E-12
34.00042	0.00000967	-6.69E-06	-2.53E-13	5.93E-13	-3.42E-12	2.71E-12
34.50023	-2.44E-06	0.00000119	-1.18E-13	2.67E-13	-1.7E-12	1.35E-12
35.00004	-6.08E-06	0.00000385	-5.54E-14	1.21E-13	-8.49E-13	6.71E-13
35.50048	-3.85E-06	0.00000259	-2.47E-14	5.54E-14	-4.24E-13	3.34E-13

36.00028	-5.04E-07	4.28E-07	-1.4E-14	2.56E-14	-2.09E-13	1.67E-13
36.50009	0.00000124	-7.77E-07	-1.04E-14	1.29E-14	-1.08E-13	8.28E-14
37.00053	0.00000121	-8.09E-07	-2.78E-15	4.47E-15	-5.92E-14	4.19E-14
37.50034	4.45E-07	-3.19E-07	-3.72E-15	3.75E-15	-2.74E-14	1.94E-14
38.00014	-1.62E-07	9.16E-08	-3.25E-15	3.32E-15	-2.01E-14	1.19E-14
38.50058	-3.2E-07	2.11E-07	3.47E-15	-3.69E-15	-1.23E-14	6.93E-15
39.00039	-1.89E-07	1.31E-07	3.72E-15	3.63E-15	-4.14E-15	5.19E-15
39.5002	-1.43E-08	1.48E-08	2.41E-15	3.64E-15	-4.15E-15	2.09E-15
40.00001	6.93E-08	-4.44E-08	2.28E-15	3.63E-15	4.11E-15	-2.02E-15
40.50044	6.18E-08	-4.21E-08	2.28E-15	3.62E-15	4.09E-15	2.05E-15
41.00025	2.01E-08	-1.49E-08	2.28E-15	3.62E-15	4.09E-15	2.02E-15
41.50006	-1.04E-08	6.11E-09	2.28E-15	3.62E-15	4.09E-15	2.02E-15
42.0005	-1.69E-08	1.13E-08	2.28E-15	3.62E-15	4.09E-15	2.02E-15
42.50031	-9.19E-09	6.48E-09	2.28E-15	3.63E-15	4.09E-15	2.02E-15
43.00011	-1.23E-10	3.69E-10	2.28E-15	3.62E-15	4.09E-15	2.02E-15
43.50055	3.82E-09	-2.47E-09	2.28E-15	3.62E-15	4.09E-15	2.02E-15
44.00036	3.14E-09	-2.15E-09	2.28E-15	3.61E-15	4.09E-15	2.02E-15
44.50017	8.82E-10	-6.72E-10	2.28E-15	3.62E-15	4.09E-15	2.02E-15
45.0006	-6.3E-10	3.79E-10	2.28E-15	3.62E-15	4.09E-15	2.02E-15
45.50041	-8.9E-10	5.96E-10	2.28E-15	3.64E-15	4.09E-15	2.02E-15
46.00022	-4.44E-10	3.16E-10	2.28E-15	3.62E-15	4.09E-15	2.02E-15
46.50003	2.51E-11	-1.86E-12	2.28E-15	3.63E-15	4.09E-15	2.02E-15
47.00047	2.1E-10	-1.36E-10	2.28E-15	3.64E-15	4.09E-15	2.02E-15
47.50027	1.59E-10	-1.1E-10	2.28E-15	3.61E-15	4.09E-15	2.02E-15
48.00008	3.75E-11	-2.94E-11	2.28E-15	3.63E-15	4.09E-15	2.02E-15
48.50052	-3.76E-11	2.31E-11	2.28E-15	3.62E-15	4.09E-15	2.02E-15
49.00033	-4.66E-11	3.14E-11	2.28E-15	3.62E-15	4.09E-15	2.02E-15
49.50014	-2.13E-11	1.53E-11	2.28E-15	3.61E-15	4.09E-15	2.02E-15
50.00057	2.78E-12	-1.1E-12	2.28E-15	3.63E-15	4.09E-15	2.02E-15
50.50038	1.14E-11	-7.48E-12	2.28E-15	3.63E-15	4.09E-15	2.02E-15
51.00019	7.98E-12	-5.53E-12	2.28E-15	3.62E-15	4.09E-15	2.02E-15
51.50063	1.54E-12	-1.26E-12	2.28E-15	3.61E-15	4.09E-15	2.02E-15
52.00043	-2.19E-12	1.37E-12	2.28E-15	3.62E-15	4.09E-15	2.02E-15
52.50024	-2.42E-12	1.64E-12	2.28E-15	3.61E-15	4.09E-15	2.02E-15
53.00005	-1E-12	7.26E-13	2.28E-15	3.63E-15	4.09E-15	2.02E-15
53.50049	2.27E-13	-1.14E-13	2.28E-15	3.62E-15	4.09E-15	2.02E-15
54.0003	6.13E-13	-4.04E-13	2.28E-15	3.62E-15	4.09E-15	2.02E-15
54.5001	3.94E-13	-2.76E-13	2.28E-15	3.62E-15	4.09E-15	2.02E-15
55.00054	5.52E-14	-4.91E-14	2.28E-15	3.62E-15	4.09E-15	2.02E-15
55.50035	-1.24E-13	7.85E-14	2.28E-15	3.64E-15	4.09E-15	2.02E-15
56.00016	-1.22E-13	8.25E-14	2.28E-15	3.62E-15	4.09E-15	2.02E-15
56.5006	-4.55E-14	3.51E-14	2.28E-15	3.64E-15	4.09E-15	2.02E-15
57.0004	1.64E-14	-7.97E-15	2.28E-15	3.62E-15	4.09E-15	2.02E-15

57.50021	3.24E-14	-2.02E-14	2.28E-15	3.64E-15	4.09E-15	2.02E-15
58.00002	1.87E-14	-1.35E-14	2.28E-15	3.62E-15	4.09E-15	2.02E-15
58.50046	-8.9E-17	-2.16E-15	2.28E-15	3.62E-15	4.09E-15	2.02E-15
59.00026	-8.92E-15	6.14E-15	2.28E-15	3.62E-15	4.09E-15	2.02E-15
59.50007	-6.97E-15	5.84E-15	2.28E-15	3.64E-15	4.09E-15	2.02E-15
60.00051	-5.19E-16	1.8E-16	2.28E-15	3.64E-15	4.09E-15	2.02E-15
60.50032	3.06E-15	-4.66E-15	2.28E-15	3.62E-15	4.09E-15	2.02E-15
61.00013	1.62E-15	-2.06E-15	2.28E-15	3.62E-15	4.09E-15	2.02E-15
61.50056	-1.37E-15	1.48E-15	2.28E-15	3.61E-15	4.09E-15	2.02E-15
62.00037	-1.39E-15	2.46E-15	2.28E-15	3.63E-15	4.09E-15	2.02E-15
62.50018	1.37E-15	-1E-15	2.28E-15	3.62E-15	4.09E-15	2.02E-15
63.00062	4.44E-16	-4.3E-17	2.28E-15	3.61E-15	4.09E-15	2.02E-15
63.50043	-2.61E-16	4.76E-16	2.28E-15	3.63E-15	4.09E-15	2.02E-15
64.00023	-3.3E-16	4.64E-16	2.28E-15	3.62E-15	4.09E-15	2.02E-15
64.50004	2.88E-16	-4.18E-16	2.28E-15	3.65E-15	4.09E-15	2.02E-15
65.00048	-1.17E-16	-2.94E-16	2.28E-15	3.63E-15	4.09E-15	2.02E-15
65.50029	-1.12E-16	8.86E-16	2.28E-15	3.62E-15	4.09E-15	2.02E-15
66.00009	-9.02E-17	8.56E-16	2.28E-15	3.62E-15	4.09E-15	2.02E-15
66.50053	-7.75E-17	3.7E-16	2.28E-15	3.62E-15	4.09E-15	2.02E-15
67.00034	1.27E-16	-6.31E-16	2.28E-15	3.65E-15	4.09E-15	2.02E-15
67.50015	3.46E-16	-7.07E-16	2.28E-15	3.64E-15	4.09E-15	2.02E-15
68.00059	4.23E-16	-7.73E-16	2.28E-15	3.62E-15	4.09E-15	2.02E-15
68.50039	-1.36E-16	-6.97E-16	2.28E-15	3.65E-15	4.09E-15	2.02E-15
69.0002	-1.79E-16	-7.22E-16	2.28E-15	3.62E-15	4.09E-15	2.02E-15
69.50001	-1.67E-16	-7.1E-16	2.28E-15	3.61E-15	4.09E-15	2.02E-15
70.00045	-1.67E-16	-7.14E-16	2.28E-15	3.62E-15	4.09E-15	2.02E-15
70.50026	-1.67E-16	-7.15E-16	2.28E-15	3.64E-15	4.09E-15	2.02E-15
71.00006	-1.67E-16	-7.22E-16	2.28E-15	3.64E-15	4.09E-15	2.02E-15
71.5005	-1.67E-16	-7.28E-16	2.28E-15	3.62E-15	4.09E-15	2.02E-15
72.00031	-1.67E-16	-7.29E-16	2.28E-15	3.64E-15	4.09E-15	2.02E-15
72.50012	-1.67E-16	-7.34E-16	2.28E-15	3.62E-15	4.09E-15	2.02E-15
73.00055	-1.67E-16	-7.46E-16	2.28E-15	3.64E-15	4.09E-15	2.02E-15
73.50036	-1.67E-16	-7.41E-16	2.28E-15	3.64E-15	4.09E-15	2.02E-15
74.00017	-1.67E-16	-7.35E-16	2.28E-15	3.63E-15	4.09E-15	2.02E-15
74.50061	-1.67E-16	-7.33E-16	2.28E-15	3.62E-15	4.09E-15	2.02E-15
75.00042	-1.67E-16	-7.32E-16	2.28E-15	3.62E-15	4.09E-15	2.02E-15
75.50022	-1.67E-16	-7.42E-16	2.28E-15	3.63E-15	4.09E-15	2.02E-15
76.00003	-1.67E-16	-7.37E-16	2.28E-15	3.64E-15	4.09E-15	2.02E-15
76.50047	-1.67E-16	-7.32E-16	2.28E-15	3.61E-15	4.09E-15	2.02E-15
77.00028	-1.67E-16	-7.27E-16	2.28E-15	3.64E-15	4.09E-15	2.02E-15
77.50009	-1.67E-16	-7.24E-16	2.28E-15	3.63E-15	4.09E-15	2.02E-15
78.00052	-1.67E-16	-7.24E-16	2.28E-15	3.61E-15	4.09E-15	2.02E-15
78.50033	-1.67E-16	-7.39E-16	2.28E-15	3.62E-15	4.09E-15	2.02E-15

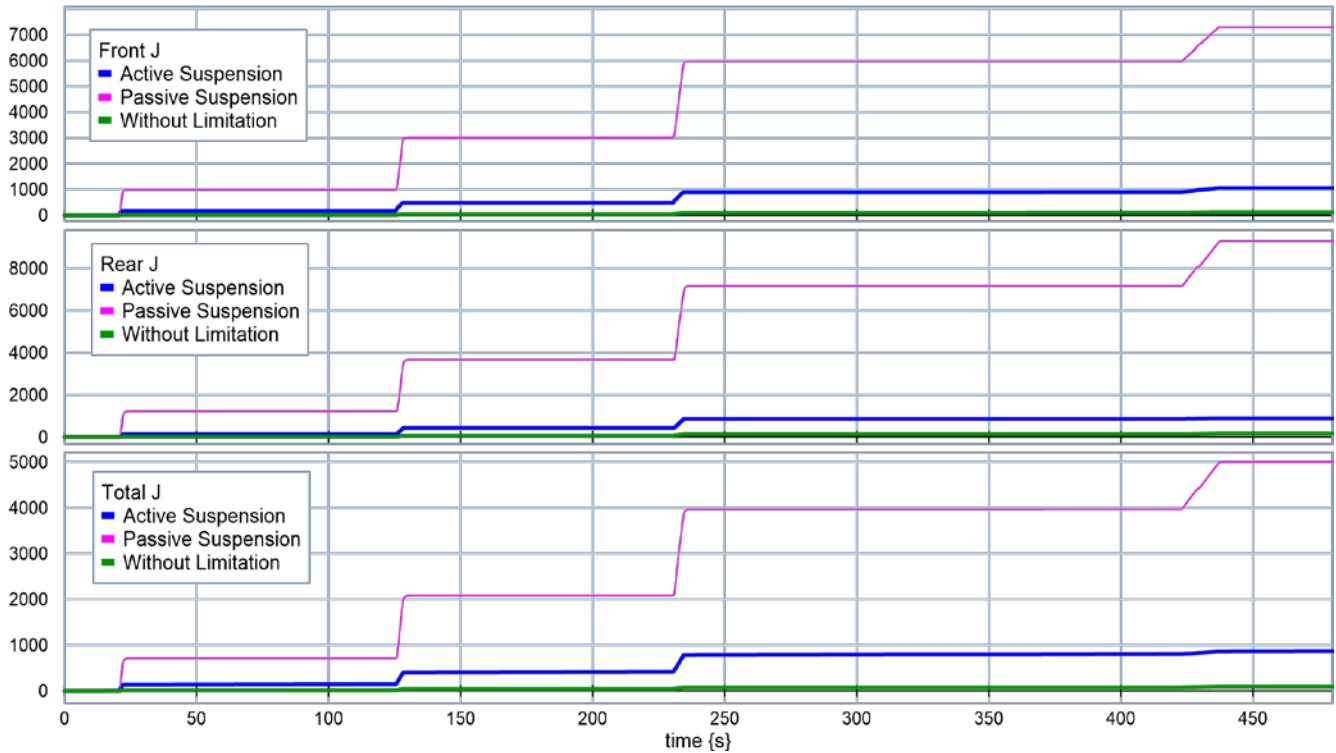
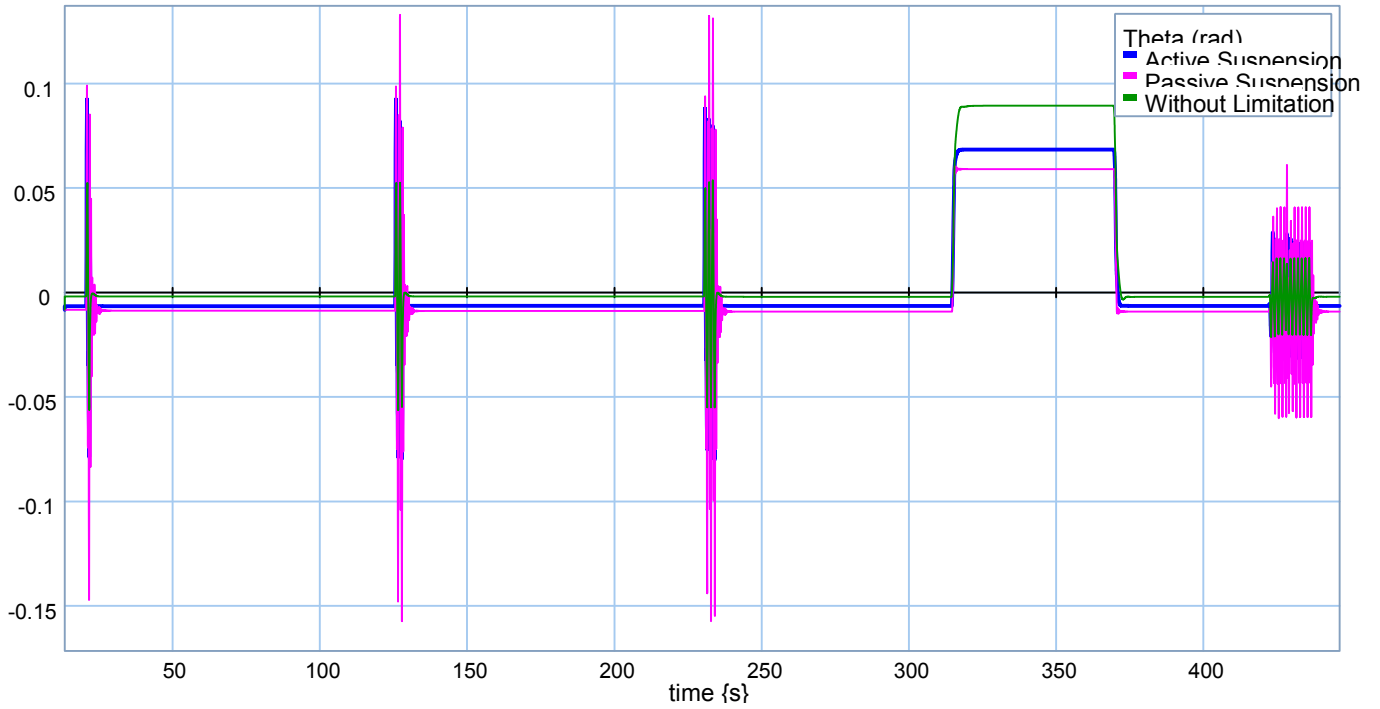
79.00014	-1.67E-16	-7.34E-16	2.28E-15	3.64E-15	4.09E-15	2.02E-15
79.50058	-1.67E-16	-7.22E-16	2.28E-15	3.63E-15	4.09E-15	2.02E-15
80.00038	-1.67E-16	-7.43E-16	2.28E-15	3.62E-15	4.09E-15	2.02E-15
80.50019	-1.67E-16	-7.36E-16	2.28E-15	3.65E-15	4.09E-15	2.02E-15
81	-1.67E-16	-7.41E-16	2.28E-15	3.62E-15	4.09E-15	2.02E-15
81.50044	-1.67E-16	-7.27E-16	2.28E-15	3.64E-15	4.09E-15	2.02E-15
82.00025	-1.67E-16	-7.22E-16	2.28E-15	3.61E-15	4.09E-15	2.02E-15
82.50005	-1.67E-16	-7.32E-16	2.28E-15	3.62E-15	4.09E-15	2.02E-15
83.00049	-1.67E-16	-7.37E-16	2.28E-15	3.63E-15	4.09E-15	2.02E-15
83.5003	-1.67E-16	-7.32E-16	2.28E-15	3.62E-15	4.09E-15	2.02E-15
84.00011	-1.67E-16	-7.35E-16	2.28E-15	3.64E-15	4.09E-15	2.02E-15
84.50055	-1.67E-16	-7.27E-16	2.28E-15	3.61E-15	4.09E-15	2.02E-15
85.00035	-1.67E-16	-7.23E-16	2.28E-15	3.62E-15	4.09E-15	2.02E-15
85.50016	-1.67E-16	-7.37E-16	2.28E-15	3.64E-15	4.09E-15	2.02E-15
86.0006	-1.67E-16	-7.36E-16	2.28E-15	3.64E-15	4.09E-15	2.02E-15
86.50041	-1.67E-16	-7.35E-16	2.28E-15	3.63E-15	4.09E-15	2.02E-15
87.00021	-1.67E-16	-7.27E-16	2.28E-15	3.62E-15	4.09E-15	2.02E-15
87.50002	-1.67E-16	-7.23E-16	2.28E-15	3.61E-15	4.09E-15	2.02E-15
88.00046	-1.67E-16	-7.42E-16	2.28E-15	3.64E-15	4.09E-15	2.02E-15
88.50027	-1.67E-16	-7.36E-16	2.28E-15	3.62E-15	4.09E-15	2.02E-15
89.00008	-1.67E-16	-7.4E-16	2.28E-15	3.62E-15	4.09E-15	2.02E-15
89.50051	-1.67E-16	-7.27E-16	2.28E-15	3.62E-15	4.09E-15	2.02E-15
90.00032	-1.67E-16	-7.22E-16	2.28E-15	3.63E-15	4.09E-15	2.02E-15
90.50013	-1.67E-16	-7.42E-16	2.28E-15	3.63E-15	4.09E-15	2.02E-15
91.00057	-1.67E-16	-7.36E-16	2.28E-15	3.61E-15	4.09E-15	2.02E-15
91.50038	-1.67E-16	-7.42E-16	2.28E-15	3.64E-15	4.09E-15	2.02E-15
92.00018	-1.67E-16	-7.35E-16	2.28E-15	3.62E-15	4.09E-15	2.02E-15
92.50062	-1.67E-16	-7.27E-16	2.28E-15	3.62E-15	4.09E-15	2.02E-15
93.00043	-1.67E-16	-7.23E-16	2.28E-15	3.62E-15	4.09E-15	2.02E-15
93.50024	-1.67E-16	-7.37E-16	2.28E-15	3.63E-15	4.09E-15	2.02E-15
94.00004	-1.67E-16	-7.35E-16	2.28E-15	3.64E-15	4.09E-15	2.02E-15
94.50048	-1.67E-16	-7.35E-16	2.28E-15	3.62E-15	4.09E-15	2.02E-15
95.00029	-1.67E-16	-7.27E-16	2.28E-15	3.64E-15	4.09E-15	2.02E-15
95.5001	-1.67E-16	-7.23E-16	2.28E-15	3.62E-15	4.09E-15	2.02E-15
96.00054	-1.67E-16	-7.42E-16	2.28E-15	3.62E-15	4.09E-15	2.02E-15
96.50034	-1.67E-16	-7.36E-16	2.28E-15	3.62E-15	4.09E-15	2.02E-15
97.00015	-1.67E-16	-7.41E-16	2.28E-15	3.64E-15	4.09E-15	2.02E-15
97.50059	-1.67E-16	-7.27E-16	2.28E-15	3.63E-15	4.09E-15	2.02E-15
98.0004	-1.67E-16	-7.22E-16	2.28E-15	3.62E-15	4.09E-15	2.02E-15
98.50021	-1.67E-16	-7.43E-16	2.28E-15	3.64E-15	4.09E-15	2.02E-15
99.00001	-1.67E-16	-7.36E-16	2.28E-15	3.63E-15	4.09E-15	2.02E-15
99.50045	-1.67E-16	-7.42E-16	2.28E-15	3.64E-15	4.09E-15	2.02E-15
100.0003	-1.67E-16	-7.27E-16	2.28E-15	3.62E-15	4.09E-15	2.02E-15

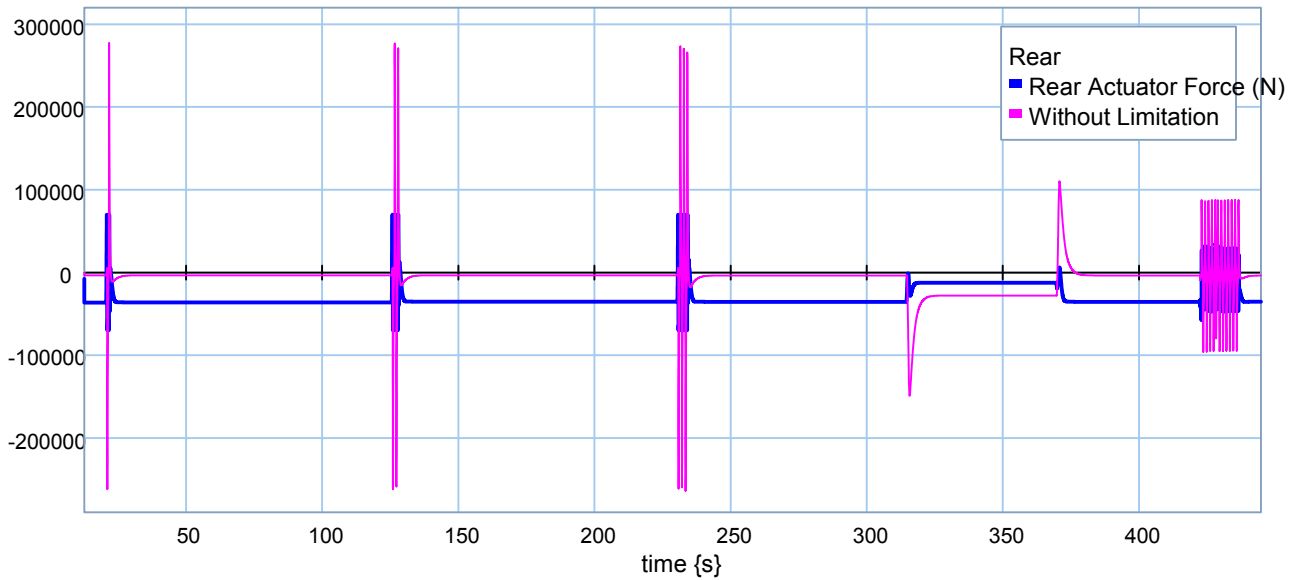
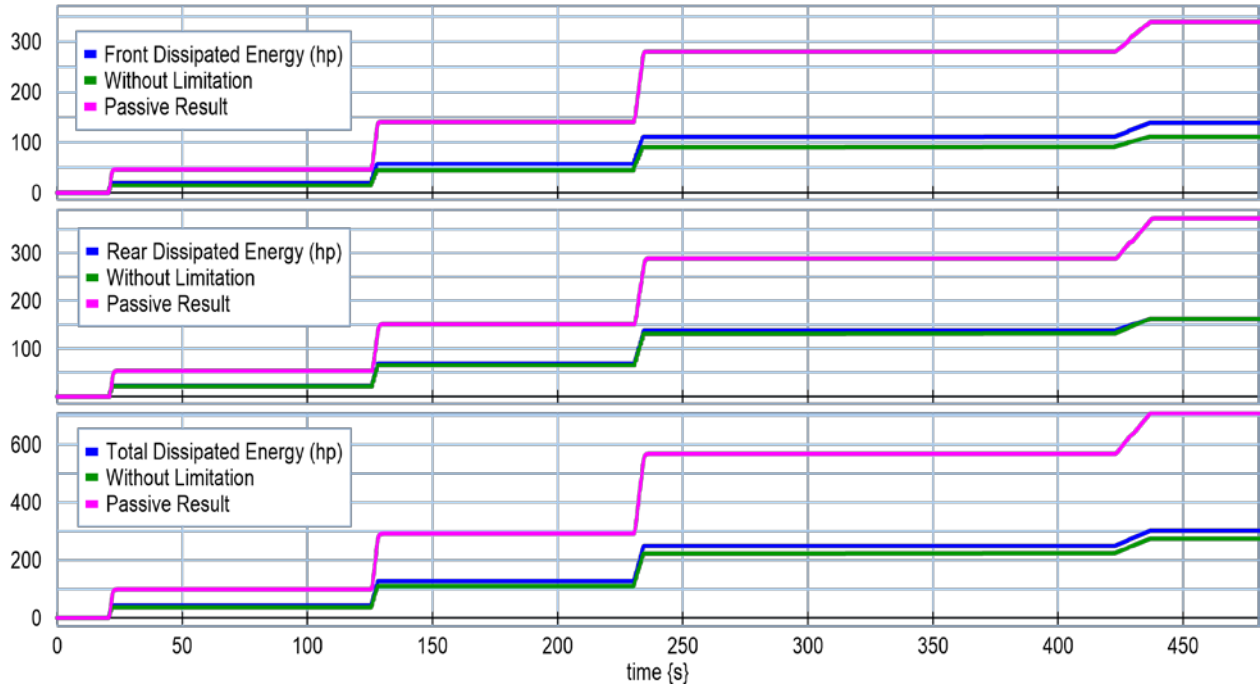
Time	Passive Suspension		QuarterCar Approach		HalfCar Approach	
	Vtf	Vtr	Vtf	Vtr	Vtf	Vtr
0.00	7.017E03	-3.511E03	-2.270E03	-1.201E02	-6.230E05	2.960E05
0.50	7.017E03	-3.511E03	-2.688E03	-1.372E02	-1.601E04	-3.180E06
1.00	7.017E03	-3.511E03	-2.068E03	-1.222E02	-8.130E05	-5.820E06
1.50	7.017E03	-3.511E03	-2.017E03	-1.207E02	-5.720E05	2.260E05
2.00	7.017E03	-3.511E03	-2.048E03	-1.208E02	-5.470E05	2.690E05
2.50	7.017E03	-3.511E03	-2.068E03	-1.210E02	-5.550E05	2.680E05
3.00	7.017E03	-3.511E03	-2.073E03	-1.211E02	-5.600E05	2.660E05
3.50	7.017E03	-3.511E03	-2.073E03	-1.211E02	-5.610E05	2.650E05
4.00	7.017E03	-3.511E03	-2.073E03	-1.211E02	-5.620E05	2.650E05
4.50	7.017E03	-3.511E03	-2.073E03	-1.211E02	-5.620E05	2.650E05
5.00	7.017E03	-3.511E03	-2.073E03	-1.211E02	-5.620E05	2.650E05
5.50	7.017E03	-3.511E03	-2.073E03	-1.211E02	-5.620E05	2.650E05
6.00	7.017E03	-3.511E03	-2.073E03	-1.211E02	-5.620E05	2.650E05
6.50	7.017E03	-3.511E03	-2.073E03	-1.211E02	-5.620E05	2.650E05
7.00	7.017E03	-3.511E03	-2.073E03	-1.211E02	-5.620E05	2.650E05
7.50	7.017E03	-3.511E03	-2.073E03	-1.211E02	-5.620E05	2.650E05
8.00	7.017E03	-3.511E03	-2.073E03	-1.211E02	-5.620E05	2.650E05
8.50	7.017E03	-3.511E03	-2.073E03	-1.211E02	-5.620E05	2.650E05
9.00	7.017E03	-3.511E03	-2.073E03	-1.211E02	-5.620E05	2.650E05
9.50	7.017E03	-3.511E03	-2.073E03	-1.211E02	-5.620E05	2.650E05
10.00	7.017E03	-3.511E03	-2.073E03	-1.211E02	-5.620E05	2.650E05
10.50	7.017E03	-3.511E03	-2.073E03	-1.211E02	-5.620E05	2.650E05
11.00	7.017E03	-3.511E03	-2.073E03	-1.211E02	-5.620E05	2.650E05
11.50	7.017E03	-3.511E03	-2.073E03	-1.211E02	-5.620E05	2.650E05
12.00	7.017E03	-3.511E03	-2.073E03	-1.211E02	-5.620E05	2.650E05
12.50	7.017E03	-3.511E03	-2.073E03	-1.211E02	-5.620E05	2.650E05
13.00	7.017E03	-3.511E03	-2.073E03	-1.211E02	-5.620E05	2.650E05
13.50	7.017E03	-3.511E03	-2.073E03	-1.211E02	-5.620E05	2.650E05
14.00	7.017E03	-3.511E03	-2.073E03	-1.211E02	-5.620E05	2.650E05
14.50	7.017E03	-3.511E03	-2.073E03	-1.211E02	-5.620E05	2.650E05
15.00	7.017E03	-3.511E03	-2.073E03	-1.211E02	-5.620E05	2.650E05
15.50	7.017E03	-3.511E03	-2.073E03	-1.211E02	-5.620E05	2.650E05
16.00	7.017E03	-3.511E03	-2.073E03	-1.211E02	-5.620E05	2.650E05
16.50	7.017E03	-3.511E03	-2.073E03	-1.211E02	-5.620E05	2.650E05
17.00	7.017E03	-3.511E03	-2.073E03	-1.211E02	-5.620E05	2.650E05
17.50	7.017E03	-3.511E03	-2.073E03	-1.211E02	-5.620E05	2.650E05
18.00	7.017E03	-3.511E03	-2.073E03	-1.211E02	-5.620E05	2.650E05
18.50	7.017E03	-3.511E03	-2.073E03	-1.211E02	-5.620E05	2.650E05
19.00	7.017E03	-3.511E03	-2.073E03	-1.211E02	-5.620E05	2.650E05
19.50	7.017E03	-3.511E03	-2.073E03	-1.211E02	-5.620E05	2.650E05

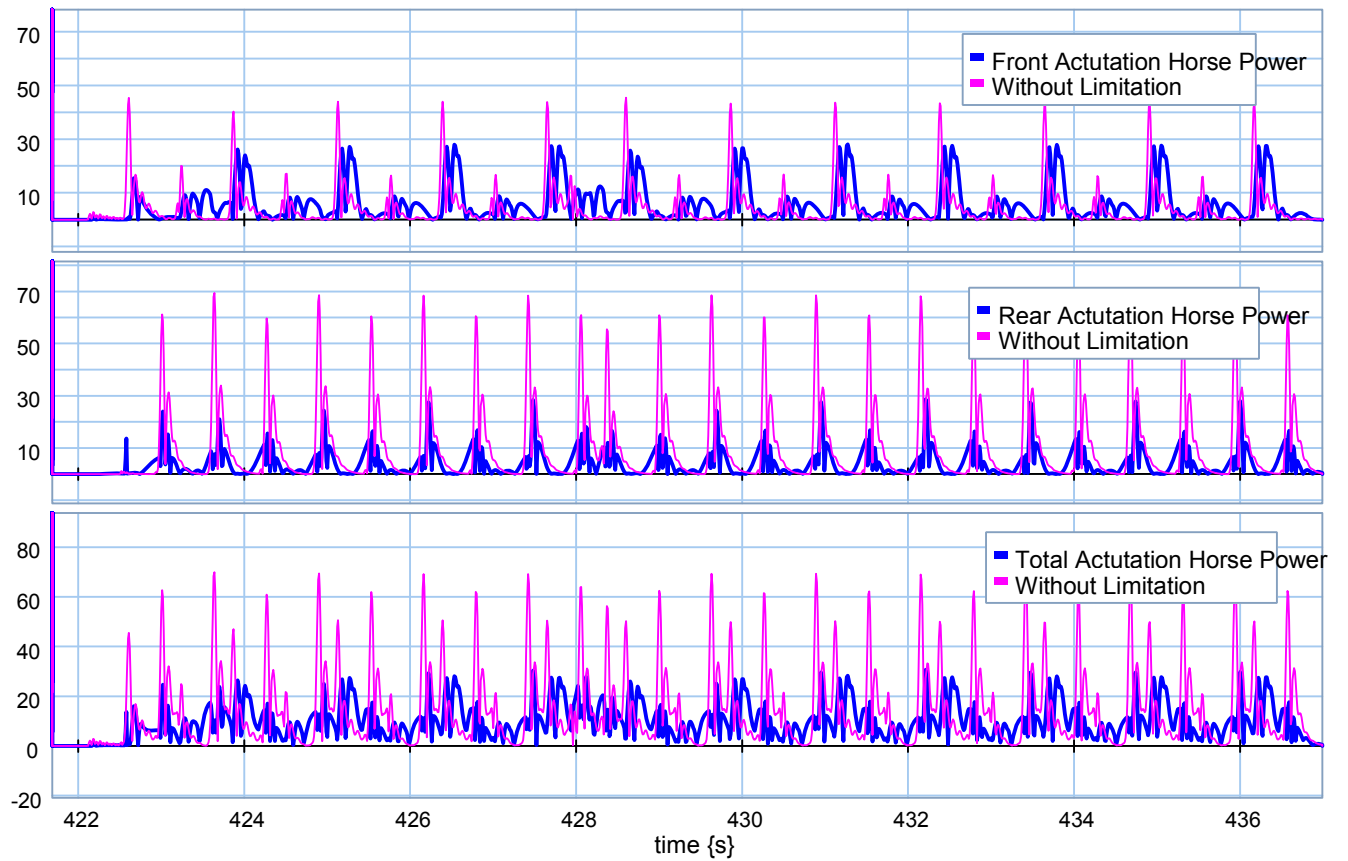
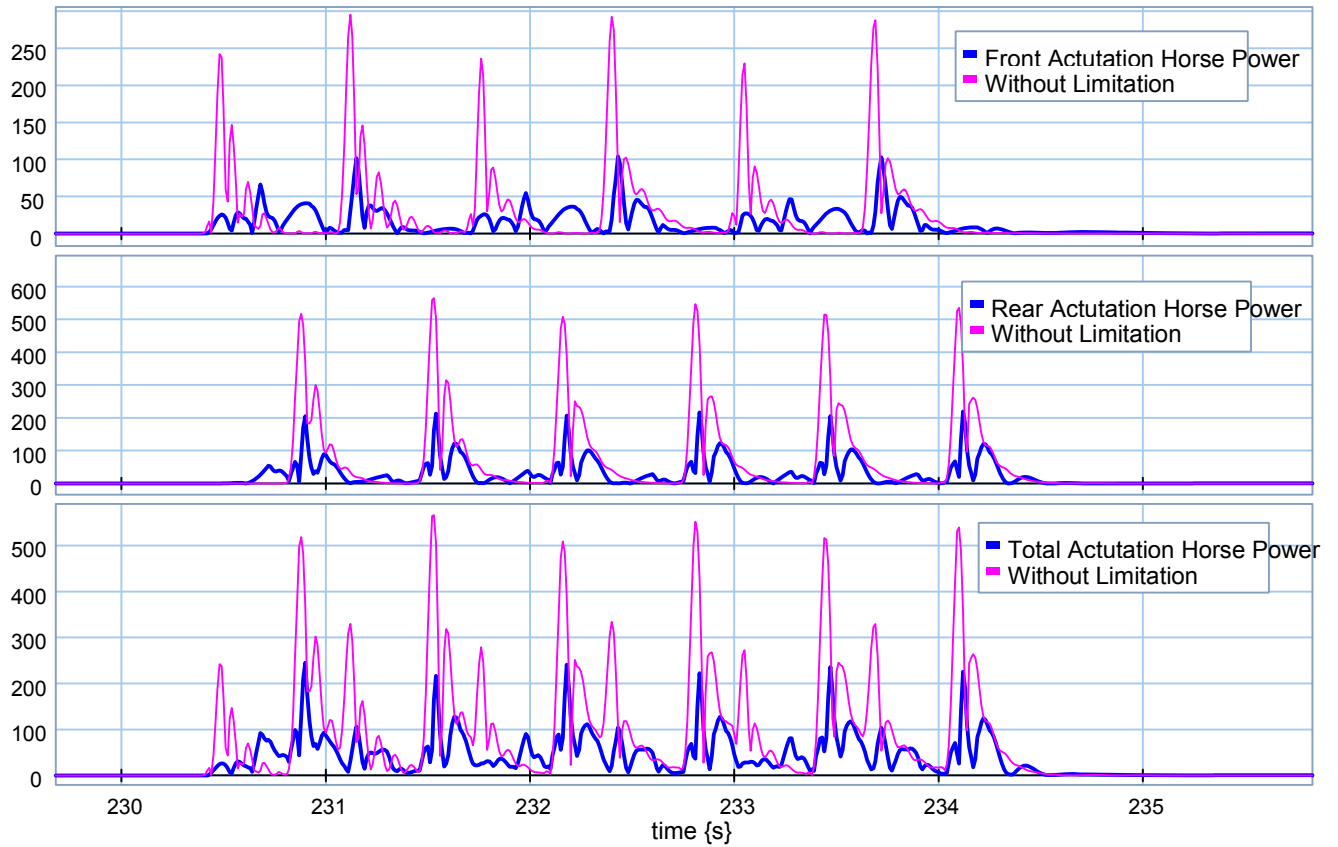
20.00	7.017E03	-3.511E03	-2.073E03	-1.211E02	-5.620E05	2.650E05
20.50	7.017E03	-3.511E03	-2.073E03	-1.211E02	-5.620E05	2.650E05
21.00	4.383E03	-5.744E02	-6.272E04	-2.153E02	5.947E04	-3.679E03
21.50	-1.315E02	-5.191E02	-2.754E03	-7.992E03	-2.592E03	4.228E03
22.00	5.320E02	-2.736E02	-4.026E03	-1.734E02	-2.395E03	-9.846E04
22.50	5.286E02	2.790E03	-2.162E03	-1.248E02	2.280E05	9.510E05
23.00	2.517E02	9.702E03	-1.942E03	-1.204E02	7.460E05	6.320E05
23.50	4.141E03	6.464E03	-2.005E03	-1.205E02	-1.260E05	4.810E05
24.00	-1.259E03	5.266E04	-2.056E03	-1.209E02	-4.720E05	3.080E05
24.50	2.256E03	-3.789E03	-2.072E03	-1.210E02	-5.500E05	2.590E05
25.00	6.663E03	-5.411E03	-2.074E03	-1.211E02	-5.590E05	2.560E05
25.50	8.546E03	-5.099E03	-2.073E03	-1.211E02	-5.590E05	2.600E05
26.00	8.253E03	-4.138E03	-2.073E03	-1.211E02	-5.590E05	2.630E05
26.50	7.312E03	-3.394E03	-2.073E03	-1.211E02	-5.600E05	2.640E05
27.00	6.741E03	-3.149E03	-2.073E03	-1.211E02	-5.600E05	2.640E05
27.50	6.692E03	-3.251E03	-2.073E03	-1.211E02	-5.600E05	2.640E05
28.00	6.890E03	-3.445E03	-2.073E03	-1.211E02	-5.610E05	2.640E05
28.50	7.060E03	-3.566E03	-2.073E03	-1.211E02	-5.610E05	2.640E05
29.00	7.107E03	-3.586E03	-2.073E03	-1.211E02	-5.610E05	2.640E05
29.50	7.072E03	-3.551E03	-2.073E03	-1.211E02	-5.610E05	2.640E05
30.00	7.024E03	-3.513E03	-2.073E03	-1.211E02	-5.610E05	2.640E05
30.50	7.002E03	-3.497E03	-2.073E03	-1.211E02	-5.610E05	2.640E05
31.00	7.004E03	-3.500E03	-2.073E03	-1.211E02	-5.610E05	2.640E05
31.50	7.016E03	-3.509E03	-2.073E03	-1.211E02	-5.610E05	2.640E05
32.00	7.025E03	-3.515E03	-2.073E03	-1.211E02	-5.610E05	2.640E05
32.50	7.026E03	-3.516E03	-2.073E03	-1.211E02	-5.610E05	2.640E05
33.00	7.024E03	-3.515E03	-2.073E03	-1.211E02	-5.610E05	2.640E05
33.50	7.021E03	-3.513E03	-2.073E03	-1.211E02	-5.610E05	2.640E05
34.00	7.020E03	-3.512E03	-2.073E03	-1.211E02	-5.610E05	2.640E05
34.50	7.020E03	-3.512E03	-2.073E03	-1.211E02	-5.610E05	2.640E05
35.00	7.021E03	-3.513E03	-2.073E03	-1.211E02	-5.610E05	2.640E05
35.50	7.021E03	-3.513E03	-2.073E03	-1.211E02	-5.610E05	2.640E05
36.00	7.021E03	-3.513E03	-2.073E03	-1.211E02	-5.610E05	2.640E05
35.60	7.021E03	-3.513E03	-2.073E03	-1.211E02	-5.610E05	2.640E05
37.00	7.021E03	-3.513E03	-2.073E03	-1.211E02	-5.610E05	2.640E05
37.50	7.021E03	-3.513E03	-2.073E03	-1.211E02	-5.610E05	2.640E05
38.00	7.021E03	-3.513E03	-2.073E03	-1.211E02	-5.610E05	2.640E05
38.50	7.021E03	-3.513E03	-2.073E03	-1.211E02	-5.610E05	2.640E05
39.00	7.021E03	-3.513E03	-2.073E03	-1.211E02	-5.610E05	2.640E05
39.50	7.021E03	-3.513E03	-2.073E03	-1.211E02	-5.610E05	2.640E05
40.00	7.021E03	-3.513E03	-2.073E03	-1.211E02	-5.610E05	2.640E05
40.50	7.021E03	-3.513E03	-2.073E03	-1.211E02	-5.610E05	2.640E05
41.00	7.021E03	-3.513E03	-2.073E03	-1.211E02	-5.610E05	2.640E05

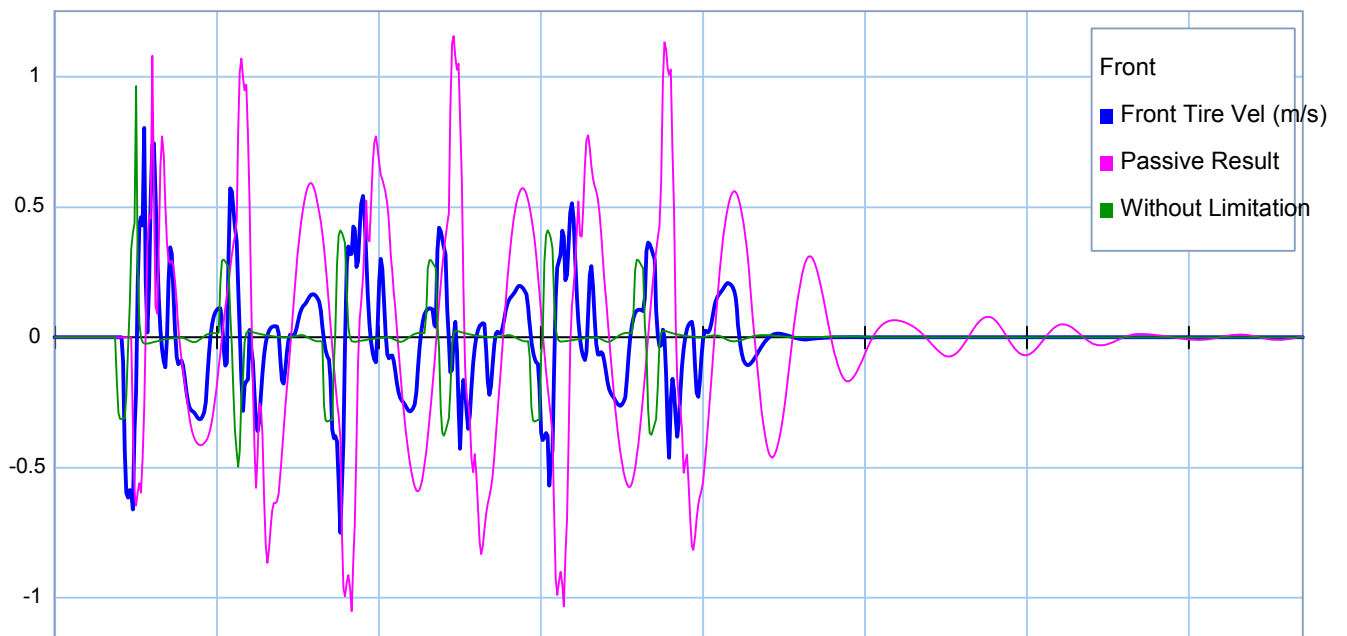
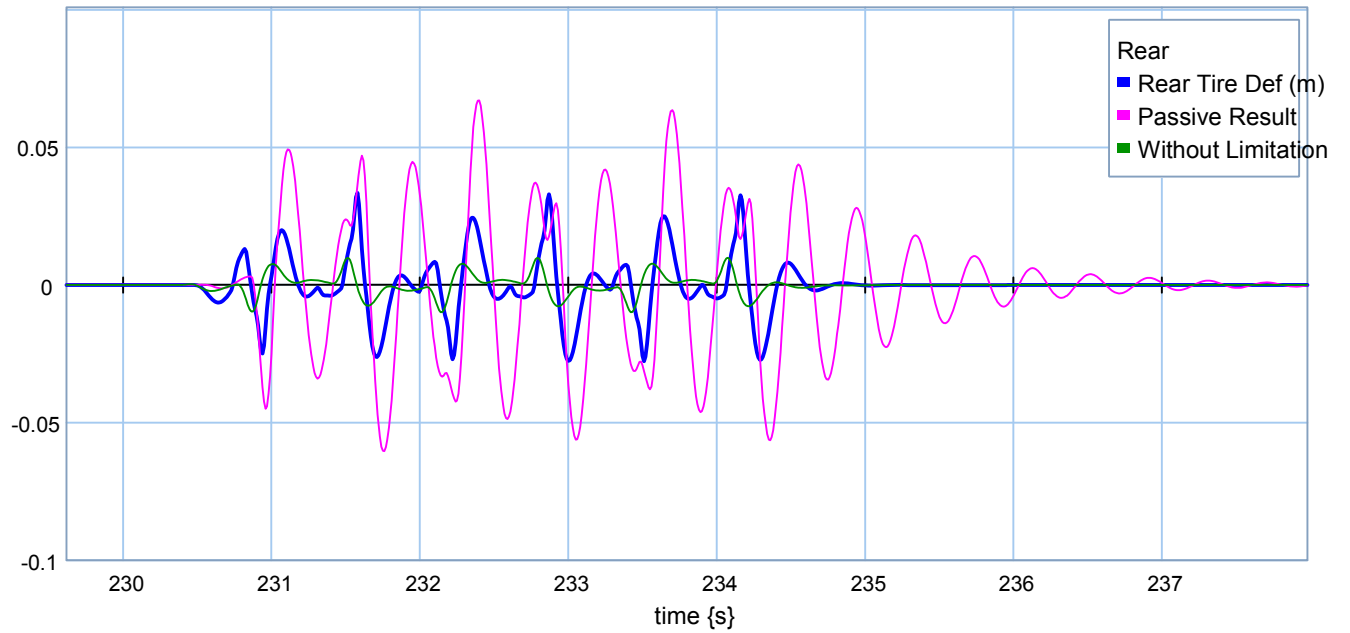
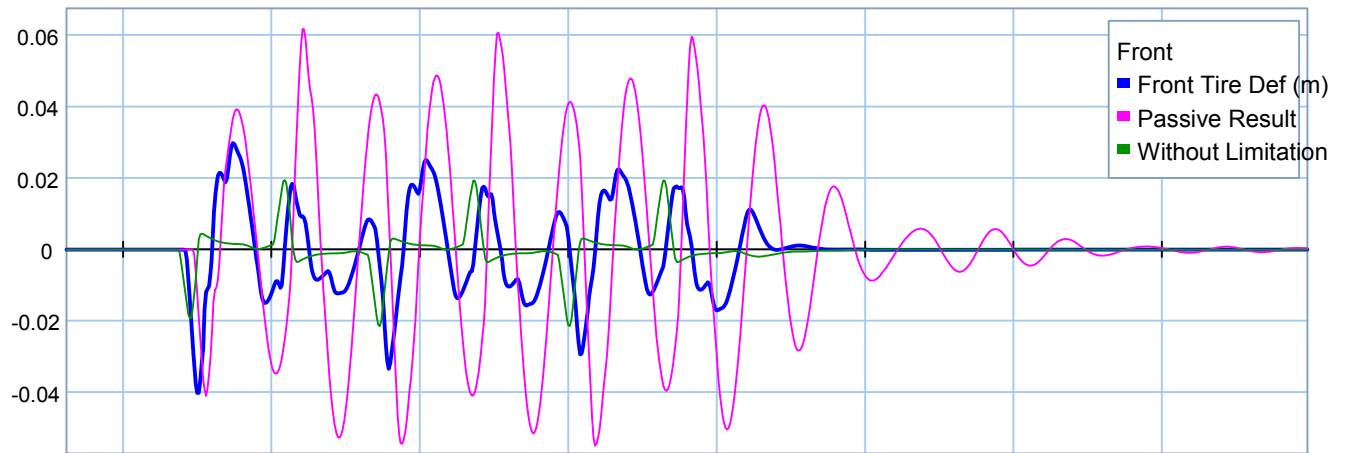
Appendix K: Non-Linear Half-Car Model, Road Holding Scenario Energy Analysis

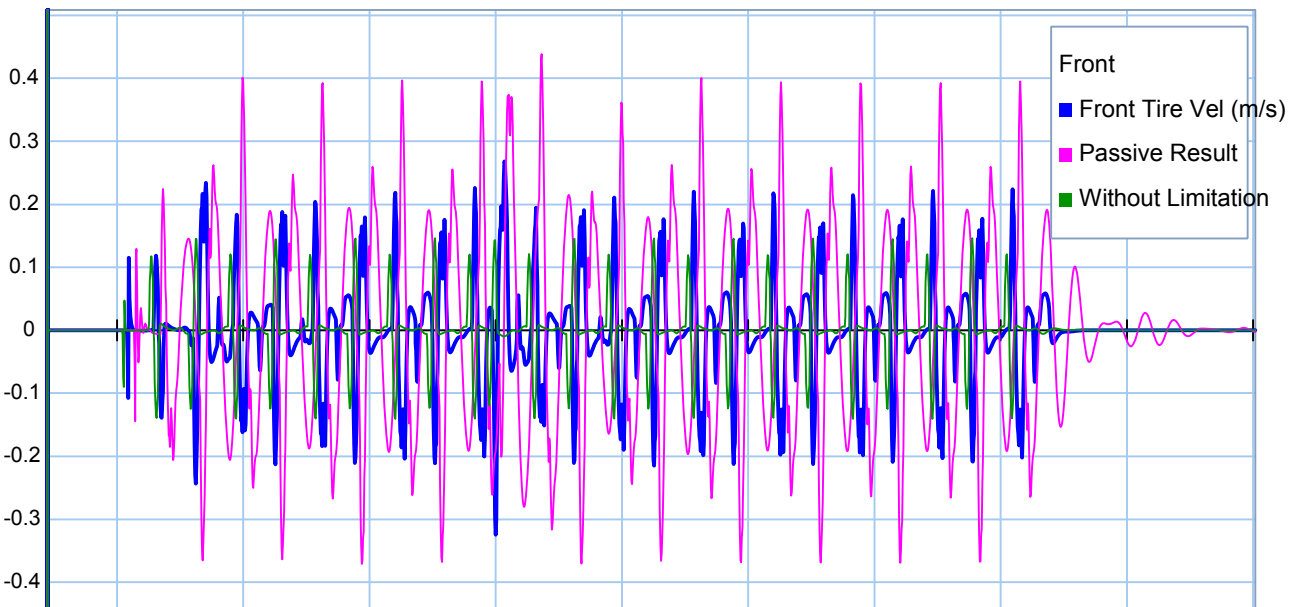
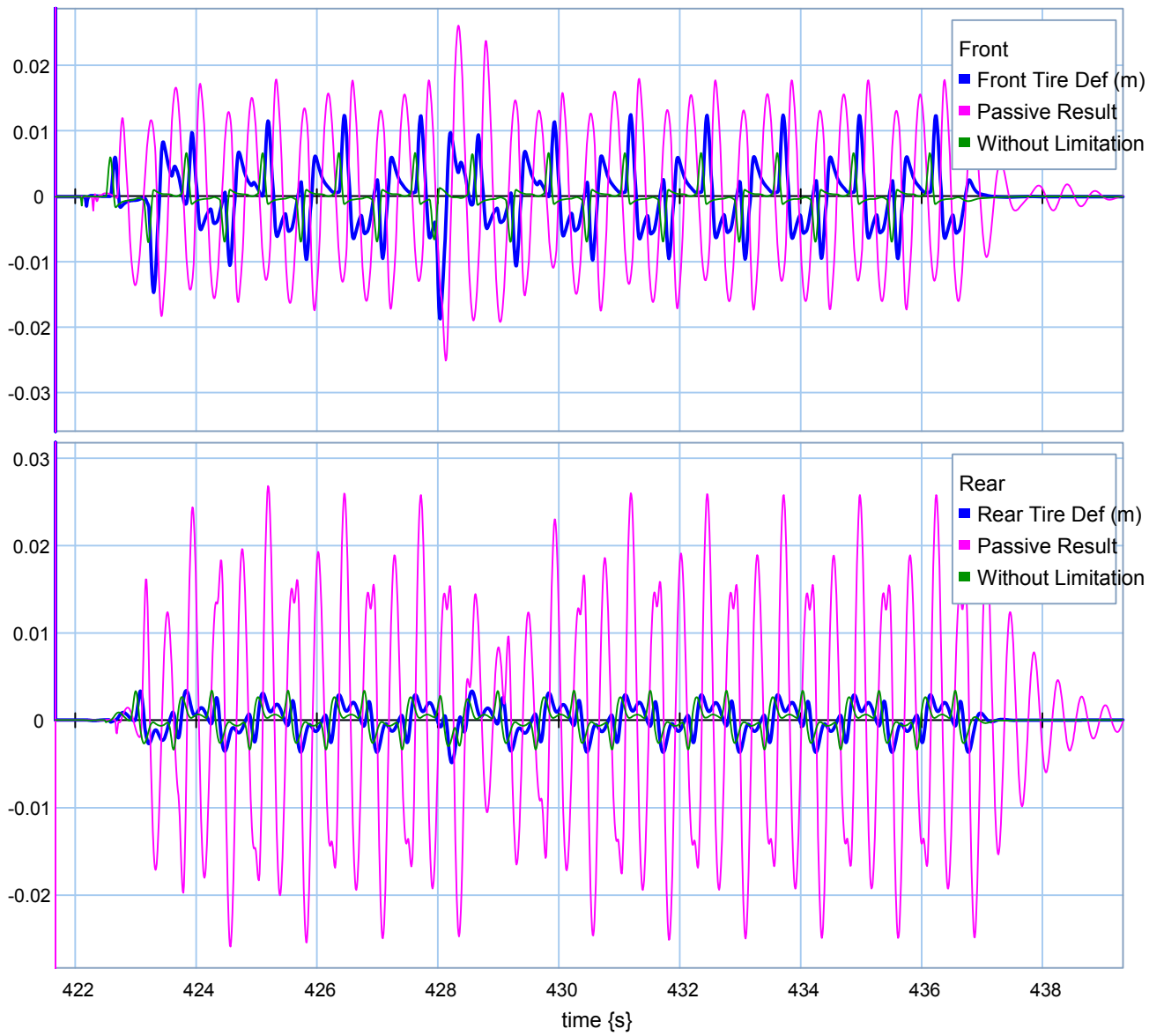
❖ Quarter-Car Active Suspension Units

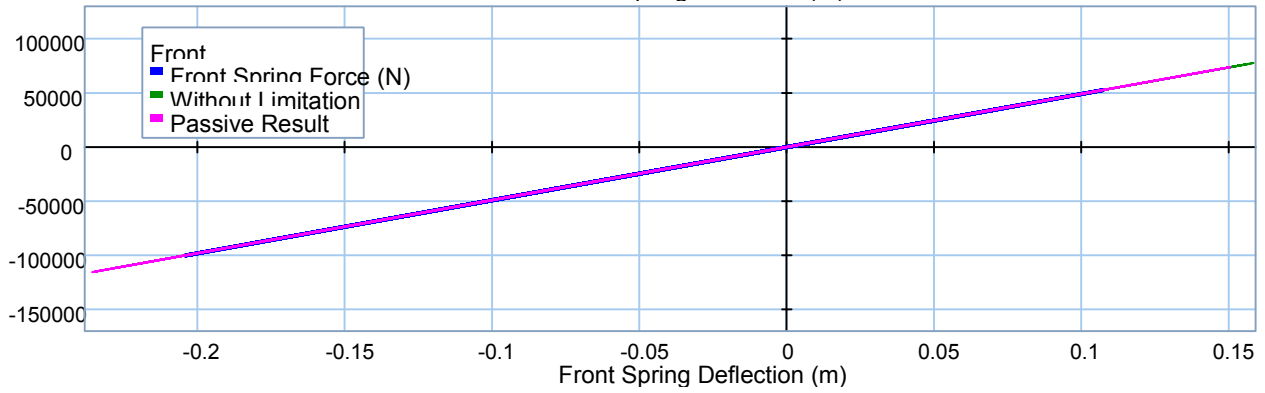
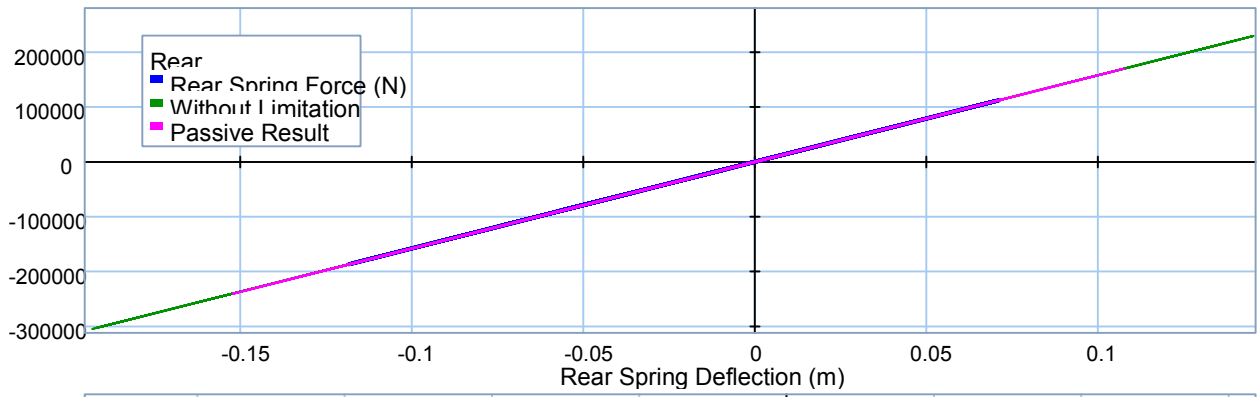




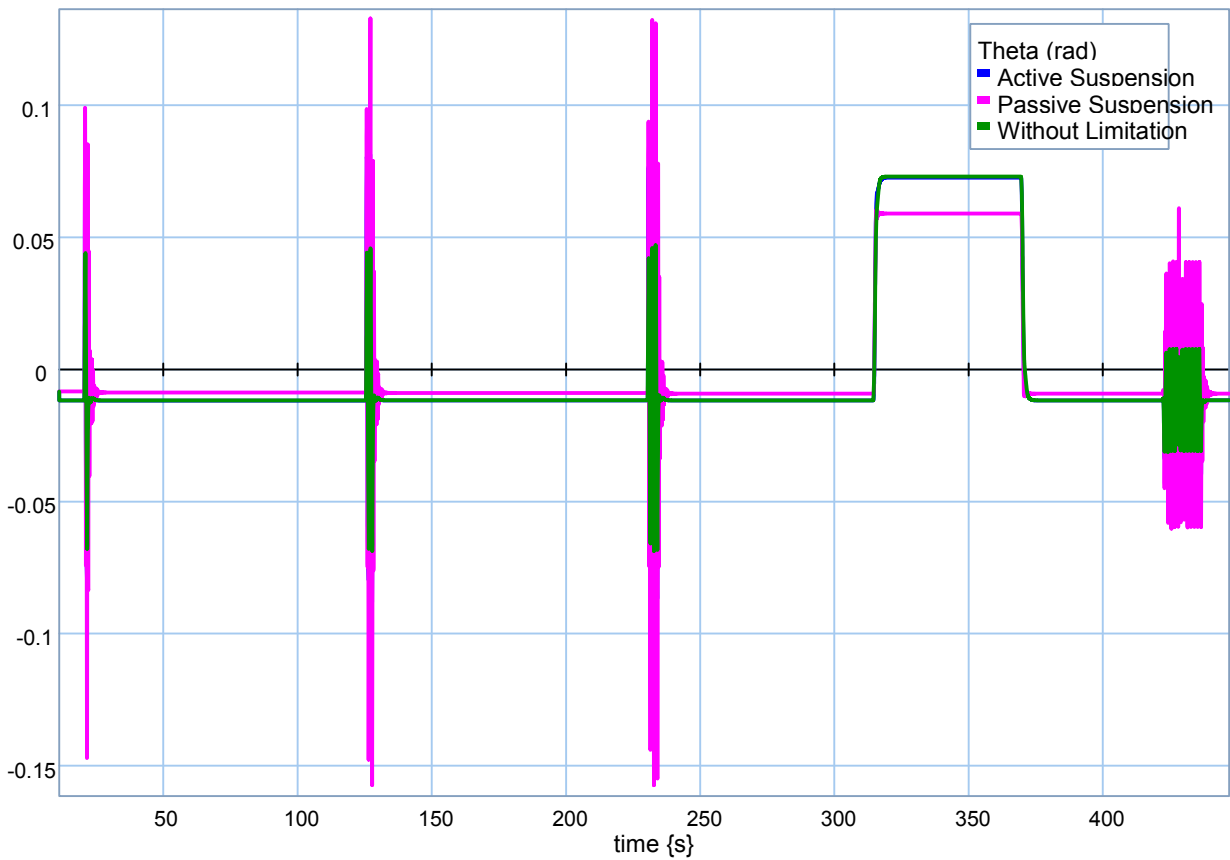


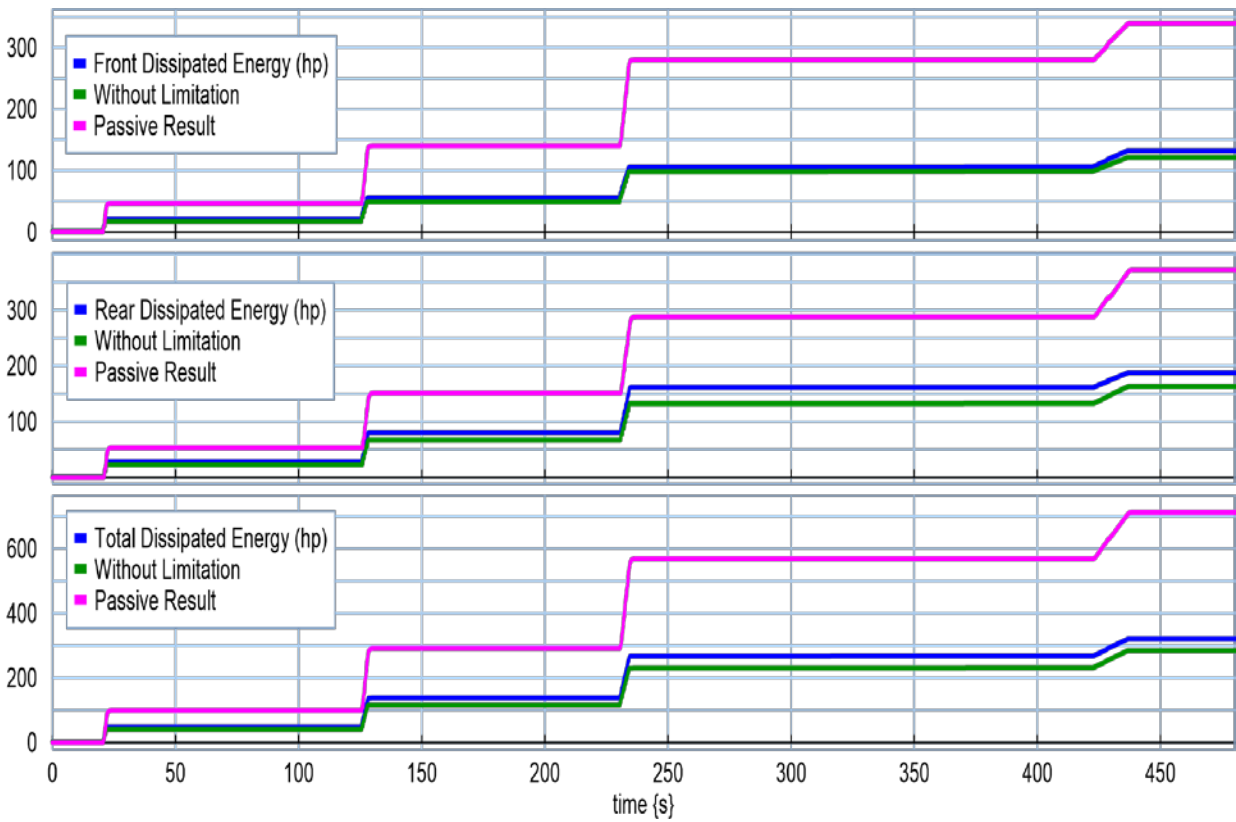
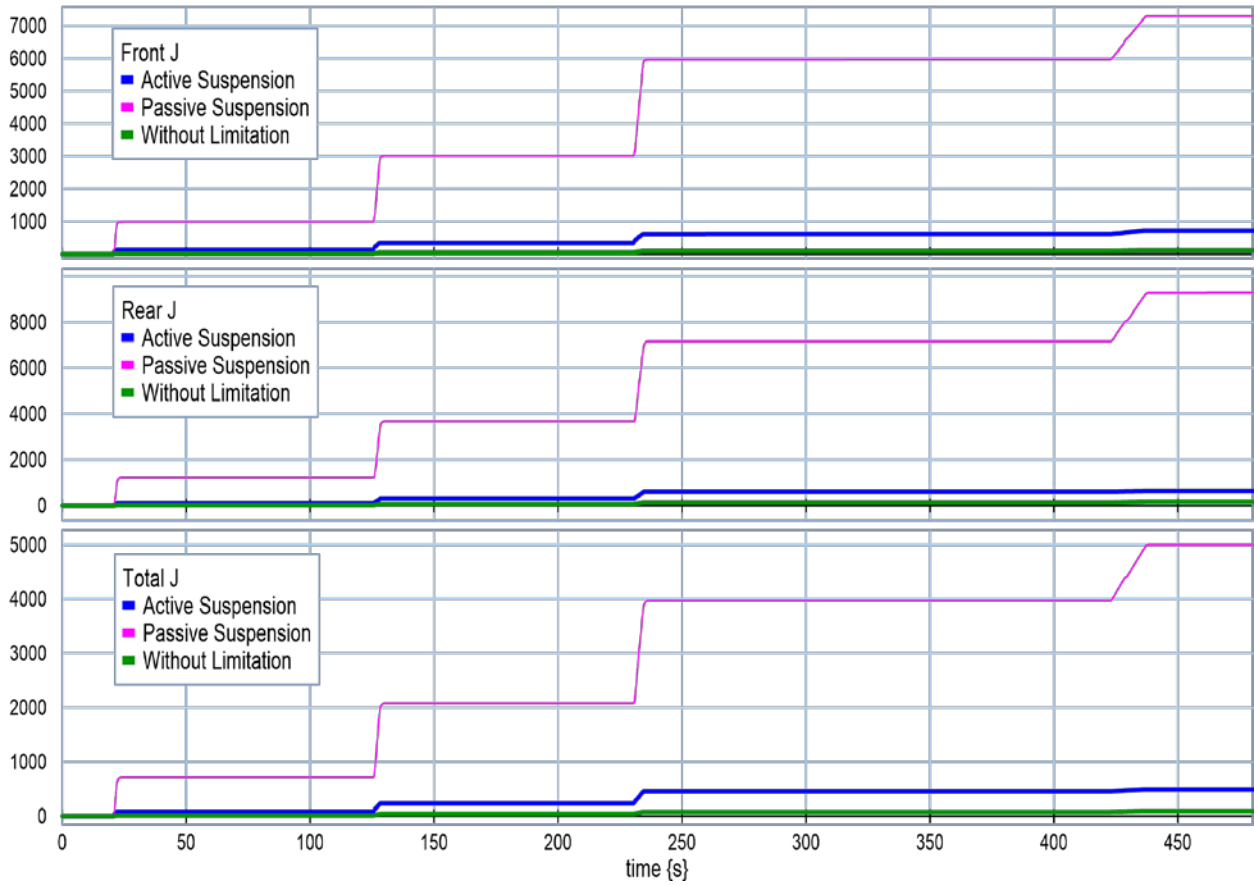


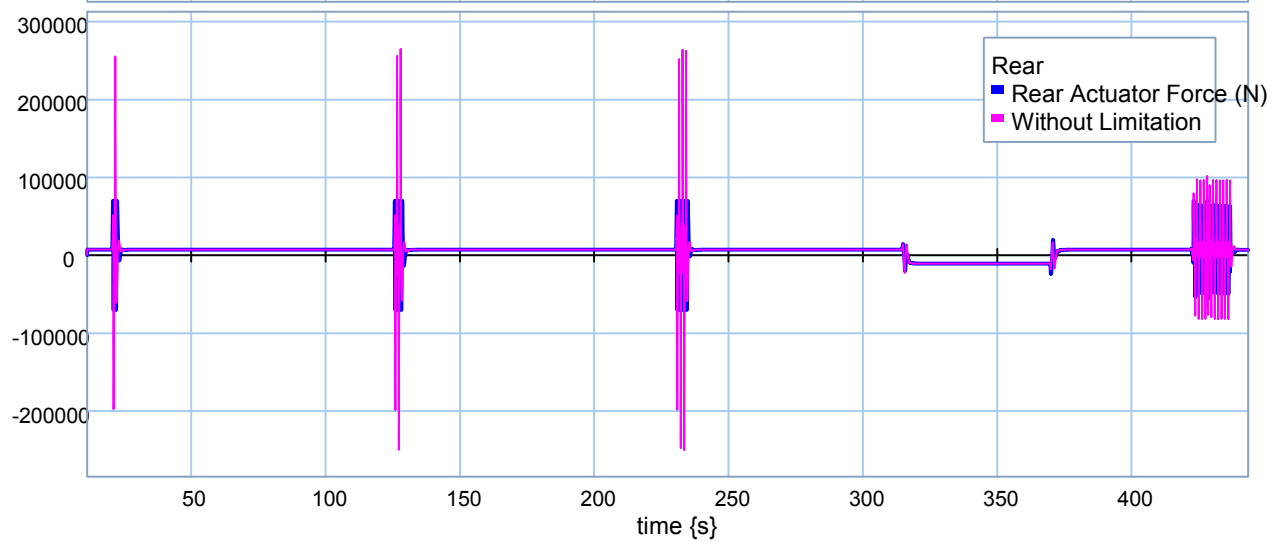
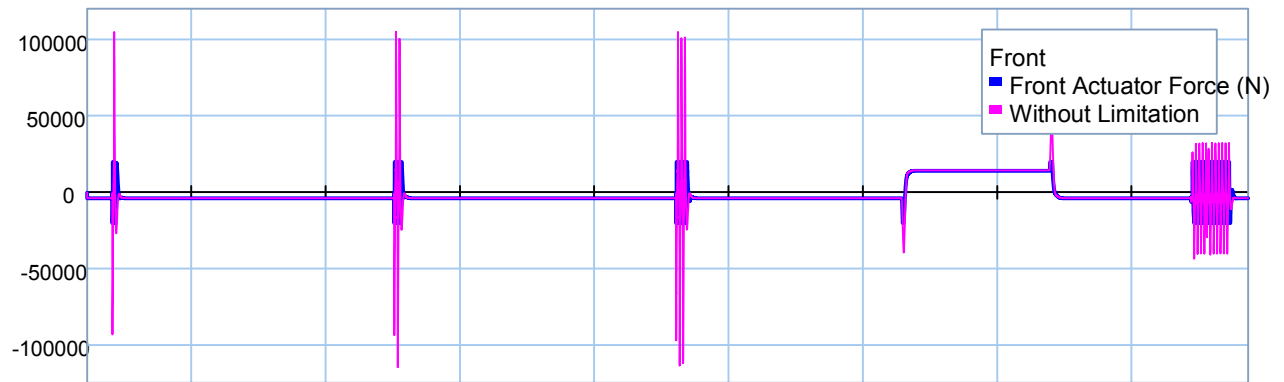
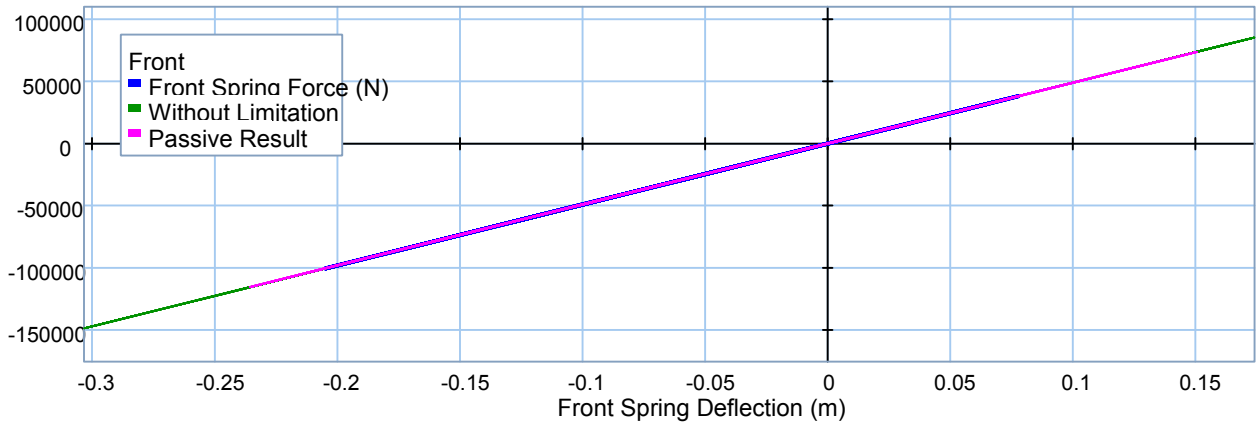
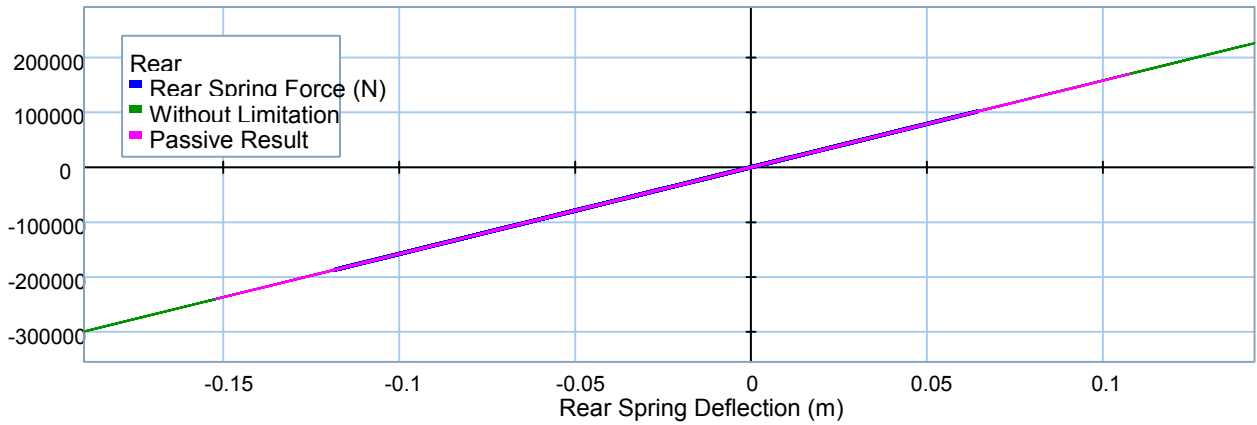


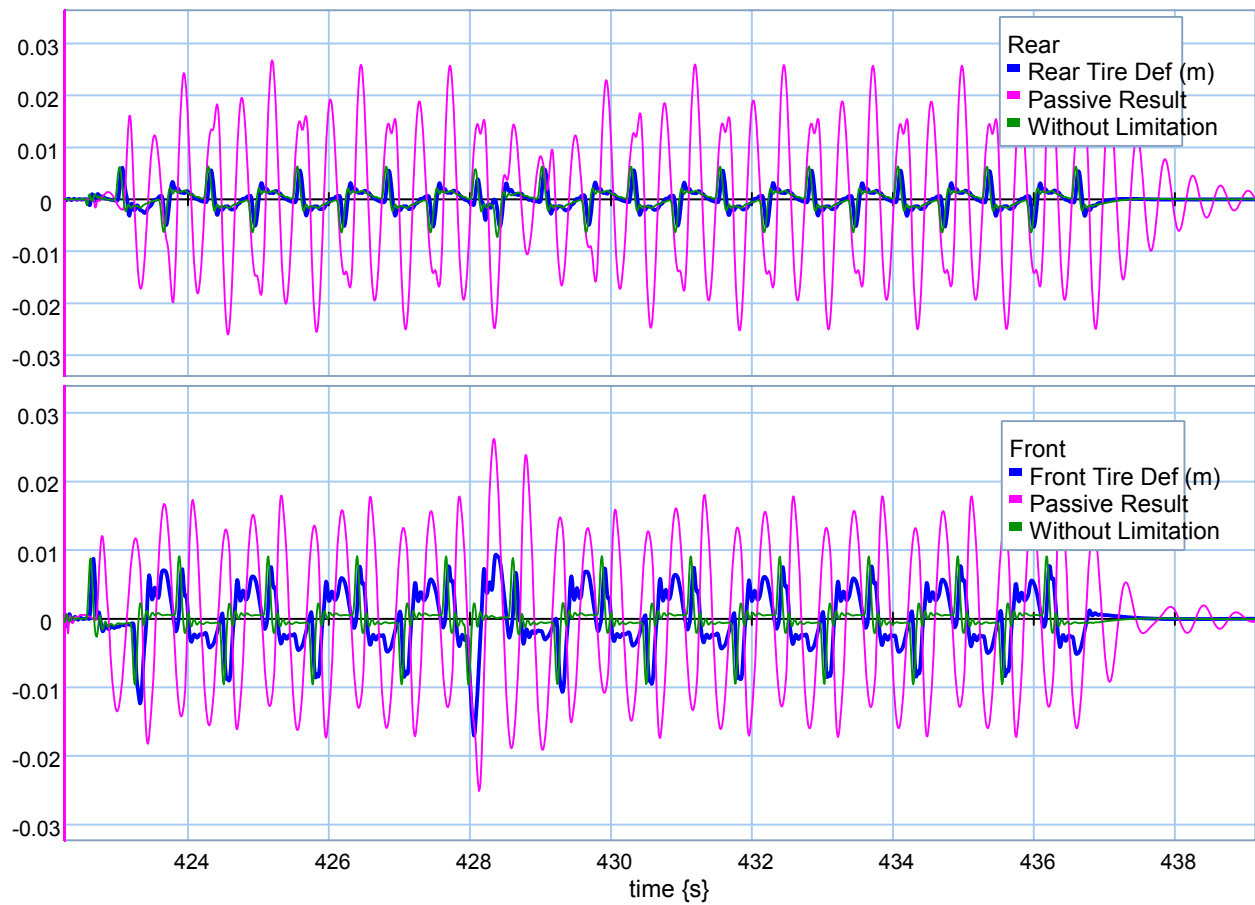
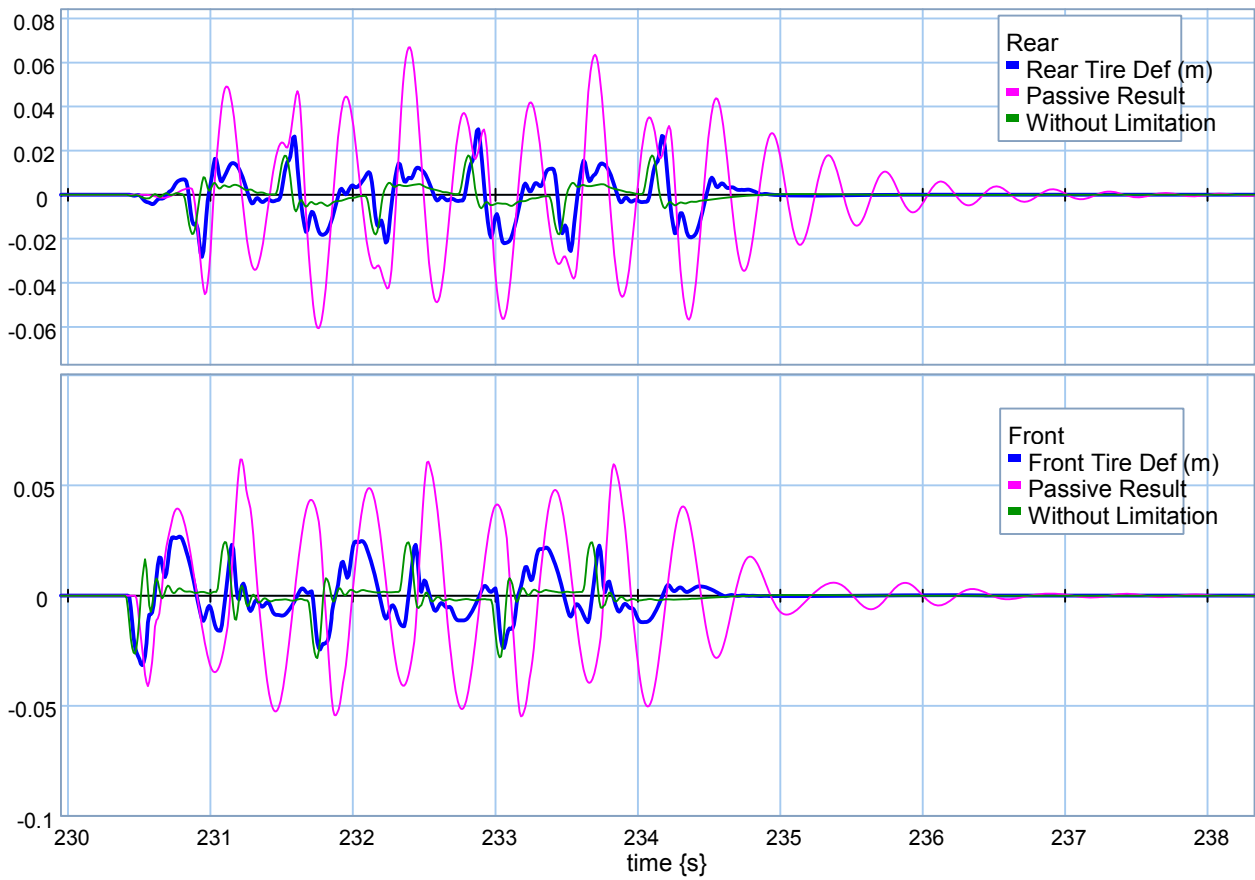


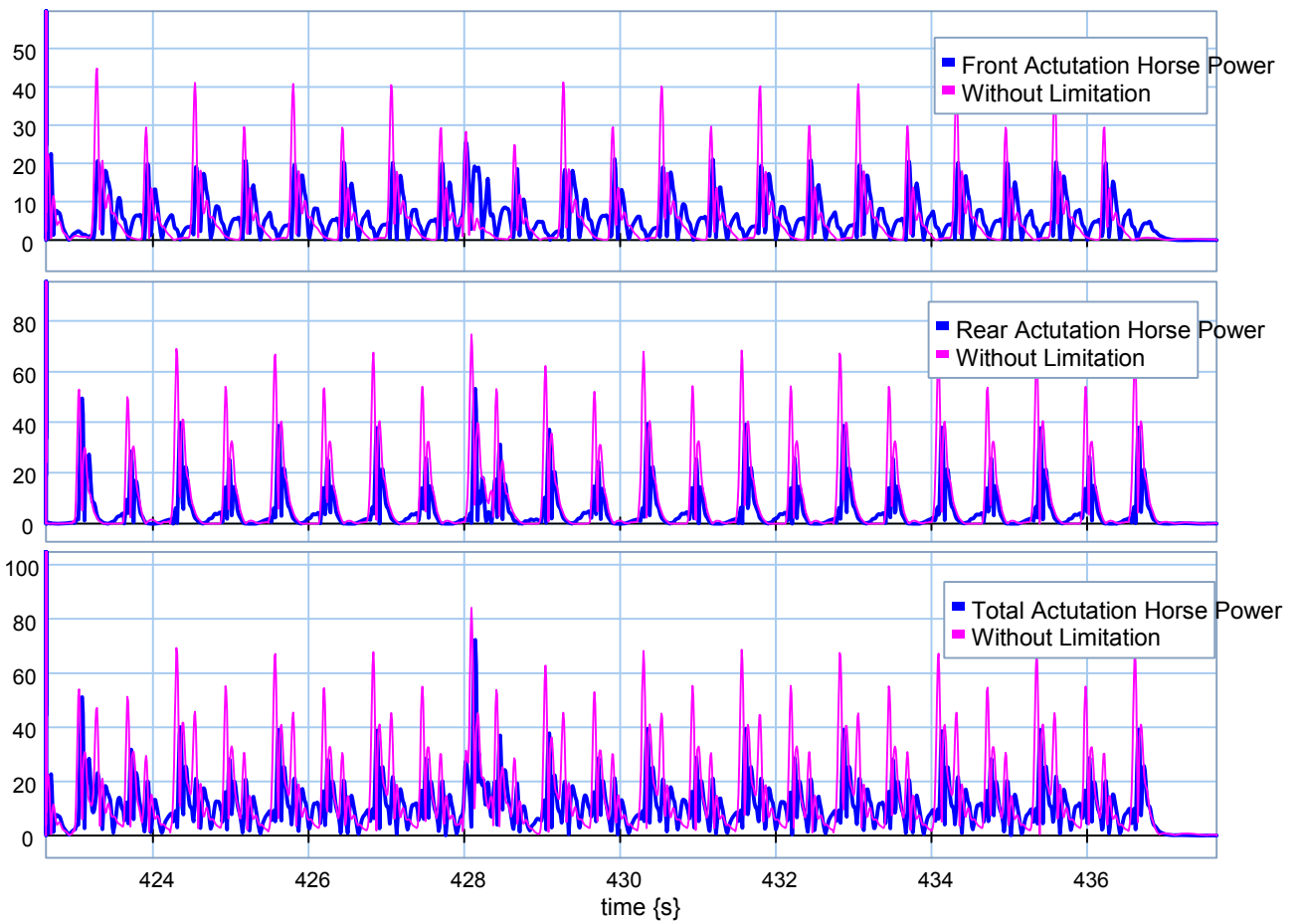
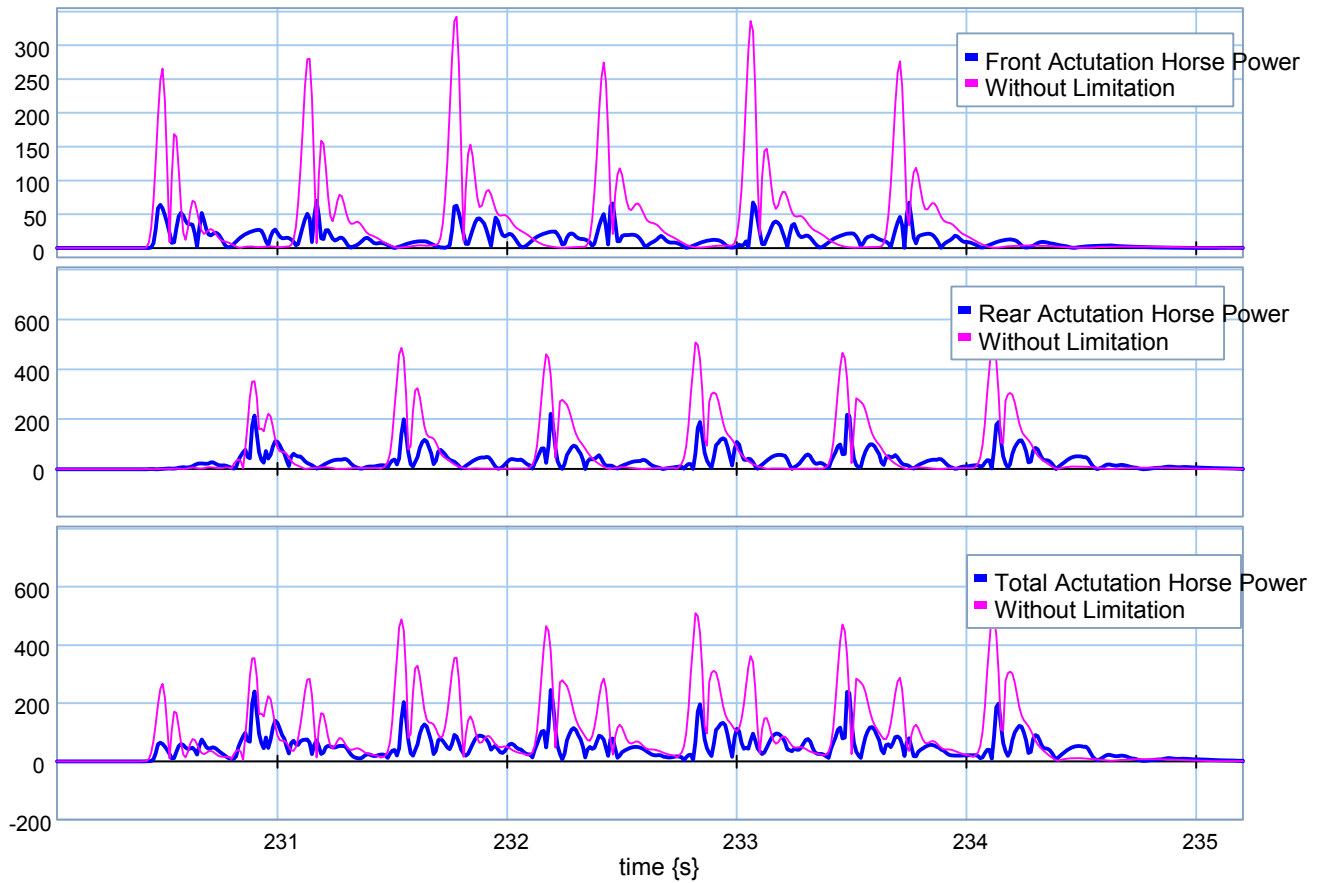
❖ HalfCar Active Suspension Units.

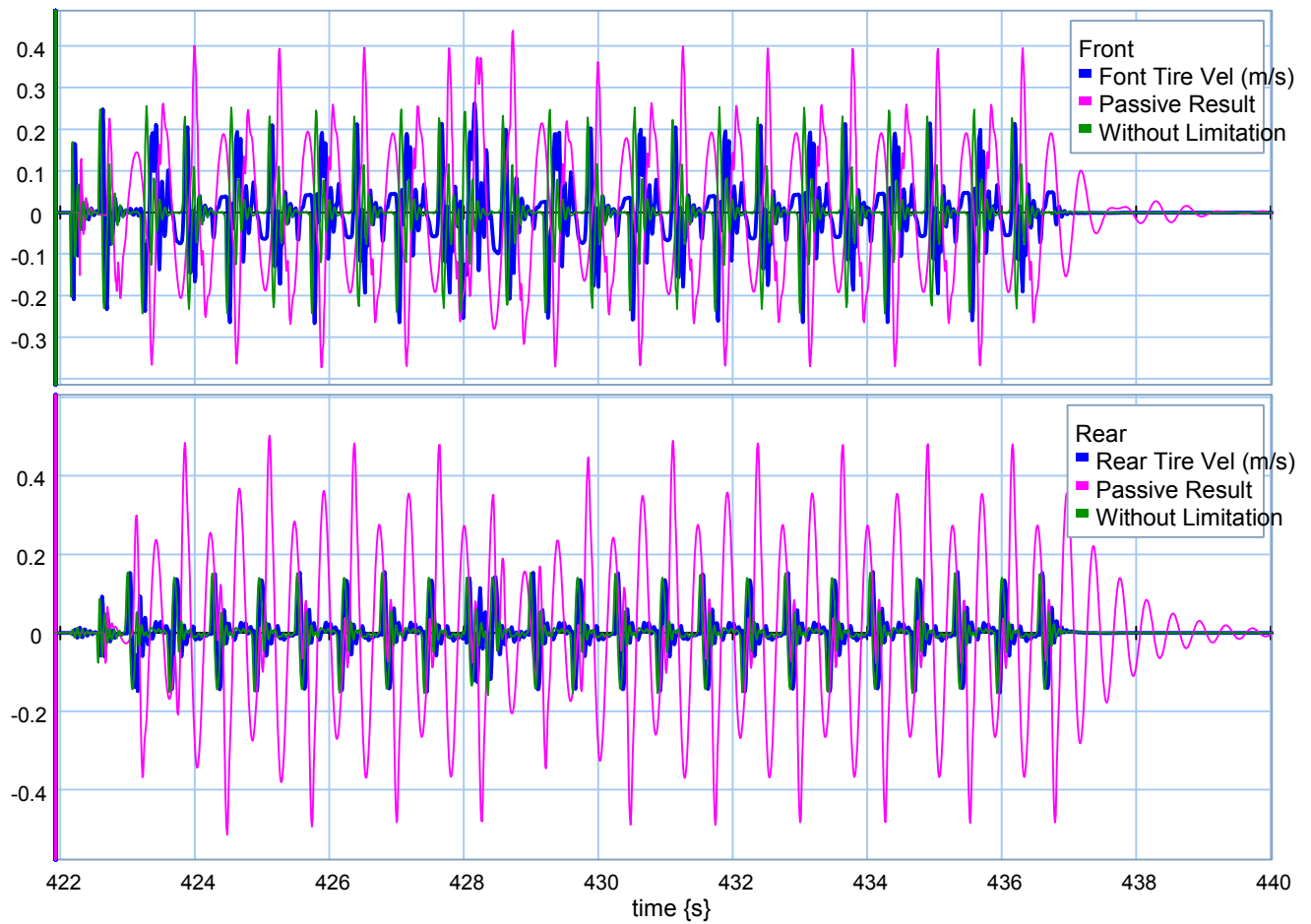
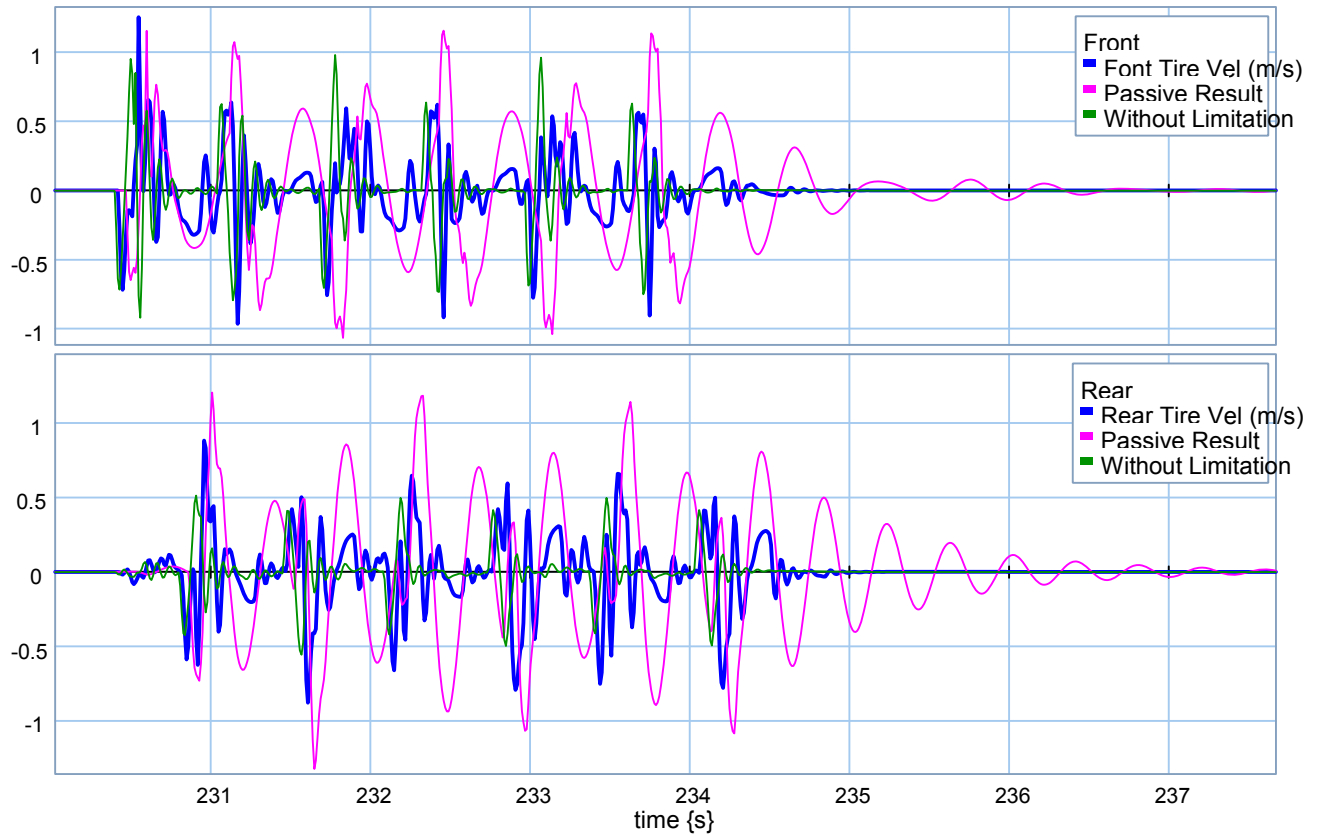












AppendixL: Properties Matrices for Halfar Active Suspension Approach.

$$A := \left[\left[\begin{array}{cccccccc} 0 & a & 0 & -1 & 0 & 1 & 0 & 0 \end{array} \right], \right. \\
 \left[\begin{array}{cccccccc} -\frac{a.ksf}{J} & -\frac{a^2.bsf + b^2.bsr}{J} & 0 & \frac{a.bsf}{J} & \frac{b.ksr}{J} & \frac{-a.bsf + b.bsr}{J} & 0 & -\frac{b.bsr}{J} \end{array} \right], \\
 \left[\begin{array}{cccccccc} 0 & 0 & 0 & 1 & 0 & 0 & 0 & 0 \end{array} \right], \\
 \left[\begin{array}{cccccccc} \frac{ksf}{Muf} & \frac{a.bsf}{Muf} & -\frac{kbf}{Muf} & -\frac{btf + bsf}{Muf} & 0 & \frac{a.bsf}{Muf} & 0 & 0 \end{array} \right], \\
 \left[\begin{array}{cccccccc} 0 & -b & 0 & 0 & 0 & 1 & 0 & -1 \end{array} \right], \\
 \left[\begin{array}{cccccccc} -\frac{ksf}{Ms} & \frac{-a.bsf + b.bsr}{Ms} & 0 & \frac{bsf}{Ms} & -\frac{ksr}{Ms} & -\frac{bsf + bsr}{Ms} & 0 & \frac{bsr}{Ms} \end{array} \right], \\
 \left[\begin{array}{cccccccc} 0 & 0 & 0 & 0 & 0 & 0 & 0 & 1 \end{array} \right], \\
 \left. \left[\begin{array}{cccccccc} 0 & -\frac{b.bsr}{Mur} & 0 & 0 & \frac{ksr}{Mur} & \frac{bsr}{Mur} & -\frac{ktr}{Mur} & -\frac{btr + bsr}{Mur} \end{array} \right] \right] \\
 \\
 B := \left[\begin{array}{cc} 0 & 0 \\ \frac{a}{J} & -\frac{b}{J} \\ 0 & 0 \\ -\frac{1}{Muf} & 0 \\ 0 & 0 \\ \frac{1}{Ms} & \frac{1}{Ms} \\ 0 & 0 \\ 0 & -\frac{1}{Mur} \end{array} \right] \qquad L := \left[\begin{array}{cc} 0 & 0 \\ 0 & 0 \\ -1 & 0 \\ -\frac{btf}{Muf} & 0 \\ 0 & 0 \\ 0 & 0 \\ 0 & -1 \\ 0 & \frac{btr}{Mur} \end{array} \right]$$

$$Q := \begin{bmatrix} q_{1,1} & q_{1,2} & q_{1,3} & q_{1,4} & q_{1,5} & q_{1,6} & q_{1,7} & q_{1,8} \\ q_{2,1} & q_{2,2} & q_{2,3} & q_{2,4} & q_{2,5} & q_{2,6} & q_{2,7} & q_{2,8} \\ q_{3,1} & q_{3,2} & q_{3,3} & q_{3,4} & q_{3,5} & q_{3,6} & q_{3,7} & q_{3,8} \\ q_{4,1} & q_{4,2} & q_{4,3} & q_{4,4} & q_{4,5} & q_{4,6} & q_{4,7} & q_{4,8} \\ q_{5,1} & q_{5,2} & q_{5,3} & q_{5,4} & q_{5,5} & q_{5,6} & q_{5,7} & q_{5,8} \\ q_{6,1} & q_{6,2} & q_{6,3} & q_{6,4} & q_{6,5} & q_{6,6} & q_{6,7} & q_{6,8} \\ q_{7,1} & q_{7,2} & q_{7,3} & q_{7,4} & q_{7,5} & q_{7,6} & q_{7,7} & q_{7,8} \\ q_{8,1} & q_{8,2} & q_{8,3} & q_{8,4} & q_{8,5} & q_{8,6} & q_{8,7} & q_{8,8} \end{bmatrix}$$

$$q_{1,1} := \rho^2 + \rho l \cdot \left(\frac{(a.ksf)^2}{J^2} \right) + \frac{ksf^2}{Ms^2}$$

$$q_{1,2} := \rho l \cdot \left(\frac{((a^2).bsf + (b^2).bsr)(a.ksf)}{J^2} \right) + \frac{ksf(a.bsfc + b.bsr)}{Ms^2}$$

$$q_{1,3} := 0$$

$$q_{1,4} := -\rho l \cdot \left(\frac{a.bsfc(a.ksf)}{J^2} \right) - \frac{ksfbsfc}{Ms^2}$$

$$q_{1,5} := -\rho l \cdot \left(\frac{b.ksr(a.ksf)}{J^2} \right) + \frac{ksfksr}{Ms^2}$$

$$q_{1,6} := -\rho l \cdot \left(\frac{(-a.bsfc + b.bsr)(a.ksf)}{J^2} \right) + \frac{ksf(bsfc + bsr)}{Ms^2}$$

$$q_{1,7} := 0$$

$$q_{1,8} := \rho l \cdot \left(\frac{b.bsr(a.ksf)}{J^2} \right) - \frac{ksfbsr}{Ms^2}$$

$$q_{2,1} := \rho l \cdot \left(\frac{((a^2).bsfc + (b^2).bsr)(a.ksf)}{J^2} \right) + \frac{ksf(a.bsfc + b.bsr)}{Ms^2}$$

$$q_{2,2} := \rho^3 + \rho l \cdot \left(\frac{((a^2).bsfc + (b^2).bsr)^2}{J^2} \right) + \frac{(a.bsfc + b.bsr)^2}{Ms^2}$$

$$q_{2,3} := 0$$

$$q_{2,4} := -\rho l \cdot \left(\frac{a.bsfc((a^2).bsfc + (b^2).bsr)}{J^2} \right) - \frac{(a.bsfc + b.bsr)bsfc}{Ms^2}$$

$$\begin{aligned}
q_{2,5} &:= -\rho l \cdot \left(\frac{b.ksr \left((a^2).bsf + (b^2).bsr \right)}{J^2} \right) + \frac{(a.bs f + b.bsr) ksr}{Ms^2} \\
q_{2,6} &:= -\rho l \cdot \left(\frac{(-a.bs f + b.bsr) \left((a^2).bsf + (b^2).bsr \right)}{J^2} \right) + \frac{(a.bs f + b.bsr) (bsf + bsr)}{Ms^2} \\
q_{2,7} &:= 0 \\
q_{2,8} &:= \rho l \cdot \left(\frac{b.bsr \left((a^2).bsf + (b^2).bsr \right)}{J^2} \right) - \frac{(a.bs f + b.bsr) bsr}{Ms^2} \\
q_{3,1} &:= 0 \\
q_{3,2} &:= 0 \\
q_{3,3} &:= \rho^4 \\
q_{3,4} &:= 0 \\
q_{3,5} &:= 0 \\
q_{3,6} &:= 0 \\
q_{3,7} &:= 0 \\
q_{3,8} &:= 0 \\
q_{4,1} &:= -\rho l \cdot \left(\frac{a.bs f (a.ksf)}{J^2} \right) - \frac{ksf bsf}{Ms^2} \\
q_{4,2} &:= -\rho l \cdot \left(\frac{a.bs f \left((a^2).bsf + (b^2).bsr \right)}{J^2} \right) - \frac{(a.bs f + b.bsr) bsf}{Ms^2} \\
q_{4,3} &:= 0 \\
q_{4,4} &:= \rho l \cdot \left(\frac{(a.bs f)^2}{J^2} \right) + \rho^5 + \frac{bsf^2}{Ms^2} \\
q_{4,5} &:= \rho l \cdot \left(\frac{b.ksr (a.bs f)}{J^2} \right) - \frac{bsf ksr}{Ms^2} \\
q_{4,6} &:= \rho l \cdot \left(\frac{(-a.bs f + b.bsr) (a.bs f)}{J^2} \right) - \frac{bsf (bsf + bsr)}{Ms^2} \\
q_{4,7} &:= 0 \\
q_{4,8} &:= -\rho l \cdot \left(\frac{b.bsr (a.bs f)}{J^2} \right) + \frac{bsf bsr}{Ms^2} \\
q_{5,1} &:= -\rho l \cdot \left(\frac{b.ksr (a.ksf)}{J^2} \right) + \frac{ksf ksr}{Ms^2} \\
q_{5,2} &:= -\rho l \cdot \left(\frac{b.ksr \left((a^2).bsf + (b^2).bsr \right)}{J^2} \right) + \frac{(a.bs f + b.bsr) ksr}{Ms^2} \\
q_{5,3} &:= 0 \\
q_{5,4} &:= \rho l \cdot \left(\frac{b.ksr (a.bs f)}{J^2} \right) - \frac{bsf ksr}{Ms^2}
\end{aligned}$$

$$\begin{aligned}
q_{5,5} &:= \rho l \cdot \left(\frac{(b.ksr)^2}{J^2} \right) + \rho 6 + \frac{ksr^2}{Ms^2} \\
q_{5,6} &:= \rho l \cdot \left(\frac{(-a.bsf + b.bsr)(b.ksr)}{J^2} \right) + \frac{ksr(bsf + bsr)}{Ms^2} \\
q_{5,7} &:= 0 \\
q_{5,8} &:= -\rho l \cdot \left(\frac{b.bsr(b.ksr)}{J^2} \right) - \frac{ksr bsr}{Ms^2} \\
q_{6,1} &:= -\rho l \cdot \left(\frac{(-a.bsf + b.bsr)(a.ksf)}{J^2} \right) + \frac{ksf(bsf + bsr)}{Ms^2} \\
q_{6,2} &:= -\rho l \cdot \left(\frac{(-a.bsf + b.bsr)((a^2).bsf + (b^2).bsr)}{J^2} \right) + \frac{(a.bsf + b.bsr)(bsf + bsr)}{Ms^2} \\
q_{6,3} &:= 0 \\
q_{6,4} &:= \rho l \cdot \left(\frac{(-a.bsf + b.bsr)(a.bsf)}{J^2} \right) - \frac{bsf(bsf + bsr)}{Ms^2} \\
q_{6,5} &:= \rho l \cdot \left(\frac{(-a.bsf + b.bsr)(b.ksr)}{J^2} \right) + \frac{ksr(bsf + bsr)}{Ms^2} \\
q_{6,6} &:= \rho 7 + \rho l \cdot \left(\frac{(-a.bsf + b.bsr)^2}{J^2} \right) + \frac{(bsf + bsr)^2}{Ms^2} \\
q_{6,7} &:= 0 \\
q_{6,8} &:= -\rho l \cdot \left(\frac{b.bsr(-a.bsf + b.bsr)}{J^2} \right) - \frac{(bsf + bsr) bsr}{Ms^2} \\
q_{7,1} &:= 0 \\
q_{7,2} &:= 0 \\
q_{7,3} &:= 0 \\
q_{7,4} &:= 0 \\
q_{7,5} &:= 0 \\
q_{7,6} &:= 0 \\
q_{7,7} &:= \rho 8 \\
q_{7,8} &:= 0 \\
q_{8,1} &:= \rho l \cdot \left(\frac{b.bsr(a.ksf)}{J^2} \right) - \frac{ksf bsr}{Ms^2} \\
q_{8,2} &:= \rho l \cdot \left(\frac{b.bsr((a^2).bsf + (b^2).bsr)}{J^2} \right) - \frac{(a.bsf + b.bsr) bsr}{Ms^2} \\
q_{8,3} &:= 0 \\
q_{8,4} &:= -\rho l \cdot \left(\frac{b.bsr(a.bsf)}{J^2} \right) + \frac{bsf bsr}{Ms^2} \\
q_{8,5} &:= -\rho l \cdot \left(\frac{b.bsr(b.ksr)}{J^2} \right) - \frac{ksr bsr}{Ms^2}
\end{aligned}$$

$$q_{8,6} := -\rho l \cdot \left(\frac{b.bsr(-a.bsf + b.bsr)}{J^2} \right) - \frac{(bsf + bsr) bsr}{Ms^2}$$

$$q_{8,7} := 0$$

$$q_{8,8} := \rho g + \rho l \cdot \left(\frac{(b.bsr)^2}{J^2} \right) + \frac{bsr^2}{Ms^2}$$

$$N := \begin{bmatrix} n_{1,1} & n_{1,2} \\ n_{2,1} & n_{2,2} \\ n_{3,1} & n_{3,2} \\ n_{4,1} & n_{4,2} \\ n_{5,1} & n_{5,2} \\ n_{6,1} & n_{6,2} \\ n_{7,1} & n_{7,2} \\ n_{8,1} & n_{8,2} \end{bmatrix}$$

$$n_{1,1} := -\rho l \cdot \left(\frac{a.ksf a}{J^2} \right) - \frac{ksf}{Ms^2}$$

$$n_{2,1} := -\rho l \cdot \left(\frac{((a^2).bsf + (b^2).bsr) a}{J^2} \right) - \frac{a.bsf + b.bsr}{Ms^2}$$

$$n_{3,1} := 0$$

$$n_{4,1} := \rho l \cdot \left(\frac{a.bsf a}{J^2} \right) + \frac{bsf}{Ms^2}$$

$$n_{5,1} := \rho l \cdot \left(\frac{b.ksr a}{J^2} \right) - \frac{ksr}{Ms^2}$$

$$n_{6,1} := \rho l \cdot \left(\frac{(-a.bsf + b.bsr) a}{J^2} \right) - \frac{bsf + bsr}{Ms^2}$$

$$n_{7,1} := 0$$

$$n_{8,1} := -\rho l \cdot \left(\frac{b.bsr a}{J^2} \right) + \frac{bsr}{Ms^2}$$

$$n_{1,2} := \rho l \cdot \left(\frac{a.ksf b}{J^2} \right) - \frac{ksf}{Ms^2}$$

$$n_{2,2} := \rho l \cdot \left(\frac{((a^2).bsf + (b^2).bsr) b}{J^2} \right) - \frac{a.bsaf + b.bsr}{Ms^2}$$

$$n_{3,2} := 0$$

$$n_{4,2} := -\rho l \cdot \left(\frac{a.bsfb}{J^2} \right) + \frac{bsf}{Ms^2}$$

$$n_{5,2} := -\rho l \cdot \left(\frac{b.ksrb}{J^2} \right) - \frac{ksr}{Ms^2}$$

$$n_{6,2} := -\rho l \cdot \left(\frac{(-a.bsaf + b.bsr) b}{J^2} \right) - \frac{bsf + bsr}{Ms^2}$$

$$n_{7,2} := 0$$

$$n_{8,2} := \rho l \cdot \left(\frac{b.bsr b}{J^2} \right) + \frac{bsr}{Ms^2}$$

$$R := \begin{bmatrix} r_{1,1} & r_{1,2} \\ r_{2,1} & r_{2,2} \end{bmatrix}$$

$$r_{1,1} := \rho l \cdot \left(\frac{a^2}{J^2} \right) + \frac{1}{Ms^2}$$

$$r_{1,2} := -\rho l \cdot \left(\frac{ba}{J^2} \right) + \frac{1}{Ms^2}$$

$$r_{2,1} := -\rho l \cdot \left(\frac{ba}{J^2} \right) + \frac{1}{Ms^2}$$

$$r_{2,2} := \rho l \cdot \left(\frac{b^2}{J^2} \right) + \frac{1}{Ms^2}$$

AppendixM: Continuous Algebraic Riccati Equation (CARE)

Considered plant:

$$\dot{x} = A \cdot x + B_1 \cdot d + B_2 \cdot u$$

$$z = C_1 \cdot x + D_{12} \cdot u$$

where:

$$A \in R^{n \times n}$$

$$B_1 \in R^n$$

$$B_2 \in R^n$$

$$d \in R \text{ (disturbance)}$$

$$u \in R \text{ (control input)}$$

$$z \in R^m \text{ (wants to be minimized)}$$

$$C_1 \in R^{m \times n}$$

$$D_{12} \in R^{m \times 1}$$

The controller in the LQR problem is designed to minimize the following performance index:

$$J = \int^{\infty} z^T \cdot z \, dt$$

$$J = \int^{\infty} [x^T C_1^T C_1 x + 2x^T C_1^T D_{12} u + u^T D_{12}^T D_{12} u] dt$$

All initial conditions are considered zero.

$$u = -(D_{12}^T D_{12})^{-1} B_2^T P x - (D_{12}^T D_{12})^{-1} (C_1^T D_{12})^T x$$

$$u = -(D_{12}^T D_{12})^{-1} [B_2^T P + (D_{12}^T D_{12})^{-1} (C_1^T D_{12})^T] x$$

$$A^T P + P A + C_1^T C_1 - (B_2^T P + D_{12}^T C_1)^T (D_{12}^T D_{12})^{-1} (B_2^T P + D_{12}^T C_1) = 0$$

The optimal value of the performance index with the above control input is:

$$J_{optimal} = x_0^T P x_0$$

AppendixN: Codes used in 2θSim Model

❖ Code used in one of the actuator units:

```
equations
  upperlimit=70000;
  lowerlimit=-70000;

  mR=-1;
  flow = p.f;
  p.e = RearGains*mR*x;

  if abs(RearGains*mR*x) <= upperlimit then
    p.e = RearGains*mR*x;
  end;

  if RearGains*mR*x > upperlimit then
    p.e = upperlimit;
  end;

  if RearGains*mR*x < lowerlimit then
    p.e = lowerlimit;
  end;
```

❖ Code used for slipping force:

```
equations
  if w_r<0.0 then
    v_kmax = -kmax;
  else
    v_kmax = kmax;
  end;

  if vel<0.0 then
    v_vmin = -vmin;
  else
    v_vmin = vmin;
  end;

  if abs(vel)<vmin then
```

```

        kappa_uncut = p.f/v_vmin;
    else
        kappa_uncut = p.f/vel;
    end;

    if abs(kappa_uncut) > 1.0 then
        kappa_lim =sign(kappa_uncut);
    else
        kappa_lim =kappa_uncut;
    end;

    if vel> 0.0 then
        kappa = kappa_lim;
    else
        kappa = -kappa_lim;
    end;

//Calculate Traction Force
    if abs(kappa)<max_slip then
        p.e = sign(kappa)*abs(Fz)*mu*abs(kappa)/max_slip;
    else
        p.e = sign(kappa)*abs(Fz)*mu;
    end;

    out = kappa;

```

❖ Code used for rolling force:

```

equations
    Fz_lbf = -Fz/4.448222/n_tire;
    max_fz = sign(p.f)*(-2.218283 + 0.005669*Fz_lbf + 0.233637*Fz_lbf/P -
0.000033886*(Fz_lbf^2)/P)*4.448222*n_tire;

    if abs(p.f)<v_min then
        p.e = max_fz*(abs(p.f)/v_min);
    else
        p.e = max_fz;
    end;

```